UNIVERSIDAD COMPLUTENSE DE MADRID
FACULTAD DE FARMACIA

TESIS DOCTORAL

Quantitative proteomics and immunoproteomics to explore host and Candida albicans complex interplay : focus on macrophage and antibody responses

Proteómica cuantitativa e inmunoproteómica dirigidas al estudio de la interacción entre el hospedador y Candida albicans : respuesta mediada por macrófagos y por anticuerpos

MEMORIA PARA OPTAR AL GRADO DE DOCTOR

PRESENTADA POR

Catarina Oliveira Vaz

Directoras

Concha Gil García
Lucía Monteoliva Díaz

Madrid

UNIVERSIDAD
COMPLUTENSE
MADRID

Quantitative proteomics and immunoproteomics to explore host and *Candida albicans* complex interplay: focus on macrophage and antibody responses

---

Proteómica cuantitativa e inmunoproteómica dirigidas al estudio de la interacción entre el hospedador y *Candida albicans:* respuesta mediada por macrófagos y por anticuerpos

Memoria para optar al grado de Doctor

Presentada por:
Catarina Oliveira Vaz

Directoras:
Dra. Concha Gil García
Dra. Lucía Monteoliva Díaz

Departamento de Microbiología y Parasitología
Facultad de Farmacia
Universidad Complutense de Madrid
Madrid, 2019

UNIVERSIDAD COMPLUTENSE MADRID

DECLARACIÓN DE AUTORÍA Y ORIGINALIDAD DE LA TESIS PRESENTADA PARA OBTENER EL TÍTULO DE DOCTOR

D./Dña. Catarina Oliveira Vaz,
estudiante en el Programa de Doctorado Microbiología y Parasitología,
de la Facultad de Farmacia de la Universidad Complutense de Madrid, como autor/a de la tesis presentada para la obtención del título de Doctor y titulada:

Quantitative proteomics and immunoproteomics to explore host and Candida albicans complex interplay: focus on macrophage and antibody responses //
Proteómica cuantitativa e inmunoproteómica dirigida al estudio de la interacción entre el hospedador y Candida albicans: respuesta mediada por macrófagos y por anticuerpos

y dirigida por: Concha Gil Garcia y Lucía Monteoliva Díaz

DECLARO QUE:

La tesis es una obra original que no infringe los derechos de propiedad intelectual ni los derechos de propiedad industrial u otros, de acuerdo con el ordenamiento jurídico vigente, en particular, la Ley de Propiedad Intelectual (R.D. legislativo 1/1996, de 12 de abril, por el que se aprueba el texto refundido de la Ley de Propiedad Intelectual, modificado por la Ley 2/2019, de 1 de marzo, regularizando, aclarando y armonizando las disposiciones legales vigentes sobre la materia), en particular, las disposiciones referidas al derecho de cita.

Del mismo modo, asumo frente a la Universidad cualquier responsabilidad que pudiera derivarse de la autoría o falta de originalidad del contenido de la tesis presentada de conformidad con el ordenamiento jurídico vigente.

En Madrid, a 16 de julio de 2019

Fdo.: Catarina Oliveira Vaz

Esta DECLARACIÓN DE AUTORÍA Y ORIGINALIDAD debe ser insertada en la primera página de la tesis presentada para la obtención del título de Doctor.

Dª. GLORIA MOLERO MARTÍN-PORTUGUÉS, DIRECTORA DEL DEPARTAMENTO DE MICROBIOLOGÍA Y PARASITOLOGÍA DE LA FACULTAD DE FARMACIA DE LA UNIVERSIDAD COMPLUTENSE DE MADRID,

CERTIFICA: Que Doña Catarina Oliveira Vaz ha realizado en el Departamento de Microbiología y Parasitología de la Universidad Complutense de Madrid bajo la dirección de las Doctoras Concha Gil García y Lucía Monteoliva, el trabajo que presenta para optar al grado de Doctor con el título:

Quantitative proteomics and immunoproteomics to explore host and *Candida albicans* complex interplay: focus on macrophage and antibody responses // Proteómica cuantitativa e inmunoproteómica dirigidas al estudio de la interacción entre el hospedador y *Candida albicans:* respuesta mediada por macrófagos y por anticuerpos

Y para que así conste, firmo la presente certificación en Madrid, 2019

Fdo. Prof. Dra. Dª. Gloria Molero Martín-Portugués

ESTA TESIS DOCTORAL HA SIDO POSIBLE GRACIAS A LA CONCESÍON DE LA BECA PREDOCTORAL:

- Beca del programa europeo *Marie Curie Initial Training Network* (FP7-PEOPLE-2013-ITN ImResFun, Grant agreement ID: 606786) durante el período Marzo 2014 – Febrero 2017.

EL TRABAJO DESCRITO HA ESTADO INCLUIDO EN LOS SIGUIENTES PROYECTOS:

- "*Molecular Mechanisms of Fungal Pathogen-Host Interactions*" del programa europeo *Marie Curie Initial Training Network* (FP7-PEOPLE-2013-ITN ImResFun).

-"Estudio de proteínas de *Candida* y de macrófago relacionados con apoptosis y señalización mediante proteómica dirigida. Nuevos métodos de inmunoprevención y diagnóstico" Proyecto BIO2015-65147-R del Ministerio Español de la Economia y Competitividad (MINECO).

- Proyecto InGEMICS-CM B2017/BMD-3691 de la Comunidad Autónoma de Madrid .

-Plataforma en Red de Recursos Biomoleculares y Bioinformáticos PRB3 (PT17/0019/0012) del Instituto de Salud Carlos III (ISCIII).

EL TRABAJO PRESENTADO HA SIDO DESAROLLADO EN COLABORACION CON:

- Unidad de Proteómica da la Universidad Complutense de Madrid, Madrid, España.

- Profesor Ole Jensen Y Dr. Pavel Shliaha del Departamento de Bioquimica y Biologia Molecular, de la Universidad Syddansk, Odense, Dinamarca.

- Profesor Uwe Groß, Dr. Oliver Bader y Dr. Emilia Gomez del Instituto de Microbiologia Medica del Centro Médico Universitario de Göttingen, Göttingen, Alemania.

Aos meus pais, ao meu irmão Necas, à minha Inês.
Ao João

ACKNOWLEDGEMENTS

De forma muy especial a mis dos jefas Concha Gil y Lucia Monteoliva que me han apoyado en todos los momentos. Muchas gracias por haberme dado mucha fuerza e ilusión para seguir adelante con el trabajo, y por ayudarme a ver el trabajo de forma más optimista. Muchas gracias por confiar en mí y por haberme transmitido todo el conocimiento, especialmente de proteómica un tema totalmente desconocido para mí cuando llegué al departamento.

A la tercera jefa Gloria Molero, muchas gracias por todo tu apoyo y consejos.

Al Departamento de Microbiología y Parasitología que me ha acogido con los brazos abiertos. Ha sido un placer compartir este lugar de trabajo con personas con muchísimo conocimiento, muchísima ilusión por la ciencia y por saber siempre más. A todos los profesores, pos-docs, técnicos y personal de la secretaría, he aprendido muchísimo con todos vosotros.

A todos los miembros de la Unidad 1. Especialmente a Jose que ha sido como mi jefe cuando llegué, me ha enseñado muchísimas técnicas nuevas. Muchas gracias por haberme apoyado y por la alegría que transmitías al laboratorio. De forma muy especial también a Aida, muchas gracias por haberme enseñado a hacer inmunoproteómica, por todas las discusiones científicas, estadísticas y por las pelis de viernes, que juntamente con Ahinara hacían cambiar el mundo. He aprendido muchísimo con nuestras conversaciones. A todos los TFM y TFG que traían mucha alegría y buena disposición. A Elvira, Ana, Vital, Perce, Victoria y Raquel.

Tengo que agradecer de forma muy muy especial y verdadera a mi compañera de doctorado *"mi arma"* Ahinara. Muchas gracias por haberme enseñado español, por tu amistad, alegría y cariño. Hemos compartido muchas experiencias y momentos, unos más alegres y otros más tristes, pero eso nos ha dado el ánimo para terminar todo este proceso. Muchas gracias por tu verdadera amistad. ¡Tu ayuda ha sido indispensable para todo!¡Voy a echarte mucho de menos!

¡A Mónica, aún que has estado poco tiempo en laboratorio creamos una amistad muy buena y cercana! ¡¡¡Muchas gracias por tu apoyo y palabras de ánimo y fuerza!!!

A la Unidad de Proteomica, Maria Luisa, Felipe, Ines, Lola, Enrique y Ebrahim. Muchas gracias por vuestra ayuda y partilla de conocimientos proteomico y estadístico.

A Inma, Mar y Almudena, por toda la ayuda siempre con una sonrisa.

A Benito, a Jose y a Elena por toda la ayuda y buena disposición.

A Mercedes por tu risa y alegría que contagia¡!

A las chicas de la U4, Belen, Sonia, Monica y Vero con quien bajamos al café y al sol. A todos los miembros de la U2 y U3.

To all IMRESFUN members both PIs (Karl Kuchler, Steffen Rupp, Per Ljungdahl, Uwe Groß, Julian Naglik, Hana Sychrová, Renate Spohn, Attila Gacser, Toni Gabaldon, Thomas Lion and Leif Schauser) and students (Raju, Debora, Fitz, Emilia, Mariana, Vicent, Claudia, Tanmoy, Ernst, Leonel, Nathalie, Nitesh and Andreas). Thank you for turning my first three years of PhD into amazing years where I had the opportunity to learn with the best researchers of this field. It was an amazing experience, all the meetings, courses, and conferences allowed me to develop a variety of skills. I really spent great and funny moments with all of you.

A special thanks to the people that host me during my secondments: Ole Jensen and Pavel Shliaha from the Odense University in Denmark, Leif Schauser and Nitesh from Qiagen in Denmark and Julian Naglik and Mariana. Thank you for hosting me, I learned a lot during these short stays.

A todos os portugueses que conheci em Madrid e que ajudaram de alguma forma a diminuir as saudades de casa e que encherem muitos fins de tarde e noites de boa disposição, boas conversas e muita alegria. Obrigada à Bebé, ao Santo, à Nuna, ao Rochinha, à Joana Castro à Diana e à Fonte.

De forma muito especial à minha marida Carol. Obrigada pela companhia, amizade, boa disposição, por me ouvires e apoiares quando as coisas não estavam tão bem e obrigada por todos os risos e brincadeiras nos momentos mais alegres. Sem dúvida que esta etapa foi muito mais fácil contigo ao lado. Obrigada!

To Pia, it was so nice meeting you, thank you for all the great time we spent together! I hope we can meet again and again in Madrid or any other place!!

A todos os meus amigos que embora longe geograficamente (uns mais do que outros) estiveram sempre perto, num cantinho do meu coração. À Joana Cunha por teres sabido sempre de forma tão tua e maravilhosa dar-me a força para enfrentar tudo e deixar-me desabafar sobre tudo (e com várias repetições do mesmo) e por estares sempre presente! Obrigada pelos nossos momentos que me deram tanta força para seguir em frente! À Ana Xavier que me mostrou que a distância não abala uma verdadeira amizade e por me dar a segurança de estar sempre comigo *no matter what*. Sem dúvida que sem vocês isto sería muito mais difícil. Não tenho palavras para descrever a nossa amizade. Obrigada por serem pessoas maravilhosas.

Ao núcleo duro: Lisa, Davide, Joaninha, Raquel, Jé, Mika, Samy e Nuno. Tudo é mais fácil quando acompanhada de amigos como vocês. À minha Lili obrigada por todo o teu carinho, amizade, obrigada pelos nossos momentos. À Joana Pereira a minha alma gémea científica e minha querida amiga.

Às professorinhas Paula Sampaio e Célia Pais porque sem elas esta aventura nunca teria sido possível.

Aos meus pais. Obrigada por estarem sempre presentes, por todos os conselhos e ajudas e por me ouvirem sempre que preciso. A conclusão desta etapa é em grande parte vossa. Sem a vossa ajuda, apoio e palavras de força a conclusão desta etapa não teria sido possível. E, finalmente agradeço muito todos aqueles miminhos e aquelas comidinhas que me faziam porque sabiam que tinha saudades. Obrigada por tudo!

Ao meu irmão Nequinhas. Por toda a tua força e determinação e por estares sempre presente. Sempre que precisei de alguma coisa, o que quer que fosse pude contar contigo. Sei que houve momentos melhores e piores enquanto estive fora, mas conseguiste superá-los sempre! Obrigada e sabes que tenho muito orgulho em ti!

Obrigada à minha Inês, cresceste muito desde que saí de Braga espero que continues a crescer dessa forma tão bonita. A minha tia Nini obrigada por estares sempre presente, por toda a tua ajuda e apoio e por todos aqueles miminhos que me davas para trazer para Madrid. Ao Filipe, sempre pronto para uma boa conversa. À minha tia Graça obrigada pela tua ajuda incansável e sempre com esse sorriso que tanto nos contagia. À minha tia Pi também sempre disponível. Às minhas avós.

Ao João. Sem dúvida que esta etapa se tornou mais fácil, mais feliz e infinitamente melhor depois de decidirmos que a vida era melhor se a seguíssemos juntos. Foi tudo graças à tua preserverança. Obrigada por estares sempre ao meu lado, por me ouvires sempre que preciso e por seres a melhor pessoa que já conheci. Obrigada por estes anos incríveis! Conhecemos muitos sítios, conhecemos ainda melhor Madrid e Dublin, cidades que vão ficar sempre num cantinho do nosso coração. Obrigada por me teres dado a conhecer a pessoa maravilhosa que és. Obrigada por me aturares, principalmente nesta parte final.

"Saudades, só portugueses
Conseguem senti-las bem,
Porque têm essa palavra
Para dizer que as têm"

Fernando Pessoa

Muchas gracias! Thank you! Obrigada!

TABLE OF CONTENTS

LIST OF FIGURES

FIGURES IN GENERAL INTRODUCTION (GI)

FIGURES IN CHAPTER 1 (C1)

FIGURES IN CHAPTER 2 (C2)

FIGURES IN GENERAL DISCUSSION (GD)

LIST OF TABLES

TABLES IN GENERAL INTRODUCTION (GI)

TABLES IN CHAPTER 1 (C1)

TABLES IN CHAPTER 2 (C2)

LIST OF ABBREVIATIONS

Abbreviation	Meaning
ºC	degrees Celsius
2-DE	2 dimensional electrophoresis
2D-DIGE	2D difference gel electrophoresis
ACN	acetonitrile
ADP	adenosine diophosphate
ALS	agglutinin-like sequence
APCs	antigen-presenting cells
ATP	adenosine triphosphate
BCA	bicinchoninic acid
BSI	bloodstream infections
CAGTA	*C. albicans* germ tube antibody
CARD9	caspase recruitment domain-containing protein 9
CCCP	carbonyl cyanide m-chlorophenyl hydrazine
CFW	calcofluor white
CGD	*Candida* genome database
CHAPS	3-[(3-cholamidopropyl) dimethylammonio]-1-propanesulfonate hydrate
CID	collision induced dissociation
CLRs	c-type lectin receptor
CPP	calcium phosphate precipitation
CTLDs	c-type lectin like domains
CWPs	cell-wall proteins
DCs	dendritic cells
DDA	data-dependent analysis
DIA	data-independent acquisition
DMEM	Dulbecco's modified Eagle's medium
DMSO	dimethyl sulfoxide
DNA	deoxyribonucleic acid
DTE	dithioerytritol
DTT	dithiothreitol
ECMM	European Confederation of Medical Mycology
EDTA	ethylenediaminetetraacetic acid
ELISA	enzyme-linked immunosorbent assay
ER	endoplasmic reticulum
ESEM	environmental scanning electron microscopy
EVs	extracellular vesicles
FA	formic acid
FBS	fetal bovine serum
FSB	5'-p-fluorosulfonylbenzoyladenosine
GAFFI	global action fund for fungal infections
G-CSF	granulocyte colony-stimulating factor
GlcNac	n-acetylglucosamine
GM-CSF	granulocyte-macrophage colony-stimulating factor

GO	gene ontology
GPI	glycophosphatidylinositol
GUT	gastrointestinal induced transition
h	hour
HCD	higher energy collisional dissociation
HEPES	4-(2-hydroxyethyl)-1-piperazineethanesulfonic acid
HILIC	hydrophilic interaction liquid chromatography
HIV	human immunodeficiency virus
HPLC	high performance liquid chromatography
HRP	horseradish peroxidase
IA	iodoacetamide
IC	invasive candidiasis
ICU	intensive care unit
IFN-γ	interferon γ
IgG	immunoglobulin g
IL	interleukin
IMAC	immobilized metal affinity chromatography
IPA	ingenuity pathway analysis
iTRAQ	isobaric tag for relative and absolute quantitation
KTRs	killer toxin receptors
LC	liquid chromatography
LDH	lactate dehydrogenase
LIMMA	linear models for microarray data
LPS	lipopolysaccharide
LTQ	linear trap quadrupole
m/z	mass-to-charge
MALDI-TOF	matrix-assisted laser desorption ionization–time of flight mass spectrometry
MHC	major histocompatibility complex
min	minutes
miRNA / miR	microrna
MOIs	multiplicity of infection
MOPS	(n-morpholino) propanesulfonic acid
mRNA	messenger rna
MS	mass-spectrometry
MS/MS	tandem mass spectrometry
NADPH	dihydronicotinamide-adenine dinucleotide phosphate
NK	natural killer cells
NSAF	normalized spectral abundance factor
OD	optical density
ORFs	open reading frames
PAMPs	pathogen-associated molecular patterns
PBS	phosphate buffer saline
PCR	polymerase chain reaction

PEP	posterior error probability
PI	propidium iodide
Pir	proteins with internal repeats
PMA	phorbol 12-myristate 13-acetate
PMSF	phenylmethanesulfonyl fluoride
pre-mRNA	primary RNA transcript
PRRs	pattern recognition receptors
PTMs	post-translational modifications
RIPA	radioimmunoprecipitation assay
RNA	ribonucleic acid
RNS	reactive nitrogen species
ROS	reactive oxygen species
RP	reverse phase
RP-LC-ESI-MS/MS	reversed-phase liquid chromatography-electrospray ionization tandem mass spectrometry
rpm	revolutions per minute
RT-PCR	quantitative real time polymerase chain reaction
SD	standard deviation
SD	synthetic defined
SDS-PAGE	sodium dodecyl sulphate polyacrylamide gel electrophoresis
sec	seconds
SILAC	stable isotope labelling by aminoacids in cell culture
SIMAC	sequential elution from imac
SRM	selected reaction monitoring
STE	ser/thr
TCEP	tris (2-carboxyethyl)phosphine
TFA	trifluoroacetic acid
Th	t-helper
TiO2	titanium dioxide
TIR	toll-interleukin 1 (il-1) receptor
TLR	toll-like receptor
TMT	tandem mass tags
TNF-α	tumor necrosis factor α
YNBS	yeast nitrogen base
YPD	yeast peptone dextrose

SUMMARY

Title

Quantitative proteomics and immunoproteomics to explore host and *Candida albicans* complex interplay: focus on macrophage and antibody responses

Introduction

Candida albicans can be part of the microbiota of healthy individuals. However, if the balance of the normal microbiota is disrupted or the immune defences are compromised a scenario of infection can arise. Invasive candidiasis (IC) is an important health-care associated fungal infection. Therefore, the study of host –pathogen complex interplay is needed to improve the knowledge on how the immune system responds to *Candida*.

Macrophages are key immune cells involved in recognition, phagocytosis and killing of the fungus. The production of antibodies against several *C. albicans* proteins has also been described during these infections.

Proteomics can be used to understand host-pathogen interactions and give information on the protein abundance and on their post translational modifications. Moreover, *C. albicans* secreted proteins analysis is crucial due to the role of these proteins in interaction with the host and their study using immunoproteomics is useful for the discovery of biomarkers for the diagnosis of IC.

Objectives

In Chapter 1, the aim is to study the mechanisms implicated in human macrophage interaction with *C. albicans* by two proteomic and phosphoproteomic approaches: one centred on ATP-binding proteins and the other based on the global proteome analysis. These can bring new insights for the development of new antifungal strategies.

In Chapter 2, the purpose is to discover biomarker candidates for the diagnosis of IC, by the analysis of *C. albicans* hyphae secreted proteins together with the characterization of the serological response to the *C. albicans* hyphal secretome in patients with IC, associated or not with catheter, using an immunoproteomic approach.

Results

In order to perform the study of differential protein abundance in macrophages and macrophages after interacting with *C. albicans*, first the analysis of human macrophage ATP-binding proteins was carried out. THP1 cell-line was used and cells were labelled with SILAC (Stable Isotope Labeling with Amino Acids in Cell Culture). After macrophages incubation with *C. albicans*, protein lysates were enriched in ATP-binding proteins using the ActivX desthiobiotin ATP probe and

analyzed by mass spectrometry (MS). Overall, 547 non-redundant proteins were quantified, including 137 ATP-binding proteins. Among the quantified proteins, 59 proteins were differentially abundant during macrophage interaction with *C. albicans*. Besides, 85 phosphopeptides were quantified and 5 were differentially abundant. More abundant proteins during interaction were involved in protein synthesis whereas less abundant proteins were related to proteolysis and ion transport. Moreover, an increase in anti-apoptotic signals over pro-apoptotic signals was observed. A high pro-inflammatory response was detected, together with no upregulation of key mi-RNAs involved in the regulation of the inflammatory response. Western blotting and selected reaction monitoring (SRM) were used to validate the abundance of two kinases (MAP2K2 and NDKA) and a peroxiredoxin (PRXD5).

A global proteomic and phosphoproteomic approach was also carried out to obtain a more holistic view of the changes in *C. albicans* infected macrophages. For that, macrophages were incubated with latex beads and with *C. albicans* at a MOI of 1 for 3 h. TMT (Tandem Mass Tag) was used for peptide labelling. A total of 6166 proteins were quantified and no statistically significant differences were observed in macrophage after interaction with beads. Overall, 89 proteins were found as differentially abundant in *C. albicans* infected macrophages. GO enrichment analysis showed that less abundant proteins were implicated in RNA splicing and more abundant proteins in cell proliferation and phosphatidylinositol biosynthetic process. Phosphopeptide enrichment led to the quantification of 9615 phosphopeptides that belong to 1842 proteins. From these, 135 phosphopeptides were differentially abundant in macrophages after interacting with *C. albicans.* Predicted protein-protein interaction network of the proteins to which these phosphopeptides belong showed proteins interacting with each other involved in different important processes, such as transcription, RNA splicing, cytoskeleton rearrangement, cell signaling and immune response.

Besides this, an MS-based proteomic approach was used for analysis of the *C. albicans* hyphae secretome after 18 h of growth in Lee medium (pH 6.7). This method enabled the identification of 301 proteins with at least 2 peptides. As expected, GO analysis of cellular component showed an enrichment in proteins from extracellular region: cell wall, cell surface, cell periphery. Furthermore, from the proteins identified in *C. albicans* hyphal secretome, 47 proteins were previously found to be immunogenic against human sera.

To carry out the immunoproteomic analysis, *C. albicans* hyphae secreted proteins were separated by two-dimensional gel electrophoresis, electroblotted onto nitrocellulose membranes, and tested by Western blotting with three distinct pools of human sera: patients with non-catheter associated IC, patients with catheter associated IC and control patients. As expected IgG

measurements showed that anti-*C. albicans* antibody levels were higher in both groups of patients with IC compared with control one. The immunoproteomic approach led to the identification of 7 antigenic proteins: **Bgl2, Eno1, Glx3, Sap5, Pgk1, Pra1 and Tdh3**. From them, Bgl2, Eno1, Glx3 and Pgk1 enabled the discrimination of patients with IC from control patients. Among this group, both Bgl2 and Glx3 did not show antigenicity in control group.

Conclusions

Both quantitative proteomic and phosphoproteomic approaches, the enrichment in ATP binding proteins and the analysis of the total proteome, revealed possible remodelling processes of macrophages after interacting with the human pathogen *C. albicans*. Among them, an increase in **anti-apoptotic signals** over pro-apoptotic was suggested together with a high **pro-inflammatory response** in macrophages after interacting with *C. albicans*. Furthermore, **RNA splicing** was found altered at the proteomic and phosphoproteomic levels. Differential phosphorylation in proteins implicated in **cytoskeleton** reorganization, **RNA splicing** and implicated in **cell survival**, **cell proliferation** and **cell cycle regulation** was also observed.

The **immunoproteomic** approach led to the identification of a group of immunogenic proteins **Bgl2, Eno1, Glx3, Sap5, Pgk1, Pra1 and Tdh3**. IgG antibodies to *C. albicans* **Bgl2, Glx3** could be interesting **biomarker candidates** for IC diagnosis.

These studies are highly important due to their possible translation to help in earlier and accurate **diagnosis** and in the development of new and more appropriate strategies of **treatment**.

RESUMEN

cuantificaron 547 proteínas, de las cuales 137 fueron proteínas de unión al ATP. Cincuenta y nueve proteínas cambiaron su abundancia tras la interacción de macrófagos con *C. albicans*. Además, se cuantificaron 85 fosfopéptidos, de los cuales 5 resultaron diferencialmente abundantes. Las proteínas más abundantes tras la interacción estaban implicadas en la síntesis de proteínas, mientras que las proteínas menos abundantes se relacionaron con la proteolisis y el transporte de iones. Se observó un aumento de las señales antiapoptóticas frente las proapoptóticas. Se detectó una elevada respuesta proinflamatoria, y una ausencia de activación de los mi-ARN involucrados en la regulación de la respuesta inflamatoria. Además, se validaran los cambios en la abundancia de tres proteínas de interés (MAP2K2, PRDX5 y NDKA) mediante *Western blot* y proteómica dirigida.

También se llevó a cabo un análisis del proteoma y fosfoproteoma total para obtener una visión global de los cambios proteómicos en macrófagos tras interaccionar con *C. albicans*. Para ello, los macrófagos se incubaron con bolitas o con células de *C. albicans*. Los péptidos fueron marcados mediante marcaje isotópico (TMT). Se cuantificaron un total de 6166 proteínas sin embargo, no se observaron diferencias significativas en los macrófagos tras la interacción con las bolitas. Se encontraron 89 proteínas diferencialmente abundantes en macrófagos infectados con *C. albicans*. El análisis GO mostró que las proteínas menos abundantes estaban implicadas en el procesamiento de ARN y las proteínas más abundantes en proliferación celular y en biosíntesis del fosfatidilinositol. El enriquecimiento de fosfopéptidos condujo a la cuantificación de 9615 fosfopéptidos, pertenecientes a 1842 proteínas, de los cuales 135 fosfopéptidos resultaron diferencialmente abundantes en macrófagos tras interaccionar con *C. albicans*. El análisis de interacciones de las proteínas a las que pertenecen estos fosfopéptidos mostró la interacción entre proteínas que participan en transcripción, procesamiento del ARN, reorganización del citoesqueleto, señalización celular y respuesta inmune.

El estudio del secretoma de hifas de *C. albicans* se realizó mediante MS. Se identificaron 301 proteínas que mostraron un enriquecimiento en proteínas de la región extracelular. De las proteínas identificadas en el secretoma de hifas de *C. albicans*, 47 proteínas ya habían sido descritas como inmunogénicas en sueros humanos.

Para el análisis inmunoproteómico, las proteínas secretadas de hifas de *C. albicans* se separaron mediante electroforesis bidimensional, se transfirieron a membranas y se analizaron mediante *Western blot* con tres grupos de sueros humanos: pacientes con IC no asociada a catéteres, pacientes con IC asociada a catéteres y pacientes control. Las mediciones de IgG mostraron que los niveles de anticuerpos frente al secretoma de *C. albicans* fueron mayores en ambos grupos de pacientes con IC en comparación con el control. La estrategia inmunoproteómica permitió

identificar 7 proteínas antigénicas: **Bgl2, Eno1, Glx3, Sap5, Pgk1, Pra1 y Tdh3**. De ellas, Bgl2, Eno1, Glx3 y Pgk1 permitieron la discriminación entre pacientes con IC y pacientes control. Las proteínas Bgl2 y Glx3 no presentaron inmunorreactividad frente al grupo control.

Conclusiones

El enriquecimiento de proteínas de unión al ATP junto al estudio del proteoma y fosfoproteoma global permitieron profundizar en el conocimiento de los posibles procesos de remodelación del macrófago tras interaccionar con *C. albicans*. Estos resultados sugieren un aumento de las **señales antiapoptóticas** frente a las proapoptóticas así como una elevada **respuesta proinflamatoria** en macrófagos tras su interacción con *C. albicans*. Además, se detectaron cambios proteómicos y fosfoproteómicos en proteínas implicadas en el **procesamiento de ARN**. También se observó la fosforilación diferencial de proteínas implicadas en reorganización del **citoesqueleto**, **procesamiento de ARN**, **proliferación**, **supervivencia celular y regulación del ciclo celular**.

La estrategia **inmunoproteómica** condujo a la identificación de proteínas inmunogénicas **Bgl2, Eno1, Glx3, Sap5, Pgk1, Pra1 y Tdh3**. Los anticuerpos IgG frente a las proteínas **Bgl2 y Glx3** son **biomarcadores potenciales** para el **diagnóstico** de IC.

Estos estudios son de relevancia por su posible utilidad en el **diagnóstico** temprano y preciso de IC y para el desarrollo de estrategias para un **tratamiento** más adecuado de estas infecciones.

GENERAL INTRODUCTION

1 Clinical importance of *Candida* infections

Invasive fungal diseases are a worldwide health problem, not only in immunocompromised patients but also increasingly in patients with chronic disorders (Schelenz *et al.*, 2015). Most people during their life time may suffer from some kind of superficial fungal infections that are usually curable with the current antifungal therapy, but millions of individuals worldwide will have life threatening invasive infections that are much more difficult to diagnose and treat (Brown *et al.*, 2012). The global action fund for fungal infections (GAFFI) highlights that over 300 million people are afflicted with a serious fungal infection and that 25 million can die. This organization estimated the most common life-threatening fungal infections and they are mentioned in **Table GI.1**:

Table GI.1 Burden of common life-threatening fungal infections estimation, (retrieved on 15/03/19 from www.gaffi.org).

Fungal infection	Estimated annual burden	Estimated deaths
Chronic pulmonary aspergillosis	> 3.000.000	> 450 000
Severe asthma with fungal sensitizations (SAFS)	> 6.500. 000	350 000 – 489 000 asthma deaths - 50% related to SAFs
Invasive candidiasis	> 700 000	> 350 000
Pneumocystic pneumonia	>500 000	> 250 000
Cryptococcal meningitis	370 000	> 125 000
Invasive aspergillosis	> 250 000	> 125 000
Disseminated histoplasmosis	> 100 000	> 80 000

Regarding the opportunistic invasive mycoses, another epidemiologic work mentions candidiasis as the second most frequent infection worldwide with more the 400 000 estimated life-threatening infections per year, right after cryptococcosis that was estimated to have a frequency of more than 1 000 000 cases per year. These are in all cases estimations based on the available data which is sometimes very limited, and this is one of the reasons why there are different values arising on the frequency of these infections (Brown *et al.*, 2012). In any case, its clinical importance is clear. The etiological agents of this fungal infection are the opportunistic pathogens from the genus *Candida*. In healthy individuals, *Candida* species belong to the normal microbiota of skin and mucosal surfaces namely oral cavity, gastrointestinal tract and vagina (Mavor *et al.*, 2005, Brown *et al.*, 2012). However, if the balance of the normal microbiota is disrupted or the immune defences are compromised, these fungi can outgrow and cause infection. These infections can be superficial or can invade the bloodstream and disseminate to internal organs. There are several risk factors for *Candida* infections, such as prior colonization with *Candida*

species, human immunodeficiency virus (HIV) infection, cancer chemotherapy, neutropenia, organ transplantation, indwelling catheters and devices, autoimmune diseases, burn, antimicrobial therapy, age, gender, abdominal surgery and perforation, trauma, heart disease, radiotherapy, therapy involving prolonged exposure to steroid drugs (Spampinato & Leonardi, 2013).

In the USA, the National Nosocomial Infections Surveillance program showed that incidence of primary *Candida* bloodstream infections (BSI) has increased by as much as 487% over the decade of the 1980's in large teaching hospitals (Vincent, 2003). The countries participating in European Confederation of Medical Mycology (ECMM) survey reported candidemia rates (0.31 to 0.44 per 10 000 patients-days) similar to other European surveys but lower than the rates reported in the USA (1,5 per 10 000 patients-days) (Tortorano *et al.*, 2006). This genus was classified as fourth on the list of nosocomial agents of sepsis in USA (Wisplinghoff *et al.*, 2004) and is associated with high morbidity and mortality. A study in Spain reviewed the epidemiology of invasive candidiasis (IC) in 26 Spanish hospitals from June 2011 and June 2012. A total of 705 cases of IC were detected during the study and a crude mortality rate of 30% was observed (Nieto *et al.*, 2015).

There are at least 15 distinct *Candida* species that cause human disease, but more that 95% of them are caused by the 5 most common pathogens: *C. albicans*; *C. glabrata*, *C. tropicalis*, *C. parapsilosis* and *C. krusei* (McCarty & Pappas, 2016). It is important to highlight the increasing medical importance that is being given to *C. auris*. This pathogen was firstly isolated from the ear canal of a patient in Japan and is often misidentified in conventional diagnostic laboratories. Furthermore, its resistance to azoles and amphotericin B is of high medical concern (Jeffery-Smith *et al.*, 2018).

Overall, *C. albicans* is the most common pathogen in most clinical settings, but non-*albicans Candida* spp. collectively could represent >50% of the bloodstream isolates in certain regions. The different incidences of non-*albicans* species are usually dependent on the antifungal pattern of treatment. In general terms some patterns can be observed. *C. glabrata* is usually the second most frequently isolated *Candida* species in USA and northwestern Europe whether this position is often occupied by *C. parapsilosis* or *C. tropicalis* in Latin America, Southern Europe, India and Pakistan (Pappas *et al.*, 2018).

2 The fungal opportunistic pathogen *C. albicans*

C. albicans belongs to the *Saccharomycetaceae* family of ascomycete fungi. This fungus is distantly related to the well-known budding yeast *Saccharomyces cerevisiae*, an extensively used model for studies in cell biology and genetics. *C. albicans* belongs to the CUG clade, which

includes *C. parapsilosis*, *C. tropicalis* and *C. auris* among others, and is a diploid organism with eight chromosome pairs. In *Candida* Genome Database (CGD) a total of 6218 ORFs in *C. albicans* are annotated at the moment, being 4379 annotated as uncharacterized open reading frames (ORFs) (there is no conclusive proof for the existence of a protein product), 1687 verified ORFS (there is empirical evidence that the ORF actually encodes a functionally characterized protein) and 152 annotated as dubious ORFs (retrieved on 04/02/2019). This data implies that most part of the predicted proteome is still unknown or has not been properly annotated yet (Vialas *et al.*, 2014, Vialas *et al.*, 2016). In this way, the characterization of the *C. albicans* proteome is of great interest to increase the knowledge on the great amount of proteins that are still annotated as uncharacterized. Peptide Atlas was generated and reported highly confident identification of proteins (63%) that corresponded to uncharacterized ORFs, according to CGD terminology. This project represented a great increase in the number of characterized *C. albicans* peptides and proteins (Vialas *et al.*, 2016).

The genus name *Candida* was used for yeast with no sexual cycle and up to now no complete sexual cycle was observed in this yeast (Kim & Sudbery, 2011). However, *C. albicans* has an elaborate mating mechanism. This species exhibits a parasexual cycle in which mating produces tetraploid cells that undergo a nonmeiotic program of concerted chromosome loss to return to a diploid or aneuploid state (Hirakawa *et al.*, 2017).

2.1 *C. albicans* virulence traits

C. albicans is equipped with a variety of commensal and virulence characteristics that help the fungus to colonize within the microbiota in the commensal phase and to invade host tissue during infection (Hofs *et al.*, 2016). Figure GI.1 summarizes these evolutionary adaptive traits, also known as virulence factors, that help *C. albicans* to be a successful pathogen during the different phases of *Candida* and host interaction (da Silva Dantas *et al.*, 2016).

Morphogenesis. *C. albicans* is a polymorphic microorganism once it has the ability to grow as a budding yeast, pseudohyphae and true hyphae (Figure GI.1). It is generally considered that pseudohyphae and hyphae are morphologies more related with invasion whereas yeast is more suited for dissemination in the bloodstream or to a more commensal state, however this is a controversial issue (Sudbery *et al.*, 2004). The yeast-to-hyphal transition is the most studied morphology transition in *C. albicans*. *In vivo* hyphal formation is mediated by a mix of environmental signals in the host, which include hypoxia, temperature, CO_2 concentration and nutrient conditions. There are several *in vitro* ways to produce the different *C. albicans*

morphologies. In detail, yeast can be induced by growing cells at temperatures around 30ºC or pH around 4; pseudohyphae can be induced by culturing cells at pH around 6, temperature of around 35ºC, in nitrogen limited growth on solid medium and high concentrations of phosphate; hyphae can be induced by adding serum to the medium, by growing cells at temperatures around 37ºC, by using specific mediums such as Lee at pH 6.7 and by the addition of N-acetylglucosamine (GlcNac). Quorum sensing molecules such as farnesol at high cell densities can promote yeast cell growth (Sudbery *et al.*, 2004). Hypha formation stimuli activate the cAMP/PKA or MAPK signaling pathway leading to the expression of master activators of hyphal formation such as Efg1 and Cph1. Moreover, it is associated with the expression of hypha associated genes such as the hyphal wall protein Hwp1, secreted aspartic proteases Sap4, Sap5 and Sap6 and hypha associated proteins such as Ece1 and Hyr1. These proteins play a special role in hyphal cells virulence, particularly in adhesion and invasion of host cells (Hofs *et al.*, 2016). This pathogen also generates stable cells and colony variants with distinct properties. The most well characterized is the white – opaque transition and it was described to be important for *C. albicans* mating (Jain *et al.*, 2008). Another *C. albicans* phenotype includes gray cells, which are smaller than conventional yeast and mate with low efficiency. In strains that are capable of white-opaque-gray switching, the transition to gray cell morphology is induced by exposure to nutrient rich growth medium (Noble *et al.*, 2017). Gastrointestinal induced transition (GUT) cells were discovered by genetic screening for fungal mediators of commensalism within the mammalian digestive tract (Pande *et al.*, 2013)

Biofilm formation. A major virulence trait of *C. albicans* is its ability to form biofilms. It usually starts by the adherence of yeast cells to a solid surface. This process is usually called seeding. Then, the biofilm starts to develop by the proliferation and early stage filamentation of the adhered cells. The next step is biofilm maturation that ends with several layers of polymorphic cells, encased in an extracellular matrix. Finally, the last step is the dispersal stage, were some yeast cells disperse from the biofilm to seed new sites (**Figure GI.1**) (Gulati & Nobile, 2016). *C. albicans* biofilms are a major source of device-associated infections. A master transcription network of six transcription regulators was described to control biofilm formation by *C. albicans in vitro* and in two different animal models (rat catheter and rat denture models): *TEC1*, *NDT80*, *ROB1*, *BRG1*, *BCR1* and *EFG1* (Nobile *et al.*, 2012). *C. albicans* biofilm cells are usually resistant to neutrophil killing (Ghosh *et al.*, 2009). It is noteworthy to mention that *C. albicans* biofilms are inherently resistant to the majority of known antifungal drugs (Gulati & Nobile, 2016). Recently, it was demonstrated that *C. albicans* biofilm extracellular vesicles (EVs) have an important role in matrix production and biofilm drug resistance (Zarnowski *et al.*, 2018).

Adhesion. The adhesion of the fungus to epithelial cells is a complex process. Initial contact events require a variety of passive forces (e.g. van der Waals forces, hydrophobic interactions) and repulsive effects. After cell-cell contact, adhesion of *C. albicans* to epithelial cells is highly dependent on hyphal expressed adhesins, such as Eap1, Iff4, Hwp1, Int1, Als3, just to mention some examples (**Figure GI.1**) (Moyes *et al.*, 2015). *C. albicans* strains lacking Hwp1 were shown to be unable to form stable attachments to human buccal epithelial cells and had a reduced capacity to cause systemic candidiasis (Staab *et al.*, 1999). The agglutinin-like sequence (*ALS*) family includes eight genes that encode large cell-surface glycoproteins and this family was characterized as having a major role in epithelial attachment. *ALS3* gene expression was shown to be upregulated during infection of oral epithelial cells *in vitro* and can be detected *in vivo* during vaginal *C. albicans* infections (Cheng *et al.*, 2005, Wachtler *et al.*, 2011). Eap1 is a glycophosphatidylinositol (GPI)-anchored protein and has structural homology with Als family, heterologous expression of this gene in *S. cerevisiae* showed adherence attachment to HEK293 epithelial cells and *eap1* Δ/Δ mutant had reduced adherence to this cell line (Li & Palecek, 2003, Li *et al.*, 2007). Iff4 is another GPI-anchored protein and it was shown that its overexpression increased *C. albicans* adherence to human epithelial cells (Fu *et al.*, 2008). Apart from GPI-anchored proteins, Mp65 and Phr1 were also linked to adherence (Naglik *et al.*, 2011).

Invasion and Damage. *C. albicans* has two mechanisms for host cell invasion: induced endocytosis and active penetration. The first one is a host driven and the second is a fungal driven process mediating fungus cell penetration in the tissue (Hofs *et al.*, 2016). The mechanism used by *Candida* cells is dependent on the invasion state, fungal morphology and the epithelial lineage to be invaded. Nevertheless, epithelial invasion is triggered by hypha associated factors, demonstrating an important connection between hypha, adhesion and invasion (Naglik *et al.*, 2017). Induced endocytosis embraces cytoskeletal reorganization, forming membrane processes that endocytose surface adherent hyphae in a clathrin-mediated mechanism (Moyes *et al.*, 2015). Active cell penetration includes hypha elongation, physical forces exerted by extending hyphae and secretion of hydrolytic enzymes known as the *SAP* family (Hofs *et al.*, 2016). Experiments using a protease inhibitor showed a reduced ability of *C. albicans* cells to damage oral epithelium (Moyes *et al.*, 2015) . Sap5 was shown to be highly expressed during infection (Naglik *et al.*, 2008). There are other fungal factors that have been implicated in the damage of epithelial cells such as the secretion of hydrolases (already mentioned above) together with lipases and phospholipases. The inhibition of *ALS3* gene inhibited adhesion, invasion and subsequent damage. Moreover, *PMT2* and *ICL1* were specifically shown to be required for invasion and damage and mutants

lacking *MKC1*, *GPD2*, *GPP1*, *EED1*, *CKA2*, *BUD2*, *RSR1* and *PGA34* invaded epithelial cells at similar rate of the wild-type but were defective on oral epithelial damage (Wachtler *et al.*, 2011). Recently, a cytolytic secreted peptide, known as Candidalysin, was described as being a critical molecular determinant of epithelial host damage (Moyes *et al.*, 2016, Wilson *et al.*, 2016).

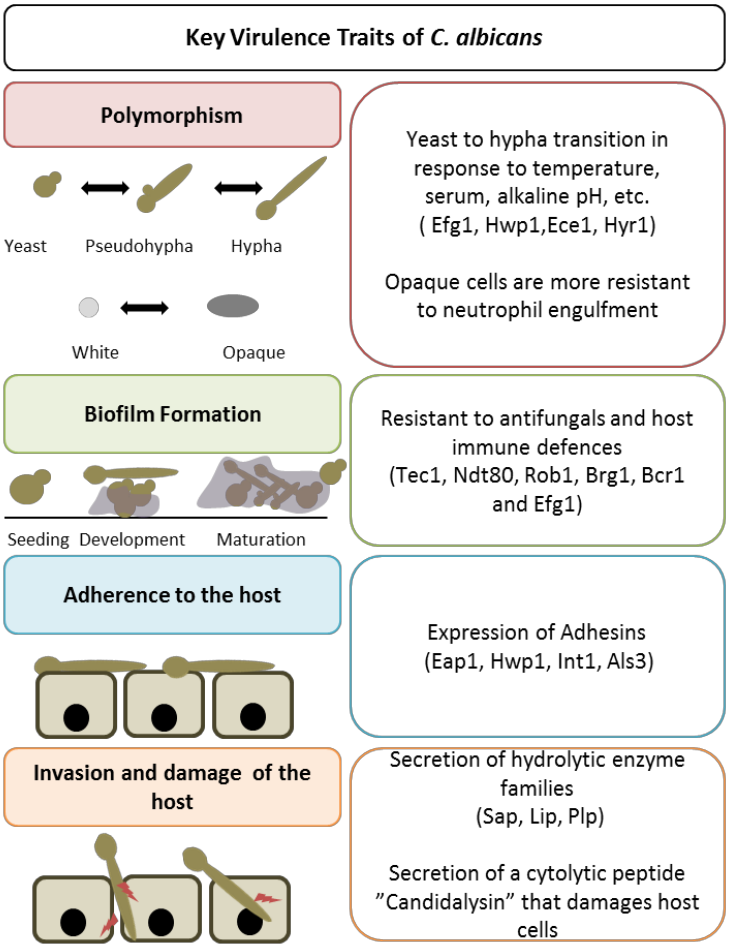

Figure GI.1 *C. albicans* virulence traits important for the establishment of the infection. Polymorphism, biofilm formation, adherence to the host together with invasion and damage of the host are among some of the most important virulence traits.

2.2 *C. albicans* cell wall and extracellular proteins

Besides the virulence traits that *C. albicans* is equipped with to successfully go from commensal to pathogen and cause infection, its cell wall is of high importance in this transition and for its recognition by immune cells.

The fungal cell wall is the outer layer of the cell and is a dynamic organelle with a composition greatly regulated in response to environmental conditions and stresses (Gow *et al.*, 2017). Due to the fact that it is not present in mammalian cells it is also a target for several antifungal drugs. *C. albicans* cell wall has two main layers: an outer layer composed by glycoproteins and an inner layer that contains skeletal polysaccharides. It is mainly composed by carbohydrates, chitin and glucans, with the outer layer predominantly consisting of *O*- and *N*- linked mannans that are covalently associated with proteins to form glycoproteins. These proteins are generally known as

cell-wall proteins (CWPs). The inner layer of the cell wall contains the polysaccharides chitin and β-1,3-glucan, which confer strength and cell shape (Gow *et al.*, 2011). The classical structure of the *C. albicans* cell wall is depicted in **Figure GI.2** (based on (Gow *et al.*, 2011)).

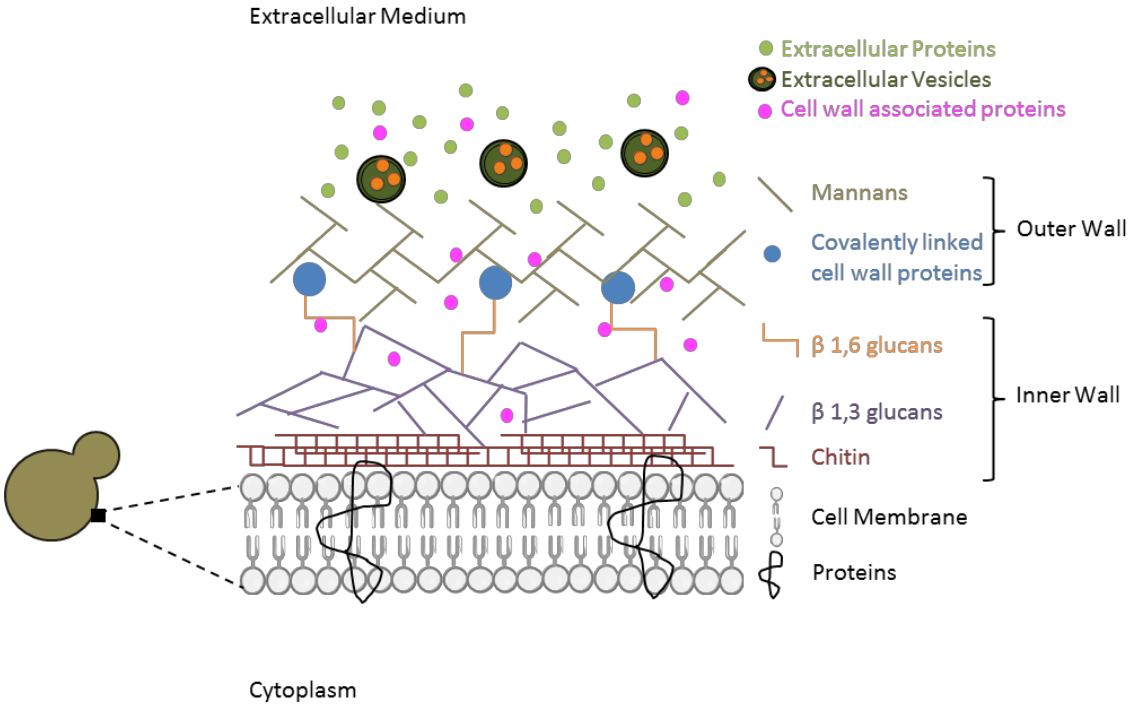

Figure GI.2 *C. albicans* cell wall composition. The outer layer is enriched in mannose polymers that are covalently associated with proteins and the inner layer is composed by chitin and β-1,3-glucan that confer strength to the cell. Outer cell wall proteins are attached to the inner wall by GPI remnants that are linked to β-1,6-glucan. Furthermore, some proteins are released to the extracellular medium by conventional and non-conventional methods of secretion.

Carbohydrates, including *N*-linked mannans, *O*-linked mannans and β-glucans, have an important role in immune recognition and the CWPs are key instruments in the adhesive interaction with host cell surfaces (Netea *et al.*, 2006, Gow & Hube, 2012). Furthermore, CWPs play key roles in cell wall assembly, as immunomodulators and in protecting the fungus from host enzymes (Nather & Munro, 2008). CWPs can be linked to polysaccharides in different ways. There are two groups that are covalently linked to them: the most abundant proteins are linked to β-1,6- glucan through a GPI remnant and the others are linked directly to β-1,3-glucan and are known as proteins with internal repeats (Pir). There is a third protein group that lacks a covalent attachment to the polysaccharides or in which proteins are bound by disulfide bridges and these proteins are generally known as cell-associated proteins (reviewed in (Gil-Bona *et al.*, 2018)).

Generally, the first contact between *C. albicans* and host cells occur predominantly at the cell surface and this is why the cell wall is very flexible in its composition. Despite this, increased importance is being attributed to a group of proteins that helps the pathogen to survive in

multiple environments and in immune recognition. *C. albicans* secretes a variety of proteins that help scavenging nutrients, degrading host proteins, lipids and glycogens and protecting against antimicrobial peptides (Klis & Brul, 2015). From them, it is important to highlight the Sap family together with extracellular lipases and phospholipases which are well known virulence factors, as previously described, to be secreted, and that are responsible for protein and lipid degradation, respectively. Also a number of proteins related to biofilm formation, such as Als family, Bgl2, Xog1 and proteins related with metal ion acquisition such as Pra1 (Klis & Brul, 2015). A study that used computer algorithms, expected that the final predicted *C. albicans* secretome was estimated to consist of up to 283 ORFs (Lee *et al.*, 2003). The Fungal Secretome Knowledge Base predicted 449 proteins to be part of the predicted secretome (Lum & Min, 2011). Another database known as Fungal Secretome Database used other algorithm, less strict once it considered entries to be secreted proteins as long as any one of the tools predicted it to be secreted, and described a putative *C. albicans* secretome of 813 proteins (Choi *et al.*, 2010).

The secretome comprises both the proteins with N-terminal secretion signal peptide and proteins that lack this signal peptide and that are exported by non-conventional routes of secretion (Nombela *et al.*, 2006, Gil-Bona *et al.*, 2015, Gil-Bona *et al.*, 2018). Eukaryotic cells use an intricate system of membrane-bound compartments and vesicles to transport proteins from the cytoplasm to the cell surface. The presence of a hydrophobic N-terminal signal sequence predetermines proteins for the secretory apparatus. These proteins are translocated across or inserted into the membrane of the endoplasmic reticulum (ER). After folding and suffer post-translational modifications within the ER, cargo proteins are loaded into coated vesicles that bud from the ER and migrate to the *cis*-Golgi where they dock and fuse. Transport through Golgi compartment to the terminal Golgi and subsequent transport to the plasma membrane is mediated by a similar migration and fusion events (Fonzi, 2009). Proteins, such as Tsa1 and Eno1, lacking N-terminal secretion signal peptide have been detected in the extracellular medium of *C. albicans* (Urban *et al.*, 2003, Pitarch *et al.*, 2006) and recently it was shown that extracellular vesicles (EVs) were carriers of proteins lacking N-terminal secretion signal peptide, including several moonlighting proteins (Gil-Bona *et al.*, 2015).

Proteomics is a powerful tool for the study of fungal secretome, and can open doors to new therapeutic and diagnostic strategies (Girard *et al.*, 2013). Sorgo and co-workers compared *C. albicans* secretome in different growth conditions (Sorgo *et al.*, 2010). In total they identified 44 secretory proteins, 29 of them have a cell wall related function, including 18 GPI-anchored proteins. They also found peptides with highly immunogenic potential. Another work by Sorgo and co-workers was performed in order to study the effect of fluconazole (antifungal drug that

inhibits ergosterol biosynthesis, detailed in other section) on *C. albicans* secretome (Sorgo *et al.*, 2011). They found 17 proteins that were fluconazole specific. Additionally, they found some proteins (Cht3, Mp65, Scw11, Sim1, Sun41, Coi1 and Tos1) to be consistently abundant in the secretome and that their secretion was not affected by the treatment, which could serve in the future as possible biomarkers of infection. After looking to the influence of fluconazole in the cell wall proteome and secretome the same group was interested in the stress caused by the temperature. Heilmann and colleagues found a decrease of the cell separation-related secretory proteins Cht3 and Eng1 at 42ºC compared to growth at lower temperatures (Heilmann *et al.*, 2013).

Ene and co-workers were interested in the secretome remodeling in different carbon source media (Ene *et al.*, 2012). Lactate- and glucose grown *C. albicans* cells displayed major differences in their secretome. They found proteins responsible for the regulation of cell wall remodeling and also with biofilm formation in the lactate- grown cells, demonstrating high plasticity of *C. albicans* secretome in response to different carbon sources (Ene *et al.*, 2012). Another work compared the secretome of an avirulent *C. albicans* mutant, *ecm33* Δ/Δ with the wild-type strain. A different protein pattern in the secretome free of vesicles and in EVs was observed in the mutant, with specific interest in the deficiency of Sap2 secretion in the mutant (Gil-Bona *et al.*, 2015). Another study performed was focused on the proteomic comparison of EVs and EVs free secretome of *C. albicans*. The authors propose that proteins lacking the signal peptide are secreted to the extracellular medium in EVs (Gil-Bona *et al.*, 2015). Besides the study of EVs protein cargo, other group focused on their characterization regarding size composition, and kinetics of internalization and immunomodulatory activity. The EVs were rapidly internalized by macrophages leading to the production of nitric oxide, IL-12, TGF-ß and IL-10 (Vargas *et al.*, 2015). Another group was interested in understanding the influence in the lack of genes responsible for phospholipid synthesis in EVs composition (Wolf *et al.*, 2015). They found that *psd1* Δ/Δ *psd2* Δ/Δ strain has much larger EVs than those from the wild-type. Additionally, they observed different protein cargo in the mutant EVs when compared to the wild-type (Wolf *et al.*, 2015). A recent work studied the functions of biofilm EVs with a panel of mutants defective in orthologues of endosomal sorting complexes required for transport subunits, which are required for normal EVs production. They found that the lack of these genes caused reduced biofilm EVs production. They suggest that EVs have an important role in biofilm matrix production and drug resistance (Zarnowski *et al.*, 2018). Recently, Luo and co-workers applied both gel and gel-free proteomics for the characterization of yeast and hyphal *C. albicans* secretome (Luo *et al.*, 2016). They also looked into the serological response of a reduced number of sera from patients with and without

Candida infections and found a group of 19 immunodominant antibodies against secreted proteins and they suggested seven secreted proteins as potential biomarkers of candidiasis (Xog1, Lip4, Asc1, Met6, Tsa1, Tpi1 and Prx1). In an attempt to look into the *C. albicans* secreted protein in an *in vivo* model, Sheehan and colleagues studied the hemolymph from *C. albicans* infected larvae (Sheehan & Kavanagh, 2019) Although it was not possible to differentiate between proteins secreted by the pathogen or just released by cell lysis, they found 101 *C. albicans* proteins in the hemolymph of *Galleria mellonella*. The proteins involved in pathogenesis were 14-3-3 homolog, Iff5, Mp65, Sse1, Rbt4, Sun41, Hsp90 and Eno1.

3 Host immune response to *Candida* infections

During infection the fungus has to face different infection stages: entering the bloodstream, surviving in the blood and escaping from the bloodstream to deep-seated organs. Physical barriers (skin and intestinal mucosal barriers) constitute the first line of defense conferred by innate immunity. The skin and mucous membrane have a commensal microbiota of saprophytic microorganisms that obstruct colonization by pathogenic microorganisms. These barriers secrete a group of peptides also called chemotactic factors that include leukotrienes and chemokines which can also be produced by leukocytes, endothelial cells, fibroblasts and smooth muscle cells after stimulation by cytokines (Blanco & Garcia, 2008, Tong & Tang, 2017). These chemotactic factors are critical factors in the defense once they enhance the effective recruitment of leucocytes to the site of infection (Blanco & Garcia, 2008). Thus, *Candida* can transit from commensal to pathogen when (i) there are perturbations of mucosal microbiota by long use of antibiotics, which gives an advantage of *Candida* over the other commensal microbiota, (ii) there is a rupture of the gastrointestinal and cutaneous barriers by a surgery or damage of central venous catheters which gives a free route of entry of *Candida* cells to the bloodstream (iii) in cases of immunosuppression by chemotherapy or corticosteroids which impairs innate immune defenses (Pappas *et al.*, 2018).

3.1 Cellular immune mechanisms against *Candida* infections: focus on macrophages

When fungi overcome physical barriers, they have to face cellular barriers. The mammalian immune system depends on both the innate and adaptive immunity. The classical view that the innate immune response was rapid, non-specific and unable of immunological memory is already outdated, mainly due to some findings showing a heightened response to a secondary infection by the same or other microorganism (Netea *et al.*, 2011, Quintin, 2018). There are several types of effector cells that protect the body and provide immunity. Among them are neutrophils,

natural killer cells (NK), dendritic cells (DCs) and macrophages that are essential for protection against fungal pathogens. Loss or defects on the fungal effector functions of these cells result in susceptibility of the host (Blanco & Garcia, 2008, Brown, 2011). Neutrophils are classically characterized by their ability to act as phagocytic cells, to release lytic enzymes from their granules and to produce reactive oxygen intermediates with antimicrobial potential (Mantovani *et al.*, 2011). NK cells are effector lymphocytes of the innate immune system that control microbial infections by limiting their spread and subsequent tissue damage and are regulatory cells engaged in reciprocal interactions with DCs, macrophages, T cells and endothelial cells (Vivier *et al.*, 2008). DCs are professional antigen-presenting cells (APCs) and are efficient stimulators of B and T lymphocytes (Banchereau & Steinman, 1998, Bourgeois *et al.*, 2010). Macrophages are particularly important phagocytic cells. On the one hand, they are one of the first cells to encounter the fungus and are able to recruit and activate other immune effector cells. On the other hand, they produce reactive oxygen species (ROS) after phagocytosis and produce a variety of cytokines that limit fungal burden (Duhring *et al.*, 2015). They also present antigens, priming T-cells (Heinsbroek & Gordon, 2009).

Finding Pattern Recognition Receptors (PRRs) changed the classical view of the non-specificity of the innate immune response. These PRRs of effector cells sense particular components of the pathogens, cell wall components and sometimes internal compounds, known as Pathogen-Associated Molecular Patterns (PAMPs) (Janeway, 1989). Figure GI.3 summarizes *C. albicans* PAMPs recognition by the PRRs present in macrophages (information collected and adapted from (Snarr *et al.*, 2017, Pappas *et al.*, 2018)).

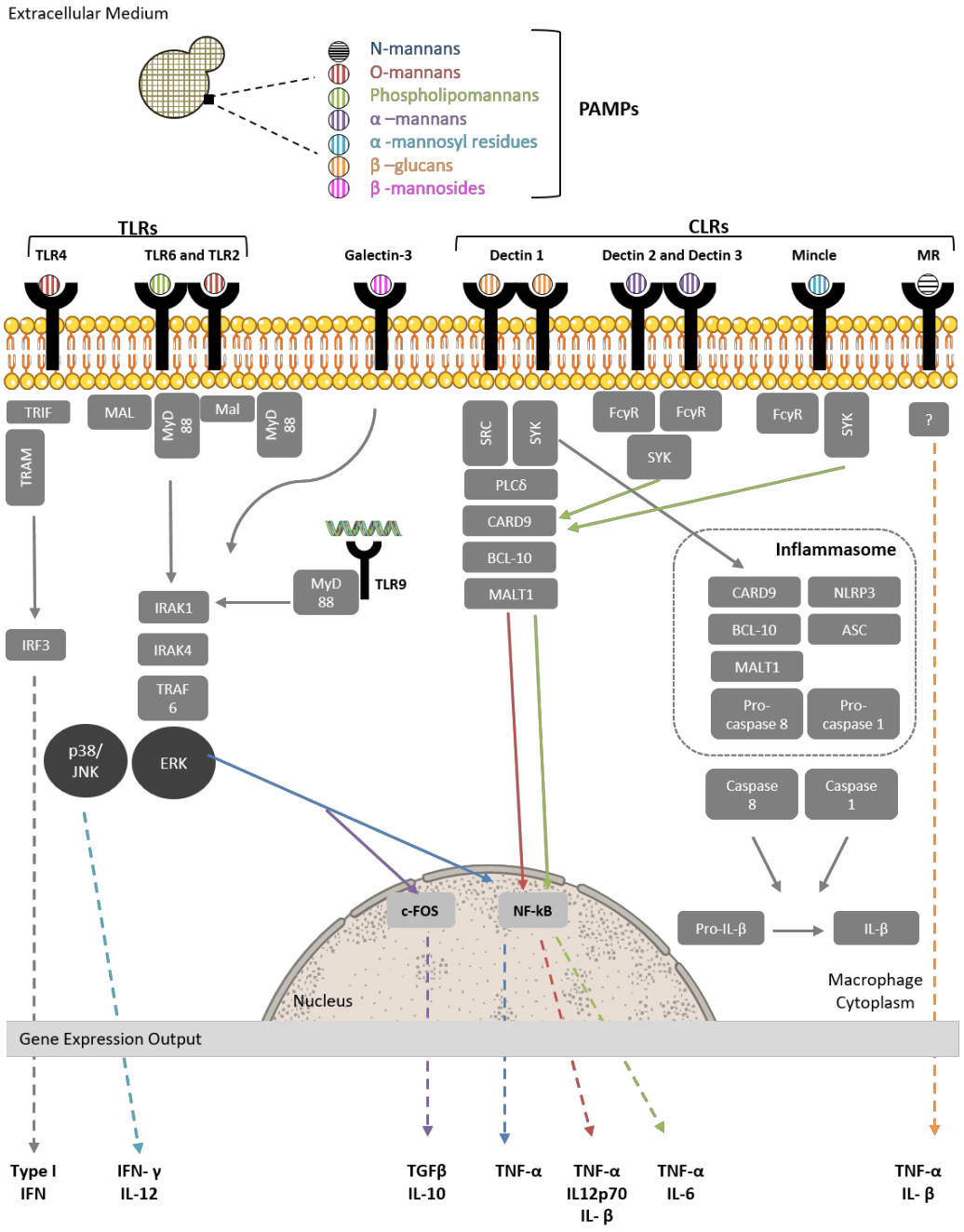

Figure GI.3 PRRs recognition of *C. albicans* PAMPs and subsequent activation of signalling pathways.
C. albicans PAMPs (N-mannans, O-mannans, phospholipomannans, α-mannans, α-mannosyl residues, β-glucans and β-mannosides) are recognized by the macrophage PRRs (TLRs, CLRs and Galectin 3). These receptors activate different signaling cascades leading to the activation of several transcription factors (NF-kB and c-Fos) that by their turn result in cytokines response (Type I IFN, IFN- γ, IL-12, TGFβ, IL-10, TNF-α, IL12p70, IL- β and IL-6) (adapted from (Pappas, *et al.*, 2018 and Bourgeois, *et al.*, 2010)).

The group of PRRs more studied due to their involvement in sensing and recognition of fungal PAMPs embrace C-Type Lectin Receptor (CLR) family such as Dectin-1, Dectin-2, Mincle, SIGNR and mannose receptor; the scavenger receptors, such as CD5 and CD36; Galectin-3 and Toll-Like Receptor (TLR) family, such as TLR2 and TLR4 (Bourgeois & Kuchler, 2012). TLRs are type I

transmembrane proteins that mediate the recognition of *Candida* PAMPs. These proteins contain transmembrane domains and intracellular toll-interleukin 1 (IL-1) receptor (TIR) domains that are required for downstream signal transduction (Kawai & Akira, 2010). This signaling transduction starts with the recruitment of a set of intracellular TIR-domain-containing adaptors (MyD88, TIRAP, TRIF, TRAM) that interact with the cytoplasmic TIR domain of the TLRs. Myeloid differentiation factor 88 (MyD88) is the universal adaptor molecule that triggers inflammatory pathways through activation of the transcription factor NF-κB that induces the expression of the inflammatory cytokine genes (Akira & Hoshino, 2003). For TLR2 and TLR4, this recruitment requires MyD88 adaptor-like protein (MAL). MYD88 and the serine/threonine kinase IL-1-receptor-associated kinase 4 (IRAK4) then interact. IRAK4 catalytic activity subsequently induces a complex with IRAK1, IRAK2, and the E3 ubiquitin ligase TNF receptor associated factor 6 (TRAF6). E3 ubiquitin-conjugated enzyme 13 (UBC13), together with either TRAF6 or an as yet unidentified E3 ligase, catalyzes the formation of K63-linked polyubiquitin chains on TRAF6 and IRAK1. TAK1-binding protein 2 (TAB2) and TAB3 recruit TGFß, activate a kinase (TAK1) to K63-linked polyubiquitylated TRAF6, which triggers p38α and Jun N-terminal kinase (JNK) mitogen-activated protein kinase (MAPK) pathways (Arthur & Ley, 2013). Netea and co-workers showed the importance of TLR2 and TLR4 receptors in the recognition of *C. albicans o*-mannans, in the host response to disseminated candidiasis (Netea *et al.*, 2002).

The second major PRR family that recognizes *Candida* PAMPs is CLRs. They are characterized by the presence of one or more C-Type Lectin Like Domains (CTLDs) (Kerrigan & Brown, 2009). Regarding *C. albicans* recognition, β-glucans are recognized by Dectin-1 and the *N*-linked mannan is recognized by the macrophage mannose receptor (MR). Dectin-1 is the most well -studied ß-glucan receptor. This receptor induces intracellular signals through a pathway mediated by spleen tyrosine kinase (SYK), caspase activation and recruitment domain-containing protein 9 (CARD9), protein kinase Cδ and RAF1 kinase signaling pathway (Netea *et al.*, 2015). DC-SIGN is another important receptor that recognizes *Candida* mannan on the dendritic cells. Galectin-3 is important for the recognition of *C. albicans* β-mannosides and mannose-binding lectin (MBL) mediates *Candida* cells opsonization and uptake (Snarr *et al.*, 2017, Pappas *et al.*, 2018). Galectin-3 is made as a monomer in the cytosol and is secreted from the cytosol via a nonclassical secretion mechanism. Secreted Galectin-3 binds to saccharide ligands on cells and extracellular matrix in the immediate milieu (Kohatsu *et al.*, 2006). Fradin and co-workers demonstrated that Galectin-3 binds to β-1,2-linked oligomannosides, an uncommon PAMP present on the surface of *C. albicans* (Fradin *et al.*, 2000).

The activation of different signaling pathways, by different PRRs culminates in pathogen engulfment, production of defensins, chemokines, cytokines, reactive oxygen species (ROS) and induction of T_H cell responses, with the ultimate objective of killing this fungus (Netea *et al.*, 2015). The release of proinflammatory mediators induces the recruitment of phagocytic cells to the site of infection, including neutrophils, macrophages and dendritic cells (Hofs *et al.*, 2016). Macrophage phagosomes, which are membrane-derived intracellular vacuoles, undergo fission and fusion events, known as phagosome maturation, leading to the formation of a phagolysosome. Generally, it has degradative properties, an acidic pH that enhances hydrolytic enzymes activity, microbicidal peptides, low carbon and nitrogen sources, and the ability to generate oxidative compounds (Vieira *et al.*, 2002). Moreover, these cells produce reactive oxygen intermediates, known as oxidative burst, mediated by dihydronicotinamide-adenine dinucleotide phosphate (NADPH) oxidase complex. This complex assembles at the phagosome membrane and transfer electrons from cytoplasmic NADPH to O_2 producing superoxide, which is then dismutated to produce hydrogen peroxide, a highly oxidative and damaging molecule (Brown, 2011). Furthermore, macrophages produce reactive nitrogen species (RNS). These cells express nitric oxide synthase, which releases nitric oxide. Nitric oxide is then transformed in peroxynitrite, which is decomposed releasing nitrogen dioxide and a hydroxyl radical (Vazquez-Torres *et al.*, 1996, Miramon *et al.*, 2013). On top of all the mechanisms macrophages have to effectively kill *C. albicans*, they also process microbial antigens, process them by proteolysis to peptide fragments and present them, activating T-cells, which are cells related to the adaptive response, together with B-lymphocytes.

3.2 Adaptive immune mechanisms against *Candida* infections

In addition to the innate immunity, the mammalian host is also equipped with two different types of adaptive immune response: humoral immunity, involving protection by antibodies, and protection by T-cells activation. Antigen presenting cells build a bridge between innate and the adaptive immune response, by presenting the fungal antigen to naïve $CD4^+$ T-cells generating a T-helper (Th) response. The last one is considered the principal mechanism of adaptive immunity (Richardson & Moyes, 2015). T helper cells exist in a variety of epigenetic states that determined their function, phenotype and form long-term immune memory (Borghi *et al.*, 2014). Th1 and Th17 cell response are important for antifungal immunity and facilitate fungal clearance through the release of cytokines such as tumor necrosis factor α (TNF-α), interferon γ (IFN-γ), interleukin 17A (IL-17A) and IL-17F. TNF-α together with IFN-γ are important cytokines against fungi and stimulate the antifungal activity of neutrophils and macrophages and also polarizes T helper cells

towards a Th1 response (Ben-Ami *et al.*, 2008). A dominant Th1 response correlates with the expression of protective immunity to fungi (Borghi *et al.*, 2014). Th1 cells start autocrine signaling through IFN-γ, which upregulates the expression of the IL-12Rβ2 receptors. This results in cells more sensitive to IL-12 which is responsible for the preservation of the Th1 response (Richardson & Moyes, 2015). Th17-type adaptive immunity was implicated in the control of fungal infections, particularly at the mucosa level, although this may be relevant only at specific mucosal sites and for specific pathogens (Brown, 2011). IL-4 and IL-13 are signals for the commitment of Th2 reactivity that, by dampening Th1 responses and promoting the alternative pathway of macrophage activation, favors fungal persistence, allergy and disease relapse. Nevertheless, Th2-dependent humoral immunity also affords some protection. The efficacy of certain vaccines that elicit protective antibody strongly indicates that antibody responses can make an important contribution to host defense against to fungi (Borghi *et al.*, 2014). There are studies showing that vaccinated mice induce antibody production and protection against disseminated candidiasis (Han & Cutler, 1995, Tso *et al.*, 2018). Mannans, mannoproteins, heat shock and stress proteins and proteases, which are part of *Candida c*ell surface, are among some the yeast epitopes known to be implicated in the protective antibody mediated response (Magliani *et al.*, 2005). Besides, the main recognized functions of antibodies are prevention of adherence, shown in a study where monoclonal antibodies generated against mannoproteins interfere with fungal adhesion to host substrates (Moragues *et al.*, 2003); and modulation of *Candida* and phagocytes interaction, shown in a study where *Candida*-opsonizing antibodies resulted in increased phagocytosis of *Candida* yeast (Montagnoli *et al.*, 2003).

3.3 *C. albicans* evasion strategies

As a metabolically flexible microorganism *C. albicans* has developed several evading strategies. An important strategy used by this fungus is to shield important PAMPs from recognition of the receptors and to degrade the complement factor C3b, which is responsible for opsonisation of microbial cells thus reducing recognition and uptake (Hofs *et al.*, 2016). Besides, it has proteins such as Pra1 (pH-regulated antigen 1) that binds to complement regulators masking fungal surface, aiding immune and complement evasion (Luo *et al.*, 2009). *C. albicans* has the ability to switch from yeast morphology to hypha to escape and kill the macrophage (Uwamahoro *et al.*, 2014, Vylkova & Lorenz, 2017). Table GI.2 shows some pairs of defence and evasion strategies of *C. albicans* to adapt to the host hostile environment and shows how intricate are host and pathogens interactions (Duhring *et al.*, 2015).

Table GI.2 Host antifungal mechanisms and *C. albicans* evading strategies (Duhring *et al.*, 2015).

Host Antifungal Mechanisms	*C. albicans* evading strategies
Limiting nutrient availability	Release of secreted aspartic proteases to liberate oligopeptides and amino acids from tissues; Switching from the glycolytic pathway to the glyoxylate cycle and gluconeogenesis to metabolize alternative carbon sources
Iron active sequestration	Iron acquisition through a reductive system, a siderophore uptake system and a heme-iron system
Zinc active sequestration	Zinc acquisition by a zyncophore system
Decrease pH	Modulate extracellular pH by actively alkalizing the surrounding environment
Inducing thermal stress	Heat shock response mediated by heat shock proteins
Inducing osmotic stress	Outer cell structure as protection from osmotic pressure Glycerol accumulation of glycerol to counteract the loss of water

4 Diagnosis of *Candida* infections

As detailed previously in general introduction, *Candida* infections cause high levels of mortality and morbidity and are of special importance in hospitalized patients. Invasive candidiasis encompasses candidemia and deep-seated candidiasis affecting organs such as kidney and spleen. Candidemia is usually diagnosed when *Candida* cells are found in the blood and deep-seated candidiasis arises from either hematogenous dissemination or direct inoculation to a sterile site (Kullberg & Arendrup, 2015). This means that when diagnosing these infections 3 scenarios should be possible to diagnose: (i) candidemia without deep-seated candidiasis; (ii) deep-seated candidiasis without candidemia and (iii) candidemia and deep-seated candidiasis (Clancy & Nguyen, 2013). Blood culture and tissue histopathology from normal sterile sites are still the standard methods for the diagnosis of these infections (reviewed in (Pitarch *et al.*, 2018)). Blood cultures are useful for the detection of viable *Candida* cells in the bloodstream, taking from 2-5 days until achieving conclusive results. Then, more time is necessary for species specific identification using conventional methods such as Vitek® or taking advantage of matrix-assisted laser desorption ionization–time of flight mass spectrometry (MALDI-TOF) such as MALDI Biotyper®. MALDI-TOF systems appear to be more reliable than conventional phenotypic methods with 96.5% of correct identifications (Lacroix *et al.*, 2014). However, blood cultures do not detect deep-seated candidiasis cases. Fungal cultures from tissue histopathology are often very invasive procedures for most patients that are in intensity care unit (ICU) and have low sensitivity due to low burden or unequal distribution of *Candida* cells (reviewed in (Pitarch *et al.*, 2018)). Although these methods are being used in the clinic on a daily basis, the delayed treatment of these infections has been minimized by the use of more rapid diagnostic techniques. Envisioning this,

the main non-culture diagnostic methods include and are depicted in **Figure GI.4** (adapted from (Pitarch *et al.*, 2018)):

- The detection of anti-mycelium antibodies, such *as C. albicans* germ tube antibody (CAGTA) test. There are two commercial available assays: one is based on an indirect immunofluorescence test (IC (CAGTA) IFA immunoglobulin G (IgG), Vircell Microbiologists) and the other is an indirect chemiluminescent immunoassay (Virclia®, Vircell Microbiologists). According to Wei and co-workers the diagnostic accuracy of this assay is moderate for invasive candidiasis (Wei *et al.*, 2018).
- The detection of mannan antigen (Platelia™ *Candida* Antigen) and anti-mannan antibodies (Platelia™ *Candida* Antibody) are highly employed in European countries and, according to Mikulska and co-workers, a combined mannan/antimannan assay sensitivity is 83% and specificity is 86% (Mikulska, 2012).
- Sera indirect measurement of β-D-glucan (Fungitel®), a component of *Candida* cell wall. According to Karageorgopoulos and co-workers the sensitivity of this assay is 76.8% and the specificity is 85.3%, with noted statistical heterogeneity (Karageorgopoulos *et al.*, 2011).
- Polymerase Chain Reaction (PCR) can be used for the detection of *Candida* DNA. A meta-analysis performed by Avni and co-workers showed that when PCR was performed to evaluate patients with suspected invasive candidiasis, the pooled sensitivity for the diagnosis was 0.95 and the pooled specificity was 0.92 (Avni *et al.*, 2011). However, there are still standardization problems for this kind of assays (Clancy & Nguyen, 2013).
- The T2*Candida*® panel detects *Candida* directly within whole blood in an automated process. In patients receiving antifungal therapy T2*Candida* identified bloodstream infections that were missed by blood cultures. This method amplifies DNA using a thermostable polymerase and target specific primers and detects amplified product by amplicon-induced agglomeration of magnetic particles and T2MR measurement. A multicentre study performed by Clancy and co-workers showed a sensitivity of 89%. (Clancy *et al.*, 2018).

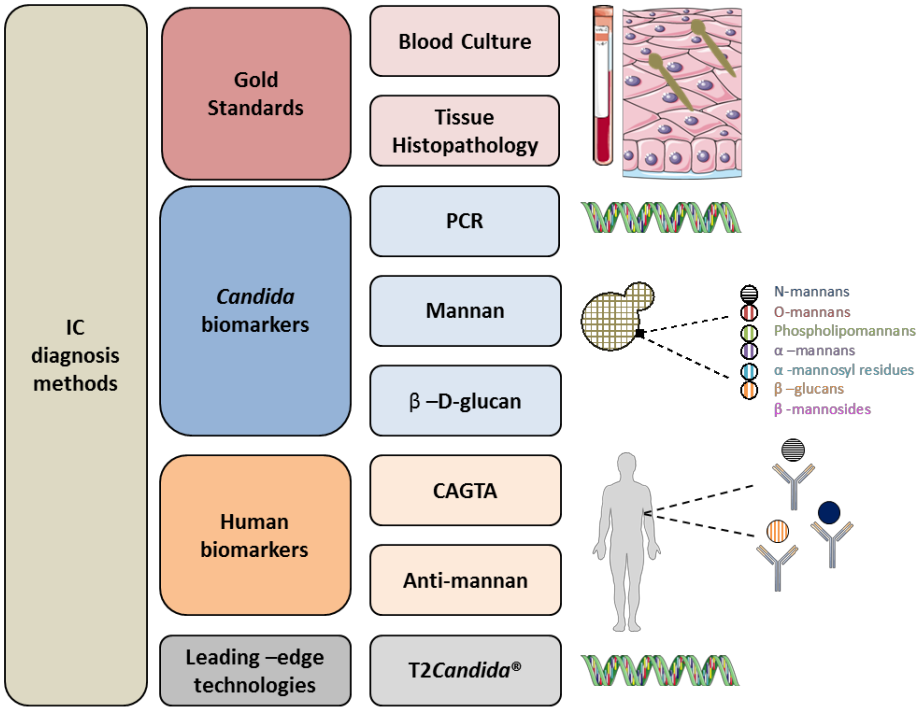

Figure GI.4 Currently available methods for IC diagnosis. Some of the most important diagnostic methods of IC include the gold standards and non-culturable tests that hold the pathogen and host derived biomarkers and leading-edge technologies (see details in text).

The intention of nonculture methods is to help in a faster, more accurate, cheaper, easier and better diagnosis of *Candida* infections. Anyhow, deep-seated candidiasis is still missed if patients never had candidemia, or when candidemia is already cleared or if falsely negative invasive sampling procedures were performed (reviewed in (Clancy & Nguyen, 2013)).

The post-genomic era is bringing new cutting-edge technologies, such as proteomics that are promising tools for the search of possible biomarkers of IC. One attractive example is the use of immunoproteomics for the discovery of new biomarkers (Pitarch *et al.*, 2004, Pitarch *et al.*, 2006, Pitarch *et al.*, 2008, Luo *et al.*, 2016). The study of the serological response to different *Candida* antigen proteins has led to the identification of a wide number of biomarker candidates (Pitarch *et al.*, 2004, Pitarch *et al.*, 2006, Mochon *et al.*, 2010, Pitarch *et al.*, 2014, Luo *et al.*, 2016). Our group showed that serum anti-Bgl2 and anti-Eno1 and also anti-Pgk1 and anti-Adh1 antibodies were biomarkers candidates of IC (Pitarch *et al.*, 2004, Pitarch *et al.*, 2006). Moreover, a group of five-IgG antibody signatures (Met6, Ssb1m Tdh3, Hsp90 and Pgk1) was suggested to have key information for prediction of the clinical outcome in IC patients (Pitarch *et al.*, 2011).

Furthermore, recent studies are investigating different host related tests as new possible diagnostic tools (Posch *et al.*, 2017). IL- 17 is an important cytokine for the defence against *C. albicans*. Krause and co-workers demonstrated that candidemic patients had significantly

higher IL-17A and kynurenine levels, compared with noncandidemic patients, suggesting their potential role as biomarkers of infection (Krause *et al.*, 2015).

Besides the great improvement in the discovery of new biomarkers of IC there is still the problem of integrating them in clinical context to reach an early diagnosis at an efficient cost and thereby optimise the antifungal treatment (Candel *et al.*, 2017).

5 Antifungal therapy of *Candida* infections

The antifungal arsenal is still limited and can be divided in four major classes (Pianalto & Alspaugh, 2016). Polyenes, such as amphotericin B, produce alterations on the membrane function and also affect mitochondrial activity by oxidative stress. Due to its high nephrotoxicity liposomal formulations were developed. Another class of antifungals highly used in clinics are azoles, which target the fungal plasma membrane, inhibiting biosynthesis of ergosterol through the inhibition of the activity of lanosterol 14-α-demethylase (ERG11 enzyme). Echinocandins, such as caspofungin, micafungin and anidulafungin, affect cell wall biosynthesis, by inhibiting β-1,3 glucan synthase and have low toxicity when compared to others. 5-Fluorocytosine, which is a fluoridated pyrimidine analogue, enters into the cytosol, is deaminated to 5-fluorouracil and subsequently converted to its active metabolite that inhibits thymidylate synthase interfering with DNA synthesis and disrupting RNA synthesis (Pianalto & Alspaugh, 2016). Figure GI.5 indicates the sites of action of the currently approved antifungal drugs (Pianalto & Alspaugh, 2016, Reales-Calderon *et al.*, 2016). It is important to remark that the antifungal therapy and the selection of the drug must be based on the immune status of the host, the site of infection, the fungal pathogen species and its susceptibility (or intrinsic resistance) to the different antifungals available and the pharmacokinetic of the drug. The resistance can be (i) primary, when the antifungal is not active against a specific species or it can be (ii) acquired, when the continuous use of these antifungal drugs led to an increase selective pressure. Figure GI.5 has also the most common mechanisms of resistance to antifungal drugs (adapted from (Reales-Calderon *et al.*, 2016). The adverse side effects, toxicity and emergence of drug resistance limit the use of these drugs. Besides the combinatorial use of different antifungal drugs that was shown to improve *Candida* eradication, different approaches are being developed for the improvement of the clinical outcome of patients with *Candida* infections.

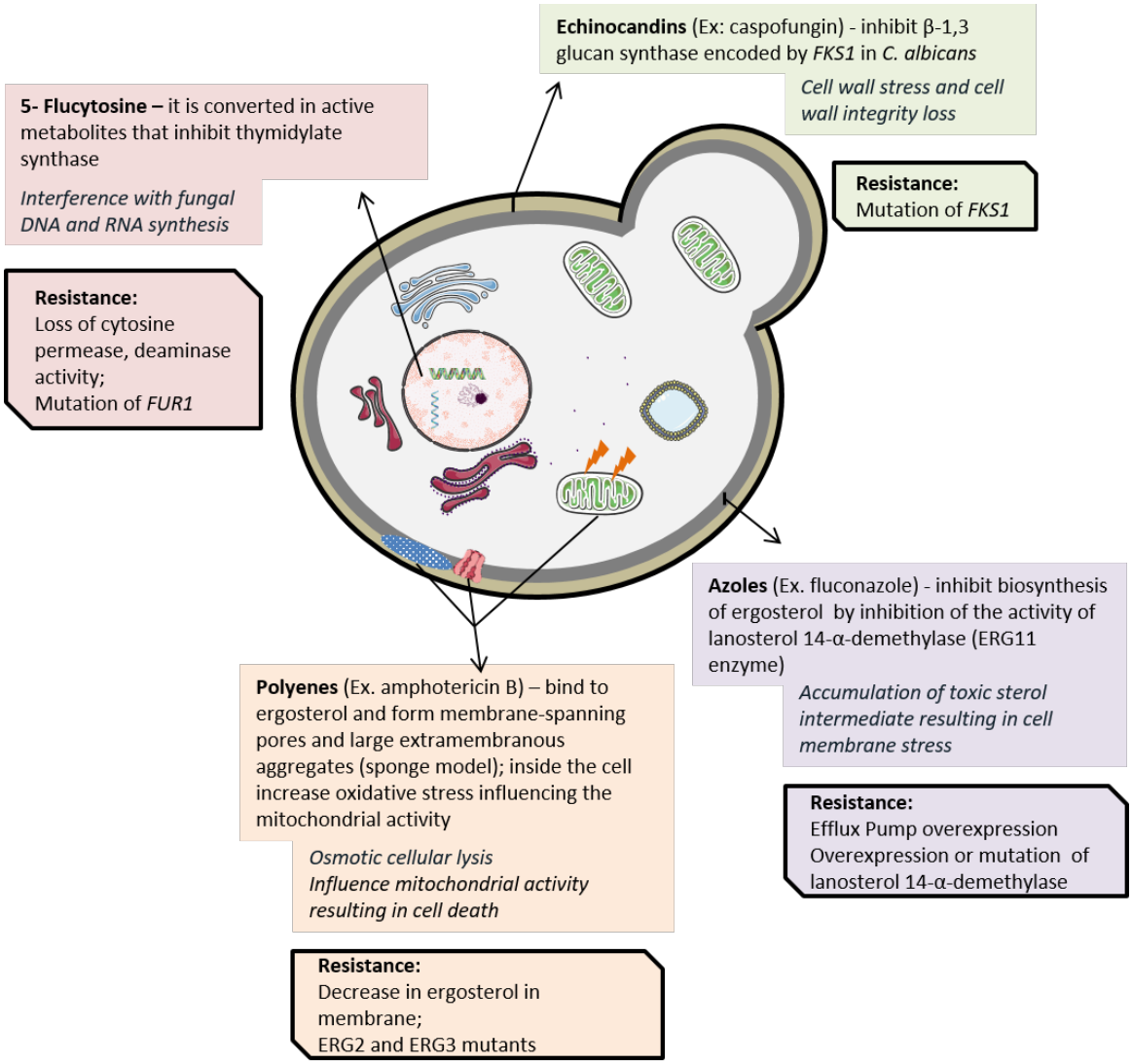

Figure GI.5 Mechanisms of action for currently approved antifungal drugs and corresponding mechanisms of drug resistance. The most important antifungal drugs can be divided in four classes: polyenes, azoles, echinocandins and 5-fluorocytosine. Each of these classes presents different mechanisms of action on the fungal cell. The fungus has developed different mechanisms of resistance to these drugs (based on (Reales-Calderón *et al.*, 2016)).

New approaches include vaccination, therapeutic antibodies, recombinant cytokines and adoptive transfer of primed immune cells. Vaccination of high-risk groups is a promising strategy to prevent invasive fungal infections in cases where the risk factors are clearly defined. There are several anti-*Candida* vaccine candidates: glycoconjugates such as diphtheria toxoid CRM197 conjugated with the alga antigen laminarin (Torosantucci *et al.*, 2005) and mannan protein conjugates (Han *et al.*, 1999); recombinant vaccines such as vaccines based on Als1 and Als3 (Ibrahim *et al.*, 2006, Spellberg *et al.*, 2006); recombinant N-terminal of *C. albicans* Hyr1 protein (Luo *et al.*, 2011); recombinant *C. albicans* Sap2 (De Bernardis *et al.*, 2012) and live attenuated vaccines such as cell wall defective *ecm33*Δ (Martinez-Lopez *et al.*, 2008), hyphal defective

C. albicans strain PCA.2 (Bistoni *et al.*, 1986); MAP kinase-defective *hog1*Δ *C. albicans* strain CNC13 (Fernandez-Arenas *et al.*, 2004).

Anti-*Candida* antibodies administered to patients can also be protective (van de Veerdonk *et al.*, 2010). A recent work by Rudkin and co-workers described the generation of fully human monoclonal antibodies to *Candida* cloned from single B cells. They showed that those antibodies had strong opsonophagocytic activity of macrophages and protection in a murine model of disseminated candidiasis (Rudkin *et al.*, 2018). Another study performed by Pachl and co-workers showed that the human recombinant monoclonal antibody against Hsp90 associated with amphotericin B produced significant clinical and culture improvement in patients with IC (Pachl *et al.*, 2006).

Cytokines are able to increase host defence against fungal infections (van de Veerdonk *et al.*, 2010). It was previously shown that the granulocyte-macrophage colony-stimulating factor (GM-CSF) was found to have anti-fungal activity, once it upregulates human chitotriosidase that cleaves fungi chitin, a component of *Candida* cell wall (van Eijk *et al.*, 2005). Other cytokines such as granulocyte colony-stimulating factor (G-CSF) and IFN-γ were found to have also important roles in antifungal activity (van de Veerdonk *et al.*, 2010).

The use of antigen primed dendritic cells and T-cells can also be a value immunotherapeutic approach. Cells can be primed *ex-vivo* and then adoptively transferred when the patient is immunocompromised. Bacci and co-workers showed that DC, from either spleen or bone marrow, transfected with yeast, but not hyphal, RNA were capable of providing protection against the fungus in allogeneic bone marrow-transplanted mice (Bacci *et al.*, 2002). Tramsen and co-workers generated anti-*Candida* T cells that were able to induce damage to *C. albicans* hyphae and significantly increased hyphal damage (Tramsen *et al.*, 2007). However, further studies are needed to look for potential adverse effects.

Thus, these approaches are based on the knowledge created on the mechanisms of host defence against *Candida* infections and underline the need to continue on studying host and pathogen interactions, with different technologies and points of view. Proteomics is a very versatile technology that can be used to find specific proteins of the host that are differentially regulated in response to the pathogen, which may help in the discovery of new therapeutic approaches (Reales-Calderon *et al.*, 2014). Moreover, it can also be useful for infection diagnosis and prognosis (Pitarch *et al.*, 2006). Ultimately, systems biology, with the integration of different –*omics* strategies can help in obtaining wider views of the host and pathogen interaction and can also bring new insights for the generation of predictions during these intricate and dynamic interactions (Tierney *et al.*, 2012).

6 Proteomics for understanding host-pathogen interactions

Host–pathogen relationships are characterized by the complex interplay between host defence mechanisms and the attempts to circumvent these defences by microorganisms (Nau *et al.*, 2002). In order to better understand these cross-talk mechanisms different global or *omics* approaches at different levels can be applied: genomics, transcriptomics, proteomics, and metabolomics just to mention some of them. All of these disciplines give different inputs towards a more integrative view that enables a more comprehensive understanding of these interactions (Tierney *et al.*, 2012). Proteomics is a highly fascinating discipline that comprises much more than proteins identification and quantification. It opens doors for the study of proteins localization, interaction, function and modifications, such as phosphorylation, glycosylation, acetylation, among others (Fields, 2001). In general terms, protein profiling can be divided in two strategies: gel- based and gel free or mass-spectrometry (MS) based proteomics (Resing & Ahn, 2005). Figure GI.6 depicts the basic differences between these two global proteomic strategies (adapted from (Belczacka *et al.*, 2019).

Gel-based proteomics involves protein separation usually by two dimensional electrophoresis (2-DE) followed by digestion and spot identification by MS whether gel-free proteomics includes protein extract digestion and peptide fractionation by liquid chromatography followed by protein identification with or without combination with metabolic or chemical labelling for protein quantification (Monteoliva & Albar, 2004, Beck *et al.*, 2011).

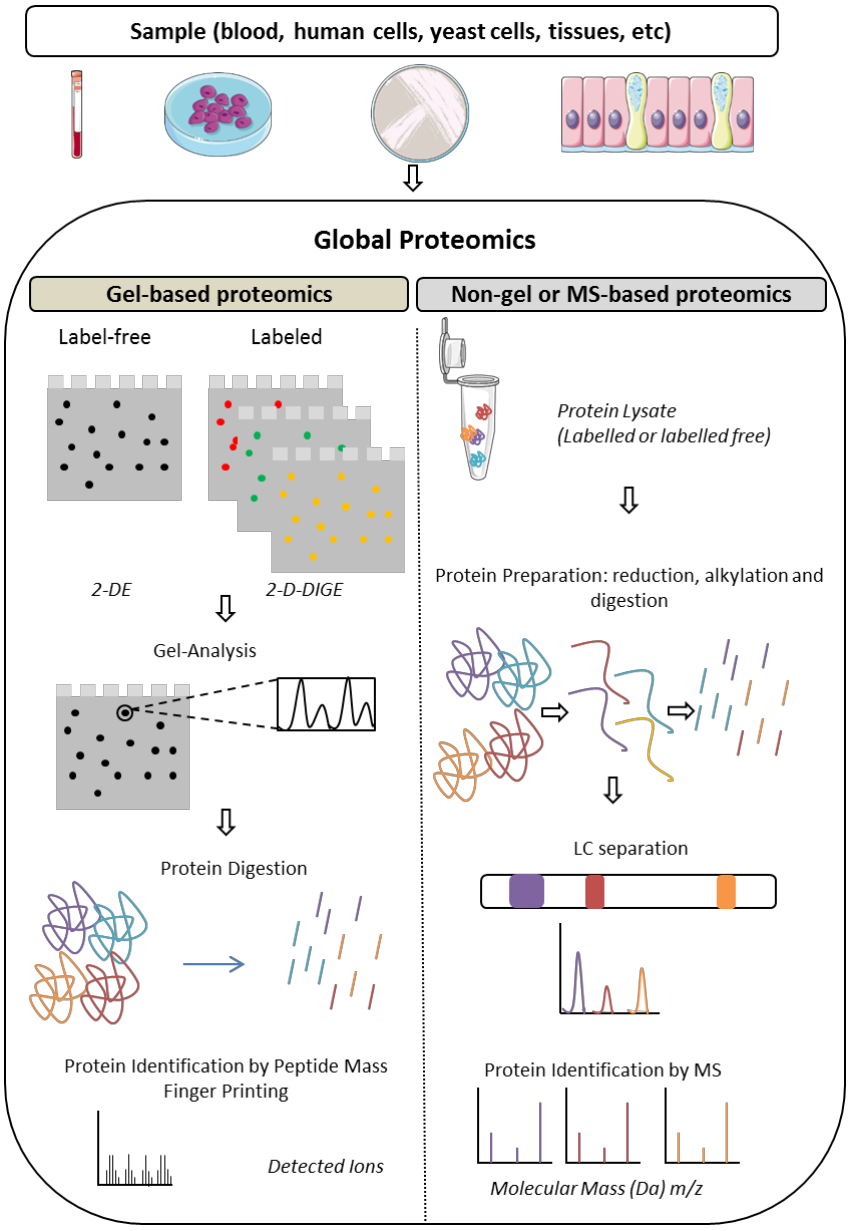

Figure GI.6 Outline of commonly used global proteomics strategies. In global proteomics protein separation prior to MS analysis can be achieved by either gel based or non-gel based approaches (based on (Belczacka *et al.*, 2009).

6.1 Gel-based proteomic approaches

2-DE combines the isoelectric separation, along a pH gradient, of the proteins according to their isoelectric point and their subsequent resolution, according their molecular weight, using a sodium dodecyl sulphate polyacrylamide gel electrophoresis (SDS-PAGE) (O'Farrell, 1975). This coupled with MS, by peptide mass fingerprinting or tandem mass spectrometry analysis, was the classical way of protein identification (**Figure GI.6**). This methodology gives a map of the intact proteins and also enables the appreciation of protein isoforms or post-translational modifications

(PTMs) (Gorg *et al.*, 2004). A work from our group used 2-DE for the analysis of macrophages after interaction with *C. albicans* (Martinez-Solano *et al.*, 2006). Several proteins such as heat-shock proteins and proteins from cytoskeletal organization were found be differentially abundant (Martinez-Solano *et al.*, 2006). Another work focused in the proteomic and genomic alteration of *C. albicans* cell after macrophage interaction (Fernandez-Arenas *et al.*, 2007). For the proteomic approach they used 2-DE and found 67 proteins differentially abundant. Functional groups of lipid and fatty acid β oxidation, glyoxylate, cell wall and actin cytoskeleton were up regulated whether carbohydrate metabolism and mitochondrial biogenesis were down regulated. The introduction of 2D difference gel electrophoresis (2D-DIGE) was very important once it enabled an increased confidence of detection and quantification of the proteins in different samples (Figure GI.6). This methodology involves a pre-labelling of the proteins from different conditions with fluorescent dyes and then labelled proteins are separated in a single 2-DE and images are acquired using specific filters (Alban *et al.*, 2003) This technology was used for the study of macrophage response to *C. albicans* (Reales-Calderon *et al.*, 2012). In this work, sub-cellular fractions of macrophages alone and macrophages after interacting with *C. albicans* were analysed by 2D-DIGE enabling the identification of new proteins involved in ER stress response, pro-inflammatory response, among others (Reales-Calderon *et al.*, 2012).

Another important 2-DE application is the identification of immunogenic proteins. This is possible by combining 2-DE with Western blotting with sera from patients with a certain disease (Pitarch *et al.*, 1999). This technique has been broadly used for biomarker discovery in patients with invasive candidiasis and is still a method used for this purpose (Pitarch *et al.*, 2006, Luo *et al.*, 2016, Pitarch *et al.*, 2016). Although enabling protein maps and the identification of protein species, gel-based proteomics has some drawbacks such as: (i) low proteome coverage; (ii) compatibility problems, due to the use of strong detergents that are not compatible with the isoelectric focusing and also (iii) low reproducibility together with (iv) the low data quality obtained (Baggerman *et al.*, 2005).

6.2 MS-based proteomic approaches

In response to the limitations above detailed regarding gel-based proteomics, other techniques, where proteins were separated based on chromatography, were developed for the analysis of protein mixtures. The development in MS workflows for proteomics, particularly new instrument configurations and higher resolving power at both MS and MS/MS levels, allowed proteome wide analysis of the abundance, modification and stability of proteins (Figure GI.6). Usually all these bottom-up workflows involve protein digestion into peptides, typically using trypsin. Then,

peptides are separated by means of chromatography and electrosprayed after which they are introduced into the vacuum of a mass spectrometer. MS involves ionizing the peptides and selecting specific precursor ions from the pool of detected peptide ions for fragmentation. The resulting product-ion mass spectra are recorded and used for peptide identification. After this, it is possible to infer the proteins that are present in the sample from the ensemble identified peptides (Aebersold & Mann, 2003, Domon & Aebersold, 2010). There are three main methods of MS analysis which are showed in **Figure GI.7** (adapted from (Aebersold & Mann, 2016, Hu *et al.*, 2016)).

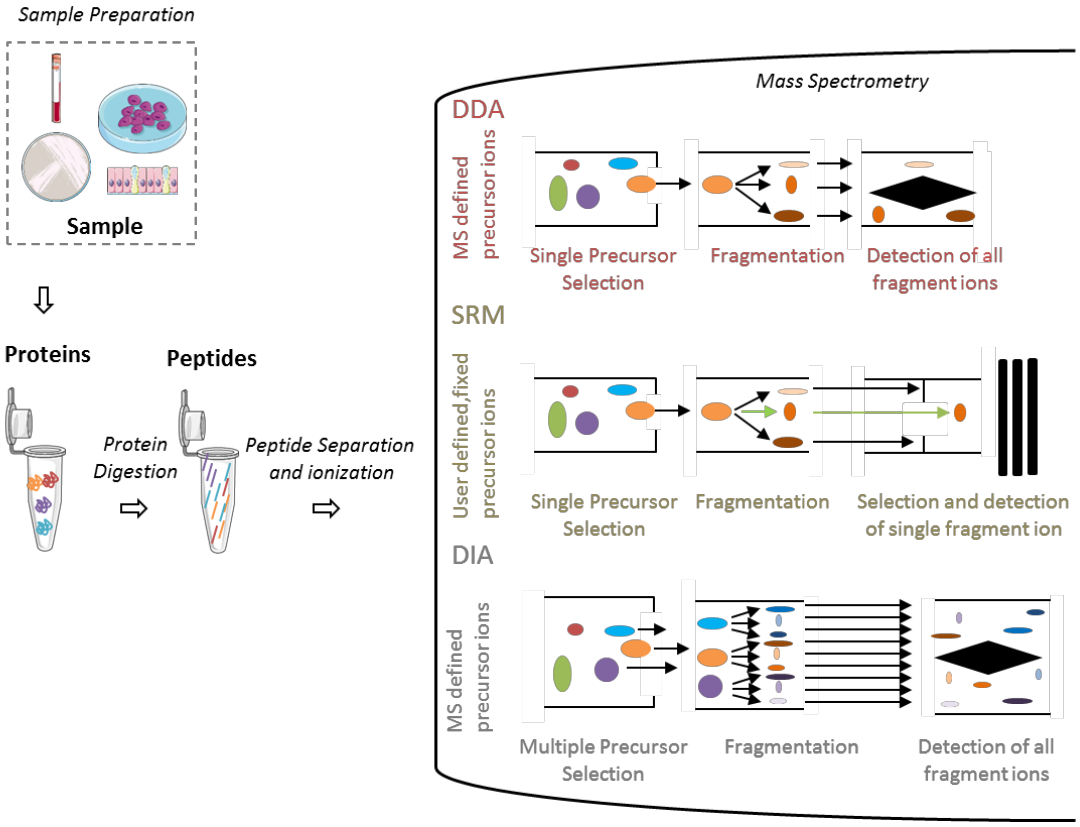

Figure GI.7 Bottom-up proteomics. Generally, bottom-up proteomic workflows have the following steps: sample preparation by digestion with trypsin, peptide separation by chromatography, ionization by electrospray and analysis by mass spectrometry. Three different methods are widely used for mass spectrometry analysis: DDA, targeted proteomics by SRM and DIA. In DDA and SRM, single precursor ions are isolated, fragmented and analysed in an MS2 scan by the mass spectrometer. In DDA mode the precursor ions are chosen sequentially by the instrument on the basis of abundance whereas in MRM the precursor ions are selected by the user. In DIA all precursor ions within a selected mass range are isolated, fragmented and analysed in a single MS2 scan.

When the precursor most abundant ions are selected automatically for tandem mass spectrometry (MS/MS), the data acquisition strategy is named as data-dependent analysis (DDA) (**Figure GI.7**). This method is very sensitive and is an unbiased and free from hypothesis once there is no need to know the identity of the expected proteins in advance. However, when

multiple samples are compared, the major drawback of the technique is that the selection of precursor ions is towards abundant peptides leading to irreproducible results of the shotgun experiments and thus incomplete MS data sets (Sabido *et al.*, 2012). In contrast to DDA, targeted proteomic approaches based on selected reaction monitoring (SRM) emerged as a potent tool due to its ability to quantify only proteins of interest with high reproducibility and high accuracy across multiple samples. In a typical SRM experiment, the proteins of interest are predetermined and known. Using pre-existing information, proteotypic peptides, which are unique and characteristic of each protein, are selectively isolated and then fragmented. The corresponding signals are measured over the chromatographic elution time window to provide better sensitivity and higher linearity for quantification, compared with other MS methods. This is done by setting the first quadrupole of a triple quadrupole instrument to the expected precursor ion m/z and the third quadrupole to the m/z ratio of an abundant fragment ion that is specific for the targeted peptide (Figure GI.7). The process is multiplexed to several fragment per peptide to increase selectivity and multiple peptide can be measured which increases throughput (Aebersold & Mann, 2016). However, this method has problems in the scale of quantification, this means that increasing the number of target peptide requires the tight control of peptide liquid chromatography (LC) elution time, for accommodating more transitions in a narrow time window, decreasing sensitivity (Shi *et al.*, 2016). Data-independent acquisition (DIA) methods were recently introduced and are based on fragmentation of all ions within a defined mass-to-charge (m/z) isolation window, independently of the relative ion abundance (Figure GI.7) (Chapman *et al.*, 2014). In this method, entire ranges of precursors are fragmented at the same time. The peptide fragmentation information is retrieved from the multiplexed MS2 spectra by targeted signal extraction on the basis of previously acquired single peptide fragmentation spectra or by the generation of “pseudo” fragment-ion spectra constructed directly from the DIA data that are then subjected to classical database searching. The advantage of this approach is that the entire range of possible precursor-ion masses can be analysed, eliminating the problem of DDA. DIA requires a priori construction of fragment-ion spectra for the query peptides to deconvolve these peptides from the DIA data (Aebersold & Mann, 2016). This method improves the depth and coverage of proteomic analysis and the overall reproducibility of the experiment (Canterbury *et al.*, 2014).

The majority of the proteomic studies compare the abundance of a specific proteome in different conditions or time-points and this highlights the importance of accurate protein quantification in the analysed samples. Protein quantification can be performed by stable isotope labelling approaches that are being broadly used for the mass-spectrometry based proteomics and include

metabolic labelling such as stable isotope labelling by amino acids in cell culture (SILAC) and $^{15}N/^{14}N$; enzymatic labelling using $^{18}O/^{16}O$ and chemical labelling using: isobaric tag for relative and absolute quantitation (iTRAQ®) and tandem mass tags (TMT®) among others (Zhu *et al.*, 2010). Figure GI. 8 depicts the main differences in the labelling methods for protein quantification (adapted from (Jazurek *et al.*, 2016)). From these, SILAC and TMT® are widely used.

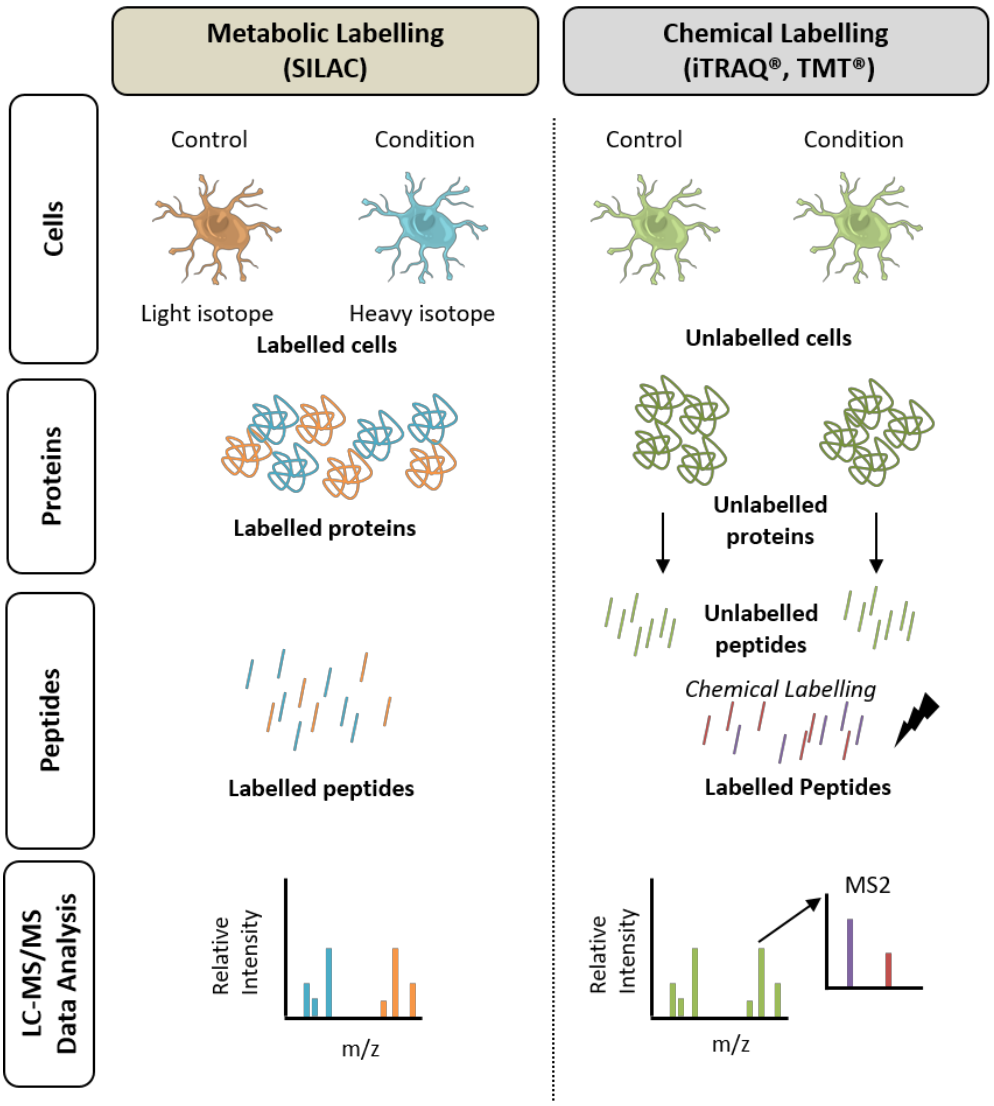

Figure GI.8 Main labelling methods for protein quantification. In metabolic methods labelling occurs at the protein level whereas in chemical methods labelling occurs at the peptide level (based on (Jazurek *et al*. 2016).

SILAC is a metabolic labelling that uses stable isotope-labelled amino acids in growth medium to encode cellular proteomes (Ong *et al.*, 2002, Ong & Mann, 2006). To accomplish proteome labelling, labelled essential amino acids are added to amino acid deficient cell culture media and they are assimilated during protein synthesis (Ong *et al.*, 2002). Then, proteins are combined, digested with trypsin and quantified (Figure GI. 8). TMT® is a chemical method composed by a set

of structural identical tags that, after proteolysis are used for peptide labelling on free amino-terminus of lysine residues. Peptides from different conditions are then combined and analysed by MS (**Figure GI. 8**)(Dayon *et al.*, 2008). These tags contain three functional parts: a reporter ion group, a mass normalization group and an amine reactive group. This last one is responsible for the reaction with the amine groups and epsilon amine groups of lysine residues to attach the tags to peptides. Labelled peptides with different isobaric tags are only possible to distinguish in MS/MS scans (Li *et al.*, 2012). The relative abundance of each reporter ion is used as a surrogate measurement for the abundance of the peptide and thus proteins from which it was derived in each sample. A major attraction of these tags is the possibility to multiplex samples. Besides this, they are suitable for any type of complex protein sample unlike SILAC which implies cell growth in labelled media. Although having these interesting advantages, this method also has some issues. One of them is incomplete labelling which highlights the importance of checking complete labelling in the experiments. Moreover, it is stated that there are some precision and accuracy problems. Accuracy problems are due to contaminant co-selection at the same time as a target peptide which results in MS/MS spectra containing reporter ions derived from mixed sources. This results in a ratio compression where observed ratios become increasingly underestimated as the expected fold change of an analyte increases (Christoforou & Lilley, 2012). Nevertheless, a benchmarking study of these methods was performed and showed that chemical labelling at the peptide level can be as robust and precise as metabolic labelling at the cellular level (Altelaar *et al.*, 2013). Our group has previously used SILAC labelling to quantify macrophage proteins and phosphoproteins by mass spectrometry to study the effect of *C. albicans* infection effects (Reales-Calderon *et al.*, 2013). Furthermore, we used TMT labelling for the study of the protein composition of THP-1 macrophages-derived EVs during interaction with *C. albicans*. The differentially abundant proteins of the EVs were involved in response to stimulus, interaction with cell and immune response (Reales-Calderon *et al.*, 2016).

6.3 Proteomic Approaches for the study of Post-Translational Modifications: focus on phosphorylation

PTMs play a crucial role in the regulation of several biological processes such as cell signalling, immune response, recognition of pathogens, among others. More than 300 types of protein PTMs are known to occur physiologically within living organisms (Huang *et al.*, 2014). From these PTMs, phosphorylation is of highly importance during signal transduction and it is believed that more than 30% of the proteins can be phosphorylated. According to Graauw and co-workers, early calculations suggested that there are approximately 100 000 potential phosphorylation sites

in the human proteome, and from those only a few part is known, emphasizing the need for sensitive, high-throughput methods, which allow the identification, characterization and monitoring of new sites of protein phosphorylation (de Graauw *et al.*, 2006). One important challenge for the application of phosphoproteomics lies on the successful extraction of the phosphopeptides from the whole lysate (de Graauw *et al.*, 2006). Numerous phosphopeptide enrichment approaches have been established and successfully employed to reveal phosphoprotein and regulated phosphorylation sites in complex biological samples: Immobilized metal affinity chromatography (IMAC), immunoprecipitation, phosphopeptide enrichment by TiO_2 and other metal oxides; calcium phosphate precipitation (CPP); sequential elution from IMAC (SIMAC), among others. IMAC is usually used for the study of phosphorylated peptides. However, studies suggested that this technique presented stronger selectivity for multiply phosphorylated peptides in biological buffers (Jensen & Larsen, 2007, Thingholm *et al.*, 2008). On the other hand, TiO_2 chromatography presented a bias towards monophosphorylated peptides (Thingholm *et al.*, 2006). Thingholm and co-workers presented a strategy that improves the number of phosphorylated peptides (Thingholm *et al.*, 2008). With this technique monophosphorylated peptides from IMAC material are eluted in acidic conditions and then, multiply phosphorylated peptides are eluted in basic conditions, and this is the reason it is named SIMAC. Subsequently, a TiO_2 chromatography is performed to remove most of the non-phosphorylated peptides from the pool of monophosphorylated peptides. Finally, the two distinct phosphorylated pools can be analysed using MS (Thingholm *et al.*, 2008). These methodologies use material in batch or microtip format with the material packed in gel-loader tips for the phosphopeptide enrichment and have some variability and selectivity issues due to manual handling steps. To tackle these limitations iron immobilized metal ion affinity chromatography columns were used for phosphoproteome analysis (Ruprecht *et al.*, 2017). This method does not suffer from these problems once it uses Fe-IMAC high performance liquid chromatography (HPLC) column for bulk phosphopeptide enrichment.

Besides the method of enrichment in phosphopeptides used additional fractionation techniques are being used to increase the capacity of phosphopeptide analysis (Wilson *et al.*, 2018). Among them, hydrophilic interaction liquid chromatography (HILIC) has previously been shown to be a successful fractionation method (Engholm-Keller *et al.*, 2012, Engholm-Keller & Larsen, 2016).

AIMS

Our group has been focusing on the study of the macrophage-*C. albicans* interactions and has previously applied proteomics approaches to identify important proteins and pathways during murine macrophage-yeast interactions (Fernandez-Arenas *et al.*, 2009, Reales-Calderon *et al.*, 2012, Reales-Calderon *et al.*, 2013). Moreover, it has also been studying the profile of IgG antibody response to *C. albicans* cytoplasmic and cell-wall proteins, with the ultimate objective of improving IC diagnosis (Pitarch *et al.*, 2006, Pitarch *et al.*, 2011, Pitarch *et al.*, 2016).

Taking these previous works into account, the key objective of this thesis is to better understand the role of the host during its interaction with the pathogen *C. albicans*, by using different proteomic approaches. These approaches may open doors for the development of new and more targeted therapies as well as a faster and sensitive diagnostic of this type of infections.

The specific purposes of this thesis are detailed below:

Chapter 1:

- To study the proteomic and phosphoproteomic alterations of the human macrophages after interaction with *C. albicans* focusing on ATP binding proteins.
- To unveil new mechanisms involved in human macrophage response to *C. albicans*, by global proteomic and phosphoproteomic studies.

Chapter 2:

- To perform the proteomic analysis of *C. albicans* hyphal secretome.
- To characterize of the serological response to the *C. albicans* hyphal secretome in patients with IC, associated or not with catheter.
- To identify biomarker candidates for the diagnosis of invasive candidiasis.

CHAPTER 1

Proteomic and phosphoproteomic approaches for the study of human macrophage remodelling after interaction with the opportunistic pathogen *Candida albicans*

*This Chapter contains supplementary figures, numbered from Supplementary Figure C1.1 to C1.7, available in the end of the thesis in **Appendix 1**

**This Chapter contains supplementary tables, numbered from Supplementary Table C1.1 to C1.7, available in the enclosed CD.

***Part of the work in this chapter was published:

Vaz C, Reales-Calderon JA, Pitarch A, Vellosillo P, Trevisan M, Hernaez ML, Monteoliva L & Gil C (2019) Enrichment of ATP Binding Proteins Unveils Proteomic Alterations in Human Macrophage Cell Death, Inflammatory Response, and Protein Synthesis after Interaction with *Candida albicans*. Journal of proteome research 18:2139-2159. **(see Appendix 2)**

Introduction

Macrophages, which are derived from monocytes circulating in the blood, are constantly patrolling tissues and non-sterile interfaces at the surfaces of epithelia, and are one of the key cells in the immune recognition and innate immune response to *C. albicans* (Erwig & Gow, 2016). As detailed in General Introduction, these cells recognize and phagocyte *C. albicans*, eliciting different immune responses through engagement of different PRRs in an infection-stage specific manner (Bourgeois *et al.*, 2010). The major PRRs implicated in the response to *C. albicans* include multiple cell-bound receptors (such as TLR2 and 4, Dectin-1, MR), soluble receptors (such as Galectin-3), and intracellular receptors (such as TLR9), that activate several signal transduction pathways, finally leading to the upregulation of costimulatory molecules and to the production of inflammatory cytokines, chemokines, antimicrobial peptides, and type I IFNs (West *et al.*, 2006). After the uptake of *Candida* cells, they are subsequently enclosed into phagolysosomes and both oxidative and non-oxidative mechanisms are activated by the macrophage to kill this pathogen (Hofs *et al.*, 2016). Besides this, macrophages are capable of restricting the availability of nutrients that are important for *C. albicans* growth (Miramon *et al.*, 2013). Although macrophages can kill some internalized *C. albicans* yeast cells, the majority survive and filament in response to the engulfment by the phagosome (O'Meara *et al.*, 2015). *C. albicans* is a strong trigger for the production of IL-1β via the Dectin-1/inflammasome activation (Uwamahoro *et al.*, 2014, Wellington *et al.*, 2014, O'Meara *et al.*, 2018).

Macrophage changes induced by *C. albicans* were a previous matter of study addressed by other groups. O'Meara and co-workers showed that some mutants were unable to induce macrophage lysis despite having significant hyphal formation. Moreover, they demonstrated that the transcriptional repression of *ALG1*, *ALG7* or *orf19.6233* caused defects on filamentation but did not block macrophage lysis (O'Meara *et al.*, 2015). Another recent work used dual RNA sequencing to study the metabolic interactions of bone-marrow-derived mouse macrophages and *C. albicans* at different time points. Among other findings, they observed a concomitant upregulation of glycolysis in both host and pathogen (Tucey *et al.*, 2018). Our research group identified differentially abundant proteins in *C. albicans*-stimulated RAW 264.7 macrophages using different proteomic approaches (Reales-Calderon *et al.*, 2012, Reales-Calderon *et al.*, 2014). Differentially abundant proteins were suggested to have pro-inflammatory and anti-apoptotic effects (Reales-Calderon *et al.*, 2012, Reales-Calderon *et al.*, 2013). Another study on human M1 (classically activated, pro-inflammatory subtype) and M2 (alternatively activated, anti-inflammatory subtype) macrophages showed that *C. albicans* induced an M1-to-M2 switch in polarization (Reales-Calderon *et al.*, 2014). Other groups used different proteomic approaches for

the analysis of macrophage and *Candida* interaction, and found new proteins involved in energy metabolism, cell survival and candidates for interaction-specific molecules (Shin *et al.*, 2005, Kitahara *et al.*, 2015).

Adenosine Triphosphate (ATP)-binding proteins include kinases, heat shock proteins as well as ATPases, and are crucial in several cellular processes, such as cell signaling, protein synthesis and metabolism (Adachi *et al.*, 2015). Despite the importance of these proteins in those pivotal cellular functions, proteomic studies of ATP-binding proteins by MS may be challenging mainly due to the fact that some ATP-binding proteins are at very low concentration in the proteome (Xiao *et al.*, 2013). The combination of MS instrumentation with powerful separation techniques or selective enrichment of these proteins and bioinformatics tools can help in the identification and quantification of low abundant proteins in complex samples (Xiao & Wang, 2014). During the last years, several procedures for selective enrichment of ATP binding proteins and kinases have been developed (Graves *et al.*, 2002, Hanoulle *et al.*, 2006, Daub *et al.*, 2008, Duncan *et al.*, 2012, Xiao & Wang, 2014). Patricelli's group presented a probe-based technology that uses biotinylated acyl phosphates of ATP or adenosine diphosphate (ADP) that irreversibly react with ATP-binding proteins on conserved lysine residues of the ATP binding pocket (Patricelli *et al.*, 2007). These probes covalently label the active site of these proteins to enable their selective enrichment using a desthiobiotin tag.

The study of the abundance of this group of proteins, together with others, can give us important information of the mechanisms being activated by the macrophage after interaction with pathogens. In addition to protein abundance, PTMs are crucial in the regulation of several biological processes, such as cell signalling, immune response, recognition of pathogens, among others. More than 300 types of protein PTMs are known to occur physiologically within living organisms. From these PTMs, serine, threonine and tyrosine phosphorylation serves as a signal transduction mechanisms enabling the cells to link extracellular signals to the regulation of adaptive and innate immune system activation (Sjoelund *et al.*, 2014). It was previously shown by our group that *C. albicans* induces changes in the phosphorylation of several peptides from murine macrophages. These changes were mainly implicated in immune response, cytoskeleton rearrangement and transcription factors (Reales-Calderon *et al.*, 2013). Another group performed a global phosphoproteomic analysis of the host response to another pathogenic fungus, *Cryptococcus neoformans*, and found that proteins in the host autophagy initiation complex were differentially phosphorylated in response to fungal infection (Pandey *et al.*, 2017). The phosphoproteome of the macrophage response to different TLR ligands was also previously profiled. They found that the activation of the different TLRs resulted in a predominance of serine

and threonine phosphorylation. They found cytoskeleton remodelling as a target of TLR signalling for all the tested ligands. More interestingly, they found that endocytosis and phagocytosis were up-regulated upon TLR4 and TLR2 stimulation but not upon TLR7 stimulation. TLR7 is located in the late endosomal compartment where it only signals in response to single-stranded DNA. (Sjoelund *et al.*, 2014). These are some examples of works that were important to increase the knowledge on host macrophages and pathogen interactions.

A better understanding of the immune response during fungal infection may help in the development of new improved therapies in the future. Envisioning this general objective, our group was interested in knowing the behavior of human macrophage cells after interacting with *C. albicans*, embracing both protein abundance and phosphorylation. To accomplish this, here we propose:

- To study the proteomic and phosphoproteomic alterations of the human macrophages after interaction with *C. albicans* focusing on ATP binding proteins.
- To unveil new mechanisms involved in human macrophage response to *C. albicans*, by global proteomic and phosphoproteomic studies.

Taken together, these two different approaches can bring new insights on the human macrophage cellular remodeling after interacting with the pathogen *C. albicans*.

Materials and Methods

1 Optimization of yeast and macrophage co-culture

1.1 *C. albicans* strain

C. albicans SC5314 strain was used in this study. This strain was grown in yeast, peptone and dextrose (YPD) plates (2% glucose, 1% yeast extract, 2% peptone and 2% agar) at 30ºC.

1.2 THP-1 cell culture and macrophage differentiation

The human acute monocytic leukemia cell line (THP-1) was cultured in Dulbecco's modified Eagle's medium (DMEM) supplemented with antibiotics (penicillin 10000 U/ml, streptomycin 10000U/ml), 2 mM L-glutamine and 10% heat-inactivated fetal bovine serum (FBS) at 37°C in a humidified atmosphere containing 5% CO_2. THP-1 cells were seeded in 24-well plastic plates at a density of $1x10^6$ cells/well in complete medium and treated with a final concentration of 30 ng/ml phorbol 12-myristate 13-acetate (PMA; Sigma-Aldrich) for 48 h to induce maturation toward

adherent macrophage-like cells. After 48 h cultures, the medium containing PMA was replaced with fresh medium without PMA to remove unattached cells.

1.3 *C. albicans*-macrophage co-culture

For interaction studies, THP-1 macrophages were incubated with *C. albicans* cells that were grown in YPD plates the day before, at multiplicity of infection (MOIs) of 1 and 5, and for different time points depending on the assays.

1.4 Environmental scanning electron microscopy (ESEM)

ESEM was performed as previously detailed (Reales-Calderon *et al.*, 2016). After macrophage interaction with *C. albicans*, cells were washed in phosphate buffer saline (PBS) containing 2.5% paraformaldehyde for 1 h at room temperature. They were incubated in 2% osmium tetroxide for 1 h and then in 2% tannic acid for 1 h. Cells were dehydrated in ethanol. They were examined at the FEI INSPECT microscope at the Museo Nacional de Ciencias Naturales (Madrid, Spain).

1.5 *C. albicans* phagocytosis assay

C. albicans yeast cells were pre-labelled with 1 µM Oregon green 488 (Molecular Probes) in the dark with gentle shaking at 30°C for 1 h. THP-1 macrophages were differentiated in 18-mm glass sterile coverslips placed into 24-well plates and confronted with the yeast cells at a MOI of 1, at 37ºC and 5% CO_2. Interaction was stopped after 45 min, 1.5 h and 3 h, and cells were then washed with ice-cold PBS and fixed with 4% paraformaldehyde for 30 min. To distinguish between internalized and attached/non-ingested yeasts, *C. albicans* cells were counterstained with 2.5 M Calcofluor white (CFW) (Sigma) for 15 min in the dark. After several washes, coverslips were mounted with specific mounting medium (Southern Biotech). The number of ingested cells (green fluorescence) and adhered/non-ingested (blue fluorescence) were counted in the fluorescence microscope (Fernandez-Arenas *et al.*, 2007). Three different replicates with two different slides were prepared for each time point. At least 500 *C. albicans* cells were scored per slide, and results were expressed as the percentage of yeast cells internalized by macrophages.

1.6 Macrophage cell damage assay

In order to evaluate the *C. albicans* damage in the THP-1 cell line macrophages, the cytotoxicity detection kit (Roche) was used. This assay is based on the measurement of lactate dehydrogenase (LDH) activity released from the cytosol of damaged cells. Macrophages were cultured in 24-well plates as stated above, and *C. albicans* cells were incubated with them in a MOI of 1 and 5 at 37ºC

and 5% CO_2. The selected time points of measurements were 3 and 6 h. After these time points, the supernatants of the cells were removed for LDH measurement. The assay was performed according to manufacturer's instructions.

2 Proteomic and phosphoproteomic analysis of human macrophage ATP-binding proteins, labeled by SILAC, after interaction with *C. albicans*

2.1 Macrophage cell line culture and SILAC labelling

THP-1 monocytes were grown in DMEM containing 10% dialyzed fetal bovine serum (FBS): i.e., either in light DMEM, containing 100 mg/l unlabeled L-arginine (Arg0) and 50 mg/l L-lysine (Lys0), or in heavy DMEM, containing 100 mg/l Arg6 (Silantes, ^{13}C labelled Arginine· HCl) and 50 mg/l Lys6 (Silantes, ^{13}C6 labeled L-Lysine HCl). After 5 cell doublings, protein lysates of the macrophage cells were analyzed by MS to ensure that all proteins were labelled. Differentiation of monocytes into macrophages was triggered by the addition of PMA. Approximately, $2x10^7$ cells were plated in 150-mm culture dishes and 30 ng/ml PMA was added, cells were incubated for two days to achieve complete differentiation. PMA was removed by washing the cells with light and heavy DMEM medium, respectively.

2.2 Fungal infection

C. albicans cells were counted using the Neubauer chamber, and $2x10^7$ cells were incubated with the macrophages (MOI of 1) for 3 h. In order to diminish the possible effect of the labelling procedure, in two biological replicates control macrophages were labelled with light DMEM and macrophages upon interaction were labelled with heavy DMEM, while in the other two biological replicates this labelling was switched over. The extracted proteins came from the same number of macrophage cells in control and interaction conditions. In each experiment, both labelled and unlabeled lysates were mixed in protein concentration ratios of 1:1.

2.3 Preparation of the protein samples for shotgun proteomics

2.3.1 Cell lysis

After the incubation time, cells were washed twice with ice-cold PBS, and 1 ml of cold modified radioimmunoprecipitation assay (RIPA) lysis buffer (150 mM sodium chloride; 50 mM Tris-HCl pH 7.5; 1% NP40; 0.25% sodium deoxycholate; proteases inhibitors (1:1000, Pierce™); 1 mM sodium orthovanadate; 5 mM sodium fluoride; 5 mM β-glycerophosphate and 5 mM sodium pyrophosphate) was added. Cells were scrapped thoroughly. Then, the cell lysate was placed on ice for 5 min, vortexed for another 5 min, and centrifuged at 15,000 rpm for 10 min and 4ºC. The

supernatant, containing the macrophage protein extract, was removed and transferred to a new tube. Protein concentration was measured using the Bradford assay.

2.3.2 Enrichment with desthiobiotin ATP probes

Protein lysates were enriched in ATP binding proteins using ActivX desthiobiotin ATP probes (Thermo Scientific), according to manufacturer instructions with some alterations. Briefly, protein lysates were desalted using Zeba spin desalting columns to remove endogenous ATP. Then, lysates were eluted in reaction buffer and supplemented with protease inhibitors. Protein concentration was determined again by the Bradford assay. For labelling with the ATP probes, 2 mM MgCl was added to 2 mg of protein lysate and incubated with 20 µM of ActivX probe in a final volume of 500 µl for 30 min at room temperature with constant mixing. Then, 500 µl of 12 M urea in lysis buffer were added to the lysate to stop the reaction. Samples were then incubated with 125 µl of high-capacity streptavidin agarose resin for 1.5 h at room temperature with constant mixing in a rotator. Beads were collected by centrifugation at 1000g for 1 min and washed twice with 4 M urea in lysis buffer. Finally, proteins were eluted by adding Laemmli reducing sample buffer and boiling for 5 min.

2.3.3 In-gel digestion

Samples in Laemmli sample buffer were loaded into a 1.5 mm thick SDS-PAGE gel with a 4% stacking gel casted over a 10% resolving gel. The run was stopped as soon as the front entered 3 mm into the resolving gel so that the whole proteome became concentrated in the stacking/resolving gel interface. Bands were stained with colloidal Coomassie Brilliant Blue staining. Gels were cut into 12 to 15 slices for protein digestion (Bonzon-Kulichenko *et al.*, 2011). In-gel digestion was carried out as described (Shevchenko *et al.*, 2006). Briefly, gel slices were cut into pieces of 1 mm^3 in size and washed with water. Proteins were reduced with 10 mM dithiothreitol (DTT) in 25 mM ammonium bicarbonate for 30 min at 56°C and then alkylated with 55 mM iodoacetamide (IA) in 25 mM ammonium bicarbonate for 15 min at 30°C. Acetonitrile (ACN) and vacuum centrifugation were applied to dry the gel pieces. They were then rehydrated with 60 ng/µl trypsin (proteomics grade; Roche Applied Science) in 25 mM ammonium bicarbonate for 45 min at 4°C. The trypsin solution was removed, and the rehydrated gel pieces were overlaid with 25 mM ammonium bicarbonate. The digestion was performed overnight at 37°C. After digestion, the supernatant was recovered. Peptides were extracted from the gel pieces with 30% ACN and 0.1% trifluoroacetic acid (TFA) for 30 min at room temperature. Peptides were desalted onto C18 OMIX cartridges and dried-down.

2.3.4 Sequential elution from immobilized metal affinity chromatography (SIMAC) for phosphopeptide enrichment

A total of 300 µg of the protein lysate enriched in ATP-binding proteins was used for phosphopeptide enrichment. Both IMAC and titanium dioxide (TiO_2) chromatography were performed as previously described (Reales-Calderon *et al.*, 2013) and summarized below.

IMAC

For each 100 µg of peptides, 40 µl of iron-coated PHOS-select^{TM} metal chelate beads (Sigma-Aldrich) were used. Beads were washed twice in loading buffer (0.1% TFA and 50% ACN) and incubated with 500 µg of peptide mixture in loading buffer for 30 min at room temperature in vibrating shaker. Then, beads were packed in the constricted end of a 200 µl GELoader tip by application of air pressure with a syringe, forming an IMAC column. The flow-through was collected for further analysis by TiO_2 chromatography. The IMAC was then washed with loading buffer, which was added to the flow-through. Both monophosphorylated peptides and contaminating non-phosphorylated peptides were eluted using acidic elution solution (1% TFA and 20% ACN) and the multiply phosphorylated peptides were eluted using basic elution solution (0.5% ammonia). The IMAC flow-through and both eluents were dried in a vacuum concentrator.

TiO_2 chromatography

A TiO_2 microcolumn was prepared by stamping out a small plug of C18 material from a C18 extraction disk and placing the plug in the constricted end of a 200 µl GELoader tip. The TiO_2 beads were first suspended in loading buffer (1 M glycolic acid in 5% TFA and 80% ACN) and then mixed with the sample and incubated for 15 min with constant mixing. This mixture was centrifuged and 90% of the supernatant was removed to minimize the volume introduced in the microcolumn. The sample was applied to the tip and the TiO_2 column was packed by the application of air pressure with a syringe. The column was washed with loading buffer and subsequently with washing buffer (80% ACN and 5% TFA). The phosphopeptides bound to the TiO_2 microcolumn were eluted using 30 µl of 0.5% ammonia followed by elution using 1 µl of 30% ACN to elute phosphopeptides bound to the C18 disk. Then, the eluent was acidified by adding 5 µl of 100% formic acid and dried in the vacuum concentrator.

2.4 MS analysis

Peptides were trapped onto a C18 SC001 2-cm precolumn (Thermo Scientific), and then eluted onto a NS-AC-11 dp3 BioSphere C18 column (75 µm inner diameter, 15 cm long, 3 µm particle

size; NanoSeparations) and separated using a 140 min gradient (0-40% buffer B for 120 min; 40%-95% buffer B for 15 min, and 95% buffer B for 5 min; buffer A: 0.1% formic acid/2% ACN; buffer B: 0.1% formic acid in ACN) at a flow-rate of 250 nL/min on a nanoEasy HPLC (Proxeon) coupled to a nanoelectrospay ion source (Proxeon). Mass spectra were acquired on a linear trap quadrupole (LTQ)-Orbitrap Velos mass spectrometer (Thermo Scientific) in the positive ion mode. Full-scan MS spectra (m/z 300–1,900) were acquired in an Orbitrap at a resolution of 60,000 at 400 m/z and the 15 most intense ions were selected for collision induced dissociation (CID) fragmentation in the linear ion trap with a normalized collision energy of 35%. Singly charged ions and unassigned charge states were rejected. Dynamic exclusion was enabled with exclusion duration of 30 s.

2.5 Quantitative data analysis

Mass spectra raw data files were searched against the SwissProt human database version 57.15 (20,266 protein entries) using MASCOT search engine (version 2.3, Matrix Science) through Proteome Discoverer (version 1.4.1.14; Thermo Fisher). Search parameters included a maximum of two missed cleavages allowed, carbamidomethylation of cysteines as a fixed modification, and oxidation of methionine, desthiobiotinylation of lysine, 13C-arginine and 13C-lysine as variable modifications. Precursor and fragment mass tolerance were set to 10 ppm and 0.8 Da, respectively. Identified peptides were validated using Percolator algorithm with a q-value threshold of 0.01. Peptide quantification from SILAC labels was performed with Proteome Discoverer v1.4 using node precursor ion quantification. For each SILAC pair, the area of the extracted ion chromatogram was determined and the “heavy/light” ratio computed.

Ratios were normalized by the median of all peptide ratios in each biological replicate. Media and standard deviation were calculated for each peptide. Protein ratios were then determined as the media of all the quantified peptides belonging to a certain protein. The quantification was analyzed at the peptide level, and peptide ratios were manually evaluated. Peptides that presented discrepant values inside each protein were discarded as soon as this elimination did not change the trend of the ratio presented, and the standard deviation was improved. By this way, an increase in the coverage of the quantified proteins was achieved.

Regarding phosphorylation, the variable modification of phosphorylation (STY) was added for peptide identification. The PhosphoRS node was used to provide a confidence measure for the localization of phosphorylation in the peptide sequences identified with this modification. The phosphorylation sites were manually corrected based on the PhosphoRS localization probability for a given residue. The phosphorylation sites assigned with a localization percentage <75% were

considered ambiguous. In addition, if the percentage was >75% but different in the biological replicates were also considered ambiguous. The phosphopeptides were treated similarly as in quantitative analysis with the exception that the quantification was performed only at peptide level. Mass spectra raw data files (both quantitative and phosphorylation files) were also searched against the SwissProt human database for the discovery of possible missing proteins.

Proteomic analysis was performed in Centro de Investigaciones Biologicas (CIB) and in the Proteomics facility of the Complutense University.

To make our findings publicly available and accessible to the community, we have deposited our dataset in ProteomeXchange Consortium via the PRIDE partner repository with the dataset identifier PXD009938 (Vizcaino *et al.*, 2016, Deutsch *et al.*, 2017).

2.6 Statistical analysis

In the SILAC experiment, the protein abundance ratio was the amount of protein in the macrophages upon interaction with *C. albicans* divided by the amount of protein in the control macrophages (without interaction with *C. albicans*). The $\log_2$-transformed mean macrophage protein abundance ratios upon *C. albicans* interaction were stratified into seven quantiles according to their distribution in the sample: Q_1 (the lower extreme values), Q_2 (the lower outlier values), Q_3 (the smaller values that extended to 1.5 times the lower quartile or 25^{th} percentile), Q_4 (the interquartile range, i.e. 25^{th} to 75^{th} percentiles), Q_5 (the larger values that extended to 1.5 times the upper quartile or 75^{th} percentile), Q_6 (the upper outlier values), and Q_7 (the upper extreme values). The first and seventh quantiles comprised those macrophage proteins that had the lowest and highest relative abundance ratios, respectively, upon interaction with *C. albicans*. The same analysis was performed for phosphorylated peptides. All quantitative data were presented as mean ± standard deviation (SD).

3 Global proteomic and phosphoproteomic analysis of human macrophages after interaction with latex beads and *C. albicans,* using TMT labelling

For this approach, the same *C. albicans* strain was used (SC5314) as well as the same macrophage cell-line (THP-1). However, due to some variability observed in the previous work, some modifications were made.

3.1 Interaction study

For the interaction, approximately $15x10^6$ THP-1 macrophage cells were incubated with *C. albicans* cells that were grown until an optical density (OD) of approximately 1 and with

polystyrene latex microspheres 4.5 micron (Alfa Aesar). *C. albicans* cells and beads were counted using the Neubauer chamber and incubated with the macrophages at a MOI of 1 for 3 h in DMEM. Four replicates were performed, and 3 conditions were compared: Macrophages alone; macrophages with beads and macrophages with *C. albicans*.

3.2 Sample preparation for proteomic and phosphoproteomic approach

3.2.1 Cell lysis

After the interaction, cells were washed twice with cold PBS. Then, 1 ml of cold RIPA medium was added and cells scrapped. Cell homogenization was performed using a milder process than before. Cells were left on ice for 40 min, slightly vortexed and then centrifuged for 10 min at 14800 rpm.

The supernatant, containing the macrophage protein extract, was removed and transferred to a new tube. Protein concentration was measured using the bicinchoninic acid (BCA) assay.

3.2.2 Protein precipitation and digestion

Proteomic and phosphoproteomic analysis were performed in the Department of Biochemistry and Molecular Biology, Syddansk University, Odense, Denmark, due to a collaboration with Professor Ole Jensen and Pavel Shliaha.

A total volume of 300 µl of the sample was mixed with 1.2 ml of acetone and proteins were precipitated for 2 h at -20 ºC and then pelleted by centrifugation at 20000 g. Samples were resuspended in 500 µl of 8 M urea 0.1 M 4-(2-hydroxyethyl)-1-piperazineethanesulfonic acid (HEPES) pH 8.0. An amount of 400 µg of protein in 150 µl were reduced and alkylated with 10 mM tris (2-carboxyethyl) phosphine (TCEP) and 40 mM chloroacetamide and digested with lysC (1:50 protease : protein ratio) at 37 ºC for 4 h. The sample was then diluted 8-fold and digested with trypsin (1:25 protease: protein ratio) at 37 ºC overnight. A total of 300 µg of peptides was desalted on 30 mg oasis HLB cartridge (Waters), and dried in the speedvac with 2 µL dimethylsulfoxide (DMSO) to prevent complete drying and quantified by BCA again.

3.2.3 Peptide labelling by TMT-11-plex and MS analysis

For the TMT labelling, 4 biological replicates of control, 3 biological replicates of macrophage after interacting with latex beads and 4 biological replicates of macrophages after interacting with *C. albicans* were analysed. Sixty µg of peptide mix was labelled with each of 11-plex TMT reagents and the sample was pulled, according to the manufacturer's instructions. After labelling, all samples were combined, desalted onto C18 OMIX cartridges (Waters) and dried-down. Fifty µg of

TMT labelled samples were analyzed by 2D-LC-MS analysis, using high pH RP fractionation as a first dimension and low pH RP chromatography as a second dimension. For high pH reverse phase (RP) fractionation peptides were separated on an Ultimate3000 HPLC system (Thermo Scientific) on ACQUITY CSH C18 1.7 µm column (300 µm X 100 mm) (Waters) with step gradient. Buffer A was H_2O, 20 mM ammonium formate, pH 9 (adjusted with NH_4OH); buffer B was 80% ACN, 20% buffer A. Thirty subfractions were collected and concatenated into 15 fractions. One extra fraction contained flow-through peptides. The fractions were dried out in a speed-vac and resolubilized in 2% ACN, 98% H_2O, 0.1% TFA. 2/3 fraction volume after resolubilization was injected for the second-dimension separation and analysis into the Ultimate3000 RSLCnano HPLC system. Samples were loaded on a cartridge precolumn PepMap 100 5x0.3 mm (Thermo Scientific) in 2% ACN, 98% H_2O, 0.1% TFA at 10 ml/min and then separated on a 1.2 m length 150 µm ID column, home-packed with InertSil ODS-3 2 µm sorbent (GLSciences). Separation was done in a gradient of ACN, 0.1% FA (buffer B) in H_2O, 0.1% formic acid (FA) (buffer A) (from 4 to 32% B in 2 h) at 0.7 µl/min at 55 ºC. Eluted peptides were identified on Orbitrap Fusion LUMOS mass spectrometer with multinotch MS3 method.

3.2.4 Phosphopeptide enrichment and MS analysis

Due to some variability observed in the previous phosphopeptide enrichment, another method was used. Phosphopeptides were enriched as previously described (Ruprecht *et al.*, 2015). The column ProPac IMAC-10 4x50 mm was charged with Fe^{3+}. Samples were loaded and the non-phosphorylated peptides were washed out in 50% ACN, 49.9% H_2O, and 0.1% TFA. Phosphopeptides were eluted by washing the column with 100% NH_4OH, 20 mM, pH 10. Immediately after elution phosphopeptide fraction was acidified by adding TFA and freeze-dried. Phosphopeptides were then separated by a linear gradient. Low pH separation was performed on 75 µM by 50 cm column with in a gradient of ACN, 0.1% FA (buffer B) in H_2O, 0.1% FA (buffer A) (from 4 to 32% B in 2 h) at 0.25 µl/min at room temperature. Eluted peptides were identified on Q-Exactive HF mass spectrometer. Full scan was performed at 400-1600 mz range with 120K resolution with 3e6 AGC target and 100 ms maximum injection time. Maximum of 12 dependent scans were performed at 60K resolution with AGC target of 1e5 and maximum injection time of 110 ms and 34 NCE. Isolation window as specified at 0.6 mz with 0.1 mz offset. Minimum AGC target was 3e3 and exclusion time was set at 11 sec.

3.3 Quantitative data analysis

Data was analyzed in Proteome Discoverer 2.1 software. A database search was performed with Mascot 2.3.2 using *Homo Sapiens* UniProt database containing only reviewed entries and canonical isoforms (retrieved on 06/11/2017). For unmodified peptide search, methionine oxidation was set as variable modification, while Cys carbamidomethylation, TMT6plex (K), and TMT6plex (N-term) were specified as fixed modifications. A maximum of two missed cleavages were permitted. The precursor and fragment mass tolerances were 10 ppm and 0.6 Da respectively. Peptides were validated by mascot percolator with a 0.01 posterior error probability (PEP) threshold. For phosphopeptide analysis the precursor and fragment mass tolerances were 10 ppm and 0.2 Da and phospho (ST), phospho (Y) modifications were additionally specified as variable modifications. The phosphorylation positions were validated using the phosphoRS algorithm. The quantification results of peptide spectrum matches were converted to peptide-level quantitation, which in turn was converted into protein quantitation using an R script (Polpitiya *et al.*, 2008). Quantitation profiles of phosphorylated peptide were normalized on the profiles of their corresponding protein expression, to verify that the observed changes of phosphorylation reflect differences in site occupancy and not in levels of protein expression.

3.4 Statistical analysis

Firstly, Linear Models for Microarray Data (limma) integrated in the Bioconductor package of R language was used for the comparison of the three conditions.

After removing beads condition from the analysis due to the lack of statistical significances found, protein abundance data was imported into the software package Perseus version 1.5 (Tyanova *et al.*, 2016) and protein intensities were $\log_2$ transformed in order to have the data more symmetric. Paired Student's T-test with the permutation-based false discovery rate (FDR) was used and the cut-off was put on *p*-value < 0.05 and 5% FDR to determine differentially abundant proteins.

The phosphorylation data was also imported in the software package Perseus version 1.5 and phosphopeptide intensities were also $\log_2$ transformed normalized to reduce systematic technical variation. The median sweeping was used as method of normalization for tandem mas tag (TMT) recommended in previous works (Kammers *et al.*, 2015, D'Angelo *et al.*, 2017) to perform limma to involve better statistical estimate. After the common processing of transformation and normalization, data was imported to perform limma included in ProStar software implemented in the R language. The *p*-values were corrected using the Benjamini–Hochberg procedure and a cut-off was set at 5% FDR. Phosphopeptides differentially abundant with *p*-value 0.01 and FDR 5% are

filtered and their and their intensities were normalized (by Z-score in Perseus) to show the heat-map of hierarchical clustering which enables the visualization of phosphopeptides intensities variation between replicates. Cluster heat-map was divided in 2 clusters to show the phosphopeptides profile and their regulation. Volcano plot was visualized by Perseus between the two dimensions ($-\log_{10}$ *p*-value vs. $\log_2$ fold change). Statistical analysis was performed in collaboration with the Proteomics unit of Complutense University of Madrid.

4 Bioinformatic analysis of differentially abundant proteins and phosphoproteins

Gene ontology (GO) enrichment analysis was performed using Genecodis (http://genecodis.cnb.csic.es/) (Carmona-Saez *et al.*, 2007, Nogales-Cadenas *et al.*, 2009, Tabas-Madrid *et al.*, 2012) and functional enrichment analysis (FunRich) tools. String software version 10.0 (http://string-db.org) was used for the study of the protein-protein interactions (Szklarczyk *et al.*, 2017). Ingenuity Pathway Analysis (IPA) (QIAGEN Bioinformatics) was used both for the prediction of possible upstream regulators and for network analysis. IPA was used during a collaboration with Doctor Leif Schauser and Nitesh Kumar Singh from QIAGEN, Aarhus, Denmark.

5 Proteomic and functional validation

5.1 Western blotting

Forty µg of protein lysate were loaded in each well of a 10% SDS-PAGE gel and electrophoretically separated. After this, proteins were transferred onto nitrocellulose membranes (GE Healthcare). Membranes were blocked with 5% skinny milk in PBS for 2 h, and incubated with primary antibodies, including anti-PRDX5 dilution 1/125 (Abcam), anti-MEK2 1/500 (Cell Signaling Technology), anti-cleaved caspase-3 1/1000 (Cell Signaling Technology), anti ERK-1/2 1/1000 (Cell Signaling Technology), anti p-ERK1/2 1/1000 (Cell Signaling Technology) or anti-Tubulin-α 1/1000 (Serotec), for 18 h at 4ºC. Membranes were washed 4 times with PBS containing 0.1% Tween-20 and incubated with IRDye® secondary antibodies for 1 h (1/4000 IRDye 800CW goat anti-mouse IgG, IRDye 680LT goat anti-mouse IgG, IRDye 800CW goat anti-rabbit IgG or IRDye 680LT goat anti-rabbit IgG, as appropriate). Membranes were then washed four times with PBS containing 0.1% Tween-20. Odyssey system (LI-COR ®) was used to detect the fluorescence signals. Protein abundance was compared between control and infected macrophages and values were given as arbitrary fluorescence units. Detection of tubulin-α was used as a loading control.

5.2 Selected reaction monitoring (SRM)

The abundance of the protein NDKA was quantified using SRM. A proteotypic peptide from NDKA that had been quantified in the shotgun approach and reached several criteria necessary for SRM was selected (FMQASEDLLK). The peptide should be proteotypic, easy to synthesize and have moderate hydrophobicity. Unpurified isotopic labelled peptide was obtained from JPT Peptide Technologies GmbH. Skyline software (Seattle Proteome Center) was used for the optimization of SRM methodology and for the analysis of the resulting MS data. Protein lysates were obtained as stated above, but without labelling the cells, enriched using ATP-probe and digested as previously shown. These SRM experiments were performed on a Q-TRAP ® 5500 LC-MS/MS system (AB Sciex). Both peaks from the endogenous and heavy peptides were evaluated manually. The area ratio (endogenous peptide area divided by heavy peptide area) was compared in both conditions (control and interaction). Three biological replicates and at least 2 technical replicates were performed.

5.3 Quantitative RT-PCR

RNA was isolated using the microRNeasy mini kit (QIAGEN) according to the manufacturer's protocol. Samples were quantified by Nanodrop 2000C (Thermo Scientific) and the presence of small RNA was confirmed using the Bioanalyzer 2100 (Agilent). Total RNA was reverse transcribed using Taqman microRNA (miRNA / miR) reverse transcription kit (Thermo Fisher Scientific) and 10 ng of total RNA from each sample. Quantitative real time polymerase chain reaction (RT-PCR) for miRNA was performed using TaqMan microRNA assays (Thermo Fisher Scientific) following the manufacturer's instructions. U6 snRNA was used as an endogenous control, and the microRNAs (miRNAs) analyzed were mmu-miR-124a, hsa-miR-146a, hsa-miR-155 and hsa-miR-21. This analysis was carried out in the Genomics facility of the Complutense University of Madrid.

5.4 Cytokine determination

For cytokines measurements, macrophages from the THP-1 cell line were incubated with or without *C. albicans* cells at a MOI of 1 for 3, 6 and 8 h. As a positive control, macrophages were treated with lipopolysaccharide (LPS; 100 ng/ml). Supernatants from untreated, LPS- or *Candida*-treated THP-1 macrophages were tested for cytokine production by enzyme-linked immuno sorbent assay (ELISA) using matched paired antibodies against different interleukins: IL-1β IL-6, IL-12p40 and TNF-α (Immunotools), according to manufacturer's instructions. Cytokine production was measured in three independent macrophage preparations.

5.5 JC-1 for mitochondrial activity measurements

For mitochondrial membrane potential measurements, a total of $3x10^5$ macrophage cells were seeded in each well of a 24-well plate. Macrophages were incubated during 3 h with beads and with *C. albicans* at a MOI of 1. Carbonyl cyanide m-chlorophenyl hydrazine (CCCP) causes the uncoupling of the proton gradient, greatly reducing red fluorescence and was used as green positive control. CCCP was added 15 min before the end of the incubation time and added at concentration of 0.1 mg/ml. Cells were detached using a solution of trypsin-ethylenediaminetetraacetic acid (EDTA) (0.05%) for 15 min, then centrifuged (2000 rpm 5 min) and incubated with JC-1 (0.5 µg/ml) during 20 min at 37ºC. Cells were analyzed by flow cytometry and cells with high mitochondrial membrane potential were detected in red and green fluorescence channels while cells with low mitochondrial membrane potential presented lower red fluorescence. Three biological replicates were performed. The flow cytometry was performed in the Centre of Flow Cytometry of the Complutense University of Madrid.

5.6 Statistical analysis

The mi-RNA expression level was calculated using $2^{-\Delta\Delta Ct}$ formula (Livak & Schmittgen, 2001). The results were represented using the relative fold-change expression compared to the control. Four biological replicates were used in this assay. For Western blotting, cytokines, SRM, miRNAs and JC-1 assays, comparisons between two groups were performed by the Student's t-test. Statistical significance was defined as * for *p*-value <0.05, ** for *p*-value <0.001 and *** for *p*-value <0.0001. Three biological replicates were performed for Western blotting and SRM-based validation assays, with exception of cleaved-caspase 3 Western blotting that was performed with two biological replicates.

The overall representation of both proteomic approaches carried out in this chapter is represented in **Figure C1.1**

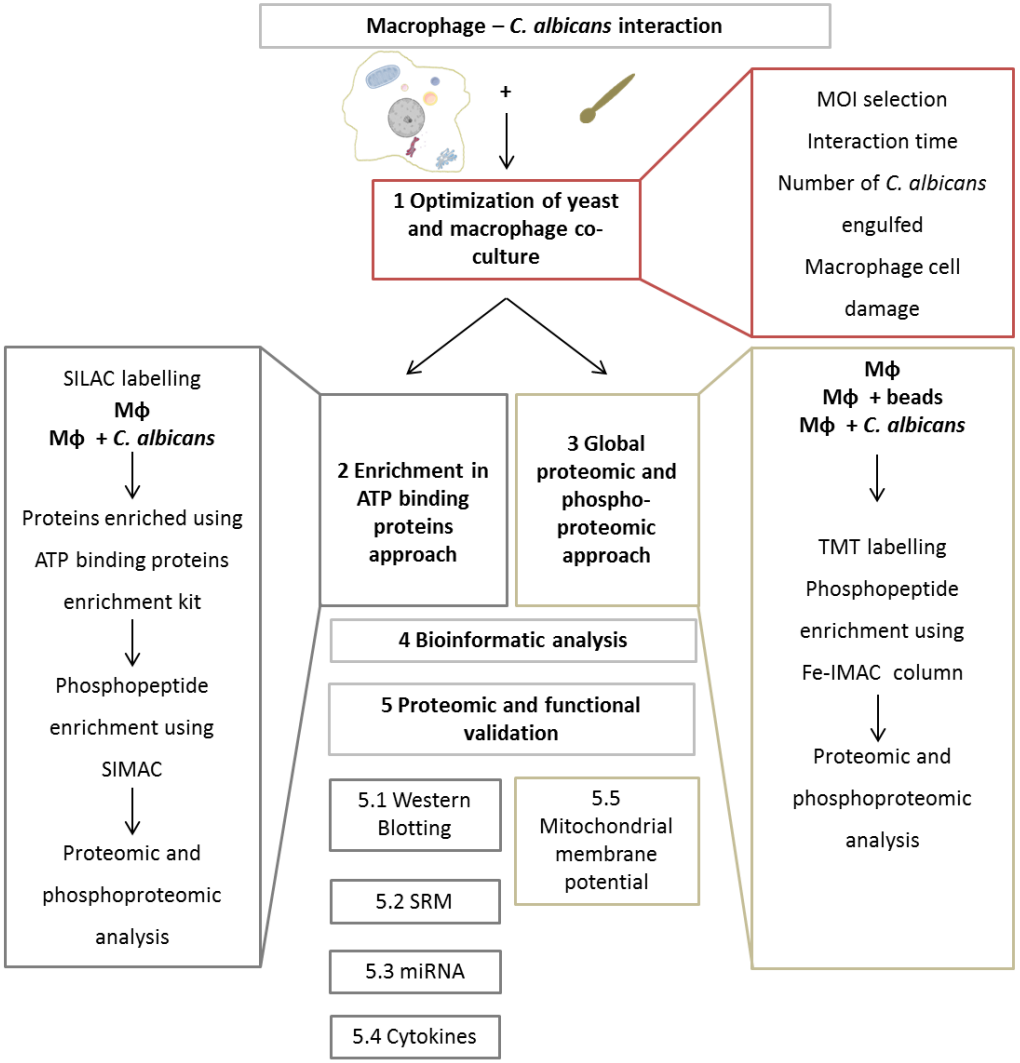

Figure C1.1 Schematic overview representing the organization of the proteomic and phosphoproteomic approaches developed in this chapter. This includes: condition set up, both MOI and time of incubation for the analysis of macrophage proteomic alterations after interaction with *C. albicans*. After this, two proteomic approaches were developed: one involves the enrichment in ATP binding macrophage proteins and the other one involves the global proteomic and phosphoproteomic analysis of the cytoplasmic extract of macrophages alone, after interaction with beads and after interaction with *C. albicans*. This outline was numbered according to the Materials and Methods section.

Results

1 Co-culture of THP-1 macrophages with *C. albicans*

The optimal conditions were set up to characterize differentially abundant proteins from human macrophages upon *C. albicans* infection. The damage of *C. albicans* in the THP-1 macrophages was evaluated by LDH measurements in two MOIs (Figure C1.2A). *C. albicans* produced more damage to THP-1 cells in a MOI of 5 than in a MOI of 1. Damage increased over time of incubation at both MOIs. A MOI of 1 was selected due to the lowest observed damage. After MOI selection,

phagocytic activity was measured. *C. albicans* cells ingested or associated with macrophages were discriminated using differential staining with Oregon green and calcofluor white. THP-1 macrophages showed an increase in their phagocytic activity over time (from 45 min to 3 h), almost 70% of *Candida* cells being engulfed after 3 h of interaction (Figures C1.2B and C). Taking into account these results and some studies performed before by our laboratory (Fernandez-Arenas *et al.*, 2007, Fernandez-Arenas *et al.*, 2009, Reales-Calderon *et al.*, 2013, Reales-Calderon *et al.*, 2014), the MOI of 1 and the time point of 3 h were the conditions used for the quantitative proteomic assay. With these conditions, it was assured that 70% of *C. albicans* cells were engulfed and most macrophages were viable. Macrophage-*C. albicans* co-culture in the selected conditions was visualized by ESEM (Figure C1.2D). As shown, after 3 h of interaction *C. albicans* cells were already in hypha form and at different stages of interaction with the macrophage.

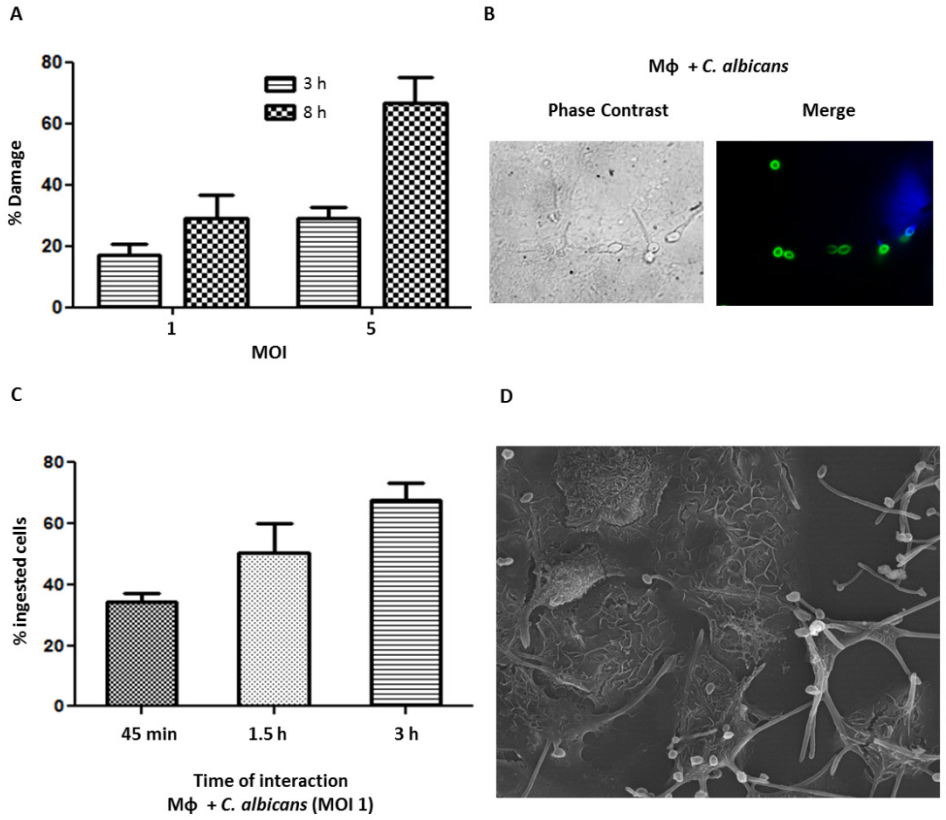

Figure C1.2 THP-1 macrophage interaction with *C. albicans* cells. (A) Lactate dehydrogenase cytotoxicity assay to measure the damage of *Candida* cells in THP1 macrophages after 3h and 8h of interaction with *C. albicans* cells and at a MOI of 1 and 5. (B) Fluorescence microscopy images of THP1 macrophages exposed to labeled *C. albicans* strain SC5314 (Oregon green 488) in green, for 3h. Intracellular and external/adhered *C. albicans* cells were distinguished based on fluorescence after co-staining with Calcofluor white in blue, which does not enter or stain macrophages. (C) Phagocytic activity of macrophages at different times of interaction. (D) Environmental scanning electronic microscopy (ESEM) of macrophage and *C. albicans* co-culture after 3h of interaction.

2 Enrichment of ATP-binding proteins for the study of proteomic alteration in human macrophages after interacting with *C. albicans*

2.1 Quantitative proteomic analysis of macrophage proteins after interaction with *C. albicans*

A quantitative shotgun proteomic approach using SILAC and LC-MS/MS was used to study the changes in the abundance of macrophage proteins enriched after using the ActivX desthiobiotin ATP probes upon interaction with *C. albicans* cells during 3 h at a MOI of 1. Protein lysate was enriched in ATP-binding proteins and samples were analyzed by LC-MS/MS. Four biological replicates and two technical replicates of each were analyzed by MS. **Figure C1.3** represents the general workflow of the approach used.

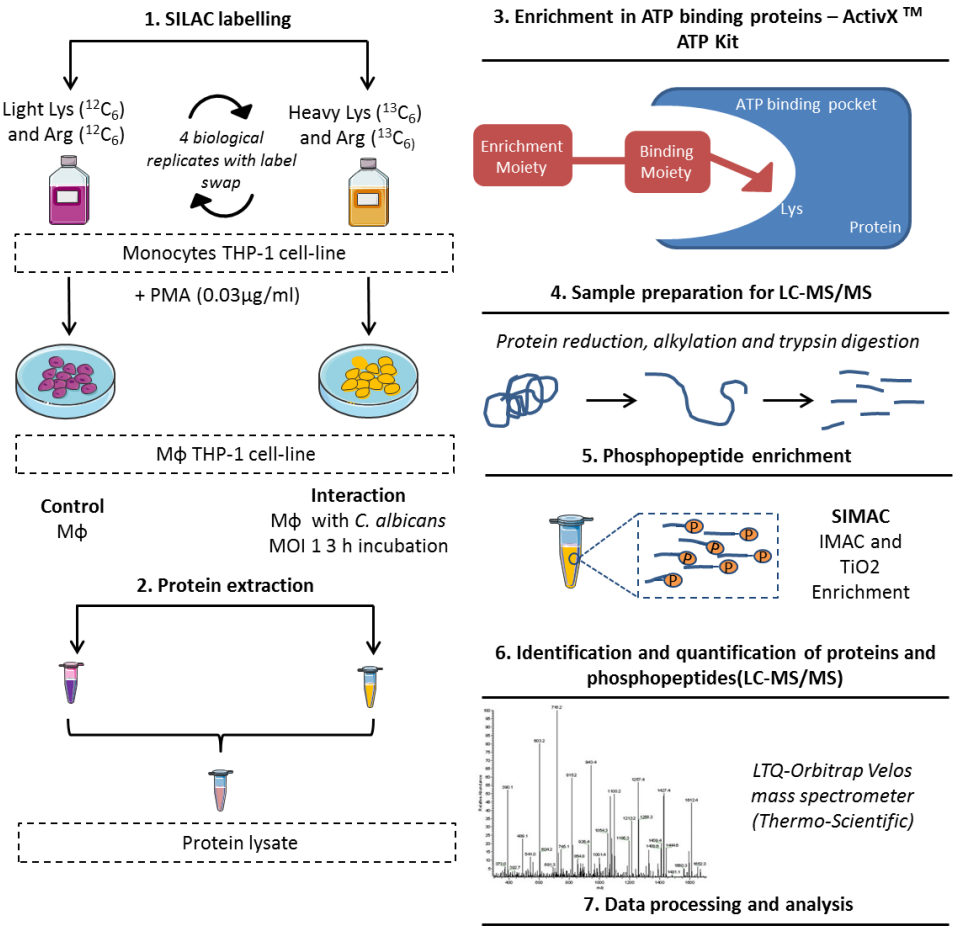

Figure C1.3 Experimental design for the analysis of the macrophage sub-proteome and phosphoproteome after ATP-binding enrichment. Four biological replicates of THP-1 monocytes were labelled with light and heavy stable isotope-containing media, producing proteins and peptides distinguishable by mass. After protein labelling monocytes, were differentiated by adding PMA and two conditions analyzed: Macrophages alone (Mϕ) and Mϕ with *C. albicans* at a MOI of 1 and during 3 h. Proteins were extracted and due to their previous labelling the protein lysate was mixed. Then, proteins were enriched using the ActivX™ ATP Kit. Proteins after the enrichment were analyzed by LC-MS/MS. Furthermore proteins were subjected to phosphopeptide enrichment and the resulting phosphopeptides were also analyzed by LC-MS/MS.

A total of 1043 proteins was identified, corresponding to 710, 664, 664 and 709 proteins in each replicate, respectively (**Supplementary Table C1.1).** A total of 547 non-redundant proteins was quantified in at least two biological replicates with a SD <0.3 (**Supplementary Table C1.2**). The molecular functions enriched on the 547 quantified proteins were mainly protein binding (271 proteins), nucleotide binding (203 proteins) and ATP binding (136 proteins). Furthermore, the total number of quantified proteins was enriched in 10 major biological processes, such as gene expression (87 proteins), cellular protein metabolic process (76 proteins), and translation (65 proteins). Regarding the cellular component, most of the proteins were located in cytoplasm (341 proteins), followed by nucleus (205 proteins), and mitochondria (105 proteins) (**Supplementary Figure C1.1**).

Macrophage proteins extracted using the ActivX desthiobiotin ATP probes showed a very homogeneous abundance ratio. After stratification of protein abundance ratios into quantiles according to their distribution upon interaction with *C. albicans*, we found that 4 and 9 proteins had the higher and lower extreme abundance ratios, whereas 18 and 28 proteins had the higher and lower outlier abundance ratios, respectively (**Supplementary Figure C1.2 and Table C1.1**).

Table C1.1 List of proteins differentially abundant 3 h after macrophage - *C. albicans* interaction. Proteins after ATP binding enrichment are ordered by ratio average inside each category.

UniProt Code[a]	Entry Names	Gene names	Protein Names[a]	Ratio[b]	SD[b]	N Replicates[c]
Proteins more abundant after macrophage interaction with *C. albicans*						
RNA processing						
O60812	HNRC1	HNRNPCL1	Heterogeneous nuclear ribonucleoprotein C-like 1	1.8	0.218	2
P14678	RSMB	SNRPB	Small nuclear ribonucleoprotein-associated proteins B and B'	1.5	0.045	3
Q99733	NP1L4	NAP1L4	Nucleosome assembly protein 1-like 4	1.4	0.169	2
Q01081	U2AF1	U2AF1	Splicing factor U2AF 35 kDa subunit	1.3	0.289	2
P09661	RU2A	SNRPA1	U2 small nuclear ribonucleoprotein A'	1.2	0.205	2
Q9NR30	DDX21	DDX21	Nucleolar RNA helicase 2	1.2	0.293	2
Structural components of ribosome						
P32969	RL9	RPL9	60S ribosomal protein L9	1.4	0.29	4
P62854	RS26	RPS26	40S ribosomal protein S26	1.3	0.166	2
P39023	RL3	RPL3	60S ribosomal protein L3	1.3	0.272	3
Oxidative stress						
P30044	PRDX5 [d]	PRDX5	Peroxiredoxin-5	1.3	0.171	2
Q6NUK1	SCMC1	SLC25A24	Calcium-binding mitochondrial carrier protein SCaMC-1	1.5	0.175	2
ATP production and transport						

O75964	ATP5L	ATP5L	ATP synthase subunit g	1.3	0.236	3
P05141	ADT2	SLC25A5	ADP/ATP translocase 2	1.2	0.227	4
Immune response and cell signalling						
P36507	MP2K2 [d]	MAP2K2	Dual specificity mitogen-activated protein kinase kinase 2	1.3	0.067	2
P43405	KSYK	SYK	Tyrosine-protein kinase SYK	1.2	0.187	2
Metabolism						
Q9NRN7	ADPPT	AASDHPPT	L-aminoadipate-semialdehyde dehydrogenase-phosphopantetheinyl transferase	1.4	0.075	3
Q8NBX0	SCPDL	SCCPDH	Saccharopine dehydrogenase-like oxidoreductase	1.3	0.066	2
Q9Y617	SERC	PSAT1	Phosphoserine aminotransferase	1.3	0.275	2
Others [e]						
B2RPK0	HGB1A	HMGB1P1	Putative high mobility group protein B1-like 1	1.3	0.251	3
P49589	SYCC	CARS	Cysteine--tRNA ligase	1.2	0.274	2
Q96QR8	PURB	PURB	Transcriptional activator protein Pur-beta	1.2	0.285	4
Q9Y6C9	MTCH2	MTCH2	Mitochondrial carrier homolog 2	1.2	0.237	4
Proteins less abundant after macrophage interaction with *C. albicans*						
Proteolysis and peptide degradation						
Q9UHL4	DPP2	DPP7	Dipeptidyl peptidase 2	0.8	0.213	3
P14780	MMP9	MMP9	Matrix metalloproteinase-9	0.8	0.22	3
P28838	AMPL	LAP3	Cytosol aminopeptidase	0.8	0.237	4
Q96KP4	CNDP2	CNDP2	Cytosolic non-specific dipeptidase	0.8	0.076	2
P09960	LKHA4	LTA4H	Leukotriene A-4 hydrolase	0.8	0.284	4
P09622	DLDH	DLD	Dihydrolipoyl dehydrogenase	0.8	0.163	2
Transport						
Q8N5M9	JAGN1	JAGN1	Protein jagunal homolog 1	0.8	0.074	2
P51149	RAB7A	RAB7A	Ras-related protein Rab-7a	0.8	0.223	2
P84085	ARF5	ARF5	ADP-ribosylation factor 5	0.8	0.162	3
Proteasome components and protein fate						
P62333	PRS10	PSMC6	26S protease regulatory subunit 10B	0.9	0.104	3
P28065	PSB9	PSMB9	Proteasome subunit beta type-9	0.8	0.276	2
O94874	UFL1	UFL1	E3 UFM1-protein ligase 1	0.8	0.281	3
P51572	BAP31	BCAP31	B-cell receptor-associated protein 31	0.8	0.127	2
Immune response and cell signalling						
Q13188	STK3	STK3	Serine/threonine-protein kinase 3	0.8	0.061	2
Q9Y2U5	M3K2	MAP3K2	Mitogen-activated protein kinase kinase kinase 2	0.8	0.2	3
P36873	PP1G	PPP1CC	Serine/threonine-protein phosphatase PP1-gamma catalytic subunit	0.8	0.238	2
P09914	IFIT1	IFIT1	Interferon-induced protein with tetratricopeptide repeats 1	0.8	0.238	4
Q9Y6K5	OAS3	OAS3	2'-5'-oligoadenylate synthase 3	0.8	0.233	4
Cytoskeleton components/interactors and regulators						

Q15019	SEPT2	SEPT2	Septin-2	0.8	0.003	2
P46940	IQGA1	IQGAP1	Ras GTPase-activating-like protein IQGAP1	0.8	0.168	3
P20700	LMNB1	LMNB1	Lamin-B1	0.7	0.101	3
O43707	ACTN4	ACTN4	Alpha-actinin-4	0.6	0.096	3
Q68CZ2	TENS3	TNS3	Tensin-3	0.1	0.137	2
Ion transport and uptake						
Q13303	KCAB2	KCNAB2	Voltage-gated potassium channel subunit beta-2	0.8	0.093	2
P27105	STOM	STOM	Erythrocyte band 7 integral membrane protein	0.8	0.253	4
P02786	TFR1	TFRC	Transferrin receptor protein 1	0.5	0.115	2
RNA processing						
Q9Y3I0	RTCB	RTCB	tRNA-splicing ligase RtcB homolog	0.8	0.087	2
P29692	EF1D	EEF1D	Elongation factor 1-delta	0.8	0.057	2
Q96SB4	SRPK1	SRPK1	SRSF protein kinase 1	0.7	0.249	2
O43865	SAHH2	AHCYL1	Adenosylhomocysteinase 2	0.7	0.274	2
Nucleoside triphosphates synthesis						
P15531	NDKA [d]	NME1	Nucleoside diphosphate kinase A	0.8	0.228	2
P48047	ATPO	ATP5O	ATP synthase subunit O	0.7	0.098	3
Others [e]						
Q9NSE4	SYIM	IARS2	Isoleucine--tRNA ligase	0.9	0.14	3
Q96IJ6	GMPPA	GMPPA	Mannose-1-phosphate guanyltransferase alpha	0.8	0.073	2
Q9NVJ2	ARL8B	ARL8B	ADP-ribosylation factor-like protein 8B	0.8	0.215	3
Q6S8J3	POTEE	POTEE	POTE ankyrin domain family member E	0.6	0.089	2
Q01432	AMPD3	AMPD3	AMP deaminase 3	0.5	0.278	4

[a] Protein name and Uniprot Code according to Uniprot Knowledge base.
[b] Average abundance ratio from macrophages + *C. albicans* versus control macrophages and respective inter-replicate standard deviation (SD) (cut-off in 0.3).
[c] Proteins present in at least two biological replicates were considered and with a standard deviation lower than 30%.
[d] Proteins from this study that were validate by Western blot or SRM.
[e] In this category were included proteins with unknown or putative function and proteins that were not possible to include in the others categories.

Out of these 59 differentially abundant proteins, 12 were annotated as ATP binding proteins. GO term enrichment analysis showed that after ATP binding protein enrichment, both more and less abundant macrophage proteins were related to the same molecular functions, such as protein binding and nucleotide binding. Furthermore, the more abundant proteins were associated with RNA binding or peroxiredoxin activities, while the less abundant proteins were related to ATP binding or peptidase activities (**Figure C1.4A**). The more abundant proteins were involved in gene expression and RNA metabolic process, whereas the less abundant proteins were associated with proteolysis, apoptotic processes and endocytosis, among others (**Figure C1.4B**). Both more and less abundant proteins were enriched in the cytosol and mitochondrion GO terms (**Figure C1.4C**).

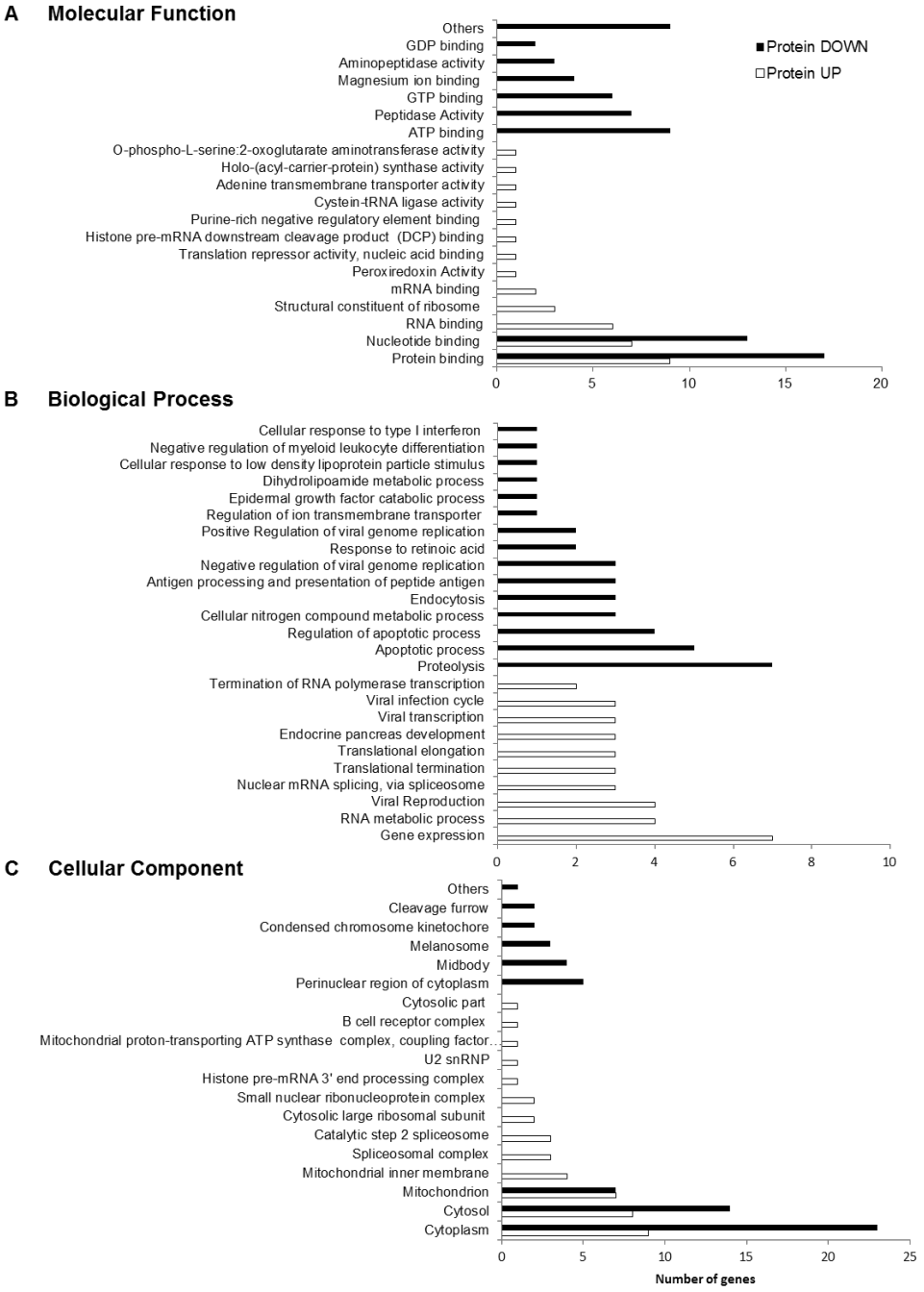

Figure C1.4 Gene Ontology (GO) analysis of the proteins considered differentially abundant after macrophage interaction with *C. albicans*. GO analysis of (A) molecular function, (B) biological process and (C) cellular component.

The more abundant mitochondrial proteins during interaction included SLC25A24 and PRDX5, which are important in the response to oxidative stress (Shiota *et al.*, 2008, Traba *et al.*, 2012).

The analysis of known and predicted protein-protein interactions was also performed with these 59 differentially abundant macrophage proteins upon *C. albicans* interaction (**Figure C1.5**).

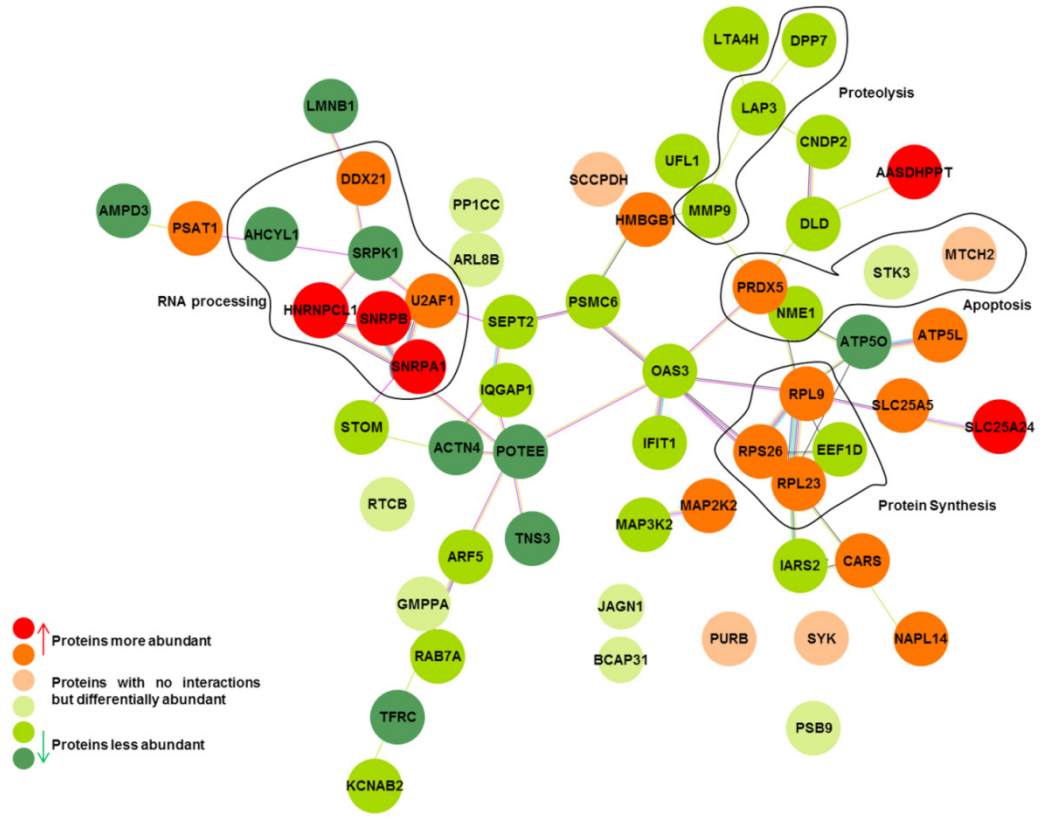

Figure C1.5 Predicted protein-protein interacting network using STRING (v10.0). Some biological processes (RNA splicing, protein synthesis, proteolysis, endocytic traffic and apoptosis) are highlighted in the network, signaling some of the interacting proteins that are involved in each process. The network protein-protein interaction *p*-value was 5.76×10^{-5}.

Forty-five protein-protein associations were found based on known or predicted interactions. Different clusters of protein associations were observed. A cluster enriched in proteins that were more abundant during *C. albicans* interaction was involved in protein synthesis. The group of proteins that were less abundant was very heterogeneous in molecular function GO terms and included a cluster of proteins involved in proteolysis and endocytic traffic. Other clusters containing both the more and less abundant proteins were related to RNA processing and apoptosis.

2.2 Analysis of the quantified proteins annotated as ATP-binding proteins

A comparison between all the proteins annotated as ATP binding in Uniprot database and the proteins quantified in this study was performed. From the 1482 proteins annotated with the ATP binding term, 137 were also present in the 547 proteins quantified in this study (**Supplementary Table C1.3**). This means that approximately 25% of all the quantified proteins were annotated as "ATP-binding". A list of all ATP binding proteins quantified and grouped by protein family is represented in **Table C1. 2**.

Table C1.2 List of ATP-binding Proteins quantified. Proteins are ordered alphabetically and by protein family.

Protein Family	UniProt Code[a]	Entry name	Gene name	Protein Name
AAA ATPase family	P17980	PRS6A	PSMC3	26S protease regulatory subunit 6A
	P35998	PRS7	PSMC2	26S protease regulatory subunit 7
	P43686	PRS6B	PSMC4	26S protease regulatory subunit 6B
	P46459	NSF	NSF	Vesicle-fusing ATPase
	P55072	TERA	VCP	Transitional endoplasmic reticulum ATPase
	P62191	PRS4	PSMC1	26S protease regulatory subunit 4
	P62195	PRS8	PSMC5	26S protease regulatory subunit 8
	P62333	PRS10	PSMC6	26S protease regulatory subunit 10B [b]
ABC transporter superfamily	Q03518	TAP1	TAP1	Antigen peptide transporter 1
	P61221	ABCE1	ABCE1	ATP-binding cassette sub-family E member 1
Actin family	P60709	ACTB	ACTB	Actin. cytoplasmic 1
	P68032	ACTC	ACTC1	Actin. alpha cardiac muscle 1
	P61163	ACTZ	ACTR1A	Alpha-centractin
	P61160	ARP2	ACTR2	Actin-related protein 2
	P61158	ARP3	ACTR3	Actin-related protein 3
Adenylate kinase family	P00568	KAD1	AK1	Adenylate kinase isoenzyme 1
	P30085	KCY	CMPK1	UMP-CMP kinase
ATPase alpha/beta chains family	P06576	ATPB	ATP5F1B	ATP synthase subunit beta
	P25705	ATPA	ATP5F1A	ATP synthase subunit alpha
	P38606	VATA	ATP6V1A	V-type proton ATPase catalytic subunit A
Class-I aminoacyl-tRNA synthetase family	P23381	SYWC	WARS	Tryptophan-tRNA ligase
	P26640	SYVC	VARS	Valine-tRNA ligase
	P47897	SYQ	QARS	Glutamine-tRNA ligase
	P49589	SYCC	CARS	Cysteine-tRNA ligase[c]
	P54136	SYRC	RARS	Arginine-tRNA ligase
	P54577	SYYC	YARS	Tyrosine-tRNA ligase
	Q9NSE4	SYIM	IARS2	Isoleucine-tRNA ligase[b]
	Q9P2J5	SYLC	LARS	Leucine-tRNA ligase
	P07814	SYEP	EPRS	Bifunctional glutamate/proline-tRNA ligase
	O43776	SYNC	NARS	Asparagine-tRNA ligase
	P12081	SYHC	HARS	Histidine-tRNA ligase
	P26639	SYTC	TARS	Threonine-tRNA ligase
	P41250	GARS	GARS	Glycine-tRNA ligase
	P49588	SYAC	AARS	Alanine-tRNA ligase
	Q9Y285	SYFA	FARSA	Phenylalanine-tRNA ligase alpha subunit
	P14868	SYDC	DARS	Aspartate-tRNA ligase
	P49591	SYSC	SARS	Serine-tRNA ligase
ClpA/ClpB family	Q9H078	CLPB	CLPB	Caseinolytic peptidase B protein homolog
	O14656	TOR1A	TOR1A	Torsin-1A

DEAD box helicase family		Q9NR30	DDX21	DDX21	Nucleolar RNA helicase 2 [c]
		O00571	DDX3X	DDX3X	ATP-dependent RNA helicase DDX3X
		P17844	DDX5	DDX5	Probable ATP-dependent RNA helicase DDX5
		Q08211	DHX9	DHX9	ATP-dependent RNA helicase A
		O43143	DHX15	DHX15	Pre-mRNA-splicing factor ATP-dependent RNA helicase DHX15
		Q13838	DX39B	DDX39B	Spliceosome RNA helicase DDX39B
		P38919	IF4A3	EIF4A3	Eukaryotic initiation factor 4A-III
		P60842	IF4A1	EIF4A1	Eukaryotic initiation factor 4A-I
		Q14240	IF4A2	EIF4A2	Eukaryotic initiation factor 4A-II
Heat shock protein 70 family		P11021	BIP	HSPA5	78 kDa glucose-regulated protein
		P11142	HSP7C	HSPA8	Heat shock cognate 71 kDa protein
		P34932	HSP74	HSPA4	Heat shock 70 kDa protein 4
		P38646	GRP75	HSPA9	Stress-70 protein
		Q92598	HS105	HSPH1	Heat shock protein 105 kDa
		Q9Y4L1	HYOU1	HYOU1	Hypoxia up-regulated protein 1
Heat shock protein 90 family		P07900	HS90A	HSP90AA1	Heat shock protein HSP 90-alpha
		P08238	HS90B	HSP90AB1	Heat shock protein HSP 90-beta
		P14625	ENPL	HSP90B1	Endoplasmin
		Q12931	TRAP1	TRAP1	Heat shock protein 75 kDa
		Q58FF6	H90B4	HSP90AB4P	Putative heat shock protein HSP 90-beta 4
Phosphofructokinase type A (PFKA) family		P17858	PFKAL	PFKL	ATP-dependent 6-phosphofructokinase
		Q01813	PFKAP	PFKP	ATP-dependent 6-phosphofructokinase
Protein kinase superfamily	AGC Ser/Thr protein kinase family	P17612	KAPCA	PRKACA	cAMP-dependent protein kinase catalytic subunit alpha
		Q15418	KS6A1	RPS6KA1	Ribosomal protein S6 kinase alpha-1
	BUD32 family	Q96S44	PRPK	TP53RK	TP53-regulating kinase
	CMGC Ser/Thr protein kinase family	Q96SB4	SRPK1	SRPK1	SRSF protein kinase 1 [b]
		P49841	GSK3B	GSK3B	Glycogen synthase kinase-3 beta
		P28482	MK01	MAPK1	Mitogen-activated protein kinase 1
		Q16539	MK14	MAPK14	Mitogen-activated protein kinase 14
	Ser/Thr protein kinase family	P19784	CSK22	CSNK2A2	Casein kinase II subunit alpha'
		P68400	CSK21	CSNK2A1	Casein kinase II subunit alpha
		P19525	E2AK2	EIF2AK2	Interferon-induced. double-stranded RNA-activated protein kinase
	STE Ser/Thr protein kinase family	Q9Y2U5	M3K2	MAP3K2	Mitogen-activated protein kinase kinase kinase 2 [b]
		P36507	MP2K2	MAP2K2	Dual specificity mitogen-activated protein kinase kinase 2 [c]
		O94804	STK10	STK10	Serine/threonine-protein kinase 10
		O95747	OXSR1	OXSR1	Serine/threonine-protein kinase OSR1
		Q13043	STK4	STK4	Serine/threonine-protein kinase 4
		Q13177	PAK2	PAK2	Serine/threonine-protein kinase PAK 2
		Q13188	STK3	STK3	Serine/threonine-protein kinase 3 [b]
		Q9H2G2	SLK	SLK	STE20-like serine/threonine-protein kinase
		Q9H2K8	TAOK3	TAOK3	Serine/threonine-protein kinase TAO3
		Q9Y6E0	STK24	STK24	Serine/threonine-protein kinase 24
	TKL Ser/Thr protein kinase	Q13418	ILK	ILK	Integrin-linked protein kinase
		Q9NWZ3	IRAK4	IRAK4	Interleukin-1 receptor-associated kinase 4

	family				
	Tyr protein kinase family. CSK subfamily	P41240	CSK	CSK	Tyrosine-protein kinase CSK
		P43405	KSYK	SYK	Tyrosine-protein kinase SYK [c]
Ribose-phosphate pyrophosphokinase family		P11908	PRPS2	PRPS2	Ribose-phosphate pyrophosphokinase 2
		P60891	PRPS1	PRPS1	Ribose-phosphate pyrophosphokinase 1
RtcB family		Q9Y3I0	RTCB	RTCB	tRNA-splicing ligase RtcB homolog [b]
		Q9Y230	RUVB2	RUVBL2	RuvB-like 2
		Q9Y265	RUVB1	RUVBL1	RuvB-like 1
Succinate/malate CoA ligase beta subunit family		Q9P2R7	SUCB1	SUCLA2	Succinate-CoA ligase
		Q96I99	SUCB2	SUCLG2	Succinate-CoA ligase
		P53396	ACLY	ACLY	ATP-citrate synthase
TCP-1 chaperonin family		P17987	TCPA	TCP1	T-complex protein 1 subunit alpha
		P40227	TCPZ	CCT6A	T-complex protein 1 subunit zeta
		P48643	TCPE	CCT5	T-complex protein 1 subunit epsilon
		P49368	TCPG	CCT3	T-complex protein 1 subunit gamma
		P50990	TCPQ	CCT8	T-complex protein 1 subunit theta
		P50991	TCPD	CCT4	T-complex protein 1 subunit delta
		P78371	TCPB	CCT2	T-complex protein 1 subunit beta
		Q99832	TCPH	CCT7	T-complex protein 1 subunit eta
Ubiquitin-activating E1 family		A0AVT1	UBA6	UBA6	Ubiquitin-like modifier-activating enzyme 6
		P22314	UBA1	UBA1	Ubiquitin-like modifier-activating enzyme 1
		Q9UBT2	SAE2	UBA2	SUMO-activating enzyme subunit 2
		Q9GZZ9	UBA5	UBA5	Ubiquitin-like modifier-activating enzyme 5
		P61088	UBE2N	UBE2N	Ubiquitin-conjugating enzyme E2 N
Proteins without Protein Family assigned		P05165	PCCA	PCCA	Propionyl-CoA carboxylase alpha chain
		P48426	PI42A	PIP4K2A	Phosphatidylinositol 5-phosphate 4-kinase type-2 alpha
		P49915	GUAA	GMPS	GMP synthase
		Q02790	FKBP4	FKBP4	Peptidyl-prolyl cis-trans isomerase FKBP4
		Q12905	ILF2	ILF2	Interleukin enhancer-binding factor 2
		Q14166	TTL12	TTLL12	Tubulin--tyrosine ligase-like protein 12
		Q9UHD1	CHRD1	CHORDC1	Cysteine and histidine-rich domain-containing protein 1
Other ATP-binding Proteins		Q9Y6K5	OAS3	OAS3	2'-5'-oligoadenylate synthase 3 [b]
		P00966	ASSY	ASS1	Argininosuccinate synthase
		O43681	ASNA	ASNA1	ATPase ASNA1
		O60488	ACSL4	ACSL4	Long-chain-fatty-acid--CoA ligase 4
		P16615	AT2A2	ATP2A2	Sarcoplasmic/endoplasmic reticulum calcium ATPase 2
		P10809	CH60	HSPD1	60 kDa heat shock protein
		P17812	PYRG1	CTPS1	CTP synthase 1
		Q13057	COASY	COASY	Bifunctional coenzyme A synthase
		P22102	PUR2	GART	Trifunctional purine biosynthetic protein adenosine-3
		P00367	DHE3	GLUD1	Glutamate dehydrogenase 1
		P54886	P5CS	ALDH18A1	Delta-1-pyrroline-5-carboxylate synthase
		P19367	HXK1	HK1	Hexokinase-1
		P12956	XRCC6	XRCC6	X-ray repair cross-complementing protein 6
		P13010	XRCC5	XRCC5	X-ray repair cross-complementing protein 5
		P15531	NDKA	NME1	Nucleoside diphosphate kinase A [b]

	P36776	LONM	LONP1	Lon protease homolog
	Q9NSD9	SYFB	FARSB	Phenylalanine--tRNA ligase beta subunit
	P00558	PGK1	PGK1	Phosphoglycerate kinase 1
	P14618	KPYM	PKM	Pyruvate kinase PKM
	P22234	PUR6	PAICS	Multifunctional protein ADE2
	P11586	C1TC	MTHFD1	C-1-tetrahydrofolate synthase
	O43615	TIM44	TIMM44	Mitochondrial import inner membrane translocase subunit TIM44
	Q12965	MYO1E	MYO1E	Unconventional myosin-Ie
	Q9NTK5	OLA1	OLA1	Obg-like ATPase 1

[a] Uniprot Code according to Uniprot Knowledge base. Proteins only with a standard deviation lower than 30% and quantified in at least 2 biological replicates.
[b] Proteins annotated as ATP-binding proteins in Uniprot database that were found in this study to be less abundant during macrophage interaction with *C. albicans*
[c] Proteins annotated as ATP-binding proteins in Uniprot database that were found in this study to be more abundant during macrophage interaction with *C. albicans*

Among them, 4 proteins (MAP2K2, KSYK, DDX21 and SYCC) were more abundant during the interaction, and 8 proteins (PRS10, SYIM, STK3, OAS3, MAP3K2, RTCB, NDKA and SRPK1) were less abundant after the interaction. In this group of differentially abundant ATP-binding proteins, 6 were kinases (MAP2K2, SYK, STK3, MAP3K2, NDKA and SRPK1). The group with more quantified proteins was the protein kinase superfamily, with 24 quantified protein kinases (Table C1.2). GO analysis on molecular function showed an over-representation of terms related to ATP binding (like nucleotide binding), ATPase activity and kinase activity (Supplementary Table C1.3). Regarding the GO analysis on cellular component, in addition to cytosol that was already expected, an over-representation on terms related to chaperonin-containing T complex, proteasome, mitochondria, extracellular vesicles was also observed. Concerning the GO analysis on the biological processes, there was an over-representation in terms such as regulation of protein localization to Cajal bodies (which are implicated in mRNA processing) (Wang *et al.*, 2016), tRNA aminoacylation for protein translation, protein folding, regulation of protein stability, and positive regulation of cellular biosynthetic process. There was also an over-representation on processes related to immune response, such as regulation of cellular response to stress and activation of innate immune response.

2.3 Phosphoproteomic analysis of macrophage proteins after interaction with *C. albicans*

The fraction enriched in ATP-binding proteins from all 4 biological replicates was further subjected to phosphopeptide enrichment. A total of 85 phosphopeptides were quantified in at least two biological replicates and with a SD < 0.3 and are listed in Supplementary Table C1.4. In some cases, two or more phosphopeptides were quantified for the same phosphorylation site (phosphosite). Therefore, 85 phosphopeptides corresponding to 70 phosphosites and 56 proteins were quantified. According to the phosphorylation probabilities given by the Proteome Discoverer

software, the phosphosites were considered ambiguous or assigned to a specific amino acid (serine, threonine and tyrosine). Sixty-one percent of the phosphosites were phosphorylated in a serine and 33% were ambiguous, whereas phosphothreonine and phosphotyrosine were less represented (3% each). Out of the 56 phosphoproteins, 25 (approximately 36%) are from proteins that were as ATP-binding proteins in UNIPROT database and 12 (21.4%) as kinases. Out of the 85 quantified phosphopeptides, 5 phosphopeptides (each one belonging to a single protein) were differentially abundant during macrophage interaction with *C. albicans* (**Table C1.3 and Supplementary Figure C1.3**). From this, 2 phosphopeptides belonging to PRKAA1 and CLN6 were more abundant during interaction, whereas 3 phosphopeptides belonging to PI4K2A, SRC and PRKCD were less abundant. Their mass spectra are shown in **Supplementary Figure C1.4**.

Table C1.3 List of phosphopeptides differentially abundant, from proteins after ATP binding enrichment, after 3 h of macrophage - *C. albicans* interaction.

UniProt Code [a]	Gene names	Protein names [a]	Phosphopeptide	Phosphosite [b]	Ratio [c]	SD [c]
Q13131	PRKAA1	5'-AMP-activated protein kinase catalytic subunit alpha-1	SGSVSNYR	ambiguous	1.58	0.22
Q9NWW5	CLN6	Ceroid-lipofuscinosis neuronal protein 6	HGs*VSADEAAR[d]	Ser31	1.40	0.29
Q9BTU6	PI4K2A	Phosphatidylinositol 4-kinase type 2-alpha	SSSESYTQSFQSr	ambiguous	0.70	0.22
P12931	SRC	Proto-oncogene tyrosine-protein kinase Src	LIEDNEy*TAR	Tyr419	0.69	0.22
Q05655	PRKCD	Protein kinase C delta type	SDSASSEPVGIYQGFEK	ambiguous	0.57	0.06

[a] Protein name and Uniprot Code according to Uniprot Knowledge base.
[b] Phosphosites were considered ambiguous in case PhosphoRS algorithm assigned a localization probability lower than 75% or if it was assigned in distinct sites in different biological replicates.
[c] Average abundance ratio from macrophages + *C. albicans* versus control macrophages and respective inter-replicate standard deviation (cut-off in 0.3). Only phosphopeptides with a standard deviation lower than 30% and quantified in at least 2 biological replicates.
[d] Asterisk indicates the phosphorylation site and the corresponding amino acid is in lower case

2.4 Protein validation

To confirm the quantitative MS data, Western blot analysis using antibodies to MAP2K2, PRDX5 and ERK1/2, and SRM of NDKA were performed. There was a significant increase in MAP2K2 and PRDX5 abundance during macrophage interaction with *C. albicans* cells in line with MS data (**Figures C1.6A and B**). Because MAP2K2 is a kinase that acts upstream ERK1/ERK2 kinases and is important for several cellular processes (Arthur & Ley, 2013), we also validated this protein by Western blotting. No significant differences in ERK1/2 abundance upon interaction were detected, confirming our proteomic data (**Figure C1.6C**). Phosphorylation of ERK1/2 was also evaluated, but no increase in its phosphorylation was observed (**Supplementary Figure C1.5**). For

SRM validation, the correspondent isotopic labelled peptide was ordered, and a calibration curve was performed (see Supplementary Figure C1.6 and Supplementary Table C1.5). The quantification of this peptide confirmed the decrease in the amount of NDKA (Figure C1.6D and Supplementary Table C1.5).

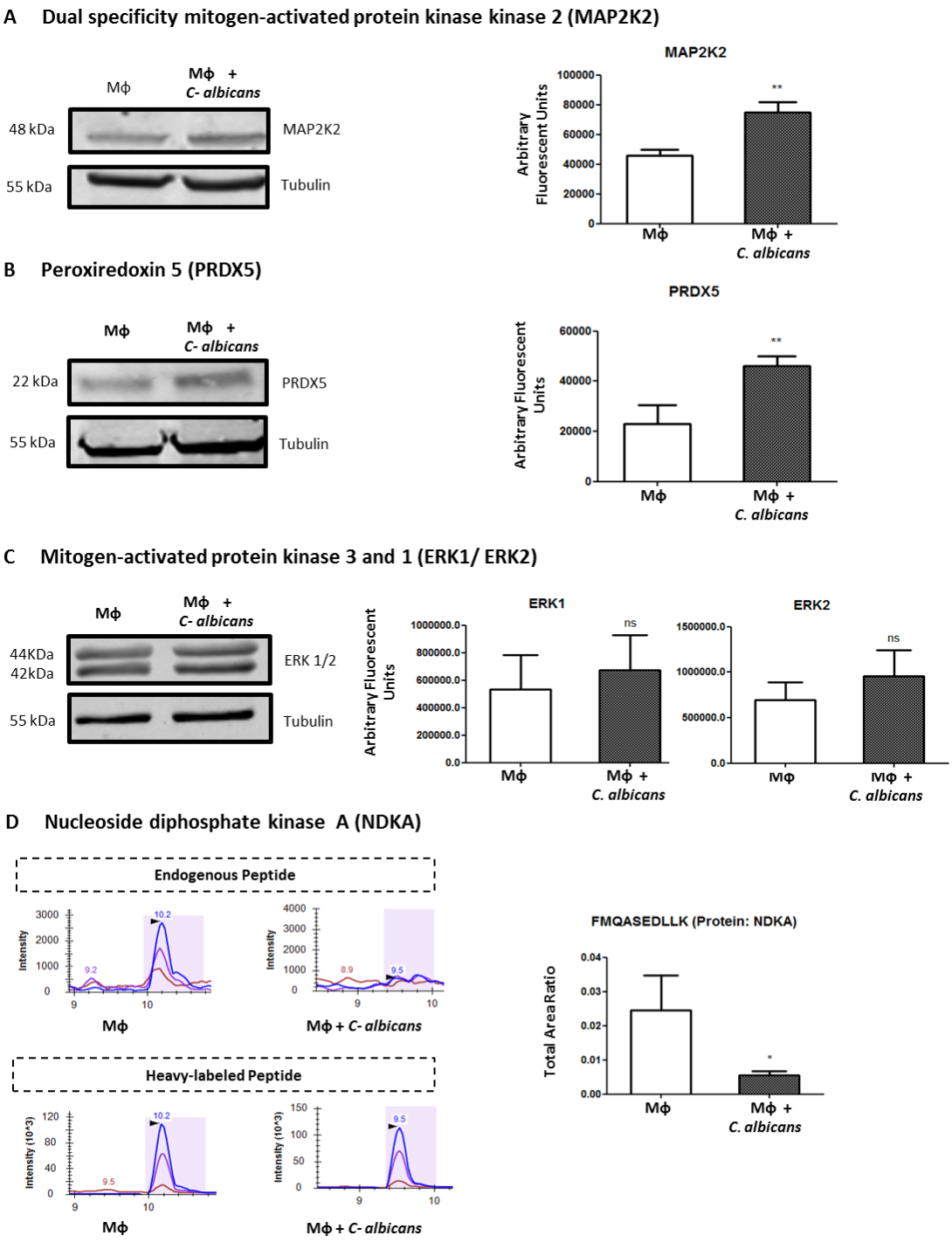

Figure C1.6 Proteomic results validation in both conditions: Mϕ (control) and Mϕ +*C. albicans* (MOI 1 and 3 h of incubation). Quantification of: (A) MAP2K2, (B) PRDX5 and (C) ERK1/2 by Western blotting and (D) NDKA by selected reaction monitoring.

2.5 Macrophage cell death mechanisms and pro-inflammatory response

Apoptosis was one of the biological processes enriched in the group of less abundant proteins. A closer look showed an increase in PRDX5, SLC25A24 and ADT2, which are anti-apoptotic proteins, and a decrease NDKA, ACTN4 and STK3, which are pro-apoptotic or anti-survival proteins (Lee *et al.*, 2001, Liu *et al.*, 2004, Yuan *et al.*, 2004, Jang *et al.*, 2008, Traba *et al.*, 2012, Lee *et al.*, 2018). In order to functionally validate these results, the apoptotic status of THP-1 macrophages after interaction with *C. albicans* was assayed by measuring caspase-3 activation by cleavage. Cells were incubated with staurosporine (as a positive control of apoptosis) and with *C. albicans* cells (at a MOI of 1 for 3 h). Activated caspase-3 was assayed by Western blotting with cell lysates and a band corresponding to the activated caspase 3 was observed in the positive control but not in macrophage-*C. albicans* interaction at 3 h (Figure C1.7A). As cleaved caspase 3 is a hallmark of apoptosis (Shalini *et al.*, 2015), this result suggests that apoptosis was not present in these conditions. In congruence with our results, it was previously described by others that *C. albicans* triggers pyroptosis during the first 6 to 8 h of interaction with macrophages (Uwamahoro *et al.*, 2014), we checked IL-1β secretion (which is secreted after caspase-1 activation) (Bergsbaken *et al.*, 2009). IL-1β was significantly more secreted in macrophages after interaction with *C. albicans* (Figure C1.7B). Furthermore, as pyroptosis is an inflammatory mechanism of cell death, (Bergsbaken *et al.*, 2009) other pro-inflammatory cytokines were evaluated. As depicted in Figures C1.7C and D, there was more secretion of pro-inflammatory cytokines IL-12p40 and TNF-α upon interaction with *C. albicans*.

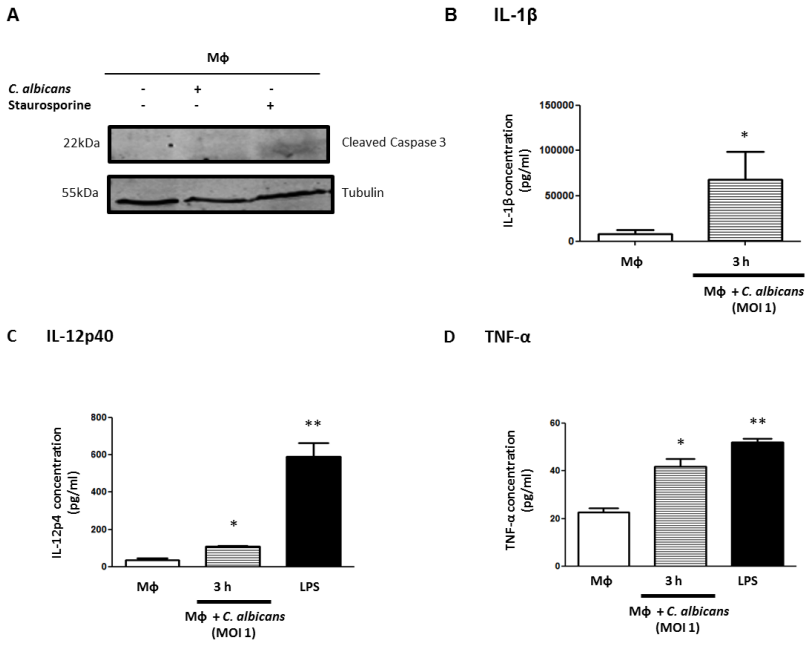

Figure C1.7 Cleaved caspase and cytokine secretion measurements. (A) Cleaved –caspase 3 was measured by Western blotting and cytokine secretion measured using Enzyme-Linked ImmunoSorbent Assay (ELISA): (B) Il-1β, (C) IL-12p40 and (D) TNF-α secretion in Mϕ (control) and Mϕ +*C. albicans* and after treatment with LPS (positive control).

To further predict potential upstream regulators implicated in the macrophage inflammatory response, the 59 differentially abundant proteins were also analyzed using the IPA software. Fifteen upstream regulators presented an activation z-score between -2 and 2 and a *p*-value of overlap < 0.05, which included CD3 complex, cytokines (oncostatin M (OSM), IL-5 and IL-6), proteins (KRAS; VEGFA; MAPK1; ESR1), miRNAs (miR-124-3p and miR-21), transcription regulators (MYCN, MYC and TP53), transmembrane receptor CD28 and rapamycin-insensitive companion of mTOR (RICTOR) (Figure C1.8A). The higher or lower z-score showed the higher probability of activation or inhibition of the upstream regulator, respectively. The IL-6 gene was predicted to be inhibited. This prompted us to assay the secretion of this cytokine at different time points (3 h, 6 h and 8 h) of THP-1 macrophage - *C. albicans* interaction. This cytokine was not secreted after interaction with yeast cells (Figure C1.8B), indicating that this gene may not be expressed under these conditions.

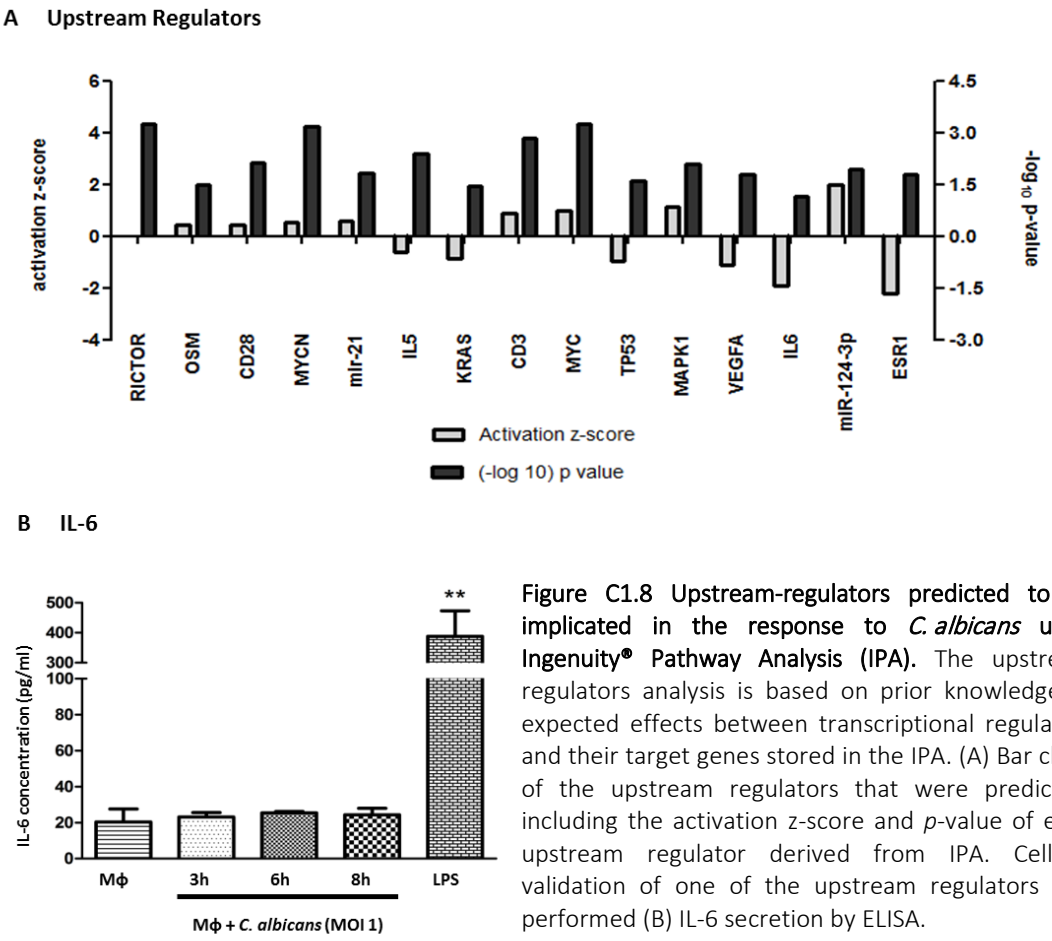

Figure C1.8 Upstream-regulators predicted to be implicated in the response to *C. albicans* using Ingenuity® Pathway Analysis (IPA). The upstream regulators analysis is based on prior knowledge of expected effects between transcriptional regulators and their target genes stored in the IPA. (A) Bar chart of the upstream regulators that were predicted, including the activation z-score and *p*-value of each upstream regulator derived from IPA. Cellular validation of one of the upstream regulators was performed (B) IL-6 secretion by ELISA.

Due to the recent evidences in the implication of miRNAs (miR) in the regulation of innate immune response (Tsitsiou & Lindsay, 2009), we also evaluated the possible activation miR-21 and miR-124 (two miRNAs that were predicted to be activated). The expression levels of miR-21

and miR-124 were evaluated together with miR-146 and miR-155 (which are activated after treatment with LPS in THP-1 cells and also after interaction with heat inactivated *C. albicans* cells (Taganov *et al.*, 2006, Monk *et al.*, 2010, Agustinho *et al.*, 2016)). MiR-21 and miR-124 were slightly, but not statistically significant, activated after treatment with LPS, and showed no significant activation in response to *C. albicans* (Figures C1.9A and B, respectively). Regarding miR-146 and miR-155, they were activated in response to LPS (Figures C1.9C and D, respectively), but also no significant activation in response to live *C. albicans* cells after 3 h and 6 h of interaction was observed.

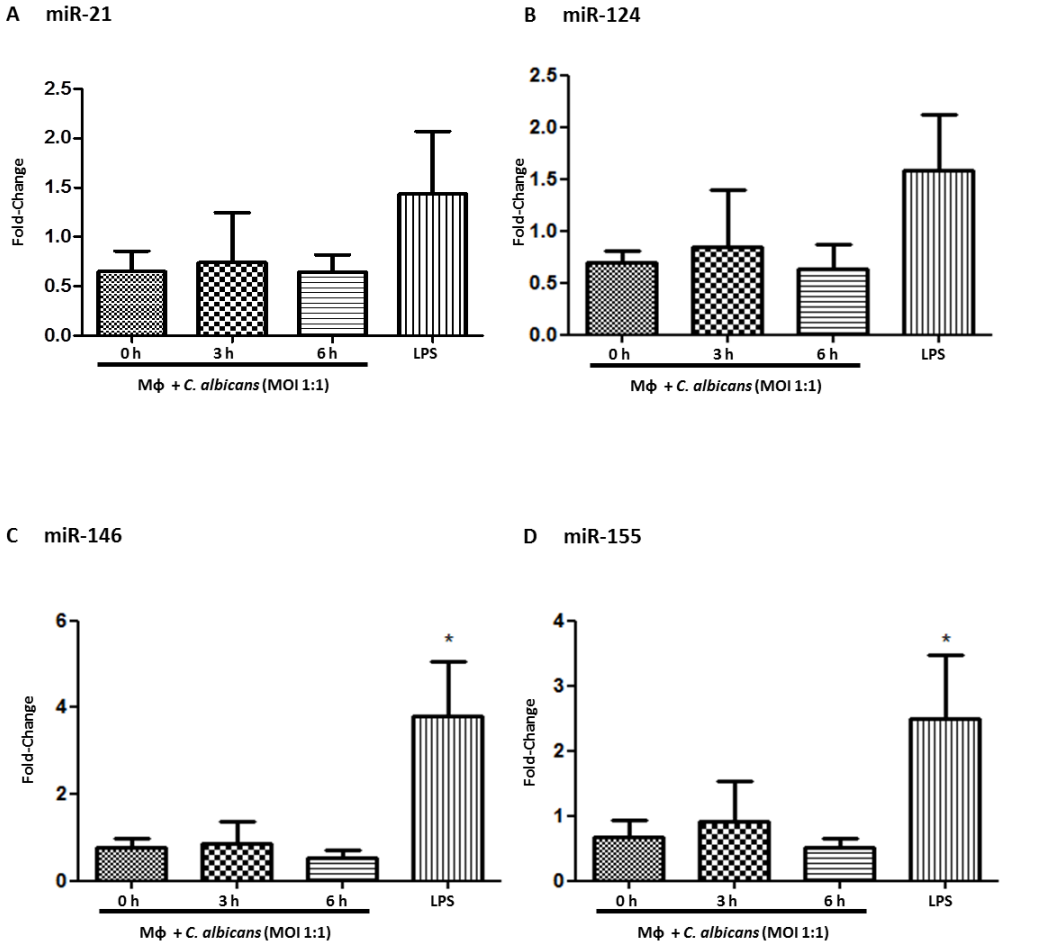

Figure C1.9 Expression levels of miRNAs in THP-1 macrophages after interaction with *C. albicans* cells. Expression levels of (A) miR-21 and (B) mir-124 that were predicted by the IPA and (c) miR-146 and (D) miR-155 that were known to be activated after treatment with LPS and were used as controls.

3 Global proteomic and phosphoproteomic analysis of macrophage after interaction with *C. albicans*

3.1 Quantitative proteomics analysis of macrophage proteins after interaction with *C. albicans*

In order to obtain a global view of the macrophage proteomic and phosphoproteomic changes after interacting with *C. albicans* we carried out a TMT based shotgun approach to analyze human

THP-1 macrophage cytoplasmic extracts in three different conditions. Besides microbes, macrophages also engulf other particulates and eliminate apoptotic cells. In order to clarify if the proteomic differences observed after macrophage interaction with *C. albicans* were attributable to the general process of phagocytosis or specifically to this fungus, we compared macrophages control; macrophages with latex beads and macrophages with *C. albicans*. Both latex beads and *C. albicans* were incubated with the macrophages for 3 h, according to the results obtained during the set-up experiments, explained previously in this Chapter.

As cytokines are potent signaling molecules that orchestrate a variety of inflammation processes they can be used to know the macrophage state of activation (Arango Duque & Descoteaux, 2014). We look into the secretion of IL-1β, a pro-inflammatory cytokine as a marker of inflammasome activation (**Figure C1.10**). The secretion of this cytokine is slightly higher, not statistically significant, when comparing macrophages after interaction with beads with macrophages control and statistically significant higher when comparing macrophages after interaction with *C. albicans* with control. This reflects a higher state of activation of the macrophage after interacting with the fungi then with the latex beads.

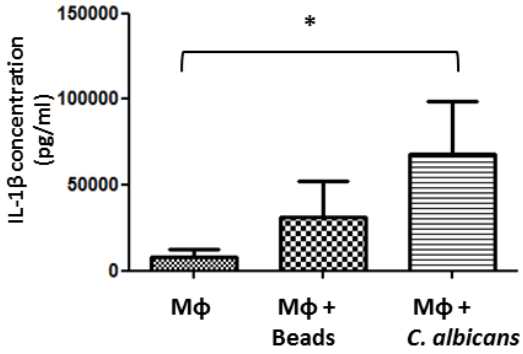

Figure C1.10 IL-1β cytokine measurements. IL-1β was measured by ELISA in the supernatant of the samples (Mϕ; Mϕ with beads and Mϕ with *C. albicans*) used for the global proteomic and phosphoproteomic approaches.

The overall workflow followed here is schematically represented in **Figure C1.11**, where TMT-11plex was used for the quantitative proteomic and phosphoproteomic analysis of 4 biological replicates of macrophages control, 3 biological replicates of macrophages with beads and 4 biological replicates of macrophages after interaction with *C. albicans*.

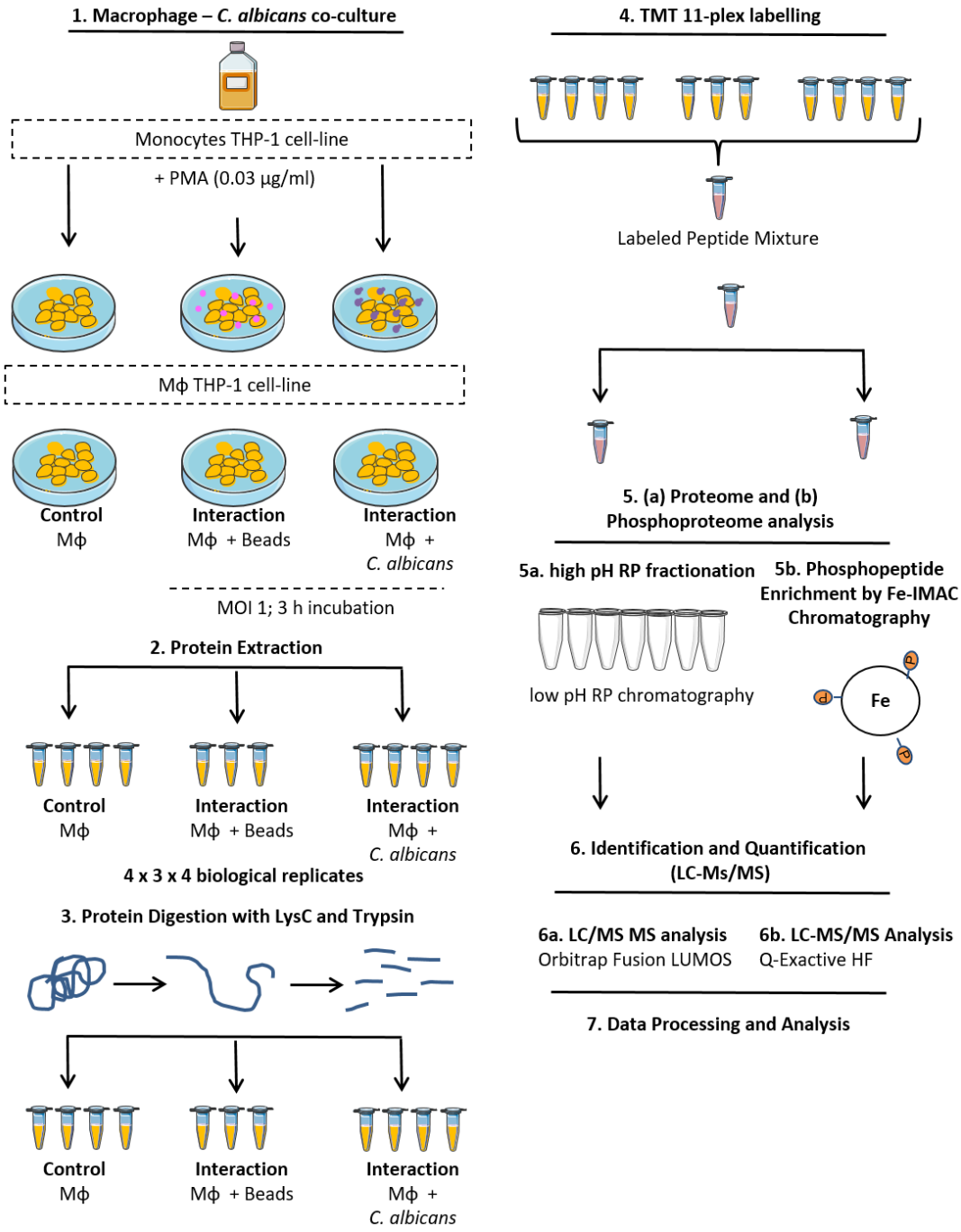

Figure C1.11 Experimental design for the analysis of the global proteome and phosphoproteome of macrophages after interaction with beads and *C. albicans*. Monocytes from the THP-1 cell line were differentiated by adding PMA and three conditions were compared macrophages alone (Mϕ); Mϕ with beads and Mϕ with *C. albicans* at a MOI of 1 and during 3 h. After interaction, cell were harvested, proteins extracted and digested with lysC and trypsin. Peptides were then labelled with TMT-11-plex and analyzed by LC-MS/MS. Part of the sample was subjected to enrichment in phosphopeptides using Fe-IMAC. Enriched phosphopeptides were analyzed by LC-MS/MS.

From this, 6166 human proteins were quantified (**Supplementary Table C1.6**). Abundances and phosphorylation were analyzed for differential expression using limma software package and no

statistically significant differences were found in macrophages alone and macrophages after interaction with beads and also macrophages after interaction with beads and with *C. albicans*. These results are congruent with IL-1β measurements, where also no statistically significant activation was observed between these conditions. Nevertheless, we observed that the interaction of the fungi with the macrophage has led to the differential abundance of proteins in the macrophage whereas beads could not. This indicated that the differences we observed are due to *C. albicans* and not only due to the phagocytosis of an inert particle. In this way, the condition of macrophages after interaction with beads was removed from the analysis. As now we had the same number of biological replicates in both conditions we used another statistical method, in Perseus software, for paired analysis of the quantitative data of the samples.

3.2 Differentially abundant proteins after macrophage interaction with *C. albicans*

As observed in the proteomic analysis of the proteome after ATP-binding proteins enrichment, also here the abundance ratios were very homogeneous. In order to look to differentially abundant proteins, we applied a paired Student's t-test (p-value < 0.05) and 89 proteins were found to have statistically significant differences comparing macrophages alone with macrophages after interaction with *C. albicans*. From these, 27 proteins were more abundant (Log_2 ratio > 0) and 62 were less abundant (Log_2 ratio <0) during interaction (**Table C1.4**).

Table C1.4 Proteins differentially abundant after macrophage interaction with *C. albicans* (3 h and MOI 1)

UniProt Code[a,b]	Entry Name	Gene Name	Protein Name[b]	*p*-value [c]	*q*-value	Log_2 (ratio)[d]
Proteins more abundant during macrophage interaction with *C. albicans*						
Cytoskeleton components/interactors and regulators						
Q8N9B5	JMY	JMY	Junction-mediating and -regulatory protein	0.0014	0.05	0.48
Q14244	MAP7	MAP7	Ensconsin	0.0004	0.04	0.35
Q13442	HAP28	PDAP1	28 kDa heat- and acid-stable phosphoprotein	0.0000	0.00	0.23
O94927	HAUS5	HAUS5	HAUS augmin-like complex subunit 5	0.0003	0.05	0.07
Immune response and/or cell signaling						
O14907	TX1B3	TAX1BP3	Tax1-binding protein 3	0.0017	0.04	0.23
Q96B36	AKTS1	AKT1S1	Proline-rich AKT1 substrate 1	0.0021	0.05	0.23
Q96C90	PP14B	PPP1R14B	Protein phosphatase 1 regulatory subunit 14B	0.0004	0.03	0.19
Q16584	M3K11	MAP3K11	Mitogen-activated protein kinase kinase kinase 11	0.0010	0.05	0.16
Q9H1I8	ASCC2	ASCC2	Activating signal cointegrator 1 complex subunit 2	0.0021	0.05	0.09
Q9UBF8	PI4KB	PI4KB	Phosphatidylinositol 4-kinase beta	0.0025	0.05	0.07
P48736	PK3CG	PIK3CG	Phosphatidylinositol 4,5-bisphosphate 3-	0.0002	0.05	0.05

			kinase catalytic subunit gamma isoform			
RNA binding						
Q96DE0	NUD16	NUDT16	U8 snoRNA-decapping enzyme	0.0018	0.04	0.22
Q5T160	SYRM	RARS2	Probable arginine--tRNA ligase, mitochondrial	0.0008	0.03	0.09
Transport						
P50238	CRIP1	CRIP1	Cysteine-rich protein 1	0.0006	0.02	0.71
Q9H0F7	ARL6	ARL6	ADP-ribosylation factor-like protein 6	0.0014	0.05	0.21
Q4J6C6	PPCEL	PREPL	Prolyl endopeptidase-like	0.0011	0.04	0.17
O43615	TIM44	TIMM44	Mitochondrial import inner membrane translocase subunit TIM44	0.0014	0.05	0.06
Metabolism						
Q9BQC3	DPH2	DPH2	2-(3-amino-3-carboxypropyl) histidine synthase subunit 2	0.0007	0.03	0.14
Q9HD40	SPCS	SEPSECS	O-phosphoseryl-tRNA(Sec) selenium transferase	0.0017	0.04	0.14
O94925	GLSK	GLS	Glutaminase kidney isoform, mitochondrial	0.0006	0.02	0.10
P41227	NAA10	NAA10	N-alpha-acetyltransferase 10	0.0014	0.05	0.06
Proteasome components and protein fate						
Q96PM5	ZN363	RCHY1	RING finger and CHY zinc finger domain-containing protein 1	0.0014	0.05	0.09
DNA repair						
P07992	ERCC1	ERCC1	DNA excision repair protein ERCC-1	0.0023	0.05	0.07
Others						
Q6P4F2	FDX2	FDX2	Ferredoxin-2, mitochondrial	0.0006	0.03	0.25
Q8N6R0	EFNMT	EEF1AKNMT	Methyltransferase-like protein 13	0.0009	0.05	0.15
Q9Y6E2	BZW2	BZW2	Basic leucine zipper and W2 domain-containing protein 2	0.0013	0.04	0.10
Q9BVQ7	SPA5L	SPATA5L1	Spermatogenesis-associated protein 5-like protein 1	0.0000	0.00	0.05
Proteins less abundant during macrophage interaction with *C. albicans*						
RNA processing						
O43809	CPSF5	NUDT21	Cleavage and polyadenylation specificity factor subunit 5	0.0019	0.04	-0.39
P51991	ROA3	HNRNPA3	Heterogeneous nuclear ribonucleoprotein A3	0.0011	0.04	-0.30
P23246	SFPQ	SFPQ	Splicing factor, proline- and glutamine-rich	0.0010	0.04	-0.18
Q12906	ILF3	ILF3	Interleukin enhancer-binding factor 3	0.0004	0.04	-0.17
Q08211	DHX9	DHX9	ATP-dependent RNA helicase A	0.0018	0.04	-0.16
O43172	PRP4	PRPF4	U4/U6 small nuclear ribonucleoprotein Prp4	0.0002	0.08	-0.15
Q9NV88	INT9	INTS9	Integrator complex subunit 9	0.0009	0.05	-0.15
O75533	SF3B1	SF3B1	Splicing factor 3B subunit 1	0.0015	0.05	-0.14
Q16630	CPSF6	CPSF6	Cleavage and polyadenylation specificity factor subunit 6	0.0020	0.05	-0.14
Q15459	SF3A1	SF3A1	Splicing factor 3A subunit 1	0.0003	0.04	-0.14
Q9BUQ8	DDX23	DDX23	Probable ATP-dependent RNA helicase DDX23	0.0008	0.03	-0.14
Q13769	THOC5	THOC5	THO complex subunit 5 homolog	0.0013	0.05	-0.13
Q13247	SRSF6	SRSF6	Serine/arginine-rich splicing factor 6	0.0024	0.05	-0.12
O75643	U520	SNRNP200	U5 small nuclear ribonucleoprotein 200	0.0019	0.04	-0.12

			kDa helicase			
Q7L014	DDX46	DDX46	Probable ATP-dependent RNA helicase DDX46	0.0007	0.03	-0.12
Q15393	SF3B3	SF3B3	Splicing factor 3B subunit 3	0.0011	0.04	-0.11
Q9Y6V7	DDX49	DDX49	Probable ATP-dependent RNA helicase DDX49	0.0005	0.03	-0.10
Q92945	FUBP2	KHSRP	Far upstream element-binding protein 2	0.0002	0.06	-0.09
Q69YN4	VIR	VIRMA	Protein virilizer homolog	0.0023	0.05	-0.09
Q96GQ7	DDX27	DDX27	Probable ATP-dependent RNA helicase DDX27	0.0003	0.05	-0.08
Cytoskeleton components/interactors and regulators						
P42167	LAP2B	TMPO	Lamina-associated polypeptide 2	0.0011	0.04	-0.22
Q6ZMZ3	SYNE3	SYNE3	Nesprin-3	0.0020	0.05	-0.19
P20700	LMNB1	LMNB1	Lamin-B1	0.0007	0.03	-0.18
P42166	LAP2A	TMPO	Lamina-associated polypeptide 2, isoform alpha	0.0007	0.03	-0.11
P50281	MMP14	MMP14	Matrix metalloproteinase-14	0.0024	0.05	-0.10
P84095	RHOG	RHOG	Rho-related GTP-binding protein RhoG	0.0017	0.04	-0.09
Q9UL63	MKLN1	MKLN1	Muskelin	0.0002	0.07	-0.06
Transport						
Q96HR9	REEP6	REEP6	Receptor expression-enhancing protein 6	0.0022	0.05	-0.19
P12270	TPR	TPR	Nucleoprotein TPR	0.0010	0.04	-0.17
Q13423	NNTM	NNT	NAD(P) transhydrogenase, mitochondrial	0.0015	0.05	-0.15
Q9BW27	NUP85	NUP85	Nuclear pore complex protein Nup85	0.0005	0.03	-0.13
O60830	TI17B	TIMM17B	Mitochondrial import inner membrane translocase subunit Tim17-B	0.0015	0.05	-0.13
Structural Components of ribosome						
Q13601	KRR1	KRR1	KRR1 small subunit processome component homolog	0.0014	0.05	-0.18
Q13428	TCOF	TCOF1	Treacle protein	0.0010	0.05	-0.12
Q9BV38	WDR18	WDR18	WD repeat-containing protein 18	0.0016	0.04	-0.11
P62899	RL31	RPL31	60S ribosomal protein L31	0.0021	0.05	-0.10
DNA binding/ processing and nucleosome						
O94776	MTA2	MTA2	Metastasis-associated protein MTA2	0.0005	0.03	-0.18
Q86YP4	P66A	GATAD2A	Transcriptional repressor p66-alpha	0.0003	0.04	-0.15
P12956	XRCC6	XRCC6	X-ray repair cross-complementing protein 6	0.0001	0.05	-0.16
P11387	TOP1	TOP1	DNA topoisomerase 1	0.0021	0.05	-0.15
Q9Y5B9	SP16H	SUPT16H	FACT complex subunit SPT16	0.0017	0.04	-0.13
Q9GZS1	RPA49	POLR1E	DNA-directed RNA polymerase I subunit RPA49	0.0000	0.00	-0.12
Q8NFD5	ARI1B	ARID1B	AT-rich interactive domain-containing protein 1B	0.0024	0.05	-0.12
Q12824	SNF5	SMARCB1	SWI/SNF-related matrix-associated actin-dependent regulator of chromatin subfamily B member 1	0.0005	0.03	-0.12
A6NHR9	SMHD1	SMCHD1	Structural maintenance of chromosomes flexible hinge domain-containing protein 1	0.0023	0.05	-0.11
Q9H9Y6	RPA2	POLR1B	DNA-directed RNA polymerase I subunit RPA2	0.0009	0.05	-0.11
Q92769	HDAC2	HDAC2	Histone deacetylase 2	0.0007	0.03	-0.10
O96019	ACL6A	ACTL6A	Actin-like protein 6A	0.0010	0.05	-0.10
P30876	RPB2	POLR2B	DNA-directed RNA polymerase II subunit RPB2	0.0002	0.06	-0.07

Metabolism						
O15121	DEGS1	DEGS1	Sphingolipid delta (4)-desaturase DES1	0.0007	0.03	-0.15
P19440	GGT1	GGT1	Glutathione hydrolase 1 proenzyme	0.0000	0.00	-0.10
Immune response and cell signaling						
Q96QC0	PP1RA	PPP1R10	Serine/threonine-protein phosphatase 1 regulatory subunit 10	0.0011	0.04	-0.14
P12931	SRC	SRC	Proto-oncogene tyrosine-protein kinase Src	0.0025	0.05	-0.11
Lipid biosynthesis						
P33121	ACSL1	ACSL1	Long-chain-fatty-acid--CoA ligase 1	0.0006	0.02	-0.14
Proteasome components and protein fate						
P25788	PSA3	PSMA3	Proteasome subunit alpha type-3	0.0002	0.05	-0.12
DNA repair						
P29372	3MG	MPG	DNA-3-methyladenine glycosylase	0.0013	0.04	-0.07
Others						
P05556	ITB1	ITGB1	Integrin beta-1	0.0010	0.04	-0.16
Q9ULV3	CIZ1	CIZ1	Cip1-interacting zinc finger protein	0.0001	0.00	-0.14
P09958	FURIN	FURIN	Furin	0.0013	0.05	-0.12
P08754	GNAI3	GNAI3	Guanine nucleotide-binding protein G(k) subunit alpha	0.0023	0.05	-0.11
Q96JM3	CHAP1	CHAMP1	Chromosome alignment-maintaining phosphoprotein 1	0.0023	0.05	-0.09
Q96HR3	MED30	MED30	Mediator of RNA polymerase II transcription subunit 30	0.0005	0.03	-0.09

[a] Proteins are ordered by $\log_2$ (ratio) inside each category
[b] Uniprot code according to Uniprot Knowledge base.
[c] *P*-value calculated in Perseus software using permutation based FDR paired Student's T-test
[d] $\log_2$ of the abundance ratio from macrophage after interaction with *C. albicans* versus macrophage control

To access both the cellular component and the biological process of the differentially quantified proteins, GO analysis was performed using the FunRich tool. When analyzing the cellular components of the group of more abundant proteins, we observe an enrichment in proteins from mitochondrial matrix, cytoskeleton, microtubules and rough endoplasmic reticulum membrane. In the group of less abundant proteins, GO analysis showed an enrichment in proteins from the spliceosome catalytic subunit and complex. Furthermore, an enrichment in membrane, nucleus, nucleoplasm and nuclear specks (small sub-nuclear membraneless organelles, retrieved on Uniprot database), in less abundant proteins, was also observed. This GO analysis is depicted in Figure C1.12.

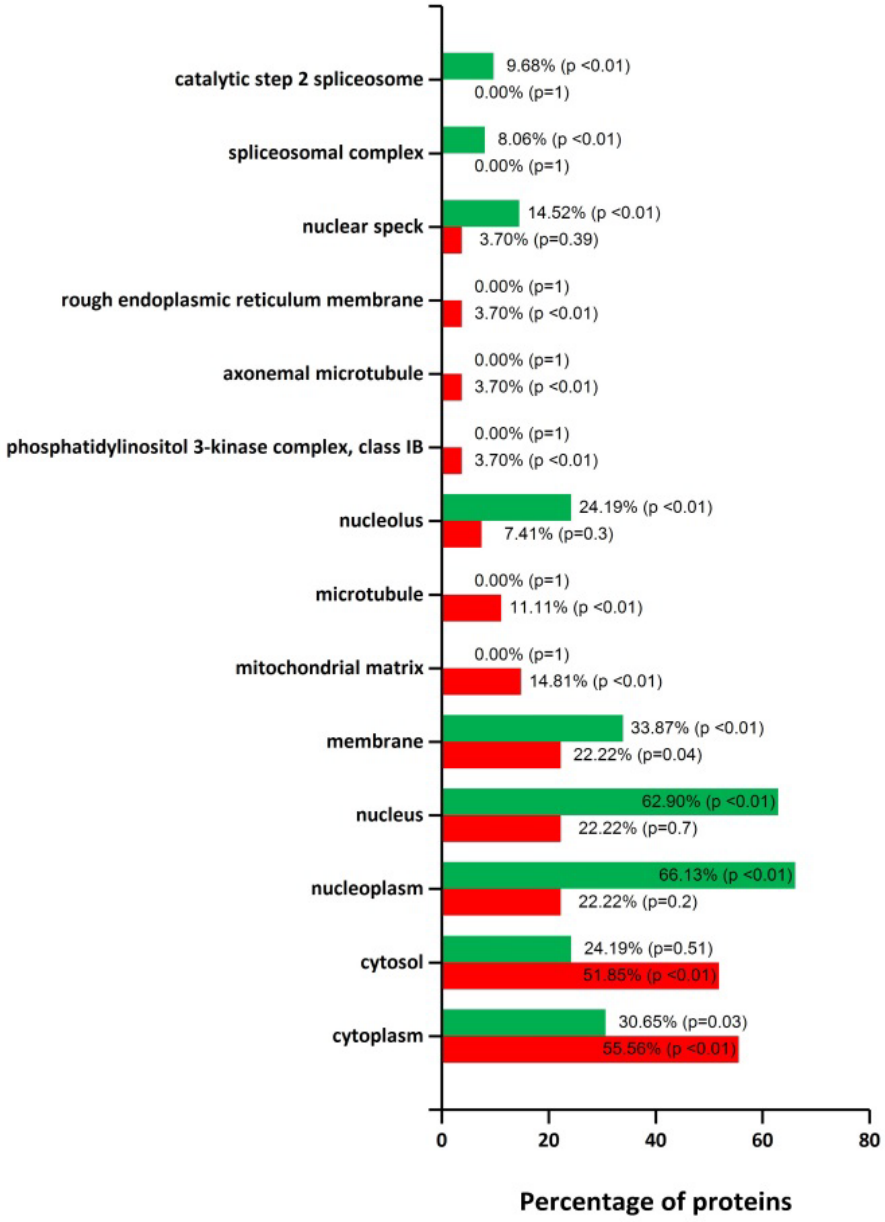

Figure C1.12 GO analysis of the cellular component of the proteins differentially abundant after macrophage interaction with *C. albicans*. In red are more abundant proteins and in green less abundant proteins after macrophage interaction with *C. albicans*.

Due to the role of mitochondria in the metabolic reprogramming undergone by macrophages in response to different pathogens, we decided to take a closer look to the proteins present in this organelle. As observable in **Figure C1.13**, there are proteins more and less abundant in the mitochondria and they have distinct functions, from amino acids metabolism to protein transport and ROS production.

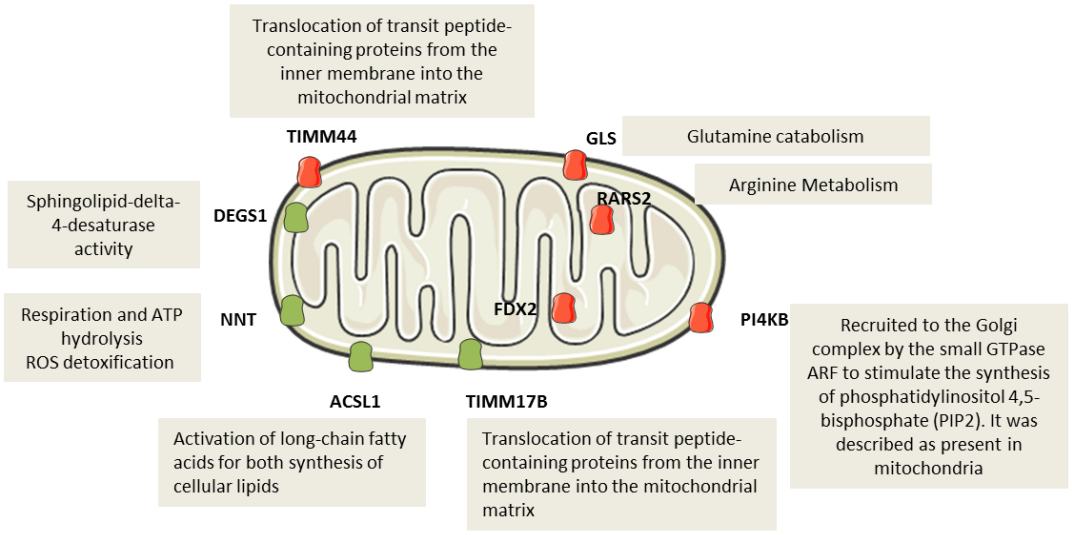

Figure C1.13 Proteins annotated as located in the mitochondria (retrieved from UniProt database). Schematic representation of the differentially abundant proteins located in the mitochondria and respective functions. Proteins are color coded according to their abundance: red for more abundant and green for less abundant after macrophage interaction with *C. albicans*.

Mitochondrial membrane potential was also analyzed in the different conditions. For that, we used JC-1 probe for flow-cytometry measurements. In cases of high mitochondrial membrane potential JC-1 spontaneously forms complexes known as J-aggregates with intense red fluorescence. In cases of low mitochondrial membrane potential JC-1 remains in the monomeric form, showing only the green fluorescence (Reers *et al.*, 1995). This means mitochondrial polarization is indicated by an increase in the red/green fluorescence intensity ratio. Mitochondrial membrane potential was measured in macrophages control, macrophages incubated with beads and with *C. albicans.* A positive green control with macrophages incubated with CCCP (membrane depolarizing agent) was included. As depicted in **Figure C1.14,** there is a trend of increasing the mitochondrial potential after macrophage interaction with beads and with *C. albicans,* although these differences were not statistically significant. **Figure C1.14A** represents the flow cytometry plots with percentage of macrophages cells (gated by cell size, FSC and granularity, SSC) with red (FL-2) and green fluorescence (FL-1). Cells positive for red and green fluorescence (UR) were counted and the percentage compared in the three conditions. **Figure C1.14B** represents the quantitative results of JC-1 flow-cytometry measurements. Furthermore, **Figure C1.14C** shows some representative fluorescence micrographs of macrophages alone and after incubation with *C. albicans* stained with JC-1. An increase in the proportion of cells with higher membrane mitochondrial potential is observed when macrophages interact with *C. albicans*, as observed in the flow cytometry results.

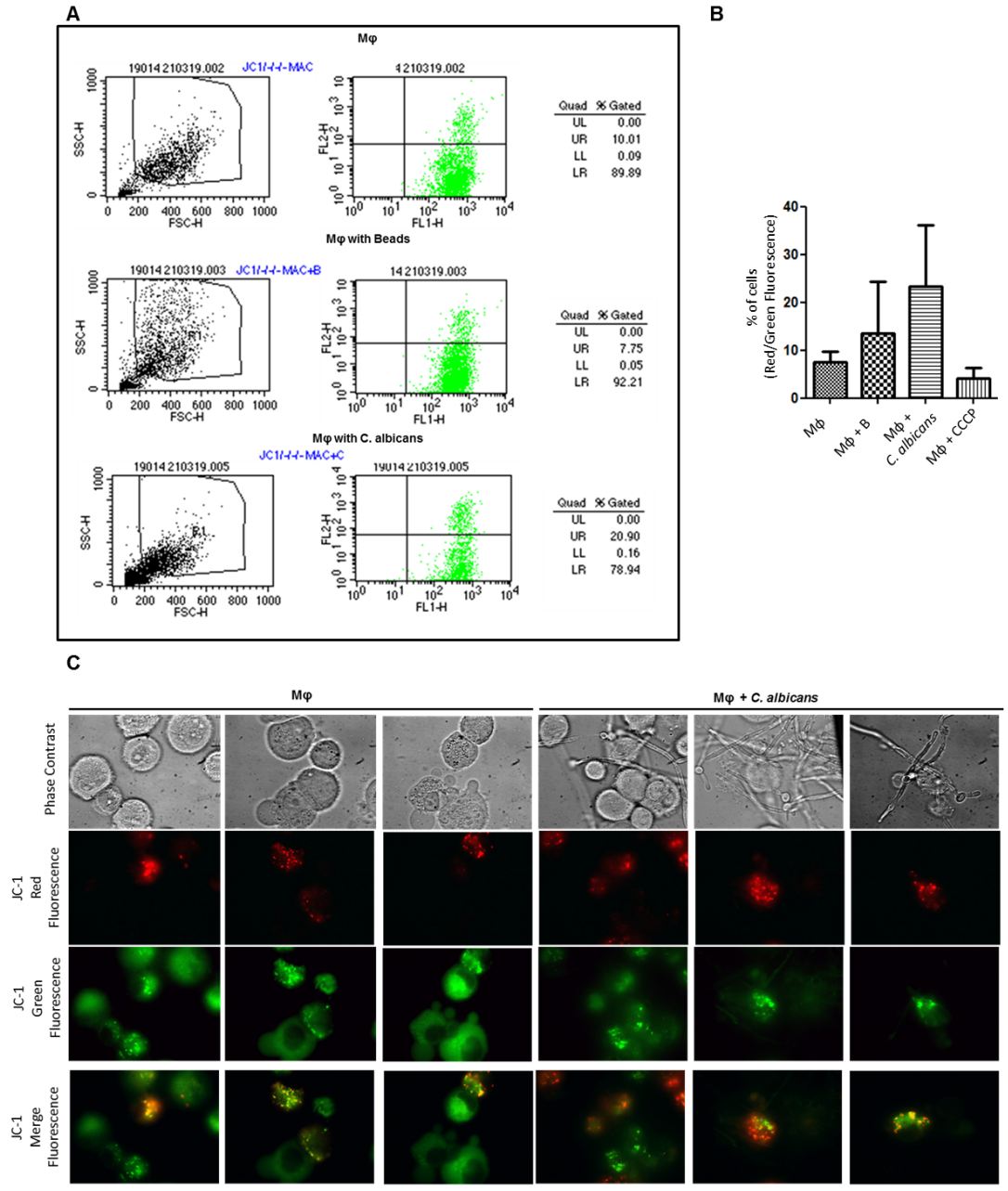

Figure C1.14 Mitochondrial membrane potential measurements with JC-1 probe. The three conditions were analyzed ((Mϕ; Mϕ with beads and Mϕ with *C. albicans*). (A) Flow cytometry dot plots representing both macrophage region and red/green fluorescence positive macrophages (UR). (B) Flow cytometry quantification of the percentage of cells with ratio of red/green fluorescent signal. This reflects mitochondrial polarization with JC-1. CCCP was used as green positive control. Three biological replicates were performed. (C) Representative microscopy fluorescence images of the macrophages alone and with *C. albicans* are shown. In cells with high mitochondrial membrane potential, JC-1 forms complexes with intense red fluorescence.

GO enrichment analysis of the biological processes was also performed comparing the differentially abundant proteins. Figure C1.15 shows this analysis, and clearly the two groups of proteins were involved in very distinct processes. The group more abundant proteins was enriched in phosphatidylinositol biosynthetic process, cell proliferation and natural killer cell chemotaxis. Although not statistically significant, also some proteins, both more and less abundant, were implicated in innate immune response and signal transduction. The group of less abundant proteins was enriched in processes such as mRNA processing and RNA splicing. It is noteworthy to point out that the GO enrichment of the more abundant proteins does not show a very significant enrichment in a specific biological process, showing that the proteins are implicated in different processes. Contrarily, the less abundant proteins were markedly enriched in categories related to RNA processing and RNA splicing.

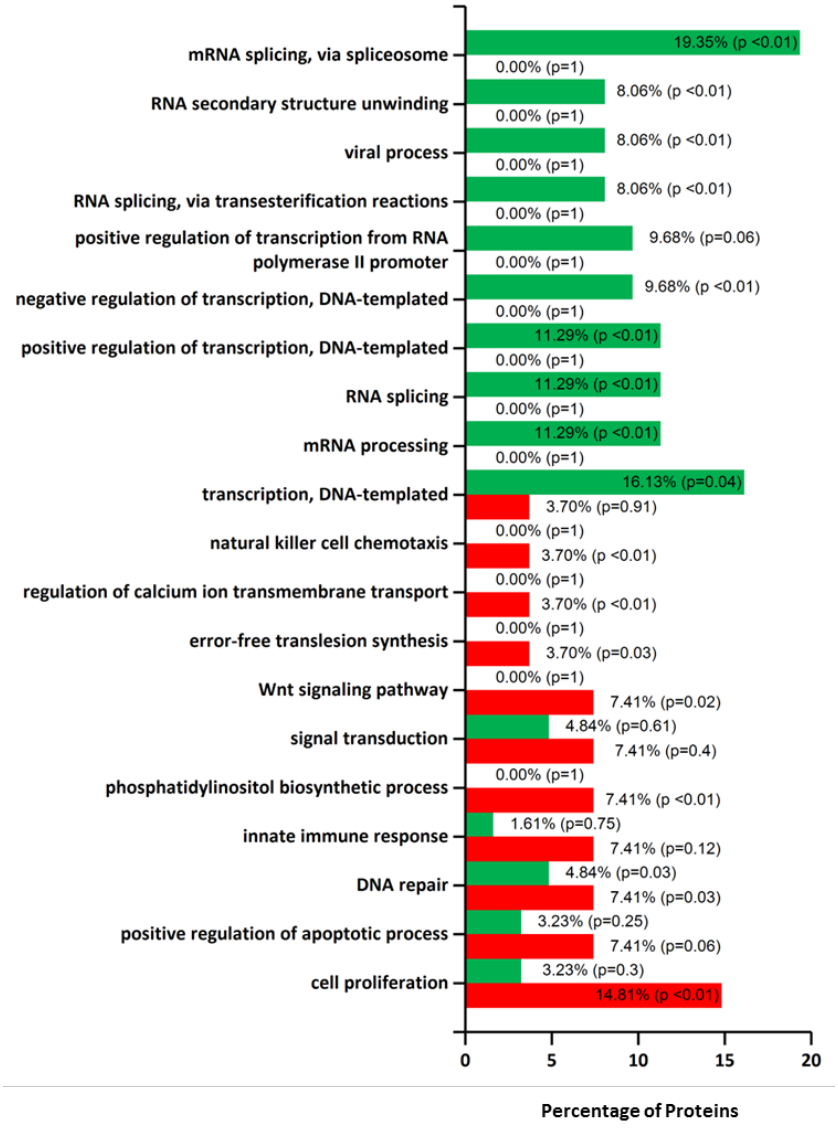

Figure C1.15 GO analysis of biological process of the differentially abundant proteins after macrophage interaction with *C. albicans*. In red are more abundant proteins and in green less abundant proteins after macrophage interaction with *C. albicans*.

To assess protein – protein interactions between the differentially abundant proteins, the interaction analysis was performed using STRING (**Supplementary Figure C1.7**). The interaction network presented 229 connections and also shows what was previously observed in the GO enrichment analysis, which is that the more abundant proteins were in their majority not interacting with each other. Interestingly, if we analyze the predicted protein-protein interaction network of the group of less abundant proteins (**Figure C1.16A**) we observed that they were highly interacting with each other, particularly the group of proteins implicated in RNA processing and splicing (21 proteins, **Figure C1.16B).**

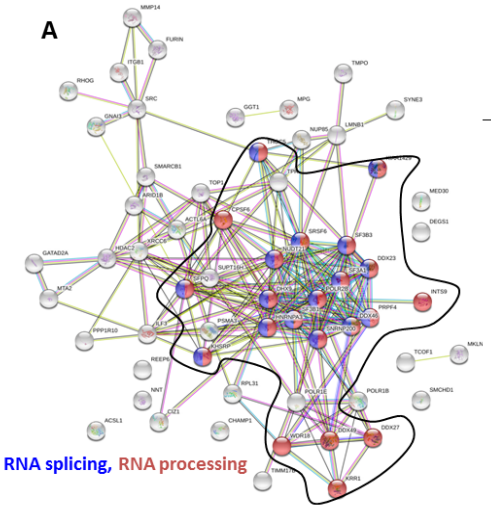

B

Uniprot Accession	Gene Name	Protein Name	Log_2 (ratio)
P30876	POLR2B	DNA-directed RNA polymerase II subunit RPB2	-0.07
Q96GQ7	DDX27	Probable ATP-dependent RNA helicase DDX27	-0.08
Q69YN4	VIRMA	Protein virilizer homolog	-0.09
Q92945	KHSRP	Far upstream element-binding protein 2	-0.09
Q9Y6V7	DDX49	Probable ATP-dependent RNA helicase DDX49	-0.10
Q15393	SF3B3	Splicing factor 3B subunit 3	-0.11
Q7L014	DDX46	Probable ATP-dependent RNA helicase DDX46	-0.12
O75643	SNRNP200	U5 small nuclear ribonucleoprotein 200 kDa helicase	-0.12
Q13247	SRSF6	Serine/arginine-rich splicing factor 6	-0.12
Q13769	THOC5	THO complex subunit 5 homolog	-0.13
Q9BUQ8	DDX23	Probable ATP-dependent RNA helicase DDX23	-0.14
Q15459	SF3A1	Splicing factor 3A subunit 1	-0.14
Q16630	CPSF6	Cleavage and polyadenylation specificity factor subunit 6	-0.14
O75533	SF3B1	Splicing factor 3B subunit 1	-0.14
Q9NV88	INTS9	Integrator complex subunit 9	-0.15
O43172	PRPF4	U4/U6 small nuclear ribonucleoprotein Prp4	-0.15
Q08211	DHX9	ATP-dependent RNA helicase A	-0.16
P23246	SFPQ	Splicing factor, proline- and glutamine-rich	-0.18
Q13601	KRR1	KRR1 small subunit processome component homolog	-0.18
P51991	HNRNPA3	Heterogeneous nuclear ribonucleoprotein A3	-0.30
O43809	NUDT21	Cleavage and polyadenylation specificity factor subunit 5	-0.39

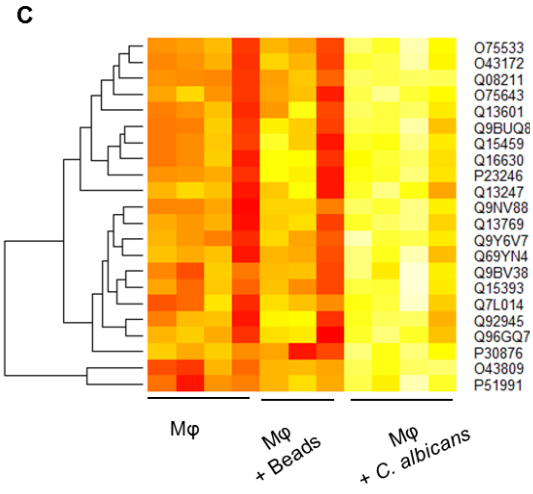

Figure C1.16 Proteins involved in RNA processing. (A) Predicted protein–protein interactions network of the proteins less abundant during macrophage interaction with *C. albicans*, showing RNA splicing and mRNA processing as processes with proteins highly interacting with each other. (B) Proteins related with RNA processing indicating their protein description retrieved on Uniprot database and the protein abundance after macrophages interaction with *C. albicans* (log_2 (ratio)). (C) Heat map with proteins (rows) implicated in RNA splicing and processing presented in the table. Protein intensities of each biological replicate and in each condition (columns). From red to yellow means from higher to lower protein intensities.

Moreover, **Figure C1.16C** represents the heat map of this group of proteins with their respective intensities in the three conditions: macrophages, macrophages after interaction with beads and

macrophages after interaction with *C. albicans*. A clear difference was observed between macrophages alone and macrophages after interaction with *C. albicans*. When comparing macrophages with beads no differences were observed.

3.3 Phosphoproteomic analysis of macrophage proteins after interaction with *C. albicans*

In an effort to identify pathways that could be activated during macrophage interaction with *C. albicans* we also analyzed the quantitative changes of the phosphoproteome of the macrophage infected with this pathogen. Regarding the analysis of the phosphorylated peptides, their abundances were normalized against the abundance of the proteins. A total of 9615 phosphopeptides belonging to 1842 proteins was quantified (**Supplementary Table C1.6**). In general terms, more differences were observed in phosphorylation than in abundance data. For differential abundance analysis, phosphopeptides were considered differentially phosphorylated if the *p*-value < 0.01 and FDR < 0.05. Using this statistical filter, 135 phosphopeptides were considered differentially abundant, being 95 phosphopeptides more abundant and 40 less abundant after macrophage interaction with *C. albicans* (**Supplementary Table C1.7**). **Figure C1.17A** represents the volcano plot with the $\log_2$ ratio against their $-\log_{10}$ *p*-value of the phosphopeptides and a cluster analysis represented with the heat-map divided in 2 clusters to show the phosphopeptides profile and their $\log_2$ (ratio) in both conditions (**Figure C1.17B**). The 95 more abundant phosphopeptide corresponded to 70 proteins whereas the 40 less abundant phosphopeptides corresponded to 36 proteins.

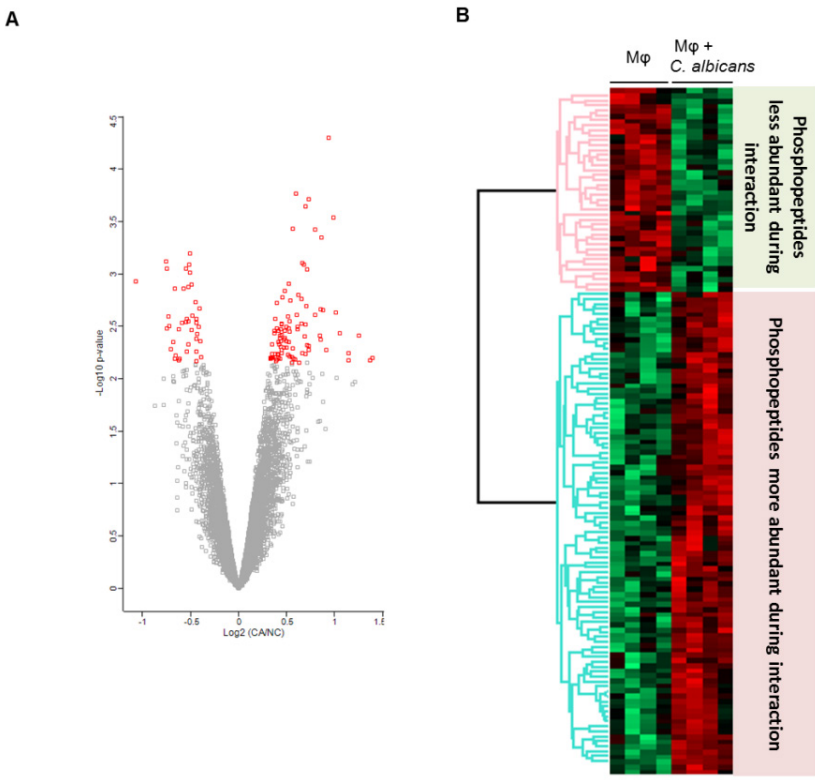

Figure C1.17 Phosphoproteome analyses of macrophage proteins after interaction with *C. albicans*. (A) Volcano Plot (Log_2 vs $-\log_{10}$*p*-value) of the phosphopeptides quantified in this study. Red dots represent the phosphopeptides considered differentially abundant during macrophage interaction with *C. albicans*. (B) Cluster heat-map was divided in 2 clusters to show phosphoproteins profile in the two conditions (Mϕ and Mϕ with *C. albicans*). Both Volcano plot and cluster heat-map were performed in Perseus software.

As the majority of the phosphosites still have unknown effect at the cellular level, we decided to perform a protein-protein interaction network with the phosphoproteins of the differentially abundant phosphopeptides in order to investigate possible biological processes activated during interaction. **Figure C1.18** depicts the predicted protein-protein interaction network obtained and some protein clusters with different functions. Among them, we observed proteins involved in RNA transcription, RNA splicing, cytoskeleton rearrangement as well as cell signaling and immune response. Strikingly, several proteins involved in RNA splicing were more phosphorylated during interaction. Complementarily, we used the website Phosphosite Plus® to look into known phosphorylation effects of the phosphopeptides quantified in this study. From the quantified phosphopeptides, 12 phosphosites presented known effects in the cell (**Table C1.5**). Interestingly, *C. albicans*-infected macrophages showed differences in phosphosites implicated in important processes: phosphosites belonging to 5 proteins (PECAM, FYN ,CEP131, CFL1 and CD44) had roles in cell motility and cytoskeleton rearrangement; phosphosites belonging to 6 proteins (CSF1R, LMNA, NOLC1, PPP6R2, PLCG1 and C5AR1) had distinct functions related with cell survival and cell signaling through cell surface receptors. Finally, the phosphosite of EEF2K is known to reduce protein synthesis.

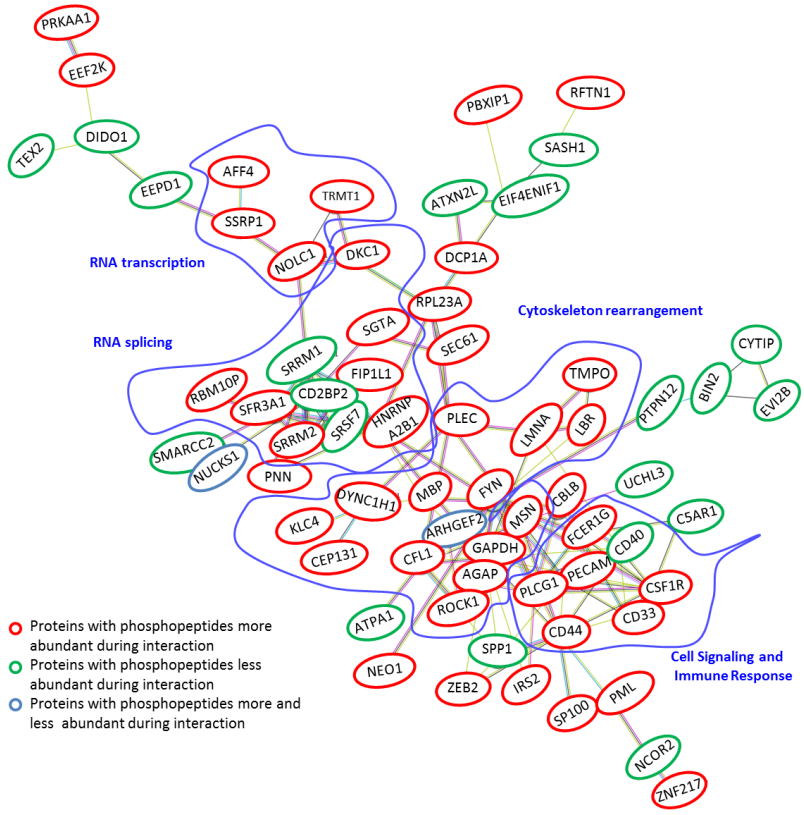

Figure C1.18 Protein–protein interaction network with the proteins with differentially abundant phosphopeptides during macrophage interaction with *C. albicans*. Some biological processes (RNA transcription, RNA splicing, cytoskeleton rearrangement, cell signaling and immune response) are highlighted in the network, signaling some of the interacting proteins that are involved in each process. The network protein-protein interaction *p*-value was 2.54×10^{-6}.

Table C1.5 Differentially abundant phosphopeptides with phosphosites that present known effects in the cell.

Uniprot Acession[a]	Gene Name[a]	Protein Descriptions	Phosphopeptide Sequence[b]	Phosphosite[c]	Effect[c]	Log_2 (ratio)[d]
Cytoskeletal Organization						
P16284	PECAM1	Platelet endothelial cell adhesion molecule	DTETV**Y**SEVR	Y713	cell adhesion and cell motility	1.4
P06241	FYN	Tyrosine-protein kinase Fyn	DG**S**LNQSSGYR	S21	cell motility	0.7
Q9UPN4	CEP131	Centrosomal protein of 131	RSN**S**TTQVSQPR	S78	cytoskeletal reorganization	0.6
P23528	CFL1	Cofilin-1	S**S**TPEEVK	S24	cytoskeletal reorganization	0.4
P16070	CD44	CD44 antigen	KP**S**GLNGEASK	S697	cell motility	0.4
Cell Survival and Cell Signalling						
P07333	CSF1R	Macrophage colony-stimulating factor 1 receptor	D**Y**TNLPSSSR	Y923	cell survival and proliferation	0.6
P02545	LMNA	Prelamin-A/C OS=Homo sapiens	LRL**S**PSPTSQR**S**R	S392	cell cycle regulation	0.6
Q14978	NOLC1	Nucleolar and coiled-body phosphoprotein 1	N**S**EEEEEEK	S563		0.5
O75170	PPP6R2	Serine/threonine-protein phosphatase 6 regulatory subunit 2	CS**S**PVDTECSHAEGSR	S771	cell cycle regulation	0.4
P19174	PLCG1	1-phosphatidylinositol 4,5-bisphosphate phosphodiesterase gamma-1	EG**S**FESR	S1248	cell cycle regulation	0.4
P21730	C5AR1	C5a anaphylatoxin chemotactic receptor 1	**S**F**T**RSTVDTMAQK	S334	cell activation and receptor desensitization	-0.5
Protein Degradation						
O00418	EEF2K	Eukaryotic elongation factor 2 kinase	ESENSGDSGYP**S**EK	S445	Protein degradation induced	0.5

[a] Uniprot accession and gene name according to Uniprot Knowledge base

[b] In bold and underlined the phosphosite(s) given by the PhosphoRS algorithm

[c] Effect of phosphosite according to PhosphositePlus database.

[d] Log_2 of the ratio from macrophages interacting with *C. albicans* versus macrophages control. Values normalized against the protein amount of the respective protein

Discussion

The current approaches to treat fungal infections are still limited and are mainly pathogen-directed therapeutics (Pappas *et al.*, 2018). Envisioning this limitation, the study of the immune response may give us new clues on how this pathogen can be more efficiently killed, and consequently improve the currently available therapeutic strategies. Furthermore, increasing efforts are being done to develop specific ways to modulate the immune system as new therapeutic strategies (Zwolanek *et al.*, 2014, Carpino *et al.*, 2017).

Macrophages are cells from the innate immune system that play an important role in the host response and elimination of pathogens (Bourgeois *et al.*, 2010). They are extremely important cells in response to cytokines and PAMPs and perform a wide range of biological functions, such as pathogen phagocytosis, antigen presenting and bridging innate and adaptive immunity (Dill *et al.*, 2015).

There are several stages generally accepted for the intricate relation between macrophage and *C. albicans*. As depicted in **Figure C1.19** (adapted from (da Silva Dantas *et al.*, 2016)), the macrophage target the fungal cell recognizes and engulf it. Then, the yeast cell is delivered to the phagosomal vesicle which fuses with lysosomes, forming a mature phagosome. The phagolysosome uses several oxidative and non-oxidative mechanisms to try to kill the fungus. On the *Candida* site, it can alkalinize the phagosome and induce its own lytic expulsion (Bain *et al.*, 2012). Moreover, it can form hypha which induces macrophage pyroptosis and lysis (da Silva Dantas *et al.*, 2016).

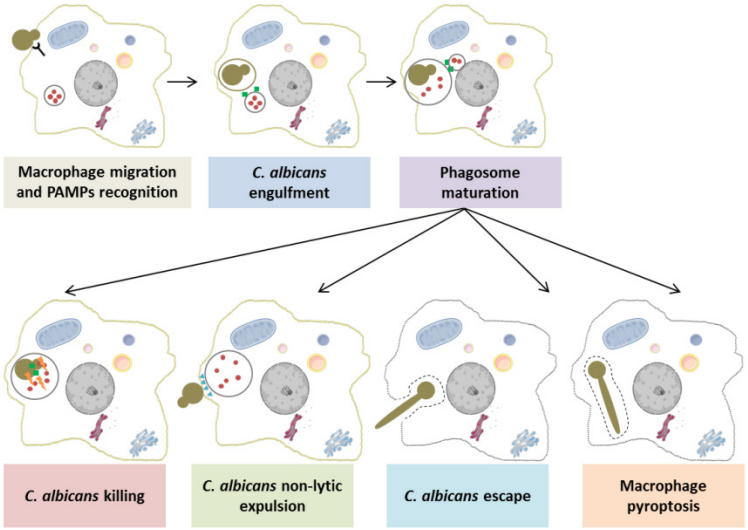

Figure C1.19 Macrophage and *C. albicans* phases of interaction. The fungus is recognized by macrophages PRRs and engulfed. Then, *C. albicans* cell is delivered to the phagosomal vesicle that undergoes several steps of maturation. Here, the fungi can be killed by oxidative and nitrosative mechanisms. *C. albicans* can interfere with the phagolysosome and induce its own non-lytic expulsion. It can also form hypha and induce pyroptosis, which causes macrophage lysis (based on (Silva-Dantas, A. *et al.*, 2016).

Here, we used two different proteomic and phosphoproteomic approaches to deepen the knowledge on the proteomic alterations the macrophage produces after interacting with *C. albicans*. For that, the immortalized monocyte-like cell line, derived from the peripheral blood of a childhood case of acute monocytic leukemia, THP-1 cell – line was used. THP-1 monocytes can be differentiated by the administration of PMA, inducing typical hallmarks of macrophages, represented by cell adhesion, spread morphology; increased granularity and irregular nucleus shape (Gatto *et al.*, 2017). Although it has some limitations such as up-regulation of specific genes during the differentiation process that might overwhelm mild effects of specific stimuli, it has been widely used for the study of interaction with several pathogens (Chanput *et al.*, 2014, Kaewseekhao *et al.*, 2015, Singh *et al.*, 2015, Duan *et al.*, 2017). Several studies comparing this cell line with human PBMC-derived macrophages showed relatively similar response patterns (Chanput *et al.*, 2014). Our group used this cell line for the study of THP-1-derived EVs both from control and from *Candida* infected macrophages. Besides studying the protein cargo of the EV's, we found that both types of EV's increased the secretion of pro-inflammatory cytokines and candidacidal activity of macrophages (Reales-Calderon *et al.*, 2016).

Here, we were particularly interested in unravelling new mechanisms activated by macrophages after interaction with *C. albicans*. THP-1-derived macrophages were incubated with *C. albicans* cells during 3 h and a MOI of 1. At this time of interaction, a reduced damage was ensured, so 70% of the macrophages were not impaired and around 70% of yeast cells were engulfed by the macrophages (see Figure C1.2 in results section). This evaluation of human macrophage interaction with *C. albicans* is in agreement with our previous studies with murine macrophage cell lines and was peremptory to select the ratio and time of incubation (Fernandez-Arenas *et al.*, 2007, Reales-Calderon *et al.*, 2013). After optimizing the best co-culturing conditions two different strategies were designed. One consisted in performing an ATP-binding enrichment for the study of these proteins which are highly involved in cell signaling and that are at low concentration in the cell. The second one was the development of a deep shotgun analysis of the whole proteome and phosphoproteome where both peptide fractionation and highly sensitive mass spectrometers were used for the study of *C. albicans* infected macrophages. A summary of the proteomic and phosphoproteomic alterations observed in both approaches are depicted in Figure C1.20.

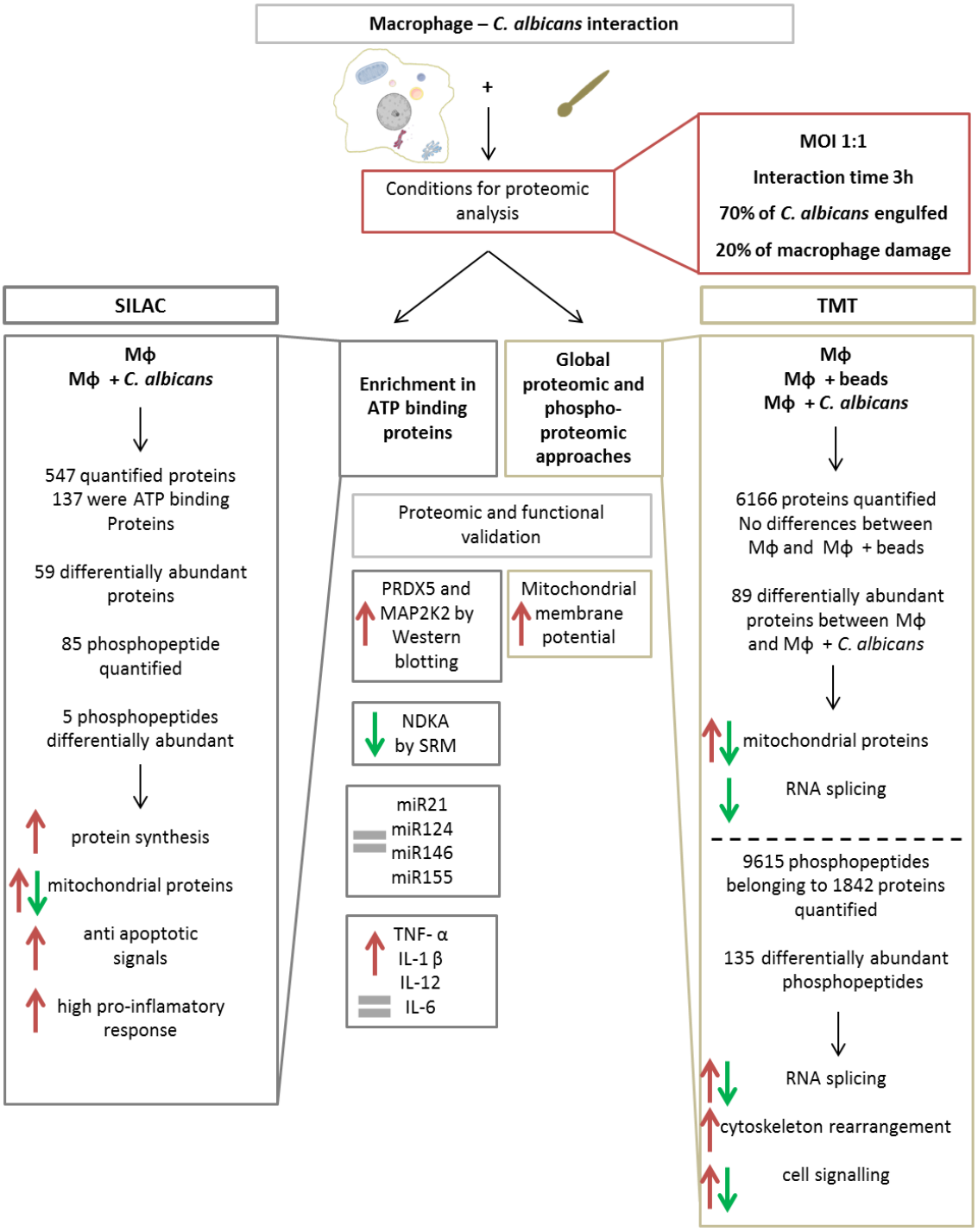

Figure C1.20 Schematic overview representing the main results obtained in both proteomic and phosphoproteomic approaches developed in this chapter. Here are depicted the conditions for the analysis of macrophage proteomic alterations after interaction with *C. albicans* together with the main results obtained in the two proteomic approaches developed: one involves the enrichment in ATP binding macrophage proteins and the other one involves the global proteomic and phosphoproteomic analysis of the cytoplasmic extract of macrophages alone, after interaction with beads and after interaction with *C. albicans.*

In one approach we applied an ATP binding protein enrichment kit and we were able to quantify 547 proteins. Among these, around 25% of the proteins were annotated as ATP binding proteins. A total of 59 proteins were considered differentially abundant. Macrophage proteomic alterations include an increase in proteins implicated in protein synthesis. Furthermore, an increase in antiapoptotic signals over pro-apoptotic signals was suggested together with a high pro-inflammatory response. In the other approach, the global proteomic and phosphoproteomic study of the macrophage after interaction with beads and with *C. albicans* was performed. A total of 6166 proteins was quantified. Although no differences were observed when comparing macrophages after interacting with beads with the other conditions, 89 proteins were considered differentially abundant when comparing macrophages control with macrophages after interacting with *C. albicans*. The proteomic analysis showed among other processes, a striking enrichment in less abundant proteins related with RNA splicing. The phosphoproteome analysis led to a quantification of 9615 phosphopeptides that belong to 1842 proteins. From these, 135 were differentially abundant during interaction. The differentially abundant phosphopeptides were implicated in different processes including RNA splicing, cytoskeleton rearrangement and cell signaling. Both works showed proteins more and less abundant that belong to the mitochondria. The processes studied in these complementary works will be further discussed.

1 *C. albicans* recognition and cell signaling

Macrophages have different receptors that recognize *C. albicans* PAMPs prior to its internalization. In the global proteomic approach several receptors were found to be differentially phosphorylated during the conditions of interaction studied. The C-type mannose receptor 2 (MRC2) was found to be differentially phosphorylated during macrophage interaction with *C. albicans,* although the effect of this phosphorylation is not known. This is an endocytic receptor with three distinct types of domains at its extracellular region, a single transmembrane region and a cytoplasmic tail. The extracellular region binds different ligands, among them sugars terminating in mannose, fucose and *N*-acetylglucosamine and microbial antigens (Gazi *et al.*, 2011). In another work it was shown that the *N*-linked mannosyl residues of *C. albicans* bind to the mannose receptor (Netea *et al.*, 2006).

CD40 is a surface glycoprotein of the TNF-receptor superfamily and it is important in cell-cell interaction and plays a role in the defense against *C. albicans* infection. Netea and co-workers observed that in early time points of infection no differences between the outgrowth of *C. albicans* in the organs of CD40L knock out and control mice. In late stages of infection the elimination of the yeast was impaired in knockout mice, indicating a more involvement of this

protein in later stages of infection (Netea *et al.*, 2002). This may explain why at 3 h of incubation we see a reduction in the phosphorylation of this protein, indicating that this protein was not particularly involved in the response to *C. albicans*. Probably longer times points should be analyzed to see if there was an increase in the phosphorylation of this receptor.

CD33 was found to be more phosphorylated during macrophage interaction with *C. albicans.* This receptor is implicated in the recognition of syalylated glycoproteins, and leads to the phosphorylation, by Src-like kinases such as LCK, of two immunoreceptor tyrosine-based inhibitory motifs (ITIMs) located in CD33 cytoplasmic tail (Paul *et al.*, 2000). Nevertheless, more studies are needed in order to unravel its role in the recognition of sialic acids present in the cell surface of *C. albicans*.

PRKAA1, also known as AMPKα, is protein sensor of energy status that maintains cellular energy homeostasis (Bae *et al.*, 2011). It was found to have differentially phosphorylated peptides in both approaches. In the ATP binding enrichment work, we observe a phosphorylated peptide with no specific phosphosite attributed, the phosphopeptide was from S494 until R501 (SGSVSNYR). In In the second work we observed that the S508 was the phosphosite attributed to be differentially phosphorylated. The phosphorylation of Thr183 is known to activate this kinase and the phosphorylation of S496 was found to inhibit the enzymatic activity (Lizcano *et al.*, 2004, Pandey *et al.*, 2017). It was previously shown that the activation of this kinase was implicated in phagocytosis of both bacteria (Bae *et al.*, 2011) and fungi (like the pathogen *Cryptococcus neoformans*) (Pandey *et al.*, 2017). Furthermore, it was suggested by other group that AMPK signaling was activated in murine macrophages upon ATP treatment and they observed the inflammasome activation and pyroptosis of these macrophages (Zha *et al.*, 2016). This is in congruence with the increase in secretion of IL-1β in macrophages upon interaction with *C. albicans*. Besides, phosphorylation of AMPKα in Ser487/491 was found to reduce AMPK activity (Hawley *et al.*, 2014). Further studies would be needed to know the cellular effects of these phosphopeptides.

2 *C. albicans* phagocytosis and macrophage cytoskeleton rearrangement

An increase in the phosphorylation of several proteins implicated in cytoskeleton rearrangement, microtubules and cell adhesion was observed during macrophage interaction with *C. albicans*. This remodeling is expected once phagocytosis of *C. albicans* carries along important changes in macrophage cytoskeleton and microtubules. Proteomic alterations in these processes were previously observed during macrophage interaction with *C. albicans* (Fernandez-Arenas *et al.*, 2009, Reales-Calderon *et al.*, 2013, Reales-Calderon *et al.*, 2014)

C. albicans phagocytosis involves macrophages recognition of PAMPs by the PRRs of the phagocytic cell. During this work, we evaluated macrophage engulfment of *C. albicans* cells and we observed that after 3 h interaction and with a MOI of 1 around 70% of the *C. albicans* cells were engulfed. C-type lectin receptors, such as Dectin 2 and Mincle, play an important role in this internalization. These receptors can signal directly or through their association with ITAM-bearing adaptor chains such as FcRγ. Then, they can activate SYK, leading to large-scale changes in transcription of multiple genes, reorganization of the actin cytoskeleton through activation of GTPases and activation of NF-κB through different routes. One of the well-known pathways activated by C-type lectin receptor signaling involves phosphoinositide 3-kinase (PI3K) that genarates membrane associated phosphatidylinositol-3,4,5-triphosphate (PIP3) to activate its downstream enzyme phospholipase PLCγ. Induction of the inositol triphosphate (IP3) and diacylglycerol (DAG) pathway through PLCγ activation leads to calcium ions release as a second messenger and activation of PKC isoforms (Figure C1.21) (Plato *et al.*, 2013). PI3K was found more abundant during macrophage interaction with *C. albicans*. In the ATP binding enrichment SYK was also found more abundant, although in the global proteomic approach no significant changes were observed. Moreover, FcRγ and PLCG1 were also found to have differentially abundant phosphopeptides. Furthermore, we observed an increase in the phosphorylation of Rho type GTPases activator proteins such as ARHGAP12 and ARHGEF2. Finally, several proteins differentially phosphorylated were found to be involved in the cytoskeleton rearrangement such as CFL1, FYN, MSN, PLEC and ROCK1.

Moreover, we found CSF1 receptor also to be more phosphorylated during interaction. This protein was previously linked to actin cytoskeleton rearrangement and chemotaxis. This receptor activation leads to the local accumulation of PI3K lipid products at the plasma membrane. This is critical to downstream regulation of the actin cytoskeleton (Rougerie *et al.*, 2013). As commented above, PI3K (catalytic subunit γ) was found to be more abundant during macrophage interaction with *C. albicans*. CD44 activation was found differentially phosphorylated and this receptor also implicated in the cytoskeleton reorganization, as observed in a work where macrophages internalized *Staphylococcus aureus* (Li *et al.*, 2017).

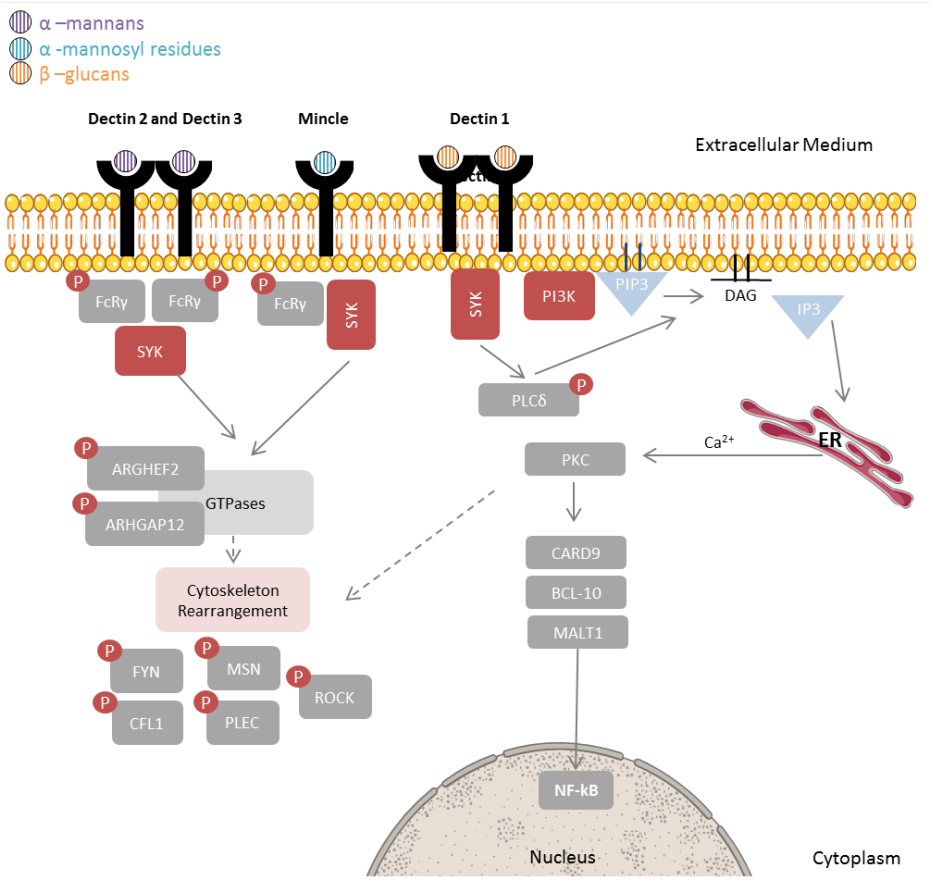

Figure C1.21 Proteomic and phosphoproteomic data regarding the cell signaling pathway activated by CTLRs that lead to cytoskeleton rearrangement. Proteins in a grey box represent proteins with no changes in the abundance. Proteins in red box represent proteins found to be more abundant in at least one of the proteomic experiments. Proteins containing a circle with P represent proteins that have phosphopeptides found to be more abundant during macrophage interaction with *C. albicans*.

During *C. albicans* phagocytosis, phagosomes acquire microbicidal and lytic enzymes that are delivered by membrane fusion and fission events with different endolysosomal compartments. This leads to an acidification of the phagosome lumen, forming a microbicidal phagolysosome (Okai *et al.*, 2015). Rab GTPases regulate vesicle recruitment and the modulation of vesicular transport through interaction with cytoskeletal components. We observed RAB8B to be more phosphorylated during interaction. In the ATP binding proteins enrichment work we observed RAB7 to be less abundant during interaction and CLN6 (see **Table C1.3** in results section) presented a phosphopeptide to be less abundant. However, in the ATP binding enrichment approach, we could not normalize the phosphorylation with the abundance of the protein. RAB7 has been shown to associate with the phagosomal membrane and plays a role in mediating interaction with late lysosomal compartments (Vieira *et al.*, 2002). More studies should be performed in the future to evaluate the importance of these results.

It is important also to mention that *C. albicans* modulates phagosome maturation. Our group performed a comparative analysis of the intracellular trafficking of virulent/avirulent *C. albicans*

strains and supported the model where *C. albicans* is able to evade trafficking, by subverting the lysosomal system (Fernandez-Arenas *et al.*, 2009). Another group showed how *C. albicans* cell wall could influence phagosome maturation. They showed that the loss of cell wall *O*-mannan leads to exposure of β-glucan facilitating recognition of Dectin 1 which was associated with enhanced phagosome maturation (Bain *et al.*, 2014). This phenomenon was previously observed during macrophage-*Mycobacterium tuberculosis* interaction.(Via *et al.*, 1997, Vergne *et al.*, 2004)

3 Mitochondrial proteins and oxidative stress response

Macrophages are phagocytic cells that produce and release reactive oxygen species (ROS) in response to phagocytosis (Forman & Torres, 2001). Mitochondria are important to ATP as well as ROS production (Liu & Ho, 2017). Proteins from the mitochondria were found differentially abundant in both studies (Figure C1.22).

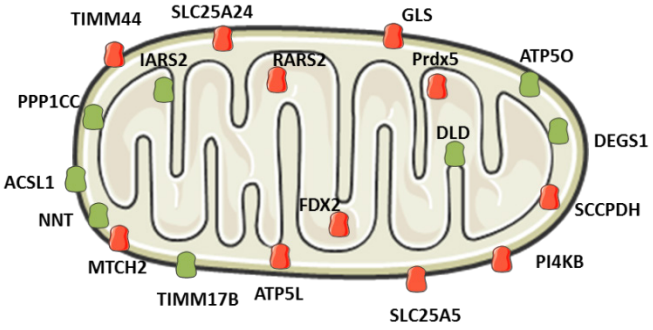

Figure C1.22 Proteins annotated as located in the mitochondria in both approaches (retrieved from UniProt database). Schematic representation of the differentially abundant proteins. Proteins are color coded according to their abundance: red for more abundant and green for less abundant after macrophage interaction with *C. albicans*.

The study with the enrichment in ATP-binding proteins showed two mitochondrial proteins involved in response to oxidative stress (PRDX5 and SLC25A24) to be more abundant upon interaction with *C. albicans*. PRDX5, a protein that protects cells from DNA damage and inhibits stress-induced apoptosis (Yuan *et al.*, 2004) was previously shown to be more abundant in LPS-treated macrophages (Choi *et al.*, 2013). We validated the increase in its abundance using Western blot (see Figure C1.6 in results section). SLC25A24 may also play a role in protecting cells against oxidative stress-induced cell death (Traba *et al.*, 2012). Moreover, NNT was found to be less abundant, and the knock down of this protein was previously implicated with an increased production of ROS (Meimaridou *et al.*, 2012). Shui and co-workers previously observed significant changes in redox-related proteins implicated in oxidative burst in order to kill intracellular mycobacteria. They observed an increase in the abundance of several proteins, including PRDX5, that counteract the effect of oxidative stress (Shui *et al.*, 2009). We can hypothesize that the higher abundance of proteins that neutralize the oxidative burst may be a host-driving response to protect itself from the ROS it is producing to kill *Candida* cells. Nevertheless, we may not

discard the possibility that it can also be a pathogen-driven response (to reduce the production of ROS and decrease the killing power of the macrophages).

Other mitochondrial proteins differentially abundant were quantified among them, proteins involved in the production and transport of ATP (ATP5L, ATPO and SLC25A5) as well as proteins implicated in the uptake of calcium to them mitochondria (SCMC1).

In the global proteomic approach performed, the GO analysis showed that the more abundant proteins were enriched in mitochondria matrix (see **Figure C1.12** in results section). Also both more and less abundant proteins from the mitochondria were quantified as differentially abundant. Interestingly, one of the mitochondrial proteins found to be more abundant during interaction was RARS which is implicated in arginine metabolism and L-Arginine was reported to be a necessary substrate for macrophage fungistatic action (Granger *et al.*, 1988). Glutamine catabolism has also emerged as a prominent process in macrophage reprogramming after pathogen interaction. In LPS-primed macrophages, glutamine was suggested to contribute to succinate accumulation and is required for IL-1β production and NOS generation (Jha *et al.*, 2015, Sander & Garaude, 2018). In congruence with this observation, we found the mitochondrial glutaminase, GLS, to be more abundant during macrophage interaction with *C. albicans*. As mitochondria has been implicated in innate and adaptive immunity (Liu & Ho, 2017) , we took a more careful look into the mitochondrial membrane potential after macrophage interaction with latex beads and with C. albicans cells. Fluorescence microscopy together with flow cytometry showed an increase, although not statistically significant, in the proportion of cells with higher mitochondrial potential during macrophage interaction with live *C. albicans* cells (see **Figure C1.14** in results section). This is in congruence with previous studies where activation of macrophages with LPS lead to an increase in the mitochondrial membrane potential and in ROS production (Mills *et al.*, 2016). Nevertheless, due to the high variability found in this assay more studies are necessary, using other probes for example, to confirm this trend. ROS production is an important mechanism applied by the macrophage to kill pathogens. It was a previously described in *A. thaliana* that even a slight decrease in the mitochondrial potential caused a significant decrease of ROS production (Miwa & Brand, 2003). Tucey and co-workers suggested that macrophages increased the glycolytic metabolism in response to *C. albicans*. Moreover, they observed mitochondrial hyperpolarization right before glucose deprivation dependent cell death (Tucey *et al.*, 2018). On the other hand mitochondrial dysfunction has been linked with bacterial infections (West, 2017), especially in later stages of infection (Marriott *et al.*, 2005). Longer time-points should be tested in the future to see if there is a later decrease in the mitochondrial membrane potential.

4 Host proteins involved in mRNA processing and translation

In the ATP binding enrichment approach a cluster with proteins differentially abundant involved in mRNA processing was observed. Interestingly, in the global proteome work, a majority of proteins less abundant during interaction, together with differentially phosphorylated proteins implicated in the same processes were observed. In eukaryotic cells, the primary RNA transcript (pre-mRNA), synthesized in the nucleus by RNA polymerase II undergoes several modifications before being transported into the cytoplasm where translation occurs (Baralle & Baralle, 2018). One of the important steps important in the mRNA maturations is the splicing, where non coding sequences (introns) are removed and coding sequences (exons) are ligated together. Some exons are constitutively spliced, meaning that they are present in every mRNA produced, but many can be alternatively spliced to generate different forms from a given pre-mRNA. These events increase the number of protein species produced from a single gene and are catalyzed by the spliceosome. Two unique spliceosomes coexist in most eukaryotes the U2-dependent spliceosome which catalyzes the removal of U2-type introns, which has as main building blocks the U1, U2, U4/U6 and U5 snRNPs, and a less abundant U12-dependent spliceosome (Will & Luhrmann, 2011). There are several splicing factors and accessory proteins involved in the splicing regulation-so called intronic and exonic splicing enhancers or silencers – that can have positive or negative effects on splice-site usage. Exonic splicing enhancers are often bound by serine-arginine containing proteins (SR proteins) whereas exonic splicing silencers are typically bound by hnRNPs (Wahl *et al.*, 2009). As observable in Figure C1.23 several proteins implicate in this process were found differentially abundant, mainly less abundant, and phosphorylated, mainly more phosphorylated.

Due to the great number of proteins found in both studies performed and the fact that this differences in RNA splicing were not statistically significant when macrophages interact with beads, we explored the relationship of host mRNA processing in other infection scenarios. We found that events like this were thoroughly studied during macrophage interaction with virus and bacteria. Several studies suggest that bacterial infections induce alternative splicing of host RNAs. *Mycobacterium tuberculosis* was found to alter the global patterns of alternate splicing in the macrophages (Kalam *et al.*, 2017). In another study, it was found that the *Shigella* protein IpaH9.8, which is a nuclear translocating effector, has the ability to interact with U2AF affecting the expression of a subset of genes encoding pro-inflammatory chemokines and cytokines (Okuda *et al.*, 2005). Other group provided strong evidence of global changes in the alternate splicing during bacterial infection with both *Salmonella* and *Listeria* (Pai *et al.*, 2016). Though, little is known about how fungal infections influence host mRNA processing.

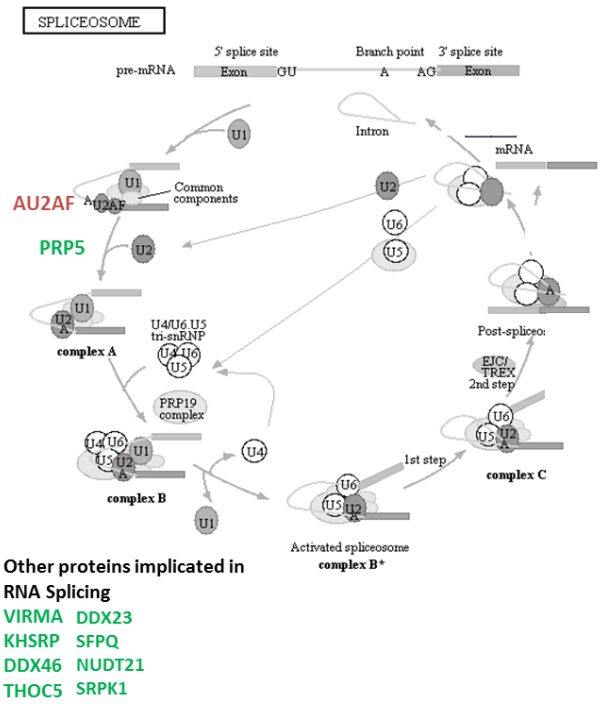

small nuclear ribonucleoproteins (snRNPs)			
U1	U2	U4/U6	U5
SNRPA	SF3A1*	PRPF4	BRR2
	SF3B1		PRP28
			CD2BP2*
		SNRNP200	
SNRPB			

Associated Proteins	
SR (associated with ESE)	hnRNPs (associated with ESS)
SRRM1*	HNRNPA2B1*
SRRM2*	HNRNPUL2 *
SRSF7*	HNRNPA3
SRSF6	HNRNPCL1

Figure C1.23 Proteomic and phosphoproteomic alterations in RNA splicing in macrophages after interaction with *C. albicans.* Schematic representation of the spliceosome (retrieved on Kegg Pathway on 16/05/19) together with the differentially abundant proteins and proteins with differentially phosphorylated peptides found in both studies. Proteins names are color coded (red for more abundant and green for less abundant). Phosphorylation data is represented by the symbol *. It is also color coded (red for protein with more abundant phosphopeptides and green for protein with less abundant phosphopeptides). ESE means exonic splicing enhancers and ESS means exonic splicing silencers.U1, U2 U4/U6 and U5 are small nuclear ribonucleoprotein complexes that form the spliceosome.

A previous study showed some genes involved in RNA processing to be down-regulated after THP1 monocytes co-culture with *C. albicans* (Barker *et al.*, 2005). Remarkably, Muñoz and co-workers were recently interested in the host and *C. albicans* transcriptional dynamics (Munoz *et al.*, 2019). They used single cell RNA-sequencing for both host and pathogen different subpopulations. Besides other analysis, they calculated the frequency of previously annotated splicing events and identified differential isoform usage between infected macrophages. They detected differential splicing between macrophages in 144 genes, among them Dectin-2. The authors point that these events may indicate different potentials to respond to fungal infections (Munoz *et al.*, 2019). Interestingly, our proteomic and phosphoproteomic data suggests RNA splicing as a process highly affected in *C. albicans* infected macrophages. It is not clear yet if this is a host or a pathogen-driven process and the importance of this to the outcome of the infection. Further studies should be addressed in order to look into the proteins that maybe alternatively spliced and analyze their importance in killing this pathogen. Another striking fact was noticing that most of the infection scenarios where RNA splicing was previously found to be altered were

in macrophages infected with virus and some facultative intracellular bacteria which are known to use the host machinery in their favor. This should be addressed in the future to try to gain comprehensive understanding of the regulatory networks that are similar and different in the host response to *Candida* and other microbial infections.

From all the proteins found in both approaches, the splicing factor subunit SF3A1 came to our attention because it was found to be less abundant but more phosphorylated in a phosphopeptide with unknown function during macrophage interaction with *C. albicans*. The role of this protein in the regulation of mRNA splicing and a connection with innate immune system was previously investigated. O'Connor and co-workers showed that inhibition of SF3A1 in the presence of LPS diminished production of numerous cytokines and chemokines (O'Connor *et al.*, 2015). They also found that innate immune signaling pathways were among the most significantly altered pathways at the level of mRNA splicing when SF3A1 is inhibited. They showed that SF3A acts to promotes inflammation in part by inhibiting the production of a negatively acting splice form of the TLR signaling adaptor MyD88 (O'Connor *et al.*, 2015). It would be interesting to investigate the role of this protein during macrophage and *C. albicans* and discover the specific role of the phosphopeptide differentially quantified. We believe that more functional studies are necessary to define the role of splicing in the macrophage response to *C. albicans.*

Regarding protein translational process, in the ATP binding enrichment approach, we observed an increase in ribosomal proteins, such as RPS26, RPL3, RPL9 and DDX21. The other approach showed an increase in the phosphorylation of two proteins of the ribosome (RBM10 and RPL23A) together with a decrease of the phosphorylation of translational inhibitor EIF4ENIF1. EEF2K, known to reduce protein synthesis, was more phosphorylated. A general increase in these ribosomal proteins may be a mechanism of the host cells to meet the increasing need of proteins and of new protein isoforms to fight the fungal infection.

5 Macrophage cell death and inflammatory response to *C. albicans*

In the ATP binding enrichment approach, we observed enrichment of proteins related to apoptosis. We found that anti-apoptotic signals were up-regulated in THP-1 macrophages infected with *C. albicans*, as compared to pro-apoptotic signals. Knowing that caspase-3 is one of the executioners of apoptosis, we measured its cleavage by Western blotting and no cleavage of this protein was observed after THP-1 macrophage interaction with *C. albicans* (McIlwain *et al.*, 2013). A previous work from our research group reported no apoptosis in RAW 264.7 macrophages incubated with *C. albicans* (Reales-Calderon *et al.*, 2013).The way by which macrophages activate cell death mechanisms as a consequence of uptaking *C. albicans* cells has

been studied previously. Uwamahoro and co-workers showed that *C. albicans* triggers pyroptosis during the first 6 to 8 h of interaction (Uwamahoro *et al.*, 2014). In concordance to our results, they observed no evidence of activation of caspase-3 by *C. albicans* early post-infection. More recently, another group suggested that neutralization of the phagosome by *C. albicans* is an important signal in activating the macrophage inflammasome (Vylkova & Lorenz, 2017). The pro-inflammatory cytokine IL-1β is released as a result of *C. albicans* driven NL3PR inflammasome activation and has been used as a measurement of pyroptotic cell death in the immune cell in response to microbial pathogens (Wellington *et al.*, 2012, O'Meara *et al.*, 2015, Vylkova & Lorenz, 2017). An increase of this cytokine was observed also in our conditions of interaction with *C. albicans*, suggesting that pyroptosis could be activated in response to *C. albicans*. However, further validation confirming caspase-1-dependent IL-1β release would be needed to confirm this phenomenon in this cell line. We were also interested in knowing whether other pro-inflammatory cytokines were secreted. Both TNF-α and IL-12 were significantly more secreted after 3 h of interaction with *C. albicans*. This pathogen is known to trigger a pro-inflammatory response of the macrophages, including the release of these cytokines (Netea *et al.*, 2008). The IPA software was used to predict upstream regulators that could help us finding other regulators of the pro-inflammatory response. This analysis is based on prior knowledge of expected effects between transcriptional regulators and their target genes that are stored in Ingenuity® Knowledge Base (taking into account previously published datasets derived from different animal models) (Kramer *et al.*, 2014). Our analysis revealed 15 regulators with a significant overlap between our dataset and the genes that are regulated by a transcription regulator. In order to validate some of these predictions, we evaluated the secretion of IL-6 and the activation of miR-21 and miR-124. The analysis performed by IPA presented a negative activation z-score of IL-6 and in accordance with this, no secretion of IL-6 was observed. IL-6 is a pro-inflammatory cytokine and was previously observed not to be secreted after interaction with *C. albicans* (Reales-Calderon *et al.*, 2014, Estrada-Mata *et al.*, 2015). Recently, mi-RNAs have been implicated in immune response, particularly as post-transcriptional regulators of the inflammatory response. There are several mi-RNAs that regulate TLR signaling pathways. Monk and co-workers showed that miR-155, miR-146a, miR-146b, miR-125a and miR-455 were upregulated after treatment with LPS and after interaction with heat killed *C. albicans* cells (Monk *et al.*, 2010). Another group was interested in the impact of *C. albicans* cell morphology (heat killed yeast and hyphal cells) in the differential regulation of host mi-RNAs (Agustinho *et al.*, 2016). They suggested that Dectin-1 may be orchestrating miR-155 up-regulation in a SYK-dependent manner. Since our proteomic approach was performed with live *C. albicans* cells, we investigated the differential mi-RNAs

regulation upon interaction with live *Candida* cells. The selected mi-RNAs were those predicted to be up-regulated by IPA (miR-21 and miR-124) and those found to be induced upon LPS activation and after interaction with heat killed *C. albicans* cells (miR-146 and miR-155) (Taganov *et al.*, 2006). Because we used live cells, our time points were shorter than others. We found that miR-21 and miR-124 were slightly, but not significantly, up-regulated after treatment with LPS. After interaction with *C. albicans*, none of these mi-RNAs were statistically significant upregulated. In our conditions and time points, the results were different from the predicted by IPA. Both miR-146 and miR-155 were confirmed to be upregulated after macrophage treatment with LPS. This was in concordance with the other work where miR-146 was shown to be involved in the mechanism of negative feedback regulation of TLR (Taganov *et al.*, 2006). Interestingly, after macrophage interaction with live *C. albicans* cells no upregulation of these mi-RNAs was observed at these time points. Although longer time points would be needed to determine whether this behavior is maintained, we can hypothesize that these miR were not yet activated because macrophages might need a much higher pro-inflammatory response to kill *C. albicans*, or because this fungus may be inducing a longer pro-inflammatory response to destroy the macrophage. The inflammatory effect induced by live *C. albicans* cells was previously suggested by our group as virulence trait responsible for tissue damage in the host (Martinez-Solano *et al.*, 2009, Reales-Calderon *et al.*, 2013). It is important to underscore the need of follow-up studies to reveal whether this is a host-driven or pathogen-driven mechanism.

In conclusion, the ATP-binding enrichment together with the global proteomic and phosphoproteomic approaches revealed new insights in macrophage remodeling after interaction with this pathogen. Here we suggest some of them (Figure C1.24):

- Phosphorylation of the mannose receptor (MR) which is known to be PRR of *C. albicans* mannans.
- Increase in the phosphorylation of proteins implicated in cytoskeleton rearrangement, such as FYN, which occurs after *C. albicans* phagocytosis
- Proteins differentially abundant of the mitochondria were quantified together with an increase in the membrane mitochondrial potential ($\Delta\psi m$), although not statistically significant, which was previously described to lead to the production of ROS in order to kill the pathogen.
- A striking number of differentially abundant proteins (mainly less abundant) and of differentially phosphorylated (mainly more phosphorylated) involved in RNA splicing was observed which indicates that this process is being highly affected by *C. albicans.*

- An increase in the abundance of proteins involved in protein synthesis was observed together with a decrease in proteolysis which may be a mechanism of the macrophage to meet the need of proteins to fight the fungal infection and to produce more protein isoforms.

- An increase in anti-apoptotic signals over pro-apoptotic signals was observed. Furthermore the production of IL-1β suggests, as previously described that macrophages could be dying by pyroptosis.

- High pro-inflammatory response was observed by the production of several pro-inflammatory cytokines such as TNF-α and IL-12 together with the lack of activation of mi-RNA involved in the regulation of the pro-inflammatory response.

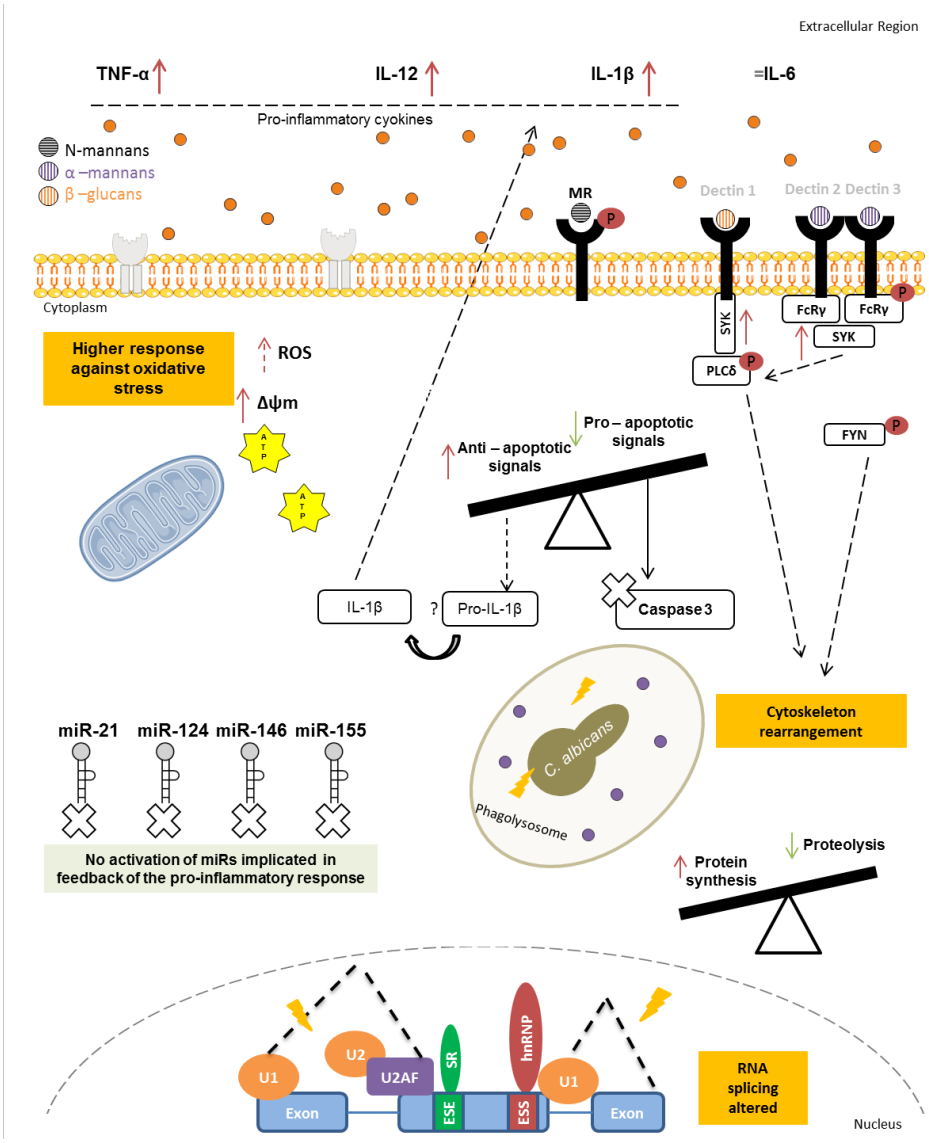

Figure C1.24 Schematic overview of macrophage possible remodeling after interaction with *C. albicans*. The differentially abundant proteins, together with the cytokines, are color coded with red for more abundant and green for less abundant after macrophage interaction with *C. albicans*. Proteins with a P circled in red represent proteins with more abundant phosphopeptides. Cytokines and miR that do not present differences after interaction are depicted in grey. Dotted arrows represent suggested connections. Δψm means membrane mitochondrial potential. More details describing some of the processes suggested to be remodeled after interaction in the text.

CHAPTER 2

Immunoproteomic study of the *Candida albicans* hyphal secretome for the discovery of diagnostic biomarker candidates of invasive candidiasis

*This Chapter contains supplementary tables, numbered from Supplementary Table C2.1 to C2.4, which are available in the enclosed CD.

Introduction

As previously commented, *C. albicans* is a polymorphic fungus. Depending on the growth conditions it can vary among yeast, pseudohyphae and hyphae morphologies. In experimental infections, patient biopsies and in histological analysis hyphae are the most observed morphology of this fungus which is frequently linked to their better ability to adhere and invade than yeast cells. Yeast cells are usually associated to bloodstream dispersion (Wilson *et al.*, 2016).

There are several important risk factors for *Candida* infections:

- Continued treatment with broad spectrum antibiotics, which increases *Candida* gut colonization.
- Breach of the gastrointestinal and cutaneous barriers, by organ transplant, central venous catheters, which collectively enable *Candida* cells to translocate from mucocutaneous sites into the bloodstream.
- Iatrogenic immunosuppression, such as chemotherapy or corticosteroid therapy, which decreases innate immune defences in tissues, facilitating *Candida* invasion from the bloodstream into organs (Pappas *et al.*, 2018).

It is known that colonization is a prerequisite to acquire these infections, being responsible for the majority of IC cases (Nucci & Anaissie, 2001). Furthermore, catheter-related bloodstream infections are common and present life-threatening complications (Phua *et al.*, 2019).

High morbidity and mortality can be attributed in some extent to the difficulty in its early and accurate diagnosis. Early detection is therefore essential to increase the possibility of a better and successful antifungal therapy, leading to a better outcome of the disease. The gold standard for diagnosing these infections is still blood culture with subsequent species identification by different methods, such as MALDI-TOF (reviewed in (Posch *et al.*, 2017)). This is considered a sensitive method only for the detection of viable cells especially at later stages of the infection, but it is not useful for the diagnosis of deep-seated candidiasis that is not accompanied by candidemia, and it can take 2-5 days to achieve a conclusive result. Direct observation of *C. albicans* in tissue (tissue histopathology) is also used but it is an invasive method for ICU patients. There is a general effort being made for the discovery of biomarkers, including the detection of biomolecules both from pathogen and from the host. These can be used as a faster diagnostic method once there is no need to culture the microorganism (reviewed in (Pitarch *et al.*, 2018)). Non-culture methods mainly include the detection of *Candida* mannans and 1,3 β-D-glucans as well as the detection of host derived biomarkers such as human antibodies against *Candida* antigens (proteins and carbohydrates) (Clancy & Nguyen, 2013). PCR-based technologies are also used for *Candida* DNA amplification. These last ones represent non-culture methods with

high specificity and sensitivity, but lack standardization protocols (Pfaller & Castanheira, 2016). The T2 Magnetic Resonance (T2MR®) is a new class of infectious disease diagnostic method. This method amplifies DNA using a thermostable polymerase and target specific primers, and detects the amplified products by amplicon-induced agglomeration of magnetic particles and T2MR measurement. It detects the 5 most common pathogenic *Candida* species and has shown a sensitivity of 89% and specificity of 98% (Mylonakis *et al.*, 2015, Clancy & Nguyen, 2018). However, this method has some drawbacks such as elevated costs, quick expiration date of its reagents and its sensitivity may decrease in the absence of intact *Candida* cells in whole-blood samples (Neely *et al.*, 2013).

Immunoproteomics is a widely used technique to screen for panels of biomarkers of infectious diseases. It enables the characterization of the pathogen immunome, which is a subset of the proteome that is a target for the immune system (Pitarch *et al.*, 2006). This approach involves the separation of the proteins by 2-DE, their electroblotting to a membrane, incubation with sera from different patients and further identification of protein spots by MALDI-TOF-MS. Our group has been taking advantage of this technique and making an effort to develop new biomarkers of invasive candidiasis (IC) and also to remark that using multiple biomarkers should be the path to choose for the development of better diagnosis (Pitarch *et al.*, 2006, Pitarch *et al.*, 2011, Pitarch *et al.*, 2014, Pitarch *et al.*, 2016). Previously, our group showed that serum anti-Bgl2, anti-Eno1 and anti-Pgk1 antibodies are biomarker candidates of IC (Pitarch *et al.*, 2004, Pitarch *et al.*, 2006). Also, our group developed and validated an antibody set for IC prognosis against the *C. albicans* proteins Ssb1, Gap1/Tdh3, Pgk1 and Met6 (Pitarch *et al.*, 2011). In another work, it was suggested that serum IgG antibody directed against Hsp90 and Eno1 may be useful for IC diagnosis in non-neutropenic patients (Pitarch *et al.*, 2014). The majority of immunoproteomic studies for the search of new biomarkers for IC were performed with intracellular proteins or proteins from the cell surface of *C. albicans* (Pitarch *et al.*, 2004, Pitarch *et al.*, 2006). A recent immunoproteomic study presented a 2-DE based secretome analysis of *C. albicans* in yeast to hyphae transition and showed a higher number of proteins identified in the hyphal form (Luo *et al.*, 2016). These proteins presented more immunogenicity than the yeast derived ones. This study, although using a reduced number of sera, identified a core set of 19 antibodies against secreted proteins of *C. albicans,* seven of which could represent potential diagnostic markers for candidemia (Xog1, Lip4, Asc1, Met6, Tsa1, Tpi1, and Prx1) (Luo *et al.*, 2016).

C. albicans secretes proteins with different functions, among them: secreted aspartyl proteases (Saps) that degrade host tissues; Pra1 and Zrt1 that sequester ions (Citiulo *et al.*, 2012). Moreover, these proteins were shown to interact with the host (Wu *et al.*, 2013). Proteins can be

secreted either by the classical secretory pathway or by non-classical pathways (Nombela *et al.*, 2006, Gil-Bona *et al.*, 2015). Recently, our group described the secretion of classical cytoplasmic proteins, lacking signal peptide, inside EVs. Some of these proteins were moonlighting, meaning they have different functions depending on their location (Gil-Bona *et al.*, 2015). Fungal vesicles were also shown to interact with the host (Nimrichter *et al.*, 2016). In this way, it is important to underline the potential of these secreted proteins as biomarkers for the diagnosis of IC. With the ultimate purpose of developing new biomarkers that help in a better and faster diagnosis which is essential for a quicker implementation of appropriate therapeutics, here we propose:

- To perform the proteomic analysis of *C. albicans* hyphal secretome.
- To characterize of the serological response to the *C. albicans* hyphal secretome in patients with IC, associated or not with catheter.
- To identify biomarker candidates for the diagnosis of invasive candidiasis.

Materials and Methods

1 Hyphal *C. albicans* secretome extraction

1.1 Microorganism and growth conditions

C. albicans strain SC5314 was used in this study and maintained in YPD plates (20 g/L glucose, 10 g/L yeast extract, 20 g/L peptone and 20 g/L agar) at 30º C. To set up the best conditions for secretome extraction, cells from a *C. albicans* colony were grown overnight in SD medium supplemented with amino acids (20 g/L of glucose, 5 g/L of ammonium sulfate, 1.7 g/L of nitrogen base, 1.92 g/L of amino acids mix without uracil, 0.1g/L of uracil) on a rotatory shaker at 180 rpm and 30 ºC. OD was measured and pre-inoculum was adjusted to 0.1 and incubated for 6 h. Cells were recovered, washed in phosphate buffer saline (PBS) and counted in Neubauer chamber. Then, $5x10^5$ cells/ml were incubated during 18 h at 180 rpm and 37ºC in three different media, for the selection of the best one:

-YNBS medium (5 g/L of ammonium sulfate, 1.7 g/L of nitrogen base, 20 g/L of sucrose, and 75mM 3-(N-morpholino) propanesulfonic acid (MOPS), pH 7.4) supplemented with 5 M of N-acetylglucosamine (GlcNac) (Sorgo *et al.*, 2010). This medium will be named as YNBS + GlcNac medium.

-Salt medium (4.5 g/L NaCl, 0.85 g/L yeast nitrogen base, 2.5 g/L ammonium sulfate, pH 7.4) supplemented with 2.5 mM GlcNac (Yin, 2008). This medium will be named as Salt + GlcNac medium.

-Lee medium pH 6.7 (MgSO4 0.2 g/L; K_2HPO_4 2.5g/L; $(NH_4)_2SO_4$ 5 g/L; NaCl 5 g/L; L-alanine 0.5 g/L; L-leucine 1.3 g/L; L-lysine 1 g/L; L-methionine 0.1 g/L; L-ornithine 0.07 g/L; L-phenylalanine 0.5 g/L; L-proline 0.5 g/L; L-threonine 0.5 g/L; glucose (50%) 25 ml/L; biotin (0.01%) 10 ml/L) (Lee *et al.*, 1975). This medium will be named as Lee medium (pH 6.7).

1.2 Isolation of secreted proteins

After optimizing the best conditions ten secretome extractions, each one using 2.5 L of Lee medium, were performed. For that, cells were grown as previously explained. After 18 h incubation at 37ºC, at 100 rpm, to reduce cell breakage, cells were centrifuged at 5000 rpm for 40 min (no break used in the centrifugation) at 4ºC and the supernatant recovered. From this moment forward all steps were performed on ice. Hypha morphology was confirmed by microscopy and cell lysis by propidium iodide (PI) staining. The supernatant was double filtered (0.45 µm low protein binding, Millipore) to eliminate cells that were not removed by centrifugation. One tablet of proteases inhibitors dissolved in MiliQ water and 0.1 M phenylmethanesulfonyl fluoride (PMSF) were added to the filtrate. One ml of the filtrate was plated and when more than one colony grew on YPD plates the supernatant was discarded.

Supernatant containing the secreted proteins was concentrated approximately 100 times using centrifugal filter devices (Centricon Plus-70 10 kDa pore, Millipore). The supernatant was frozen until precipitation. Precipitation was performed by incubation of the sample with a fourth part of trichloroacetic acid (100% w/v) during 1 h in ice. Then, it was centrifuged at 10 000 g for 30 min at 4ºC. Supernatant was discarded and ultrapure water was added to the pellet and vortexed. After this, chilled washing buffer from the 2D Clean Up kit (GE Healthcare) was added with 5 µl of wash additive, vortexed and left at -20 ºC overnight. In the next day, the sample was centrifuged, and the supernatant discarded. The pellet was dried, no longer than 5 minutes, and resuspended in rehydration buffer (urea 7 M; thiourea 2 M; 2% 3-[(3-Cholamidopropyl) dimethylammonio]-1-propanesulfonate hydrate (CHAPS)). A summary of the secretome extraction procedure is represented in Figure C2.1

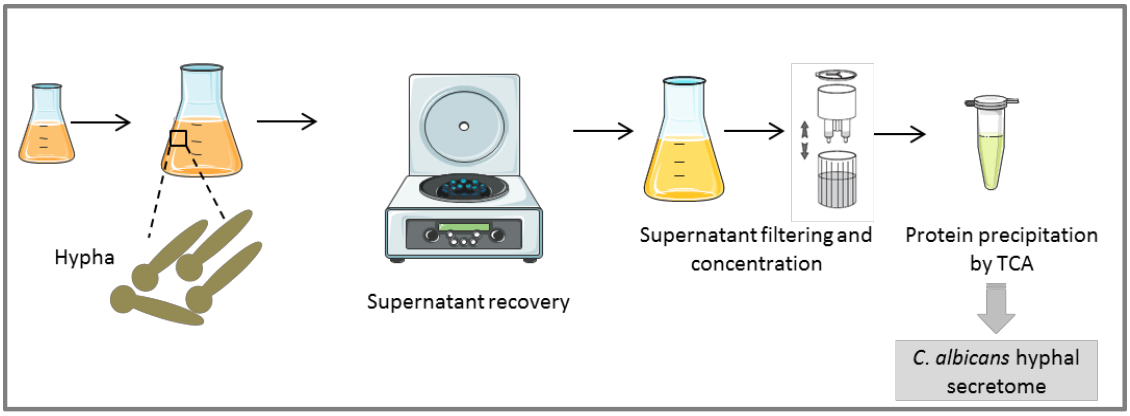

Figure C2.1 Schematic overview of secretome extraction procedure. *C .albicans* cells were grown during 18 h, at 100 rpm and at 37 ºC. The supernatant recovered, filtered and concentrated using centrifugal filter devices. Proteins were precipitated by TCA and quantified.

2 Protein analysis by SDS-PAGE

2.1 One-Dimensional Gel Electrophoresis

The protein pattern of the different secretomes extracted was compared by SDS-PAGE in a 10% polyacrylamide gel. Gel was stained using the Coomassie blue method. Briefly, gel was fixed with a fixing solution (50% methanol and 10% glacial acetic acid). Then, it was stained 1 h at room temperature with agitation with a staining solution (0.1% Coomassie brilliant blue R-250, 50% methanol, 10% glacial acetic acid) and destained with a destaining solution (40% methanol and 10% acetic glacial solution). Silver staining was used after Coomassie blue destaining. For that, a kit was used (BioRad). Briefly, gel was incubated in oxidizer solution for 20 min. Then, washed three times in MiliQ water (10 min each washing). After this, the gel was incubated in silver reagent for 20 min and washed once with MiliQ water. The developer solution was used several times until bands were developed. Different secretomes were pooled in two batches (S1 and S2).

2.2 Two-Dimensional Gel Electrophoresis (2-DE) and Immunoblot Analysis

2-DE was carried out adapting the protocol from previous works (Pitarch *et al.*, 2006, Luo *et al.*, 2016). The amount of 100 µg of protein was actively rehydrated in 7 cm IPG strips (Immobiline DryStrip, GE Healthcare) that covered a pH range of 3-11 (NL). Isoelectric focusing was performed using IPGphor device (Amersham Biosciences) and the following program was used for analytical gels: (i) 30 V, 3.5 h, step and hold (ii) 60 V, 3.5 h, step and hold; (iii) 300 V, 3 h, gradient; (iv) 600 V, 4 h, gradient; (v) 1000 V, 4 h, gradient; (vi) 8000 V, 4 h, gradient; (vii) 8000 V, 6 h, step and hold and (viii) 500 V, step and hold. 190 µg of protein were used for preparative gels. A similar program was selected for the isoelectric focusing for the preparative gels. The only modification was at step (vi) where the proteins were at 8000 V for 9.5 h, step and hold. IPG strips were

reduced and alkylated. For that, strips were incubating first in balancing solution (Tris-HCl 50 mM, pH 6.5; urea 6 M, glycerol 30%; SDS 2%) with DTT 20 mg/ml during 30 min in agitation and then with iodoacetamide 25 mg/ml during 30 min with agitation. The second dimension was carried out using a 10% polyacrylamide gel and in an electrophoresis unit (Bio Rad). The electrophoresis was carried out at 50 V. For protein spot identification by MALDI-TOF MS the preparative gel was stained with colloidal Coomassie blue (Dyballa & Metzger, 2009). Briefly, proteins were fixed to the gel with a fixing solution (50% methanol, 2% phosphoric acid) during 30 min, then, the gel was washed with distilled water twice during 10 min each, and the gel was equilibrated using an equilibrating solution (33% methanol, 3% phosphoric acid, 17% ammonium sulfate) during 40 min. Then, a Coomassie brilliant blue G-250 6.6% solution in methanol was added to reach 0.066% of dye. After an overnight incubation, the dye excess was eliminated with successive washes with distillate water.

For Western blotting, after electrophoresis, proteins were transferred to a nitrocellulose membrane (GE Healthcare) at 100 V for 1 h. Blots were then stained with Sypro™ Ruby Protein Blot Stain, following manufacturer instructions. Membranes were scanned using Typhon scanner (GE Healthcare) for Sypro Ruby staining (488 nm, 610 BP30, PMT between 400 and 600, sensitivity normal). After staining, membranes were blocked overnight in PBS with 5% of skin milk at 4 ºC with agitation. Membranes were incubated with the different human serum pools (detailed below) at three dilutions 1:500, 1:250 and 1:100 (in TPBS - PBS with 0.1% Tween) for 2 h at room temperature with gentle agitation. After 4 washing steps (20 min each) with TPBS, membranes were incubated with IRDye 800 W conjugated goat (polyclonal) anti-human IgG antibody (LI-COR Biosciences) at a dilution of 1:5000 during 1 h at room temperature with gentle agitation. After 4 washing steps with TPBS (15 min each) Odyssey system was used to detect the fluorescence signals.

2.3 Serum samples

Sera were obtained through a collaboration with Professor Uwe Groß, Oliver Bader and Emilia Gomez from the Institute for Medical Microbiology, University Medical Center Göttingen in Germany. Serum samples were classified and pooled in three groups:

(i) Group 1-12 sera from patients with non-catheter associated IC

(ii) Group 2-11 sera from patients with catheter associated IC

(iii) Group 3-11 patients without IC from similar hospital wards as the infected ones.

Although lacking the exact source where the patients acquired the infection, *C. albicans* isolation site was known. In this way, if it was from blood, a sterile liquid or organ, the serum was pooled in

the first group. In case it was isolated from catheter it was pooled in the second group. Regarding the control group an effort was made to have patients from the same hospital ward as the other two groups. The use of these sera in diagnostic research areas has ethical clearance and was approved by the University Ethics Committee (Evaluierung serologischer Marker für die Diagnostik invasiver Mykosen".UMG-17/9/08). Sera were stored at -80ºC until use. Detailed clinical information is shown in Table C2.1.

Table C2.1 Characteristics of the subjects included in this study.

	Age	Sex	Hospital Ward	*C. albicans* isolation site
Group 1 Non-catheter associated IC	44	female	anaesthesiology	swab intraperitoneal
	76	male	anaesthesiology	swab abdominal zone
	41	male	anaesthesiology	blood culture
	68	female	general surgery	pleura
	61	male	general surgery	swab thorax
	29	male	general surgery	blood culture
	19	female	neurology	abdomen
	63	male	neurology	blood culture
	87	female	oral and maxillofacial surgery	tissue peritoneum
	74	female	oral and maxillofacial surgery	blood culture
	80	female	thoracic and cardiovascular surgery	blood culture
	72	male	thoracic and cardiovascular surgery	swab pleura
	Age	**Sex**	**Hospital Ward**	***C. albicans* isolation site**
Group 2 Catheter associated IC	73	female	anaesthesiology	venous catheter
	57	male	anaesthesiology	central venous catheter
	42	male	anaesthesiology	central venous catheter
	33	male	anaesthesiology	central venous catheter
	71	male	general surgery	venous catheter
	27	male	general surgery	urine catheter
	76	female	neurology	venous catheter
	46	female	neurology	central venous catheter
	82	male	neurology	catheter
	70	male	neurology	venous catheter
	70	male	neurology	venous catheter tip
	Age	**Sex**	**Hospital Ward**	
Group 3 Control Patients	78	male	anaesthesiology	
	54	female	neurology	
	42	female	neurology	
	67	male	neurology	
	29	male	neurology	
	58	female	trauma surgery	
	46	female	trauma surgery	
	43	female	trauma surgery	
	69	male	trauma surgery	
	33	male	trauma surgery	
	21	male	trauma surgery	

3 ELISA for IgG antibody quantification against the hyphal *C. albicans* secretome

Indirect ELISA was performed as described previously (Pitarch *et al.*, 2008, Huertas *et al.*, 2017) for measuring the serum IgG antibodies against hyphal *C. albicans* secretome. For the coating step, 5 µg/ml of hyphal *C. albicans* secretome in 0.1 M carbonate/sodium bicarbonate pH 9.6 buffer was incubated overnight at 4ºC, and then washed three times with washing buffer (PBS with 0.05% Tween - 20). Wells were then blocked with blocking buffer (PBS with BSA 1%) for 2 h at 37 ºC. After this step, wells were washed three times with washing buffer and incubated with serial dilutions (from 1:250 until 1:1024000) of the different serum pools for 2 h at 37 ºC. Sera serial dilutions were performed in assay buffer (PBS with 0.05% Tween and 0.1% BSA). After this, wells were thoroughly washed six times with washing buffer. Wells were then incubated with a secondary horseradish peroxidase (HRP)-labelled anti-human IgG antibody (GE Healthcare) at a dilution of 1:3000 in assay buffer at 37 ºC for 1 h and rinsed again three times. Then, wells were washed once with PBS and developed with *o*-phenylenediamine dihydrochloride tablets (SIGMAFAST^{TM} OPD, Sigma) at a final concentration of 0.4 mg/ml OPD, 0.4 mg/ml urea hydrogen peroxide, and 0.05 M phosphate-citrate, pH 5.0. These tablets are substrates of the horseradish peroxidase that was used to label the antihuman IgG antibodies. The reaction was stopped by the addition of 50 µl of 3 N sulfuric acid and read on a microplate reader at 490 nm (Bio-Rad). Background was defined in wells coated with *C. albicans* hyphal secretome to which the secondary antibody was added but the primary antibody not. The IgG reactive titer was defined as the inverse of the greatest dilution at which the optical density was twofold greater than the background (Clancy *et al.*, 2008). Antibody titers were $\log_2$ transformed to approximate normal distribution prior to data analysis. The differences in the mean $\log_2$ IgG titers were assessed using one-way ANOVA with Tukey's multiple comparison correction and p-value < 0.05 was considered significant.

4 Protein analysis by mass spectrometry (MS)

4.1 MALDI-TOF MS for protein spot identification

Protein spots of interest were manually excised from a preparative gel. Proteins selected for analysis were in-gel reduced, alkylated and digested with trypsin as previously described (Sechi & Chait, 2000). Briefly, samples were reduced with 10 mM dithioerytritol (DTE) in 25 mM ammonium bicarbonate for 30 min at 56 ºC and subsequently alkylated with 25 mM iodoacetamide in 25 mM ammonium bicarbonate for 15 min in the dark. Finally, samples were digested with 12.5 ng/µl sequencing grade trypsin (Roche) in 25 mM ammonium bicarbonate (pH 8.5) overnight at 37 ºC. After digestion, the supernatant was collected and 1 µl was spotted onto

a MALDI target plate and allowed to air-dry at room temperature. Then, 0.6 µl of a 3 mg/ml of α-cyano-4-hydroxycinnamic acid matrix (Sigma) in 50% acetonitrile were added to the dried peptide digest spots and allowed again to air-dry at room temperature. MALDI-TOF MS analyses were performed in a 4800 Plus Proteomics Analyzer MALDI-TOF mass spectrometer (Applied Biosystems) at the Proteomics Center from the Complutense University of Madrid. The MALDI-TOF operated in positive reflector mode with an accelerating voltage of 20000 V. All mass spectra were calibrated internally using peptides from the auto digestion of trypsin.

For protein identification *Candida* Genome Database (CGD) Assembly 22 (12421 sequences; 6015970 residues) was carried out using MASCOT 2.3 (www.matrixscience.com) through the software Global Protein Server v 3.6 (ABSciex). Search parameters were carbamidomethyl cysteine as fixed modification and oxidized methionine as variable modification; peptide mass tolerance, 100 ppm (PMF) and 1 missed trypsin cleavage site. In all protein identification, the probability scores were greater than the score fixed by Mascot as significant with a *p*-value < 0.05.

4.2 LC-MS/MS for secretome analysis

4.2.1 Protein digestion

Firstly, 20 µg of both secretome pools, S1 and S2, were in-gel digested. This digestion is performed by doing a one dimensional SDS-PAGE with a larger stacking gel. Protein bands were cut from the interface between stacking and resolving gel to carry out in gel trypsin digestion. Briefly, protein bands with the proteins were reduced with DTT, alkylated with iodoacetamide and digested with a 1/20 (w/w) ratio of recombinant trypsin (Roche) overnight at 37ºC, according to Sechi and Chait (Sechi & Chait, 2000). Finally, samples were freeze-dried in Speed-vac and resuspended in 2% ACN, 0.1% formic acid before the nano LC-MS/MS analysis. Samples were stored at -20 ºC until further analysis.

For the identification of the proteins from the upper left zone of the preparative 2-DE gel, four bands were cut and in-gel digested with trypsin, as detailed above.

4.2.2 MS analysis

Peptides were analyzed by reversed-phase liquid chromatography-electrospray ionization tandem mass spectrometry (RP-LC-ESI-MS/MS) in an EASY-nLC 1000 System coupled to the Q-Exactive HF mass spectrometer through the nano-Easy spray source (Thermo Scientific). Peptides were loaded first onto a Acclaim PepMap 100 Trapping column (Thermo Scientific, 20mm x 75 µm ID, 3 µm C18 resin with 100 Å pore size) using buffer A (mobile phase A: 2% acetonitrile and 0.1% formic acid) and then were separated and eluted on a C18 resin analytical column NTCC (Nikkyo Technos

Co., Ltd. de 150 mm x 75 µm ID, 3 µm C18 resin with 100 Å pore size) with an integrated spray tip. A 150 min gradient of 5% to 35% buffer B (100% acetonitrile, 0.1% formic acid) in buffer A at a constant flow rate of 250 nl/min was used. Data acquisition was performed with a Q-Exactive HF. Data were acquired using an ion spray voltage 1.8 KV and ion transfer temperature of 250 ºC. All data were acquired using data-dependent acquisition (DDA) and in positive mode with Xcalibur 4.0 software. For MS2 scan, the top 15 most abundant precursors with charges of 2 to 4+ in MS 1 scans were selected for higher energy collisional dissociation (HCD) fragmentation with a dynamic exclusion of 20 s. The MS1 scans were acquired at *m/z* range of 350–1600 Da with mass resolution of 60,000 and automatic gain control (AGC) target of 3E6 at a maximum ion time (ITmax) of 60 ms. The threshold to trigger MS2 scans was 2E3; the normalized collision energy (NCE) was 27%; the resolved fragments were scanned at mass resolution of 30,000 and AGC target value of 1E5 in a ITmax of 100 ms. This analysis was performed in the Proteomic Facility from the Complutense University of Madrid.

4.2.2 LC-MS/MS protein identification and database searches

Peptide identification from raw data was carried out using Mascot v.2.6.1 search engine through the Protein Discoverer 2.2 software (Thermo Scientific). A database search was performed against CGD Assembly 21 (6221 sequences). The following parameters were used for the searches: tryptic cleavage after Arg and Lys, up to two missed cleavage sites allowed, and tolerances of 10 ppm for precursor ions and 0.02 Da for MS/MS fragment ion. The searches were performed allowing optional methionine oxidation and methionine loss plus acetyl protein N-terminal and fixed carbamidomethylation of cysteine. Search against decoy database (integrated decoy approach) was used to FDR calculate. The Mascot scores were adjusted by the Mascot percolator algorithm. The acceptance criteria for protein identification were a FDR < 1% and at least one peptide identified with high confidence (CI>95%). Moreover, only proteins present in both replicates (S1 and S2) and identified with at least two peptides were selected for further analysis. The mass spectrometry proteomics data have been deposited to the ProteomeXchange Consortium via the PRIDE (Perez-Riverol *et al.*, 2019) partner repository with the dataset identifier PXD013933 and 10.6019/PXD013933.

4.2.3 Bioinformatic analysis of identified proteins

NSAF (normalized spectral abundance factor) was calculated for each protein (Zybailov *et al.*, 2006). CGD was the main database used for the functional classification. Signal peptide was predicted using SignalP4.1 (http://www.cbs.dtu.dk/services/SignalP/). For the prediction the

software bases on its prediction on a combination of several artificial neural networks. The presence of signal peptide was confirmed in CGD database. Venn diagrams were performed using the Venny 2.1 tool (http://bioinfogp.cnb.csic.es/tools/venny/). Glycosylation sites were predicted using NetNGlyc 1.0 Server Prediction (examines the sequence context of Asn-Xaa-Ser/Thr) and NetNGlyc 4.0 Server Prediction (produces predictions of the type GalNac *O*-glycosylation).

Results

1 Optimization of the conditions for *C. albicans* hyphal secretome extraction

To setup the best conditions for the isolation of *C. albicans* hyphal secretome, *C. albicans* was grown during 18 h in distinct mediums: YNBS + GlcNac, Salt medium+ GlcNac and Lee medium (pH 6.7). Two criteria were taken into account to choose the best medium: cell integrity measured by propidium iodide and the protein recovered after protein precipitation.

Regarding cell integrity, representative figures of propidium iodide measurements are shown in Figure C2.2. Propidium iodide is a fluorescent red probe that does no enter in live cells but when the cell membrane loses its integrity, it enters the cell and binds to the DNA. Due to the difficulty to calculate an accurate percentage of cell lysis, caused by the long filaments after 18 h of *C. albicans* growth, several photos were taken and cells counted when possible. Percentages were calculated based on that. After cell growth during 18 h in the different media, they presented around 5% of cell lysis in YNBS + GlcNac, around 3% in Salt medium +GlcNac and around 7% in Lee medium (pH 6.7).

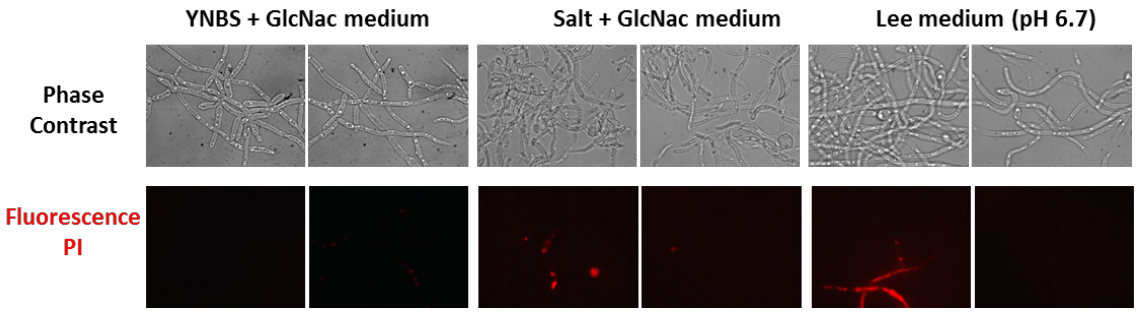

Figure C2.2 Optimization of the best conditions for extraction of secreted proteins from hyphal *C. albicans*. Morphology and cell lysis evaluation by PI measurement (red fluorescence) in the three different cell growth media used in this study: YNBS + GlcNac, Salt +GlcNac and Lee (pH 6.7).

Cell morphology was also evaluated. As demonstrated in Figure C2.2, in the three media hypha morphology was observed. After cell integrity measurements, secreted proteins were obtained from 500 ml of the different media, concentrated and quantified. In samples from the YNBS + GlcNac, a sediment appeared after supernatant concentration using the centrifugal filter units.

This did not allow protein recovery. Due to this problem this medium was excluded. Regarding the protein amount obtained from cells grown in the other media (Lee medium pH 6.7 and Salt medium + GlcNac) similar amounts of protein yield, 16.8 µg and 17.1 µg respectively, were obtained and the protein patterns are depicted in **Figure C2.3A**. In order to analyse the secreted proteins from these two media, proteins were digested with trypsin into peptides and analysed by MS. Q-TRAP was the mass spectrometer used and only one sample of each media was performed during this set up experiment. When analysing the proteins identified, a slightly higher number of proteins from Lee medium (pH 6.7) (115 proteins) was identified when compared with Salt medium + GlcNac (100 proteins). A total of 43 proteins were common to both media (**Figure C2.3B)**. Although in Lee medium (pH 6.7) there was a slightly higher percentage of cell lysis, analysis in SignalP 4.1 showed a higher percentage of secreted proteins with signal peptide (23.4%) than in Salt medium + GlcNac (2%) (**Table C2.2).** The identified proteins in each medium are indicated in **Table C2.2**. Due to the higher number of proteins with signal peptide, Lee medium (pH 6.7) was used for secretome extraction.

A

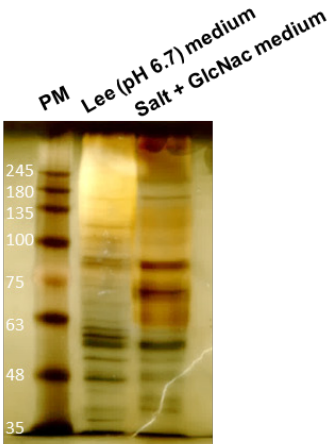

B

Medium	Protein Yield (from 500ml)	Unique Proteins Identified
Lee (pH 6.7)	16.8 µg	72
Salt + GlcNac	17.1 µg	57

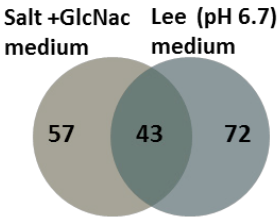

Figure C2.3 Analysis of secreted proteins after concentration and precipitation in Salt +GlcNac and Lee (pH 6.7) media. (A) Protein Pattern of the proteins extracted from Salt +GlcNac and Lee (pH 6.7) media. PM means protein marker. (B) Comparison of the protein yield and proteins identified in Salt + GlcNac and Lee (pH 6.7) medium and respective Venn diagram showing unique and shared proteins among both media. Gel was firstly stained with Coomassie blue then destained and Silver stained.

Table C2.2 Preliminary analysis of the secreted proteins identified after cell growth in Lee medium (pH 6.7) and Salt + GlcNac medium.

Lee Medium (pH 6.7)	Salt + GlcNac Medium
23.4% of Proteins with signal peptide	2% of proteins with signal peptide
Aat1, Acb1, Ado1,Als3, Ams1, Ape2, Arg1, Asc1, Bgl2, Bmh1, Cat1, Cdc19, Cip1, Cit1, Cof1, Coi1, Crd2, Crh11, Csa2, Csh1, Cyc1, Cyp1, Cyp5, Dag7, Ece1, Ecm33, Eno1, Erg20, Fba1, Fum11, Gcv3, Gcy1, Glr1, Glx3, Gnd1, Gpm1, Gre3, Grp2, Hbr2, Hex1, Hom2, Hpt1, Hsp70, Hxk2, Hyr1, Idi1, Ino1,	Acb1, Aco1, Ade12, Adh1, Ahp1, Ald5, Anb1, Ape2, Aro3, Aro4, Asn1, Asr2, Asr3, Atp2, Bat22, Cat1, Cdc19, Cef3, Cip1, Cmd1, Cof1, Csh1, Cyc1, Cyp1, Dak2, Eft2, Egd1, Egd2, Eno1, Erg10, Fba1, Fum12, Gcv3, Gdh3, Glk1, Glr1, Glx3, Gnd1, Gpm1, Grp2, Hem13, His1, Hom2, Hpt1, Hsp60, Hsp70, Hxk2,

Ipp1, Kar2, Lpd1, Mal2, Mbf1, Mcr1, Met6, Mmd1, Mp65, Ntf2, Orf19.1239, Orf19.1738.1, Orf19.1862, Orf19.2269, Orf19.2769, Orf19.3053, Orf19.3226, Orf19.3475, Orf19.3499, Orf19.4609, Orf19.5078, Orf19.6701, Orf19.715, Orf19.7214 Orf19.7322, Orf19.7578, Osm1, Pbr1, Pdc11, Pfy1, Pga4, Pga45, Pgi1, Pgk1, Pgm2, Phr1 Pmm1, Pra1, Rbp1, Rbt4, Rdi1, Rpl10a, Sah1, Sam2, Sap5, Sim1, Smt3, Snz1, Sod3, Sod5 Sol3, Ssa2, Sun41, Tal1, Tdh3, Tfs1, Tkl1, Tma19, Tos1, Tpi1, Tpm2, Trr1, Ttr1, Ubi3, Xog1, Ynk1, Yrb1, Zwf1	Idp1, Ilv5, Imh3, Ipp1, Kar2, Krs1, Mdg1, Mdh1-1, Met6, Nhp6a, Orf19.2244, Orf19.3475, Orf19.4216, Orf19.4609, Orf19.6147, Orf19.7215.3, Orf19.7263, Osm1, Pdc11, Pdi1, Pgi1, Pgk1, Pma1, Pmi1, Pmm1, Pst3, Rpl10a, Rpl12, Rpl82, Rpp2a, Rpp2b, Rps19a, Sah1, Ser1, Sod1, Ssa2, Ssc1, Sti1, Tal1, Tdh3, Thr4, Tif3, Tkl1, Tma19, Tpi1, Tpm2, Trr1 Tsa1b, Wh11, Xyl2, Ynk1, Yst1, Zwf1

Highlighted in yellow are proteins that presented signal peptide in both SignalP 4.1 and in *Candida* Genome Database (CGD).

2 Gel free LC-MS/MS analysis of the *C. albicans* hyphal secretome in Lee medium

After medium selection, the protocol was further optimized by reducing shaking conditions of cell growth and removing the centrifugation break in order to obtain minimal cell lysis.

Ten fluorescence images were taken before each secretome secretion to have an idea of the cell lysis percentage, which was lower than previously. Some representative fluorescence images are depicted in **Figure C2.4A.** Nevertheless, it is important to emphasize that the major objective of this work was not to do a thorough analysis of the *C. albicans* hyphal secretome but to have an enriched fraction of secreted proteins and study their immunogenicity. A Coomassie blue-stained gel with all secretome samples is presented in **Figure C2.4B**. Secretome protein patterns were very similar among the different replicates. The upper smear indicates the presence of glycosylated proteins. Secretomes were batched in two distinct samples (S1 and S2) and used for the different analysis.

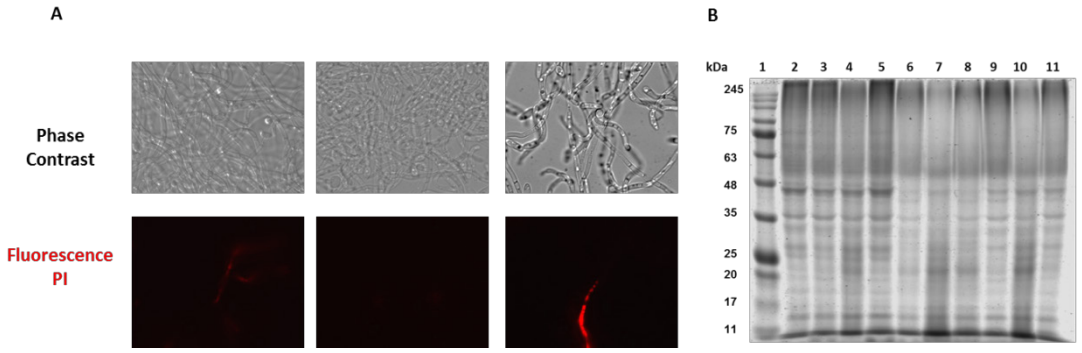

Figure C2.4 Secretome in Lee (pH 6.7) medium. (A) Representative fluorescence images from cell lysis measured using PI in secretome extraction performed in this study. (B) Coommassie blue stained gel with the different secretomes extracted. An ammount of 10ug of protein from each extraction was loaded in a 10% acrylamide/bis acrylamide gel. Lane 1 was loaded with the protein marker and Lane 2 to Lane 11 were loaded with the different secretomes extracted from 18 h culture of *C. albicans* in Lee medium (pH 6.7).

Secreted proteins from S1 and S2 were in-gel digested and further analysed by LC-MS/MS. With this analysis, 301 proteins were identified in both replicates and with at least 2 peptides (Supplementary Table C2.1). NSAF was used to rank proteins regarding their relative abundance within a particular run being its values between 0 and 1. The closer to 1 indicates the higher protein levels. Figure C2.5A represents the NSAF correlation between the proteins identified in both replicates and Figure C2.5B the protein ranking of the 50 more abundant proteins.

A

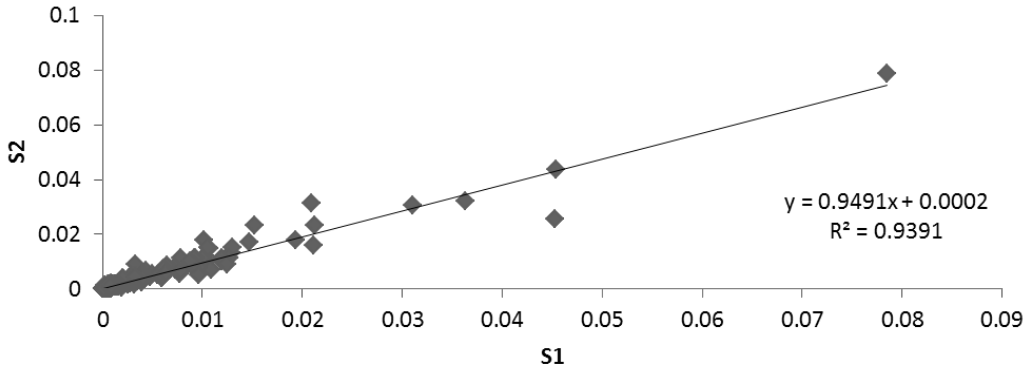

B

Rank	Systematic Name	Standard Name	Assembly 19/21 Identifier	NSAF	Signal peptide	Rank	Systematic Name	Standard Name	Assembly 19/21 Identifier	NSAF	Signal peptide
1	C1_08500C_A	Eno1	orf19.395	0.079		26	C5_00370W_A	Cof1	orf19.953.1	0.009	
2	C6_00750C_A	Pgk1	orf19.3651	0.045		27	C1_01350C_A	Tif	orf19.3324	0.009	
3	C6_03030W_A	Sap5	orf19.5585	0.035	x	28	C4_07180W_A	Ubi3	orf19.3087	0.009	
4	C7_02380C_A	Cyp1	orf19.6472	0.034		29	C4_06570C_A	Pdc11	orf19.2877	0.009	
5	C4_01750C_A	Fba1	orf19.4618	0.031		30	C5_04270C_A	Sah1	orf19.3911	0.009	
6	C2_10030C_A	Mp65	orf19.1779	0.026	x	31	C5_02860C_A	Grp2	orf19.4309	0.009	
7	C1_13860C_A	Gnd1	orf19.5024	0.022		32	C6_02240C_A	Rpl10a	orf19.3465	0.009	
8	C3_07440W_A	Tpi1	orf19.6745	0.019		33	C1_02480W_A	Pmm1	orf19.2937	0.008	
9	C3_06870W_A	Tdh3	orf19.6814	0.019		34	C2_08810C_A	Ipp1	orf19.3590	0.008	
10	C3_06180C_A	Tsa1	orf19.7417	0.019		35	C1_04300C_A	Ssa2	orf19.1065	0.008	
11	C4_03470C_A	Ece1	orf19.3374	0.016		36	C1_02590C_A	Snz1	orf19.2947	0.007	
12	C4_06980W_A	Pra1	orf19.3111	0.014	x	37	C7_02570C_A	Rbp1	orf19.6452	0.007	
13	CR_03720W_A	Tal1	orf19.4371	0.014		38	C1_13480W_A	Hsp70	orf19.4980	0.007	
14	C2_05460W_A	Cdc19	orf19.3575	0.013		39	C2_10110W_A	Cyc1	orf19.1770	0.007	
15	CR_10350C_A	Trx1	orf19.7611	0.013		40	C7_00750W_A	Acb1	orf19.7043.1	0.007	
16	C1_07900W_A	Coi1	orf19.5063	0.013	x	41	C1_03510C_A	orf19.3053	orf19.3053	0.007	
17	C1_08030W_A	Pfy1	orf19.5076	0.012		42	C4_02410C_A	Ahp1	orf19.2762	0.007	
18	C3_06360C_A	Cyp5	orf19.7421	0.012	x	43	C3_05000W_A	Rdi1	orf19.5968	0.006	
19	CR_06340C_A	Pgi1	orf19.3888	0.011		44	CR_10100C_A	Ino1	orf19.7585	0.006	
20	C1_03220C_A	Bmh1	orf19.3014	0.011		45	C1_13940W_A	Sim1	orf19.5032	0.006	x
21	C2_03270W_A	Gpm1	orf19.903	0.011		46	C1_02990C_A	Xog1	orf19.2990	0.006	x
22	CR_01620C_A	Met6	orf19.2551	0.010		47	C7_01250W_A	Asc1	orf19.6906	0.006	
23	CR_04510W_A	Hxk2	orf19.542	0.010		48	C1_03190C_A	Ecm33	orf19.3010.1	0.005	x
24	C5_02890W_A	Ynk1	orf19.4311	0.010		49	C2_03100W_A	Eft2	orf19.5788	0.005	
25	C7_00110W_A	Sod3	orf19.7111.1	0.010		50	C3_05130C_A	Thi4	orf19.5986	0.005	

Figure C2.5 Proteins identified in both samples (S1 and S2) with at least two peptides in the gel-free LC-MS/MS analysis. (A) Correlation of NSAFs from the proteins from both samples. (B) Protein ranking of the 50 most abundant proteins according to the NSAFs average of the two samples.

GO analysis of the identified proteins was also performed. The most significant biological process represented were carbohydrate metabolic process that includes both proteins involved in the glycolytic process such as Tdh3, Eno1 and Fba1 and proteins involved in cell wall polymers metabolism such as Cht3, Bgl2 and Kre9. Some of the other important processes in which the identified proteins were enriched are depicted in **Figure C2.6A**, such as:

- interaction with the host (Aco1, Als1, Cat1, Cdc19, Ece1, Eno1, Fba1, Gpm1, Hsp70, Kex1, Met6, Mp65, Pgk1, Pra1, Sap4, Ssa2, Ssb1, Tdh3, Tpi1, Tsa1, Tup1 and Yhb1);
- cellular response to oxidative stress (Ahp1, Cat1, Cip1, Crm1, Gcy1, Gnd1, Grx3, Mcr1, Mxr1, Orf19.2262, Orf19.3319, Orf19.4150, Orf19.518, Orf19.6816, Orf19.86, Pet9, Prx1, Pst2, Pst3, Sod1, Sod2, Sod3, Svf1, Tma19, Trr1, Trx1, Tsa1, Ttr1, Yhb1 and Ynk1);
- pathogenesis (Als1, Asc1, Bgl2, Bmh1, Cat1, Ece1, Ecm33, Het1, Hex1, Hsp90, Kex1, Leu2, Mbf1, Mnn2, Mnt1, Mp65, Msi3, Phr2, Pst2, Pst3, Rbe1, Rhd3, Sap4, Sap5, Slk19, Sod1, Tup1, Ttr1, Utr2, Vps21 and Yhb1).

Regarding their location in the cell, GO analysis showed an enrichment in proteins from the extracellular part of the cell (**Figure C2.6B**).

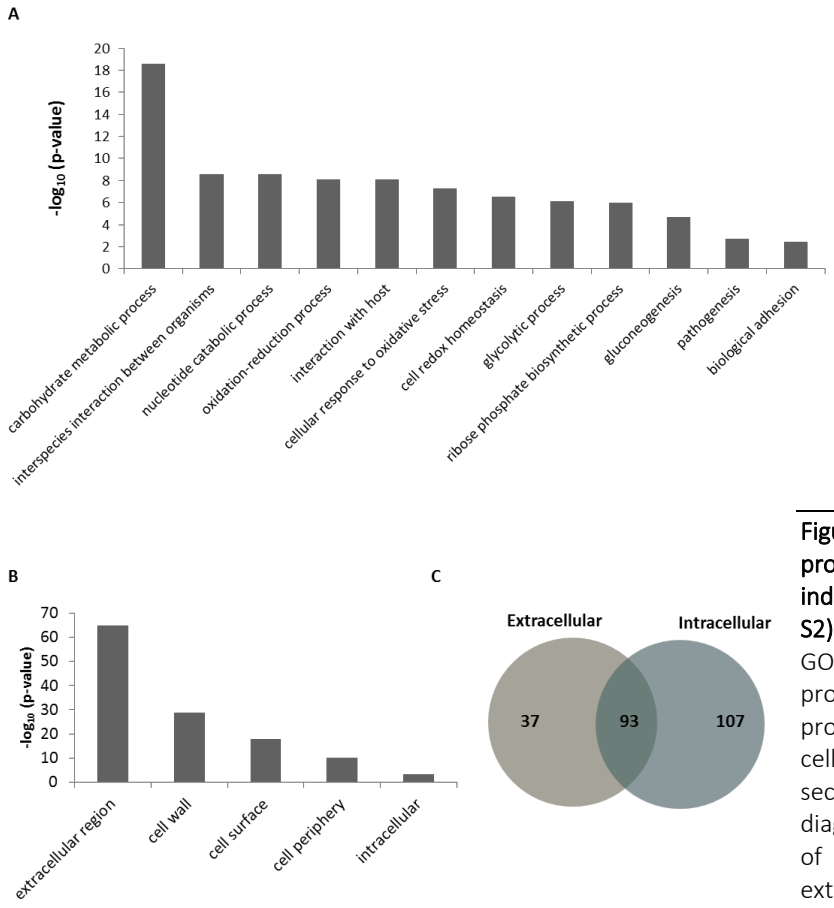

Figure C2.6 GO analysis of the proteins identified in in both independent replicates (S1 and S2) with at least 2 peptides. (A) GO enrichment in biological process of the secreted proteins. (B) GO enrichment in cellular component of the secreted proteins. (C) Venn diagram showing the number of proteins annotated as extracellular or intracellular and in both locations.

There were also proteins annotated in intracellular region or in both locations. Thus, a comparison between the proteins that were annotated in the extracellular and intracellular part of the cell was performed. As shown in the Venn diagram in **Figure C2.6C** and in **Table C2.3**, 37 proteins were annotated as present only in the extracellular region, 93 proteins were annotated in both localizations, and 107 proteins were annotated only in the inside of the cell.

Table C2.3 List of the identified proteins in both samples (S1 and S2) with at least two peptides classified regarding their localization: present in the extracellular regions (extracellular region, cell surface, cell wall and cell periphery), in the intracellular region, or present in both locations.

Proteins in:	No of Proteins	Protein Names
Extracellular region, cell surface, cell wall & cell periphery	37	Ade8, **Als1**, **Bgl2**, Cht1, Cht3, Cip1, Coi1, **Ece1**, **Ecm33**, Gcy1, **Grp2**, Hex1, Kre9, Mal2, Mdg1, Met15, **Mp65**, Nit3, Ofr1, Orf19.1394, Orf19.3053, Orf19.6809, Orf19.6867, Orf19.7322, Pga12, **Pga4**, **Pra1**, Pst2, Rbe1, Rbp1, Rhd3, **Sah1**, Sap10, Sap8, **Slk19**, Sol3, Xyl2
Intracellular	107	**Ade17**, Aha1, Ams1, Anb1, Arf2, Arg1, Arg3, Arg4, Aro2, **Asc1**, Bfr1, Bud7, Cit1, Cmd1, Cpr6, Crm1, Cyc1, Dtd2, Ecm4, Egd1, Eif4e, Erg10, Erg20, Etr1, Fbp1, Fum11, Gcv3, Grs1, Grx3, Het1, His1, Hom2, Hta3, **Hxk2**, Idh1, Kex1, Krs1, Lat1, Lsc1, Lys21, Mca1, Mcr1, **Mdh1**, Mmd1, Mrf1, Mxr1, Npt1, Ntf2, Orf19.1355, Orf19.1448.1, Orf19.1738.1, Orf19.1815, Orf19.2930, Orf19.3319, Orf19.3681, Orf19.3932, Orf19.4150, Orf19.4382, Orf19.4898, Orf19.518, Orf19.5322, Orf19.5943.1, Orf19.5961, Orf19.6559, Orf19.6596, Orf19.6701, Orf19.6872, Orf19.7152, **Orf19.7196**, **Orf19.7214**, Orf19.7297, Orf19.7330, Orf19.7368, Orf19.7404, Orf19.7531, Orf19.7578, Orf19.86, Orf19.904, Pol30, Rdi1, Rnr21, Rpl10a, Rpl12, Rpl30, Rpp0, Rps12, Rps19a, Rps21b, Rps22a, Sbp1, Sec14, Skp1, Sno1, Snz1, Sod2, Sod3, Sub2, Sui1, Tfs1, Thi4, **Tif1**, Tub1, Tub2, Tup1, Uba1, Yhb1, Ykt6
Shared	93	Aat21, Abp1, Acb1, **Aco1**, Ahp1, Ape3, **Atp1**, **Atp2,** Bmh1, Cam1, Cat1, **Cdc19**, Cdc3, Cof1, Cyp1, Cyp5, **Eft2**, Egd2, Emp24, Eng1, **Eno1**, **Fba1**, Fdh1, Gdh3, **Gnd1**, Gpd2, Gph1, **Gpm1**, Gsp1, **Hem13**, Hsp12, **Hsp70**, **Hsp90**, **Ino1**, **Ipp1**, Kel1, Leu2, Lpd1, Lsp1, **Mdh1-1**, **Met6**, Mir1, Mlc1, Mnt1, Orf19.1085, Orf19.1862, Orf19.1946, Orf19.3915, Orf19.4395, Orf19.4597, Orf19.5342, **Pdc11**, Pet9, Pfy1, **Pgi1**, **Pgk1**, Phr2, Pin3, Pmm1, **Por1**, **Prx1**, Pst3, Rho1, Rib3, Rpl14, Rpl6, Rps20, Sam2, Sap4, Sap5, Sec4, Sim1, Smt3, Sod1, Spe3, **Ssa2**, **Ssb1**, **Tal1**, **Tdh3**, Tma19, **Tpi1**, Tpm2, Trr1, Trx1, **Tsa1**, Ttr1, Ubi3, Ugp1, **Utr2**, Vps21, **Xog1**, Ynk1, Ypt1

CGD and its GO tool were used for this analysis. In bold proteins that were previously described as immunogenic (Torosantucci *et al*., 1993, Gil-Navarro *et al*., 1997, Martinez *et al*., 1998, Pardo *et al*., 2000, Pitarch *et al*., 1999, 2004, 2006, 2008, 2011, 2014, 2016, Mochon *et al*., 2010, Luo *et al*., 2016, (Giraldo, 2013). Highlighted in yellow are the proteins with signal peptide.

As expected, in the group of proteins classified as present in the extracellular region, 43% of the proteins presented signal peptide while in the group of proteins annotated as present in both locations 11% of the proteins present signal peptide. Unsurprisingly, only 4 proteins annotated as intracellular presented prediction of signal peptide and all of them corresponded to uncharacterized ORFs. Moreover, both proteins classified as present in the extracellular region

and in both location presented higher percentage of immunogenic proteins (27% and 31%, respectively) comparing to the ones located intracellularly (6.5%).

3 Antibody responses against *C. albicans* hyphal secretome in sera from patients with and without IC

Making an attempt to characterize the different anti-*Candida* hyphal secretome IgG antibody patterns, three different pools of sera from patients were compared. Twelve sera from patients with non-catheter associated IC (Group 1) were pooled whereas 11 sera from patients with catheter associated IC were pooled in another group. A third group of 11 sera from control patients, without IC, was also used. Clinical details of the patients or shown in **Table C2.1** (in Materials and Methods section). Serum IgG antibody levels against hyphal *C. albicans* secretome (both S1 and S2) were measured by indirect ELISA. As expected, both groups of patients with IC (associated and non-associated with catheters) presented higher IgG antibody levels against the *C. albicans* hyphal secretome than the group of control patients (**Figure C2.7A)**. Interestingly, the group of sera from patients with catheter associated IC showed higher levels of serum IgG antibody, but not statistically significant, against hyphal *C. albicans* secreted proteins than the group of sera from patients with non-catheter associated IC. IgG titers were measured for the three groups (**Figure C2.7B**). The mean $\log_2$ IgG titers were significantly higher in both groups with IC (14.5 for group 1 and 16.5 for group 2) than in group control (11.5) against *C. albicans* hyphal secretome.

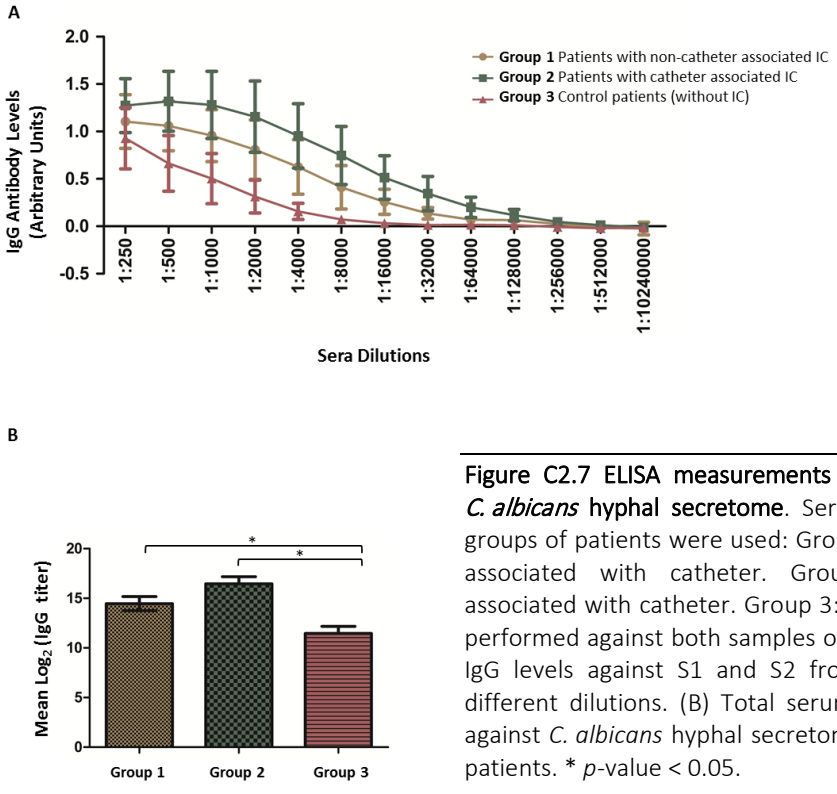

Figure C2.7 ELISA measurements of IgG antibodies against *C. albicans* hyphal secretome. Serum pools from the three groups of patients were used: Group 1: patients with IC non-associated with catheter. Group 2: Patients with IC associated with catheter. Group 3: patients control. This was performed against both samples of secretome S1 and S2. (A) IgG levels against S1 and S2 from the different pools at different dilutions. (B) Total serum titers of IgG antibodies against *C. albicans* hyphal secretome in groups 1, 2 and 3 of patients. * *p*-value < 0.05.

This prompted us to further analyze the serological response from different patient groups, using immunoproteomics. After separating the secreted proteins by 2-DE gels, they were blotted into a nitrocellulose membrane and stained using Sypro staining. After confirming protein blotting, membranes were incubated with the three different serum pools in 3 sequential dilutions (1:500, 1:250 and 1:100). Representative immunoblots with the different sera groups are shown in Figure C2.8 (A, B and C).

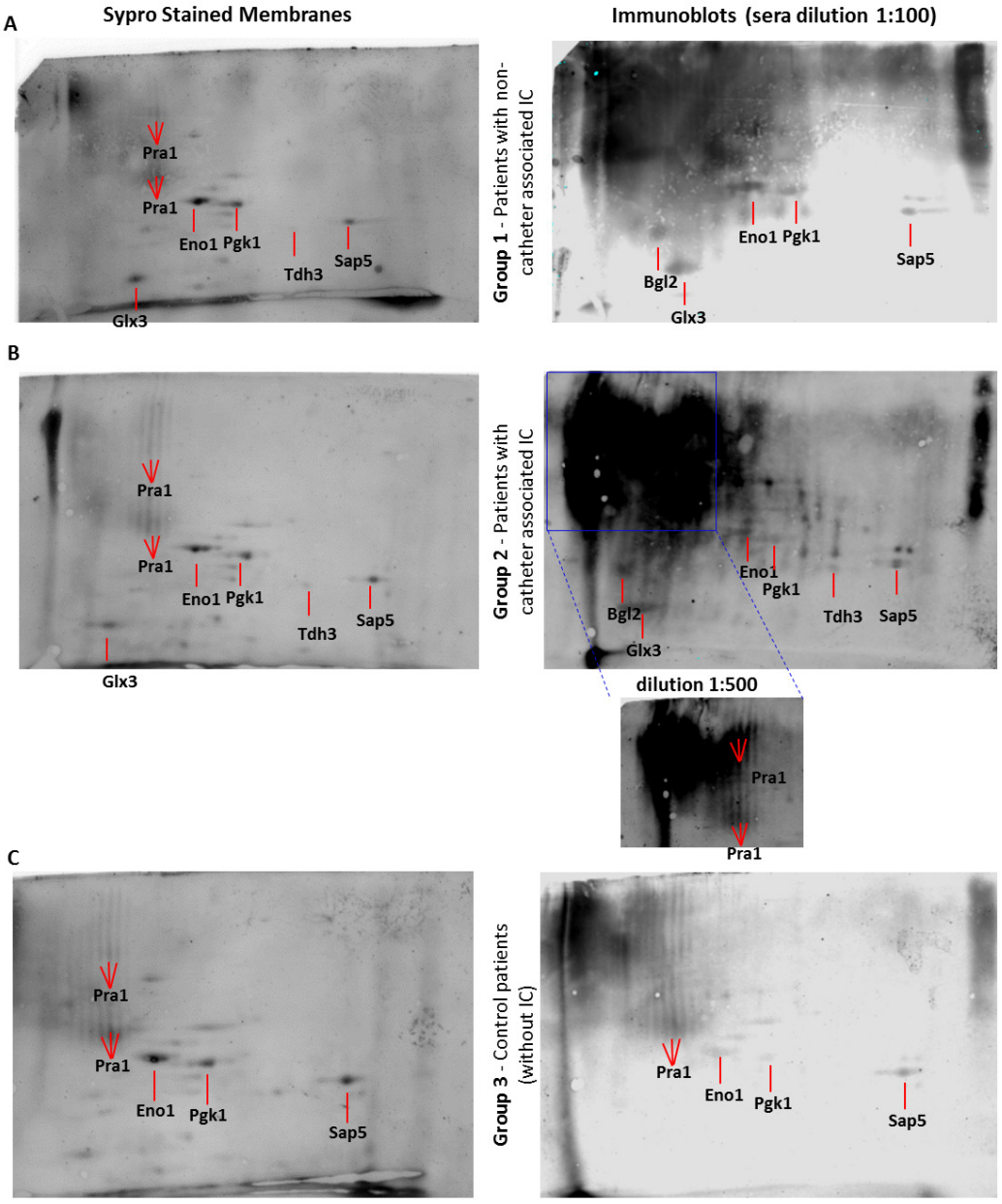

Figure C2.8 Comparison of serum IgG antibody reactivity profiles by 2-DE followed by Western blotting. Sypro stained membranes and immunoblots at a dilution of 1:100 are represented with (A) Group 1: patients with non-catheter associated IC (B) Group 2: patients with catheter associated IC and (C) Group 3: control patients. In (B) it is also depicted a part of the membrane with a lower dilution of sera (1:500) where defined spots of reactivity instead of the smear are possible to observe (the smear appears due to high reactivity in the upper left zone). In the left side representative Sypro-stained membranes are depicted and in the right side membranes after incubation with the sera. Lines in red position the immunoreactive proteins identified by MALDI-TOF.

In this figure it is possible to observe (i) Sypro stained membranes of the proteins, showing a similar protein pattern in all the membranes and on the right side (ii) immunoblots after incubation with different serum groups, showing the different patterns of immunoreactivity. The overall comparison of the immunoblots showed a higher pattern of immunoreactivity of the *C. albicans* hyphal secreted proteins to both groups of patients with IC when compared to the group of control patients. This finding was expectable due to the significantly higher titers obtained in the ELISA measurements.

To further analyze the protein spots that were immunoreactive, *C. albicans* hyphal secretome was separated in a 2-DE preparative gel, i.e. with more protein load, and the spots were identified by MALDI-TOF-MS. A total of seven immunoreactive *C. albicans* proteins involved in interaction with the host and metabolism were identified on 2-DE gel (**Figure C2.9**).

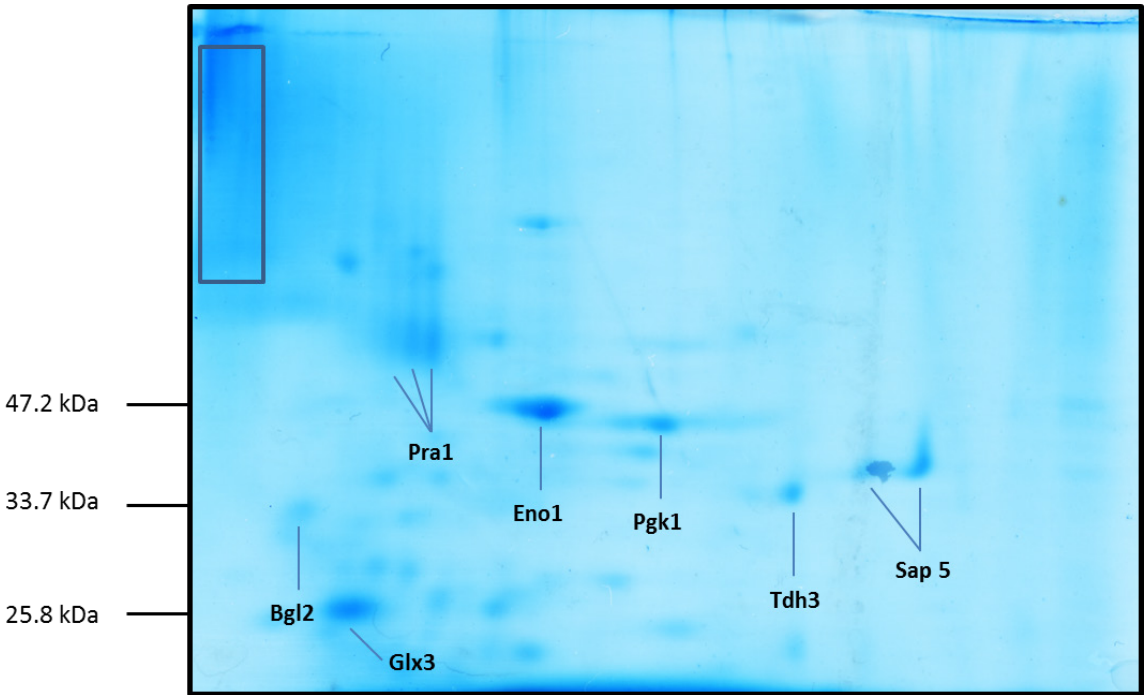

Figure C2.9 Coomassie blue stained 2-DE preparative gel. Preparative gel used for MALDI-TOF-MS identification. The seven immunoreactive proteins are represented here. The upper-left zone that was cut for protein identification is inside the rectangle depicted here.

Unfortunately, several spots presented high levels of immunoreactivity but were not possible to be identified due to their low amount of protein. This is clearly depicted in **Figure C2.8B**, where *C. albicans* hyphal proteins were exposed to serum pool from Group 2 and several spots were highly immunoreactive, but no proteins were detectable in the preparative gel. Regarding the identification by MALDI-TOF-MS, **Table C2.4** shows the identified proteins and their respective antigenicity patterns, and they are also represented in **Figure C2.9**. The identified proteins can be divided in cell wall proteins (Bgl2), metabolic enzymes localized in the cell surface (Eno1, Glx3,

Pgk1 and Tdh3) and proteins involved in the interaction with the host (Pra1 and Sap5). As it is possible to observe, Glx3 together with Bgl2 presented high levels of immunoreactivity against *C. albicans* hyphal secretome in both group of patients with IC but not in group control. Eno1, Pgk1, Pra1 were proteins that presented high levels of immunoreactivity in both group of patients with IC and lower levels of reactivity group control. Sap5 presented similar levels of immunoreactivity in Group 1 and 3 of patients and higher in Group 2. Interestingly, some of the proteins, Pra1 and Sap5 were identified in different spots, indicating possible different species of the same protein. Additionally, Pra1 was the identified protein that presented the highest immunoreactivity, especially in Group 2. Interestingly, in this study Tdh3 was immunoreactive in Group 2 but not in Group 1 and 3.

Table C2.4 Recognition patterns of hyphal *C. albicans* secreted proteins by sera from patients: with non - catheter associated IC (Group 1); with catheter associated IC (Group 2) and control patients (Group 3).

Immunoreactive proteins[a]			IgG antibody reactivity levels[b]			LC-MS/MS			MALDI-TOF-MS		
Standard name	Systematic name	Description	Group 1	Group 2	Group 3	No. of peptides	Ranking according to NSAF	NSAF	No. of matched/ unmatched peptides	Mascot score	% of sequence coverage
Bgl2	C4_02250C_A	Cell wall 1,3-beta-glucosyltransferase	+++	+++	-	8	55	0.0045	10/58	213	20
Eno1	C1_08500C_A	Enolase	++++	+++	+	30	1	0.0786	9/61	157	32
Glx3	C3_02610C_A	Glutathione-independent glyoxalase	+++	+++	-	NI	NI	NI	12/56	276	61
Pgk1	C6_00750C_A	Phosphoglycerate kinase	+++	++	+	38	2	0.0446	21/47	460	48
Pra1[d]	C4_06980W_A	pH Regulated Antigen	ND	+++++[c]	+++	10	12	0.0141	11/57 9/59 10/58 7/61 7/60 5/63	240 218 229 75 115 96	29 16 20 8 11 7
Sap5[d]	C6_03030W_A	Secreted aspartyl proteinase	++	+++	++	26	3	0.0354	14/54 28/43 39/38 6/62	272 815 1220 60	39 60 67 18
Tdh3	C3_06870W_A	NAD-linked glyceraldehyde-3-phosphate	-	+	-	27	9	0.0186	16/53	140	51

[a] Standard name, systematic name and description of the protein according to CGD.

[b] Levels of reactivity were given to the spots. From less to more reactivity: +; ++; +++;+++++. When no reactivity was observed: - and ND in case it was not possible to determine.

[c] This proteins has a higher level of immunogenicity thatn the represented by the symbol +++++.

[d] Proteins that were identified in different spots of the preparative gel. NI means that this protein was identified by LC-MS/MS but did not pass the statistical filters

As shown in **Figure C2.8**, the upper-left corner of the membranes presented high levels of immunoreactivity mainly when *C. albicans* hypha secretome was incubated with sera from both groups of patients with IC. This is mainly attributed to heavy glycosylated proteins (Chaffin, 2008, Luo *et al.*, 2016). In an endeavor to identify the mixture of the proteins that was in this corner of the gel (**Figure C2.9**), proteins from this zone of the gel were digested and identified by LC-MS/MS. The list of identified proteins and respective MS data is shown in **Supplementary Table C2.2.** The more abundant proteins (NSAF higher than 0.01) identified in the upper-left corner are shown in **Table C2.5.** The majority of these proteins are described to be in the cell wall (Tos1, Ecm33, Sim1, Sun41, Cht3 and Mp65) and in the cell surface or extracellular medium (Rbt4 and Pra1). According to two tools used to predict glycosylation sites, all of the proteins present in the table had at least one predicted glycosylation site. Ecm33, Pra1, Scw1, Sim1 and Sun41 were predicted by both servers to have glycosylation sites. With exception of Cht3 and Scw11 that have high molecular weight (60 kDa and 54.4 kDa, respectively) all of the other proteins presented molecular weights that are lower than the zone in-gel digested for protein identification. This also indicates that these proteins might be glycosylated.

Table C2.5 Proteins identified by LC-MS/MS from the left upper corner of the 2-DE gel of *C. albicans* hyphal secretome.

Systematic Name	Standard Name	Description	NetNGlyc 1.0 Server Prediction	NetNGlyc 4.0 Server Prediction	NSAF	Nr Peptides	MW
C1_07030C_A	Rbt4	Pry family protein	no	yes	0.19	11	37.4
C2_10030C_A	**Mp65**	Cell surface mannoprotein	no	yes	0.15	13	39.3
C6_00820W_A	Sun41	Cell wall glycosidase	yes	yes	0.12	11	43.7
C3_01550C_A	**Tos1**	Protein similar to alpha agglutinin anchor subunit	no	yes	0.10	15	49.4
C1_03190C_A	**Ecm33**	GPI-anchored cell wall protein	yes	yes	0.03	6	43.5
CR_10110W_A	Cht3	Major chitinase	no	yes	0.03	7	60
C4_06980W_A	**Pra1**	Cell surface protein that sequesters zinc from host tissue	yes	yes	0.02	7	33.1
C3_02610C_A	**Glx3**	Glutathione-independent glyoxalase	yes	no	0.02	12	25.8
C1_13940W_A	Sim1	Adhesin-like protein	yes	yes	0.01	9	39.4
C5_04110W_A	Scw11	Cell wall protein	yes	yes	0.01	10	54.4

Here are presented only the more abundant proteins (NSAF higher than 0.01).
Proteins in bold were previously described as immunogenic (Torosantucci *et al*., 1993, Pitarch *et al*., 2004, 2008, 2011, 2014,2016, Mochon *et al*., 2010 and Luo *et al*., 2016, (Giraldo, 2013)).

Discussion

Invasive candidiasis (IC) is a common fungal infection in ICU patients that have their immune defences reduced due to underlying diseases (Quindos, 2014). This pathogen is known to be a polymorphic microorganism that depending on the surrounding conditions can grow in the form of yeast, pseudohyphae and hypha (Gow & Hube, 2012), being the hyphal form more correlated with the state of epithelial and endothelial cell invasion (Gow & Hube, 2012). Previous works shown that this pathogen can secrete different proteins which have important roles such as degrading host proteins, lipids and glycogen or to acquire zinc or other ions and to provide protection against microbial peptides (Klis & Brul, 2015, Gil-Bona *et al.*, 2018). Proteins can be secreted by the classical secretory pathway or by alternative routes of exportation, such as extracellular vesicles. A recent work showed that biofilms with *C. albicans* defective mutants in the endosomal sorting complexes produced less EVs and these biofilms presented more sensitivity to antifungal drugs, which helped to understand the role in EVs in cell-cell signalling (Zarnowski *et al.*, 2018).

Taking into account the important role of secreted proteins and their role during interaction with the host, we decided to characterize the serological response to *C. albicans* hyphal secretome in patients with IC, associated and non-associated with catheters. To approach this, Lee medium was selected for *C. albicans* cell growth mainly due to identification of more proteins with signal peptide than in other media. This medium was previously used to induce hyphal morphology in *C. albicans* (Lee *et al.*, 1975, Nantel *et al.*, 2002, Pitarch *et al.*, 2002).

1 *C. albicans* hyphal secretome analysis revealed proteins involved in interaction with host and antigenic proteins

Using MS-based proteomics, we decided to analyse *C. albicans* hyphal secreted proteins. This strategy rendered the identification of 301 proteins. The NSAF, which ranks protein spectral abundance inside each sample, was calculated for each protein of both S1 and S2 and showed that the secretome samples were very similar to each other in terms of protein relative abundance (see Figure C2.5 in results section). GO enrichment analysis showed that the identified extracellular proteins were implicated in different processes involved in interaction with the host, such as pathogenesis, cellular response to oxidative stress, induction by symbiont of host defence response and adhesion to the host. In fact, in this secretome proteins from Sap family (Sap5, Sap4, Sap10 and Sap8) which is a well-known protein family known to be implicated in degradation of human proteins were detected (Naglik *et al.*, 2003). Different proteins from the cell wall were also identified in this secretome, such as some GPI-anchored cell wall proteins

(Ecm33, Pga4, Rhd3, Utr2) and some non-covalent cell wall proteins (Kre9, Bgl2, Eng1, Mp65, Cht1, Cht2). The presence of cell wall proteins in secretome was previously noticed in other works (Sorgo *et al.*, 2010, Luo *et al.*, 2016) and it is congruent with the fact that some of them may be detached from the cell wall during cell growth. Another proteins were identified such as Als1 and Xog1 which are involved in cell adherence and biofilm formation (Chaffin, 2008). Our group was previously interested in the protein cell-wall protein Ecm33. This protein was suggested to be required for cell wall integrity, morphogenesis and virulence in *C. albicans* (Martinez-Lopez *et al.*, 2004). Our group described that *ecm33/ecm33* mutant was found to be unable to regenerate the cell wall from protoplasts and to activate cell wall integrity pathway. The mutant was also found to be hypersensitive to temperature, osmotic and oxidative stress (Gil-Bona *et al.*, 2016).

Only 12% of the identified proteins had signal peptide. However, as it is shown in Table C2.3 (in results section) several proteins were described as located both intra- and extracellular regions suggesting that a great number of proteins were secreted by non-canonical mechanisms. As previously proposed by our group, these proteins can be secreted inside EVs (Nombela *et al.*, 2006, Gil-Bona *et al.*, 2015). In fact, when comparing the proteins identified in this study with the proteins identified in both EVs and EVs free secretome from *C. albicans* (Gil-Bona et al., 2015), we observe that 16 proteins were common to all conditions (Bgl2, Cht1, Cht3, Coi1, Cyp5, Ecm33, Eng1, Mp65, orf19.4952.1, Pga4, Phr2, Rbe1, Rhd3, Sim1, Utr2, Xog1). Only 4 proteins were common between our secretome and the EVs free secretome described (Asc1, Hex1, Sap10, Sap8). Interestingly, other 16 proteins were common only between EVs secretome and our secretome (Cyp1, Eft2, Eno1, Gpm1, Hsp70, Met6, Mnt1, Pdc11, Pgk1, Por1, Rho1, Sah1, Ssa2, Tal1, Tdh3, Ykt6). Some of these proteins are moonlighting, such as Tdh3, which is a well-known housekeeping enzyme, named glyceraldehyde-3 phosphate dehydrogenase that is important in glycolysis. This protein was also found to be present in the cell surface of *C. albicans* and was found to be immunogenic (Gil-Navarro *et al.*, 1997). Furthermore, it was also shown in different works that serum proteins bind to the *C. albicans* cell surface through several moonlighting proteins, such as enolase (Eno1) and the elongation factor 2 (Eft2) (reviewed in (Karkowska-Kuleta & Kozik, 2014)).

It is possible that the proteins typically classified as intracellular were present in the supernatant due to some cell lysis that could occur during cell incubation and growth. Nevertheless, this does not constitute an important problem in this work once the main objective of this work was to identify immunoreactive proteins in samples enriched in secreted proteins.

To our knowledge, there are three studies on hyphal *C. albicans* secretome (Sorgo *et al.*, 2010, Heilmann *et al.*, 2013, Luo *et al.*, 2016) and a recent review from our group compiles the proteins

identified in these and in others studies on whole secretome from yeast forms as well as EVs free secretome (Gil-Bona *et al.*, 2018). Comparing the 301 proteins identified in this study with the previous ones, we observed that 192 proteins were already described in at least one of the studies and 111 were newly identified as present in the supernatant of *C. albicans* hyphal cells (**Figure C2.10A** and **Supplementary Table C2.3**). A recent study compared the proteomic composition of planktonic and biofilm EVs from *C. albicans*, where the planktonic cells were in the hyphal form (Zarnowski *et al.*, 2018). As the present study was performed with whole secretome, it comprises secreted proteins by the classical secretory pathway and by non-conventional pathways. We compared the proteins from this study that were not found in the previous studies of hyphal secretome, and out of the 111, 48 proteins were common to Zarnwoski study and 63 were only present in our study (**Figure C2.10B)**.

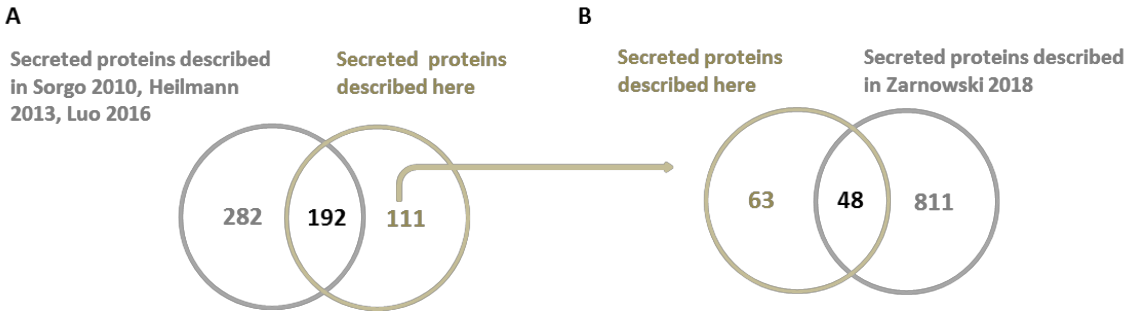

Figure C2.10 Venn Diagrams comparing secreted proteins described here and in other studies. In (A) a comparison between proteins identified in hyphal secretomes here and in previously studies (Sorgo *et al.*, 2010, Heilmann *et al.*, 2013 and Luo *et al.*, 2016). In (B) a comparison between proteins identified here and not in the previous studies (111 proteins) with proteins in EVs from hyphal cells (Zarnowski *et al.*, 2018).

It is noteworthy that 4 out of these 63 secreted proteins were already identified in gel-based proteomics (Dut1, orf19.6596, orf.7196, and Pbr1) by Luo and co-workers (Luo *et al.*, 2016). The comparison with Zarnowski work may give us an indication that a part of the proteins identified in this study were secreted by non-conventional pathways of secretion (Nombela *et al.*, 2006, Gil-Bona *et al.*, 2015, Zarnowski *et al.*, 2018). There are several explanations that can elucidate the differences in the protein composition of the secretome, such as cell growth media, time of incubation, temperature of incubation, differences in the extraction protocol and type of mass spectrometers used for protein identification. With the MS technology evolving so quickly there is increasing detection sensitivity and more proteins can be identified in fungal secretomes.

Surfome analysis, by trypsin cell surface shaving, is another type of study that can give us important information about proteins that interact with the host, once they are localized in the cell surface (Gil-Bona *et al.*, 2015, Marin *et al.*, 2015, Gil-Bona *et al.*, 2018).Interestingly, some of

the proteins identified in this secretome were previously identified in *C. albicans* surfome, such as Cip1, Cmd1, Egd1, Hnt1, Hsp12, Mdg1, orf19.5943.1, orf19.7196 and orf19.7368 (Martinez-Gomariz *et al.*, 2009, Hernaez *et al.*, 2010, Vialas *et al.*, 2012, Gil-Bona *et al.*, 2015, Marin *et al.*, 2015) (Supplementary Table C2.4). As these proteins are non-covalently attached to the cell surface, they may have detached during the incubation time.

Additionally, the global proteomic analysis performed on the *C. albicans* secreted proteins enabled the identification of 47 proteins previously characterized as immunogenic (Table C2.6). As observable in Table C2.6 the majority of the proteins that were antigenic did not present signal peptide but were observed in both the extra- and intracellular part of the cell.

Table C2.6 Proteins identified by LC-MS/MS and previously found to be immunogenic.

Systematic name[1]	Standard name[1]	Description[1]	Cell localization[2]	Signal peptide[1]	References[3]
CR_08210C_A	Aco1	Aconitase	Shared	No	Pardo 2000, Pitarch 2004, Pitarch 2008, Pitarch 2011, Pitarch 2014, Pitarch 2016, Luo 2016
CR_04090C_A	Ade17	5-Aminoimidazole-4-carboxamide ribotide transformylase	Intracellular	No	Pitarch 2004, Pitarch 2008, Pitarch 2011, Pitarch 2016
C6_03700W_A	Als1	Cell-surface adhesin	Extracellular	yes	Mochon 2010
C7_01250W_A	Asc1	40S ribosomal subunit similar to G-beta subunits	Intracellular	No	Pitarch 2004, Pitarch 2008, Pitarch 2011, Pitarch 2014, Pitarch 2016, Luo 2016
C1_04610W_A	Atp1	ATP synthase alpha subunit	Shared	No	Pitarch 2004
C4_00270W_A	Atp2	F1 beta subunit of F1F0 ATPase complex	Shared	No	Pitarch 2004
C4_02250C_A	Bgl2	Cell wall 1,3-beta-glucosyltransferase	Extracellular	Yes	Pitarch 2006
C2_05460W_A	Cdc19	Pyruvate kinase at yeast cell surface	Shared	No	Pardo 2000, Pitarch 2004, Mochon, 2010, Pitarch 2011, Pitarch 2014, Pitarch 2016, Luo 2016
C4_03470C_A	Ece1	Extent of Cell Elongation Protein	Extracellular	yes	Mochon
C1_03190C_A	Ecm33	GPI-anchored cell wall	Extracellular	yes	Parra 2013

		protein			
C2_03100W_A	Eft2	Elongation Factor 2 (eEF2)	Shared	No	Pitarch 2004, Pitarch 2011, Pitarch 2016, Luo 2016
C1_08500C_A	Eno1	Enolase	Shared	No	Martinez 1998, Pitarch 1999, Pitarch 2004, Pitarch 2006, Pitarch 2008, Pitarch 2011, Pitarch 2014, Pitarch 2016, Luo 2016
C4_01750C_A	Fba1	Fructose-bisphosphate aldolase	Shared	No	Pitarch 2004, Pitarch 2006, Pitarch 2008, Pitarch 2011, Pitarch 2014, Pitarch 2016, Luo 2016
C1_13860C_A	Gnd1	6-phosphogluconate dehydrogenase	Shared	No	Pitarch 2016
C2_03270W_A	Gpm1	Phosphoglycerate mutase	Shared	No	Pardo 2000, Pitarch 2004, Pitarch 2011, Pitarch 2016
C5_02860C_A	Grp2	NAD(H)-linked methylglyoxal oxidoreductase involved in regulation of methylglyoxal and pyruvate levels	Extracellular	No	Pitarch 2004, Pitarch 2008, Pitarch 2011, Pitarch 2014, Pitarch 2016
C3_04060C_A	Hem13	Coproporphyrinogen III oxidase	Shared	No	Pitarch 2004, Pitarch 2011
C1_13480W_A	Hsp70	Putative Hsp70 chaperone	Shared	No	Pitarch 2011, Pitarch 2016
C7_02030W_A	Hsp90	Essential chaperone	Shared	No	Pitarch 2004, Pitarch 2011, Pitarch 2014, Pitarch 2016
CR_04510W_A	Hxk2	Hexokinase II	Intracellular	No	Pitarch 2004, Pitarch 2016
CR_10100C_A	Ino1	Inositol-1-phosphate synthase	Shared	No	Pitarch 2004, Pitarch 2016
C2_08810C_A	Ipp1	Putative inorganic pyrophosphatase	Shared	No	Pitarch 2004, Pitarch 2014, Pitarch 2016
CR_00540C_A	Mdh1	Mitochondrial malate dehydrogenase	Intracellular	Yes	Pitarch 2014, Pitarch 2016
C4_01900C_A	Mdh1-1	Predicted malate dehydrogenase precursor	Shared	No	Pitarch 2004, Pitarch 2008, Pitarch 2011

CR_01620C_A	Met6	Essential 5-methyltetrahydropteroyltriglutamate-homocysteine methyltransferase	Shared	No	Pardo 2000, Pitarch 2004, Pitarch 2006, Pitarch 2008, Pitarch 2011, Pitarch 2014, Pitarch 2016, Luo 2016
C2_10030C_A	Mp65	Cell surface mannoprotein	Extracellular	Yes	Torosantucci 1993
C1_06100C_A	Msi3	Essential HSP70 family protein	Intracellular	No	Pitarch 2004, Pitarch 2011, Pitarch 2014, Pitarch 2016
C7_03860W_A	orf19.7196	Putative vacuolar protease	Intracellular	Yes	Luo 2016
C1_14060W_A	orf19.7214	Glucan 1,3-beta-glucosidase	Intracellular	No	Mochon 2010
C4_06570C_A	Pdc11	Pyruvate decarboxylase	Shared	No	Pitarch 2004. Pitarch 2008, Pitarch 2011, Pitarch 2014, Pitarch 2016
C5_05390C_A	Pga4	GPI-anchored cell surface protein	Extracellular	Yes	Mochon 2010
CR_06340C_A	Pgi1	Glucose-6-phosphate isomerase	Shared	No	Pitarch 2004, Pitarch 2011, Pitarch 2016
C6_00750C_A	Pgk1	Phosphoglycerate kinase	Shared	No	Martinez 1998, Pitarch 1999, Pitarch 2004, Pitarch 2006, Pitarch 2008, Pitarch 2011, Pitarch 2014, Pitarch 2016
C1_04100C_A	Por1	Mitochondrial outer membrane porin	Shared	No	Pitarch 2004
C4_06980W_A	Pra1	pH regulated antigen	Extracellular	Yes	Viudes 2004
C7_02810W_A	Prx1	Thioredoxin peroxidase	Shared	No	Luo 2016
C5_04270C_A	Sah1	S-adenosyl-L-homocysteine hydrolase	Extracellular	No	Pitarch 2004, Pitarch 2014, Pitarch 2016
C3_07310C_A	Slk19	Alkaline-induced protein of plasma membrane	Extracellular	no	Mochon 2010
C1_04300C_A	Ssa2	HSP70 family chaperone	Shared	No	Pitarch 2004, Pitarch 2008
CR_08090W_A	Ssb1	HSP70 family heat shock protein	Shared	No	Pitarch 2004, Pitarch 2011, Pitarch 2014, Pitarch 2016
CR_03720W_A	Tal1	Transaldolase	Shared	No	Luo 2016
C3_06870W_A	Tdh3	NAD-linked glyceraldehyde-3-phosphate dehydrogenase	Shared	No	Pitarch 2004, Pitarch 2006, Pitarch 2011, Pitarch 2014,

					Pitarch 2016
C1_01350C_A	Tif	Translation initiation factor	Intracellular	No	Pitarch 2004
C3_07440W_A	Tpi1	Triose-phosphate isomerase	Shared	No	Pitarch 2004, Pitarch 2006, Pitarch 2011, Pitarch 2014, Pitarch 2016, Luo 2016
C3_06180C_A	Tsa1	TSA/alkyl hydroperoxide peroxidase C (AhPC) family protein	Shared	No	Pitarch 2011, Pitarch 2016, Luo 2016
C3_01730C_A	Utr2	Putative GPI anchored cell wall glycosidase	Extracellular	yes	Mochon
C1_02990C_A	Xog1	Exo-1,3-beta-glucanase	Shared	Yes	Luo 2016

[1] Names, description and prediction of signal peptide according to CGD

[2] Localization according to GO enrichment performed in CGD. "Shared" means the protein was described intra- and extracellularly. "Extracellular" embraces extracellular region, cell surface, cell wall and cell periphery.

[3] Previous studies where these proteins were shown to be antigenic in humans

2 Different serum profiles of IgG antibodies were detected against the *C. albicans* hyphal secretome

Catheter-related bloodstream infections are among the most frequent infections acquired in hospitals (Chaves *et al.*, 2018). Due to this we pooled the serum from patients according to *C. albicans* isolation site: if they were isolated from catheter they were pooled in Group 2 and if they were isolated from other sites, such as abdominal zone, blood they were pooled in Group 1. After this, we were interested in evaluating the IgG antibody levels against *C. albicans* hyphal secretome in the different serum pools. As expected, IgG measurements showed that anti-*C. albicans* antibody levels were higher in both groups of patients with IC (Group 1 and 2) compared with control one (Group 3), showing that the patients with IC presented a stronger antibody response to this infection. Interestingly, in this study, the antibody response was higher in the pool of patients with catheter associated IC (Group 2) than the group of patients with non - catheter associated IC (Group 1). *C. albicans* in the catheter can enter directly in blood and this could explain why we observed stronger IgG response. Group 1 is composed by *C. albicans* isolation sites corresponding to blood and deep-seated candidiasis and this means the amount of *C. albicans* cells in blood might be lower resulting in lower antibody levels against them. Due to the lack of information regarding patient history, more studies are needed to prove this hypothesis. Moreover, it is important to remark that the interest behind pooling the patients in this way was to discover new proteins that could be more immunogenic in one group than the other, and with this, find new possible biomarkers for the diagnosis of IC.

3 A group of seven *C. albicans* immunogenic proteins: Bgl2, Eno1, Glx3, Pgk1, Pra1, Sap5 and Tdh3 were identified by immunoproteomics

An immunoproteomic approach was performed where *C. albicans* hyphal secreted proteins were separated by 2-DE gel and electroblotted. After this, immunoblotting with three different serum pools was done. Congruently with the IgG antibody levels measured by ELISA, the group of patients with catheter associated IC showed higher antibody levels against the *C. albicans* hyphal secretome than the group of patients with non-catheter associated IC.

With this approach, we were able to identify 7 immunoreactive proteins: Bgl2, Eno1, Glx3, Sap5, Pgk1, Pra1 and Tdh3 (see **Table C2.4** in results section). From this protein set Bgl2, Eno1, Glx3 and Pgk1 were immunoreactive proteins that enabled the discrimination of patients with IC, associated and non-associated with catheter, from patients without IC. From this group, Bgl2 and Glx3 did not present reactivity in the control group whereas Eno1 and Pgk2 presented low levels of reactivity in the control group. The other three immunoreactive proteins, Sap5, Pra1 and Tdh3, enabled the discrimination of patients with catheter associated IC from control patients, but not patients with non-catheter associated IC from control patients. Sap5 and Pra1 proteins presented some reactivity levels in control group. It is important to mention that in our work we observed in same cases low levels of immunoreactivity when incubating *C. albicans* hyphal secreted proteins with control sera. This is maybe due to the fact that *C. albicans* is commensal in most humans, which means that there is a basal level of antibodies against these proteins.

Interestingly, Bgl2 brought our attention because it was identified in LC-MS/MS in a much lower ranking position that the others (Nr 55, NSAF 0.0045) and it produced high levels of IgG antibodies in both groups with IC and no immunoreactivity in control group. In the preparative gel it is also possible to see that this protein has lower abundance that others identified (see **Figure C2.9** in results section). Bgl2 is a protein localized in the cell wall. It is a 1,3-beta-glucosyltransferase that splits and links β-1,3 glucan molecules, resulting in a β-1,3-glucan chain elongated with a β-1,6 glucan at the transfer site (Sarthy *et al.*, 1997). This protein was also described to function in the delivery and accumulation of glucan for biofilm matrix building (Taff *et al.*, 2012). It was previously observed in the secretome of both yeast and hyphal secretomes (Sorgo *et al.*, 2010, Ene *et al.*, 2012, Heilmann *et al.*, 2013, Gil-Bona *et al.*, 2015, Luo *et al.*, 2016). Bgl2 was also described as an immunogenic protein in other works (Pitarch *et al.*, 2006, Mochon *et al.*, 2010). Furthermore, anti-Bgl2 antibodies were previously proposed as potential diagnostic biomarker of IC (Pitarch *et al.*, 2006).

Both Eno1 and Pgk1 were identified in upper ranking positions (1 and 2 respectively; NSAF 0.0786 and 0.0446, respectively) indicating that they are abundant proteins. They also appeared as very

abundant proteins in the preparative gel (see Figure C2.9 in results section). These proteins also enabled the differentiation from patients with IC from the control patients. Eno1 is known to be one of the most abundant cytosolic enzymes with a known role in the glycolytic pathway. Currently, it is also known to be a multifunctional protein and to be secreted to the extracellular medium. It was suggested to have a role in the colonization of mammalian intestinal epithelium (Silva *et al.*, 2014). Eno1 was also found to bind to human plasminogen (Jong *et al.*, 2003). Plasminogen is abundant in human plasma and extracellular fluids and its active form, plasmin, is important for the degradation of extracellular matrix proteins, blood clot dissociation and cellular migration. Pathogens recruit the host plasminogen resulting in an increased invasive capacity for the microorganisms (Jong *et al.*, 2003). This protein was also found to be immunogenic (Martinez *et al.*, 1998, Pitarch *et al.*, 1999, Pitarch *et al.*, 2006, Pitarch *et al.*, 2008, Luo *et al.*, 2016). Pgk1 is a phosphoglycerate kinase involved in the glycolysis. As Eno1, it was found both in the cytoplasm and in the cell wall (Alloush *et al.*, 1997). Furthermore, this protein was shown to bind to plasminogen (Crowe *et al.*, 2003) and to be immunogenic (Martinez *et al.*, 1998, Pitarch *et al.*, 1999, Pitarch *et al.*, 2004, Pitarch *et al.*, 2016).

Glx3 was detected by LC-MS/MS but it was not included in the list of identified proteins due to the statistical filters applied. However, it was detected and abundant in the preparative gel (see Figure C2.9 in results section). Interestingly, it was found to be highly immunoreactive in the groups with IC and it did not present immunoreactivity in control patients. Glx3 is a glyoxalase that converts methylglyoxal to *D*-lactate (Hasim *et al.*, 2014). Most significantly, it is a very abundant protein in the biofilm extracellular matrix. *C. albicans glx3Δ* mutant showed impaired growth on media with glycerol. The mutant has impaired filamentation and biofilm formation (Cabello *et al.*, 2019). In addition to being present in biofilm matrix it was also observed in yeast and hyphal secretomes (Luo *et al.*, 2016). Regarding data from its antigenicity, Glx3 was previously described as an immunogenic protein (Pitarch *et al.*, 2004, Pitarch *et al.*, 2011, Pitarch *et al.*, 2016).

Sap5 is part of large family of secreted aspartyl proteases which are known to be associated with *C. albicans* virulence. This protein was ranked as third in LC-MS/MS identification and it was also found to be abundant in the preparative gel (see Figure C2.9 in results section). The main function of Saps is to degrade proteins. It was also shown that they may play a role in biofilm associated bloodstream infections caused by *C. albicans* (Joo *et al.*, 2013). This protein was found in the *C. albicans* hyphal secretome (Sorgo *et al.*, 2010, Luo *et al.*, 2016). It was previously found to be an immunogenic protein. As it was observed here when comparing reactivity levels of this protein in patients with non-catheter associated IC and control, also previously no statistical differences

between patients with IC and controls were found (Mochon *et al.*, 2010). Nevertheless, it is worth to reference that Mochon and co-workers expressed *C. albicans* proteins in *E.coli*, and this means they lack post-translational modifications (Mochon *et al.*, 2010).

Pra1 is a cell-wall associated protein. In this work, we observed that this protein was more immunoreactive in patients with catheter associated IC when compared to control ones. However it did not enabled the clear differentiation between non-catheter associated IC with control patients. It was ranked in twelfth according to its NSAF and it was found to be abundant in the preparative gel with characteristics of glycosylation (see Figure C2.9 in results section). This protein elicits a strong immune response in infected patients. Moreover, a monoclonal antibody directed towards this protein was shown to confer protection (Viudes *et al.*, 2004). A previous study shows that *C. albicans* secretes Pra1 to sequester zinc from host cells and the protein re-associates with the fungus through a co-expressed zinc transporter, Zrt1 (Citiulo *et al.*, 2012). Recently, it was shown that Pra1 binds and complexes the complement molecules C3 and blocks C3 conversion by the host C3 convertases. It was further proved that Pra1 block the C3a antifungal activity (Luo *et al.*, 2018). Tdh3 is a glyceraldehyde 3-phosphate dehydrogenase involved in the glycolysis pathway that was also found in the *C. albicans* cell wall (Gil-Navarro *et al.*, 1997). This protein allowed the differentiation of patients with catheter-associated IC from control but not between non-catheter associated IC from control. The reactivity levels were low. This protein was ranked in the ninth position of abundance and it was also detectable in the preparative gel (see Figure C2.9 in results section). This protein was also previously found in both yeast and hyphal secretomes (Luo *et al.*, 2016). Likewise, it was found to be immunogenic (Gil-Navarro *et al.*, 1997, Pitarch *et al.*, 1999, Pitarch *et al.*, 2004, Pitarch *et al.*, 2016).

In order to prove the validity of these immunoreactive proteins as biomarkers of IC further studies analyzing the antibody response in unpooled sera are needed.

In addition to the immunoreactive proteins that were identified by MALDI-TOF-MS, the upper-left corner of the immunoblots presented much higher levels of reactivity than in the rest of the blot. This area corresponds to the more acidic part and higher molecular mass of the gel where the more glycosylated proteins are often present. In spite of being difficult to correlate the antigenicity levels to a specific identifiable protein due to the high background, the group of proteins in Table C2.5 was predicted by at least one tool to have one glycosylation site. Furthermore, Mp65, Sun41 and Cht3, which are proteins known to be in the cell surface, were previously described to be glycosylated (McCreath *et al.*, 1995, Gomez *et al.*, 1996, Hiller *et al.*, 2007). Particularly, Mp65 was found to be highly released in mycelial forms of *C. albicans* and to stimulate cell-mediated immune response (Bromuro *et al.*, 1994).

C. albicans glycosylated cell wall proteins are covalently attached to structural polysaccharides in two ways: GPI anchored proteins, which are linked to β-1,6 glucan through a glycophosphatidylinositol remnant, and Pir proteins, which are directly linked to β-1,3 glucan (Chaffin, 2008). Glycosylated proteins can carry different types of antigenic epitopes. Some oligosaccharides can also be antigenic. Another type are glycopeptide epitopes defined by antibodies which recognize specific oligosaccharide structures and adjacent amino acid residues. There are peptidic epitopes which represent either relatively short sequences of the polypeptide chains or include amino acid residues brought into proximity due to the secondary structure of the proteins (Lisowska, 2002). Recently, the role of glycosylation in the recognition of protein antigens by antibodies was studied. For that, Luo and co-workers studied the immunoreactivity of Sap6 on the glycosylation status and they found that anti-Sap6 antibody signal was drastically reduced after deglycosylation. Furthermore, they observed that Mp65 and other cell wall proteins in the upper-left corner of 2-DE gels showed reduced antibody recognition by sera of candidemia patients after deglycosylation (Luo *et al.*, 2016).

Overall, this study gave new insights in the serological response of patients with IC associated and non-associated with catheters. Furthermore, it led to the identification of immunogenic proteins. An overview of the main findings obtained in this work is presented in Figure C2.10.

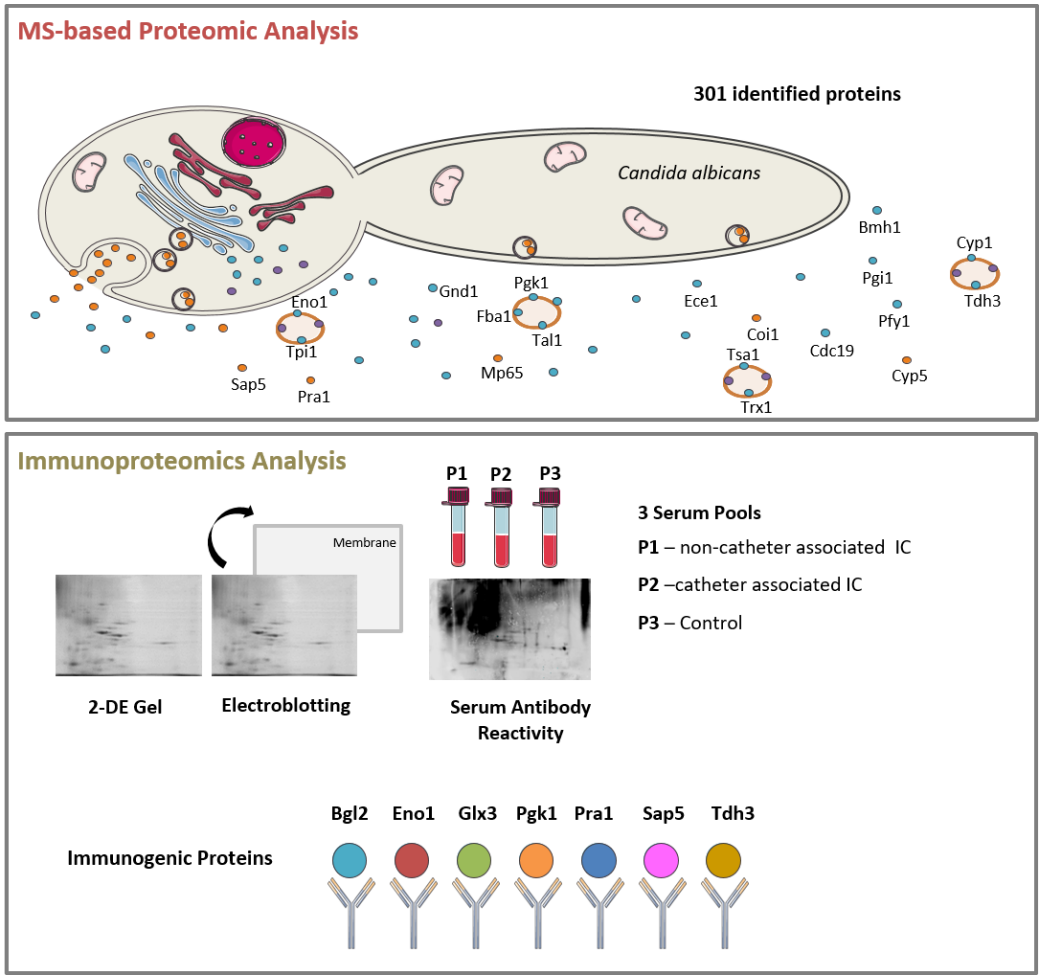

Figure C2.10 Schematic representation of the main findings regarding the MS-based proteomic immunoproteomic approaches. The 20 more abundant proteins identified in the MS-based proteomic approach are represented. They are orange if they have and blue if they lack signal peptide. In case proteins were previously described as present in EVs (reviewed in Gil-bona *et al*. 2018), they were depicted here in EVs. The immunoproteomics approach is also schematically represented with the group of proteins found to be immunogenic (Bgl2, Eno1, Glx3, Pgk1, Pra1, Sap5 and Tdh3).

Nevertheless, it is important to highlight the need of multicentric studies with larger patient cohorts to determine the diagnostic performance of these assays in cases of deep-seated candidiasis. Furthermore, it is important to evaluate their diagnostic utility combined with other assays or with clinical prediction algorithms (reviewed in (Pitarch *et al.*, 2018)).

GENERAL DISCUSSION

Host-pathogen interactions stand as a complex interplay between the host defence mechanisms and the infecting microorganisms. The human body has evolved with different strategies of immune tolerance to the commensal microbiota as well as different immune defense mechanisms to eliminate pathogens. Yet, the incidence of fungal infections is rising and becoming a serious threat to the public health (Swidergall, 2019). Therefore, new, holistic and innovative approaches are needed to improve the knowledge of how the immune system interacts and responds to these pathogens. Currently, we are witnessing the increasing application of proteomic approaches for the study of host-pathogen interactions. **Figure GD.1** represents some of the different proteomic approaches that are currently being used to increase this knowledge.

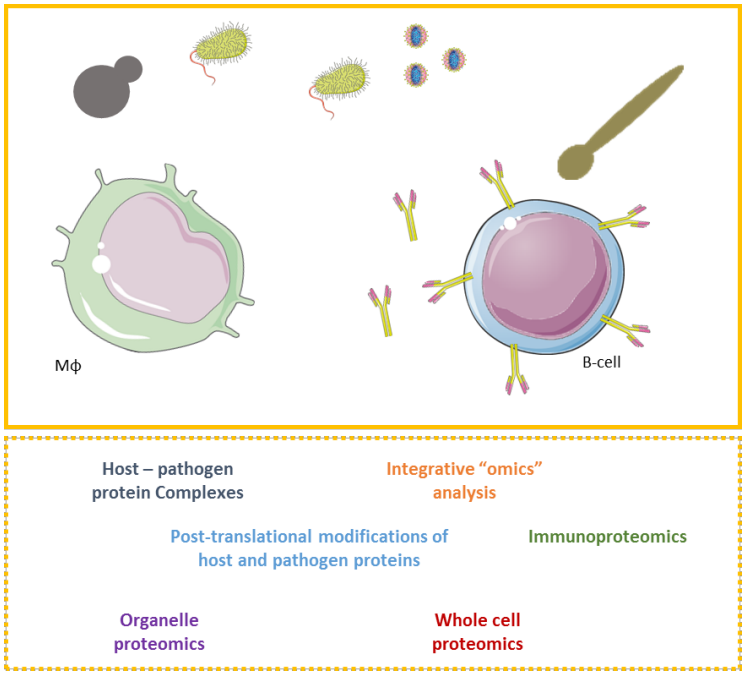

Figure GD.1 Proteomic approaches usually used for the study of host - pathogen interactions. The proteomic study of host-pathogen interactions can be performed at different levels and using distinct proteomic strategies.

Proteomic approaches can be used to evaluate the level of protein expression in different conditions of interaction, as well as the post-translational modifications that occur during these interactions. They also stand as important methods to build host-pathogen protein–protein interaction networks. Together with specific enrichments, they can enlighten the function and role of specific organelles in this interaction. Besides, they can bring important insights in the characterization of the serological response to a specific immunome.

During this general discussion, an attempt to integrate the distinct proteomic approaches carried out to study the different levels of host and pathogen interactions will be made. On the one hand, the proteomic and phosphoproteomic approaches, one centered on the enrichment in macrophage ATP binding proteins and the other focused on the analysis of the global proteome, for a better understanding of macrophages and *C. albicans* interactions. On the other hand, the MS-based analysis of *C. albicans* hypha secretome together with the immunoproteomic approach

used for the characterization of the serological response to this secretome in patients with IC (Figure GD.2).

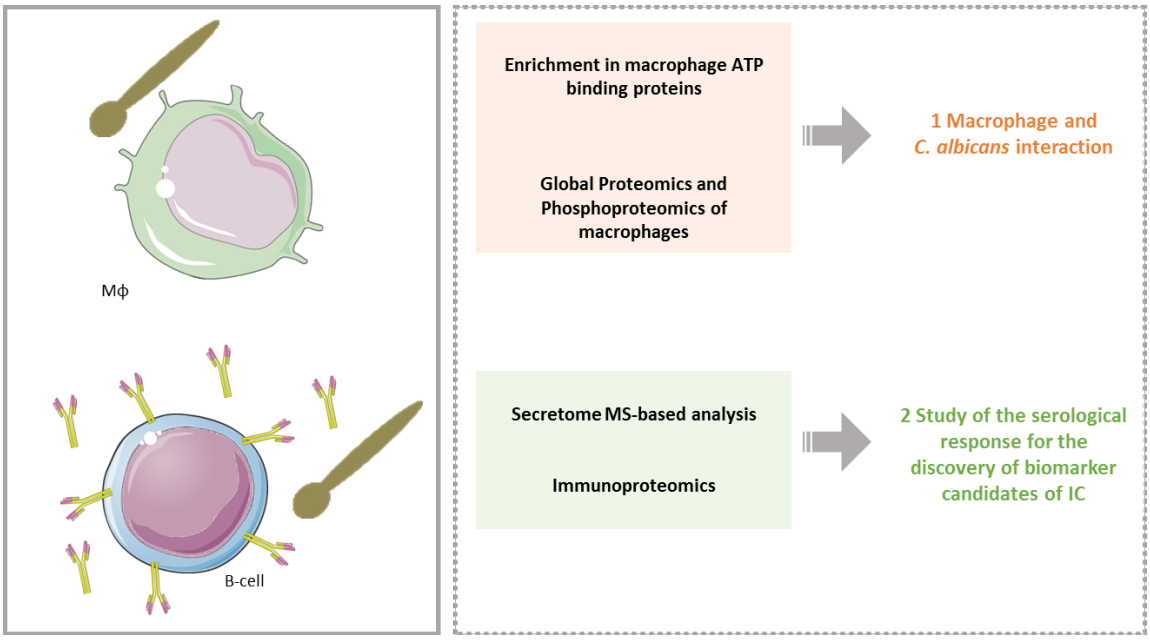

Figure GD.2 Specific proteomic strategies used in this thesis. Different proteomic approaches were carried out to characterize the macrophage role in their interaction with *C. albicans* and to characterize the serological response to the *C. albicans* hyphal secretome.

1 Macrophage and *C. albicans* interaction

Previous works of our group used the murine cell line RAW 264.7 for the study of macrophage interaction with *C. albicans.* They used 2-DE for the study of macrophage proteins after interacting 45 min with *C. albicans* (Martinez-Solano *et al.*, 2006). They found changes in proteins of cytoskeletal organization, oxidative stress and protein biosynthesis. Furthermore, they found that the elongation factor Eef2p was modified in some of its different protein species. Another work studying macrophage interaction with heat inactivated *C. albicans* showed an overall activation of an anti-inflammatory response (Martinez-Solano *et al.*, 2009). Moreover, another study with sub-cellular fractionation identified new proteins involved in this interaction such as Galectin-3, and some ER related proteins (Reales-Calderon *et al.*, 2012). With the development of LC-MS approaches, our group then used SILAC and SIMAC methodology for the study of protein and phosphopeptide alterations. An increase in both the pro-inflammatory response and in anti-apoptotic signals was observed in murine macrophages after interacting with *C. albicans* (Reales-Calderon *et al.*, 2013).

In Chapter 1 of this thesis, the major proteomic and phosphoproteomic alterations together with their biological significance were addressed during the intricate interplay between human macrophages and the pathogenic fungus *C. albicans.* The main purpose of developing the present

approaches is to continue developing a comprehensive understanding of the cellular remodelling that occurs in *C. albicans* infected macrophages from a human cell line.

1.1 Application of an ATP affinity probe for the proteomic study of human macrophage interaction with *C. albicans*

ATP-binding proteins, among them kinases, are essential in several cellular processes including cell signaling, differentiation, apoptosis and others (Patricelli *et al.*, 2007). They are also highly involved in complex cellular functions and pathways, ranging from metabolic regulation to tumorigenesis or immune response. The study of these proteins can be performed by using immunoblot; however, the global study of their abundance levels can hardly be achieved with the use of conventional methods. This limitation can be partially overcome by combining MS with powerful separation techniques or by selective enrichment of these proteins from cellular extracts (Xiao & Wang, 2014). There are different methods for the enrichment in ATP-binding proteins. Activity-based protein profiling uses chemically reactive affinity probes to study a specific family of subproteome based on their unique structural or functional similarities. Generally, the entire proteome is treated with a chemical affinity probe, which incorporates an enrichment tag that facilitates downstream purification (Xiao & Wang, 2014). Hanoulle and co-workers made use of an ATP analogue: 5'-ρ-fluorosulfonylbenzoyladenosine (FSBA) that binds proteins by affinity in their nucleotide-binding site and then reacts covalently with side chains of proximate nucleophilic amino acids. They report a global functional and chemical technique, FSBA-combined fractional diagonal chromatography that allows the identification of nucleotide-binding proteins while characterizing the sequences neighbouring their binding sites (Hanoulle *et al.*, 2006). Patricelli group presented a probe-based technology that uses biotinylated acyl phosphates of ATP that covalently label the active site of ATPases, including chaperones, kinases and metabolic enzymes, to enable their selective enrichment using a desthiobiotin tag (Patricelli *et al.*, 2007). This ATP-probe based technology was used to develop a kinase enrichment kit commercialized by Thermo Scientific Pierce that utilizes ActivX™ ATP or ADP Probes. In 2013, Xiao group introduced another isotope-coded ATP-affinity probe as an acylating agent to simultaneously enrich and incorporate isotope label to ATP binding proteins. This method can be applied with any biological samples, including clinical samples (Xiao *et al.*, 2013). Recently, the same group introduced an MRM-based kinome profiling assay that fights some of the low sensitivity and reproducibility problems of shot-gun approaches (Guo *et al.*, 2014).

We took advantage of ActivX™ ATP probe and enriched cytoplasmic extracts of macrophages control and macrophages after interacting with *C. albicans*. In this study, we found that the overall ratio abundances of the proteins quantified after this enrichment was very homogeneous. With this approach, 547 non-redundant macrophage proteins were quantified and 137 were annotated in Uniprot as "ATP-binding proteins" (around 25%). Proteins that were quantified and not annotated as ATP binding proteins could be either proteins that were interacting with the ATP binding proteins or proteins that resulted from unspecific binding with the probe. The protein family with more quantified ATP-binding proteins was the protein kinase superfamily (with 24 quantified protein kinases). Out of these 24 protein kinases, 13 proteins were included in the Ser/Thr (STE) protein kinase family. The preference to this protein kinase family was previously observed by Lemeer and co-workers (Lemeer *et al.*, 2013). They performed a comparison between two enrichment methods (ATP-affinity probe and kinobeads). They found a higher number of tyrosine kinases enriched with kinobeads, while more kinases from the STE kinase group were enriched with the ATP affinity probe. They detailed that small molecules inhibitors immobilized in kinobeads were originally developed to target tyrosine kinases, whereas the reaction mechanism of the ATP probe was distinct (Lemeer *et al.*, 2013).

From the quantified proteins, 59 were differentially abundant. From the differentially abundant ATP-binding proteins 6 were kinases (MAP2K2, SYK, STK3, MAP3K2, NDKA and SRPK1), most of them involved in signaling pathways. Macrophage proteomic alterations included an increase of protein synthesis. Besides, macrophages showed changes in mitochondrial proteins involved in the response to oxidative stress. Regarding cell death mechanisms an increase of antiapoptotic signals was suggested. Furthermore, a high pro-inflammatory response together with no up-regulation of key mi-RNAs involved in the regulation of this response was observed. Besides, we analyzed the phosphopeptides of this sub-proteome because ATP-binding proteins represent one superfamily of proteins, including kinases, which are known to be highly phosphorylated when signaling cascades are activated after interaction with the pathogens. This enrichment could allow us getting more information, other than protein abundance. The method used for the phosphopeptide enrichment was SIMAC. This method is based on an initial enrichment and separation of mono- and multi-phosphorylated peptides using IMAC and a subsequent enrichment of the mono-phosphorylated peptides using TiO_2 chromatography (Thingholm *et al.*, 2008). It combines the advantages of IMAC and TiO_2. This was the main reason for using this methodology instead of only TiO_2. Moreover, a comparison between SIMAC and TiO_2 was performed and they were able to identify more than double of phosphorylation sites and to recover 3-fold more of multiple phosphorylated peptides than using TiO_2 alone (Thingholm *et al.*,

2008). With SIMAC, we were able to quantify 85 phosphopeptides and 5 were differentially abundant. The reason we believe we did not obtain a higher number of identifications was due to the fact that we did the phosphopeptide enrichment on the ATP binding proteins sub-proteome which could have decreased it.

1.2 Global proteomic and phosphoproteomic approaches to study macrophage remodeling after interaction with *C. albicans*

We were also interested in understanding the global changes in *C. albicans* infected macrophages and to know if these changes were specific for the pathogen or resulted from a general phagocytic event. To achieve this, a proteomic and phosphoproteomic TMT based approach was carried out. A condition where macrophages were co-incubated with inert latex beads in the same conditions as *C. albicans* was included. We also performed some optimization in order to try to diminish the inter-replicate variability observed in the ATP binding enrichment approach. *C. albicans* was used from a liquid culture at OD of 1 (beginning of exponential phase) instead from a plate were the cells can be at different growth phases. IL-1β was checked to evaluate macrophage activation for samples used in the proteomic analysis. Moreover, cell homogenization was performed with a mild process to further avoid *C. albicans* cell lysis. Due to the higher number of conditions, TMT was the peptide labelling method used once it has higher capability of multiplexing than SILAC. With this approach we were able to quantify 6166 human proteins and 9615 phosphopeptides. First statistical analysis showed that the condition of macrophages co-incubated with beads did not give statistically significant changes. This may be due to the fact the ratio 1 macrophage to 1 bead is too low for significant proteomic changes. This correlates with the IL-1β measurements, where also no statistically significant differences were observed when comparing the secretion of this cytokine in macrophages after interacting with beads and macrophages control; and also, when comparing in macrophages after interacting with beads and macrophages after interacting with *C. albicans*. In any case, this suggested that the proteomic changes observed after macrophage interaction with *C. albicans* were due to the pathogen and not only due to the process phagocytosis. Future works could be performed with higher ratios of beads in order to try to better distinguish between general and *C. albicans* specific effects.

With this shot-gun approach, from the 6166 proteins quantified 89 proteins were found to be differentially abundant. The protein fold-change values were not very high also in this work.

As observed in the approach of ATP binding enrichment, also here proteins differentially abundant from the mitochondria were quantified. Furthermore, GO analysis showed an

enrichment in more abundant proteins from the mitochondrial matrix. A higher proportion of cells with higher mitochondrial membrane potential was suggested. This is important once higher mitochondrial potential is highly correlated with ROS production (Suski *et al.*, 2018). Although a high variability in this assay was observed and more studies are needed to confirm these results. This TMT-based approach revealed that the more abundant proteins after macrophage interaction with *C. albicans* were involved in different biological processes such as cell proliferation and phosphatidylinositol biosynthetic process. Interestingly, less abundant proteins were highly interacting with each other and involved in RNA splicing and processing. For the phosphopeptide enrichment Fe-IMAC was used. This methodology is more reproducible than the enrichments that use stage tips or batch incubations like TiO_2 or Ti-IMAC beads. These formats suffer from a high degree of variability due to the manual handling steps which increase variability. Moreover, the enrichment efficiency and selectivity is largely dependent on the bead-to-sample ratio (Ruprecht *et al.*, 2017). This methodology uses Fe-IMAC columns and it was showed that column enrichment did not suffered from bead-to-sample ratio issues and scaled linearly from 100 µg to 5 mg of digest. Furthermore, Fe-IMAC columns were shown to enable the identification of more phosphopeptide than Ti-IMAC and TiO_2 (Ruprecht *et al.*, 2015). With this phosphopeptide enrichment, a total of 134 phosphopeptides were found to be differentially abundant. Furthermore, an interesting network of the phosphoproteins was presented, depicting proteins involved in RNA splicing, RNA transcription as well as cytoskeleton rearrangement and cell signaling.

Overall, both proteomic approaches brought us relevant and complementary biological information. These strategies can help to better understand these host-pathogen dynamics and lead to the development of new antifungal therapies or to modulate the immune response in response to fungal infections. Over the past years, MS-based proteomics used data-dependent acquisition (DDA) strategies, such as the shotgun approaches. The main drawback of DDA is that it stochastically samples the most abundant peptides and misses the rest. Besides this, DDA was until now the preferred method due to its flexibility, breadth of detection and the simplicity of its setup and analysis. DIA is an emerging method that samples all peptides within the selected mass ranges, allowing identification of all sufficiently abundant peptides and this constitutes the main advantage over DDA (reviewed in (Aebersold & Mann, 2016)). The use of this methodology for the study of host-pathogen interactions can bring new and valuable information.

Increasing the knowledge in the dynamic mechanisms that happen during this interaction is, from our point of view, crucial to open doors for the development of novel and more efficient antifungal therapies. The current therapies are mainly focused on the pathogen, nevertheless

new approaches are arising. Administration of cytokines was shown to enhance protection against *Candida* infections (Polak-Wyss, 1991). Although controversial, it also being studied if host receptors blockage can be beneficial to treat these infections (Filler, 2013). Zwolanek and co-workers suggested the inhibition of the Tec kinase to combat invasive microbial infections (Zwolanek *et al.*, 2014). It is our belief that although being yet elusive, holistic approaches, using proteomics and other *omic* techniques can give us valuable insights to approach treatment by targeting the host. The results obtained here, made us look into the possible clinical uses of miRNAs and RNA splicing. Interestingly, new experimental treatments targeting host miRNA are being investigated (Drury *et al.*, 2017). Furthermore, defects in RNA splicing can have pathological consequences and many human genetic diseases are associated with splicing defects. Currently there are several tools being developed to target and alter splicing (Havens *et al.*, 2013).

2 Study of the serological response for the discovery of biomarker candidates of IC

Besides treating fungal infections, also its early diagnosis is of highly importance. These bring us to the second important interaction studied here that entailed the characterization of the host serological response to hyphal C*: albicans* secreted proteins. Adaptive immune responses to *C. albicans* are crucial for the successful eradication of the fungal infection. The role of Th1 and Th17 cellular response is considered of great importance for protection against these infections. On the other hand, the importance of antibody response to *C. albicans* has been neglected in the past. This happened because different experiments gave different degrees of importance to antibody-mediated immune response (reviewed in (Richardson & Moyes, 2015)). For example, some works showed that depletion of B cells did not increase susceptibility to *C. albicans* infections (Carrow *et al.*, 1984). Nowadays, more importance has been given to antibody response. For instance, it was shown that antibodies against *C. albicans* mannan could protect mice against *Candida* infections (Zhang *et al.*, 2006). This importance is reflected mainly in the study of several different anti-*Candida* vaccines (reviewed in (Tso *et al.*, 2018)) and in the development of diagnostic methods that are based on the antibody response to *C. albicans* antigens, such as the commercially available CAGTA® (Vircell) assays that detect IgG antibodies to *C. albicans* cell surface antigens from germ tubes (Parra-Sanchez *et al.*, 2017). Our group and others have been making a great effort in the discovery of specific antigenic *C. albicans* proteins that could be used in the future as immunoassays that evaluate serum antibody response directly to these proteins and aid in IC diagnosis. Swoboda and co-workers performed a *C. albicans* cDNA library and found that alcohol dehydrogenase and pyruvate kinase sequences, together with other cDNA sequences with unknown function at that time, were recognized as being among the

strongest antigens (Swoboda *et al.*, 1993). Ardizzoni and co-workers performed an antibody array with 10 well-known immunogenic proteins (Bgl2, Eno1, Pgk1, Fba1, Adh1, Als3, Hwp1, Hsp90 and Grp2) and found that Bgl2, Eno1, Pgk1 and Grp2 presented higher IgG levels in IC than in non-IC patients (Ardizzoni *et al.*, 2014). Mochon and co-workers performed a *C. albicans* cell surface protein microarray and evaluated the antibody profile of patients with candidemia and controls. For that, they used sera from patients with candidemia and negative controls and they were able to identify 13 cell surface antigens capable of distinguish acute candidemia from healthy individuals and uninfected hospital patients with commensal colonization (Cdr1, Cfl91, Cdr4, Als9, Cdc19, Nik1, Chs8, Rta4, Sln1, Trk1, Yor1, Csc25 and Ras2) (Mochon *et al.*, 2010). These are some examples of the effort that is being made towards the discovery of new biomarkers that do not need to culture the microorganism to diagnose IC. Our group has been widely using the combination of two-dimensional gel electrophoresis along with immunoblot analysis and further identification by MALDI-TOF-MS for the identification of antigenic *C. albicans* cytoplasmic and cell-wall proteins (Pitarch *et al.*, 2006, Pitarch *et al.*, 2011, Pitarch *et al.*, 2016).

In Chapter 2, we carried out an MS-based proteomic approach for the overall analysis of the *C. albicans* hyphal secretome in Lee medium (pH 6.7) and an immunoproteomic approach for the study of the serological response to *C. albicans* secreted proteins in patients with catheter and non-catheter associated IC.

2.1 Analysis of the *C. albicans* hyphal secretome and immunoproteomic study for the identification of potential diagnostic biomarkers of IC

MS-based proteomics can analyze peptide mixtures by digesting (usually with trypsin) complex protein samples in a much easier way than by a gel dependent manner. As explained in Chapter 2, the analysis of the whole secretome entails the concentration of cultured medium without the cells followed by protein analysis. Taking advantage of this approach we were able to identify 301 proteins present in the secretome of hyphal *C. albicans*. Among them, we were able to identify proteins implicated in interaction with the host, cellular response to oxidative stress and pathogenesis. Moreover, some of them were previously described as immunogenic. The global view of the proteins in *C. albicans* secretome is highly relevant once extracellular proteins are involved in biofilm formation, cell nutrient acquisition and cell wall integrity maintenance. These proteins interact with the host and include virulence factors (Gil-Bona *et al.*, 2018) and can give us important insights on proteins that can be used for IC diagnosis.

Despite the clear returns that MS-based proteomics bring, several advantages are still attributed to gel-based proteomics. Among them, the fact that densitometric analysis of the protein spots provides more direct quantitative results than peptide intensity-based calculation and it is also a

more appropriate technique for the study of protein species (Kim & Cho, 2019). Gel-based immunoproteomics is a widely used methodology for serological screenings of several microbial infections, in particular IC. The combination of 2-DE with Western blot assays using specific antibodies raised against *C. albicans* antigens was reported as a very sensitive methodology for the detection of immunoreactive *C. albicans* proteins (Pitarch *et al.*, 1999) and was used in this work. Moreover, its importance was previously proved for the discovery of possible biomarkers of infection (Pitarch *et al.*, 2006, Luo *et al.*, 2016).

With this work, new insights were given in the serological response to hyphal secreted *C. albicans* proteins. We observed higher serological response in the group of patients with catheter associated IC. Nevertheless, more studies are needed, using the sera separately, to corroborate that the entrance of *C. albicans* directly to the bloodstream, producing a scenario of candidemia instead of deep-seated candidiasis, may result in higher levels of antibody response. Interestingly, 7 proteins were found to be highly immunoreactive (Bgl2, Eno1, Glx3, Sap5, Pra1, Pgk1 and Tdh3). Specially promising are Glx3 and Bgl2 which were the proteins that, with our sera pools, presented high immunogenicity in the groups of patients with IC and no immunogenicity in the pool of control patients. High levels of anti Bgl2p antibody levels in sera from patients with IC were previously observed and were significantly different from patients control and suggested as an independent biomarker to diagnose IC (Pitarch *et al.*, 2006). Our group had previously showed that serum anti-Bgl2, anti-Eno1, anti-Glx3, anti-Pgk1 and anti-Tdh31 antibodies were biomarker candidates of IC (Pitarch *et al.*, 2004, Pitarch *et al.*, 2006). This brings us to one limitation of this approach: only the soluble and more abundant proteins can be resolved on the immunoblot. Specifically, one of the limitations observed during this work was the observation of highly immunogenic proteins that were not possible to identify by MALDI-TOF-MS due to its low abundance in the gel. This culminates with the identification of several proteins that were previously found to be immunogenic, once they are abundant and soluble. Nevertheless, this method provides a robust way of screening the antibody reactivity profiles of serum (Fulton & Twine, 2013). An alternative methodology is the use of protein microarray-based methodology to profile antibody response. Mochon and co-workers developed a cell surface protein microarray and profile the serological response on the protein array with sera from different patients (Mochon *et al.*, 2010). The chip-based technology has the advantage of using the entire theoretical proteome of the organism and reduced volume of serum (Fulton & Twine, 2013). Nevertheless, constraints on recombinant protein expression could arise (Kudva *et al.*, 2008). Another possible strategy are immuno-affinity capture technologies, where antibodies from patient sera are immobilized on protein A- or protein G-coupled columns and then immunogenic

proteins from fungal cell lysates or from secretome are captured and effectively enriched on the columns. After eluting the immunocaptured antigens, these proteins are digested and identified by MS/MS (Kniemeyer *et al.*, 2016). This technique overcomes the problem of the 2-DE where only some proteins are effectively resolved in the gel. On the other hand, it also has some drawbacks such as unspecific binding and the fact that MS analysis is more complex than from 2-DE (reviewed in (Tjalsma *et al.*, 2008)). However, to our knowledge this technique was not yet used with *C. albicans*.

All of these results highlight the fact that the use of breakthrough technologies such as proteomics and their diverse and different approaches may help in the basic study of the mechanisms of host immunity and fungal pathogenesis. Figure GD.3 schematically represents our contribution with these works.

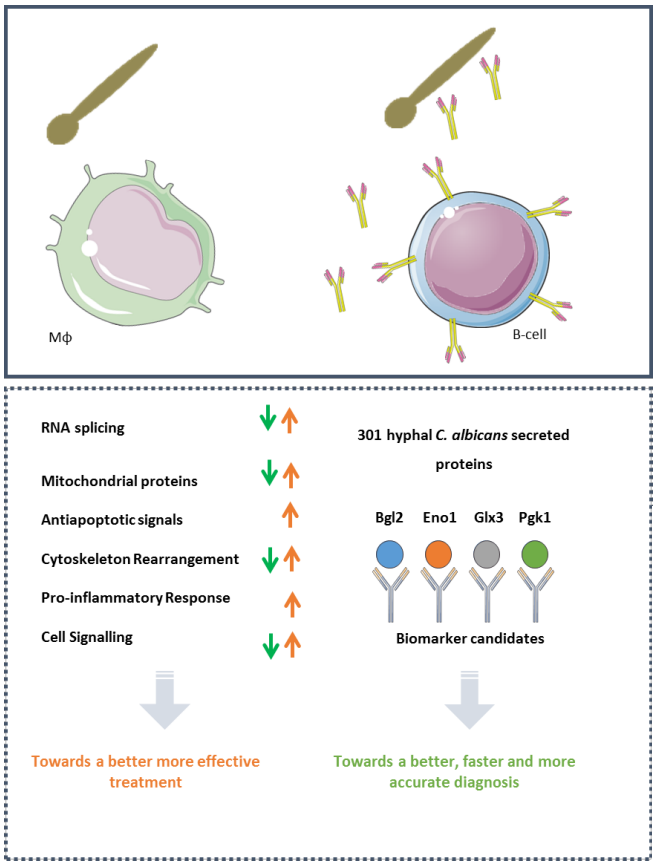

Figure GD.3 Contributions made with this thesis. Different proteomic approaches led to the study of mechanisms altered in macrophages after interaction with *C. albicans*, to the identification of secreted proteins, and of immunoreactive proteins. IgG antibodies against Bgl2, Eno1, Glx3 and Pgk1 are biomarker candidates of IC.

These studies can be translated in the future to the clinical practice and aid in the three more important fields when dealing with a disease: effective prevention, early and accurate diagnosis and appropriate treatment.

CONCLUSIONS

1. Both proteomic and phosphoproteomic approaches, the one focused on the ATP binding proteins and the other based on the analysis of the global proteome, enabled the study of the important proteomic remodelling in human PMA-activated THP-1 macrophages after 3 h of interaction with *C. albicans* with a MOI of 1. Both proteomic and phosphoproteomic approaches showed generally homogenous ratios in protein abundance when comparing macrophages control with *C. albicans* infected macrophages, suggesting that pre-activation with PMA may overwhelm this specific stimulus.

2. The ATP-binding enrichment approach was developed successfully and revealed that 25% of all quantified proteins were annotated as ATP binding proteins. From the 12 ATP-binding proteins differentially abundant, 6 were kinases (MAP2K2, SYK, STK3, MAP3K2, NDKA and SRPK1), most of them involved in signaling pathways.

3. Antiapoptotic signals were more abundant than proapoptotic signals, in line with the lack of cleaved caspase-3, in human macrophages after interaction with *C. albicans*.

4. Macrophages presented a high pro-inflammatory response after interacting with *C. albicans*, by an increase in the secretion of IL-1β, TNF-α and IL-12 cytokines. Furthermore, there was a lack of activation of mi-RNAs that could be involved in the regulation of the inflammatory response in immune cells.

5. The global proteomic and phosphoproteomic approach unveiled that *C. albicans* induced important macrophage proteomic alterations that were not detected when macrophages interacted with latex beads. A group of 89 proteins and 135 phosphopeptides were differentially abundant in *C. albicans* infected macrophages.

6. RNA splicing was found altered at both proteomic and phosphoproteomic levels in macrophages after interaction with *C. albicans.* Less abundant proteins were enriched in RNA processing and RNA splicing, suggesting a different regulation of this process during macrophage interaction with *C. albicans*.

7. Phosphoproteomic analysis of *C. albicans* infected macrophages showed an increase in the abundance of phosphopeptides from several proteins implicated in biologically relevant processes such as cytoskeleton rearrangement and proteins important in cell survival, cell proliferation and cell cycle regulation.

8. Both proteomic approaches, the one focused on the ATP binding proteins sub-proteome and the other focused on the global proteome, performed in macrophages after interacting with *C. albicans* unveiled differentially **more and less abundant proteins from the mitochondria**, suggesting that this organelle, highly important in ROS production, could be implicated in macrophage response to *Candida albicans*.

9. MS-based proteomic analysis of ***C. albicans*** **hyphal secretome lead to the identification of 301 proteins**, 47 of them previously described as immunogenic proteins in humans. This sub-proteome was unsurprisingly enriched in proteins previously described in the **extracellular region** and 59 proteins were, to our knowledge, newly identified in *C. albicans* hyphae secretome.

10. **Higher IgG antibody levels** together with **significantly higher IgG titers** against *C. albicans* hyphal secretome were detected in the pool of patients with IC than in control group, as expected. Interestingly, higher IgG antibody levels were found in the pool of patients with catheter associated IC than in the pool of patients with non-catheter associated IC.

11. The study of the serological response to *C. albicans* hyphal secretome in patients with IC rendered the identification of *C. albicans* **Bgl2, Eno1, Glx3, Sap5, Pgk1, Pra1 and Tdh3 as immunoreactive proteins**. Highly immunogenic proteins detected mainly in the immunoblots from the pool of patients with catheter associated IC were not possible to identify, due to their low abundance in the gel.

12. This **immunoproteomic study reinforces that serum IgG antibodies to *C. albicans*** Bgl2, Eno1, Glx3 and Pgk1 are biomarker candidates for IC diagnosis, with special interest in **Bgl2 and Glx3** that did not show any immunoreactivity in immunoblots from control patients.

REFERENCES

Adachi J, Kishida M, Watanabe S, Hashimoto Y, Fukamizu K & Tomonaga T (2015) Proteome-Wide Discovery of Unknown ATP-Binding Proteins and Kinase Inhibitor Target Proteins Using an ATP Probe (vol 13, pg 5461, 2014). *Journal of proteome research* **14**: 1333-1333.

Aebersold R & Mann M (2003) Mass spectrometry-based proteomics. *Nature* **422**: 198-207.

Aebersold R & Mann M (2016) Mass-spectrometric exploration of proteome structure and function. *Nature* **537**: 347-355.

Agustinho DP, de Oliveira MA, Tavares AH, Derengowski L, Stolz V, Guilhelmelli F, Mortari MR, Kuchler K & Silva-Pereira I (2016) Dectin-1 is required for miR155 upregulation in murine macrophages in response to *Candida albicans*. *Virulence* 1-12.

Akira S & Hoshino K (2003) Myeloid differentiation factor 88-dependent and -independent pathways in toll-like receptor signaling. *The Journal of infectious diseases* **187 Suppl 2**: S356-363.

Alban A, David SO, Bjorkesten L, Andersson C, Sloge E, Lewis S & Currie I (2003) A novel experimental design for comparative two-dimensional gel analysis: two-dimensional difference gel electrophoresis incorporating a pooled internal standard. *Proteomics* **3**: 36-44.

Alloush HM, Lopez-Ribot JL, Masten BJ & Chaffin WL (1997) 3-phosphoglycerate kinase: a glycolytic enzyme protein present in the cell wall of *Candida albicans*. *Microbiology* **143 (Pt 2)**: 321-330.

Altelaar AF, Frese CK, Preisinger C, Hennrich ML, Schram AW, Timmers HT, Heck AJ & Mohammed S (2013) Benchmarking stable isotope labeling based quantitative proteomics. *Journal of proteomics* **88**: 14-26.

Arango Duque G & Descoteaux A (2014) Macrophage cytokines: involvement in immunity and infectious diseases. *Frontiers in Immunology* **5**: 491.

Ardizzoni A, Posteraro B, Baschieri MC*, et al.* (2014) An antibody reactivity-based assay for diagnosis of invasive candidiasis using protein array. *International Journal of Immunopathology and Pharmacology* **27**: 403-412.

Arthur JS & Ley SC (2013) Mitogen-activated protein kinases in innate immunity. *Nature reviews Immunology* **13**: 679-692.

Avni T, Leibovici L & Paul M (2011) PCR diagnosis of invasive candidiasis: systematic review and meta-analysis. *Journal of Clinical Microbiology* **49**: 665-670.

Bacci A, Montagnoli C, Perruccio K, Bozza S, Gaziano R, Pitzurra L, Velardi A, d'Ostiani CF, Cutler JE & Romani L (2002) Dendritic cells pulsed with fungal RNA induce protective immunity to *Candida albicans* in hematopoietic transplantation. *The Journal of Immunology* **168**: 2904-2913.

Bae HB, Zmijewski JW, Deshane JS, Tadie JM, Chaplin DD, Takashima S & Abraham E (2011) AMP-activated protein kinase enhances the phagocytic ability of macrophages and neutrophils. *Federation of American Societies for Experimental Biology Journal* **25**: 4358-4368.

Baggerman G, Vierstraete E, De Loof A & Schoofs L (2005) Gel-based versus gel-free proteomics: a review. *Combinatorial Chemistry & High Throughput Screening* **8**: 669-677.

Bain JM, Lewis LE, Okai B, Quinn J, Gow NA & Erwig LP (2012) Non-lytic expulsion/exocytosis of *Candida albicans* from macrophages. *Fungal genetics and biology : FG & B* **49**: 677-678.

Bain JM, Louw J, Lewis LE*, et al.* (2014) *Candida albicans* hypha formation and mannan masking of beta-glucan inhibit macrophage phagosome maturation. *MBio* **5**: e01874.

Banchereau J & Steinman RM (1998) Dendritic cells and the control of immunity. *Nature* **392**: 245-252.

Baralle M & Baralle FE (2018) The splicing code. *Biosystems* **164**: 39-48.

Barker KS, Liu T & Rogers PD (2005) Coculture of THP-1 human mononuclear cells with *Candida albicans* results in pronounced changes in host gene expression. *The Journal of infectious diseases* **192**: 901-912.

Beck M, Claassen M & Aebersold R (2011) Comprehensive proteomics. *Current opinion in biotechnology* **22**: 3-8.

Belczacka I, Latosinska A, Metzger J, Marx D, Vlahou A, Mischak H & Frantzi M (2019) Proteomics biomarkers for solid tumors: Current status and future prospects. *Mass spectrometry reviews* **38**: 49-78.

Ben-Ami R, Lewis RE & Kontoyiannis DP (2008) Immunocompromised hosts: immunopharmacology of modern antifungals. *Clinical Infectious Diseases* **47**: 226-235.

Bergsbaken T, Fink SL & Cookson BT (2009) Pyroptosis: host cell death and inflammation. *Nature reviews Microbiology* **7**: 99-109.

Bistoni F, Vecchiarelli A, Cenci E, Puccetti P, Marconi P & Cassone A (1986) Evidence for macrophage-mediated protection against lethal *Candida albicans* infection. *Infection and immunity* **51**: 668-674.

Blanco JL & Garcia ME (2008) Immune response to fungal infections. *Veterinary Immunology and Immunopathology* **125**: 47-70.

Bonzon-Kulichenko E, Perez-Hernandez D, Nunez E*, et al.* (2011) A robust method for quantitative high-throughput analysis of proteomes by 18O labeling. *Molecular & Cellular Proteomics* **10**: M110 003335.

Borghi M, Renga G, Puccetti M, Oikonomou V, Palmieri M, Galosi C, Bartoli A & Romani L (2014) Antifungal Th Immunity: Growing up in Family. *Frontiers in Immunology* **5**: 506.

Bourgeois C & Kuchler K (2012) Fungal pathogens-a sweet and sour treat for toll-like receptors. *Frontiers in cellular and infection microbiology* **2**: 142.

Bourgeois C, Majer O, Frohner IE, Tierney L & Kuchler K (2010) Fungal attacks on mammalian hosts: pathogen elimination requires sensing and tasting. *Current opinion in microbiology* **13**: 401-408.

Bromuro C, Torosantucci A, Gomez MJ, Urbani F & Cassone A (1994) Differential release of an immunodominant 65 kDa mannoprotein antigen from yeast and mycelial forms of Candida albicans. *Journal of Medical and Veterinary Mycology* **32**: 447-459.

Brown GD (2011) Innate antifungal immunity: the key role of phagocytes. *Annual review of immunology* **29**: 1-21.

Brown GD, Denning DW, Gow NA, Levitz SM, Netea MG & White TC (2012) Hidden killers: human fungal infections. *Science Translational Medicine* **4**: 165rv113.

Cabello L, Gomez-Herreros E, Fernandez-Pereira J, Maicas S, Martinez-Esparza MC, de Groot PWJ & Valentin E (2019) Deletion of GLX3 in *Candida albicans* affects temperature tolerance, biofilm formation and virulence. *FEMS yeast research* **19**.

Candel FJ, Pazos Pacheco C, Ruiz-Camps I, Maseda E, Sanchez-Benito MR, Montero A, Puig M, Gilsanz F, Aguilar J & Matesanz M (2017) Update on management of invasive candidiasis. *Revista Española de Quimioterapia* **30**: 397-406.

Canterbury JD, Merrihew GE, MacCoss MJ, Goodlett DR & Shaffer SA (2014) Comparison of data acquisition strategies on quadrupole ion trap instrumentation for shotgun proteomics. *Journal of the American Society for Mass Spectrometry* **25**: 2048-2059.

Carmona-Saez P, Chagoyen M, Tirado F, Carazo JM & Pascual-Montano A (2007) GENECODIS: a web-based tool for finding significant concurrent annotations in gene lists. *Genome Biology* **8**: R3.

Carpino N, Naseem S, Frank DM & Konopka JB (2017) Modulating Host Signaling Pathways to Promote Resistance to Infection by *Candida albicans*. *Frontiers in cellular and infection microbiology* **7**: 481.

Carrow EW, Hector RF & Domer JE (1984) Immunodeficient CBA/N mice respond effectively to *Candida albicans*. *Clinical Immunology and Immunopathology* **33**: 371-380.

Chaffin WL (2008) *Candida albicans* cell wall proteins. *Microbiology and Molecular Biology Reviews* **72**: 495-544.

Chanput W, Mes JJ & Wichers HJ (2014) THP-1 cell line: An in vitro cell model for immune modulation approach. *International immunopharmacology* **23**: 37-45.

Chapman JD, Goodlett DR & Masselon CD (2014) Multiplexed and data-independent tandem mass spectrometry for global proteome profiling. *Mass spectrometry reviews* **33**: 452-470.

Chaves F, Garnacho-Montero J, Del Pozo JL*, et al.* (2018) Diagnosis and treatment of catheter-related bloodstream infection: Clinical guidelines of the Spanish Society of Infectious Diseases and Clinical Microbiology and (SEIMC) and the Spanish Society of Spanish Society of Intensive and Critical Care Medicine and Coronary Units (SEMICYUC). *Medicina Intensiva* **42**: 5-36.

Cheng G, Wozniak K, Wallig MA, Fidel PL, Trupin SR & Hoyer LL (2005) Comparison between *Candida albicans* agglutinin-like sequence gene expression patterns in human clinical specimens and models of vaginal candidiasis. *Infection and immunity* **73**: 1656-1663.

Choi HI, Chung KJ, Yang HY, Ren L, Sohn S, Kim PR, Kook MS, Choy HE & Lee TH (2013) Peroxiredoxin V selectively regulates IL-6 production by modulating the Jak2-Stat5 pathway. *Free Radical Biology and Medicine* **65**: 270-279.

Choi J, Park J, Kim D, Jung K, Kang S & Lee YH (2010) Fungal secretome database: integrated platform for annotation of fungal secretomes. *BMC Genomics* **11**: 105.

Christoforou AL & Lilley KS (2012) Isobaric tagging approaches in quantitative proteomics: the ups and downs. *Analytical and bioanalytical chemistry* **404**: 1029-1037.

Citiulo F, Jacobsen ID, Miramon P, Schild L, Brunke S, Zipfel P, Brock M, Hube B & Wilson D (2012) *Candida albicans* scavenges host zinc via Pra1 during endothelial invasion. *PLoS pathogens* **8**: e1002777.

Clancy CJ & Nguyen MH (2013) Finding the "missing 50%" of invasive candidiasis: how nonculture diagnostics will improve understanding of disease spectrum and transform patient care. *Clinical Infectious Diseases* **56**: 1284-1292.

Clancy CJ & Nguyen MH (2018) T2 magnetic resonance for the diagnosis of bloodstream infections: charting a path forward. *Journal of Antimicrobial Chemotherapy* **73**: iv2-iv5.

Clancy CJ, Nguyen ML, Cheng S, Huang H, Fan G, Jaber RA, Wingard JR, Cline C & Nguyen MH (2008) Immunoglobulin G responses to a panel of *Candida albicans* antigens as accurate and early markers for the presence of systemic candidiasis. *Journal of Clinical Microbiology* **46**: 1647-1654.

Clancy CJ, Pappas PG, Vazquez J*, et al.* (2018) Detecting Infections Rapidly and Easily for Candidemia Trial, Part 2 (DIRECT2): A Prospective, Multicenter Study of the T2*Candida* Panel. *Clinical Infectious Diseases* **66**: 1678-1686.

Crowe JD, Sievwright IK, Auld GC, Moore NR, Gow NA & Booth NA (2003) *Candida albicans* binds human plasminogen: identification of eight plasminogen-binding proteins. *Molecular microbiology* **47**: 1637-1651.

D'Angelo G, Chaerkady R, Yu W*, et al.* (2017) Statistical Models for the Analysis of Isobaric Tags Multiplexed Quantitative Proteomics. *Journal of proteome research* **16**: 3124-3136.

da Silva Dantas A, Lee KK, Raziunaite I, Schaefer K, Wagener J, Yadav B & Gow NA (2016) Cell biology of *Candida albicans*-host interactions. *Current opinion in microbiology* **34**: 111-118.

Daub H, Olsen JV, Bairlein M, Gnad F, Oppermann FS, Korner R, Greff Z, Keri G, Stemmann O & Mann M (2008) Kinase-selective enrichment enables quantitative phosphoproteomics of the kinome across the cell cycle. *Molecular cell* **31**: 438-448.

Dayon L, Hainard A, Licker V, Turck N, Kuhn K, Hochstrasser DF, Burkhard PR & Sanchez JC (2008) Relative quantification of proteins in human cerebrospinal fluids by MS/MS using 6-plex isobaric tags. *Analytical chemistry* **80**: 2921-2931.

De Bernardis F, Amacker M, Arancia S, Sandini S, Gremion C, Zurbriggen R, Moser C & Cassone A (2012) A virosomal vaccine against candidal vaginitis: immunogenicity, efficacy and safety profile in animal models. *Vaccine* **30**: 4490-4498.

de Graauw M, Hensbergen P & van de Water B (2006) Phospho-proteomic analysis of cellular signaling. *Electrophoresis* **27**: 2676-2686.

Deutsch EW, Csordas A, Sun Z*, et al.* (2017) The ProteomeXchange consortium in 2017: supporting the cultural change in proteomics public data deposition. *Nucleic acids research* **45**: D1100-D1106.

Dill BD, Gierlinski M, Hartlova A, Arandilla AG, Guo M, Clarke RG & Trost M (2015) Quantitative proteome analysis of temporally resolved phagosomes following uptake via key phagocytic receptors. *Molecular & cellular proteomics : MCP* **14**: 1334-1349.

Domon B & Aebersold R (2010) Options and considerations when selecting a quantitative proteomics strategy. *Nature biotechnology* **28**: 710-721.

Drury RE, O'Connor D & Pollard AJ (2017) The Clinical Application of MicroRNAs in Infectious Disease. *Frontiers in Immunology* **8**: 1182.

Duan Z, Chen X, Du L, Liu C, Zeng R, Chen Q & Li M (2017) Inflammation Induced by *Candida parapsilosis* in THP-1 Cells and Human Peripheral Blood Mononuclear Cells (PBMCs). *Mycopathologia* **182**: 1015-1023.

Duhring S, Germerodt S, Skerka C, Zipfel PF, Dandekar T & Schuster S (2015) Host-pathogen interactions between the human innate immune system and *Candida albicans*-understanding and modeling defense and evasion strategies. *Frontiers in microbiology* **6**: 625.

Duncan JS, Whittle MC, Nakamura K*, et al.* (2012) Dynamic reprogramming of the kinome in response to targeted MEK inhibition in triple-negative breast cancer. *Cell* **149**: 307-321.

Dyballa N & Metzger S (2009) Fast and sensitive colloidal coomassie G-250 staining for proteins in polyacrylamide gels. *Journal of Visualized Experiments*.

Ene IV, Heilmann CJ, Sorgo AG, Walker LA, de Koster CG, Munro CA, Klis FM & Brown AJ (2012) Carbon source-induced reprogramming of the cell wall proteome and secretome modulates the adherence and drug resistance of the fungal pathogen *Candida albicans*. *Proteomics* **12**: 3164-3179.

Engholm-Keller K & Larsen MR (2016) Improving the Phosphoproteome Coverage for Limited Sample Amounts Using TiO2-SIMAC-HILIC (TiSH) Phosphopeptide Enrichment and Fractionation. *Methods in molecular biology* **1355**: 161-177.

Engholm-Keller K, Birck P, Storling J, Pociot F, Mandrup-Poulsen T & Larsen MR (2012) TiSH - a robust and sensitive global phosphoproteomics strategy employing a combination of TiO2, SIMAC, and HILIC. *Journal of proteomics* **75**: 5749-5761.

Erwig LP & Gow NA (2016) Interactions of fungal pathogens with phagocytes. *Nature reviews Microbiology* **14**: 163-176.

Estrada-Mata E, Navarro-Arias MJ, Perez-Garcia LA, Mellado-Mojica E, Lopez MG, Csonka K, Gacser A & Mora-Montes HM (2015) Members of the *Candida parapsilosis* Complex and *Candida albicans* are Differentially Recognized by Human Peripheral Blood Mononuclear Cells. *Frontiers in microbiology* **6**: 1527.

Fernandez-Arenas E, Molero G, Nombela C, Diez-Orejas R & Gil C (2004) Low virulent strains of *Candida albicans:* unravelling the antigens for a future vaccine. *Proteomics* **4**: 3007-3020.

Fernandez-Arenas E, Bleck CK, Nombela C, Gil C, Griffiths G & Diez-Orejas R (2009) *Candida albicans* actively modulates intracellular membrane trafficking in mouse macrophage phagosomes. *Cellular microbiology* **11**: 560-589.

Fernandez-Arenas E, Cabezon V, Bermejo C, Arroyo J, Nombela C, Diez-Orejas R & Gil C (2007) Integrated proteomics and genomics strategies bring new insight into Candida albicans response upon macrophage interaction. *Molecular & cellular proteomics : MCP* **6**: 460-478.

Fields S (2001) Proteomics. Proteomics in genomeland. *Science* **291**: 1221-1224.

Filler SG (2013) Can host receptors for fungi be targeted for treatment of fungal infections? *Trends in microbiology* **21**: 389-396.

Fonzi WA (2009) The protein secretory pathway of *Candida albicans*. *Mycoses* **52**: 291-303.

Forman HJ & Torres M (2001) Redox signaling in macrophages. *Molecular Aspects of Medicine* **22**: 189-216.

Fradin C, Poulain D & Jouault T (2000) Beta-1,2-linked oligomannosides from *Candida albicans* bind to a 32-kilodalton macrophage membrane protein homologous to the mammalian lectin galectin-3. *Infection and immunity* **68**: 4391-4398.

Fu Y, Luo G, Spellberg BJ, Edwards JE, Jr. & Ibrahim AS (2008) Gene overexpression/suppression analysis of candidate virulence factors of *Candida albicans*. *Eukaryotic cell* **7**: 483-492.

Fulton KM & Twine SM (2013) Immunoproteomics: current technology and applications. *Methods in molecular biology* **1061**: 21-57.

Gatto F, Cagliani R, Catelani T, Guarnieri D, Moglianetti M, Pompa PP & Bardi G (2017) PMA-Induced THP-1 Macrophage Differentiation is Not Impaired by Citrate-Coated Platinum Nanoparticles. *Nanomaterials (Basel)* **7**.

Gazi U, Rosas M, Singh S, Heinsbroek S, Haq I, Johnson S, Brown GD, Williams DL, Taylor PR & Martinez-Pomares L (2011) Fungal recognition enhances mannose receptor shedding through dectin-1 engagement. *The Journal of biological chemistry* **286**: 7822-7829.

Ghosh S, Navarathna DHMLP, Roberts DD, Cooper JT, Atkin AL, Petro TM & Nickerson KW (2009) Arginine-Induced Germ Tube Formation in *Candida albicans* Is Essential for Escape from Murine Macrophage Line RAW 264.7. *Infection and immunity* **77**: 1596-1605.

Gil-Bona A, Monteoliva L & Gil C (2015) Global Proteomic Profiling of the Secretome of *Candida albicans* ecm33 Cell Wall Mutant Reveals the Involvement of Ecm33 in Sap2 Secretion. *Journal of proteome research* **14**: 4270-4281.

Gil-Bona A, Amador-Garcia A, Gil C & Monteoliva L (2018) The external face of *Candida albicans*: A proteomic view of the cell surface and the extracellular environment. *Journal of proteomics* **180**: 70-79.

Gil-Bona A, Reales-Calderon JA, Parra-Giraldo CM, Martinez-Lopez R, Monteoliva L & Gil C (2016) The Cell Wall Protein Ecm33 of *Candida albicans* is Involved in Chronological Life Span, Morphogenesis, Cell Wall Regeneration, Stress Tolerance, and Host-Cell Interaction. *Frontiers in microbiology* **7**: 64.

Gil-Bona A, Llama-Palacios A, Parra CM, Vivanco F, Nombela C, Monteoliva L & Gil C (2015) Proteomics unravels extracellular vesicles as carriers of classical cytoplasmic proteins in *Candida albicans*. *Journal of proteome research* **14**: 142-153.

Gil-Bona A, Parra-Giraldo CM, Hernaez ML, Reales-Calderon JA, Solis NV, Filler SG, Monteoliva L & Gil C (2015) *Candida albicans* cell shaving uncovers new proteins involved in cell wall integrity, yeast to hypha transition, stress response and host-pathogen interaction. *Journal of proteomics*.

Gil-Navarro I, Gil ML, Casanova M, O'Connor JE, Martinez JP & Gozalbo D (1997) The glycolytic enzyme glyceraldehyde-3-phosphate dehydrogenase of *Candida albicans* is a surface antigen. *Journal of bacteriology* **179**: 4992-4999.

Giraldo CMP (2013) Estudio Proteomico de la superficie celular de *Candida* spp: aplicaciones biomédicas. Thesis, Universidad Complutense de Madrid.

Girard V, Dieryckx C, Job C & Job D (2013) Secretomes: the fungal strike force. *Proteomics* **13**: 597-608.

Gomez MJ, Torosantucci A, Arancia S, Maras B, Parisi L & Cassone A (1996) Purification and biochemical characterization of a 65-kilodalton mannoprotein (MP65), a main target of anti-*Candida* cell-mediated immune responses in humans. *Infection and immunity* **64**: 2577-2584.

Gorg A, Weiss W & Dunn MJ (2004) Current two-dimensional electrophoresis technology for proteomics. *Proteomics* **4**: 3665-3685.

Gow NA & Hube B (2012) Importance of the Candida albicans cell wall during commensalism and infection. *Current opinion in microbiology* **15**: 406-412.

Gow NA, van de Veerdonk FL, Brown AJ & Netea MG (2011) *Candida albicans* morphogenesis and host defence: discriminating invasion from colonization. *Nature reviews Microbiology* **10**: 112-122.

Gow NAR, Latge JP & Munro CA (2017) The Fungal Cell Wall: Structure, Biosynthesis, and Function. *Microbiol Spectr* **5**.

Granger DL, Hibbs JB, Jr., Perfect JR & Durack DT (1988) Specific amino acid (L-arginine) requirement for the microbiostatic activity of murine macrophages. *J Clin Invest* **81**: 1129-1136.

Graves PR, Kwiek JJ, Fadden P, Ray R, Hardeman K, Coley AM, Foley M & Haystead TA (2002) Discovery of novel targets of quinoline drugs in the human purine binding proteome. *Molecular pharmacology* **62**: 1364-1372.

Gulati M & Nobile CJ (2016) *Candida albicans* biofilms: development, regulation, and molecular mechanisms. *Microbes and Infection* **18**: 310-321.

Guo L, Xiao Y, Fan M, Li JJ & Wang Y (2014) Profiling Global Kinome Signatures of the Radioresistant MCF-7/C6 Breast Cancer Cells Using MRM-based Targeted Proteomics. *Journal of proteome research*.

Han Y & Cutler JE (1995) Antibody response that protects against disseminated candidiasis. *Infection and immunity* **63**: 2714-2719.

Han Y, Ulrich MA & Cutler JE (1999) *Candida albicans* mannan extract-protein conjugates induce a protective immune response against experimental candidiasis. *The Journal of infectious diseases* **179**: 1477-1484.

Hanoulle X, Van Damme J, Staes A, Martens L, Goethals M, Vandekerckhove J & Gevaert K (2006) A new functional, chemical proteomics technology to identify purine nucleotide binding sites in complex proteomes. *Journal of proteome research* **5**: 3438-3445.

Hasim S, Hussin NA, Alomar F, Bidasee KR, Nickerson KW & Wilson MA (2014) A glutathione-independent glyoxalase of the DJ-1 superfamily plays an important role in managing metabolically generated methylglyoxal in *Candida albicans*. *The Journal of biological chemistry* **289**: 1662-1674.

Havens MA, Duelli DM & Hastings ML (2013) Targeting RNA splicing for disease therapy. *Wiley Interdisciplinary Reviews: RNA* **4**: 247-266.

Hawley SA, Ross FA, Gowans GJ, Tibarewal P, Leslie NR & Hardie DG (2014) Phosphorylation by Akt within the ST loop of AMPK-alpha 1 down-regulates its activation in tumour cells. *Biochemical Journal* **459**: 275-287.

Heilmann CJ, Sorgo AG, Mohammadi S, Sosinska GJ, de Koster CG, Brul S, de Koning LJ & Klis FM (2013) Surface stress induces a conserved cell wall stress response in the pathogenic fungus *Candida albicans*. *Eukaryotic cell* **12**: 254-264.

Heinsbroek SE & Gordon S (2009) The role of macrophages in inflammatory bowel diseases. *Expert Reviews in Molecular Medicine* **11**: e14.

Hernaez ML, Ximenez-Embun P, Martinez-Gomariz M, Gutierrez-Blazquez MD, Nombela C & Gil C (2010) Identification of *Candida albicans* exposed surface proteins in vivo by a rapid proteomic approach. *Journal of proteomics* **73**: 1404-1409.

Hiller E, Heine S, Brunner H & Rupp S (2007) *Candida albicans* Sun41p, a putative glycosidase, is involved in morphogenesis, cell wall biogenesis, and biofilm formation. *Eukaryotic cell* **6**: 2056-2065.

Hirakawa MP, Chyou DE, Huang D, Slan AR & Bennett RJ (2017) Parasex Generates Phenotypic Diversity de Novo and Impacts Drug Resistance and Virulence in *Candida albicans*. *Genetics* **207**: 1195-1211.

Hofs S, Mogavero S & Hube B (2016) Interaction of *Candida albicans* with host cells: virulence factors, host defense, escape strategies, and the microbiota. *Journal of Microbiology* **54**: 149-169.

Hu A, Noble WS & Wolf-Yadlin A (2016) Technical advances in proteomics: new developments in data-independent acquisition. *F1000Research* **5**.

Huang J, Wang F, Ye M & Zou H (2014) Enrichment and separation techniques for large-scale proteomics analysis of the protein post-translational modifications. *Journal of chromatography A* **1372C**: 1-17.

Huertas B, Prieto D, Pitarch A, Gil C, Pla J & Diez-Orejas R (2017) Serum Antibody Profile during Colonization of the Mouse Gut by *Candida albicans*: Relevance for Protection during Systemic Infection. *Journal of proteome research* **16**: 335-345.

Ibrahim AS, Spellberg BJ, Avanesian V, Fu Y & Edwards JE, Jr. (2006) The anti-*Candida* vaccine based on the recombinant N-terminal domain of Als1p is broadly active against disseminated candidiasis. *Infection and immunity* **74**: 3039-3041.

Jain N, Hasan F & Fries BC (2008) Phenotypic Switching in Fungi. *Current Fungal Infection Reports* **2**: 180-188.

Janeway CA (1989) Approaching the Asymptote - Evolution and Revolution in Immunology. *Cold Spring Harbor Symposia on Quantitative Biology* **54**: 1-13.

Jang JY, Choi Y, Jeon YK & Kim CW (2008) Suppression of adenine nucleotide translocase-2 by vector-based siRNA in human breast cancer cells induces apoptosis and inhibits tumor growth in vitro and in vivo. *Breast Cancer Research* **10**: R11.

Jazurek M, Ciesiolka A, Starega-Roslan J, Bilinska K & Krzyzosiak WJ (2016) Identifying proteins that bind to specific RNAs - focus on simple repeat expansion diseases. *Nucleic acids research* **44**: 9050-9070.

Jeffery-Smith A, Taori SK, Schelenz S, Jeffery K, Johnson EM, Borman A, Manuel R & Brown CS (2018) *Candida auris*: a Review of the Literature. *Clinical Microbiology Reviews* **31**.

Jensen SS & Larsen MR (2007) Evaluation of the impact of some experimental procedures on different phosphopeptide enrichment techniques. *Rapid Communications in Mass Spectrometry* **21**: 3635-3645.

Jha AK, Huang SC, Sergushichev A*, et al.* (2015) Network integration of parallel metabolic and transcriptional data reveals metabolic modules that regulate macrophage polarization. *Immunity* **42**: 419-430.

Jong AY, Chen SH, Stins MF, Kim KS, Tuan TL & Huang SH (2003) Binding of *Candida albicans* enolase to plasmin(ogen) results in enhanced invasion of human brain microvascular endothelial cells. *Journal of medical microbiology* **52**: 615-622.

Joo MY, Shin JH, Jang HC, Song ES, Kee SJ, Shin MG, Suh SP & Ryang DW (2013) Expression of SAP5 and SAP9 in *Candida albicans* biofilms: comparison of bloodstream isolates with isolates from other sources. *Medical mycology* **51**: 892-896.

Kaewseekhao B, Naranbhai V, Roytrakul S, Namwat W, Paemanee A, Lulitanond V, Chaiprasert A & Faksri K (2015) Comparative Proteomics of Activated THP-1 Cells Infected with *Mycobacterium tuberculosis* Identifies Putative Clearance Biomarkers for Tuberculosis Treatment. *PloS one* **10**: e0134168.

Kalam H, Fontana MF & Kumar D (2017) Alternate splicing of transcripts shape macrophage response to *Mycobacterium tuberculosis* infection. *PLoS pathogens* **13**: e1006236.

Kammers K, Cole RN, Tiengwe C & Ruczinski I (2015) Detecting Significant Changes in Protein Abundance. *EuPA Open Proteomics* **7**: 11-19.

Karageorgopoulos DE, Vouloumanou EK, Ntziora F, Michalopoulos A, Rafailidis PI & Falagas ME (2011) beta-D-glucan assay for the diagnosis of invasive fungal infections: a meta-analysis. *Clinical Infectious Diseases* **52**: 750-770.

Karkowska-Kuleta J & Kozik A (2014) Moonlighting proteins as virulence factors of pathogenic fungi, parasitic protozoa and multicellular parasites. *Molecular Oral Microbiology* **29**: 270-283.

Kawai T & Akira S (2010) The role of pattern-recognition receptors in innate immunity: update on Toll-like receptors. *Nature immunology* **11**: 373-384.

Kerrigan AM & Brown GD (2009) C-type lectins and phagocytosis. *Immunobiology* **214**: 562-575.

Kim J & Sudbery P (2011) *Candida albicans*, a major human fungal pathogen. *Journal of Microbiology* **49**: 171-177.

Kim YI & Cho JY (2019) Gel-based proteomics in disease research: Is it still valuable? *Biochimica et Biophysica Acta (BBA) - Proteins and Proteomics* **1867**: 9-16.

Kitahara N, Morisaka H, Aoki W, Takeda Y, Shibasaki S, Kuroda K & Ueda M (2015) Description of the interaction between *Candida albicans* and macrophages by mixed and quantitative proteome analysis without isolation. *Amb Express* **5**: 1-12.

Klis FM & Brul S (2015) Adaptations of the Secretome of *Candida albicans* in Response to Host-Related Environmental Conditions. *Eukaryotic cell* **14**: 1165-1172.

Kniemeyer O, Ebel F, Kruger T, Bacher P, Scheffold A, Luo T, Strassburger M & Brakhage AA (2016) Immunoproteomics of *Aspergillus* for the development of biomarkers and immunotherapies. *PROTEOMICS – Clinical Applications* **10**: 910-921.

Kohatsu L, Hsu DK, Jegalian AG, Liu FT & Baum LG (2006) Galectin-3 induces death of *Candida* species expressing specific beta-1,2-linked mannans. *The Journal of Immunology* **177**: 4718-4726.

Kramer A, Green J, Pollard J, Jr. & Tugendreich S (2014) Causal analysis approaches in Ingenuity Pathway Analysis. *Bioinformatics* **30**: 523-530.

Krause R, Zollner-Schwetz I, Salzer HJ*, et al.* (2015) Elevated levels of interleukin 17A and kynurenine in candidemic patients, compared with levels in noncandidemic patients in the intensive care unit and those in healthy controls. *The Journal of infectious diseases* **211**: 445-451.

Kudva IT, Calderwood SB & John M (2008) Proteomics-based expression library screening - a platform technology for rapid discovery of pathogen-specific markers of infection. *Expert Opinion on Medical Diagnostics* **2**: 979-989.

Kullberg BJ & Arendrup MC (2015) Invasive Candidiasis. *The New England Journal of Medicine* **373**: 1445-1456.

Lacroix C, Gicquel A, Sendid B*, et al.* (2014) Evaluation of two matrix-assisted laser desorption ionization-time of flight mass spectrometry (MALDI-TOF MS) systems for the identification of *Candida* species. *Clinical Microbiology and Infection* **20**: 153-158.

Lee JH, Choi YJ, Park SH & Nam MJ (2018) Potential role of nucleoside diphosphate kinase in myricetin-induced selective apoptosis in colon cancer HCT-15 cells. *Food and Chemical Toxicology* **116**: 315-322.

Lee KK, Ohyama T, Yajima N, Tsubuki S & Yonehara S (2001) MST, a physiological caspase substrate, highly sensitizes apoptosis both upstream and downstream of caspase activation. *The Journal of biological chemistry* **276**: 19276-19285.

Lee KL, Buckley HR & Campbell CC (1975) An amino acid liquid synthetic medium for the development of mycelial and yeast forms of *Candida albicans*. *Sabouraudia* **13**: 148-153.

Lee SA, Wormsley S, Kamoun S, Lee AF, Joiner K & Wong B (2003) An analysis of the *Candida albicans* genome database for soluble secreted proteins using computer-based prediction algorithms. *Yeast* **20**: 595-610.

Lemeer S, Zorgiebel C, Ruprecht B, Kohl K & Kuster B (2013) Comparing immobilized kinase inhibitors and covalent ATP probes for proteomic profiling of kinase expression and drug selectivity. *Journal of proteome research* **12**: 1723-1731.

Li C, Wu Y, Riehle A, Orian-Rousseau V, Zhang Y, Gulbins E & Grassme H (2017) Regulation of *Staphylococcus aureus* Infection of Macrophages by CD44, Reactive Oxygen Species, and Acid Sphingomyelinase. *Antioxidants & Redox Signaling*.

Li F & Palecek SP (2003) EAP1, a *Candida albicans* gene involved in binding human epithelial cells. *Eukaryotic cell* **2**: 1266-1273.

Li F, Svarovsky MJ, Karlsson AJ, Wagner JP, Marchillo K, Oshel P, Andes D & Palecek SP (2007) Eap1p, an adhesin that mediates *Candida albicans* biofilm formation in vitro and in vivo. *Eukaryotic cell* **6**: 931-939.

Li Z, Adams RM, Chourey K, Hurst GB, Hettich RL & Pan C (2012) Systematic comparison of label-free, metabolic labeling, and isobaric chemical labeling for quantitative proteomics on LTQ Orbitrap Velos. *Journal of proteome research* **11**: 1582-1590.

Lisowska E (2002) The role of glycosylation in protein antigenic properties. *Cellular and Molecular Life Sciences* **59**: 445-455.

Liu PS & Ho PC (2017) Mitochondria: A master regulator in macrophage and T cell immunity. *Mitochondrion* **41**: 45-50.

Liu QY, Lei JX, LeBlanc J, Sodja C, Ly D, Charlebois C, Walker PR, Yamada T, Hirohashi S & Sikorska M (2004) Regulation of DNaseY activity by actinin-alpha4 during apoptosis. *Cell Death & Differentiation* **11**: 645-654.

Livak KJ & Schmittgen TD (2001) Analysis of relative gene expression data using real-time quantitative PCR and the 2(-Delta Delta C(T)) Method. *Methods* **25**: 402-408.

Lizcano JM, Goransson O, Toth R*, et al.* (2004) LKB1 is a master kinase that activates 13 kinases of the AMPK subfamily, including MARK/PAR-1. *Embo Journal* **23**: 833-843.

Lum G & Min XJ (2011) FunSecKB: the Fungal Secretome KnowledgeBase. *Database (Oxford)* **2011**: bar001.

Luo G, Ibrahim AS, French SW, Edwards JE, Jr. & Fu Y (2011) Active and passive immunization with rHyr1p-N protects mice against hematogenously disseminated candidiasis. *PloS one* **6**: e25909.

Luo S, Poltermann S, Kunert A, Rupp S & Zipfel PF (2009) Immune evasion of the human pathogenic yeast *Candida albicans*: Pra1 is a Factor H, FHL-1 and plasminogen binding surface protein. *Molecular immunology* **47**: 541-550.

Luo S, Dasari P, Reiher N*, et al.* (2018) The secreted *Candida albicans* protein Pra1 disrupts host defense by broadly targeting and blocking complement C3 and C3 activation fragments. *Molecular immunology* **93**: 266-277.

Luo T, Kruger T, Knupfer U*, et al.* (2016) Immunoproteomic Analysis of Antibody Responses to Extracellular Proteins of *Candida albicans* Revealing the Importance of Glycosylation for Antigen Recognition. *Journal of proteome research* **15**: 2394-2406.

Magliani W, Conti S, Arseni S, Salati A, Ravanetti L, Maffei DL, Giovati L & Polonelli L (2005) Antibody-mediated protective immunity in fungal infections. *New Microbiologica* **28**: 299-309.

Mantovani A, Cassatella MA, Costantini C & Jaillon S (2011) Neutrophils in the activation and regulation of innate and adaptive immunity. *Nature reviews Immunology* **11**: 519-531.

Marin E, Parra-Giraldo CM, Hernandez-Haro C, Hernaez ML, Nombela C, Monteoliva L & Gil C (2015) *Candida albicans* Shaving to Profile Human Serum Proteins on Hyphal Surface. *Frontiers in microbiology* **6**: 1343.

Marriott HM, Bingle CD, Read RC, Braley KE, Kroemer G, Hellewell PG, Craig RW, Whyte MK & Dockrell DH (2005) Dynamic changes in Mcl-1 expression regulate macrophage viability or commitment to apoptosis during bacterial clearance. *J Clin Invest* **115**: 359-368.

Martinez-Gomariz M, Perumal P, Mekala S, Nombela C, Chaffin WL & Gil C (2009) Proteomic analysis of cytoplasmic and surface proteins from yeast cells, hyphae, and biofilms of *Candida albicans*. *Proteomics* **9**: 2230-2252.

Martinez-Lopez R, Monteoliva L, Diez-Orejas R, Nombela C & Gil C (2004) The GPI-anchored protein CaEcm33p is required for cell wall integrity, morphogenesis and virulence in *Candida albicans*. *Microbiology* **150**: 3341-3354.

Martinez-Lopez R, Nombela C, Diez-Orejas R, Monteoliva L & Gil C (2008) Immunoproteomic analysis of the protective response obtained from vaccination with *Candida albicans* ecm33 cell wall mutant in mice. *Proteomics* **8**: 2651-2664.

Martinez-Solano L, Nombela C, Molero G & Gil C (2006) Differential protein expression of murine macrophages upon interaction with *Candida albicans*. *Proteomics* **6 Suppl 1**: S133-144.

Martinez-Solano L, Reales-Calderon JA, Nombela C, Molero G & Gil C (2009) Proteomics of RAW 264.7 macrophages upon interaction with heat-inactivated *Candida albicans* cells unravel an anti-inflammatory response. *Proteomics* **9**: 2995-3010.

Martinez JP, Gil ML, Lopez-Ribot JL & Chaffin WL (1998) Serologic response to cell wall mannoproteins and proteins of *Candida albicans*. *Clinical Microbiology Reviews* **11**: 121-141.

Mavor AL, Thewes S & Hube B (2005) Systemic fungal infections caused by *Candida* species: epidemiology, infection process and virulence attributes. *Current Drug Targets* **6**: 863-874.

McCarty TP & Pappas PG (2016) Invasive Candidiasis. *Infectious Disease Clinics of North America* **30**: 103-124.

McCreath KJ, Specht CA & Robbins PW (1995) Molecular cloning and characterization of chitinase genes from *Candida albicans*. *Proceedings of the National Academy of Sciences of the United States of America* **92**: 2544-2548.

McIlwain DR, Berger T & Mak TW (2013) Caspase functions in cell death and disease. *Cold Spring Harbor perspectives in biology* **5**: a008656.

Meimaridou E, Kowalczyk J, Guasti L*, et al.* (2012) Mutations in NNT encoding nicotinamide nucleotide transhydrogenase cause familial glucocorticoid deficiency. *Nature Genetics* **44**: 740-742.

Mikulska M (2012) The use of mannan antigen and anti-mannan antibodies in the diagnosis of invasive candidiasis. *Mycoses* **55**: 5-5.

Mills EL, Kelly B, Logan A*, et al.* (2016) Succinate Dehydrogenase Supports Metabolic Repurposing of Mitochondria to Drive Inflammatory Macrophages. *Cell* **167**: 457-470 e413.

Miramon P, Kasper L & Hube B (2013) Thriving within the host: *Candida* spp. interactions with phagocytic cells. *Medical microbiology and immunology* **202**: 183-195.

Miwa S & Brand MD (2003) Mitochondrial matrix reactive oxygen species production is very sensitive to mild uncoupling. *Biochemical Society transactions* **31**: 1300-1301.

Mochon AB, Jin Y, Kayala MA, Wingard JR, Clancy CJ, Nguyen MH, Felgner P, Baldi P & Liu H (2010) Serological profiling of a *Candida albicans* protein microarray reveals permanent host-pathogen interplay and stage-specific responses during candidemia. *PLoS pathogens* **6**: e1000827.

Monk CE, Hutvagner G & Arthur JS (2010) Regulation of miRNA transcription in macrophages in response to *Candida albicans*. *PloS one* **5**: e13669.

Montagnoli C, Bozza S, Bacci A, Gaziano R, Mosci P, Morschhauser J, Pitzurra L, Kopf M, Cutler J & Romani L (2003) A role for antibodies in the generation of memory antifungal immunity. *European journal of immunology* **33**: 1193-1204.

Monteoliva L & Albar JP (2004) Differential proteomics: an overview of gel and non-gel based approaches. *Briefings in Functional Genomics & Proteomics* **3**: 220-239.

Moragues MD, Omaetxebarria MJ, Elguezabal N, Sevilla MJ, Conti S, Polonelli L & Ponton J (2003) A monoclonal antibody directed against a *Candida albicans* cell wall mannoprotein exerts three anti-*C. albicans* activities. *Infection and immunity* **71**: 5273-5279.

Moyes DL, Richardson JP & Naglik JR (2015) *Candida albicans*-epithelial interactions and pathogenicity mechanisms: scratching the surface. *Virulence* **6**: 338-346.

Moyes DL, Wilson D, Richardson JP*, et al.* (2016) Candidalysin is a fungal peptide toxin critical for mucosal infection. *Nature* **532**: 64-+.

Munoz JF, Delorey T, Ford CB, Li BY, Thompson DA, Rao RP & Cuomo CA (2019) Coordinated host-pathogen transcriptional dynamics revealed using sorted subpopulations and single macrophages infected with *Candida albicans*. *Nature Communications* **10**: 1607.

Mylonakis E, Clancy CJ, Ostrosky-Zeichner L*, et al.* (2015) T2 magnetic resonance assay for the rapid diagnosis of candidemia in whole blood: a clinical trial. *Clinical Infectious Diseases* **60**: 892-899.

Naglik JR, Challacombe SJ & Hube B (2003) *Candida albicans* secreted aspartyl proteinases in virulence and pathogenesis. *Microbiology and Molecular Biology Reviews* **67**: 400-428, table of contents.

Naglik JR, Moyes DL, Wachtler B & Hube B (2011) *Candida albicans* interactions with epithelial cells and mucosal immunity. *Microbes and Infection* **13**: 963-976.

Naglik JR, Konig A, Hube B & Gaffen SL (2017) *Candida albicans*-epithelial interactions and induction of mucosal innate immunity. *Current opinion in microbiology* **40**: 104-112.

Naglik JR, Moyes D, Makwana J*, et al.* (2008) Quantitative expression of the *Candida albicans* secreted aspartyl proteinase gene family in human oral and vaginal candidiasis. *Microbiology* **154**: 3266-3280.

Nantel A, Dignard D, Bachewich C*, et al.* (2002) Transcription profiling of *Candida albicans* cells undergoing the yeast-to-hyphal transition. *Molecular Biology of the Cell* **13**: 3452-3465.

Nather K & Munro CA (2008) Generating cell surface diversity in *Candida albicans* and other fungal pathogens. *FEMS Microbiology Letters* **285**: 137-145.

Nau GJ, Richmond JF, Schlesinger A, Jennings EG, Lander ES & Young RA (2002) Human macrophage activation programs induced by bacterial pathogens. *Proceedings of the National Academy of Sciences of the United States of America* **99**: 1503-1508.

Neely LA, Audeh M, Phung NA*, et al.* (2013) T2 magnetic resonance enables nanoparticle-mediated rapid detection of candidemia in whole blood. *Science Translational Medicine* **5**: 182ra154.

Netea MG, Quintin J & van der Meer JW (2011) Trained immunity: a memory for innate host defense. *Cell host & microbe* **9**: 355-361.

Netea MG, Meer JW, Verschueren I & Kullberg BJ (2002) CD40/CD40 ligand interactions in the host defense against disseminated *Candida albicans* infection: the role of macrophage-derived nitric oxide. *European journal of immunology* **32**: 1455-1463.

Netea MG, Brown GD, Kullberg BJ & Gow NA (2008) An integrated model of the recognition of *Candida albicans* by the innate immune system. *Nature reviews Microbiology* **6**: 67-78.

Netea MG, Joosten LA, van der Meer JW, Kullberg BJ & van de Veerdonk FL (2015) Immune defence against *Candida* fungal infections. *Nature reviews Immunology* **15**: 630-642.

Netea MG, Van Der Graaf CA, Vonk AG, Verschueren I, Van Der Meer JW & Kullberg BJ (2002) The role of toll-like receptor (TLR) 2 and TLR4 in the host defense against disseminated candidiasis. *The Journal of infectious diseases* **185**: 1483-1489.

Netea MG, Gow NA, Munro CA*, et al.* (2006) Immune sensing of *Candida albicans* requires cooperative recognition of mannans and glucans by lectin and Toll-like receptors. *J Clin Invest* **116**: 1642-1650.

Nieto MC, Telleria O & Cisterna R (2015) Sentinel surveillance of invasive candidiasis in Spain: epidemiology and antifungal susceptibility. *Diagnostic microbiology and infectious disease* **81**: 34-40.

Nimrichter L, de Souza MM, Del Poeta M, Nosanchuk JD, Joffe L, Tavares Pde M & Rodrigues ML (2016) Extracellular Vesicle-Associated Transitory Cell Wall Components and Their Impact on the Interaction of Fungi with Host Cells. *Frontiers in microbiology* **7**: 1034.

Nobile CJ, Fox EP, Nett JE, Sorrells TR, Mitrovich QM, Hernday AD, Tuch BB, Andes DR & Johnson AD (2012) A recently evolved transcriptional network controls biofilm development in *Candida albicans*. *Cell* **148**: 126-138.

Noble SM, Gianetti BA & Witchley JN (2017) *Candida albicans* cell-type switching and functional plasticity in the mammalian host. *Nature reviews Microbiology* **15**: 96-108.

Nogales-Cadenas R, Carmona-Saez P, Vazquez M, Vicente C, Yang X, Tirado F, Carazo JM & Pascual-Montano A (2009) GeneCodis: interpreting gene lists through enrichment analysis and integration of diverse biological information. *Nucleic acids research* **37**: W317-322.

Nombela C, Gil C & Chaffin WL (2006) Non-conventional protein secretion in yeast. *Trends in microbiology* **14**: 15-21.

Nucci M & Anaissie E (2001) Revisiting the source of candidemia: skin or gut? *Clinical Infectious Diseases* **33**: 1959-1967.

O'Connor BP, Danhorn T, De Arras L, Flatley BR, Marcus RA, Farias-Hesson E, Leach SM & Alper S (2015) Regulation of Toll-like Receptor Signaling by the SF3a mRNA Splicing Complex. *Plos Genetics* **11**.

O'Farrell PH (1975) High resolution two-dimensional electrophoresis of proteins. *The Journal of biological chemistry* **250**: 4007-4021.

O'Meara TR, Veri AO, Ketela T, Jiang B, Roemer T & Cowen LE (2015) Global analysis of fungal morphology exposes mechanisms of host cell escape. *Nature Communications* **6**: 6741.

O'Meara TR, Duah K, Guo CX*, et al.* (2018) High-Throughput Screening Identifies Genes Required for *Candida albicans* Induction of Macrophage Pyroptosis. *MBio* **9**.

Okai B, Lyall N, Gow NA, Bain JM & Erwig LP (2015) Rab14 regulates maturation of macrophage phagosomes containing the fungal pathogen *Candida albicans* and outcome of the host-pathogen interaction. *Infection and immunity* **83**: 1523-1535.

Okuda J, Toyotome T, Kataoka N, Ohno M, Abe H, Shimura Y, Seyedarabi A, Pickersgill R & Sasakawa C (2005) *Shigella* effector IpaH9.8 binds to a splicing factor U2AF(35) to modulate host immune responses. *Biochemical and Biophysical Research Communications* **333**: 531-539.

Ong SE & Mann M (2006) A practical recipe for stable isotope labeling by amino acids in cell culture (SILAC). *Nature protocols* **1**: 2650-2660.

Ong SE, Blagoev B, Kratchmarova I, Kristensen DB, Steen H, Pandey A & Mann M (2002) Stable isotope labeling by amino acids in cell culture, SILAC, as a simple and accurate approach to expression proteomics. *Molecular & cellular proteomics : MCP* **1**: 376-386.

Pachl J, Svoboda P, Jacobs F*, et al.* (2006) A randomized, blinded, multicenter trial of lipid-associated amphotericin B alone versus in combination with an antibody-based inhibitor of heat shock protein 90 in patients with invasive candidiasis. *Clinical Infectious Diseases* **42**: 1404-1413.

Pai AA, Baharian G, Page Sabourin A*, et al.* (2016) Widespread Shortening of 3' Untranslated Regions and Increased Exon Inclusion Are Evolutionarily Conserved Features of Innate Immune Responses to Infection. *PLoS Genetics* **12**: e1006338.

Pande K, Chen C & Noble SM (2013) Passage through the mammalian gut triggers a phenotypic switch that promotes *Candida albicans* commensalism. *Nature Genetics* **45**: 1088-1091.

Pandey A, Ding SL, Qin QM*, et al.* (2017) Global Reprogramming of Host Kinase Signaling in Response to Fungal Infection. *Cell host & microbe* **21**: 637-649 e636.

Pappas PG, Lionakis MS, Arendrup MC, Ostrosky-Zeichner L & Kullberg BJ (2018) Invasive candidiasis. *Nature Reviews Disease Primers* **4**: 18026.

Parra-Sanchez M, Zakariya-Yousef Breval I, Castro Mendez C*, et al.* (2017) *Candida albicans* Germ-Tube Antibody: Evaluation of a New Automatic Assay for Diagnosing Invasive Candidiasis in ICU Patients. *Mycopathologia* **182**: 645-652.

Patricelli MP, Szardenings AK, Liyanage M, Nomanbhoy TK, Wu M, Weissig H, Aban A, Chun D, Tanner S & Kozarich JW (2007) Functional Interrogation of the Kinome Using Nucleotide Acyl Phosphates. *The Biochemical journal* **46**: 350-358.

Paul SP, Taylor LS, Stansbury EK & McVicar DW (2000) Myeloid specific human CD33 is an inhibitory receptor with differential ITIM function in recruiting the phosphatases SHP-1 and SHP-2. *Blood* **96**: 483-490.

Perez-Riverol Y, Csordas A, Bai J*, et al.* (2019) The PRIDE database and related tools and resources in 2019: improving support for quantification data. *Nucleic acids research* **47**: D442-D450.

Pfaller MA & Castanheira M (2016) Nosocomial Candidiasis: Antifungal Stewardship and the Importance of Rapid Diagnosis. *Medical mycology* **54**: 1-22.

Phua AI, Hon KY, Holt A, O'Callaghan M & Bihari S (2019) *Candida* catheter-related bloodstream infection in patients on home parenteral nutrition - Rates, risk factors, outcomes, and management. *Clinical Nutrition ESPEN* **31**: 1-9.

Pianalto KM & Alspaugh JA (2016) New Horizons in Antifungal Therapy. *Journal of Fungi* **2**.

Pitarch A, Nombela C & Gil C (2011) Prediction of the clinical outcome in invasive candidiasis patients based on molecular fingerprints of five anti-Candida antibodies in serum. *Molecular & cellular proteomics : MCP* **10**: M110 004010.

Pitarch A, Nombela C & Gil C (2014) Serum antibody signature directed against *Candida albicans* Hsp90 and enolase detects invasive candidiasis in non-neutropenic patients. *Journal of proteome research* **13**: 5165-5184.

Pitarch A, Nombela C & Gil C (2016) Seroprofiling at the *Candida albicans* protein species level unveils an accurate molecular discriminator for candidemia. *Journal of proteomics* **134**: 144-162.

Pitarch A, Nombela C & Gil C (2018) Diagnosis of Invasive Candidiasis: From Gold Standard Methods to Promising Leading-edge Technologies. *Current Topics in Medicinal Chemistry* **18**: 1375-1392.

Pitarch A, Sanchez M, Nombela C & Gil C (2002) Sequential fractionation and two-dimensional gel analysis unravels the complexity of the dimorphic fungus *Candida albicans* cell wall proteome. *Molecular & cellular proteomics : MCP* **1**: 967-982.

Pitarch A, Jimenez A, Nombela C & Gil C (2006) Decoding serological response to Candida cell wall immunome into novel diagnostic, prognostic, and therapeutic candidates for systemic candidiasis by proteomic and bioinformatic analyses. *Molecular & cellular proteomics : MCP* **5**: 79-96.

Pitarch A, Jimenez A, Nombela C & Gil C (2008) Serological proteome analysis to identify systemic candidiasis patients in the intensive care unit: Analytical, diagnostic and prognostic validation of anti-*Candida* enolase antibodies on quantitative clinical platforms. *PROTEOMICS – Clinical Applications* **2**: 596-618.

Pitarch A, Abian J, Carrascal M, Sanchez M, Nombela C & Gil C (2004) Proteomics-based identification of novel *Candida albicans* antigens for diagnosis of systemic candidiasis in patients with underlying hematological malignancies. *Proteomics* **4**: 3084-3106.

Pitarch A, Pardo M, Jimenez A, Pla J, Gil C, Sanchez M & Nombela C (1999) Two-dimensional gel electrophoresis as analytical tool for identifying *Candida albicans* immunogenic proteins. *Electrophoresis* **20**: 1001-1010.

Plato A, Willment JA & Brown GD (2013) C-type lectin-like receptors of the dectin-1 cluster: ligands and signaling pathways. *International reviews of immunology* **32**: 134-156.

Polak-Wyss A (1991) Protective effect of human granulocyte colony stimulating factor (hG-CSF) on *Candida* infections in normal and immunosuppressed mice. *Mycoses* **34**: 109-118.

Polpitiya AD, Qian WJ, Jaitly N, Petyuk VA, Adkins JN, Camp DG, 2nd, Anderson GA & Smith RD (2008) DAnTE: a statistical tool for quantitative analysis of -omics data. *Bioinformatics* **24**: 1556-1558.

Posch W, Heimdorfer D, Wilflingseder D & Lass-Florl C (2017) Invasive candidiasis: future directions in non-culture based diagnosis. *Expert Review of Anti-infective Therapy* **15**: 829-838.

Quindos G (2014) Epidemiology of candidaemia and invasive candidiasis. A changing face. *Revista Iberoamericana de Micología* **31**: 42-48.

Quintin J (2018) Fungal mediated innate immune memory, what have we learned? *Seminars in Cell and Developmental Biology*.

Reales-Calderon JA, Molero G, Gil C & Martinez JL (2016) The fungal resistome: a risk and an opportunity for the development of novel antifungal therapies. *Future Medicinal Chemistry* **8**: 1503-1520.

Reales-Calderon JA, Aguilera-Montilla N, Corbi AL, Molero G & Gil C (2014) Proteomic characterization of human proinflammatory M1 and anti-inflammatory M2 macrophages and their response to Candida albicans. *Proteomics* **14**: 1503-1518.

Reales-Calderon JA, Vaz C, Monteoliva L, Molero G & Gil C (2016) *Candida albicans* Modifies the Protein Composition and Size Distribution of THP1 macrophages-derived Extracellular Vesicles. *Journal of proteome research* **16**: 87-105.

Reales-Calderon JA, Martinez-Solano L, Martinez-Gomariz M, Nombela C, Molero G & Gil C (2012) Sub-proteomic study on macrophage response to *Candida albicans* unravels new proteins involved in the host defense against the fungus. *Journal of proteomics* **75**: 4734-4746.

Reales-Calderon JA, Sylvester M, Strijbis K, Jensen ON, Nombela C, Molero G & Gil C (2013) Candida albicans induces pro-inflammatory and anti-apoptotic signals in macrophages as revealed by quantitative proteomics and phosphoproteomics. *Journal of proteomics* **91**: 106-135.

Reers M, Smiley ST, Mottola-Hartshorn C, Chen A, Lin M & Chen LB (1995) Mitochondrial membrane potential monitored by JC-1 dye. *Methods in enzymology* **260**: 406-417.

Resing KA & Ahn NG (2005) Proteomics strategies for protein identification. *FEBS letters* **579**: 885-889.

Richardson JP & Moyes DL (2015) Adaptive immune responses to *Candida albicans* infection. *Virulence* **6**: 327-337.

Rougerie P, Miskolci V & Cox D (2013) Generation of membrane structures during phagocytosis and chemotaxis of macrophages: role and regulation of the actin cytoskeleton. *Immunological Reviews* 256: 222-239.

Rudkin FM, Raziunaite I, Workman H*, et al.* (2018) Single human B cell-derived monoclonal anti-*Candida* antibodies enhance phagocytosis and protect against disseminated candidiasis. *Nature Communications* 9: 5288.

Ruprecht B, Koch H, Medard G, Mundt M, Kuster B & Lemeer S (2015) Comprehensive and reproducible phosphopeptide enrichment using iron immobilized metal ion affinity chromatography (Fe-IMAC) columns. *Molecular & cellular proteomics : MCP* 14: 205-215.

Ruprecht B, Koch H, Domasinska P, Frejno M, Kuster B & Lemeer S (2017) Optimized Enrichment of Phosphoproteomes by Fe-IMAC Column Chromatography. *Methods in molecular biology* 1550: 47-60.

Sabido E, Selevsek N & Aebersold R (2012) Mass spectrometry-based proteomics for systems biology. *Current opinion in biotechnology* 23: 591-597.

Sander LE & Garaude J (2018) The mitochondrial respiratory chain: A metabolic rheostat of innate immune cell-mediated antibacterial responses. *Mitochondrion* 41: 28-36.

Sarthy AV, McGonigal T, Coen M, Frost DJ, Meulbroek JA & Goldman RC (1997) Phenotype in *Candida albicans* of a disruption of the BGL2 gene encoding a 1,3-beta-glucosyltransferase. *Microbiology* 143 (Pt 2): 367-376.

Schelenz S, Barnes RA, Barton RC, Cleverley JR, Lucas SB, Kibbler CC, Denning DW & British Society for Medical M (2015) British Society for Medical Mycology best practice recommendations for the diagnosis of serious fungal diseases. *The Lancet Infectious Diseases* 15: 461-474.

Sechi S & Chait BT (2000) A method to define the carboxyl terminal of proteins. *Analytical chemistry* 72: 3374-3378.

Shalini S, Dorstyn L, Dawar S & Kumar S (2015) Old, new and emerging functions of caspases. *Cell Death & Differentiation* 22: 526-539.

Sheehan G & Kavanagh K (2019) Proteomic Analysis of the Responses of *Candida albicans* during Infection of *Galleria mellonella* Larvae. *Journal of Fungi* 5.

Shevchenko A, Tomas H, Havlis J, Olsen JV & Mann M (2006) In-gel digestion for mass spectrometric characterization of proteins and proteomes. *Nature protocols* 1: 2856-2860.

Shi T, Song E, Nie S, Rodland KD, Liu T, Qian WJ & Smith RD (2016) Advances in targeted proteomics and applications to biomedical research. *Proteomics* 16: 2160-2182.

Shin YK, Kim KY & Paik YK (2005) Alterations of protein expression in macrophages in response to *Candida albicans* infection. *Molecules and Cells* 20: 271-279.

Shiota M, Izumi H, Miyamoto N*, et al.* (2008) Ets regulates peroxiredoxin1 and 5 expressions through their interaction with the high-mobility group protein B1. *Cancer Science* 99: 1950-1959.

Shui W, Gilmore SA, Sheu L, Liu J, Keasling JD & Bertozzi CR (2009) Quantitative proteomic profiling of host-pathogen interactions: the macrophage response to *Mycobacterium tuberculosis* lipids. *Journal of proteome research* 8: 282-289.

Silva RC, Padovan AC, Pimenta DC, Ferreira RC, da Silva CV & Briones MR (2014) Extracellular enolase of *Candida albicans* is involved in colonization of mammalian intestinal epithelium. *Frontiers in cellular and infection microbiology* 4: 66.

Singh AK, Pandey RK, Siqueira-Neto JL, Kwon YJ, Freitas LH, Shaha C & Madhubala R (2015) Proteomic-Based Approach To Gain Insight into Reprogramming of THP-1 Cells Exposed to *Leishmania donovani* over an Early Temporal Window. *Infection and immunity* 83: 1853-1868.

Sjoelund V, Smelkinson M & Nita-Lazar A (2014) Phosphoproteome profiling of the macrophage response to different toll-like receptor ligands identifies differences in global phosphorylation dynamics. *Journal of proteome research* 13: 5185-5197.

Snarr BD, Qureshi ST & Sheppard DC (2017) Immune Recognition of Fungal Polysaccharides. *Journal of Fungi* 3.

Sorgo AG, Heilmann CJ, Dekker HL, Brul S, de Koster CG & Klis FM (2010) Mass spectrometric analysis of the secretome of *Candida albicans*. *Yeast* **27**: 661-672.

Sorgo AG, Heilmann CJ, Dekker HL, Bekker M, Brul S, de Koster CG, de Koning LJ & Klis FM (2011) Effects of fluconazole on the secretome, the wall proteome, and wall integrity of the clinical fungus *Candida albicans*. *Eukaryotic cell* **10**: 1071-1081.

Spampinato C & Leonardi D (2013) *Candida* infections, causes, targets, and resistance mechanisms: traditional and alternative antifungal agents. *BioMed Research International* **2013**: 204237.

Spellberg BJ, Ibrahim AS, Avanesian V, Fu Y, Myers C, Phan QT, Filler SG, Yeaman MR & Edwards JE, Jr. (2006) Efficacy of the anti-*Candida* rAls3p-N or rAls1p-N vaccines against disseminated and mucosal candidiasis. *The Journal of infectious diseases* **194**: 256-260.

Staab JF, Bradway SD, Fidel PL & Sundstrom P (1999) Adhesive and mammalian transglutaminase substrate properties of *Candida albicans* Hwp1. *Science* **283**: 1535-1538.

Sudbery P, Gow N & Berman J (2004) The distinct morphogenic states of *Candida albicans*. *Trends in microbiology* **12**: 317-324.

Suski J, Lebiedzinska M, Bonora M, Pinton P, Duszynski J & Wieckowski MR (2018) Relation Between Mitochondrial Membrane Potential and ROS Formation. *Methods in molecular biology* **1782**: 357-381.

Swidergall M (2019) *Candida albicans* at Host Barrier Sites: Pattern Recognition Receptors and Beyond. *Pathogens* **8**.

Swoboda RK, Bertram G, Hollander H, Greenspan D, Greenspan JS, Gow NA, Gooday GW & Brown AJ (1993) Glycolytic enzymes of *Candida albicans* are nonubiquitous immunogens during candidiasis. *Infection and immunity* **61**: 4263-4271.

Szklarczyk D, Morris JH, Cook H*, et al.* (2017) The STRING database in 2017: quality-controlled protein-protein association networks, made broadly accessible. *Nucleic acids research* **45**: D362-D368.

Tabas-Madrid D, Nogales-Cadenas R & Pascual-Montano A (2012) GeneCodis3: a non-redundant and modular enrichment analysis tool for functional genomics. *Nucleic acids research* **40**: W478-483.

Taff HT, Nett JE, Zarnowski R, Ross KM, Sanchez H, Cain MT, Hamaker J, Mitchell AP & Andes DR (2012) A *Candida* biofilm-induced pathway for matrix glucan delivery: implications for drug resistance. *PLoS pathogens* **8**: e1002848.

Taganov KD, Boldin MP, Chang KJ & Baltimore D (2006) NF-kappaB-dependent induction of microRNA miR-146, an inhibitor targeted to signaling proteins of innate immune responses. *Proceedings of the National Academy of Sciences of the United States of America* **103**: 12481-12486.

Thingholm TE, Jorgensen TJ, Jensen ON & Larsen MR (2006) Highly selective enrichment of phosphorylated peptides using titanium dioxide. *Nature protocols* **1**: 1929-1935.

Thingholm TE, Jensen ON, Robinson PJ & Larsen MR (2008) SIMAC (sequential elution from IMAC), a phosphoproteomics strategy for the rapid separation of monophosphorylated from multiply phosphorylated peptides. *Molecular & cellular proteomics : MCP* **7**: 661-671.

Tierney L, Kuchler K, Rizzetto L & Cavalieri D (2012) Systems biology of host-fungus interactions: turning complexity into simplicity. *Current opinion in microbiology* **15**: 440-446.

Tierney L, Linde J, Muller S, Brunke S, Molina JC, Hube B, Schock U, Guthke R & Kuchler K (2012) An Interspecies Regulatory Network Inferred from Simultaneous RNA-seq of Candida albicans Invading Innate Immune Cells. *Frontiers in microbiology* **3**: 85.

Tjalsma H, Schaeps RM & Swinkels DW (2008) Immunoproteomics: From biomarker discovery to diagnostic applications. *PROTEOMICS – Clinical Applications* **2**: 167-180.

Tong Y & Tang J (2017) *Candida albicans* infection and intestinal immunity. *Microbiological Research* **198**: 27-35.

Torosantucci A, Bromuro C, Chiani P*, et al.* (2005) A novel glyco-conjugate vaccine against fungal pathogens. *J Exp Med* **202**: 597-606.

Tortorano AM, Kibbler C, Peman J, Bernhardt H, Klingspor L & Grillot R (2006) Candidaemia in Europe: epidemiology and resistance. *International Journal of Antimicrobial Agents* **27**: 359-366.

Traba J, Del Arco A, Duchen MR, Szabadkai G & Satrustegui J (2012) SCaMC-1 promotes cancer cell survival by desensitizing mitochondrial permeability transition via ATP/ADP-mediated matrix Ca(2+) buffering. *Cell Death & Differentiation* **19**: 650-660.

Tramsen L, Beck O, Schuster FR, Hunfeld KP, Latge JP, Sarfati J, Roger F, Klingebiel T, Koehl U & Lehrnbecher T (2007) Generation and characterization of anti-*Candida* T cells as potential immunotherapy in patients with *Candida* infection after allogeneic hematopoietic stem-cell transplant. *The Journal of infectious diseases* **196**: 485-492.

Tsitsiou E & Lindsay MA (2009) microRNAs and the immune response. *Curr Opin Pharmacol* **9**: 514-520.

Tso GHW, Reales-Calderon JA & Pavelka N (2018) The Elusive Anti-*Candida* Vaccine: Lessons From the Past and Opportunities for the Future. *Frontiers in Immunology* **9**: 897.

Tucey TM, Verma J, Harrison PF*, et al.* (2018) Glucose Homeostasis Is Important for Immune Cell Viability during *Candida* Challenge and Host Survival of Systemic Fungal Infection. *Cell Metabolism* **27**: 988-1006 e1007.

Tyanova S, Temu T, Sinitcyn P, Carlson A, Hein MY, Geiger T, Mann M & Cox J (2016) The Perseus computational platform for comprehensive analysis of (prote)omics data. *Nature methods* **13**: 731-740.

Urban C, Sohn K, Lottspeich F, Brunner H & Rupp S (2003) Identification of cell surface determinants in *Candida albicans* reveals Tsa1p, a protein differentially localized in the cell. *FEBS letters* **544**: 228-235.

Uwamahoro N, Verma-Gaur J, Shen HH*, et al.* (2014) The pathogen *Candida albicans* hijacks pyroptosis for escape from macrophages. *MBio* **5**: e00003-00014.

van de Veerdonk FL, Netea MG, Joosten LA, van der Meer JW & Kullberg BJ (2010) Novel strategies for the prevention and treatment of *Candida* infections: the potential of immunotherapy. *FEMS Microbiology Reviews* **34**: 1063-1075.

van Eijk M, van Roomen CP, Renkema GH, Bussink AP, Andrews L, Blommaart EF, Sugar A, Verhoeven AJ, Boot RG & Aerts JM (2005) Characterization of human phagocyte-derived chitotriosidase, a component of innate immunity. *International Immunology* **17**: 1505-1512.

Vargas G, Rocha JD, Oliveira DL*, et al.* (2015) Compositional and immunobiological analyses of extracellular vesicles released by *Candida albicans*. *Cellular microbiology* **17**: 389-407.

Vazquez-Torres A, Jones-Carson J & Balish E (1996) Peroxynitrite contributes to the candidacidal activity of nitric oxide-producing macrophages. *Infection and immunity* **64**: 3127-3133.

Vergne I, Fratti RA, Hill PJ, Chua J, Belisle J & Deretic V (2004) *Mycobacterium tuberculosis* phagosome maturation arrest: mycobacterial phosphatidylinositol analog phosphatidylinositol mannoside stimulates early endosomal fusion. *Molecular Biology of the Cell* **15**: 751-760.

Via LE, Deretic D, Ulmer RJ, Hibler NS, Huber LA & Deretic V (1997) Arrest of mycobacterial phagosome maturation is caused by a block in vesicle fusion between stages controlled by rab5 and rab7. *Journal of Biological Chemistry* **272**: 13326-13331.

Vialas V, Perumal P, Gutierrez D, Ximenez-Embun P, Nombela C, Gil C & Chaffin WL (2012) Cell surface shaving of *Candida albicans* biofilms, hyphae, and yeast form cells. *Proteomics* **12**: 2331-2339.

Vialas V, Sun Z, Loureiro y Penha CV, Carrascal M, Abian J, Monteoliva L, Deutsch EW, Aebersold R, Moritz RL & Gil C (2014) A *Candida albicans* PeptideAtlas. *Journal of proteomics* **97**: 62-68.

Vialas V, Sun Z, Reales-Calderon JA*, et al.* (2016) A comprehensive *Candida albicans* PeptideAtlas build enables deep proteome coverage. *Journal of proteomics* **131**: 122-130.

Vieira OV, Botelho RJ & Grinstein S (2002) Phagosome maturation: aging gracefully. *The Biochemical journal* **366**: 689-704.

Vincent JL (2003) Nosocomial infections in adult intensive-care units. *Lancet* **361**: 2068-2077.

Viudes A, Lazzell A, Perea S, Kirkpatrick WR, Peman J, Patterson TF, Martinez JP & Lopez-Ribot JL (2004) The C-terminal antibody binding domain of *Candida albicans* mp58 represents a protective epitope during candidiasis. *FEMS Microbiology Letters* **232**: 133-138.

Vivier E, Tomasello E, Baratin M, Walzer T & Ugolini S (2008) Functions of natural killer cells. *Nature immunology* **9**: 503-510.

Vizcaino JA, Csordas A, del-Toro N*, et al.* (2016) 2016 update of the PRIDE database and its related tools. *Nucleic acids research* **44**: D447-456.

Vylkova S & Lorenz MC (2017) Phagosomal Neutralization by the Fungal Pathogen *Candida albicans* Induces Macrophage Pyroptosis. *Infection and immunity* **85**.

Wachtler B, Wilson D, Haedicke K, Dalle F & Hube B (2011) From attachment to damage: defined genes of *Candida albicans* mediate adhesion, invasion and damage during interaction with oral epithelial cells. *PloS one* **6**: e17046.

Wahl MC, Will CL & Luhrmann R (2009) The spliceosome: design principles of a dynamic RNP machine. *Cell* **136**: 701-718.

Wang Q, Sawyer IA, Sung MH, Sturgill D, Shevtsov SP, Pegoraro G, Hakim O, Baek S, Hager GL & Dundr M (2016) Cajal bodies are linked to genome conformation. *Nature Communications* **7**: 10966.

Wei S, Wu T, Wu Y, Ming D & Zhu X (2018) Diagnostic accuracy of *Candida albicans* germ tube antibody for invasive candidiasis: systematic review and meta-analysis. *Diagnostic microbiology and infectious disease*.

Wellington M, Koselny K & Krysan DJ (2012) *Candida albicans* morphogenesis is not required for macrophage interleukin 1beta production. *MBio* **4**: e00433-00412.

Wellington M, Koselny K, Sutterwala FS & Krysan DJ (2014) *Candida albicans* triggers NLRP3-mediated pyroptosis in macrophages. *Eukaryotic cell* **13**: 329-340.

West AP (2017) Mitochondrial dysfunction as a trigger of innate immune responses and inflammation. *Toxicology* **391**: 54-63.

West AP, Koblansky AA & Ghosh S (2006) Recognition and signaling by toll-like receptors. *Annual review of cell and developmental biology* **22**: 409-437.

Will CL & Luhrmann R (2011) Spliceosome structure and function. *Cold Spring Harbor perspectives in biology* **3**.

Wilson D, Naglik JR & Hube B (2016) The Missing Link between *Candida albicans* Hyphal Morphogenesis and Host Cell Damage. *PLoS pathogens* **12**.

Wilson GM, Blanco R, Coon JJ & Hornberger TA (2018) Identifying Novel Signaling Pathways: An Exercise Scientists Guide to Phosphoproteomics. *Exerc Sport Sci Rev* **46**: 76-85.

Wisplinghoff H, Bischoff T, Tallent SM, Seifert H, Wenzel RP & Edmond MB (2004) Nosocomial bloodstream infections in US hospitals: analysis of 24,179 cases from a prospective nationwide surveillance study. *Clinical Infectious Diseases* **39**: 309-317.

Wolf JM, Espadas J, Luque-Garcia J, Reynolds T & Casadevall A (2015) Lipid Biosynthetic Genes Affect *Candida albicans* Extracellular Vesicle Morphology, Cargo, and Immunostimulatory Properties. *Eukaryotic cell* **14**: 745-754.

Wu H, Downs D, Ghosh K, Ghosh AK, Staib P, Monod M & Tang J (2013) *Candida albicans* secreted aspartic proteases 4-6 induce apoptosis of epithelial cells by a novel Trojan horse mechanism. *Faseb Journal* **27**: 2132-2144.

Xiao Y & Wang Y (2014) Global discovery of protein kinases and other nucleotide-binding proteins by mass spectrometry. *Mass spectrometry reviews* **35**: 601-619.

Xiao Y & Wang Y (2014) Global discovery of protein kinases and other nucleotide-binding proteins by mass spectrometry. *Mass spectrometry reviews*.

Xiao Y, Guo L & Wang Y (2013) Isotope-coded ATP probe for quantitative affinity profiling of ATP-binding proteins. *Analytical chemistry* **85**: 7478-7486.

Yin QY (2008) Exploring the fungal wall proteome by mass spectrometry. Thesis, University of Amsterdam.

Yuan J, Murrell GA, Trickett A, Landtmeters M, Knoops B & Wang MX (2004) Overexpression of antioxidant enzyme peroxiredoxin 5 protects human tendon cells against apoptosis and loss of cellular function during oxidative stress. *Biochimica et Biophysica Acta* **1693**: 37-45.

Zarnowski R, Sanchez H, Covelli AS, Dominguez E, Jaromin A, Berhardt J, Heiss C, Azadi P, Mitchell A & Andes DR (2018) *Candida albicans* biofilm-induced vesicles confer drug resistance through matrix biogenesis. *PLoS Biology* **16**: e2006872.

Zha QB, Wei HX, Li CG, Liang YD, Xu LH, Bai WJ, Pan H, He XH & Ouyang DY (2016) ATP-Induced Inflammasome Activation and Pyroptosis Is Regulated by AMP-Activated Protein Kinase in Macrophages. *Frontiers in Immunology* **7**: 597.

Zhang MX, Bohlman MC, Itatani C, Burton DR, Parren PW, St Jeor SC & Kozel TR (2006) Human recombinant antimannan immunoglobulin G1 antibody confers resistance to hematogenously disseminated candidiasis in mice. *Infection and immunity* **74**: 362-369.

Zhu W, Smith JW & Huang CM (2010) Mass spectrometry-based label-free quantitative proteomics. *Journal of Biomedicine and Biotechnology* **2010**: 840518.

Zwolanek F, Riedelberger M, Stolz V, Jenull S, Istel F, Koprulu AD, Ellmeier W & Kuchler K (2014) The non-receptor tyrosine kinase Tec controls assembly and activity of the noncanonical caspase-8 inflammasome. *PLoS pathogens* **10**: e1004525.

Zybailov B, Mosley AL, Sardiu ME, Coleman MK, Florens L & Washburn MP (2006) Statistical analysis of membrane proteome expression changes in *Saccharomyces cerevisiae*. *Journal of proteome research* **5**: 2339-2347.

APPENDIX

APPENDIX 1 - Supplementary Figures from Chapter 1

APPENDIX 2 – Publications related to the thesis

APPENDIX 3 - Other manuscripts published during the period of the thesis

APPENDIX 1 - Supplementary Data from Chapter 1

Supplementary Figure C1.1

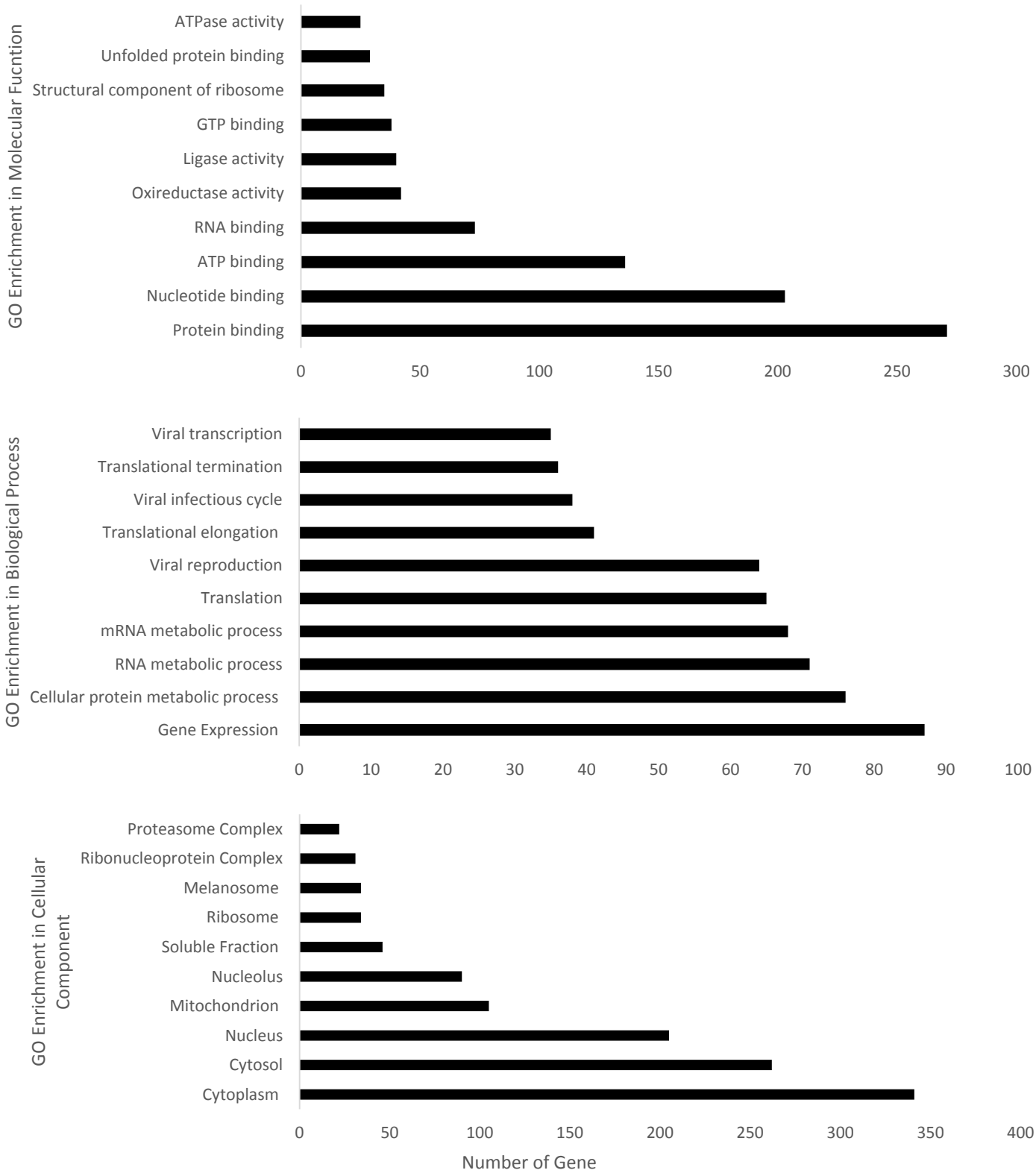

Supplementary Figure C1.1 GO analysis of proteins quantified after ATP-binding proteins enrichment.

Supplementary Figure C1.2

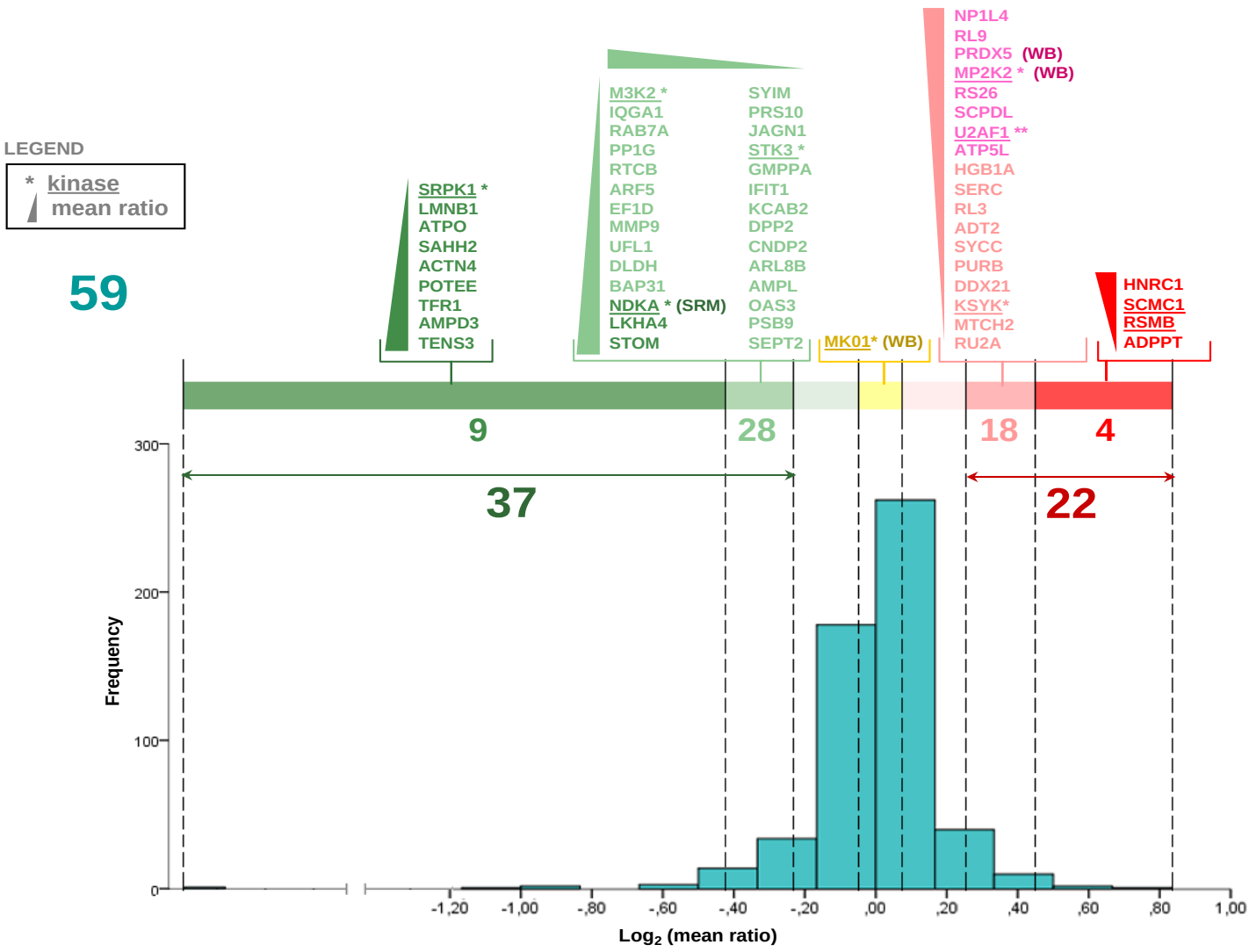

Supplementary Figure C1.2 Histogram showing log2-transformed mean of THP-1 macrophage protein abundance ratios upon C. albicans interaction. WB means the proteins were validated by Western-blotting and SRM means the protein was validated by Selected Reaction Monitoring.

Supplementary Figure C1.3

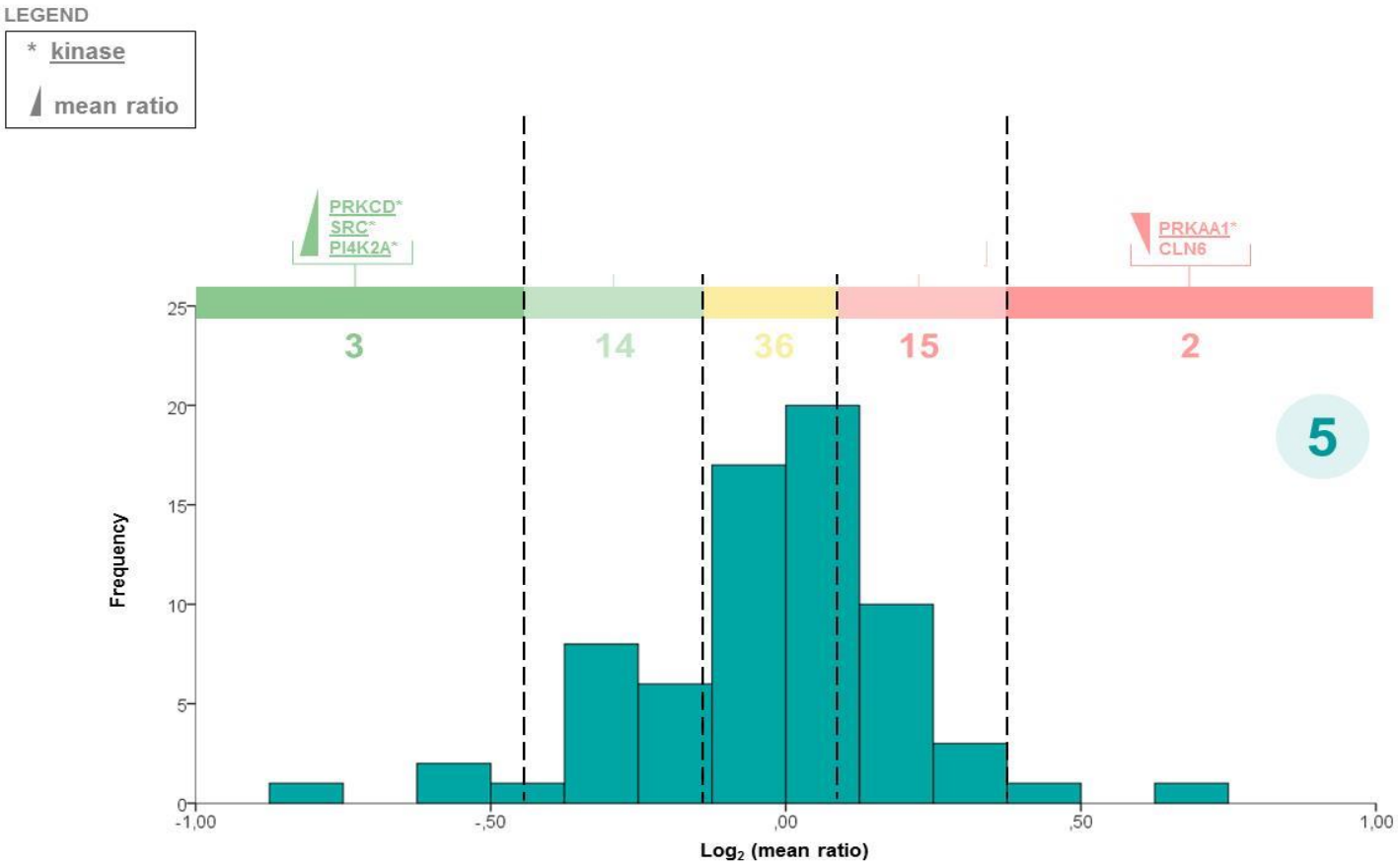

Supplementary Figure C1.3 Histogram showing log2-transformed mean of THP-1 macrophage phosphopeptide abundance ratios upon C. albicans interaction. The corresponding phosphoproteins are depicted in the present figure.

Supplementary Figure C1.4

Protein: 5'-AMP-activated protein kinase catalytic subunit alpha-1
UniProt: Code: Q13131
Phosphopeptide: SGSVSNYR
Phosphorylation Site: Ambiguous
Spectrum : S3

Protein: 5'-AMP-activated protein kinase catalytic subunit alpha-1
UniProt: Code: Q13131
Phosphopeptide: SGSVSNYR
Phosphorylation Site: Ambiguous
Spectrum : S1

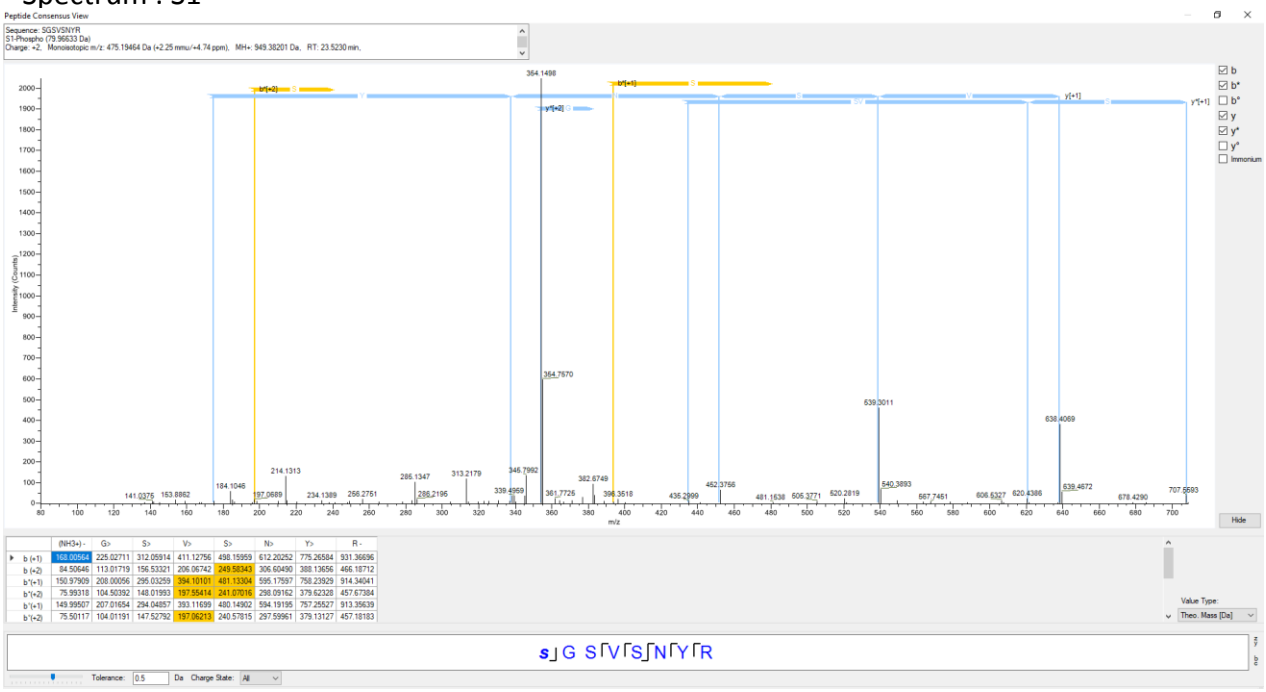

Supplementary Figure C1.4

Protein: Ceroid-lipofuscinosis neuronal protein 6

UniProt: Code: Q9NWW5

Phosphopeptide: HGsVSADEAAR

Phosphorylation Site: S3

Spectrum : S3

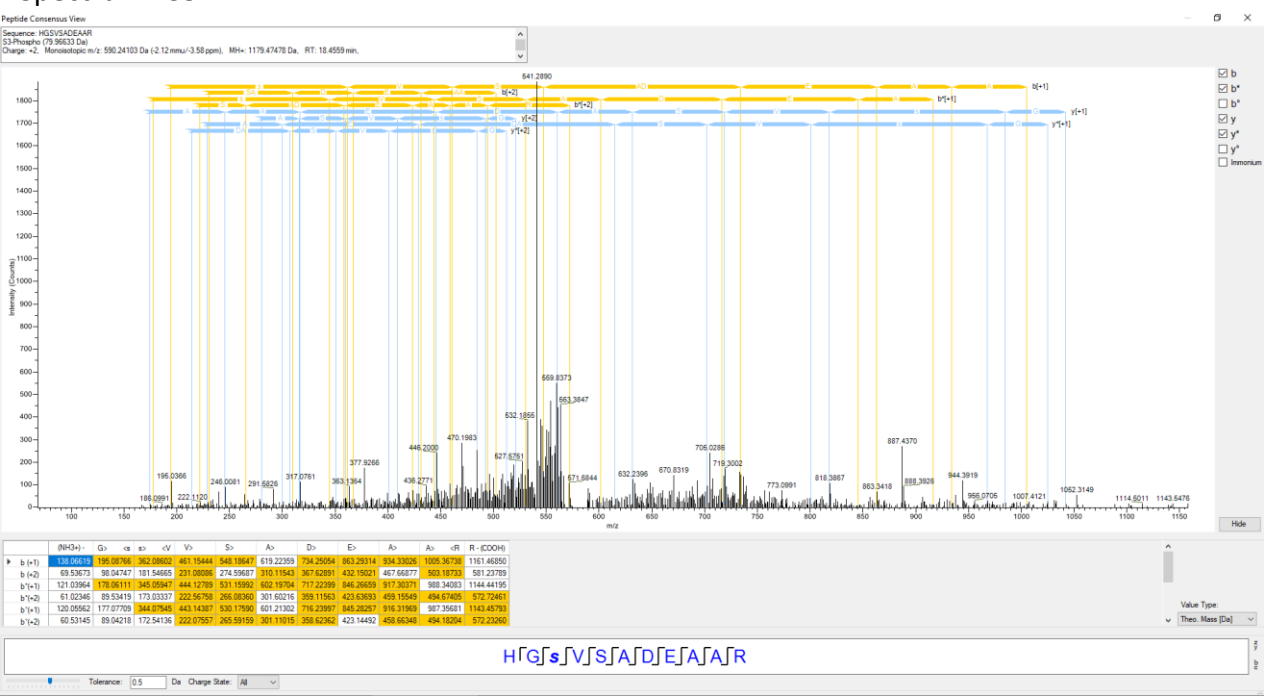

Protein: Proto-oncogene tyrosine-protein kinase Src

UniProt: Code: P12931

Phosphopeptide: LIEDNEyTAR

Phosphorylation Site: Y7

Spectrum : Y7

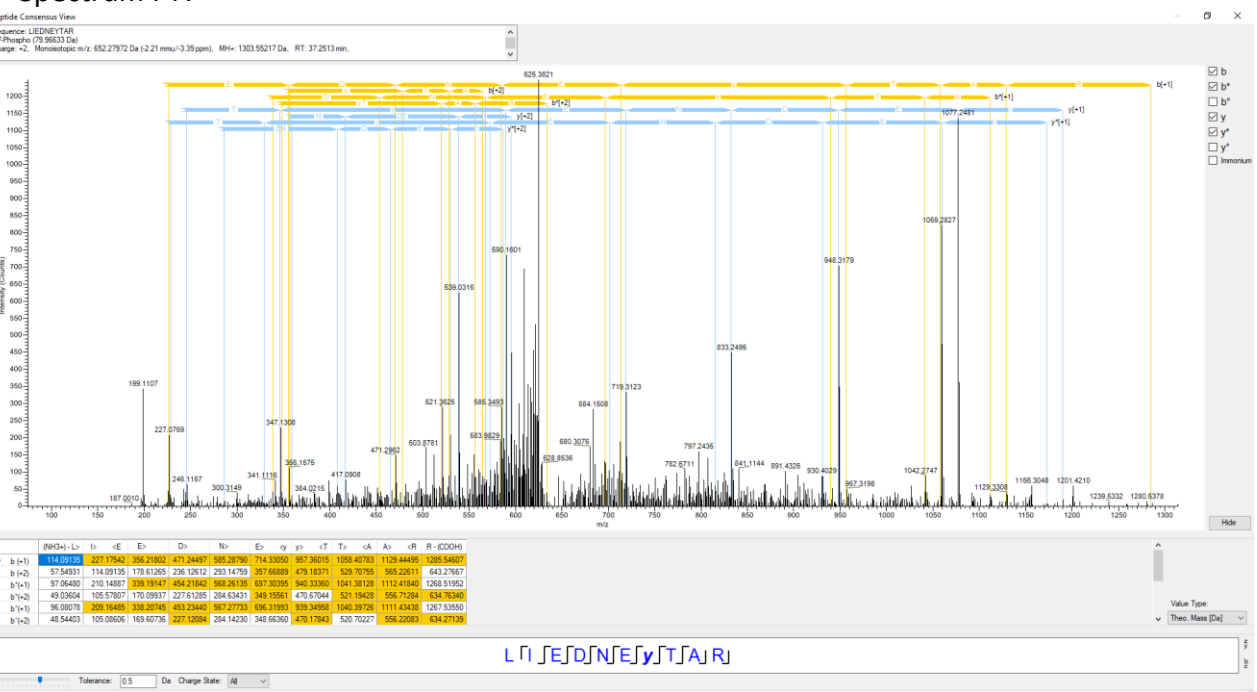

Supplementary Figure C1.4

Protein: Phosphatidylinositol 4-kinase type 2-alpha
UniProt: Code: Q9BTU6
Phosphopeptide: SSSESYTQSFQSr
Phosphorylation Site: Ambiguous
Spectrum : S3

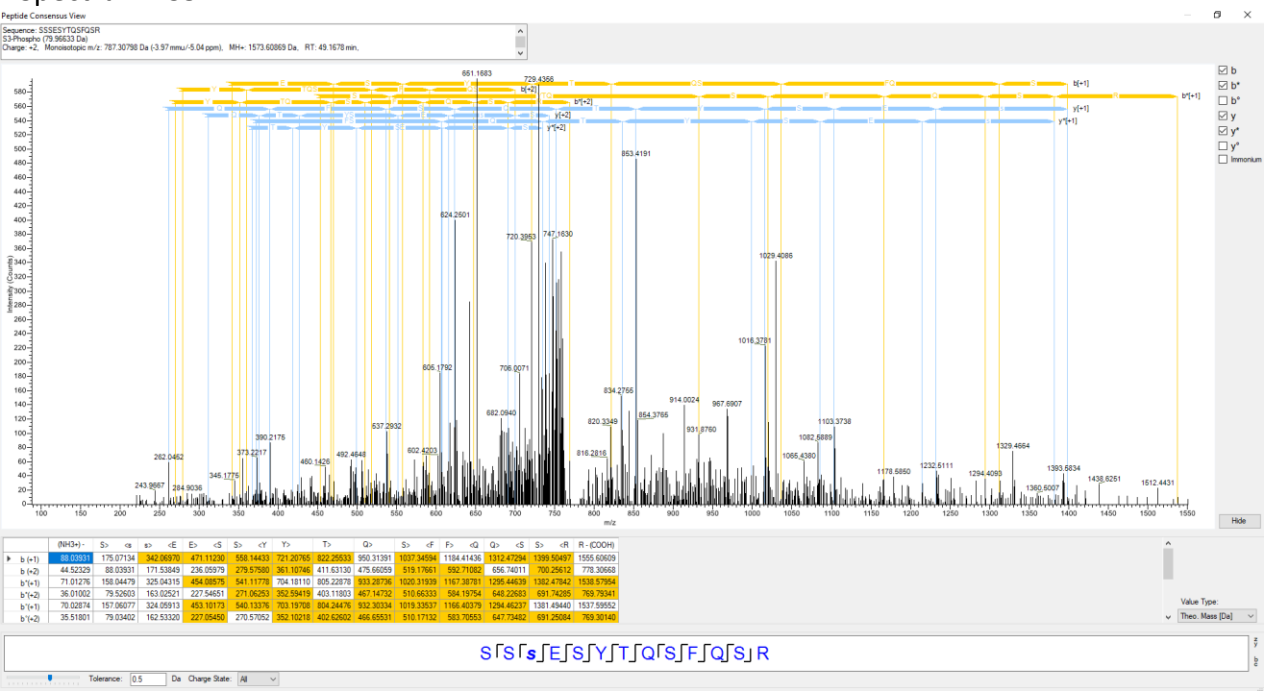

Protein: Phosphatidylinositol 4-kinase type 2-alpha
UniProt: Code: Q9BTU6
Phosphopeptide: SSSESYTQSFQSr
Phosphorylation Site: Ambiguous
Spectrum : S2

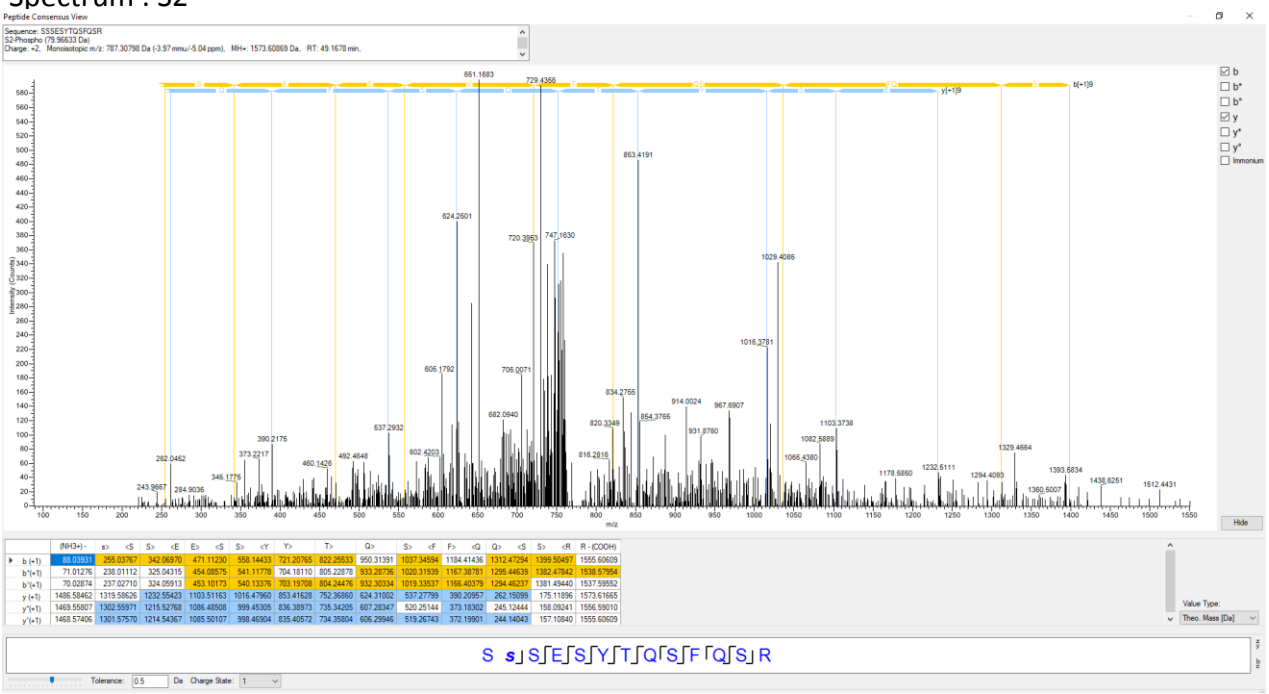

Supplementary Figure C1.4

Protein: Phosphatidylinositol 4-kinase type 2-alpha

UniProt: Code: Q9BTU6

Phosphopeptide: SSSESYTQSFQSr

Phosphorylation Site: Ambiguous

Spectrum : S1

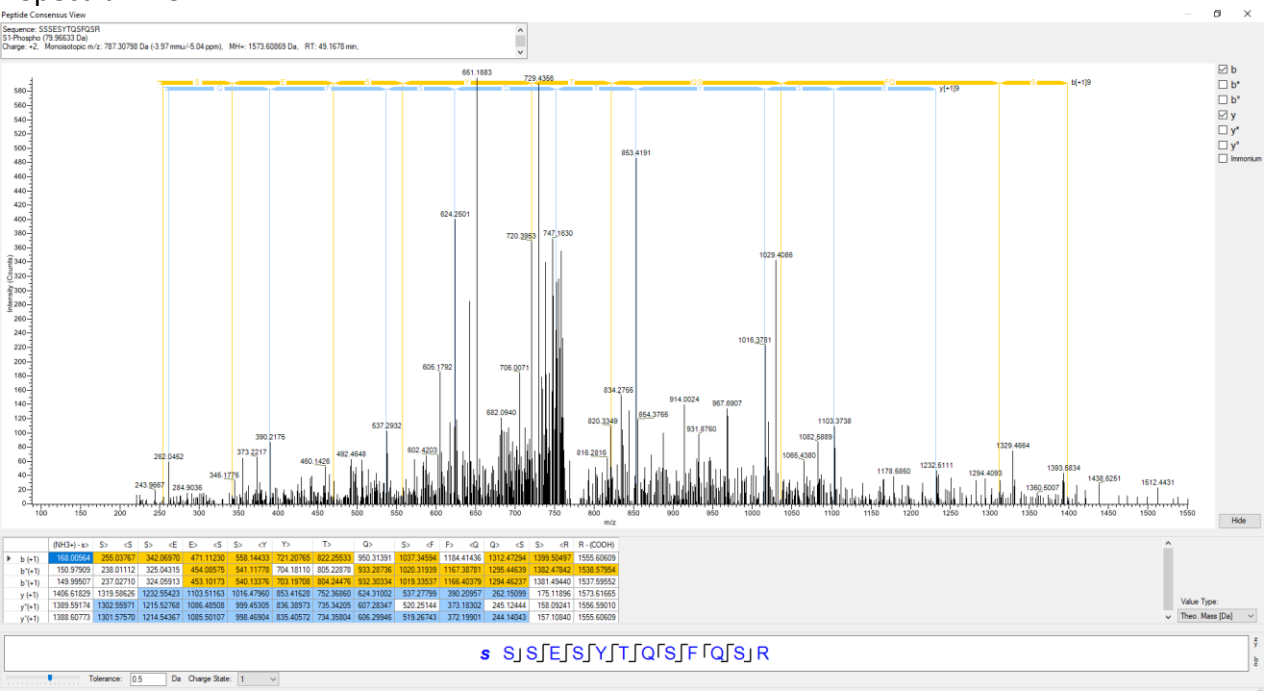

Protein: Protein kinase C delta type

UniProt: Code: Q05655

Phosphopeptide: SDSASSEPVGIYQGFEK

Phosphorylation Site: Ambiguous

Spectrum : S1

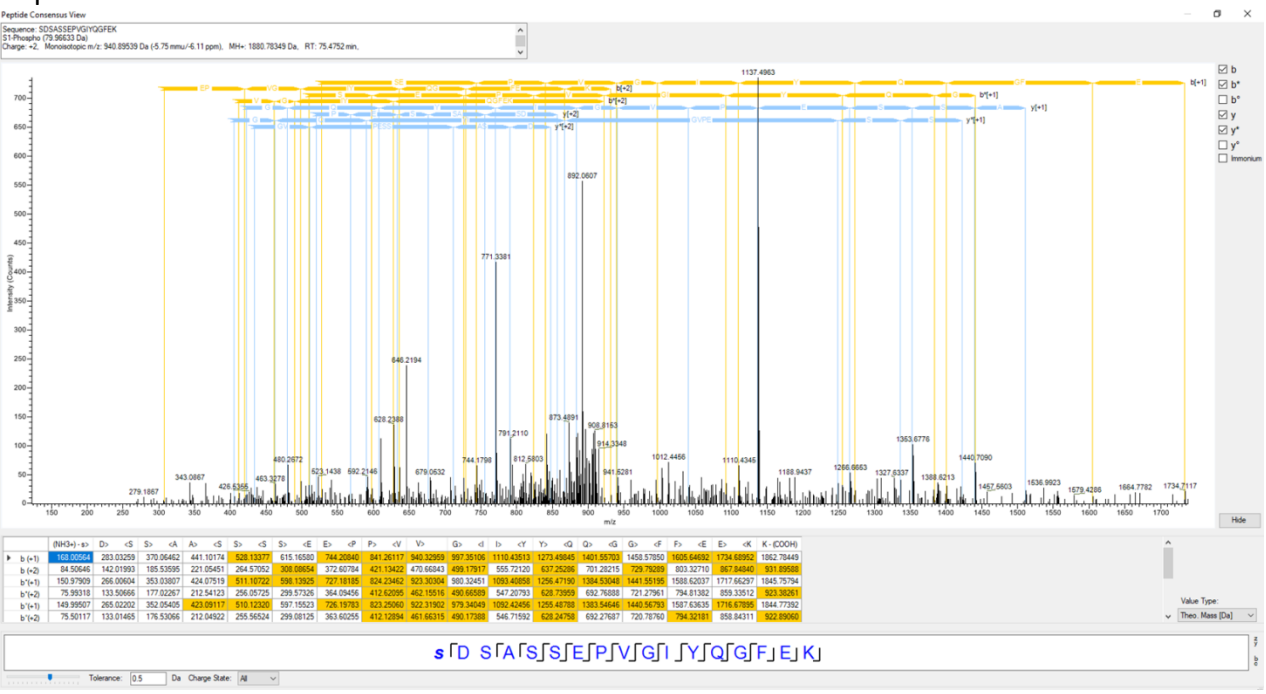

Supplementary Figure C1.4

Protein: Protein kinase C delta type
UniProt: Code: Q05655
Phosphopeptide: SDSASSEPVGIYQGFEK
Phosphorylation Site: Ambiguous
Spectrum : S3

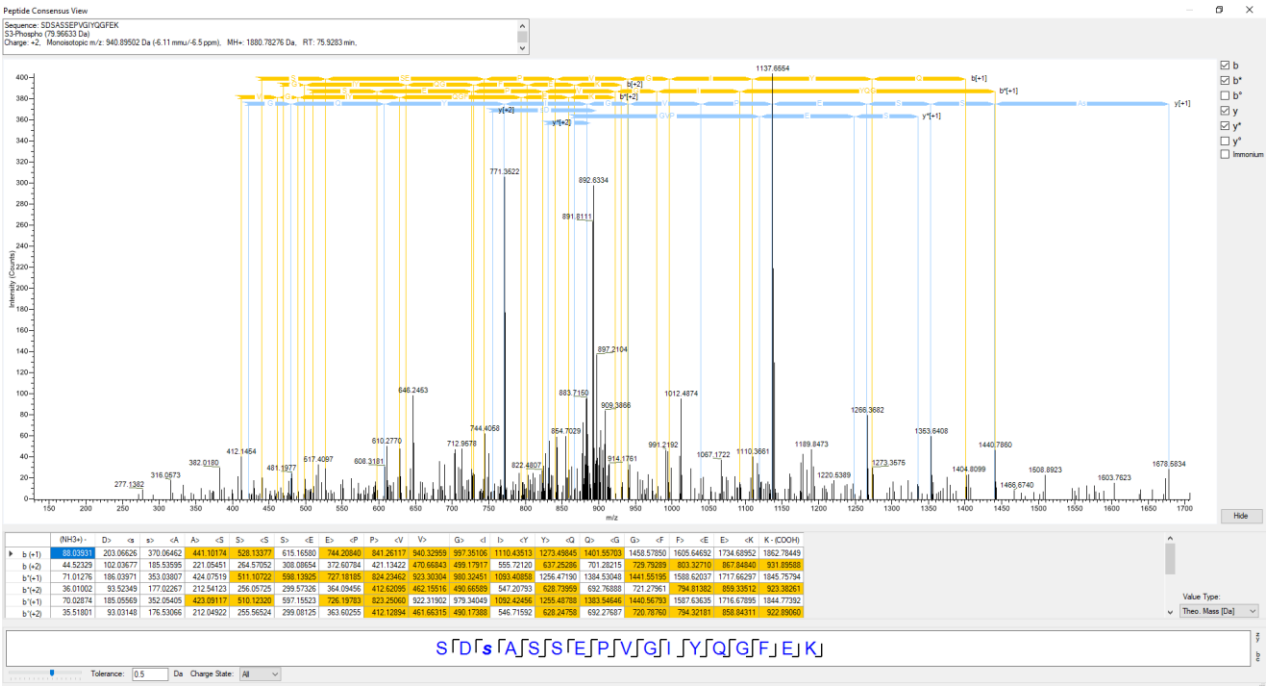

Supplementary Figure C1.4 Mass spectra of the differentially abundant phosphopeptides.

Supplementary Figure C1.5

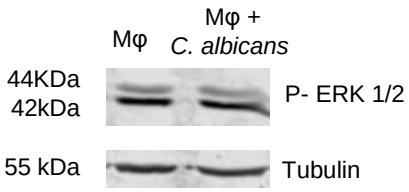

Supplementary Figure C1.5 Quantification of P-ERK1/ERK2 by Western blot

Supplementary Figure C1.6

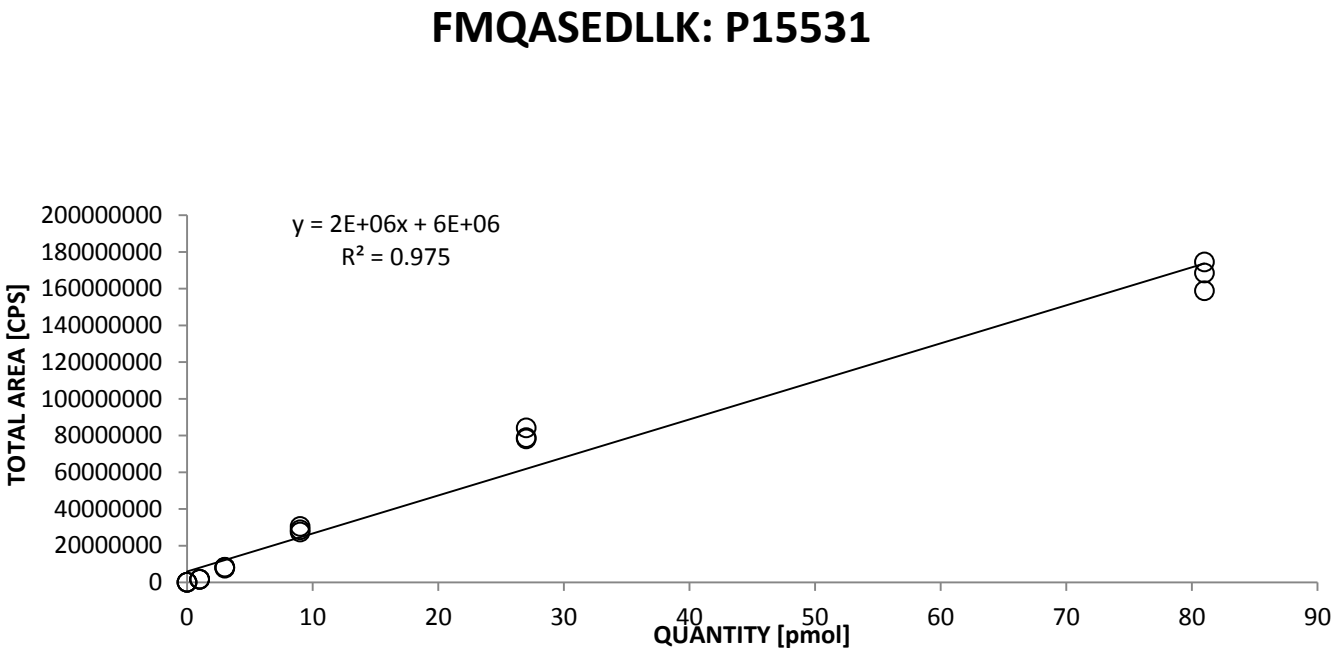

Supplementary Figure C1.6 Calibration curve of the peptide FMQASEDLLK from NDKA protein.

Supplementary Figure C1.7

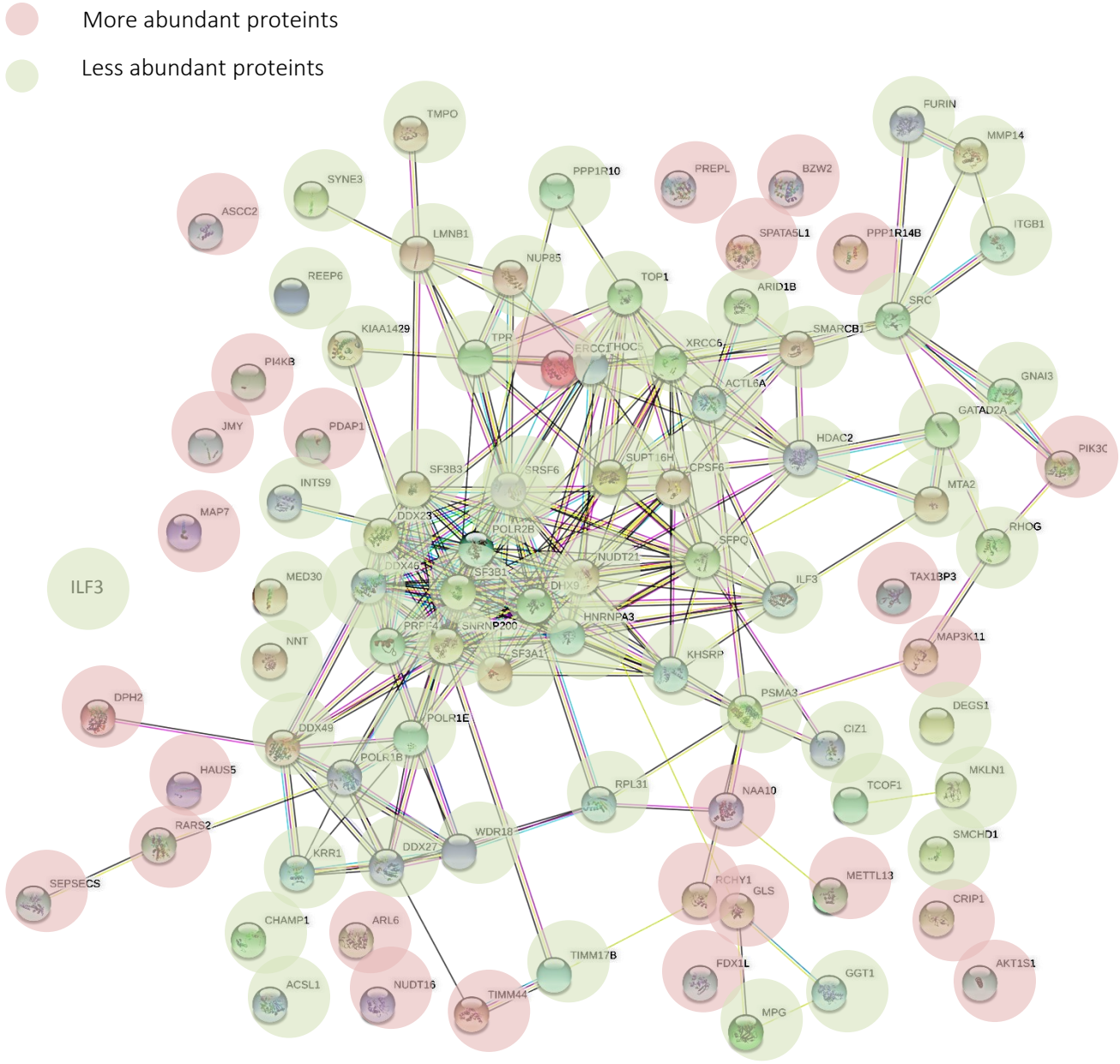

Supplementary Figure C1.7 Predicted Protein-Protein interaction network using String (v10.0) among the differentially abundant proteins from the second approach developed. The network protein-protein interaction p-value is 1.0×10^{-16} (retrieved on 15/02/19)

Appendix 2 – Publications related to the thesis

Vaz C, Reales-Calderon JA, Pitarch A, Vellosillo P, Trevisan M, Hernaez ML, Monteoliva L & Gil C (2019) Enrichment of ATP binding proteins unveils proteomic alterations in human macrophage cell death, inflammatory response and protein synthesis after interaction with *Candida albicans.* *Journal of proteome research* 18:2139-2159.

Journal of proteome research

Article

Cite This: J. Proteome Res. XXXX, XXX, XXX−XXX

pubs.acs.org/jpr

Enrichment of ATP Binding Proteins Unveils Proteomic Alterations in Human Macrophage Cell Death, Inflammatory Response, and Protein Synthesis after Interaction with *Candida albicans*

Catarina Vaz,[†,‡] Jose Antonio Reales-Calderon,[†,‡,#] Aida Pitarch,[†,‡] Perceval Vellosillo,[†] Marco Trevisan,[∥] María Luisa Hernáez,[§] Lucía Monteoliva,[*,†,‡] and Concha Gil[†,‡,§]

[†]Departamento de Microbiología y Parasitología, Facultad de Farmacia, Universidad Complutense de Madrid, 28040 Madrid, Spain

[‡]Instituto Ramón y Cajal de Investigación Sanitaria IRYCIS, 28034 Madrid, Spain

[§]Unidad de Proteómica, Universidad Complutense de Madrid, 28040 Madrid, Spain

[∥]Laboratorio de Proteómica Cardiovascular, Centro Nacional de Investigaciones Cardiovasculares Carlos III (CNIC), 28029 Madrid, Spain

Supporting Information

ABSTRACT: Macrophages are involved in the primary human response to *Candida albicans*. After pathogen recognition, signaling pathways are activated, leading to the production of cytokines, chemokines, and antimicrobial peptides. ATP binding proteins are crucial for this regulation. Here, a quantitative proteomic and phosphoproteomic approach was carried out for the study of human macrophage ATP-binding proteins after interaction with *C. albicans*. From a total of 547 nonredundant quantified proteins, 137 were ATP binding proteins and 59 were detected as differentially abundant. From the differentially abundant ATP-binding proteins, 6 were kinases (MAP2K2, SYK, STK3, MAP3K2, NDKA, and SRPK1), most of them involved in signaling pathways. Furthermore, 85 phosphopeptides were quantified. Macrophage proteomic alterations including an increase of protein synthesis with a consistent decrease in proteolysis were observed. Besides, macrophages showed changes in proteins of endosomal trafficking together with mitochondrial proteins, including some involved in the response to oxidative stress. Regarding cell death mechanisms, an increase of antiapoptotic over pro-apoptotic signals is suggested. Furthermore, a high pro-inflammatory response was detected, together with no upregulation of key mi-RNAs involved in the negative feedback of this response. These findings illustrate a strategy to deepen the knowledge of the complex interactions between the host and the clinically important pathogen *C. albicans*.

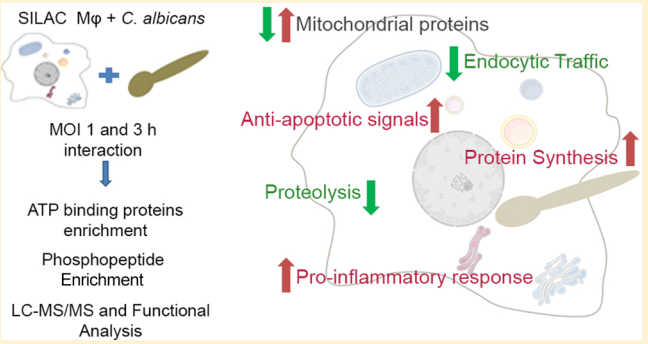

KEYWORDS: *macrophages, Candida albicans, proteomics, SILAC, ATP binding proteins*

INTRODUCTION

Candida albicans is a human opportunistic pathogen and a common commensal fungus of the mucosa from many healthy individuals. Most potentially lethal invasive infections occur in immunocompromised patients, such as those infected with HIV or individuals with neutropenia owing to immunosuppressive treatments for cancer or organ transplantation.[1] Infections caused by *Candida* spp. have high levels of morbidity and mortality particularly in critically ill patients that may be attributed to the difficulty in the early diagnosis of *Candida* infections and a limited antifungal therapy.[2] A recent epidemiologic study in Spain described a 30% of global mortality in the 705 documented cases of invasive candidiasis, and *C. albicans* was the most frequently isolated species, although an increase in non-*C. albicans* species has been observed.[3,2]

Macrophages, which are derived from monocytes circulating in the blood, are constantly patrolling tissues and nonsterile interfaces at the surfaces of epithelia, and are one of the key cells in the immune recognition and innate immune response to *C. albicans*.[1] These cells recognize and phagocyte *C. albicans*, eliciting innate immune responses through engagement of different pattern recognition receptors (PRRs) in an infection-stage specific manner.[4] Mainly, PRRs are composed of three groups: Toll-like receptors (TLRs), C-type lectin receptors (CLRs), and nod-like receptors (NODs). These PRRs, which include multiple cell-bound receptors (such as TLR2 and 4, Dectin-1, or Mannan Receptor), soluble receptors (like galectin-3), and intracellular receptors (like TLR 9), activate

Received: January 16, 2019
Published: April 15, 2019

DOI: 10.1021/acs.jproteome.9b00032
J. Proteome Res. XXXX, XXX, XXX−XXX

several signal transduction pathways, which finally lead to the upregulation of costimulatory molecules and the production of inflammatory cytokines, chemokines, antimicrobial peptides, and type I interferons (IFNs).[5] Our research group identified new differentially abundant proteins in *C. albicans*-stimulated RAW 264.7 macrophages using proteomic approaches.[6,7] Differentially abundant proteins were suggested to have pro-inflammatory and antiapoptotic effects.[6,7] Another study on human M1 (classically activated, pro-inflammatory subtype) and M2 (alternatively activated, anti-inflammatory subtype) macrophages showed that the biggest differences between them were related to cytoskeletal rearrangement and metabolic routes.[8] Other studies analyzed the interaction between macrophage and *Candida* using proteomic approaches, and found proteins involved in energy metabolism, cell survival, and candidates for interaction-specific molecules.[9,10]

Adenosine triphosphate (ATP) can bind to a group of proteins known as ATP-binding proteins. These proteins were previously studied to elucidate molecular mechanisms in cancer, identify proteins that can be therapeutic targets for the development of novel antibiotics, and profile plant proteomes.[11−14] However, their role is still poorly understood during different infection scenarios. This group of proteins include kinases, heat shock proteins, as well as ATPases, and are crucial in several cellular processes, such as cell signaling, protein synthesis, and metabolism.[15] Despite the importance of these proteins in those pivotal cellular functions, proteomic studies of ATP-binding proteins by MS are still a challenge mainly due to the fact that some ATP-binding proteins are present at very low cellular concentrations.[16] The combination of MS instrumentation with powerful separation techniques or selective enrichment of these proteins and bioinformatics tools can help in the identification and quantification of low abundant proteins in complex samples.[11] Several procedures for selective enrichment of ATP binding proteins and kinases have been developed,[11,17−20] including a probe-based technology that uses biotinylated acyl phosphates of ATP or adenosine diphosphate (ADP) that irreversibly react with protein kinases on conserved lysine residues in the ATP binding pocket.[21] These probes covalently label the active site of ATPases, including chaperones and metabolic enzymes, to enable their selective enrichment using a desthiobiotin tag. The combination of metabolic labeling, such as stable isotope labeling by amino acids in cell culture (SILAC), with affinity enrichment was proven previously to be useful for quantification of subproteomes of interest.[22,23] Moreover, protein post-translational modifications (PTMs) play a crucial role in the regulation of several biological processes, such as cell signaling, immune response, recognition of pathogens, among others. More than 300 types of protein PTMs are known to occur physiologically within living organisms. From these PTMs, the phosphorylation is highly important during signal transduction and it is believed that more than 30% of the proteins can be phosphorylated.[24]

A better understanding of the immune response during fungal infection may help in the development of new improved therapies in the future. We are particularly interested in unravelling new regulatory mechanisms activated by macrophages after interaction with *C. albicans*. Here, we study the abundances and phosphorylation levels of ATP-binding proteins in human macrophage cells after interacting with *C. albicans*. For that, SILAC was used to differentially label proteomes obtained from control macrophages and macrophages after interaction with *C. albicans*. The combined cell lysates were subjected to ATP-binding protein enrichment, and a quantitative proteomic and phosphoproteomic approaches were used to analyze the enriched extracts.

MATERIALS AND METHODS

C. albicans Strain

The *C. albicans* SC5314 strain was used in this study. This strain was grown in YPD plates (2% glucose, 1% yeast extract, 2% peptone, and 2% agar) at 30 °C.

THP-1 Cell Culture and Macrophage Differentiation

The human acute monocytic leukemia cell line (THP-1) was cultured in Dulbecco's modified eagle's medium (DMEM) supplemented with antibiotics (penicillin 10000 U/mL−streptomycin 10000 U/mL), 2 mM L-glutamine, and 10% heat-inactivated fetal bovine serum (FBS) at 37 °C in a humidified atmosphere containing 5% CO_2. THP-1 cells were seeded in 24-well plastic plates at a density of 1×10^6 cells/well in complete medium and treated with a final concentration of 30 ng/mL phorbol 12-myristate 13-acetate (PMA; Sigma-Aldrich) for 48 h to induce maturation toward adherent macrophage-like cells. After 48 h cultures, the medium containing PMA was replaced with fresh medium without PMA to remove unattached cells.

C. albicans−Macrophage Coculture

For interaction studies, THP-1 macrophages were incubated with *C. albicans* cells that were grown in YPD plates the day before, at multiplicity of infection (MOIs) of 1 and 5, and for different time points depending on the assays.

Environmental Scanning Electron Microscopy (ESEM)

ESEM was performed as previously detailed.[25] After macrophage interaction with *C. albicans*, cells were washed in PBS containing 2.5% paraformaldehyde for 1 h at room temperature. They were incubated in 2% osmium tetroxide for 1 h and then in 2% tannic acid for 1 h. Cells were dehydrated in ethanol. They were examined at the FEI INSPECT microscope at the Museo Nacional de Ciencias Naturales (Madrid, Spain).

Cytokine Determination

For cytokines measurements, macrophages from the THP-1 cell line were incubated with or without *C. albicans* cells at an MOI of 1 for 3, 6, and 8 h. As a positive control, macrophages were treated with lipopolysaccharide (LPS; 100 ng/mL). Supernatants from untreated, LPS- or *Candida*-treated THP-1 macrophages were tested for cytokine production by ELISA using matched paired antibodies against different interleukins: IL-1β, IL-6, IL-12p40, and TNF-α (Immunotools), according to manufacturer's instructions. Cytokine production was measured in three independent macrophage preparations.

C. albicans Phagocytosis Assay

C. albicans yeast cells were prelabeled with 1 μM Oregon green 488 (Molecular Probes) in the dark with gentle shaking at 30 °C for 1 h. THP-1 macrophages were differentiated in 18 mm glass sterile coverslips placed into 24-well plates and confronted with the yeast cells at a MOI of 1, at 37 °C and 5% CO_2. Interaction was stopped after 45 min, 1.5 h, and 3 h, and cells were then washed with ice-cold PBS and fixed with 4% paraformaldehyde for 30 min. To distinguish between internalized and attached/noningested yeasts, *C. albicans* cells were counterstained with 2.5 M Calcofluor white (Sigma) for 15 min in the dark. After several washes, coverslips were

DOI: 10.1021/acs.jproteome.9b00032
J. Proteome Res. XXXX, XXX, XXX−XXX

mounted with specific mounting medium (Southern Biotech). The number of ingested cells (green fluorescence) and adhered/noningested (blue fluorescence) were calculated by fluorescence microscopy.[26] Three different replicates with two different slides were prepared for each time point. At least 500 *C. albicans* cells were scored per slide, and results were expressed as the percentage of yeast cells internalized by macrophages.

Macrophage Cell Damage Assay

In order to evaluate the *C. albicans* damage in the THP-1 cell line macrophages, the cytotoxicity detection kit (Roche) was used. This assay is based on the measurement of lactate dehydrogenase (LDH) activity released from the cytosol of damaged cells. Macrophages were cultured in 24-well plates as stated above, and *C. albicans* cells were incubated with them at a MOI of 1 and 5 at 37 °C and 5% CO_2. The selected time points of measurements were 3 and 6 h. After these time points, the supernatants of the cells were removed for LDH measurement. The assay was performed according to manufacturer's instructions.

Macrophage Cell Line Culture and SILAC Labeling

THP-1 monocytes were grown in DMEM containing 10% dialyzed fetal bovine serum (FBS): i.e., either in light DMEM, containing 100 mg/L unlabeled L-arginine (Arg0) and 50 mg/L L-lysine (Lys0), or in heavy DMEM, containing 100 mg/L Arg6 (Silantes, ^{13}C labeled Arginine· HCl) and 50 mg/L Lys6 (Silantes, ^{13}C6 labeled L-Lysine·HCl). After 5 cell doublings, protein lysates of the macrophage cells were analyzed by MS to ensure that all proteins were labeled. Differentiation of monocytes into macrophages was triggered by the addition of PMA. Approximately, 20×10^6 cells were plated in 150 mm culture dishes and 30 ng/mL PMA was added, cells were incubated for 2 days to achieve complete differentiation. PMA was removed by washing the cells with light and heavy DMEM medium, respectively.

Fungal Infection for Shotgun Quantitative Proteomics

C. albicans cells were counted using the Neubauer chamber, and 20×10^6 cells were incubated with the macrophages (MOI of 1) for 3 h. In order to diminish the possible effect of the labeling procedure, in two biological replicates control macrophages were labeled with light DMEM and macrophages upon interaction were labeled with heavy DMEM, while in the other two biological replicates this labeling was switched over. The extracted proteins came from the same number of macrophage cells in control and interaction conditions. In each experiment, both labeled and unlabeled lysates were mixed in protein concentration ratios of 1:1.

Preparation of the Protein Samples for Shotgun Proteomics

Cell Lysis. After the incubation time, cells were washed twice with ice-cold PBS, and 1 mL of cold modified radioimmunoprecipitation assay (RIPA) lysis buffer (150 mM sodium chloride; 50 mM Tris-HCl pH 7.5; 1% NP40; 0.25% sodium deoxycholate; proteases inhibitors (1/1000, Pierce); 1 mM sodium orthovanadate; 5 mM sodium fluoride; 5 mM β-glycerolphosphate and 5 mM sodium pyrophosphate) was added. Cells were scrapped thoroughly. Then, the cell lysate was placed on ice for 5 min, vortexed for another 5 min, and centrifuged at 15 000 rpm for 10 min and 4 °C. The supernatant, containing the macrophage protein extract, was removed and transferred to a new tube. Protein concentration was measured using the Bradford assay.

Kinase Enrichment with ATP Probes. Protein lysates were enriched in kinases using ActivX desthiobiotin ATP probes (Thermo Scientific), according to manufacturer instructions with some alterations. Briefly, protein lysates were desalted using Zeba spin desalting columns to remove endogenous ATP. Then, lysates were eluted in reaction buffer and supplemented with protease inhibitors. Protein concentration was determined again by the Bradford assay. For labeling with the ATP probes, 2 mM MgCl was added to 2 mg of protein lysate and incubated with 20 μM of ActivX probe in a final volume of 500 μL for 30 min at room temperature with constant mixing. Then, 500 μL of 12 M urea in lysis buffer were added to the lysate to stop the reaction. Samples were then incubated with 125 μL of high-capacity streptavidin agarose resin for 1.5 h at room temperature with constant mixing. Beads were collected by centrifugation at 1000*g* for 1 min and washed twice with 4 M urea in lysis buffer. Finally, proteins were eluted by adding Laemmli reducing sample buffer and boiling for 5 min.

In-Gel Digestion. Samples in Laemmli sample buffer were loaded into a 1.5 mm thick SDS-PAGE gel with a 4% stacking gel casted over a 10% resolving gel. The run was stopped as soon as the front entered 3 mm into the resolving gel so that the whole proteome became concentrated in the stacking/resolving gel interface. Bands were stained with colloidal Coomassie Brilliant Blue staining. Gels were cut into 12 to 15 slices for protein digestion.[27] In-gel digestion was carried out as described.[28] Briefly, gel slices were cut into pieces of 1 mm^3 in size and washed with water. Proteins were reduced with 10 mM DTT in 25 mM ammonium bicarbonate for 30 min at 56 °C and then alkylated with 55 mM iodoacetamide in 25 mM ammonium bicarbonate for 15 min at 30 °C. Acetonitrile (ACN) and vacuum centrifugation were applied to dry the gel pieces. They were then rehydrated with 60 ng/μL trypsin (proteomics grade; Roche Applied Science) in 25 mM ammonium bicarbonate for 45 min at 4 °C. The trypsin solution was removed, and the rehydrated gel pieces were overlaid with 25 mM ammonium bicarbonate. The digestion was performed overnight at 37 °C. After digestion, the supernatant was recovered. Peptides were extracted from the gel pieces with 30% ACN and 0.1% trifluoroacetic acid (TFA) for 30 min at room temperature. Peptides were desalted onto C18 OMIX cartridges and dried-down.

Sequential Elution from Immobilized Metal Affinity Chromatography (SIMAC) for Phosphopeptide Enrichment. A total of 300 μg of the protein lysate enriched in ATP-binding proteins was used for phosphopeptide enrichment. Both immobilized metal affinity chromatography (IMAC) and titanium dioxide (TiO_2) chromatography were performed as previously described[7] and summarized below.

For each 100 μg of peptides, 40 μL of iron-coated PHOS-select metal chelate beads (Sigma-Aldrich) were used. Beads were washed twice in loading buffer (0.1% TFA and 50% ACN), and incubated with 500 μg of peptide mixture in loading buffer for 30 min at room temperature in vibrating shaker. Then, beads were packed in the constricted end of a 200 μL GELoader tip by application of air pressure with a syringe, forming an IMAC column. The flow-through was collected for further analysis by TiO_2 chromatography. The IMAC was then washed with loading buffer, which was added to the flow-through. Both monophosphorylated peptides and

DOI: 10.1021/acs.jproteome.9b00032
J. Proteome Res. XXXX, XXX, XXX−XXX

contaminating nonphosphorylated peptides were eluted using acidic elution solution (1% TFA and 20% ACN) and the multiply phosphorylated peptides were eluted using basic elution solution (0.5% ammonia). The IMAC flow-through and both eluents were dried in a vacuum concentrator. A TiO_2 microcolumn was prepared by stamping out a small plug of C18 material from a C18 extraction disk and placing the plug in the constricted end of a 200 μL GELoader tip. The TiO_2 beads were first suspended in loading buffer (1 M glycolic acid in 5% TFA and 80% ACN) and then mixed with the sample and incubated for 15 min with constant mixing. This mixture was centrifuged and 90% of the supernatant was removed to minimize the volume introduced in the microcolumn. The sample was applied to the tip and the TiO_2 column was packed by the application of air pressure with a syringe. The column was washed with loading buffer and subsequently with washing buffer (80% ACN and 5% TFA). The phosphopeptides bound to the TiO_2 microcolumn were eluted using 30 μL of 0.5% ammonia followed by elution using 1 μL of 30% ACN to elute phosphopeptides bound to the C18 disk. Then, the eluent was acidified by adding 5 μL of 100% formic acid and dried in the vacuum concentrator.

MS Analysis

Peptides were trapped onto a C18 SC001 2 cm precolumn (Thermo-Scientific), and then eluted onto a NS-AC-11 dp3 BioSphere C18 column (75 μm inner diameter, 15 cm long, 3 μm particle size; NanoSeparations) and separated using a 140 min gradient (0−40% buffer B for 120 min; 40%−95% buffer B for 15 min, and 95% buffer B for 5 min; buffer A: 0.1% formic acid/2% ACN; buffer B: 0.1% formic acid in ACN) at a flow-rate of 250 nL/min on a nanoEasy HPLC (Proxeon) coupled to a nanoelectrospray ion source (Proxeon). Mass spectra were acquired on a LTQ-Orbitrap Velos mass spectrometer (Thermo-Scientific) in the positive ion mode. Full-scan MS spectra (m/z 300−1900) were acquired in an Orbitrap at a resolution of 60 000 at 400 m/z and the 15 most intense ions were selected for collision induced dissociation (CID) fragmentation in the linear ion trap with a normalized collision energy of 35%. Singly charged ions and unassigned charge states were rejected. Dynamic exclusion was enabled with exclusion duration of 30 s.

Protein/Peptide Identification and Quantification

Mass spectra raw data files were searched against the SwissProt human database version 57.15 (20 266 protein entries) using MASCOT search engine (version 2.3, Matrix Science) through Proteome Discoverer (version 1.4.1.14; Thermo Fisher). Search parameters included a maximum of two missed cleavages allowed, carbamidomethylation of cysteines as a fixed modification, and oxidation of methionine, desthiobiotinylation of lysine, ^{13}C-arginine, and ^{13}C-lysine as variable modifications. Precursor and fragment mass tolerance were set to 10 ppm and 0.8 Da, respectively. Identified peptides were validated using Percolator algorithm with a q-value threshold of 0.01. Peptide quantification from SILAC labels was performed with Proteome Discoverer v1.4 using node precursor ion quantification. For each SILAC pair, the area of the extracted ion chromatogram was determined and the "heavy/light" ratio computed. Ratios were normalized by the median of all peptides ratios in each biological replicate. Media and standard deviation were calculated for each peptide. Protein ratios were then determined as the median of all the quantified peptides belonging to a certain protein. The quantification was analyzed at the peptide level, and peptide ratios were manually evaluated. Peptides that presented discrepant values inside each protein were discarded as soon as this elimination did not change the trend of the ratio presented, and the standard deviation was improved. By this way, an increase in the coverage of the quantified proteins was achieved.

Regarding phosphorylation, the variable modification of phosphorylation (STY) was added for peptide identification. The PhosphoRS node was used to provide a confidence measure for the localization of phosphorylation in the peptide sequences identified with this modification. The phosphorylation sites were manually corrected based on the PhosphoRS localization probability for a given residue. The phosphorylation sites assigned with a localization percentage <75% were considered ambiguous. In addition, if the percentage was >75% but different in the biological replicates were also considered ambiguous. The phosphopeptides were treated similarly as in quantitative analysis with the exception that the quantification was performed only at peptide level.

To make our findings publicly available and accessible to the community, we have deposited our data set in the ProteomeXchange Consortium via the PRIDE partner repository with the data set identifier PXD009938.

Western Blotting

Protein lysates were obtained as stated above but without cell labeling, and used for the proteomic validation assays. Forty μg of protein lysate were loaded in each well of a 10% SDS-PAGE gel and electrophoretically separated. After this, the proteins were transferred onto nitrocellulose membranes (Hybond-ECL; GE Healthcare). The membranes were blocked with 5% skinny milk in PBS for 2 h, and incubated with primary antibodies, including anti-PRDX5 (Abcam) (1/125), anti-MEK2 (Cell Signaling Technology) (1/500), anticleaved caspase-3 (Cell Signaling Technology) (1/1000), anti Erk-1/2 (Cell Signaling Technology) (1/1000), or anti-Tubulin-α (Serotec) (1/1000), anti P-Erk1/2 (Cell Signaling Technology) (1:1000) for 18 h at 4 °C. The membranes were washed 4 times with PBS containing 0.1% Tween-20 and incubated with IRDye secondary antibodies for 1 h (1/4000 IRDye 800CW goat antimouse IgG, IRDye 680LT goat antimouse IgG, IRDye 800CW goat antirabbit IgG, or IRDye 680LT goat antirabbit IgG, as appropriate). Membranes were then washed four times with PBS containing 0.1% Tween-20. Odyssey system (LI-COR) was used to detect the fluorescence signals. Protein abundance was compared between control and infected macrophages and values were given as arbitrary fluorescence units. Detection of tubulin-α was used as a loading control.

Selected Reaction Monitoring (SRM)

The abundance of the protein NDKA was quantified using SRM. A proteotypic peptide, which is a peptide unique to the target protein and easily detectable by mass spectrometry was selected for protein quantification.[29] The selected peptide was FMQASEDLLK because it was quantified in the shotgun approach and reached several criteria necessary for SRM. These criteria were as follows: be proteotypic and easy to synthesize and have moderate hydrophobicity. Unpurified isotopic labeled peptide was obtained from JPT Peptide Technologies GmbH. Skyline software (Seattle Proteome Center) was used for the optimization of SRM methodology and for the analysis of the resulting MS data. Protein lysates

DOI: 10.1021/acs.jproteome.9b00032
J. Proteome Res. XXXX, XXX, XXX−XXX

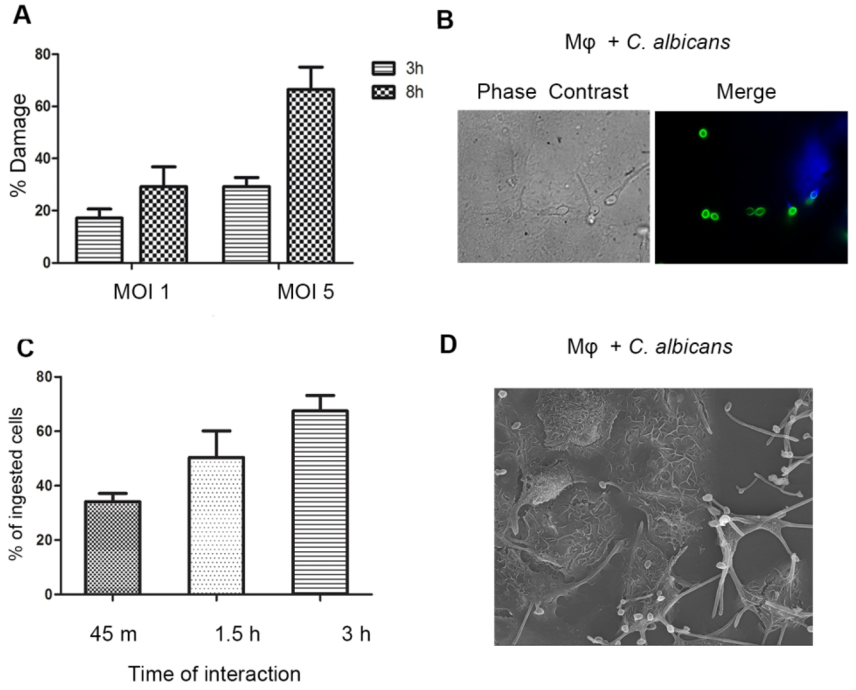

Figure 1. THP1 macrophage interaction with *C. albicans* cells. (A) Lactate dehydrogenase cytotoxicity assay to measure the damage in THP1 macrophages after 3 h and 8 h of interaction with *C. albicans* cells and at a MOI of 1 and 5. (B) Fluorescence microscopy images of THP1 macrophages exposed to labeled *C. albicans* strain SC5314 (Oregon green 488) in green, for 3 h. Intracellular and external/adhered *C. albicans* cells were distinguished based on fluorescence after costaining with Calcofluor white in blue, which does not enter or stain macrophages. (C) Phagocytic activity of macrophages at different times of interaction. (D) Environmental scanning electronic microscopy (ESEM) of macrophage and *C. albicans* coculture after 3 h of interaction.

were obtained as stated above, but without labeling the cells, enriched using ATP-probe and digested as previously shown. These SRM experiments were performed on a Q-TRAP 5500 LC−MS/MS system (AB Sciex). Both peaks from the endogenous and heavy peptides were evaluated manually. The area ratio (endogenous peptide area divided by heavy peptide area) was compared in both conditions (control and interaction). Three biological replicates and at least 2 technical replicates were performed.

Bioinformatic Analysis of the Differentially Abundant Proteins

Gene ontology (GO) enrichment analysis was performed using Genecodis (http://genecodis.cnb.csic.es/)[30−32] and Panther (http://pantherdb.org/) web tools. For GO analysis, statistical significance was set at p-value < 0.05. STRING software version 10.0 (http://string-db.org) was used for the study of the protein−protein interactions.[33] Ingenuity Pathway Analysis (IPA) (QIAGEN Bioinformatics) was used both for the prediction of possible upstream regulators and for network analysis.

Quantitative RT-PCR

RNA was isolated using the microRNeasy mini kit (QIAGEN) according to the manufacturer's protocol. Samples were quantified by Nanodrop 2000C (Thermo Fisher Scientific) and the presence of small RNA was confirmed using the Bioanalyzer 2100 (Agilent). Total RNA was reverse transcribed using Taqman microRNA reverse transcription kit (Thermo Fisher Scientific) and 10 ng of total RNA from each sample. Quantitative real time polymerase chain reaction (RT-PCR) for miRNA was performed using TaqMan microRNA assays (Thermo Fisher Scientific) following the manufacturer's instructions. U6 snRNA was used as an endogenous control, and the microRNAs (miRNAs) analyzed were mmu-miR-124a, hsa-miR-146a, hsa-miR-155, and hsa-miR-21.

Statistical Analysis

In the SILAC experiment, the protein abundance ratio was the amount of protein in the macrophages upon interaction with *C. albicans* divided by the amount of protein in the control macrophages (without interaction with *C. albicans*). The $\log_2$-transformed mean macrophage protein abundance ratios upon *C. albicans* interaction were stratified into seven quantiles according to their distribution in the sample: Q_1 (the lower extreme values), Q_2 (the lower outlier values), Q_3 (the smaller values that extended to 1.5 times the lower quartile or 25th percentile), Q_4 (the interquartile range, i.e., 25th to 75th percentiles), Q_5 (the larger values that extended to 1.5 times the upper quartile or 75th percentile), Q_6 (the upper outlier values), and Q_7 (the upper extreme values). The first and seventh quantiles comprised those macrophage proteins that had the lowest and highest relative abundance ratios, respectively, upon interaction with *C. albicans*. The same analysis was performed for phosphorylated peptides. All quantitative data were presented as mean ± standard deviation (SD).

For Western blotting, cytokines and SRM assays, comparisons between two groups were performed by the Student's t test. Statistical significance was defined as * for p-value < 0.05, ** for p-value < 0.001 and *** for p-value < 0.0001. Three biological replicates were performed for Western blotting and SRM-based validation assays, with exception of cleaved-caspase Western blotting that was performed with two biological replicates.

DOI: 10.1021/acs.jproteome.9b00032
J. Proteome Res. XXXX, XXX, XXX−XXX

Table 1. Proteins Differentially Abundant 3 h after Macrophage–*C. albicans* Interaction[a]

UniProt code[b]	entry names	gene names	protein names[b]	ratio[c]	standard deviation[c]	nr replicates[d]
Proteins more abundant after macrophage interaction with *C. albicans*						
RNA processing						
O60812	HNRC1	HNRNPCL1	Heterogeneous nuclear ribonucleoprotein C-like 1	1.8	0.218	2
P14678	RSMB	SNRPB	Small nuclear ribonucleoprotein-associated proteins B and B′	1.5	0.045	3
Q99733	NP1L4	NAP1L4	Nucleosome assembly protein 1-like 4	1.4	0.169	2
Q01081	U2AF1	U2AF1	Splicing factor U2AF 35 kDa subunit	1.3	0.289	2
P09661	RU2A	SNRPA1	U2 small nuclear ribonucleoprotein A′	1.2	0.205	2
Q9NR30	DDX21	DDX21	Nucleolar RNA helicase 2	1.2	0.293	2
Structural components of ribosome						
P32969	RL9	RPL9	60S ribosomal protein L9	1.4	0.29	4
P62854	RS26	RPS26	40S ribosomal protein S26	1.3	0.166	2
P39023	RL3	RPL3	60S ribosomal protein L3	1.3	0.272	3
Oxidative stress						
P30044	PRDX5[e]	PRDX5	Peroxiredoxin-5	1.3	0.171	2
Q6NUK1	SCMC1	SLC25A24	Calcium-binding mitochondrial carrier protein SCaMC-1	1.5	0.175	2
ATP production and transport						
O75964	ATP5L	ATP5L	ATP synthase subunit g	1.3	0.236	3
P05141	ADT2	SLC25A5	ADP/ATP translocase 2	1.2	0.227	4
Immune response and cell signaling						
P36507	MP2K2[e]	MAP2K2	Dual specificity mitogen-activated protein kinase kinase 2	1.3	0.067	2
P43405	KSYK	SYK	Tyrosine-protein kinase SYK	1.2	0.187	2
Metabolism						
Q9NRN7	ADPPT	AASDHPPT	L-aminoadipate-semialdehyde dehydrogenase-phosphopantetheinyl transferase	1.4	0.075	3
Q8NBX0	SCPDL	SCCPDH	Saccharopine dehydrogenase-like oxidoreductase	1.3	0.066	2
Q9Y617	SERC	PSAT1	Phosphoserine aminotransferase	1.3	0.275	2
Others[f]						
B2RPK0	HGB1A	HMGB1P1	Putative high mobility group protein B1-like 1	1.3	0.251	3
P49589	SYCC	CARS	Cysteine–tRNA ligase	1.2	0.274	2
Q96QR8	PURB	PURB	Transcriptional activator protein Pur-beta	1.2	0.285	4
Q9Y6C9	MTCH2	MTCH2	Mitochondrial carrier homologue 2	1.2	0.237	4
Proteins less abundant after macrophage interaction with *C. albicans*						
UniProt code[b]	entry names	gene names	protein names[b]	ratio[c]	standard deviation[c]	nr replicates[d]
Proteolysis and peptide degradation						
Q9UHL4	DPP2	DPP7	Dipeptidyl peptidase 2	0.8	0.213	3
P14780	MMP9	MMP9	Matrix metalloproteinase-9	0.8	0.22	3
P28838	AMPL	LAP3	Cytosol aminopeptidase	0.8	0.237	4
Q96KP4	CNDP2	CNDP2	Cytosolic nonspecific dipeptidase	0.8	0.076	2
P09960	LKHA4	LTA4H	Leukotriene A-4 hydrolase	0.8	0.284	4
P09622	DLDH	DLD	Dihydrolipoyl dehydrogenase	0.8	0.163	2
Transport						
Q8N5M9	JAGN1	JAGN1	Protein jagunal homologue 1	0.8	0.074	2
P51149	RAB7A	RAB7A	Ras-related protein Rab-7a	0.8	0.223	2
P84085	ARF5	ARF5	ADP-ribosylation factor 5	0.8	0.162	3
Proteasome components and protein fate						
P62333	PRS10	PSMC6	26S protease regulatory subunit 10B	0.9	0.104	3
P28065	PSB9	PSMB9	Proteasome subunit beta type-9	0.8	0.276	2
O94874	UFL1	UFL1	E3 UFM1-protein ligase 1	0.8	0.281	3
P51572	BAP31	BCAP31	B-cell receptor-associated protein 31	0.8	0.127	2
Immune response and cell signaling						
Q13188	STK3	STK3	Serine/threonine-protein kinase 3	0.8	0.061	2
Q9Y2U5	M3K2	MAP3K2	Mitogen-activated protein kinase kinase kinase 2	0.8	0.2	3
P36873	PP1G	PPP1CC	Serine/threonine-protein phosphatase PP1-gamma catalytic subunit	0.8	0.238	2
P09914	IFIT1	IFIT1	Interferon-induced protein with tetratricopeptide repeats 1	0.8	0.238	4
Q9Y6K5	OAS3	OAS3	2′-5′-oligoadenylate synthase 3	0.8	0.233	4
Cytoskeleton components/interactors and regulators						
Q15019	SEPT2	SEPT2	Septin-2	0.8	0.003	2
P46940	IQGA1	IQGAP1	Ras GTPase-activating-like protein IQGAP1	0.8	0.168	3
P20700	LMNB1	LMNB1	Lamin-B1	0.7	0.101	3
O43707	ACTN4	ACTN4	Alpha-actinin-4	0.6	0.096	3

DOI: 10.1021/acs.jproteome.9b00032
J. Proteome Res. XXXX, XXX, XXX–XXX

Table 1. continued

Proteins less abundant after macrophage interaction with *C. albicans*						
UniProt code[b]	entry names	gene names	protein names[b]	ratio[c]	standard deviation[c]	nr replicates[d]
Q68CZ2	TENS3	TNS3	Tensin-3	0.1	0.137	2
Ion transport and uptake						
Q13303	KCAB2	KCNAB2	Voltage-gated potassium channel subunit beta-2	0.8	0.093	2
P27105	STOM	STOM	Erythrocyte band 7 integral membrane protein	0.8	0.253	4
P02786	TFR1	TFRC	Transferrin receptor protein 1	0.5	0.115	2
RNA processing						
Q9Y3I0	RTCB	RTCB	tRNA-splicing ligase RtcB homologue	0.8	0.087	2
P29692	EF1D	EEF1D	Elongation factor 1-delta	0.8	0.057	2
Q96SB4	SRPK1	SRPK1	SRSF protein kinase 1	0.7	0.249	2
O43865	SAHH2	AHCYL1	Adenosylhomocysteinase 2	0.7	0.274	2
Nucleoside triphosphates synthesis						
P15531	NDKA[e]	NME1	Nucleoside diphosphate kinase A	0.8	0.228	2
P48047	ATPO	ATP5O	ATP synthase subunit O	0.7	0.098	3
Others[f]						
Q9NSE4	SYIM	IARS2	Isoleucine−tRNA ligase	0.9	0.14	3
Q96IJ6	GMPPA	GMPPA	Mannose-1-phosphate guanyltransferase alpha	0.8	0.073	2
Q9NVJ2	ARL8B	ARL8B	ADP-ribosylation factor-like protein 8B	0.8	0.215	3
Q6S8J3	POTEE	POTEE	POTE ankyrin domain family member E	0.6	0.089	2
Q01432	AMPD3	AMPD3	AMP deaminase 3	0.5	0.278	4

[a]Proteins are ordered by ratio average inside each category. [b]Protein name and Uniprot Code according to Uniprot Knowledge base. [c]Average abundance ratio from macrophages + *C. albicans* versus control macrophages and respective inter-replicate standard deviation (cutoff in 0.3). [d]Proteins present in at least two biological replicates were considered and with a standard deviation lower than 30%. [e]Proteins from this study that were validated by Western blot or SRM. [f]In this category were included proteins with unknown or putative function and proteins that were not possible to include in the other categories.

The mi-RNA expression level was calculated using $2^{-\Delta\Delta C_T}$ formula.[34] The results were represented using the relative fold-change expression compared to the control, where the control values were considered a value of 1. Four biological replicates were used in this assay.

For all the assays, conditions were tested with Student's *t* test. A *p*-value lower than 0.05 was considered statistically significant.

RESULTS

THP-1 Macrophages and *C. albicans* Coculture

The optimal conditions were set up to characterize differentially abundant proteins from human macrophages upon *C. albicans* infection. The damage of *C. albicans* in the THP-1 macrophages was evaluated by lactate dehydrogenase measurements in two MOIs (Figure 1A). *C. albicans* produced more damage to THP-1 cells in a MOI of 5 than in a MOI of 1, as expected. Damage increased over time of incubation at both MOIs. A MOI of 1 was selected due to the lowest observed damage. After MOI selection, phagocytic activity was measured. *C. albicans* cells ingested or associated with macrophages were discriminated using differential staining with Oregon green and Calcofluor white. THP-1 macrophages showed an increase in their phagocytic activity over time (from 45 min to 3 h), almost 70% of *Candida* cells being engulfed after 3 h of interaction (Figures 1B,C). Taking into account these results and some studies performed before by our laboratory,[7,8,26,35] a MOI of 1 and the time point of 3 h were the conditions used for the quantitative proteomic assay. With these conditions, it was assured that 70% of *C. albicans* cells were engulfed and most macrophages were viable. Macrophage−*C. albicans* coculture in the selected conditions was visualized by ESEM (Figure 1D). As shown, after 3 h of interaction *C. albicans* cells were already in hypha form and at different stages of interaction with the macrophage.

Quantitative Proteomic Analysis of Macrophage Proteins after Interaction with *C. albicans*

A quantitative shotgun proteomic approach using SILAC and LC−MS/MS was used to study the changes in the abundance of macrophage proteins enriched after using the ActivX desthiobiotin ATP probes upon interaction with *C. albicans* cells during 3 h at a MOI of 1. Protein lysate was enriched in ATP-binding proteins and samples were analyzed by LC−MS/MS. Four biological replicates and two technical replicates of each were analyzed by MS and a schematic workflow of the experimental procedure is reflected in Figure S1. A total of 1043 proteins were identified, corresponding to 710, 664, 664, and 709 proteins in each replicate, respectively (Table S1 and Figure S2). A total of 547 nonredundant proteins were quantified in at least two biological replicates with a SD < 0.3 (Table S2). The molecular functions enriched on the 547 quantified proteins were mainly protein binding (271 proteins), nucleotide binding (203 proteins), and ATP binding (136 proteins). Furthermore, the total number of quantified proteins was enriched in 10 major biological processes, such as gene expression (87 proteins), cellular protein metabolic process (76 proteins), and translation (65 proteins). Regarding the cellular component, most of the proteins were located in cytoplasm (341 proteins), followed by nucleus (205 proteins), and mitochondria (105 proteins) (Figure S3).

The macrophage proteins extracted using the ActivX desthiobiotin ATP probes showed a very homogeneous abundance ratio. After stratification of protein abundance ratios into quantiles according to their distribution upon interaction with *C. albicans*, we found that 4 and 9 proteins had the higher and lower extreme abundance ratios, whereas 18 and 28 proteins had the higher and lower outlier abundance

DOI: 10.1021/acs.jproteome.9b00032
J. Proteome Res. XXXX, XXX, XXX−XXX

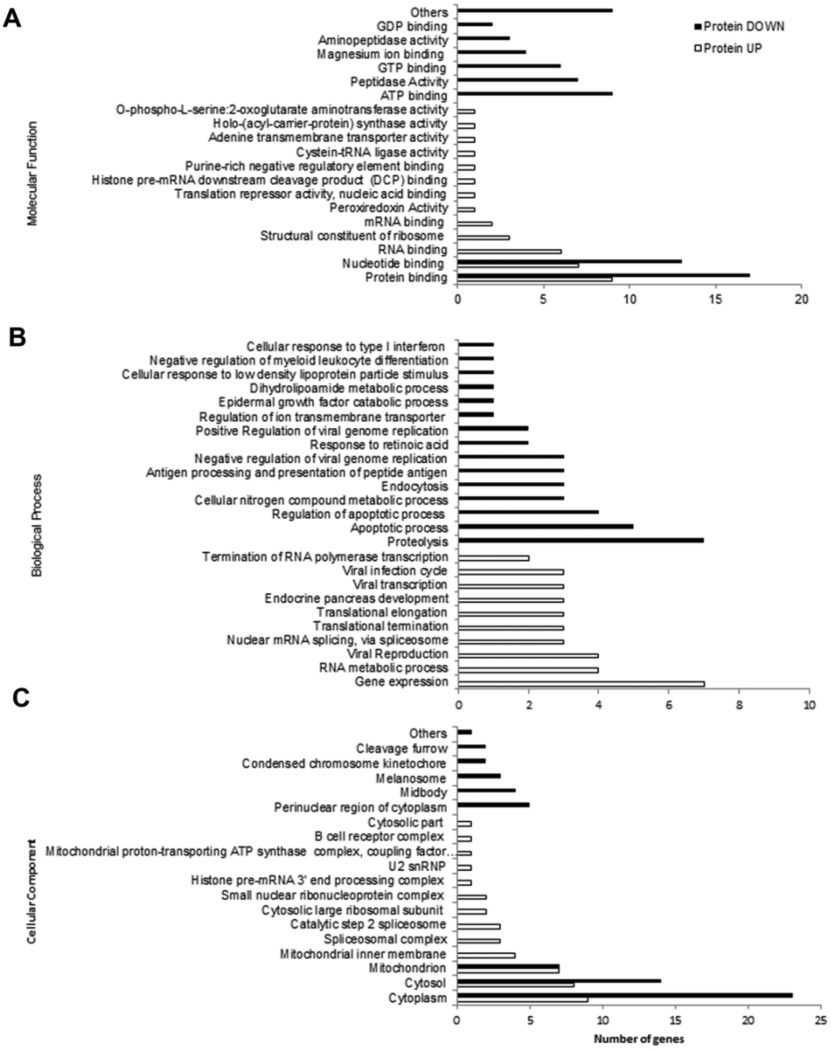

Figure 2. Gene Ontology (GO) analysis of the proteins considered differentially abundant after macrophage interaction with *C. albicans*. GO analysis of (A) molecular function, (B) biological process, and (C) cellular component.

ratios, respectively (Figure S4 and Table 1). Out of these 59 differentially abundant proteins, 12 were annotated as ATP binding proteins. GO term enrichment analysis showed that the more abundant proteins were involved in gene expression and RNA metabolic process, whereas the less abundant proteins were associated with proteolysis, apoptotic processes and endocytosis, among others. Both, the more and less abundant macrophage proteins, were related to the same molecular functions, such as protein binding and nucleotide binding. Furthermore, the more abundant proteins were associated with RNA binding or peroxiredoxin activities, while the less abundant proteins were related to ATP binding or peptidase activities. Both the more and less abundant proteins were enriched in the cytosol and mitochondrion GO terms (Figure 2). The more abundant mitochondrial proteins during interaction included SLC25A24 and PRDX5, which are important in the response to oxidative stress.[36,37]

The analysis of known and predicted protein−protein interactions was also performed with these 59 differentially abundant macrophage proteins upon *C. albicans* interaction (Figure 3). Forty-five protein−protein associations were found on the basis of known or predicted interactions. Different clusters of protein associations were observed. A cluster enriched in proteins that were more abundant during *C. albicans* interaction was involved in protein synthesis. The group of proteins that were less abundant was very heterogeneous in molecular function GO terms and included a cluster of proteins involved in proteolysis and endocytic traffic. Other clusters containing both the more and less abundant proteins were related to RNA processing and apoptosis.

Analysis of the Quantified Proteins Annotated as ATP-Binding Proteins

A comparison between all the proteins annotated as ATP binding in Uniprot database and the proteins quantified in this study was performed. From the 1482 proteins annotated with the ATP binding term, 137 were also present in the 547 proteins quantified in this study (Table S3). This means that approximately 25% of all the quantified proteins were annotated as "ATP-binding". A list of all ATP binding proteins quantified and grouped by protein family is represented in Table 2. Among them, 4 proteins (MAP2K2, KSYK, DDX21, and SYCC) were more abundant during the interaction, and 8 proteins (PRS10, SYIM, STK3, OAS3, MAP3K2, RTCB, NDKA, and SRPK1) were less abundant after the interaction. In this group of differentially abundant ATP-binding proteins,

DOI: 10.1021/acs.jproteome.9b00032
J. Proteome Res. XXXX, XXX, XXX−XXX

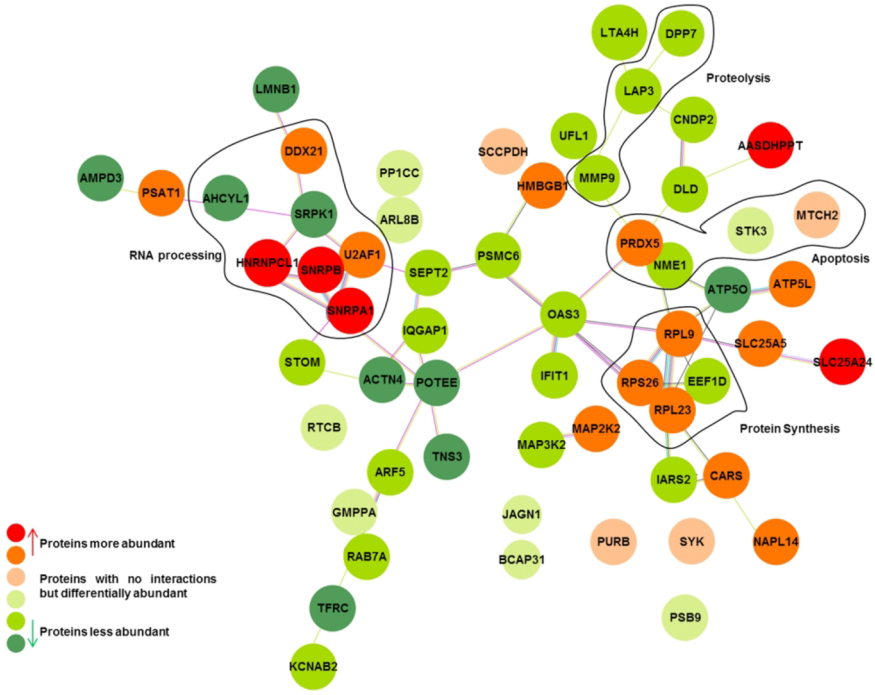

Figure 3. Predicted protein−protein interacting network using STRING (v10.0). Some biological processes (RNA splicing, protein synthesis, proteolysis, endocytic traffic, and apoptosis) are highlighted in the network, signaling some of the interacting proteins that are involved in each process. The network protein−protein interaction *p*-value was 5.76×10^{-05}.

6 were kinases (MAP2K2, SYK, STK3, MAP3K2, NDKA, and SRPK1). The group with more quantified proteins was the protein kinase superfamily, with 24 quantified protein kinases (Table 2). GO analysis on molecular function showed an over-representation of terms related to ATP binding (like nucleotide binding), ATPase activity and kinase activity (Table S3). Regarding the GO analysis on cellular component, in addition to cytosol that was already expected, an over-representation on terms related to chaperonin-containing T complex, proteasome, mitochondria or extracellular vesicles was also observed. Concerning the GO analysis on the biological processes, there was an over-representation in terms such as regulation of protein localization to Cajal bodies (which are implicated in mRNA processing),[38] tRNA amino-acylation for protein translation, protein folding, regulation of protein stability, and positive regulation of cellular biosynthetic process. There was also an over-representation on processes related to immune response, such as regulation of cellular response to stress and activation of innate immune response.

Phosphoproteomic Analysis of Macrophage Proteins after Interaction with *C. albicans*

The fraction enriched in ATP-binding proteins from all 4 biological replicates was further subjected to phosphopeptide enrichment. A total of 85 phosphopeptides were quantified in at least two biological replicates and with a SD < 0.3 and are listed in Table S4. In some cases two or more phosphopeptides were quantified for the same phosphorylation site (phosphosite). Therefore, 85 phosphopeptides corresponding to 70 phosphosites and 56 proteins were quantified. According to the phosphorylation probabilities given by the Proteome Discoverer software, the phosphosites were considered ambiguous or assigned to a specific amino acid (serine, threonine and tyrosine). Sixty-one percent of the phosphosites were phosphorylated in a serine and 33% were ambiguous, whereas phosphothreonine and phosphotyrosine were less represented (3% each). Out of the 56 phosphoproteins, 25 (approximately 36%) are from proteins that were annotated as ATP-binding proteins in Uniprot database and 12 (21.4%) as kinases. Out of the 85 quantified phosphopeptides, 5 phosphopeptides (each one belonging to a single protein) were differentially abundant during macrophage interaction with *C. albicans* (Table 3 and Figure S5). From this, 2 phosphopeptides belonging to PRKAA1 and CLN6 were more abundant during interaction, whereas 3 phosphopeptides belonging to PI4K2A, SRC and PRKCD were less abundant. Their mass spectra are shown in Figure S6.

Protein Validation

To confirm the quantitative MS data, Western blot analysis using antibodies to MAP2K2, PRDX5 and ERK1/2, and SRM of NDKA were performed. There was a significant increase in MAP2K2 (ratio between interaction and macrophages control of 1.6) and PRDX5 (ratio of 2.1) abundance during macrophage interaction with *C. albicans* cells in line with MS data (Figures 4A and 4B). Because MAP2K2 is a kinase that acts upstream ERK1/ERK2 kinases and is important for several cellular processes,[39] we also validated this protein by Western blotting. No significant differences in ERK1/2 abundance upon interaction were detected, confirming our proteomic data (Figure 4C). In addition, phosphorylation of ERK1/2 was also evaluated and no increase in phosphorylation was observed (Figure S7). For SRM validation, the correspondent isotopic labeled peptide was ordered, and a calibration curve was performed (see Figure S8 and Table S5). The quantification of this peptide confirmed the decrease in the amount of NDKA (ratio of 0.24) (Figure 4D and Table S5).

DOI: 10.1021/acs.jproteome.9b00032
J. Proteome Res. XXXX, XXX, XXX−XXX

Table 2. ATP-Binding Proteins Quantified[a]

protein family	UniProt code[b]	entry name	gene names	protein name
AAA ATPase family	P17980	PRS6A	PSMC3	26S protease regulatory subunit 6A
	P35998	PRS7	PSMC2	26S protease regulatory subunit 7
	P43686	PRS6B	PSMC4	26S protease regulatory subunit 6B
	P46459	NSF	NSF	Vesicle-fusing ATPase
	P55072	TERA	VCP	Transitional endoplasmic reticulum ATPase
	P62191	PRS4	PSMC1	26S protease regulatory subunit 4
	P62195	PRS8	PSMC5	26S protease regulatory subunit 8
	P62333	PRS10	PSMC6	26S protease regulatory subunit 10B[c]
ABC transporter superfamily	Q03518	TAP1	TAP1	Antigen peptide transporter 1
	P61221	ABCE1	ABCE1	ATP-binding cassette subfamily E member 1
Actin family	P60709	ACTB	ACTB	Actin. cytoplasmic 1
	P68032	ACTC	ACTC1	Actin. alpha cardiac muscle 1
	P61163	ACTZ	ACTR1A	Alpha-centractin
	P61160	ARP2	ACTR2	Actin-related protein 2
	P61158	ARP3	ACTR3	Actin-related protein 3
Adenylate kinase family	P00568	KAD1	AK1	Adenylate kinase isoenzyme 1
	P30085	KCY	CMPK1	UMP-CMP kinase
ATPase alpha/beta chains family	P06576	ATPB	ATP5F1B	ATP synthase subunit beta
	P25705	ATPA	ATP5F1A	ATP synthase subunit alpha
	P38606	VATA	ATP6 V1A	V-type proton ATPase catalytic subunit A
Class-I aminoacyl-tRNA synthetase family	P23381	SYWC	WARS	Tryptophan-tRNA ligase
	P26640	SYVC	VARS	Valine-tRNA ligase
	P47897	SYQ	QARS	Glutamine-tRNA ligase
	P49589	SYCC	CARS	Cysteine-tRNA ligase[d]
	P54136	SYRC	RARS	Arginine-tRNA ligase
	P54577	SYYC	YARS	Tyrosine-tRNA ligase
	Q9NSE4	SYIM	IARS2	Isoleucine-tRNA ligase[c]
	Q9P2J5	SYLC	LARS	Leucine-tRNA ligase
	P07814	SYEP	EPRS	Bifunctional glutamate/proline-tRNA ligase
	O43776	SYNC	NARS	Asparagine-tRNA ligase
	P12081	SYHC	HARS	Histidine-tRNA ligase
	P26639	SYTC	TARS	Threonine-tRNA ligase
	P41250	GARS	GARS	Glycine-tRNA ligase
	P49588	SYAC	AARS	Alanine-tRNA ligase
	Q9Y285	SYFA	FARSA	Phenylalanine-tRNA ligase alpha subunit
	P14868	SYDC	DARS	Aspartate-tRNA ligase
	P49591	SYSC	SARS	Serine-tRNA ligase
ClpA/ClpB family	Q9H078	CLPB	CLPB	Caseinolytic peptidase B protein homologue
	O14656	TOR1A	TOR1A	Torsin-1A
DEAD box helicase family	Q9NR30	DDX21	DDX21	Nucleolar RNA helicase 2[d]
	O00571	DDX3X	DDX3X	ATP-dependent RNA helicase DDX3X
	P17844	DDX5	DDX5	Probable ATP-dependent RNA helicase DDX5
	Q08211	DHX9	DHX9	ATP-dependent RNA helicase A
	O43143	DHX15	DHX15	Pre-mRNA-splicing factor ATP-dependent RNA helicase DHX15
	Q13838	DX39B	DDX39B	Spliceosome RNA helicase DDX39B
	P38919	IF4A3	EIF4A3	Eukaryotic initiation factor 4A-III
	P60842	IF4A1	EIF4A1	Eukaryotic initiation factor 4A-I
	Q14240	IF4A2	EIF4A2	Eukaryotic initiation factor 4A-II
Heat shock protein 70 family	P11021	BIP	HSPA5	78 kDa glucose-regulated protein
	P11142	HSP7C	HSPA8	Heat shock cognate 71 kDa protein
	P34932	HSP74	HSPA4	Heat shock 70 kDa protein 4
	P38646	GRP75	HSPA9	Stress-70 protein
	Q92598	HS105	HSPH1	Heat shock protein 105 kDa
	Q9Y4L1	HYOU1	HYOU1	Hypoxia up-regulated protein 1
Heat shock protein 90 family	P07900	HS90A	HSP90AA1	Heat shock protein HSP 90-alpha
	P08238	HS90B	HSP90AB1	Heat shock protein HSP 90-beta
	P14625	ENPL	HSP90B1	Endoplasmin
	Q12931	TRAP1	TRAP1	Heat shock protein 75 kDa
	Q58FF6	H90B4	HSP90AB4P	Putative heat shock protein HSP 90-beta 4

DOI: 10.1021/acs.jproteome.9b00032
J. Proteome Res. XXXX, XXX, XXX−XXX

Table 2. continued

protein family		UniProt code[b]	entry name	gene names	protein name
Phosphofructokinase type A (PFKA) family		P17858	PFKAL	PFKL	ATP-dependent 6-phosphofructokinase
		Q01813	PFKAP	PFKP	ATP-dependent 6-phosphofructokinase
Protein kinase superfamily	AGC Ser/Thr protein kinase family	P17612	KAPCA	PRKACA	cAMP-dependent protein kinase catalytic subunit alpha
		Q15418	KS6A1	RPS6KA1	Ribosomal protein S6 kinase alpha-1
	BUD32 family	Q96S44	PRPK	TP53RK	TP53-regulating kinase
	CMGC Ser/Thr protein kinase family	Q96SB4	SRPK1	SRPK1	SRSF protein kinase 1[c]
		P49841	GSK3B	GSK3B	Glycogen synthase kinase-3 beta
		P28482	MK01	MAPK1	Mitogen-activated protein kinase 1
		Q16539	MK14	MAPK14	Mitogen-activated protein kinase 14
	Ser/Thr protein kinase family	P19784	CSK22	CSNK2A2	Casein kinase II subunit alpha′
		P68400	CSK21	CSNK2A1	Casein kinase II subunit alpha
		P19525	E2AK2	EIF2AK2	Interferon-induced. double-stranded RNA-activated protein kinase
	STE Ser/Thr protein kinase family	Q9Y2U5	M3K2	MAP3K2	Mitogen-activated protein kinase kinase kinase 2[c]
		P36507	MP2K2	MAP2K2	Dual specificity mitogen-activated protein kinase kinase 2[d]
		O94804	STK10	STK10	Serine/threonine-protein kinase 10
		O95747	OXSR1	OXSR1	Serine/threonine-protein kinase OSR1
		Q13043	STK4	STK4	Serine/threonine-protein kinase 4
		Q13177	PAK2	PAK2	Serine/threonine-protein kinase PAK 2
		Q13188	STK3	STK3	Serine/threonine-protein kinase 3[c]
		Q9H2G2	SLK	SLK	STE20-like serine/threonine-protein kinase
		Q9H2K8	TAOK3	TAOK3	Serine/threonine-protein kinase TAO3
		Q9Y6E0	STK24	STK24	Serine/threonine-protein kinase 24
	TKL Ser/Thr protein kinase family	Q13418	ILK	ILK	Integrin-linked protein kinase
		Q9NWZ3	IRAK4	IRAK4	Interleukin-1 receptor-associated kinase 4
	Tyr protein kinase family. CSK subfamily	P41240	CSK	CSK	Tyrosine-protein kinase CSK
		P43405	KSYK	SYK	Tyrosine-protein kinase SYK[d]
Ribose-phosphate pyrophosphokinase family		P11908	PRPS2	PRPS2	Ribose-phosphate pyrophosphokinase 2
		P60891	PRPS1	PRPS1	Ribose-phosphate pyrophosphokinase 1
RtcB family		Q9Y3I0	RTCB	RTCB	tRNA-splicing ligase RtcB homologue[c]
		Q9Y230	RUVB2	RUVBL2	RuvB-like 2
		Q9Y265	RUVB1	RUVBL1	RuvB-like 1
Succinate/malate CoA ligase beta subunit family		Q9P2R7	SUCB1	SUCLA2	Succinate-CoA ligase
		Q96I99	SUCB2	SUCLG2	Succinate-CoA ligase
		P53396	ACLY	ACLY	ATP-citrate synthase
TCP-1 chaperonin family		P17987	TCPA	TCP1	T-complex protein 1 subunit alpha
		P40227	TCPZ	CCT6A	T-complex protein 1 subunit zeta
		P48643	TCPE	CCT5	T-complex protein 1 subunit epsilon
		P49368	TCPG	CCT3	T-complex protein 1 subunit gamma
		P50990	TCPQ	CCT8	T-complex protein 1 subunit theta
		P50991	TCPD	CCT4	T-complex protein 1 subunit delta
		P78371	TCPB	CCT2	T-complex protein 1 subunit beta
		Q99832	TCPH	CCT7	T-complex protein 1 subunit eta
Ubiquitin-activating E1 family		A0AVT1	UBA6	UBA6	Ubiquitin-like modifier-activating enzyme 6
		P22314	UBA1	UBA1	Ubiquitin-like modifier-activating enzyme 1
		Q9UBT2	SAE2	UBA2	SUMO-activating enzyme subunit 2
		Q9GZZ9	UBA5	UBA5	Ubiquitin-like modifier-activating enzyme 5
		P61088	UBE2N	UBE2N	Ubiquitin-conjugating enzyme E2 N
Proteins without Protein Family assigned		P05165	PCCA	PCCA	Propionyl-CoA carboxylase alpha chain
		P48426	PI42A	PIP4K2A	Phosphatidylinositol 5-phosphate 4-kinase type-2 alpha
		P49915	GUAA	GMPS	GMP synthase
		Q02790	FKBP4	FKBP4	Peptidyl-prolyl cis−trans isomerase FKBP4
		Q12905	ILF2	ILF2	Interleukin enhancer-binding factor 2
		Q14166	TTL12	TTLL12	Tubulin−tyrosine ligase-like protein 12
		Q9UHD1	CHRD1	CHORDC1	Cysteine and histidine-rich domain-containing protein 1
Other ATP-binding Proteins		Q9Y6K5	OAS3	OAS3	2′-5′-oligoadenylate synthase 3[c]

DOI: 10.1021/acs.jproteome.9b00032
J. Proteome Res. XXXX, XXX, XXX−XXX

Table 2. continued

protein family	UniProt code[b]	entry name	gene names	protein name
	P00966	ASSY	ASS1	Argininosuccinate synthase
	O43681	ASNA	ASNA1	ATPase ASNA1
	O60488	ACSL4	ACSL4	Long-chain-fatty-acid−CoA ligase 4
	P16615	AT2A2	ATP2A2	Sarcoplasmic/endoplasmic reticulum calcium ATPase 2
	P10809	CH60	HSPD1	60 kDa heat shock protein
	P17812	PYRG1	CTPS1	CTP synthase 1
	Q13057	COASY	COASY	Bifunctional coenzyme A synthase
	P22102	PUR2	GART	Trifunctional purine biosynthetic protein adenosine-3
	P00367	DHE3	GLUD1	Glutamate dehydrogenase 1
	P54886	P5CS	ALDH18A1	Delta-1-pyrroline-5-carboxylate synthase
	P19367	HXK1	HK1	Hexokinase-1
	P12956	XRCC6	XRCC6	X-ray repair cross-complementing protein 6
	P13010	XRCC5	XRCC5	X-ray repair cross-complementing protein 5
	P15531	NDKA	NME1	Nucleoside diphosphate kinase A[c]
	P36776	LONM	LONP1	Lon protease homologue
	Q9NSD9	SYFB	FARSB	Phenylalanine−tRNA ligase beta subunit
	P00558	PGK1	PGK1	Phosphoglycerate kinase 1
	P14618	KPYM	PKM	Pyruvate kinase PKM
	P22234	PUR6	PAICS	Multifunctional protein ADE2
	P11586	C1TC	MTHFD1	C-1-tetrahydrofolate synthase
	O43615	TIM44	TIMM44	Mitochondrial import inner membrane translocase subunit TIM44
	Q12965	MYO1E	MYO1E	Unconventional myosin-Ie
	Q9NTK5	OLA1	OLA1	Obg-like ATPase 1

[a]Proteins are ordered by alphabetical and by protein family. [b]Uniprot Code according to Uniprot Knowledge base. Proteins only with a standard deviation lower than 30% and quantified in at least 2 biological replicates. [c]Proteins annotated as ATP-binding proteins in Uniprot database that were found in this study to be less abundant during macrophage interaction with *C. albicans*. [d]Proteins annotated as ATP-binding proteins in Uniprot database that were found in this study to be more abundant during macrophage interaction with *C. albicans*.

Table 3. Phosphopeptides Differentially Abundant after 3 h of Macrophage−*C. albicans* Interaction

UniProt code[a]	gene names	protein names[a]	phosphopeptide	phosphosite[b]	ratio[c]	SD[c]
Q13131	PRKAA1	5′-AMP-activated protein kinase catalytic subunit alpha-1	SGSVSNYR	ambiguous	1.58	0.22
Q9NWW5	CLN6	Ceroid-lipofuscinosis neuronal protein 6	HGs*VSADEAAR[d]	Ser31	1.40	0.29
Q9BTU6	PI4K2A	Phosphatidylinositol 4-kinase type 2-alpha	SSSESYTQSFQSr	ambiguous	0.70	0.22
P12931	SRC	Proto-oncogene tyrosine-protein kinase Src	LIEDNEy*TAR	Tyr419	0.69	0.22
Q05655	PRKCD	Protein kinase C delta type	SDSASSEPVGIYQGFEK	ambiguous	0.57	0.06

[a]Protein name and Uniprot Code according to Uniprot Knowledge base. [b]Phosphosites were considered ambiguous in case PhosphoRS algorithm assigned a localization probability lower than 75% or if it was assigned in distinct sites in different biological replicates. [c]Average abundance ratio from macrophages + *C. albicans* versus control macrophages and respective inter-replicate standard deviation (cutoff in 0.3). Only phosphopeptides with a standard deviation lower than 30% and quantified in at least 2 biological replicates. [d]Asterisk indicates the phosphorylation site, and the corresponding amino acid is in lower case.

Macrophage Cell Death Mechanisms and Pro-inflammatory Response

Apoptosis was one of the biological processes enriched in the group of less abundant proteins. A closer look showed an increase in PRDX5, SLC25A24, and ADT2, which are antiapoptotic proteins, and a decrease NDKA, ACTN4, and STK3, which are pro-apoptotic or antisurvival proteins.[36,40−44] In order to functionally validate these results, the apoptotic status of THP-1 macrophages after interaction with *C. albicans* was assayed by measuring caspase-3 activation by cleavage. Cells were incubated with staurosporine (as a positive control of apoptosis) and with *C. albicans* cells (at a MOI of 1 for 3 h). Activated caspase-3 was assayed by Western blotting with cell lysates and a band corresponding to the activated caspase 3 was observed in the positive control but not in macrophage−*C. albicans* interaction at 3 h (Figure 5A). As cleaved caspase 3 is a hallmark of apoptosis,[45] this result suggests that apoptosis was not present in these conditions. In congruence with our results, it was previously described by others that *C. albicans* triggers pyroptosis during the first 6 to 8 h of interaction with macrophages,[46] we checked IL-1β secretion (which is secreted after caspase-1 activation).[47] IL-1β was significantly more secreted in macrophages after interaction with *C. albicans* (Figure 5B). Furthermore, as pyroptosis is an inflammatory mechanism of cell death,[47] other pro-inflammatory cytokines were evaluated. As depicted in Figures 5C and 5D, there was more secretion of pro-inflammatory cytokines IL-12p40 and TNF-α upon interaction with *C. albicans*.

To further predict potential upstream regulators implicated in the macrophage inflammatory response, the 59 differentially abundant proteins were also analyzed using the IPA software. Fifteen upstream regulators presented an activation *z*-score between −2 and 2 and a *p*-value of overlap <0.05, which included CD3 complex, cytokines (oncostatin M (OSM), IL5 and IL6), proteins (KRAS; VEGFA; MAPK1; ESR1), miRNAs

DOI: 10.1021/acs.jproteome.9b00032
J. Proteome Res. XXXX, XXX, XXX−XXX

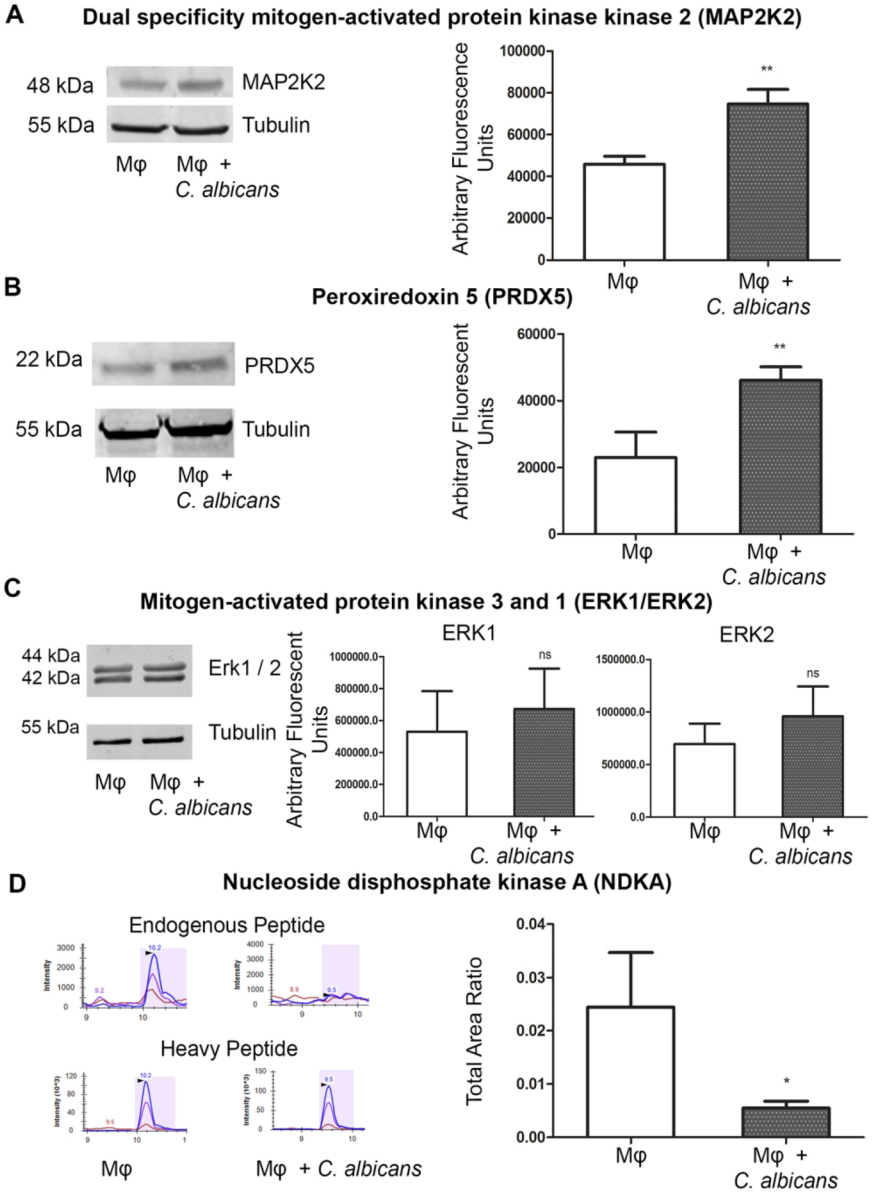

Figure 4. Proteomic results validation in both conditions: M*φ* (control) and M*φ*+ *C. albicans* (MOI 1 and 3 h of incubation). Quantification of (A) MAP2K2, (B) PRDX5, and (C) ERK1/2 by Western blotting and (D) NDKA by selected reaction monitoring.

(miR-124-3p and miR-21), transcription regulators (MYCN, MYC, and TP53), transmembrane receptor CD28 and rapamycin-insensitive companion of mTOR (RICTOR) (Figure 6A). The higher or lower *z*-score showed the higher probability of activation or inhibition of the upstream regulator, respectively. The IL-6 gene was predicted to be inhibited. This prompted us to assay the secretion of this cytokine at different time points (3, 6, and 8 h) of THP-1 macrophage−*C. albicans* interaction. This cytokine was not secreted after interaction with yeast cells (Figure 6B), indicating that this gene may not be expressed under these conditions. Due to the recent evidence in the implication of miRNAs (miR) in the regulation of innate immune response,[48] we also evaluated the possible activation miR-21 and miR-124 (two miRNAs that were predicted to be activated; Figure 6A). The expression levels of miR-21 and miR-124 were evaluated together with miR-146 and miR-155 (which are activated after treatment with LPS in THP-1 cells[24] and also after interaction with heat inactivated *C. albicans* cells[49−51]). MiR-21 and miR-124 were slightly, but not statistically significant, activated after treatment with LPS, and showed no significant activation in response to *C. albicans* (Figures 7A and 7B, respectively). Regarding miR-146 and miR-155, they were activated in response to LPS (Figures 7C and 7D, respectively), but also no significant activation in response to live *C. albicans* cells after 3 and 6 h of interaction was observed.

DISCUSSION

The current approaches to decrease fungal infections are still limited and are mainly pathogen-directed therapeutics.[52] In this way, the study of the immune response may give us new clues on how this pathogen can be killed, and consequently improve the currently available therapeutic approaches. Furthermore, increasing efforts are being done to develop specific ways to modulate the immune system as new therapeutic strategies.[53,54] Macrophages are cells from the innate immune system that play an important role in the host

DOI: 10.1021/acs.jproteome.9b00032
J. Proteome Res. XXXX, XXX, XXX−XXX

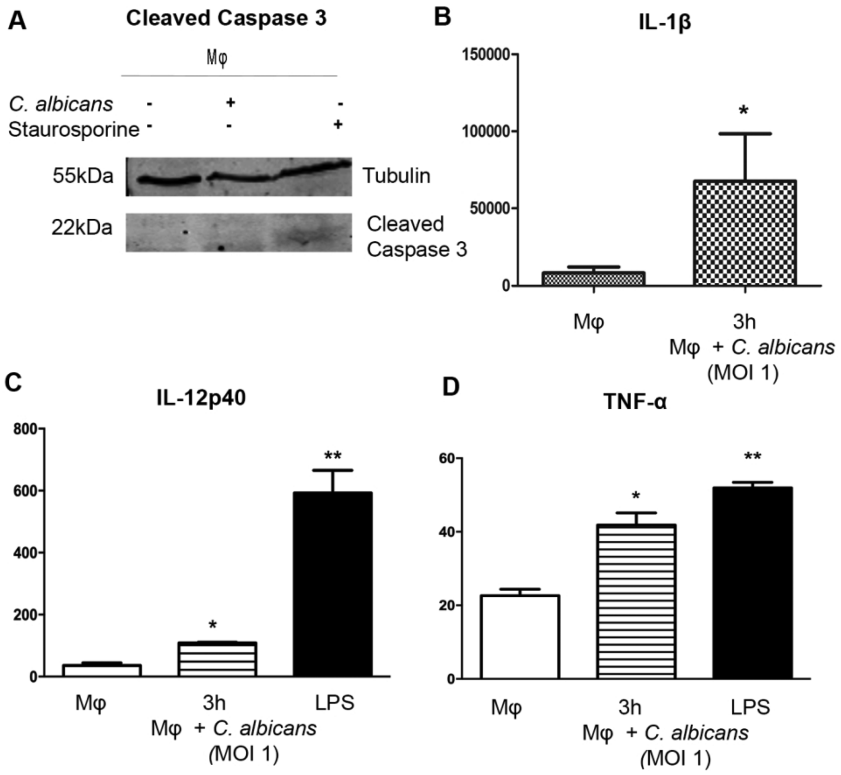

Figure 5. Caspase 3 activation and cytokine secretion measurement. Caspase activation was measured by Western blotting (A) and cytokine secretion measured using enzyme-linked immunosorbent assay (ELISA): (B) Il-1β, (C) IL-12p40, and (D) TNF-α secretion in Mφ (control) and Mφ+ *C. albicans* and after treatment with LPS (positive control).

response and elimination of pathogens.[4] ATP-binding proteins are essential in several cellular processes including cell signaling, differentiation apoptosis and others.[21] Despite this fact, proteomic studies of this group of proteins are generally difficult because they are at low abundance in the cell. In this way, we decided to perform a selective enrichment in ATP-binding proteins with an ATP probe[16] in order to get more information on this subproteome. Taking advantage of this approach, a quantitative proteomic study of human macrophage proteins after interaction with *C. albicans* cells was carried out in this work and allowed the quantification of proteins that could be involved in the response to this pathogen. In this study, THP-1-derived macrophages were incubated with *C. albicans* cells during 3 h and a MOI of 1. PMA was used for the differentiation of THP-1 monocytes. The up-regulation of specific genes during the differentiation process might overwhelm mild effects of specific stimuli. Nevertheless, this cell line was described to be very close to primary human cells and used previously for the study interaction with pathogens.[55−59] At 3 h of interaction, a reduced damage was ensured, so 70% of the macrophages were not impaired and around 70% of yeast cells were engulfed by the macrophages. This evaluation of human macrophage interaction with *C. albicans* is in agreement with our previous studies with murine macrophage cell lines and was peremptory to select the ratio and time of incubation.[7,26]

Enrichment in ATP Binding Macrophage Proteins

In this study, 547 nonredundant macrophage proteins were quantified, approximately 25% of which were annotated in Uniprot as "ATP-binding" proteins. Proteins that were quantified and not annotated as ATP binding proteins could be either proteins that were interacting with the ATP binding proteins or proteins that resulted from unspecific binding with the probe. The protein family with more quantified ATP-binding proteins was the protein kinase superfamily (with 24 quantified protein kinases). Out of these 24 protein kinases, 13 proteins were included in the Ser/Thr (STE) protein kinase family. The preference to this protein kinase family was previously observed by Lemeer and co-workers.[60] They performed a comparison between two enrichment methods (ATP-affinity probe and kinobeads). They found a higher number of tyrosine kinases enriched with kinobeads, while more kinases from the STE kinase group were enriched with the ATP affinity probe. They detailed that small molecules inhibitors immobilized in kinobeads were originally developed to target tyrosine kinases, whereas the reaction mechanism of the ATP probe was distinct.[60]

Differentially Phosphorylated Macrophage Peptides after Interaction with *C. albicans*

In addition to protein abundance, phosphorylation information can significantly enhance our knowledge on the involvement of macrophage ATP-binding proteins in different cellular mechanisms during interaction with pathogens. Furthermore, an important group of ATP binding proteins include kinases which are known to be highly phosphorylated in cell signaling processes where they are implicated.[61] Although few phosphorylation results were obtained, 5 differentially abundant phosphopeptides were found and 4 of them were key kinases in cell signaling pathways. This means that type of enrichment in ATP binding proteins, coupled with the new and more potent mass spectrometers, can be a useful tool for the study of kinase phosphorylation sites. Regarding the more abundant phosphopeptides during macrophage−*C. albicans* interaction, they corresponded to CLN6 and PRKAA1.

DOI: 10.1021/acs.jproteome.9b00032
J. Proteome Res. XXXX, XXX, XXX−XXX

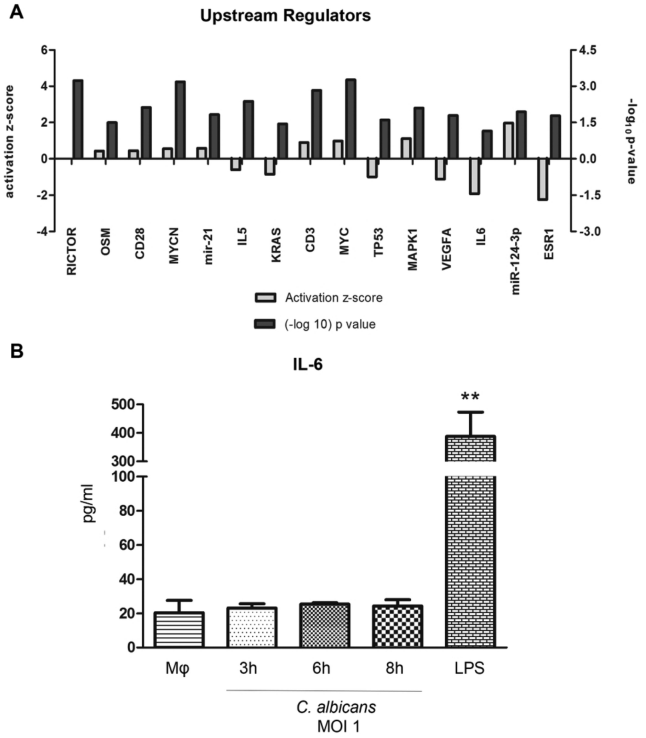

Figure 6. Upstream regulators predicted to be implicated in the response to *C. albicans* using Ingenuity Pathway Analysis (IPA). The upstream regulators analysis is based on prior knowledge of expected effects between transcriptional regulators and their target genes stored in the IPA. (A) Bar chart of the upstream regulators that were predicted, including the activation *z*-score and *p*-value of each upstream regulator derived from IPA. Cellular validation of some of the upstream regulators was performed. (B) IL-6 secretion by ELISA.

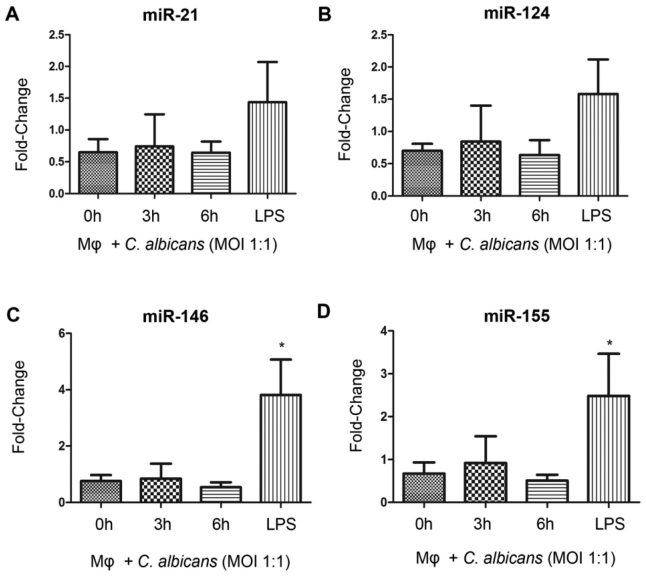

Figure 7. Expression levels of miRNAs in THP1 macrophages after interaction with *C. albicans* cells. Expression levels of (A) miR-21 and (B) mir-124 that were predicted by the IPA and (C) miR-146 and (D) miR-155 that were known to be activated after treatment with LPS and were used as controls.

Neuronal ceroid lipofuscinosis are lysosomal storage disorders and mutation in CLN genes are the cause of this disease. Among them, CLN6 is involved in endocytosis of lysosomal proteins.[62] However, little is known about this protein in other contexts. PRKAA1 presented the phosphopeptide that showed the highest increase in abundance during macrophage interaction. This protein is a sensor of energy status that maintains cellular energy homeostasis.[63] The phosphorylation of Thr183 is known to activate this kinase.[64,65] It was previously shown that the activation of this kinase was implicated in phagocytosis of both bacteria[63] and fungi (like the pathogen *Cryptococcus neoformans*).[65] Phosphorylation of AMPKα in Ser487/491 was found to reduce AMPK activity.[66] In this study, the quantified AMPKα phosphopeptide had several possible phosphosites assigned: Ser494, Ser496, and Tyr500. A search in Phosphosite Plus showed that the phosphorylation of Ser496 would be responsible for the inhibition of the enzymatic activity. However, further studies would be needed to know the cellular effects of this phosphopeptide.

The less abundant phosphopeptides during macrophage *C. albicans* interaction belonged to PRKCD, SRC and PI4K2. PRKCD and SRC are known to be activated after macrophage receptor recognition of *C. albicans* PAMPs.[4,67] During this study, both phosphopeptides were found to be less abundant during interaction. SRC was found to be less phosphorylated in the activation site (Tyr419) during interaction. Due to its implication in several fundamental processes, including cell differentiation, proliferation, migration and survival[68] in addition to its involvement in the inflammatory process,[69] deeper analysis and time course experiment would be needed to further explain these results. In any case, SRC is one of the primary kinases to be activated after receptor engagement,[4] it is plausible that after 3 h of incubation this kinase is no longer phosphorylated, once the signaling cascades are already activated. PI4K2A was previously described to be involved in the correct endocytic traffic.[70] Interestingly, the quantitative proteomic results showed that two proteins implicated in endosomal trafficking, RAB7A and TFR1, were less abundant during macrophage interaction with *C. albicans*.[71−73] These data together with the fact that our group previously supported the model where *C. albicans* evade trafficking to lytic compartments in murine macrophages[35] make us hypothesize that also during this experiment *C. albicans* may be modulating phagosome maturation. This phenomenon was previously observed during macrophage−*Mycobacterium tuberculosis* interaction.[71,72]

Mitochondrial Proteins and Oxidative Stress Response

In general, the overall quantification of the ATP binding proteins subproteome enriched with this method presents slight changes in its abundance upon interaction with *Candida*. This may be due to the preactivation with PMA needed to differentiate monocytes into macrophages. Macrophages are phagocytic cells that produce and release reactive oxygen species (ROS) in response to phagocytosis.[74] Two mitochondrial proteins involved in response to oxidative stress (PRDX5 and SLC25A24) were found to be more abundant upon interaction with *C. albicans*. PRDX5, a protein that protects cells from DNA damage and inhibits stress-induced apoptosis,[40] was previously shown to be more abundant in LPS-treated macrophages.[75] We validated the increase in its abundance using Western blot. SLC25A24 may also play a role in protecting cells against oxidative stress-induced cell death.[36] Another group previously observed significant changes in redox-related proteins implicated in oxidative burst in order to

DOI: 10.1021/acs.jproteome.9b00032
J. Proteome Res. XXXX, XXX, XXX−XXX

kill intracellular mycobacteria. They observed an increase in the abundance of several proteins that counteract the effect of oxidative stress.[76] We can hypothesize that the higher abundance of proteins that neutralize the oxidative burst may be a host-driving response to protect itself from the ROS production because after 3 h of interaction *Candida* cells are already producing hypha, which promotes phagolysosome rupture. Nevertheless, we may not discard the possibility that it can also be a pathogen-driven response (to reduce the production of ROS and decrease the killing power of the macrophages). In addition to being of highly importance to ATP production and electron transport chain, mitochondria were recently implicated in innate and adaptive immunity.[77] Knowing this, we took a more careful look to the quantified proteins located in the mitochondria. In general terms, we observed an increase in the mechanisms that protect cell against oxidative stress as well as transport of ATP to the cytoplasm. This behavior is understandable once macrophages increase the amount of ROS to kill *C. albicans*. So, the increase in abundance of these proteins could play a role in the phagocyte protection against the produced oxidative stress. Furthermore, the higher demand of metabolites and proteins could explain the need of the mitochondria to increase the transport of ATP to the cytosol.

Host Proteins Involved in mRNA Processing and Translation

HNRNPCL1, a heterogeneous nuclear ribonucleoprotein, was the protein with the highest differential abundance in our study. HNRNPs are operationally defined as proteins that bind to RNA[78] and are responsible for packing and stabilizing them.[79] Little is known about HNRNPCL1. Nevertheless, HNRNPC was one of the first HNRNPs found to be involved in RNA splicing.[80] The depletion of these C proteins from splicing extracts abolished splicing activity. Thus, we can hypothesize that HNRNPCL1, which has a 90.8% identity with HNRNPC, may have a similar role to HNRNPC. Interestingly, an increase in the abundance of several HNRNPs was previously observed in THP-1 cells infected with *Leishmania* parasites.[55] String analysis showed a cluster of (more and less abundant) proteins involved in RNA processing. Further validation and functional studies are necessary to define the role of splicing proteins in the macrophage response to *C. albicans*.

Another group of differentially more abundant proteins were ribosomal proteins (RPS26, RPL3, RPL9, and DDX21). A higher abundance of these proteins may be a mechanism of the host cells to meet the increasing need of proteins to fight the fungal infection. In line with the upregulation of the protein synthesis process, a decrease in the abundance of proteins involved in proteolysis (MMP9, LAP3, DPP7, and DLD) was observed.

Macrophage Cell Death and Inflammatory Response to *C. albicans*

We also observed enrichment of proteins related to apoptosis. We found that antiapoptotic signals were up-regulated in THP-1 macrophages infected with *C. albicans*, as compared to pro-apoptotic signals. Knowing that caspase-3 is one of the executioners of apoptosis, we measured its cleavage by Western blotting and no cleavage of this protein was observed after THP-1 macrophage interaction with *C. albicans*.[81] A previous work from our research group reported no apoptosis in RAW 264.7 macrophages incubated with *C. albicans*.[7] The way by which macrophages activate cell death mechanisms as a consequence of uptaking *C. albicans* cells has been studied previously. Uwamahoro and co-workers showed that *C. albicans* triggers pyroptosis during the first 6 to 8 h of interaction.[46] In concordance to our results, they observed no evidence of activation of caspase-3 by *C. albicans* early postinfection. More recently, another group suggested that neutralization of the phagosome by *C. albicans* is an important signal in activating the macrophage inflammasome.[82] The pro-inflammatory cytokine IL-1β is released as a result of *C. albicans* driven NL3PR inflammasome activation and has been used as a measurement of pyroptotic cell death in the immune cell in response to microbial pathogens.[82−84] An increase of this cytokine was observed after 3 h of interaction with *C. albicans*, suggesting that pyroptosis could be activated in response to *C. albicans*. However, further validation confirming caspase-1-dependent IL-1β release would be needed to confirm this phenomenon in this cell line. We were also interested in knowing whether other pro-inflammatory cytokines were secreted. Both TNF-α and Il-12 were significantly more secreted after 3 h of interaction with *C. albicans*. This pathogen is known to trigger a pro-inflammatory response of the macrophages, including the release of these cytokines.[85] The IPA software was used to predict upstream regulators of the pro-inflammatory response. This analysis is based on prior knowledge of expected effects between transcriptional regulators and their target genes that are stored in Ingenuity Knowledge Base (taking into account previously published data sets derived from different animal models).[86] This analysis suggested 15 potential regulators of gene expression for the genes encoding the proteins identified in this. In order to validate some of these predictions, we evaluated the secretion of IL-6 and the activation of miR-21 and miR-124. The analysis performed by IPA presented a negative activation *z*-score of IL-6 and in accordance with this, no secretion of IL-6 was observed. IL-6 is a pro-inflammatory cytokine and was previously observed not to be secreted after interaction with *C. albicans*.[8,87] Recently, mi-RNAs have been implicated in immune response, particularly as post-transcriptional regulators of the inflammatory response. There are several mi-RNAs that regulate TLR signaling pathways. Monk and co-workers showed that miR-155, miR-146a, miR-146b, miR-125a and miR-455 were upregulated after treatment with LPS and after interaction with heat killed *C. albicans* cells.[51] Another group was interested in the impact of *C. albicans* cell morphology (heat killed yeast and hyphal cells) in the differential regulation of host mi-RNAs.[50] They suggested that dectin-1 may be orchestrating miR-155 up-regulation in a Syk-dependent manner. Since our proteomic approach was performed with live *C. albicans* cells, we investigated the differential mi-RNAs regulation upon interaction with live *Candida* cells. The selected mi-RNAs were those predicted to be up-regulated by IPA (miR-21 and miR −124) and those found to be induced upon LPS activation and after interaction with heat killed *C. albicans* cells (miR-146 and miR-155).[49] Because we used live cells, our time points were shorter than others. We found that miR-21 and miR-124 were slightly, but not significantly, up-regulated after treatment with LPS. After interaction with *C. albicans*, none of these mi-RNAs were statistically significant upregulated. In our conditions and time points, the results were different from the predicted by IPA. Both miR-146 and miR-155 were confirmed to be upregulated after macrophage treatment with LPS. This was in con-

DOI: 10.1021/acs.jproteome.9b00032
J. Proteome Res. XXXX, XXX, XXX−XXX

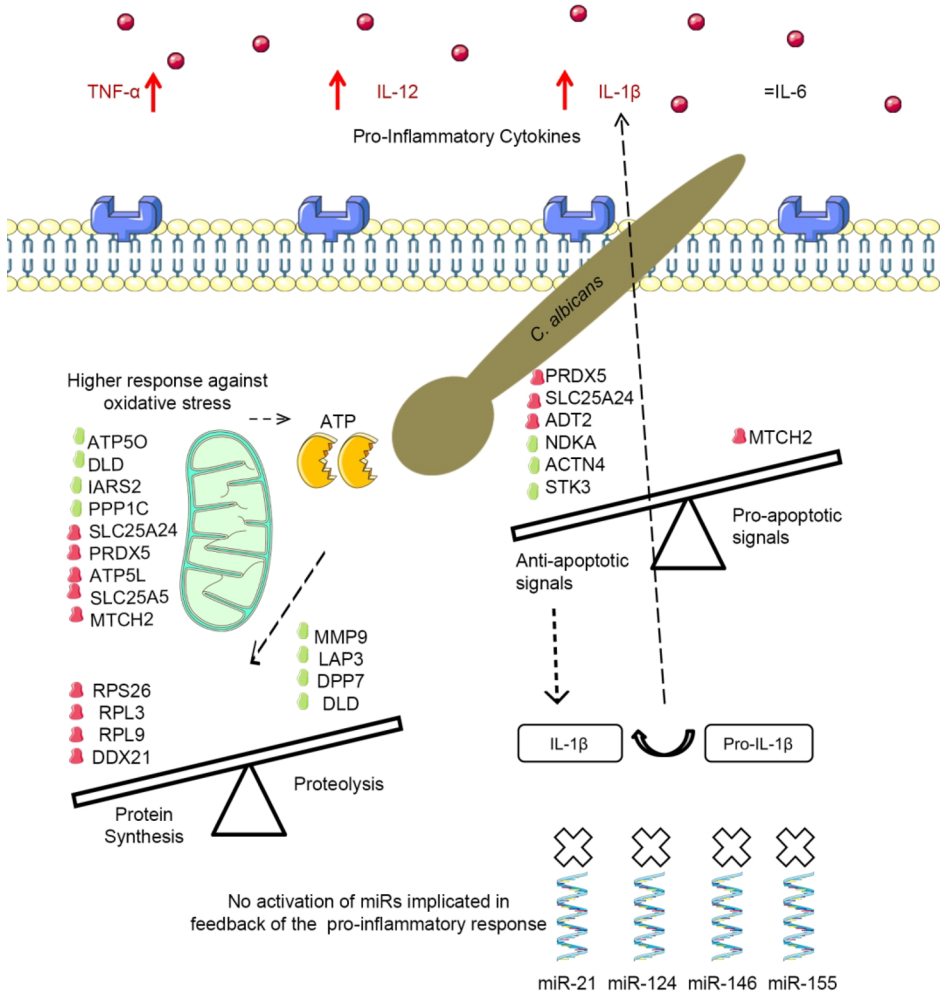

Figure 8. Schematic overview of macrophage possible remodeling after interaction with *C. albicans*. The differentially abundant proteins, together with the cytokines, are color coded with red for more abundant and green for less abundant after macrophage interaction with *C. albicans*. The cytokines and the miR that do not present differences after interaction are depicted in gray. The text describes some of the processes suggested to be remodeled after interaction.

cordance with the other work where miR-146 was shown to be involved in the mechanism of negative feedback regulation of TLR.[49] Interestingly, after macrophage interaction with live *C. albicans* cells, no upregulation of these mi-RNAs was observed at these time points. Although longer time points would be needed to determine whether this behavior is maintained, we can hypothesize that these miR were not yet activated because macrophages might need a much higher pro-inflammatory response to kill *C. albicans*, or because this fungus may be inducing a longer pro-inflammatory response to destroy the macrophage. The inflammatory effect induced by live *C. albicans* cells was previously suggested by our group as virulence trait responsible for tissue damage in the host.[7,88] It is important to underscore the need of follow-up studies to reveal whether this is a host-driven or pathogen-driven mechanism.

CONCLUDING REMARKS

The ATP-binding enrichment together with the SILAC proteomic and phosphoproteomic approach revealed new insights into the possible remodeling processes altered upon macrophage interaction with this human pathogen. A summary of these processes is depicted in Figure 8. Interestingly, an increase in the abundance of proteins involved in protein synthesis was observed together with an increase in the abundance of mitochondrial proteins responsible for macrophage response against oxidative stress. Regarding the cell death mechanisms, antiapoptotic signals were more abundant than pro-apoptotic signals, in line with the lack of caspase-3 cleavage during interaction. A high pro-inflammatory response of the macrophage was observed, by the secretion of TNF-α and IL-12 cytokines together with the lack of activation of some mi-RNAs involved in the control of the pro-inflammatory response. Phosphorylation together with quantitative proteomic results suggested a possible reduction of the endosomal trafficking inside the macrophage. This study constitutes a valuable way to better understand cellular mechanism of response or readjustments and is important for the future development of new therapeutic approaches.

ASSOCIATED CONTENT

Supporting Information

The Supporting Information is available free of charge on the ACS Publications website at DOI: 10.1021/acs.jproteome.9b00032.

Figures S1−S8 (PDF)
Table S1 (XLSX)

DOI: 10.1021/acs.jproteome.9b00032
J. Proteome Res. XXXX, XXX, XXX−XXX

Table S2 (XLSX)
Table S3 (XLSX)
Table S4 (XLSX)
Table S5 (XLSX)

AUTHOR INFORMATION

Corresponding Author

*E-mail: luciamon@ucm.es. Phone: +34913941748. Fax: +34913941745.

ORCID

Catarina Vaz: 0000-0002-0174-9748
Marco Trevisan: 0000-0002-7129-0602
Lucía Monteoliva: 0000-0003-4949-0664
Concha Gil: 0000-0003-3137-2600

Present Address

#Singapore Immunology Network (SIgN), A*STAR; 8A Biomedical Grove, Level 4, Immunos (Biopolis), 138648 Singapore.

Notes

The authors declare no competing financial interest.
The data set from this paper has been deposited in the ProteomeXchange Consortium via the PRIDE partner repository with the data set identifier PXD009938.[89,90]

ACKNOWLEDGMENTS

This study was supported by the Marie Curie Initial Training Network (FP7-PEOPLE-2013-ITN ImResFun), the project BIO2015-65147-R from Spanish Ministry of Economy and Competitiveness (MINECO), InGEMICS-CM B2017/BMD-3691 from the Comunidad de Madrid, Spanish Network for the Research in Infectious Diseases (REIPI RD16/0016/0011) and PRB3 (PT17/0019/0012) from the ISCIII. InGEMICS-CM, REIPI and PRB3 are cofinanced by European Development Regional Fund ERDF "A way to achieve Europe". These results are lined up with the Human Infectious Diseases HPP initiative from the Human Proteome Project (HID-HPP). The ESEM was performed in Museo Nacional de Ciencias Naturales. The proteomics analyses were performed in Centro de Investigaciones Biológicas (CIB) and Proteomics Facility of Complutense University of Madrid (UCM), both members of ProteoRed-ISCIII network. The miRNA analysis was carried out in Genomics Facility of Complutense University of Madrid. The authors would like to thank Leif Schauser and Nitesh Kumar Singh from QIAGEN (Aarhus) IMRESFUN consortium partners for their help in IPA analysis.

ABBREVIATIONS

CLRs, c-type lectin receptors; DMEM, Dulbecco's modified Eagle's medium; ELISA, enzyme-linked immunosorbent assay; ESEM, environmental scanning electron microscopy; FBS, fetal bovine serum; GO, gene ontology; IFNs, interferons; IL, interleukin; IPA, Ingenuity Pathway Analysis; LDH, lactate dehydrogenase; LPS, lipopolysaccharide; MOI, multiplicity of infection; NODs, nod-like receptors; PBS, phosphate buffer saline; PMA, phorbol 12-myristate 13-acetate; PRRs, pattern recognition receptors; RIPA, radio immunoprecipitation assay buffer; ROS, reactive oxygen species; RT-PCR, real time polymerase chain reaction; SD, standard deviation; STE, ser/thr protein kinase family; TLRs, toll-like receptors; TR, transcription regulator; YPD, yeast peptone dextrose.

REFERENCES

(1) Erwig, L. P.; Gow, N. A. Interactions of fungal pathogens with phagocytes. *Nat. Rev. Microbiol.* **2016**, *14* (3), 163−76.
(2) Pfaller, M. A.; Castanheira, M. Nosocomial Candidiasis: Antifungal Stewardship and the Importance of Rapid Diagnosis. *Med. Mycol.* **2015**, *54* (1), 1−22.
(3) Nieto, M. C.; Telleria, O.; Cisterna, R. Sentinel surveillance of invasive candidiasis in Spain: epidemiology and antifungal susceptibility. *Diagn. Microbiol. Infect. Dis.* **2015**, *81* (1), 34−40.
(4) Bourgeois, C.; Majer, O.; Frohner, I. E.; Tierney, L.; Kuchler, K. Fungal attacks on mammalian hosts: pathogen elimination requires sensing and tasting. *Curr. Opin. Microbiol.* **2010**, *13* (4), 401−8.
(5) West, A. P.; Koblansky, A. A.; Ghosh, S. Recognition and signaling by toll-like receptors. *Annu. Rev. Cell Dev. Biol.* **2006**, *22*, 409−37.
(6) Reales-Calderon, J. A.; Martinez-Solano, L.; Martinez-Gomariz, M.; Nombela, C.; Molero, G.; Gil, C. Sub-proteomic study on macrophage response to *Candida albicans* unravels new proteins involved in the host defense against the fungus. *J. Proteomics* **2012**, *75* (15), 4734−46.
(7) Reales-Calderon, J. A.; Sylvester, M.; Strijbis, K.; Jensen, O. N.; Nombela, C.; Molero, G.; Gil, C. *Candida albicans* induces pro-inflammatory and anti-apoptotic signals in macrophages as revealed by quantitative proteomics and phosphoproteomics. *J. Proteomics* **2013**, *91*, 106−35.
(8) Reales-Calderon, J. A.; Aguilera-Montilla, N.; Corbi, A. L.; Molero, G.; Gil, C. Proteomic characterization of human proinflammatory M1 and anti-inflammatory M2 macrophages and their response to *Candida albicans*. *Proteomics* **2014**, *14* (12), 1503−18.
(9) Shin, Y. K.; Kim, K. Y.; Paik, Y. K. Alterations of protein expression in macrophages in response to *Candida albicans* infection. *Mol. Cells* **2005**, *20* (2), 271−9.
(10) Kitahara, N.; Morisaka, H.; Aoki, W.; Takeda, Y.; Shibasaki, S.; Kuroda, K.; Ueda, M. Description of the interaction between *Candida albicans* and macrophages by mixed and quantitative proteome analysis without isolation. *AMB Express* **2015**, *5* (41), 1−12.
(11) Xiao, Y.; Wang, Y. Global discovery of protein kinases and other nucleotide-binding proteins by mass spectrometry. *Mass Spectrom. Rev.* **2016**, *35*, 601−619.
(12) Guo, L.; Xiao, Y.; Fan, M.; Li, J. J.; Wang, Y. Profiling Global Kinome Signatures of the Radioresistant MCF-7/C6 Breast Cancer Cells Using MRM-based Targeted Proteomics. *J. Proteome Res.* **2015**, *14*, 193.
(13) Wolfe, L. M.; Veeraraghavan, U.; Idicula-Thomas, S.; Schurer, S.; Wennerberg, K.; Reynolds, R.; Besra, G. S.; Dobos, K. M. A chemical proteomics approach to profiling the ATP-binding proteome of *Mycobacterium tuberculosis*. *Mol. Cell. Proteomics* **2013**, *12* (6), 1644−60.
(14) Villamor, J. G.; Kaschani, F.; Colby, T.; Oeljeklaus, J.; Zhao, D.; Kaiser, M.; Patricelli, M. P.; van der Hoorn, R. A. Profiling protein kinases and other ATP binding proteins in *Arabidopsis* using Acyl-ATP probes. *Mol. Cell. Proteomics* **2013**, *12* (9), 2481−96.
(15) Adachi, J.; Kishida, M.; Watanabe, S.; Hashimoto, Y.; Fukamizu, K.; Tomonaga, T. Proteome-Wide Discovery of Unknown ATP-Binding Proteins and Kinase Inhibitor Target Proteins Using an ATP Probe (vol 13, pg 5461, 2014). *J. Proteome Res.* **2015**, *14* (2), 1333−1333.
(16) Xiao, Y.; Guo, L.; Wang, Y. Isotope-coded ATP probe for quantitative affinity profiling of ATP-binding proteins. *Anal. Chem.* **2013**, *85* (15), 7478−86.
(17) Graves, P. R.; Kwiek, J. J.; Fadden, P.; Ray, R.; Hardeman, K.; Coley, A. M.; Foley, M.; Haystead, T. A. Discovery of novel targets of quinoline drugs in the human purine binding proteome. *Molecular pharmacology* **2002**, *62* (6), 1364−72.
(18) Daub, H.; Olsen, J. V.; Bairlein, M.; Gnad, F.; Oppermann, F. S.; Korner, R.; Greff, Z.; Keri, G.; Stemmann, O.; Mann, M. Kinase-selective enrichment enables quantitative phosphoproteomics of the kinome across the cell cycle. *Mol. Cell* **2008**, *31* (3), 438−48.

DOI: 10.1021/acs.jproteome.9b00032
J. Proteome Res. XXXX, XXX, XXX−XXX

(19) Hanoulle, X.; Van Damme, J.; Staes, A.; Martens, L.; Goethals, M.; Vandekerckhove, J.; Gevaert, K. A new functional, chemical proteomics technology to identify purine nucleotide binding sites in complex proteomes. *J. Proteome Res.* **2006**, *5* (12), 3438−45.
(20) Duncan, J. S.; Whittle, M. C.; Nakamura, K.; Abell, A. N.; Midland, A. A.; Zawistowski, J. S.; Johnson, N. L.; Granger, D. A.; Jordan, N. V.; Darr, D. B.; Usary, J.; Kuan, P. F.; Smalley, D. M.; Major, B.; He, X.; Hoadley, K. A.; Zhou, B.; Sharpless, N. E.; Perou, C. M.; Kim, W. Y.; Gomez, S. M.; Chen, X.; Jin, J.; Frye, S. V.; Earp, H. S.; Graves, L. M.; Johnson, G. L. Dynamic reprogramming of the kinome in response to targeted MEK inhibition in triple-negative breast cancer. *Cell* **2012**, *149* (2), 307−21.
(21) Patricelli, M. P.; Szardenings, A. K.; Liyanage, M.; Nomanbhoy, T. K.; Wu, M.; Weissig, H.; Aban, A.; Chun, D.; Tanner, S.; Kozarich, J. W. Functional Interrogation of the Kinome Using Nucleotide Acyl Phosphates. *Biochemistry* **2007**, *46*, 350−358.
(22) Ong, S. E.; Mann, M. A practical recipe for stable isotope labeling by amino acids in cell culture (SILAC). *Nat. Protoc.* **2006**, *1* (6), 2650−60.
(23) Blagoev, B.; Kratchmarova, I.; Ong, S. E.; Nielsen, M.; Foster, L. J.; Mann, M. A proteomics strategy to elucidate functional protein-protein interactions applied to EGF signaling. *Nat. Biotechnol.* **2003**, *21* (3), 315−8.
(24) Huang, J.; Wang, F.; Ye, M.; Zou, H. Enrichment and separation techniques for large-scale proteomics analysis of the protein post-translational modifications. *Journal of chromatography. A* **2014**, *1372C*, 1−17.
(25) Reales-Calderon, J. A.; Vaz, C.; Monteoliva, L.; Molero, G.; Gil, C. *Candida albicans* Modifies the Protein Composition and Size Distribution of THP1 macrophages-derived Extracellular Vesicles. *J. Proteome Res.* **2017**, *16* (1), 87−105.
(26) Fernandez-Arenas, E.; Cabezon, V.; Bermejo, C.; Arroyo, J.; Nombela, C.; Diez-Orejas, R.; Gil, C. Integrated proteomics and genomics strategies bring new insight into *Candida albicans* response upon macrophage interaction. *Mol. Cell. Proteomics* **2007**, *6* (3), 460−78.
(27) Bonzon-Kulichenko, E.; Perez-Hernandez, D.; Nunez, E.; Martinez-Acedo, P.; Navarro, P.; Trevisan-Herraz, M.; Ramos Mdel, C.; Sierra, S.; Martinez-Martinez, S.; Ruiz-Meana, M.; Miro-Casas, E.; Garcia-Dorado, D.; Redondo, J. M.; Burgos, J. S.; Vazquez, J. A robust method for quantitative high-throughput analysis of proteomes by 18O labeling. *Mol. Cell. Proteomics* **2011**, *10* (1), M110.003335.
(28) Shevchenko, A.; Tomas, H.; Havlis, J.; Olsen, J. V.; Mann, M. In-gel digestion for mass spectrometric characterization of proteins and proteomes. *Nat. Protoc.* **2006**, *1* (6), 2856−60.
(29) Picotti, P.; Aebersold, R. Selected reaction monitoring-based proteomics: workflows, potential, pitfalls and future directions. *Nat. Methods* **2012**, *9* (6), 555−66.
(30) Carmona-Saez, P.; Chagoyen, M.; Tirado, F.; Carazo, J. M.; Pascual-Montano, A. GENECODIS: a web-based tool for finding significant concurrent annotations in gene lists. *Genome Biol.* **2007**, *8* (1), R3.
(31) Nogales-Cadenas, R.; Carmona-Saez, P.; Vazquez, M.; Vicente, C.; Yang, X.; Tirado, F.; Carazo, J. M.; Pascual-Montano, A. GeneCodis: interpreting gene lists through enrichment analysis and integration of diverse biological information. *Nucleic Acids Res.* **2009**, *37*, W317−22.
(32) Tabas-Madrid, D.; Nogales-Cadenas, R.; Pascual-Montano, A. GeneCodis3: a non-redundant and modular enrichment analysis tool for functional genomics. *Nucleic Acids Res.* **2012**, *40*, W478−83.
(33) Szklarczyk, D.; Morris, J. H.; Cook, H.; Kuhn, M.; Wyder, S.; Simonovic, M.; Santos, A.; Doncheva, N. T.; Roth, A.; Bork, P.; Jensen, L. J.; von Mering, C. The STRING database in 2017: quality-controlled protein-protein association networks, made broadly accessible. *Nucleic Acids Res.* **2017**, *45* (D1), D362−D368.
(34) Livak, K. J.; Schmittgen, T. D. Analysis of relative gene expression data using real-time quantitative PCR and the 2(-Delta Delta C(T)) Method. *Methods* **2001**, *25* (4), 402−8.
(35) Fernandez-Arenas, E.; Bleck, C. K.; Nombela, C.; Gil, C.; Griffiths, G.; Diez-Orejas, R. *Candida albicans* actively modulates intracellular membrane trafficking in mouse macrophage phagosomes. *Cell. Microbiol.* **2009**, *11* (4), 560−89.
(36) Traba, J.; Del Arco, A.; Duchen, M. R.; Szabadkai, G.; Satrustegui, J. SCaMC-1 promotes cancer cell survival by desensitizing mitochondrial permeability transition via ATP/ADP-mediated matrix Ca(2+) buffering. *Cell Death Differ.* **2012**, *19* (4), 650−60.
(37) Shiota, M.; Izumi, H.; Miyamoto, N.; Onitsuka, T.; Kashiwagi, E.; Kidani, A.; Hirano, G.; Takahashi, M.; Ono, M.; Kuwano, M.; Naito, S.; Sasaguri, Y.; Kohno, K. Ets regulates peroxiredoxin1 and 5 expressions through their interaction with the high-mobility group protein B1. *Cancer Sci.* **2008**, *99* (10), 1950−9.
(38) Wang, Q.; Sawyer, I. A.; Sung, M. H.; Sturgill, D.; Shevtsov, S. P.; Pegoraro, G.; Hakim, O.; Baek, S.; Hager, G. L.; Dundr, M. Cajal bodies are linked to genome conformation. *Nat. Commun.* **2016**, *7*, 10966.
(39) Arthur, J. S.; Ley, S. C. Mitogen-activated protein kinases in innate immunity. *Nat. Rev. Immunol.* **2013**, *13* (9), 679−92.
(40) Yuan, J.; Murrell, G. A.; Trickett, A.; Landtmeters, M.; Knoops, B.; Wang, M. X. Overexpression of antioxidant enzyme peroxiredoxin 5 protects human tendon cells against apoptosis and loss of cellular function during oxidative stress. *Biochim. Biophys. Acta, Mol. Cell Res.* **2004**, *1693* (1), 37−45.
(41) Jang, J. Y.; Choi, Y.; Jeon, Y. K.; Kim, C. W. Suppression of adenine nucleotide translocase-2 by vector-based siRNA in human breast cancer cells induces apoptosis and inhibits tumor growth in vitro and in vivo. *Breast Cancer Res.* **2008**, *10* (1), R11.
(42) Lee, J. H.; Choi, Y. J.; Park, S. H.; Nam, M. J. Potential role of nucleoside diphosphate kinase in myricetin-induced selective apoptosis in colon cancer HCT-15cells. *Food Chem. Toxicol.* **2018**, *116*, 315−322.
(43) Liu, Q. Y.; Lei, J. X.; LeBlanc, J.; Sodja, C.; Ly, D.; Charlebois, C.; Walker, P. R.; Yamada, T.; Hirohashi, S.; Sikorska, M. Regulation of DNaseY activity by actinin-alpha4 during apoptosis. *Cell Death Differ.* **2004**, *11* (6), 645−54.
(44) Lee, K. K.; Ohyama, T.; Yajima, N.; Tsubuki, S.; Yonehara, S. MST, a physiological caspase substrate, highly sensitizes apoptosis both upstream and downstream of caspase activation. *J. Biol. Chem.* **2001**, *276* (22), 19276−85.
(45) Shalini, S.; Dorstyn, L.; Dawar, S.; Kumar, S. Old, new and emerging functions of caspases. *Cell Death Differ.* **2015**, *22* (4), 526−39.
(46) Uwamahoro, N.; Verma-Gaur, J.; Shen, H. H.; Qu, Y.; Lewis, R.; Lu, J.; Bambery, K.; Masters, S. L.; Vince, J. E.; Naderer, T.; Traven, A. The pathogen *Candida albicans* hijacks pyroptosis for escape from macrophages. *mBio* **2014**, *5* (2), e00003−14.
(47) Bergsbaken, T.; Fink, S. L.; Cookson, B. T. Pyroptosis: host cell death and inflammation. *Nat. Rev. Microbiol.* **2009**, *7* (2), 99−109.
(48) Tsitsiou, E.; Lindsay, M. A. microRNAs and the immune response. *Curr. Opin. Pharmacol.* **2009**, *9* (4), 514−20.
(49) Taganov, K. D.; Boldin, M. P.; Chang, K. J.; Baltimore, D. NF-kappaB-dependent induction of microRNA miR-146, an inhibitor targeted to signaling proteins of innate immune responses. *Proc. Natl. Acad. Sci. U. S. A.* **2006**, *103* (33), 12481−6.
(50) Agustinho, D. P.; de Oliveira, M. A.; Tavares, A. H.; Derengowski, L.; Stolz, V.; Guilhelmelli, F.; Mortari, M. R.; Kuchler, K.; Silva-Pereira, I. Dectin-1 is required for miR155 upregulation in murine macrophages in response to *Candida albicans*. *Virulence* **2017**, *8*, 1−12.
(51) Monk, C. E.; Hutvagner, G.; Arthur, J. S. Regulation of miRNA transcription in macrophages in response to *Candida albicans*. *PLoS One* **2010**, *5* (10), No. e13669.
(52) Pappas, P. G.; Lionakis, M. S.; Arendrup, M. C.; Ostrosky-Zeichner, L.; Kullberg, B. J. Invasive candidiasis. *Nat. Rev. Dis Primers* **2018**, *4*, 18026.
(53) Carpino, N.; Naseem, S.; Frank, D. M.; Konopka, J. B. Modulating Host Signaling Pathways to Promote Resistance to

DOI: 10.1021/acs.jproteome.9b00032
J. Proteome Res. XXXX, XXX, XXX−XXX

Infection by *Candida albicans*. *Front. Cell. Infect. Microbiol.* **2017**, *7*, 481.
(54) Zwolanek, F.; Riedelberger, M.; Stolz, V.; Jenull, S.; Istel, F.; Koprulu, A. D.; Ellmeier, W.; Kuchler, K. The non-receptor tyrosine kinase Tec controls assembly and activity of the noncanonical caspase-8 inflammasome. *PLoS Pathog.* **2014**, *10* (12), No. e1004525.
(55) Singh, A. K.; Pandey, R. K.; Siqueira-Neto, J. L.; Kwon, Y. J.; Freitas, L. H.; Shaha, C.; Madhubala, R. Proteomic-Based Approach To Gain Insight into Reprogramming of THP-1 Cells Exposed to *Leishmania donovani* over an Early Temporal Window. *Infect. Immun.* **2015**, *83* (5), 1853−1868.
(56) Duan, Z.; Chen, X.; Du, L.; Liu, C.; Zeng, R.; Chen, Q.; Li, M. Inflammation Induced by *Candida parapsilosis* in THP-1 Cells and Human Peripheral Blood Mononuclear Cells (PBMCs). *Mycopathologia* **2017**, *182* (11−12), 1015−1023.
(57) Kaewseekhao, B.; Naranbhai, V.; Roytrakul, S.; Namwat, W.; Paemanee, A.; Lulitanond, V.; Chaiprasert, A.; Faksri, K. Comparative Proteomics of Activated THP-1 Cells Infected with *Mycobacterium tuberculosis* Identifies Putative Clearance Biomarkers for Tuberculosis Treatment. *PLoS One* **2015**, *10* (7), No. e0134168.
(58) Barker, K. S.; Liu, T.; Rogers, P. D. Coculture of THP-1 human mononuclear cells with *Candida albicans* results in pronounced changes in host gene expression. *J. Infect. Dis.* **2005**, *192* (5), 901−12.
(59) Chanput, W.; Mes, J. J.; Wichers, H. J. THP-1 cell line: An in vitro cell model for immune modulation approach. *Int. Immunopharmacol.* **2014**, *23* (1), 37−45.
(60) Lemeer, S.; Zorgiebel, C.; Ruprecht, B.; Kohl, K.; Kuster, B. Comparing immobilized kinase inhibitors and covalent ATP probes for proteomic profiling of kinase expression and drug selectivity. *J. Proteome Res.* **2013**, *12* (4), 1723−31.
(61) Oppermann, F. S.; Gnad, F.; Olsen, J. V.; Hornberger, R.; Greff, Z.; Keri, G.; Mann, M.; Daub, H. Large-scale proteomics analysis of the human kinome. *Mol. Cell. Proteomics* **2009**, *8* (7), 1751−64.
(62) Sun, G.; Yao, F.; Tian, Z.; Ma, T.; Yang, Z. A first CLN6 variant case of late infantile neuronal ceroid lipofuscinosis caused by a homozygous mutation in a boy from China: a case report. *BMC Med. Genet.* **2018**, *19* (1), 177.
(63) Bae, H. B.; Zmijewski, J. W.; Deshane, J. S.; Tadie, J. M.; Chaplin, D. D.; Takashima, S.; Abraham, E. AMP-activated protein kinase enhances the phagocytic ability of macrophages and neutrophils. *FASEB J.* **2011**, *25* (12), 4358−68.
(64) Lizcano, J. M.; Goransson, O.; Toth, R.; Deak, M.; Morrice, N. A.; Boudeau, J.; Hawley, S. A.; Udd, L.; Makela, T. P.; Hardie, D. G.; Alessi, D. R. LKB1 is a master kinase that activates 13 kinases of the AMPK subfamily, including MARK/PAR-1. *EMBO J.* **2004**, *23* (4), 833−843.
(65) Pandey, A.; Ding, S. L.; Qin, Q. M.; Gupta, R.; Gomez, G.; Lin, F.; Feng, X.; Fachini da Costa, L.; Chaki, S. P.; Katepalli, M.; Case, E. D.; van Schaik, E. J.; Sidiq, T.; Khalaf, O.; Arenas, A.; Kobayashi, K. S.; Samuel, J. E.; Rivera, G. M.; Alaniz, R. C.; Sze, S. H.; Qian, X.; Brown, W. J.; Rice-Ficht, A.; Russell, W. K.; Ficht, T. A.; de Figueiredo, P. Global Reprogramming of Host Kinase Signaling in Response to Fungal Infection. *Cell Host Microbe* **2017**, *21* (5), 637−649.
(66) Hawley, S. A.; Ross, F. A.; Gowans, G. J.; Tibarewal, P.; Leslie, N. R.; Hardie, D. G. Phosphorylation by Akt within the ST loop of AMPK-alpha 1 down-regulates its activation in tumour cells. *Biochem. J.* **2014**, *459*, 275−287.
(67) Netea, M. G.; Joosten, L. A.; van der Meer, J. W.; Kullberg, B. J.; van de Veerdonk, F. L. Immune defence against *Candida* fungal infections. *Nat. Rev. Immunol.* **2015**, *15* (10), 630−42.
(68) Zhang, Y.; Tu, Y.; Zhao, J.; Chen, K.; Wu, C. Reversion-induced LIM interaction with Src reveals a novel Src inactivation cycle. *J. Cell Biol.* **2009**, *184* (6), 785−92.
(69) Byeon, S. E.; Yi, Y. S.; Oh, J.; Yoo, B. C.; Hong, S.; Cho, J. Y. The Role of Src Kinase inMacrophage-Mediated Inflammatory Responses. *Mediators Inflammation* **2012**, *2012*, 1−18.
(70) Minogue, S.; Waugh, M. G.; De Matteis, M. A.; Stephens, D. J.; Berditchevski, F.; Hsuan, J. J. Phosphatidylinositol 4-kinase is required for endosomal trafficking and degradation of the EGF receptor. *J. Cell Sci.* **2006**, *119* (3), 571−580.
(71) Via, L. E.; Deretic, D.; Ulmer, R. J.; Hibler, N. S.; Huber, L. A.; Deretic, V. Arrest of mycobacterial phagosome maturation is caused by a block in vesicle fusion between stages controlled by rab5 and rab7. *J. Biol. Chem.* **1997**, *272* (20), 13326−13331.
(72) Vergne, I.; Fratti, R. A.; Hill, P. J.; Chua, J.; Belisle, J.; Deretic, V. *Mycobacterium tuberculosis* phagosome maturation arrest: mycobacterial phosphatidylinositol analog phosphatidylinositol mannoside stimulates early endosomal fusion. *Mol. Biol. Cell* **2004**, *15* (2), 751−60.
(73) Rothenberger, S.; Iacopetta, B. J.; Kuhn, L. C. Endocytosis of the transferrin receptor requires the cytoplasmic domain but not its phosphorylation site. *Cell* **1987**, *49* (3), 423−31.
(74) Forman, H. J.; Torres, M. Redox signaling in macrophages. *Mol. Aspects Med.* **2001**, *22* (4−5), 189−216.
(75) Choi, H. I.; Chung, K. J.; Yang, H. Y.; Ren, L.; Sohn, S.; Kim, P. R.; Kook, M. S.; Choy, H. E.; Lee, T. H. Peroxiredoxin V selectively regulates IL-6 production by modulating the Jak2-Stat5 pathway. *Free Radical Biol. Med.* **2013**, *65*, 270−9.
(76) Shui, W.; Gilmore, S. A.; Sheu, L.; Liu, J.; Keasling, J. D.; Bertozzi, C. R. Quantitative proteomic profiling of host-pathogen interactions: the macrophage response to *Mycobacterium tuberculosis* lipids. *J. Proteome Res.* **2009**, *8* (1), 282−9.
(77) Liu, P. S.; Ho, P. C. Mitochondria: A master regulator in macrophage and T cell immunity. *Mitochondrion* **2018**, *41* (2018), 45−50.
(78) Tazi, J.; Bakkour, N.; Stamm, S. Alternative splicing and disease. *Biochim. Biophys. Acta, Mol. Basis Dis.* **2009**, *1792* (1), 14−26.
(79) Geuens, T.; Bouhy, D.; Timmerman, V. The hnRNP family: insights into their role in health and disease. *Hum. Genet.* **2016**, *135* (8), 851−867.
(80) Choi, Y. D.; Grabowski, P. J.; Sharp, P. A.; Dreyfuss, G. Heterogeneous nuclear ribonucleoproteins: role in RNA splicing. *Science* **1986**, *231* (4745), 1534−9.
(81) McIlwain, D. R.; Berger, T.; Mak, T. W. Caspase functions in cell death and disease. *Cold Spring Harbor Perspect. Biol.* **2013**, *5* (4), a008656.
(82) Vylkova, S.; Lorenz, M. C. Phagosomal Neutralization by the Fungal Pathogen *Candida albicans* Induces Macrophage Pyroptosis. *Infect. Immun.* **2017**, DOI: 10.1128/IAI.00832-16.
(83) O'Meara, T. R.; Veri, A. O.; Ketela, T.; Jiang, B.; Roemer, T.; Cowen, L. E. Global analysis of fungal morphology exposes mechanisms of host cell escape. *Nat. Commun.* **2015**, *6*, 6741.
(84) Wellington, M.; Koselny, K.; Krysan, D. J. *Candida albicans* morphogenesis is not required for macrophage interleukin 1beta production. *mBio* **2013**, *4* (1), e00433−12.
(85) Netea, M. G.; Brown, G. D.; Kullberg, B. J.; Gow, N. A. An integrated model of the recognition of *Candida albicans* by the innate immune system. *Nat. Rev. Microbiol.* **2008**, *6* (1), 67−78.
(86) Kramer, A.; Green, J.; Pollard, J., Jr.; Tugendreich, S. Causal analysis approaches in Ingenuity Pathway Analysis. *Bioinformatics* **2014**, *30* (4), 523−30.
(87) Estrada-Mata, E.; Navarro-Arias, M. J.; Perez-Garcia, L. A.; Mellado-Mojica, E.; Lopez, M. G.; Csonka, K.; Gacser, A.; Mora-Montes, H. M. Members of the *Candida parapsilosis* Complex and *Candida albicans* are Differentially Recognized by Human Peripheral Blood Mononuclear Cells. *Front. Microbiol.* **2016**, *6*, 1527.
(88) Martinez-Solano, L.; Reales-Calderon, J. A.; Nombela, C.; Molero, G.; Gil, C. Proteomics of RAW 264.7 macrophages upon interaction with heat-inactivated *Candida albicans* cells unravel an anti-inflammatory response. *Proteomics* **2009**, *9* (11), 2995−3010.
(89) Vizcaíno, J. A.; Csordas, A.; del-Toro, N.; Dianes, J. A.; Griss, J.; Lavidas, I.; Mayer, G.; Perez-Riverol, Y.; Reisinger, F.; Ternent, T.; Xu, Q.-W.; Wang, R.; Hermjakob, H. 2016 update of the PRIDE database and related tools. *Nucleic Acids Res.* **2016**, *44*, D447−D456.
(90) Deutsch, E. W.; Csordas, A.; Sun, Z.; Jarnuczak, A.; Perez-Riverol, Y.; Ternent, T.; Campbell, D. S.; Bernal-Llinares, M.; Okuda, S.; Kawano, S.; Moritz, R. L.; Carver, J. J.; Wang, M.; Ishihama, Y.;

DOI: 10.1021/acs.jproteome.9b00032
J. Proteome Res. XXXX, XXX, XXX−XXX

Bandeira, N.; Hermjakob, H.; Vizcaíno, J. A. The ProteomeXchange Consortium in 2017: supporting the cultural change in proteomics public data deposition. *Nucleic Acids Res.* **2017**, *45*, D1100−D1106.

DOI: 10.1021/acs.jproteome.9b00032
J. Proteome Res. XXXX, XXX, XXX−XXX

APPENDIX 3 - Other manuscripts published during the period of the thesis

Reales-Calderon JA, Vaz C, Monteoliva L, Molero G & Gil C (2016) *Candida albicans* modifies the protein composition and size distribution of THP-1 macrophages-derived extracellular vesicles. *Journal of proteome research* 1:87-105.

Llopis-Torregrosa, Vaz C, Monteoliva L, Ryman K, Engstrom Y, Gacser A, Gil C, Ljungdahl P & Sychrova H (2019) Trk1-mediated potassium uptake contributes to cell-surface properties and virulence of *Candida glabrata. Scientific Reports* 9:7529.

Journal of proteome research

Article

pubs.acs.org/jpr

Candida albicans Modifies the Protein Composition and Size Distribution of THP-1 Macrophage-Derived Extracellular Vesicles

Jose Antonio Reales-Calderón,[†,‡,§] Catarina Vaz,[‡,§] Lucía Monteoliva,[‡,§] Gloria Molero,[*,‡,§] and Concha Gil[*,‡,§]

[‡]Departamento de Microbiología II, Facultad de Farmacia, Universidad Complutense de Madrid Plaza de Ramón y Cajal s/n, Madrid 28040, Spain

[§]Instituto Ramón y Cajal de Investigación Sanitaria (IRYCIS), Madrid 28034, Spain

Supporting Information

ABSTRACT: The effectiveness of macrophages in the response to systemic candidiasis is crucial to an effective clearance of the pathogen. The secretion of proteins, mRNAs, noncoding RNAs and lipids through extracellular vesicles (EVs) is one of the mechanisms of communication between immune cells. EVs change their cargo to mediate different responses, and may play a role in the response against infections. Thus we have undertaken the first quantitative proteomic analysis on the protein composition of THP-1 macrophage-derived EVs during the interaction with *Candida albicans*. This study revealed changes in EVs sizes and in protein composition, and allowed the identification and quantification of 717 proteins. Of them, 133 proteins changed their abundance due to the interaction. The differentially abundant proteins were involved in functions relating to immune response, signaling, or cytoskeletal reorganization. THP-1-derived EVs, both from control and from *Candida*-infected macrophages, had similar effector functions on other THP-1-differenciated macrophages, activating ERK and p38 kinases, and increasing both the secretion of proinflammatory cytokines and the candidacidal activity; while in THP-1 nondifferenciated monocytes, only EVs from infected macrophages increased significantly the TNF-α secretion. Our findings provide new information on the role of macrophage-derived EVs in response to *C. albicans* infection and in macrophages communication.

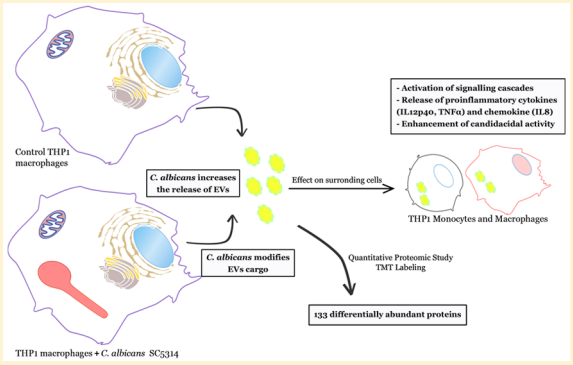

KEYWORDS: *macrophages, Candida albicans, extracellular vesicles, inflammation, tandem mass tagging, immune response*

1. INTRODUCTION

Candida albicans is a commensal microorganism that colonizes the skin and the mucosal surfaces in a high percentage of healthy individuals. However, when the immune defenses of the individuals are disrupted, this fungus can outgrow and cause symptoms of disease, producing mucocutaneous or invasive candidiasis. *C. albicans* causes more than 400 000 cases of invasive candidiasis cases per year, with a mortality rate up to 75%.[1]

In the host, an effective innate immune response is essential for fungal clearance. There are several effector cells such as natural killer cells, dendritic cells, neutrophils, and macrophages. Macrophages constitute the main phagocyte population and are important cytokines producers, initiating both innate immune and adaptive immune responses.[2] After recognition of the cell wall or the internal components of pathogens by pattern recognition receptors (PRRs) such as Toll-like receptors (TLRs) and C-type lectin receptors (CLRs), a myriad of intracellular cascades are activated. Integration of simultaneously activated signaling pathways occurs at the level of signaling adaptors and transcription factors, which are shared between overlapping signaling pathways. This results in cytokine responses, oxidative burst, and arachidonic acid release, which consequently activate the adaptive response and ultimately determine the outcome of the infection.[3]

In a wide number of organisms, from bacteria to eukaryotes, communication between cells involves the cellular secretion of proteins to the extracellular environment that bind to the neighboring cells receptors and initiate signaling cascades. Besides the classical secretion pathway of proteins, another mechanism to export proteins out of the cell is through extracellular vesicles (EVs); the most studied are apoptotic blebs, microvesicles (MVs), and exosomes.[4] The secretion of EVs is a very conserved process throughout evolution.[5] Cells from different organisms, from eukaryotes (amoebae, parasites, fungi, and mammals) to prokaryotic cells, have been proven to release EVs to the extracellular environment.[6−8] In mammals, EVs have been purified from different cell lines and body fluids under physiological and pathological situations. Their origin is very diverse, and these EVs have been classified based either on

Special Issue: The Immune System and the Proteome 2016

Received: July 1, 2016

DOI: 10.1021/acs.jproteome.6b00605
J. Proteome Res. XXXX, XXX, XXX−XXX

their size (microparticles, MVs, nanoparticles, and nanovesicles) or on their location in/outside the cell (ectosomes, exosomes, exovesicles, and exosome-like vesicles). EV cargo usually includes membrane and cytosolic proteins, mRNA and noncoding RNAs, and lipids.[5]

The term MVs generally refers to 100 nm up to 1 μm vesicles that are formed by budding from the plasma membrane. Recently, exosomes were introduced as a type of communication among immune cells for antigen presentation and immune activation.[9] These small (30−90 nm) EVs result from the fusion of multivesicular bodies with the plasma membrane, which are then released to the external microenvironment.[10] They are known to be released by several cell types, such as B- and T-lymphocytes, dendritic cells, mast cells, astrocytes, neurons, and macrophages. Recent studies have shown that macrophages can be activated by exosomes.[9,11−13] The mechanism of action of exosomes in vivo is poorly understood. Exosomes from antigen-presenting cells (APCs) could stimulate T cells directly or could be captured by other professional APCs. As previous studies have described, EVs participate in the intercellular communication and change the cargo to mediate different immune responses, and thus we hypothesized that macrophage-derived EVs may have a different composition depending on the stimulus and may play a role in the pathogenesis of *C. albicans* infection and in the macrophage activity against the yeast.

There are few studies that have performed proteomic analysis of the exosomes secreted by several cell types,[9,14−16] usually without discrimination between exosomes and MVs.

Our group has widely studied the proteins involved in the macrophage response against *C. albicans* using proteomic approaches. Studies in the murine macrophage cell line RAW 264.7 showed that the presence of *C. albicans* induces inflammatory and anti-apoptotic signaling in these macrophages,[17] while the analyses on the differential protein expression in human M1 and M2 macrophages revealed that *C. albicans* induces a different response in either type of human monocyte-derived macrophages.[18] In the current work, the first quantitative proteomic approach was developed for the differential analysis of the EVs secreted by macrophages infected and noninfected with *C. albicans* cells to identify and characterize the composition and their possible effect on other macrophages and monocytes. Therefore, the human acute monocytic leukemia cell line (THP-1) was differentiated into macrophages. Subsequently, control macrophages and macrophages after 3 h of interaction with *C. albicans* at a multiplicity of infection (MOI) of 1 were used to isolate EVs according to previous works.[6,7] The proteins in EVs from THP-1 differentiated macrophage control and those treated with *C. albicans* were analyzed by TMT (tandem mass tagging) for peptide labeling and LC−MS/MS for proteomic analysis. Also, the effect of these EVs on other THP-1 monocytes and differentiated macrophages was studied.

Our findings provide a new insight into the role of circulating macrophage-derived EVs in *C. albicans* infections and their signaling effect on the recipient cells, showing a different abundance of EVs populations and different protein composition of EVs depending on the stimulus that the macrophage is responding to.

2. EXPERIMENTAL PROCEDURES

2.1. *Candida albicans* Strain

The *C. albicans* strain used was a clinical isolate (SC5314)[19] and was maintained on solid YPD medium (1% D-glucose, 1% Difco Yeast Extract, and 2% agar) and incubated at 30 °C for 1 day before use.

2.2. THP-1 Cell Culture and Macrophage Differentiation

The human acute monocytic leukemia cell line (THP-1) was cultured in DMEM medium supplemented with antibiotics (penicillin 100 U/mL−streptomycin 100 μg/mL), L-glutamine (2 mM), and 10% heat-inactivated fetal bovine serum (FBS) at 37 °C in a humidified atmosphere containing 5% CO_2.

DMEM medium, fetal bovine serum (FBS), L-glutamine, and antibiotics (penicillin−streptomycin) were obtained from GIBCO BRL (Grand Island, NY).

THP-1 monocytes were seeded onto 145 mm plastic plates at a density of 40 × 10^6 cells/plate in complete medium and treated with a final concentration of 30 ng/mL phorbol 12-myristate 13-acetate (PMA) (Sigma-Aldrich, Steinheim, Germany) for 24 h to induce maturation toward adherent macrophage-like cells. After 24 h, the medium containing PMA was replaced with fresh medium not containing PMA to remove unattached cells; THP-1 cells were cultured in medium without PMA for 48 h more.

2.3. *Candida albicans*-Macrophage Coculture

For interaction studies, PMA-induced THP-1 macrophages were incubated with *C. albicans* in fresh DMEM media supplemented with 1% FBS at a MOI (macrophage/yeast ratio) of 1 during 3 h at 37 °C. Then, supernatants were collected and centrifuged to eliminate cells. After this, supernatants were filtered through a 0.2 μm pore size Nalgene Disposable Filter Unit (Thermo Fisher Scientific) to remove smaller debris.

2.4. Isolation of Extracellular Vesicles

Three independent experiments were done with THP-1 macrophages samples. Control (MC) and after interaction with *C. albicans* (MI) were used to isolate EVs according to Rodrigues et al.[20] with some modifications updated in our lab.[6,7] The number of macrophages used for each sample was ∼9 × 10^8. In brief, the supernatant of 20 Petri dishes (size 150 mm × 15 mm) with ∼45 × 10^6 macrophages each was collected and concentrated using a Centricon Plus-70 filter (cutoff filter 100 kDa, Millipore). The concentrated supernatant was ultracentrifuged at 100 000*g* for 1 h at 4 °C. Isolated EVs were washed in PBS twice, and samples were solubilized in 0.5 M triethylammonium bicarbonate (TEAB) buffer supplemented with a protease inhibitor cocktail.

The workflow of the current study is represented in the Supplemental Figure S1A.

2.5. Visualization and Measurement of EVs

2.5.1. Environmental Scanning Electron Microscopy.

Environmental scanning electron microscopy (ESEM) is a relatively new technique that turns possible the examination of practically any material, including biological tissues, wet or dry. In this study, ESEM was used to visualize the interaction between THP-1 macrophages and *C. albicans* after 3 h of interaction. In brief, THP-1 monocytes were differentiated in macrophages in 24-well plates with a glass coverslip into the well. After 72 h, the differentiated macrophages were coincubated with *C. albicans* at a MOI of 1 during 3 h at 37

DOI: 10.1021/acs.jproteome.6b00605
J. Proteome Res. XXXX, XXX, XXX−XXX

°C and 5% CO_2. Then, cells were washed three times with PBS and fixed in a phosphate buffer containing 2.5% paraformaldehyde during 1 h at room temperature. After that, samples were incubated for 1 h in 2% osmium tetroxide (TAAB Laboratories, U.K.) and then for 1 h in 2% tannic acid. After two washes with PBS, samples were serially dehydrated in ethanol. Critical point drying was performed and samples were sputter-coated with gold and examined in the FEI INSPECT microscope (FEI Company, Oregon-USA) at the Museo Nacional de Ciencias Naturales (Madrid, Spain).

2.5.2. Transmission Electron Microscopy. Transmission electron microscopy (TEM) was used to visualize EVs isolated from both MC and MI. Samples were fixed in a buffer containing 2.5% glutaraldehyde and 0.1 M cacodylate at room temperature for 2 h and then incubated in 4% paraformaraldehyde, 1% glutaraldehyde, and 0.1% PBS overnight at 4 °C. After that, samples were incubated for 90 min in 2% osmium tetroxide (TAAB Laboratories, U.K.), serially dehydrated in ethanol, and embedded in EMBed-812 resin (Electron Microscopy Sciences). Thin sections (50−70 nm) were obtained by ultracut and observed in a JEOL JEM 1010 transmission electron microscope operating at 100 kV, and pictures were taken with Megaview II camera. TEM images were analyzed with Soft Imaging Viewer Software. TEM was carried out in Centro Nacional de Microscopía Electrónica (ICTS)-UCM.

2.5.3. Measurement of EV Size by Dynamic Light Scattering. EV sizes (*z*-average diameter) were measured by dynamic light scattering (DLS) using ZetaSizer (Nano ZS, Malvern). Vesicles in a liquid phase undergo Brownian motion, and this produces light-scattering fluctuations, which give information on the size and heterogeneity of a sample.[21,22] For that, three biological replicates of EVs (from both MC-derived and MI-derived) were obtained by ultracentrifugation and diluted in PBS; then, samples were transferred to a disposable cuvette, and 10 measurements for each were performed with refractive index at 1.33 and absorption at 0.01. Data analysis was performed using the Zetasizer Software 7.11 (Malvern). DLS was carried out at the spectroscopy and correlation facility of the Complutense University of Madrid (UCM).

2.6. Quantitative Proteomic Analysis

2.6.1. Sample Preparation and Digestion. The proteomic analysis was performed in the proteomics facility of The Spanish National Center for Biotechnology (CNB-CSIC) and at the proteomics facility of the Complutense University-Scientific Park of Madrid (UCM-PCM); both of them belong to ProteoRed, PRB2-ISCIII.

The amount of protein in each sample was quantified using RC/DC protein assay (BioRad) prior TMT labeling. For digestion, 40 μg of protein from each condition was precipitated by methanol/chloroform method, as described in Wessel et al.,[23] and pellets were resuspended and denatured in 20 μL of 6 M guanidine hydrochloride/100 mM HEPES, pH 7.5 (SERVA Electrophoresis), reduced with 2 μL of 50 mM tris (2-carboxyethyl) phosphine (TCEP, AB SCIEX), pH 8.0, at 60 °C for 60 min, followed by the addition of 2 μL of 200 mM cysteine-blocking reagent methylmethanethiosulfonate (MMTS, Pierce) for 10 min at room temperature. Samples were diluted to 120 μL to reduce guanidine concentration with 50 mM TEAB. Digestions were initiated by adding 3 μL (1 μg/μL) of sequence-grade-modified trypsin (Sigma-Aldrich) to each sample in a ratio 1/20 (w/w), which were then incubated at 37 °C overnight on a shaker. Digested samples were evaporated to dryness in a vacuum concentrator.

2.6.2. TMT Labeling. Digested samples were labeled with the TMTsixplex Isobaric Mass Tagging Kit (Thermo Scientific, Rockford, IL) previously reconstituted with 42 μL of anhydrous acetonitrile (ACN). Three biological replicates of each condition were analyzed in this study. The TMT labeling was performed as described in Supplemental Figure S1B. After 2 h of incubation at room temperature, the reactions were quenched adding 8 μL of 5% hydroxylamine and incubating for 15 min. Finally, samples were combined at equal peptide amounts by adding 100 μL of 50% ACN, and sample-labeled digestion was evaporated to dryness in a vacuum concentrator. The digested, labeled, and pooled peptide mixture was desalted using a Sep-PAK C18 Cartridge (Waters) following manufacturer's indications; the cleaned tryptic peptides were evaporated to dryness and kept at −20 °C for further analysis.

2.6.3. Liquid Chromatography and Mass Spectrometer Analysis. A 1.5 μg aliquot of the each peptide fraction was subjected to 2D-nano LC−ESI−MS/MS analysis using a nano liquid chromatography system (Eksigent Technologies nanoLC Ultra 1D plus, AB SCIEX, Foster City, CA) coupled to a high-speed Triple TOF 5600 mass spectrometer (AB SCIEX, Foster City, CA) with a Nanospray III Source. The analytical column used was a silica-based reverse-phase column C18 ChromXP 75 μm × 15 cm, 3 μm particle size, and 120 Å pore size (Eksigent Technologies, AB SCIEX, Foster City, CA). The trap column was a C18 ChromXP (Eksigent Technologies, AB SCIEX, Foster City, CA), 3 μm particle diameter, 120 Å pore size, switched online with the analytical column. The loading pump delivered a solution of 0.1% formic acid in water at 2 μL/min. The nanopump provided a flow-rate of 300 nL/min and was operated under gradient elution conditions using 0.1% formic acid in water as mobile phase A and 0.1% formic acid in acetonitrile as mobile phase B. Gradient elution was performed using a 120 min gradient ranging from 2 to 90% mobile phase B. Injection volume was 5 μL.

Data acquisition was performed with a TripleTOF 5600 System (AB SCIEX, Concord, ON). Data were acquired using an ionspray voltage floating (ISVF) 2800 V, curtain gas (CUR) 20, interface heater temperature (IHT) 150, ion source gas 1 (GS1) 20, and declustering potential (DP) 85 V. All data were acquired using information-dependent acquisition (IDA) mode with Analyst TF 1.5 software (AB SCIEX, USA). For IDA parameters, 0.25 s MS survey scan in the mass range of 350−1250 Da was followed by 30 MS/MS scans of 150 ms in the mass range of 100−1800 (total cycle time: 4.04 s). Switching criteria were set to ions greater than mass to charge ratio (m/z) 350 and smaller than m/z 1250 with charge state of 2−5 and an abundance threshold of more than 90 counts (cps). Former target ions were excluded for 20 s. IDA rolling collision energy (CE) parameters script was used for automatically controlling the CE.

All mass spectrometry proteomics data have been deposited to the ProteomeXchange Consortium (http://proteomecentral.proteomexchange.org) via the PRIDE partner repository[24] with the provisional Submission Reference: 1-20160630-150406.

2.6.4. Data Analysis. MS/MS spectra were exported to .mgf format using (Peak View v1.2.0.3) and searched using MASCOT 2.4.0, OMSSA 2.1.9, X!TANDEM 2013.02.01.1, and Myrimatch 2.2.140 against a composite target/decoy database built from the *Homo sapiens* and *Bos taurus* reference proteomes at Uniprot Knowledgebase containing 67911 (2015/02) and

DOI: 10.1021/acs.jproteome.6b00605
J. Proteome Res. XXXX, XXX, XXX−XXX

5993 (2015/06) sequences, respectively, plus all proteins sequences in the *Candida* Genome Database (assembly 22) and some commonly occurring contaminants. Decoy sequences were obtained by reversing target protein sequences. Search engines were configured to match potential peptide candidates with mass error tolerance of 25 ppm and fragment ion tolerance of 0.02 Da, allowing for up to two missed tryptic cleavage sites and a maximum isotope error (^{13}C) of 1, considering fixed MMTS modification of cysteine and variable oxidation of methionine, pyroglutamic acid from glutamine or glutamic acid at the peptide N-terminus, acetylation of the protein N-terminus, and TMT-modified lysine or peptide N-terminus. Search engine results were depleted of bovine proteins by removing hits to any peptide sequences in a reference exclusion peptide list. Score distribution models were used to compute peptide−spectrum match p values,[25] and spectra recovered by an FDR* $\leq$ 0.01 (peptide-level) filter were selected for quantitative analysis. Isobaric reporter ion intensities were corrected according to specifications of reagent purity supplied by the manufacturer. Approximately 15% of the lowest quality signals were removed prior to further analysis. Differential regulation was measured using linear models,[26] and statistical significance was measured using q values (FDR). The exclusion peptide list was obtained from a FDR $\leq$ 0.1 analysis of a sample of fetal bovine serum using X!TANDEM and a composite target/decoy database built from the *Bos taurus* reference proteome to exclude from the analyses any potential contamination from FBS EVs.

2.7. Bioinformatic Analysis

Gene Ontology classifications and enrichments were performed using the software STRAP[27] and FunRich.[28] Signal Peptide Predictor (SignalP) 4.1 was used to analyze the presence of signal peptide in the identified proteins (http://www.cbs.dtu.dk/services/SignalP); this program predicts the presence and location of signal peptide cleavage sites in amino acids sequences based on a combination of several artificial neural networks.[29] Besides, SecretomeP 2.0 was used to predict the nonclassically secreted proteins (http://www.cbs.dtu.dk/services/SecretomeP). This software uses an algorithm that gives a score to each protein, when the protein has a score above 0.5, and it does not simultaneously get a prediction of containing a Signal Peptide, it is considered indicative of nonclassical secretion.[30] Exocarta was used as the database to compare the identified proteins and also with the TOP 100 exosomal proteins present in it.[31]

2.8. Western Blotting Validation Analysis

Twenty-five μg of protein per well were separated onto 10% SDS-polyacrylamide minigels and transferred to Hybond-ECL nitrocellulose membranes (Amersham Biosciences). The Western blotting was performed with Odyssey system (Infrared Imaging System (LI-COR Biosciences, Lincoln, NE). The membranes were incubated for 1 h with primary antibody 1/2000 anti-Vimentin (SIGMA), 1/500 peroxiredoxin-5 (Abcam), and 1/250 transferrin receptor (TFRC) (Thermo Fisher) for the proteomic validation and 1/2000 ERK1/2, phospho-ERK1/2, p38, and phospho-p38 (Cell Signaling) for the activation assays. Then, membranes were washed four times in PBS with 0.1% Tween-20. After this, the membranes were incubated with a fluorescently labeled secondary antibody 1/5000 IRDye 800CW-conjugated Goat (polyclonal) anti-Rabbit IgG and 1/5000 IRDye-680-conjugated Goat (polyclonal) anti-Mouse IgG, highly cross-absorbed (LI-COR Biosciences) for 1 h at room temperature and protected from light. Membranes were washed again and scanned for fluorescence detection with Odyssey system (LI-COR Biosciences).

Data were expressed as mean ± SD. The unpaired Student's t test was used to compare differences between groups, and $p < 0.05$ was considered significant.

2.9. In Vitro Stimulation of THP-1 Macrophages

2.9.1. Observation of EV Internalization. To see the EV internalization, MC-derived and MI-derived EVs were incubated with PKH26 (2× PKH dye solution, 4×10^{-6} M in diluent C) (Sigma) for 5 min at 25 °C. The reaction was quenched with complete medium. Then, THP-1 macrophages previously differentiated onto 24 plates with a coverslip inside were coincubated with/without 100 μg/mL of PKH-labeled EVs. After 1 h, cells were washed with ice-cold PBS and fixed in 4% paraformaldehyde for 30 min. Nuclei were stained with DAPI and washed three times with PBS. Coverslips were prepared for microscopy by mounting them on slides in Fluoromount G, and images were acquired by fluorescence microscopy with FITC (excitation/emission BP 480/30 and BP 535/40, respectively) and UV filters (excitation/emission BP 365/12 and long pass 397, respectively).

2.9.2. Evaluation of MAP Kinase Pathways Activation. The phosphorylation of ERK and p38 was evaluated in THP-1 macrophages untreated or coincubated with 100 ng/mL LPS or with 100 μg/mL of MC-derived and MI-derived EVs during 1 h. After this time point, macrophages were washed and proteins were obtained with RIPA buffer. Proteins were quantified with Bradford, and 25 μg of each sample were used to perform the Western blotting, as detailed above.

2.9.3. Cytokine Measurement. THP-1 macrophages were stimulated with 100 μg/mL of MC-derived and MI-derived EVs or 100 ng/mL LPS during 24 h at 37 °C in a 5% CO_2 atmosphere. After this time, supernatants were collected and clarified by centrifugation and tested for cytokine production by ELISA using matched paired antibodies specific for IL-10, IL12p40, TNF-α, and IL-8 (Immunotools) according to manufacturer's instructions. Cytokine production was measured in a total of three independent macrophage preparations, and the statistical significance of the differences between control and *C. albicans*- treated macrophages was evaluated by using the Student's t test.

2.9.4. Effect on Candidacidal Activity. After 24 h of coincubation with/without MC-derived, MI-derived EVs or LPS, candidacidal activity in vitro was carried out by a growth inhibition assay by CFU measurement, as previously reported.[32] In brief, THP-1 macrophages stimulated for 24 h with 100 μg/mL of EVs obtained from untreated and *C. albicans*-stimulated macrophages or 100 ng/mL LPS during 24 h at 37 °C in a 5% CO_2 atmosphere were cocultured with *C. albicans* at a MOI of 1 during 3 h at 37 °C in a 5% CO_2 atmosphere. As a control, the same amount of yeast was grown in complete media during 3 h. After this time, samples were diluted 1:200 and 1:2000 in distilled water and plated on YED agar in duplicate. After 24−48 h at 30 °C, CFU were counted. Three independent experiments were carried out, and the statistical significance of the differences in the candidacidal activity referred to the unstimulated (control) macrophages was evaluated by using the Student t test.

DOI: 10.1021/acs.jproteome.6b00605
J. Proteome Res. XXXX, XXX, XXX−XXX

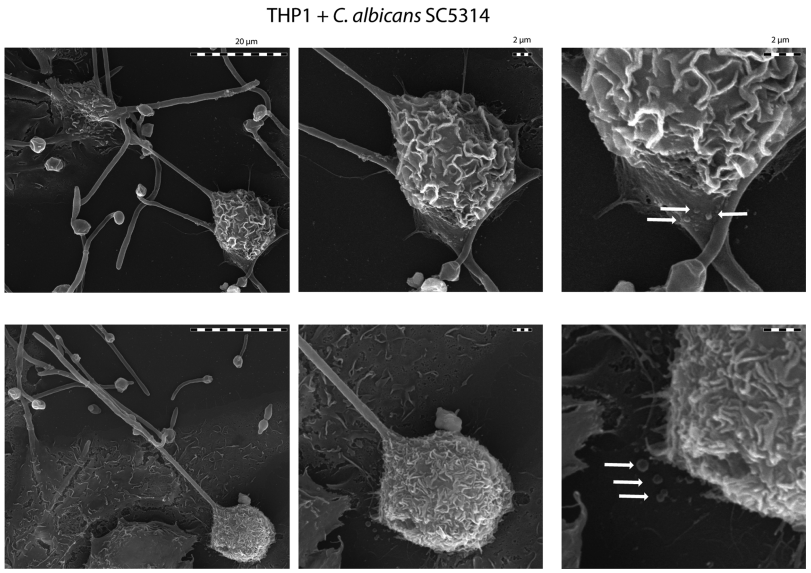

Figure 1. EV secretion in macrophages infected with *C. albicans*. THP-1 macrophages were differentiated and cocultured with *C. albicans* at a MOI of 1. Cells were washed, fixed, and treated to perform the environmental scanning electron microscopy (ESEM) analysis. Representative pictures of ESEM are shown, and the zones of interest were magnified to show the rounded protrusions in the cell surface similar to EVs (marked with an arrow). Scale bars: 20 and 2 μm.

3. RESULTS

3.1. *C. albicans* Induces an Increase in the Release of EVs in THP-1 Macrophages and Changes in the Different EVs Populations

Macrophages cocultured during 3 h with *C. albicans* at an MOI of 1 were visualized using an environmental scanning electron microscopy (ESEM). As we can see in Figure 1, the ESEM pictures showed rounded protrusions in the cell surface with an approximated size of 100 nm that may be EVs from THP-1 macrophages.

To visualize these macrophage-derived EVs, transmission electron microscopy (TEM) was performed. An equal amount of macrophages was used to compare the secretion of EVs between uninfected (MC) and *C. albicans*-infected (MI) macrophages. After 3 h of interaction with the yeast at a MOI of 1, supernatants from infected and uninfected macrophages were collected and EVs were concentrated as detailed in the Experimental Procedures. Samples were ultracentrifuged to purify the EVs, and different aliquots of the samples were used to embed in resin for TEM analysis or used for the DLS analysis to determine and quantify the size of the different macrophage-derived EVs. In Figure 2A, representative images from macrophage-derived EVs are shown. The number of EVs in the control THP-1 macrophages seems lower than that in the macrophages after the interaction with *C. albicans*, suggesting an increase in the secretion of EVs in macrophages in response to the interaction with the yeast. This enhancement can also be observed in TEM images depicted in Figure 2A and might be supported by the measurement of the protein amount obtained from the same number of MC and MI macrophages, showing a 68% increase of the total amount of protein after the interaction with *C. albicans* (Figure 2B), although more experiments have to be done to demonstrate the increase in the number of EVs. The increase in EV protein amount has already been described in human macrophages derived from monocytes stimulated with β-glucan.[16]

Regarding the morphologies and the different sizes observed in TEM images, it can be seen that after the interaction with *C. albicans* macrophages secrete more diverse EVs. Most of them are spherical, typical form of vesicles, but others are nonspherical vesicles, and some of them hold another vesicle inside (Figure 2A).

To evaluate the macrophage-derived EVs size, we performed dynamic light scattering (DLS) analysis. In all the replicates, both in EVs derived from macrophage control and from infected macrophages, a heterogeneous population was observed, with a polydispersity index (PDI) average of 0.5 and 0.53, respectively. Three different size subpopulations were observed under both conditions: a first subpopulation with an average size of ∼10 nm; a second subpopulation with an average size of ∼40 nm; and the third subpopulation with an average size of ∼369 nm (Figure 2C). The size of the second subpopulation can be correlated with the term exosomes, representing EVs with sizes between 30 and 100 nm and the third subpopulation with the term MVs for EVs with a diameter exceeding 100 nm (Figure 2C). As can be observed in Figure 2C, the population ranging from 100 to 1000 nm has a higher percentage of intensity in the MI-derived EV sample, a fact not observed in human macrophages derived from PMBCs stimulated with β-glucan.[16]

3.2. Identification of THP-1 EVs Proteins

Three replicates of EVs secreted by THP-1 cells, both control and infected during 3 h with *C. albicans*, were obtained, and 40 μg of proteins from each EVs were labeled with the TMT isobaric mass tags. A pool of all of the samples was analyzed using a 2D-nano LC−ESI−MS/MS coupled to high-speed Triple-TOF 5600 MS. After the exclusion of the contaminant proteins and the ambiguous proteins that can belong to the serum, a total of 797 redundant proteins were identified in the macrophage EVs. Of these, 719 proteins were well-assigned to *Homo sapiens* and 4 to *C. albicans*, and 73 were not clearly discriminated between human and the possible serum proteins because of their homology. For this reason, all of the subsequent bioinformatic analysis was performed by removing

DOI: 10.1021/acs.jproteome.6b00605
J. Proteome Res. XXXX, XXX, XXX−XXX

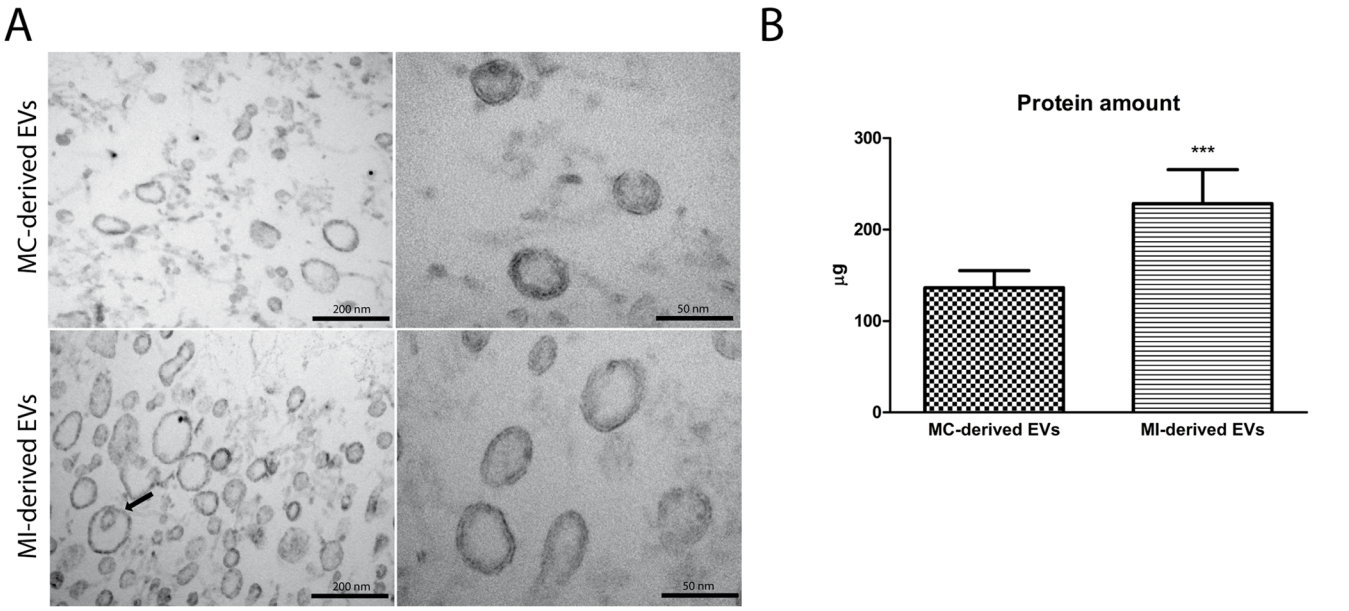

	Size (nm)		
	1-25	**26-100**	**101-1000**
MC-derived EVs	37.60	33.40	19.33
MI-derived EVs	31.57	35.93	31.30

Figure 2. Characterization of THP-1 EVs. EVs from control macrophages (MC) and macrophages cocultured with *C. albicans* at a MOI of 1 (MI) were purified by ultracentrifugation and visualized by TEM, total protein amount in macrophage-derived EVs was measured, and the size was measured by dynamic light scattering (DLS). (A) Transmission electron micrographs of MC- and MI-derived EVs. Scale bars: 200 and 50 nm. (B) Total protein amount in macrophage-derived EVs measured by Bradford using the same number of macrophage cells. (C) Particle size distributions of MC- and MI-derived EVs by DLS. Frequencies (%) by size (nm) of recovered EVs are represented. The table shows the percentages of intensity for the three different populations of EVs detected by DLS.

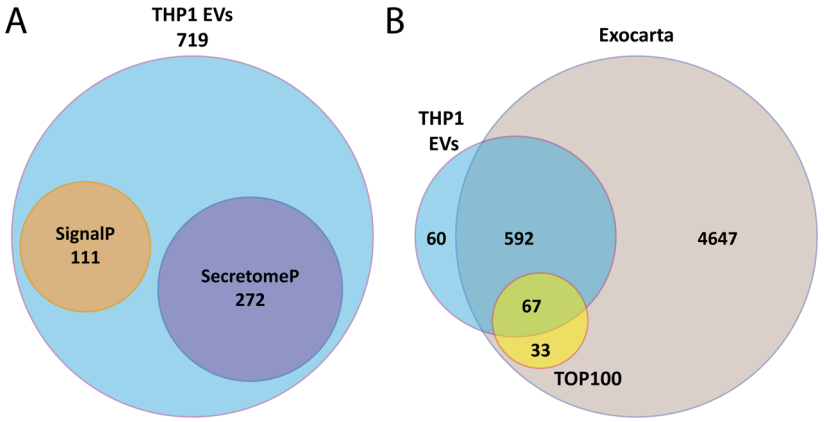

Figure 3. Analysis of the proteins identified in the THP-1-derived EVs. (A) Bioinformatic analysis using SignalP and SecretomeP of the proteins present in the macrophage-derived EVs. (B) Comparison of the proteins identified in THP-1-derived EVs with Exocarta database and the top 100 proteins of the same database.

the nonconfidently identified proteins. Supplemental Table S1 shows 720 proteins identified, where 2 of them were the same protein with different Uniprot access. Thus 719 identified proteins were confidently assigned.

DOI: 10.1021/acs.jproteome.6b00605
J. Proteome Res. XXXX, XXX, XXX−XXX

Table 1. Functional Classification of the Differentially Abundant Proteins in the EVs of THP-1 Macrophages after the Interaction with *C. albicans*

Swiss Prot[a]	Protein ID[a]	protein name[a]	fold change (log_2)[b]	*p* value[c]	*q* value[c]	N replicates[d]	N peptides[d]
		Immune Response					
P61769	B2M	beta-2-microglobulin	0.56	0.00	0.03	3	4
P13501	CCL5	C−C motif chemokine 5	−1.22	0.00	0.00	3	6
P36222	CHI3L1	chitinase-3-like protein 1	2.66	0.00	0.00	3	14
Q9BZP6	CHIA	acidic mammalian chitinase	−1.58	0.00	0.00	3	1
Q96RQ9	IL4I1	L-amino-acid oxidase	−0.53	0.01	0.04	3	7
P01033	TIMP1	metalloproteinase inhibitor 1	−1.27	0.00	0.03	2	1
		Signal Transduction					
P08758	ANXA5	annexin A5	0.62	0.00	0.00	3	9
Q7Z5R6	APBB1IP (RIAM)	amyloid beta A4 precursor protein-binding family B member 1-interacting protein	0.95	0.03	0.12	2	2
P09211	GSTP1	glutathione S-transferase P	−0.51	0.04	0.13	3	2
Q13418	ILK	integrin-linked protein kinase	−0.96	0.01	0.05	3	1
P08134	RHOC	Rho-related GTP-binding protein RhoC	−1.24	0.00	0.01	3	1
P61981	YWHAG	14−3−3 protein gamma	−0.61	0.01	0.07	3	2
		Stress Response/Oxidoreductase Activity					
Q92598	HSPH1	heat shock protein 105 kDa	−0.64	0.01	0.07	3	4
P13489	RNH1	ribonuclease inhibitor	−0.77	0.02	0.08	3	1
		Cytoskeletal Components and Actin Binding Proteins					
P60709	ACTB	actin, cytoplasmic 1	−0.68	0.00	0.03	3	2
K7EM38	ACTG1	actin, cytoplasmic 2 (fragment)	−0.75	0.02	0.08	3	1
O43707	ACTN4	alpha-actinin-4	−0.54	0.00	0.01	3	15
Q13554	CAMK2B	aalcium/calmodulin-dependent protein kinase type II subunit beta	0.77	0.03	0.11	3	1
Q01518	CAP1	adenylyl cyclase-associated protein 1	0.51	0.05	0.16	3	1
P60953	CDC42	cell division control protein 42 homologue	−0.91	0.01	0.06	3	1
P60981	DSTN	destrin	0.71	0.04	0.15	3	1
Q02241	KIF23	kinesin-like protein KIF23	−1.04	0.01	0.07	2	1
P04264	KRT1	keratin, type II cytoskeletal 1	−0.65	0.00	0.00	3	15
P13645	KRT10	keratin, type I cytoskeletal 10	−0.72	0.00	0.00	3	14
P02545	LMNA	prelamin-A/C	0.52	0.00	0.01	3	18
O14950	MYL12B	myosin regulatory light chain 12B	0.84	0.00	0.00	3	3
Q12965	MYO1E	unconventional myosin-Ie	0.54	0.00	0.03	3	9
P07737	PFN1	profilin-1	−0.53	0.00	0.02	3	9
Q15019	SEPT2	septin-2	−0.77	0.01	0.04	3	1
P08670	VIM	vimentin	0.58	0.00	0.00	3	30
		Extracellular Matrix Structural Protein					
P02452	COL1A1	collagen alpha-1(I) chain	−0.98	0.00	0.02	3	1
P08123	COL1A2	collagen alpha-2(I) chain	−1.81	0.00	0.00	3	1
P12109	COL6A1	collagen alpha-1(VI) chain	−0.70	0.01	0.06	3	3
P02751	FN1	fibronectin	−0.92	0.00	0.00	3	19
		Transport					
P56385	ATP5I	ATP synthase subunit e, mitochondrial	0.62	0.02	0.08	3	2
O00299	CLIC1	chloride intracellular channel protein 1	−0.65	0.00	0.01	3	7
P13073	COX4I1	cytochrome *c* oxidase subunit 4 isoform 1, mitochondrial	0.74	0.01	0.04	3	2
P69905	HBA1	hemoglobin subunit alpha	−0.59	0.02	0.08	3	1
Q13303	KCNAB2	voltage-gated potassium channel subunit beta-2	1.54	0.00	0.00	3	5
O00629	KPNA4	importin subunit alpha-3	1.69	0.01	0.05	2	1
Q8WUM4	PDCD6IP	programmed cell death 6-interacting protein	−0.56	0.00	0.02	3	7
P61026	RAB10	Ras-related protein Rab-10	−0.82	0.00	0.03	3	2
Q8WUD1	RAB2B	Ras-related protein Rab-2B	−1.17	0.00	0.02	3	1
O76094	SRP72	signal recognition particle subunit SRP72	−1.12	0.01	0.07	2	1
Q07955	SRSF1	Serine/arginine-rich splicing factor 1	0.53	0.00	0.01	3	12
P02786	TFRC	transferrin receptor protein 1	−1.30	0.00	0.00	3	1
Q99816	TSG101	tumor susceptibility gene 101 protein	−0.50	0.04	0.15	3	3
P14927	UQCRB	cytochrome *b*-c1 complex subunit 7	0.54	0.01	0.07	3	3
P55072	VCP	transitional endoplasmic reticulum ATPase	−0.67	0.00	0.00	3	33

DOI: 10.1021/acs.jproteome.6b00605
J. Proteome Res. XXXX, XXX, XXX−XXX

Table 1. continued

Swiss Prot[a]	Protein ID[a]	protein name[a]	fold change (log_2)[b]	*p* value[c]	*q* value[c]	N replicates[d]	N peptides[d]
		Metabolism					
P04745	AMY1A	alpha-amylase 1	−0.84	0.01	0.07	3	1
P08243	ASNS	asparagine synthetase [glutamine-hydrolyzing]	−0.82	0.02	0.08	3	1
P42126	ECI1	enoyl-CoA delta isomerase 1, mitochondrial	0.87	0.04	0.15	2	1
P13929	ENO3	beta-enolase	−0.82	0.01	0.04	3	1
P49327	FASN	fatty acid synthase	−0.63	0.00	0.02	3	8
P14324	FDPS	farnesyl pyrophosphate synthase	−0.58	0.03	0.10	3	4
P00367	GLUD1	glutamate dehydrogenase 1, mitochondrial	0.59	0.02	0.09	3	4
P00338	LDHA	L-lactate dehydrogenase A chain	−0.65	0.00	0.02	3	3
Q08431	MFGE8	lactadherin	−0.91	0.00	0.00	3	4
P14780	MMP9	matrix metalloproteinase-9	−0.84	0.00	0.00	3	8
P17858	PFKL	ATP-dependent 6-phosphofructokinase, liver type	−0.78	0.01	0.05	3	3
Q15126	PMVK	phosphomevalonate kinase	−0.99	0.00	0.02	3	1
P00491	PNP	purine nucleoside phosphorylase	0.93	0.01	0.05	3	1
P22314	UBA1	ubiquitin-like modifier-activating enzyme 1	−0.51	0.01	0.07	3	5
		Protein Fate					
O15372	EIF3H	eukaryotic translation initiation factor 3 subunit H	0.74	0.01	0.06	3	2
Q13151	HNRNPA0	heterogeneous nuclear ribonucleoprotein A0	1.29	0.00	0.03	2	1
P62937	PPIA	peptidyl-prolyl *cis*−*trans* isomerase A	−0.50	0.01	0.05	3	5
Q9UNM6	PSMD13	26S proteasome non-ATPase regulatory subunit 13	1.70	0.00	0.00	2	1
		Nucleic Acid Processing					
Q9BTT0	ANP32E	acidic leucine-rich nuclear phosphoprotein 32 family member E	−1.87	0.00	0.00	3	1
O75531	BANF1	barrier-to-autointegration factor	0.80	0.00	0.00	3	4
Q9Y224	C14orf166	UPF0568 protein C14orf166	0.55	0.02	0.08	3	5
P35659	DEK	protein DEK	0.97	0.00	0.02	3	2
P22087	FBL	rRNA 2′-*O*-methyltransferase fibrillarin	0.50	0.01	0.06	3	6
O14979	HNRNPDL	heterogeneous nuclear ribonucleoprotein D-like	0.70	0.05	0.16	3	1
P43243	MATR3	matrin-3	0.53	0.01	0.04	3	9
P38159	RBMX	RNA-binding motif protein, X chromosome	−0.60	0.03	0.10	3	2
Q9Y3B4	SF3B6	splicing factor 3B subunit 6	−0.96	0.03	0.11	2	1
Q01130	SRSF2	serine/arginine-rich splicing factor 2	0.59	0.01	0.04	3	3
P84103	SRSF3	serine/arginine-rich splicing factor 3	0.75	0.00	0.00	3	4
Q16629	SRSF7	serine/arginine-rich splicing factor 7	0.65	0.00	0.02	3	3
P31948	STIP1	stress-induced-phosphoprotein 1	−0.55	0.01	0.04	3	7
P62995	TRA2B	transformer-2 protein homologue beta	0.57	0.00	0.03	3	5
P23381	WARS	tryptophan−tRNA ligase, cytoplasmic	−0.54	0.05	0.16	3	4
		Structural Component of the Ribosome/Ribosome Synthesis					
O43861	ATP9B	probable phospholipid-transporting ATPase IIB	1.16	0.00	0.01	3	1
P62906	RPL10A	60S ribosomal protein L10a	0.67	0.00	0.02	3	4
P26373	RPL13	60S ribosomal protein L13	1.04	0.00	0.00	3	6
P40429	RPL13A	60S ribosomal protein L13a	0.84	0.00	0.00	3	7
P50914	RPL14	60S ribosomal protein L14	0.72	0.00	0.00	3	5
P61313	RPL15	60S ribosomal protein L15	0.77	0.00	0.00	3	4
P18621	RPL17	60S ribosomal protein L17	0.70	0.00	0.00	3	10
Q02543	RPL18A	60S ribosomal protein L18a	0.58	0.00	0.01	3	8
P84098	RPL19	60S ribosomal protein L19	0.86	0.00	0.00	3	6
P46778	RPL21	60S ribosomal protein L21	0.76	0.00	0.00	3	4
P62750	RPL23A	60S ribosomal protein L23a	0.66	0.00	0.00	3	7
P83731	RPL24	60S ribosomal protein L24	0.72	0.00	0.00	3	7
P61254	RPL26	60S ribosomal protein L26	0.67	0.00	0.00	3	6
P61353	RPL27	60S ribosomal protein L27	0.72	0.00	0.00	3	7
P46776	RPL27A	60S ribosomal protein L27a	0.52	0.01	0.04	3	6
P46779	RPL28	60S ribosomal protein L28	0.90	0.00	0.00	3	5
P47914	RPL29	60S ribosomal protein L29	0.86	0.00	0.00	3	2
P39023	RPL3	60S ribosomal protein L3	0.59	0.00	0.00	3	18
P62910	RPL32	60S ribosomal protein L32	0.88	0.00	0.00	3	6
P49207	RPL34	60S ribosomal protein L34	0.90	0.00	0.00	3	3
P42766	RPL35	60S ribosomal protein L35	0.79	0.00	0.00	3	3
P18077	RPL35A	60S ribosomal protein L35a	0.77	0.00	0.00	3	5
P83881	RPL36A	60S ribosomal protein L36a	0.83	0.01	0.07	3	1

DOI: 10.1021/acs.jproteome.6b00605
J. Proteome Res. XXXX, XXX, XXX−XXX

Table 1. continued

Swiss Prot[a]	Protein ID[a]	protein name[a]	fold change (log_2)[b]	p value[c]	q value[c]	N replicates[d]	N peptides[d]
		Structural Component of the Ribosome/Ribosome Synthesis					
Q969Q0	RPL36AL	60S ribosomal protein L36a-like	−0.86	0.02	0.07	3	1
P36578	RPL4	60S ribosomal protein L4	0.59	0.00	0.00	3	15
P46777	RPL5	60S ribosomal protein L5	0.58	0.00	0.02	3	5
Q02878	RPL6	60S ribosomal protein L6	1.05	0.00	0.00	3	11
P18124	RPL7	60S ribosomal protein L7	0.75	0.00	0.00	3	11
P62424	RPL7A	60S ribosomal protein L7a	0.74	0.00	0.00	3	13
P62917	RPL8	60S ribosomal protein L8	1.17	0.00	0.00	3	7
P32969	RPL9	60S ribosomal protein L9	0.52	0.00	0.03	3	7
P05388	RPLP0	60S acidic ribosomal protein P0	0.67	0.00	0.00	3	10
P05386	RPLP1	60S acidic ribosomal protein P1	0.65	0.02	0.08	3	1
P62280	RPS11	40S ribosomal protein S11	0.53	0.01	0.04	3	5
P62277	RPS13	40S ribosomal protein S13	0.90	0.00	0.00	3	9
P62841	RPS15	40S ribosomal protein S15	1.29	0.00	0.00	3	3
P62269	RPS18	40S ribosomal protein S18	0.64	0.00	0.00	3	9
P39019	RPS19	40S ribosomal protein S19	0.73	0.00	0.00	3	11
P15880	RPS2	40S ribosomal protein S2	0.85	0.00	0.00	3	10
P62266	RPS23	40S ribosomal protein S23	0.78	0.00	0.00	3	5
P62847	RPS24	40S ribosomal protein S24	0.86	0.00	0.00	3	4
P62851	RPS25	40S ribosomal protein S25	0.83	0.00	0.00	3	4
P62854	RPS26	40S ribosomal protein S26	0.76	0.00	0.01	3	2
P62857	RPS28	40S ribosomal protein S28	0.93	0.00	0.00	3	2
P62273	RPS29	40S ribosomal protein S29	1.06	0.00	0.01	3	1
P23396	RPS3	40S ribosomal protein S3	0.59	0.00	0.00	3	13
P61247	RPS3A	40S ribosomal protein S3a	0.55	0.00	0.01	3	17
P62753	RPS6	40S ribosomal protein S6	0.65	0.00	0.00	3	9
P62241	RPS8	40S ribosomal protein S8	0.82	0.00	0.00	3	9
		Other Functions					
Q5H9B9	BMP2KL	putative BMP-2-inducible kinase-like protein	1.03	0.00	0.03	3	1
P00488	F13A1	coagulation factor XIII A chain	−0.68	0.03	0.12	3	1

[a]Protein name and accession number according to Uniprot Knowledgebase. [b]Fold-change abundance was averaged by calculating the log_2 of the geometrical mean of EVs from THP-1 macrophages + *C. albicans* versus THP-1 control macrophages. [c]p values and q values were obtained using MASCOT 2.4.0, OMSSA 2.1.9, X!TANDEM 2013.02.01.1, and Myrimatch 2.2.140 searches. [d]Only protein identifications supported by at least two high confident peptides (confidence >95%) or one high confident peptide in three replicates were considered.

The majority of the identified proteins were membrane-associated (~40%), accordingly to previous works,[16,33] and almost 60% of them have a Gene Ontology annotation related to extracellular/vesicular/exosome.

To evaluate the possibility of the identified proteins to be secreted through classical or nonclassical pathways, each protein was analyzed by SignalP and SecretomeP software (Figure 3A). While SignalP predicts the signal peptide necessary to be secreted through the classical ER/Golgi pathway, the SecretomeP software determines the putative export through one of the nonclassical secretory pathways. Supplemental Table S2 shows the score assigned to the identified proteins according to both prediction software. Using SignalP predictor, 111 macrophage-derived EVs proteins have signal peptide sequence necessary to the conventional protein secretion. Besides, the SecretomeP predictor detects 272 proteins with a score above 0.5 and without a signal peptide predicted in their sequence, determining that these proteins can be classified as putative nonclassically secreted proteins. Interestingly, 47% of EVs proteins were not predicted to be secreted.

The identified proteins were also compared with the Exocarta database, which includes most of the exosomal proteins identified in several studies (Figure 3B). Compared with the database, 659 proteins had been reported in human ExoCarta.[31] Of the top 100-ranked proteins presented in Exocarta, 67 of them have been identified in our study (Figure 3B). Sixty proteins were not present in the database. Seven of these proteins were involved in immunity-related system processes: galectin-9 (LGALS9), tumor necrosis factor alpha-induced protein 8-like protein 2 (TNFAIP8L2), acidic mammalian chitinase (CHIA), chitinase-3-like protein 1 (CHI3L1), CD97 antigen, IFI30, and C−C motif chemokine 5 (CCL5).

3.3. Quantification of THP-1 EV Proteins

The high-throughput quantitative proteomic analysis was performed with three independent biological replicates that were labeled with the six isobaric tags of TMT, allowing the analysis and comparison of the three replicates in the same MS/MS run to minimize random effects and to increase fidelity (two technical replicates were performed). Differential regulation was measured using linear models, and statistical significance was measured using q values (FDR). After removing all of the low-quality results and the duplicated proteins, 717 unique proteins were quantified with good statistics among the three replicates (Supplemental Table S1).

Next, we used the ±0.5 cutoff of values for the quantified proteins. From these proteins, 133 showed differential abundance between control and infected macrophages (Table

DOI: 10.1021/acs.jproteome.6b00605
J. Proteome Res. XXXX, XXX, XXX−XXX

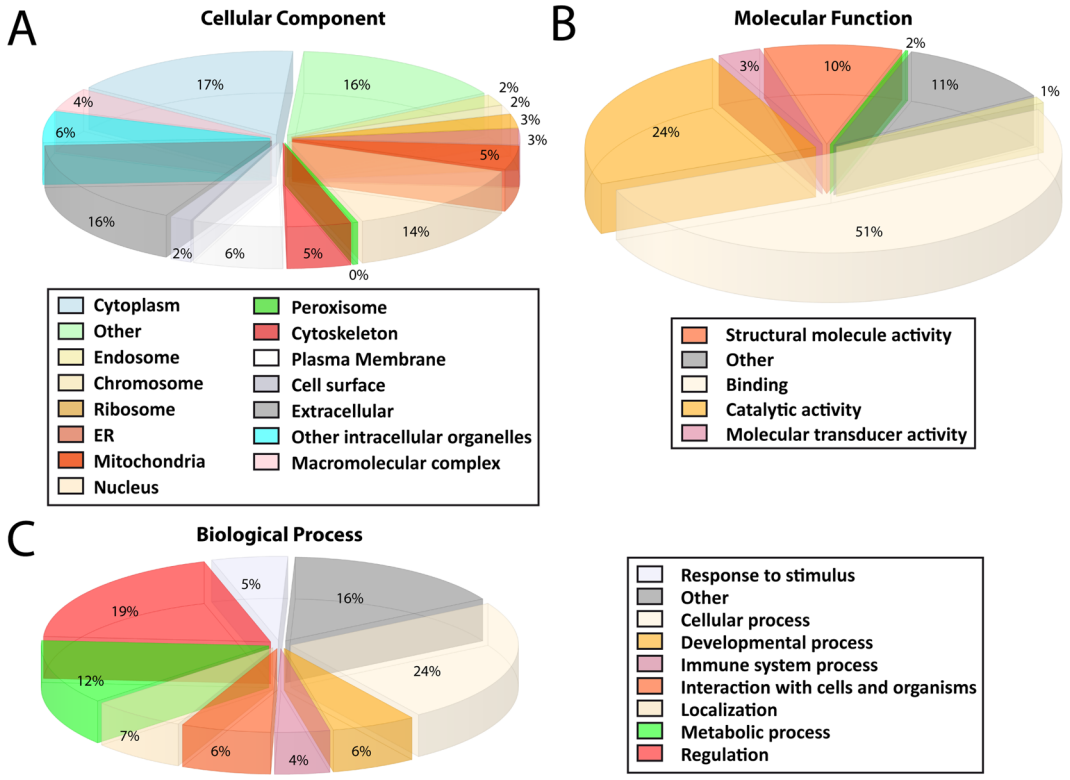

Figure 4. Gene Ontology analysis of the THP-1-derived EVs identified proteins. Gene Ontology (GO) analysis of the identified proteins was performed using STRAP (Software Tool for Rapid Annotation of Proteins). (A) Pie chart showing ontology analysis on Cellular Components (CC). (B) Pie chart of GO analysis on Molecular Functions (MF). (C) Pie chart of GO analysis on Biological Processes (BP).

1); there were 82 more abundant and 51 less abundant proteins in EVs of THP-1 macrophages after 3 h of interaction with *C. albicans*.

3.3.1. Classification/Functional Profiles of the Quantified THP-1 EVs Proteins. The 717 quantified proteins in the macrophage-derived EVs were then classified based on their localization in the cell (cellular component), their molecular function, and the biological process in which they are involved (Figure 4). STRAP analysis showed that the extracellular/exosome one was the second more enriched annotation, with >60% of the proteins annotated with this term. Cytoplasmic location is the most common (476) annotation, followed by extracellular/exosome (472), then nucleus (402), and then the plasma membrane (184) (Figure 4A). The enrichment in molecular function revealed that the majority of the proteins possess protein binding activity (595). Other well-represented molecular functions were: catalytic activity (274), structural molecule activity (112), molecular transducer or signal transducer activity (35), and antioxidant activity (12) (Figure 4B). Regarding the enrichment in biological processes, most of the EVs proteins were related to regulation (493), metabolism (319), interaction with cells and organisms (163), response to stimulus (138), localization (127), and immune system processes (100) (Figure 4C). Some of the proteins are annotated in more than one cellular component, molecular function, or biological process.

Then, subcellular and functional categories of the EVs proteins identified and quantified in the THP-1 cell line were compared with the proteomic data from the Vesiclepedia Exosome Database[34] using FunRich software.[28] Using this data set, we could find differences in some of the categories between THP-1 EVs and Vesiclepedia Exosome Database. Regarding the cellular component, membrane proteins were underrepresented in our EVs, while proteins belonging to phagocytic cup, cytoskeleton and lysosomal lumen, among others, were enriched (Supplemental Figure S2A). In functional categories, we detected an increase in the secretion of proteins related to superoxide dismutase activity and sterol transferase, and nucleocytoplasmic transporter activities (Supplemental Figure S2B). The most relevant changes compared with Vesiclepedia were observed in the biological processes assigned to proteins. Enrichment in the intracellular signaling cascades, immune cell migration, and cell maturation was observed, while for other processes the fold change was very low compared with the overrepresented processes (Supplemental Figure S2C).

3.3.2. Differentially Secreted Proteins in EVs. As indicated above, the interaction with *C. albicans* modified the protein composition and the abundance of the different size populations of THP-1 macrophage-derived EVs. The TMT labeling used for protein quantification allowed us to identify and quantify 133 proteins that showed differential abundance in macrophage EVs after the interaction with the yeast. Eighty-two proteins showed an increase in the abundance, and 51 proteins were less abundant in macrophage-derived EVs after *C. albicans* interaction. The classifications of the differentially abundant proteins secreted by macrophage-derived EVs are summarized in Table 1.

STRAP cellular component showed that the more abundant proteins of the macrophage-derived EVs after *C. albicans* interaction were proteins located in the nucleus and in the ribosome. On the other side, an increase in terms related to the extracellular space in the less abundant proteins was observed (Figure 5A). In the analysis of the molecular function, both groups of the differentially abundant proteins showed similar

DOI: 10.1021/acs.jproteome.6b00605
J. Proteome Res. XXXX, XXX, XXX−XXX

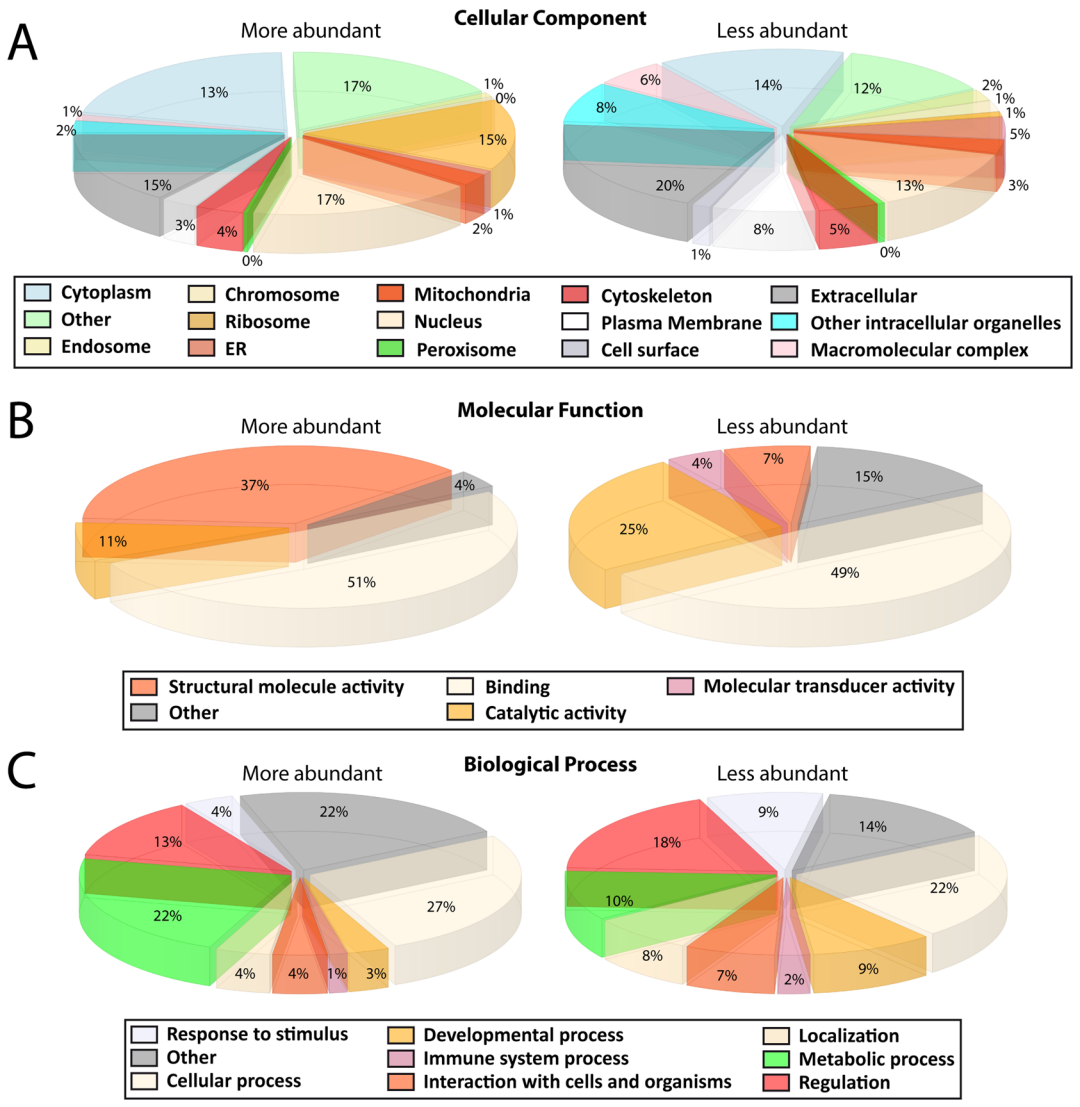

Figure 5. Gene Ontology analysis of the differentially abundant proteins of THP-1-derived EVs after the interaction with *C. albicans*. Gene Ontology (GO) analysis of the 133 differentially abundant proteins from Macrophages Control (MC) and Macrophages infected with *C. albicans* (MI) derived EVs was performed using STRAP (Software Tool for Rapid Annotation of Proteins). (A) Pie charts showing GO analysis on Cellular Components of the more abundant and less abundant proteins (CC). (B) Pie charts of GO analysis on Molecular Functions (MF). (C) Pie charts of GO analysis on Biological Processes (BP).

functions, although with different percentages (Figure 5B). The most important biological functions for the differentially abundant proteins are response to stimulus, metabolic processes, interaction with cells and organisms, and immune system processes (Figure 5C).

Supplemental Figures S3–S5 describe in more depth the differences in cellular component, molecular function, and biological processes of the differentially abundant proteins based on FunRich analysis software. Figure S3 shows the comparison between more and less abundant groups of proteins, and Figures S4 and S5 show, respectively, the comparison of the more abundant and the less abundant proteins with the database. In summary, for the proteins that increase in their abundance, 50% of the proteins are structural components of the ribosome, the protein metabolism is the more represented molecular function, and proteins related to MHC class I and II functions appear. Also, there is an increase in proteins from the nucleolus and the centrosome. For the proteins that decrease in their abundance, the lysosome, the cytoskeleton, and the extracellular matrix are the main cellular components represented, while GTPase activity, cell growth, energy pathways, and metabolism are the molecular functions in which most of the proteins that decrease in abundance are involved.

To validate the proteomics results, Western blots were performed for three selected proteins, Vimentin, Peroxiredoxin-5, and Transferrin receptor. The quantification of these three proteins by Western blotting confirmed the alteration in protein content in macrophage-derived EVs observed in our MS/MS results (Figure 6).

3.4. Effector Functions of Macrophage-Derived EVs in Response to *C. albicans*

The effect of both MI- and MC-derived EVs on surrounding PMA-induced THP-1 macrophages was analyzed by treating macrophages with 100 μg/mL of MC-derived and MI-derived EVs and subsequent measurement of the phosphorylation of ERK1/2 and p38. To see how these EVs were interacting with macrophages, EVs were labeled with PKH26 and macrophages

DOI: 10.1021/acs.jproteome.6b00605
J. Proteome Res. XXXX, XXX, XXX−XXX

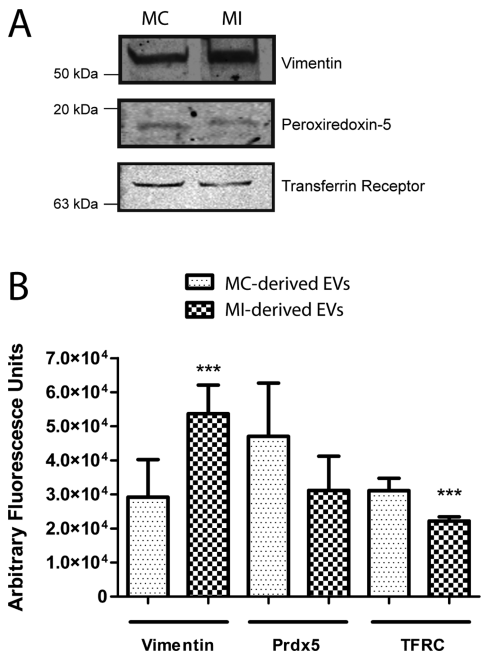

Figure 6. Validation of the differential secretion of THP-1 proteins after the interaction with *C. albicans* by Western blotting. Western blot representative captures (A) and quantification (in arbitrary fluorescence units) (B) of the levels of Vimentin, Peroxiredoxin 5, and Transferrin Receptor in Macrophages Control (MC) and Macrophages infected with *C. albicans* (MI) derived EVs. Statistically significant differences are indicated (***, $p < 0.001$).

with DAPI and observed in a fluorescence microscope. As observable in Figure 7A, both types of vesicles were internalized by macrophages. Qualitatively, MI-derived EVs seem to be more intensively internalized than the MC-derived ones. Figure 7B shows that the treatment of THP-1 macrophages during 1 h with macrophages-derived EVs (both MC and MI) leads to a significant phosphorylation/activation of ERK2 and p38 kinases compared with the untreated macrophages, although the phosphorylation is less intense than the positive control of THP-1 macrophages treated with LPS.

The activation of these kinases leads to the secretion of different cytokines. Figure 8A shows that after 24 h the secretion of the pro-inflammatory cytokines TNF-α, IL-12 was highly stimulated by MC- and MI-derived EVs, although it was less intense than the LPS-treated positive control. In the case of the chemokine IL-8, the secretion was higher, even higher than the LPS control. However, no differences were detected in the secretion of IL-10 or in IFN-γ (data not shown). To check if the PMA differentiation was altering the THP-1 macrophages response, monocytes were also incubated with EVs and LPS. As observed in Figure 8A, monocytes secreted a higher amount of TNF-α in response to MI-derived stimulus, even higher than LPS. Secretion of IL-12 and IL-8 was also higher but with similar levels for both kinds of EVs.

The increased secretion of pro-inflammatory cytokines could be related to the intensification in the macrophage responsiveness against *C. albicans*. To study if macrophages stimulated with the EVs were able to destroy *C. albicans* better than the untreated ones, candidacidal activity was examined for macrophages treated with the three stimuli and for control macrophages for 24 h. As can be observed in Figure 8B, candidacidal activity of EVs prestimulated macrophages was higher than the control without stimulation. It was also higher than LPS-stimulated macrophages although not statistically significant. This experiment shows that both types of EVs are a positive stimulus for macrophages against *C. albicans* infections.

4. DISCUSSION

It has been described that innate immunity is the first line of defense against microbial infections and of tissue damage remodeling, where macrophages and neutrophils were the most important cell types acting against fungal infections. Macrophage activation plays an important role in the *C. albicans* destruction, for both murine and human macrophages.[17,18,35,36] The activation of signaling cascades and their effects along the interaction produce pro-inflammatory mediators with direct effects in the neighboring cells through different mechanisms. The secretion of the mediators can be performed directly via classical secretion or by vesicle-mediated secretion. There is evidence that macrophages can be activated by exosomes that belong to other infected macrophages;[12,14,15] for this reason we decided to study the protein composition of THP-1 macrophage -derived EVs and the differences in their composition due to the interaction with *C. albicans*. A previous study on human macrophages derived from monocytes revealed differences in protein abundance and protein composition of EVs upon stimulation with β-glucan,[16] but this is the first study using live *C. albicans* cells.

The protein cargo of these macrophage-derived EVs was studied by LC−MS/MS together with the different abundance of these proteins in THP-1 macrophages after the coincubation with *C. albicans* (MI) compared with unstimulated macrophages (MC). Quantitative proteomic and posterior bioinformatic analysis allowed the identification and quantification of the proteins potentially involved in the communication of macrophages with other effector cells during candidiasis.

Vesicles were observed by ESEM. Micrographs revealed spherical structures in THP-1 macrophages after the engulfment of *C. albicans* (Figure 1) that can be exosomes or other type of EVs, such as MVs. The isolation of these EVs by concentration and ultracentrifugation and posterior SEM analysis revealed that these structures were very diverse in sizes and form and that there seemed to be an increase in the number and changes in the subpopulations of the EVs in the MI with respect to MC. The significant increase in the protein concentration, 68% more in MI-derived EVs compared to the MC-derived ones for the same number of THP-1 macrophages, might be in concordance with the observed increase in the number of vesicles, but more accurate measurements have to be done to demonstrate this increase. The differences observed by TEM in MI-derived EVs size with respect to the control were supported by the size measurements in both samples, where the percentage of intensity of the vesicles with 101−1000 nm in MI-derived sample almost doubled the MC-derived ones.

The quantitative proteomic study allowed the identification of 791 proteins; of these, 719 were unambiguous proteins for *Homo sapiens* and 717 of them were identified quantified with good statistics (Supplementary Table S1). The comparison with different databases allowed us to describe proteins not previously identified in EVs. The comparison with Exocarta showed that ∼90% of the quantified proteins have been found in previous studies in exosomes, where 60 were related to EVs for the first time.

The comparison between proteins in MI- and MC-derived EVs showed 133 differentially abundant proteins, 82 with increased and 51 with decreased abundance in the presence of

DOI: 10.1021/acs.jproteome.6b00605
J. Proteome Res. XXXX, XXX, XXX−XXX

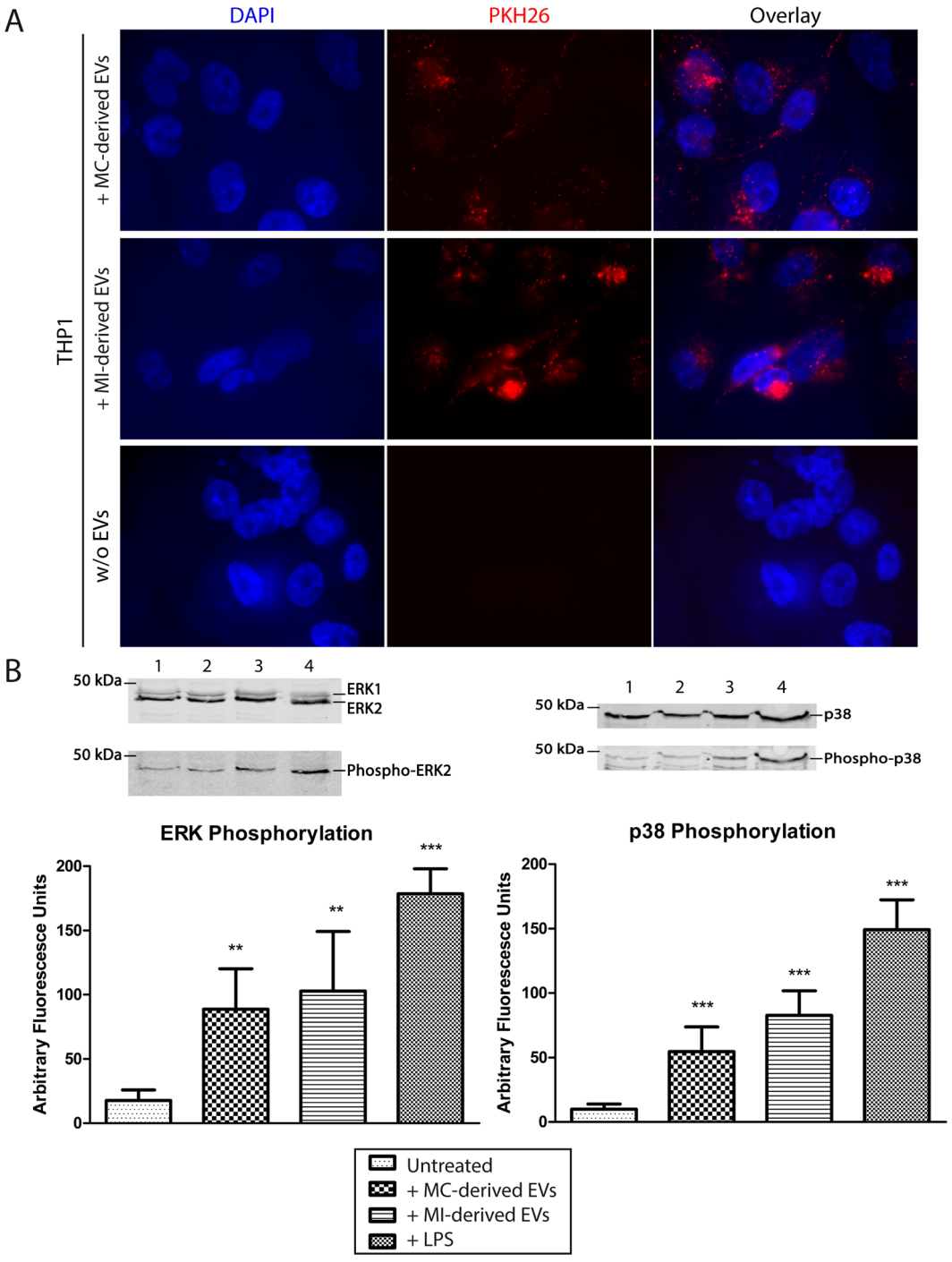

Figure 7. Effect of EVs in THP-1 macrophages. Differentiated THP-1 macrophages were coincubated with Macrophages Control (MC) and Macrophages infected with *C. albicans* (MI) derived EVs during 1 h. (A) Representative images of PKH 26-labeled EVs phagocyted by THP-1 macrophages; nuclei from macrophages are stained with DAPI. (B) After the incubation with MC- or MI-derived EVs or with LPS, THP-1 proteins were extracted and 30 μg of proteins was used to measure ERK and p38 phosphorylation. Samples were loaded in the lines as follows (1: untreated THP-1; 2: THP-1 + MC-derived EVs; 3: THP-1 + MI-derived EVs; 4: THP-1 + LPS). Western blotting representative images and the quantification (Arbitrary Fluorescence Units) of the phosphorylation levels of ERK and p38 are shown. Statistically significant differences are indicated (**, $p < 0.01$; ***, $p < 0.001$).

C. albicans (Table 1). The proteins that were differentially abundant in EVs were involved in functions related to immune response, signal transduction, stress response, cytoskeleton remodeling and metabolism, among others.

4.1. Proteins Involved in Immune Response

The chitinase-3-like protein 1 (CHI3L1) was the most differentially secreted protein. It binds to chitin with high affinity but has no chitinase activity registered. It has been described as an inflammation-associated inducible protein that enhances bacterial adhesion and invasion into macrophages and epithelial cells.[37] CHI3L1 secretion is increased in monocytes/macrophages, neutrophils, fibroblasts, granulocytes, epithelial, and tumor cells upon stimulation by inflammatory mediators,[37−39] and it stimulates the production of inflammatory

DOI: 10.1021/acs.jproteome.6b00605
J. Proteome Res. XXXX, XXX, XXX−XXX

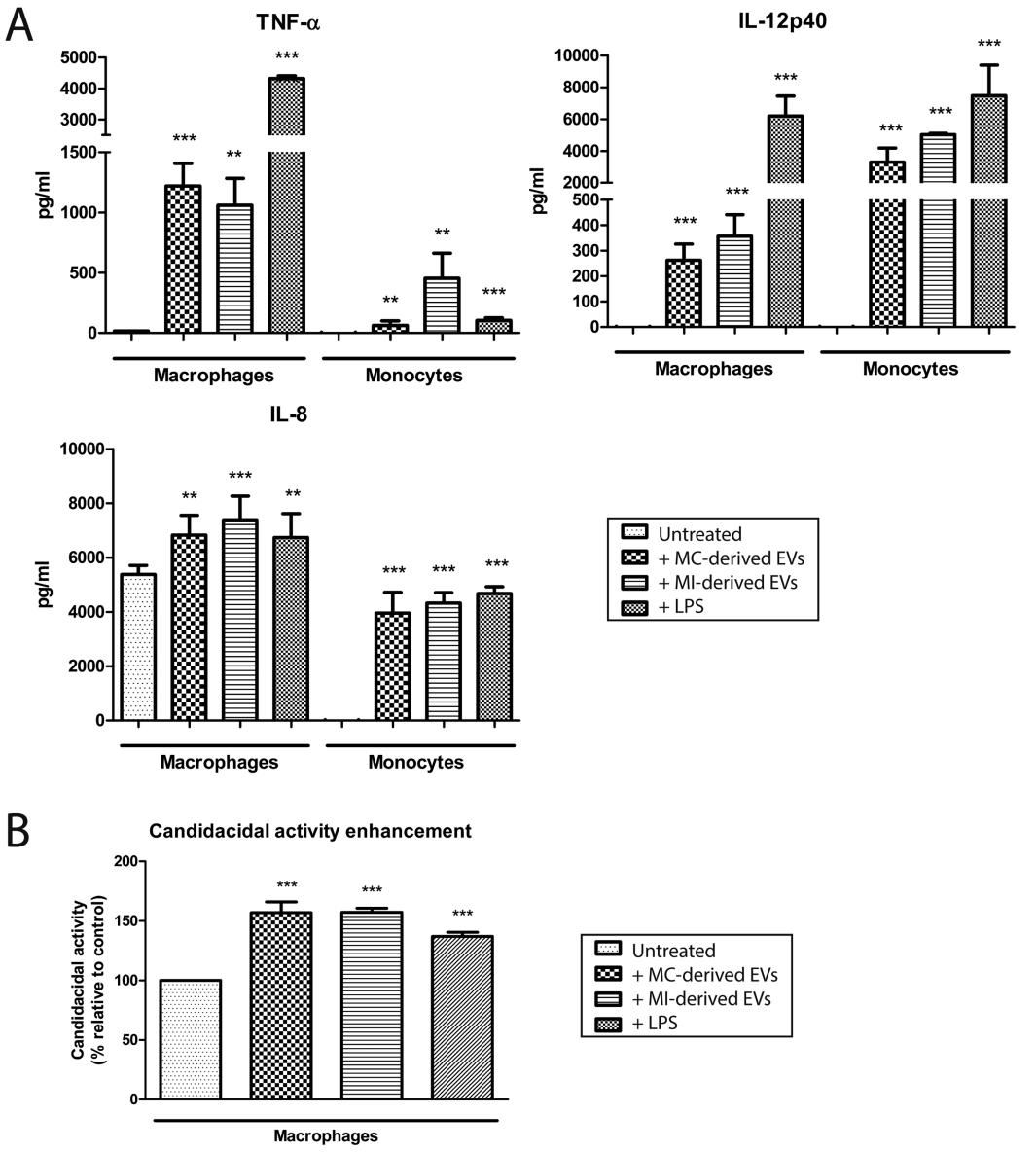

Figure 8. Cytokine profile and candidacidal activity of THP-1 cells stimulated with EVs. (A) TNFα, IL-12p40, and IL8 levels in THP-1 monocytes and macrophages exposed either to MC-, MI-derived EVs or LPS (as positive control) determined by ELISA. Monocytes and macrophages were treated with MC- and MI-derived EVs (100 μg/mL) or LPS (10 ng/mL) for 24 h. Data are represented as mean ± SD and statistical significance relative to the corresponding untreated macrophages that were used as negative control (*, $p < 0.05$; **, $p < 0.01$; ***, $p < 0.001$). (B) Candidacidal activity of THP-1 macrophages stimulated with either MC- or MI-derived EVs or LPS was exposed to *C. albicans* at a MOI of 1 during 3 h. Candidacidal activity was determined by plating *Candida* at 1/200 and 1/2000, and colony forming units (CFU) were counted. Data are relativized to untreated macrophages and represented as mean ± SD and statistical significance relative to the corresponding untreated macrophages (***, $p < 0.001$).

mediators (e.g., CLC2, CXCL2, and MMP9), being considered as an acute-phase reactant. CHI3L1 has been proposed as a pro-inflammatory marker[40] because it is more stimulated in M1 macrophages.[41] The specific function of this protein is unknown, but it is very important in cell proliferation and differentiation, inflammation and matrix remodeling, and activation of the immune responses.[42] With respect to infections, the CHI3L1secretion by macrophages and epithelial cells enhances the recognition and interaction of chitin-containing pathogens (such as fungi), leading to a pro-inflammatory response,[43,44] and it is also increased in *Plasmodium falciparum* infection.[45] Our results reinforce the importance of the secretion of CHI3L1 for the innate immune response against *C. albicans*.

Another important secreted protein is C−C motif chemokine 5 (CCL5), also known as RANTES, and its abundance in EVs decreases during interaction. This chemokine is secreted by macrophages, T cells, platelets, fibroblasts, epithelial cells, and some tumor cells, playing an important role in inflammatory diseases and tumors[46] acting as a molecular signal to induce cellular migration during inflammation. CCL5 is a signal peptide-containing cytokine that is secreted via classical pathway. However, the decrease in the level of this protein in the EVs may not indicate a decrease in the pro-inflammatory signals and neither does the secretion of the chemokine by the classical pathway because their immune activities can be performed by other chemokines.[47,48]

DOI: 10.1021/acs.jproteome.6b00605
J. Proteome Res. XXXX, XXX, XXX−XXX

Another chitinase, the acidic mammalian chitinase (CHIA/AMCase), is less abundant in MI-derived EVs. AMCase, as other chitinases, is secreted by macrophages in response to chitin-containing pathogens such as *Candida* and *Aspergillus*[49] against certain bacteria[50] and in nematode infections.[51] Its real function and its effect in the inflammation are under investigation. The expression of AMCase during macrophage differentiation and polarization does not significantly change.[52] Its activity has been described to be important in allergic inflammation and asthma.[53] This protein is secreted via classical pathway and has not been previously identified as secreted via EV-mediated secretion.

Interleukin-4-induced 1 (IL4I1) was less abundant in EVs after the interaction. This protein is a secreted L-amino acid oxidase that catalyzes the oxidation of L-phenylalanine and some other amino acids and inhibits T-cell proliferation in vitro.[54] IL4I1 protein expression has been observed in macrophages and dendritic cells under the influence of pro-inflammatory and T helper type 1 (Th1) mediators in vitro and contributes to the downregulation of Th1 inflammation.[55] Also, Yue et al. showed that IL4I1 protein was markedly increased by Th2 cytokines and promoted alternatively activated M2 macrophages that inhibit T cell activation.[56] Thus the decrease in IL4I1 can contribute to the pro-inflammatory effect of the macrophage-derived EVs in response to *C. albicans* infection.

One of the relevant functions related to EVs and immune responses are the pro-survival signals. Different proteins related to apoptosis have been identified in macrophage-derived EVs. Vimentin is one of the proteins that increases in EVs after *C. albicans* interaction. Its increase in MI-EVs was validated by Western blotting (Figure 5). This protein was previously identified as important for both murine[17,36] and human macrophages[18] in response to the fungus, while its expression was decreased during the interaction with heat-inactivated *C. albicans*.[35] This cytoskeletal protein is involved in attachment, migration, cell signaling, inflammation, and apoptosis and has bactericidal activity in vitro,[57−59] and its secretion is related to the enhancement of the bactericidal activity through the secretion of pro-inflammatory cytokines.[58] The increase in Vimentin secretion via EVs could be enhancing both the pro-inflammatory effect and the pro-survival effect in the surrounding cells.

The increase in DEK secretion in EVs after the interaction with the yeast could be related to its chemotactic activity. Activated macrophages secrete DEK, which acts as a chemoattractant factor for cytotoxic T lymphocytes, neutrophils, and natural killer cells.[60] Saha et al. report that DEK secreted by one cell can be uptaken by another cell, then translocated to the nucleus to develop its function (bind to cruciform and superhelical DNA and induce positive supercoils into closed circular DNA; also splice site selection during mRNA processing), playing an important role in the pro-survival signals.[61]

The increase in Vimentin and protein DEK in MI-derived EVs might be augmenting the effect on not only the pro-inflammatory and chemoattractant signals but also the pro-survival signals, suggesting an important role of these EVs in the macrophage response against *C. albicans* and in the THP-1 macrophages survival.

4.2. Proteins Involved in Signal Transduction

Several signaling proteins that have different abundance in EVs can play a significant role in *C. albicans* infection and contention. Three members of the Rho family of GTPases, belonging to the Ras superfamily (Cdc42, RhoC, and RIAM), which are reduced in abundance, are known to organize the actin cytoskeleton and regulate the phagocytic oxidative burst in macrophages.[62] Rho GTPases act as dualistic functions activating (GTP-bound) or inactivating (GDP-bound). This switch regulates different events during phagocytosis and the pathogen establishment, but the role of Cdc42 and RhoC in the macrophage-derived EVs and their decrease after the coculture remain unclear. RIAM (APBB1IP) has been implicated in the APC-T cell interaction. The knockdown of RIAM in THP-1 macrophages abrogated the increased $\alpha M\beta 2$ integrin affinity and the phagocytosis of complement-opsonized particles induced by Rap1 activation. Moreover, this protein has been described as a regulator of complement-dependent phagocytosis.[63] Thus its reduced abundance in MI-derived EVs might be a *C. albicans* defense mechanism.

Another important protein with reduced release by macrophage-EVs is the integrin-linked kinase (ILK); this protein is involved in cell−matrix interactions, cytoskeletal organization, and cell signaling, and it has also been related to apoptosis. ILK deletion resulted in apoptotic cell death in the lens epithelium,[64] and thus it could be a pro-apoptotic signal. These results about integrins and their related proteins are in disagreement with the result found in a previous work with macrophages stimulated with β-glucan.[16] In this work, integrins and the related proteins are increased in response to β-glucan. Moreover, the differentially abundant proteins found in EVs in response to β-glucan are different from the ones obtained in our experiments when THP-1 macrophages are in contact with *C. albicans*. It has already been described that alive *C. albicans* cells induce different response in macrophages than dead cells,[35] and thus these different results in EVs proteins in response to alive cells are in agreement with previous results.

4.3. EV Effect on Neighboring Macrophages and Monocytes

EVs are internalized by neighboring cells, being able to stimulate them and induce the phosphorylation of ERK2 and p38 kinases, leading to the secretion of pro-inflammatory cytokines (Figures 7 and 8A). The stimulatory effects were less marked than in the LPS-stimulated positive control for THP-1 macrophages, and the effect was not different between MI- and MC-derived EVs. However, in the case of monocytes, the stimuli induced by both EVs were higher compared with the LPS-positive control, supporting the roles of the differentially abundant proteins in these EVs. In the case of TNF-α secretion, the MI-derived EVs induced a statistically significant higher level, even higher than the one induced in the LPS control. Thus these results allow us to hypothesize that THP-1-infected macrophages send EVs to stimulate circulating monocytes to respond against *C. albicans* with a higher TNF-α secretion. Similar results have been observed with EVs from *Leishmania*-infected macrophages, which increase cytokine production in naïve macrophages.[13]

The candidacidal activity on THP-1 macrophages was enhanced by both populations of EVs, with no significant differences, suggesting a mechanism of unspecific enhancement of the immune response mediated by these EVs. It is remarkable that the effect of both kinds of EVs, in a similar quantity (with respect to protein concentration) was similar, even a slightly higher than the LPS standard activation conditions. We hypothesize that the expected differential effect

DOI: 10.1021/acs.jproteome.6b00605
J. Proteome Res. XXXX, XXX, XXX−XXX

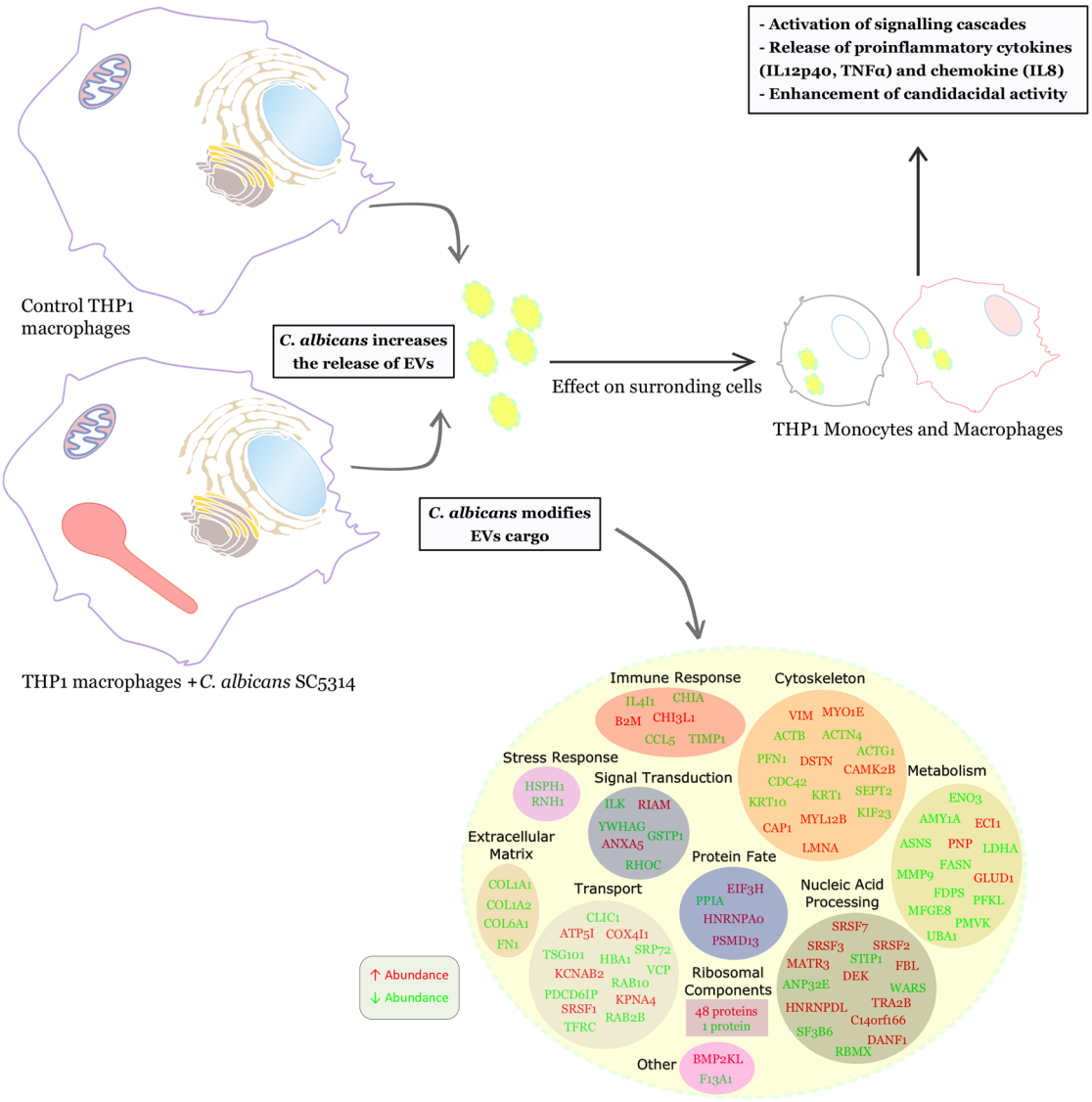

Figure 9. Summary of the results described in the manuscript. THP-1 MC- and MI-derived EVs were analyzed by TMT. The differentially abundant proteins are represented grouped by functions using red or green color depending on their variation tendency. The text describes the effects on THP-1 monocytes and differentiated macrophages from MC- and MI-derived EVs.

on neighboring monocytes and macrophages upon *C. albicans* infection might be due to the increase in the number of EVs that the macrophages that meet *C. albicans* release so as to signal other macrophages that there is danger of infection.

5. CONCLUDING REMARKS

These findings support the concept that EVs transport different signals with a wide range of impact on the recipient cells and that the signal carried by these EVs is changed by the interaction with *C. albicans* as it is by the interaction with other microorganisms. The main results of this approach are summarized in Figure 9.

The studies on the EVs cargo, particularly on the protein composition, will provide supporting information of how immune cells communicate with other surrounding cells in response to infections.

■ ASSOCIATED CONTENT

Supporting Information

The Supporting Information is available free of charge on the ACS Publications website at DOI: 10.1021/acs.jproteome.6b00605.

Figure S1. Experimental and TMT labeling designs followed in this study. Figure S2. Gene Ontology analysis of the THP-1-derived EVs compared to Vesiclepedia database. Figure S3. FunRich analysis of the differentially abundant proteins in the THP-1-derived EVs in response to *C. albicans*. Figure S4. FunRich analysis of the proteins that increase their abundance in the THP-1-derived EVs in response to *C. albicans*. Figure S5. FunRich analysis of the proteins that decrease their abundance in the THP-1-derived EVs in response to *C. albicans*. (PDF)

Table S1. Proteins identified and quantified in the EVs of the THP-1 macrophages after the interaction with *C. albicans*. (XLSX)

DOI: 10.1021/acs.jproteome.6b00605
J. Proteome Res. XXXX, XXX, XXX−XXX

Table S2. Scores of SignalP and SecretomeP software obtained for the proteins identified in the EVs of the THP-1 macrophages after the interaction with *C. albicans*. (XLSX)

AUTHOR INFORMATION

Corresponding Authors

* (G.M.) Tel: +34 91 394 2084. Fax: +34 91 394 1745. E-mail: gloros@ucm.es.
* (C.G.) Tel: +34 91 394 1743. Fax: +34 91 394 1745. E-mail: conchagil@ucm.es.

Present Address

†J.A.R.-C.: Singapore Immunology Network (SIgN), A*STAR 8A Biomedical Grove, Level 4, Immunos (Biopolis) Singapore, 138648. Tel: + 65 6407 0776. E-mail: Jose_Reales@immunol.a-star.edu.sg.

Author Contributions

The manuscript was written through contributions of all authors. All authors have given approval to the final version of the manuscript.

Notes

The authors declare no competing financial interest.

ACKNOWLEDGMENTS

This study was supported by grants from the Instituto de Salud Carlos III (Spanish Network for Research on Infectious Diseases, REIPI RD12/0015), Ministerio de Economía y Competitividad (Spanish Ministry of Economy and Competitiveness) (BIO2012-31767 and BIO2015-65147-R), and Comunidad Autónoma de Madrid (S2010/BMD2414 (PROMPT)) and the Marie Curie Initial Training Network (FP7-PEOPLE-2013-ITN ImResFun). The proteomic analysis was performed at the proteomics facility of the Universidad Complutense de Madrid (UCM) and in the proteomics facility of the Spanish National Center for Biotechnology (CNB-CSIC); both facilities belong to ProteoRed, PRB2-ISCIII, supported by grant PT13/0001. The transmission electron microscopy was carried out in Centro Nacional de Microscopía Electrónica (ICTS)-UCM and the environmental scanning electron microscopy at the Museo Nacional de Ciencias Naturales. Dynamic Light Scattering was carried out at the Correlation Spectroscopy facility of the Universidad Complutense de Madrid (UCM).

ABBREVIATIONS

EVs, extracellular vesicles; MVs, microvesicles; TMT, tandem mass tagging; MOI, multiplicity of infection; TEM, transmission electron microscopy; ESEM, environmental scanning electron microscopy; DLS, dynamic light scattering

REFERENCES

(1) Brown, G. D.; Denning, D. W.; Gow, N. A.; Levitz, S. M.; Netea, M. G.; White, T. C. Hidden killers: human fungal infections. *Sci. Transl. Med.* **2012**, *4* (165), 165rv13.

(2) Netea, M. G.; Joosten, L. A. Master and commander: epigenetic regulation of macrophages. *Cell Res.* **2016**, *26* (2), 145−6.

(3) Bourgeois, C.; Majer, O.; Frohner, I. E.; Tierney, L.; Kuchler, K. Fungal attacks on mammalian hosts: pathogen elimination requires sensing and tasting. *Curr. Opin. Microbiol.* **2010**, *13* (4), 401−8.

(4) Denzer, K.; Kleijmeer, M. J.; Heijnen, H. F.; Stoorvogel, W.; Geuze, H. J. Exosome: from internal vesicle of the multivesicular body to intercellular signaling device. *J. Cell Sci.* **2000**, *113* (Pt 19), 3365−74.

(5) Raposo, G.; Stoorvogel, W. Extracellular vesicles: Exosomes, microvesicles, and friends. *J. Cell Biol.* **2013**, *200* (4), 373−383.

(6) Reales-Calderon, J. A.; Corona, F.; Monteoliva, L.; Gil, C.; Martinez, J. L. Quantitative proteomics unravels that the post-transcriptional regulator Crc modulates the generation of vesicles and secreted virulence determinants of *Pseudomonas aeruginosa*. *J. Proteomics* **2015**, *127* (Pt B), 352−64.

(7) Gil-Bona, A.; Llama-Palacios, A.; Parra, C. M.; Vivanco, F.; Nombela, C.; Monteoliva, L.; Gil, C. Proteomics unravels extracellular vesicles as carriers of classical cytoplasmic proteins in *Candida albicans*. *J. Proteome Res.* **2015**, *14* (1), 142−53.

(8) Brown, L.; Wolf, J. M.; Prados-Rosales, R.; Casadevall, A. Through the wall: extracellular vesicles in Gram-positive bacteria, mycobacteria and fungi. *Nat. Rev. Microbiol.* **2015**, *13* (10), 620−630.

(9) Hassani, K.; Olivier, M. Immunomodulatory impact of *Leishmania*-induced macrophage exosomes: a comparative proteomic and functional analysis. *PLoS Neglected Trop. Dis.* **2013**, *7* (5), e2185.

(10) Keerthikumar, S.; Chisanga, D.; Ariyaratne, D.; Al Saffar, H.; Anand, S.; Zhao, K.; Samuel, M.; Pathan, M.; Jois, M.; Chilamkurti, N.; Gangoda, L.; Mathivanan, S. ExoCarta: A Web-Based Compendium of Exosomal Cargo. *J. Mol. Biol.* **2016**, *428* (4), 688−92.

(11) Singh, P. P.; Smith, V. L.; Karakousis, P. C.; Schorey, J. S. Exosomes isolated from mycobacteria-infected mice or cultured macrophages can recruit and activate immune cells in vitro and in vivo. *J. Immunol.* **2012**, *189* (2), 777−85.

(12) Wang, J.; Yao, Y.; Xiong, J.; Wu, J.; Tang, X.; Li, G. Evaluation of the inflammatory response in macrophages stimulated with exosomes secreted by *Mycobacterium avium*-infected macrophages. *BioMed Res. Int.* **2015**, *2015*, 658421.

(13) Cronemberger-Andrade, A.; Aragao-Franca, L.; de Araujo, C. F.; Rocha, V. J.; Borges-Silva, M. d. C.; Figueiras, C. P.; Oliveira, P. R.; de Freitas, L. A.; Veras, P. S.; Pontes-de-Carvalho, L. Extracellular vesicles from *Leishmania*-infected macrophages confer an anti-infection cytokine-production profile to naive macrophages. *PLoS Neglected Trop. Dis.* **2014**, *8* (9), e3161.

(14) Zhu, Y.; Chen, X.; Pan, Q.; Wang, Y.; Su, S.; Jiang, C.; Li, Y.; Xu, N.; Wu, L.; Lou, X.; Liu, S. A Comprehensive Proteomics Analysis Reveals a Secretory Path- and Status-Dependent Signature of Exosomes Released from Tumor-Associated Macrophages. *J. Proteome Res.* **2015**, *14* (10), 4319−31.

(15) Wang, J. J.; Chen, C.; Xie, P. F.; Pan, Y.; Tan, Y. H.; Tang, L. J. Proteomic analysis and immune properties of exosomes released by macrophages infected with Mycobacterium avium. *Microbes Infect.* **2014**, *16* (4), 283−91.

(16) Cypryk, W.; Ohman, T.; Eskelinen, E. L.; Matikainen, S.; Nyman, T. A. Quantitative proteomics of extracellular vesicles released from human monocyte-derived macrophages upon beta-glucan stimulation. *J. Proteome Res.* **2014**, *13* (5), 2468−77.

(17) Reales-Calderon, J. A.; Sylvester, M.; Strijbis, K.; Jensen, O. N.; Nombela, C.; Molero, G.; Gil, C. *Candida albicans* induces pro-inflammatory and anti-apoptotic signals in macrophages as revealed by quantitative proteomics and phosphoproteomics. *J. Proteomics* **2013**, *91*, 106−35.

(18) Reales-Calderon, J. A.; Aguilera-Montilla, N.; Corbi, A. L.; Molero, G.; Gil, C. Proteomic characterization of human proinflammatory M1 and anti-inflammatory M2 macrophages and their response to *Candida albicans*. *Proteomics* **2014**, *14* (12), 1503−18.

(19) Gillum, A. M.; Tsay, E. Y.; Kirsch, D. R. Isolation of the *Candida albicans* gene for orotidine-5′-phosphate decarboxylase by complementation of S. cerevisiae ura3 and E. coli pyrF mutations. *Mol. Gen. Genet.* **1984**, *198* (1), 179−82.

(20) Rodrigues, M. L.; Nimrichter, L.; Oliveira, D. L.; Frases, S.; Miranda, K.; Zaragoza, O.; Alvarez, M.; Nakouzi, A.; Feldmesser, M.; Casadevall, A. Vesicular polysaccharide export in *Cryptococcus neoformans* is a eukaryotic solution to the problem of fungal trans-cell wall transport. *Eukaryotic Cell* **2007**, *6* (1), 48−59.

DOI: 10.1021/acs.jproteome.6b00605
J. Proteome Res. XXXX, XXX, XXX−XXX

(21) Oliveira, D. L.; Nakayasu, E. S.; Joffe, L. S.; Guimaraes, A. J.; Sobreira, T. J.; Nosanchuk, J. D.; Cordero, R. J.; Frases, S.; Casadevall, A.; Almeida, I. C.; Nimrichter, L.; Rodrigues, M. L. Characterization of yeast extracellular vesicles: evidence for the participation of different pathways of cellular traffic in vesicle biogenesis. *PLoS One* **2010**, *5* (6), e11113.
(22) Eisenman, H. C.; Frases, S.; Nicola, A. M.; Rodrigues, M. L.; Casadevall, A. Vesicle-associated melanization in *Cryptococcus neoformans*. *Microbiology* **2009**, *155* (Pt 12), 3860−7.
(23) Wessel, D.; Flugge, U. I. A method for the quantitative recovery of protein in dilute solution in the presence of detergents and lipids. *Anal. Biochem.* **1984**, *138* (1), 141−3.
(24) Vizcaino, J. A.; Cote, R. G.; Csordas, A.; Dianes, J. A.; Fabregat, A.; Foster, J. M.; Griss, J.; Alpi, E.; Birim, M.; Contell, J.; O'Kelly, G.; Schoenegger, A.; Ovelleiro, D.; Perez-Riverol, Y.; Reisinger, F.; Rios, D.; Wang, R.; Hermjakob, H. The PRoteomics IDEntifications (PRIDE) database and associated tools: status in 2013. *Nucleic Acids Res.* **2013**, *41* (Database issue), D1063−9.
(25) Ramos-Fernandez, A.; Paradela, A.; Navajas, R.; Albar, J. P. Generalized method for probability-based peptide and protein identification from tandem mass spectrometry data and sequence database searching. *Mol. Cell. Proteomics* **2008**, *7* (9), 1748−54.
(26) Lopez-Serra, P.; Marcilla, M.; Villanueva, A.; Ramos-Fernandez, A.; Palau, A.; Leal, L.; Wahi, J. E.; Setien-Baranda, F.; Szczesna, K.; Moutinho, C.; et al. A DERL3-associated defect in the degradation of SLC2A1 mediates the Warburg effect. *Nat. Commun.* **2014**, *5*, 5.
(27) Bhatia, V. N.; Perlman, D. H.; Costello, C. E.; McComb, M. E. Software tool for researching annotations of proteins: open-source protein annotation software with data visualization. *Anal. Chem.* **2009**, *81* (23), 9819−23.
(28) Benito-Martin, A.; Peinado, H. FunRich proteomics software analysis, let the fun begin! *Proteomics* **2015**, *15* (15), 2555−6.
(29) Petersen, T. N.; Brunak, S.; von Heijne, G.; Nielsen, H. SignalP 4.0: discriminating signal peptides from transmembrane regions. *Nat. Methods* **2011**, *8* (10), 785−786.
(30) Bendtsen, J. D.; Kiemer, L.; Fausboll, A.; Brunak, S. Non-classical protein secretion in bacteria. *BMC Microbiol.* **2005**, *5*, 58.
(31) Keerthikumar, S.; Chisanga, D.; Ariyaratne, D.; Al Saffar, H.; Anand, S.; Zhao, K.; Samuel, M.; Pathan, M.; Jois, M.; Chilamkurti, N.; Gangoda, L.; Mathivanan, S. ExoCarta: A Web-Based Compendium of Exosomal Cargo. *J. Mol. Biol.* **2016**, *428*, 688.
(32) Diez-Orejas, R.; Molero, G.; Moro, M. A.; Gil, C.; Nombela, C.; Sanchez-Perez, M. Two different NO-dependent mechanisms account for the low virulence of a non-mycelial morphological mutant of *Candida albicans*. *Med. Microbiol. Immunol.* **2001**, *189* (3), 153−160.
(33) Thery, C.; Regnault, A.; Garin, J.; Wolfers, J.; Zitvogel, L.; Ricciardi-Castagnoli, P.; Raposo, G.; Amigorena, S. Molecular characterization of dendritic cell-derived exosomes: Selective accumulation of the heat shock protein hsc73. *J. Cell Biol.* **1999**, *147* (3), 599−610.
(34) Ung, T. H.; Madsen, H. J.; Hellwinkel, J. E.; Lencioni, A. M.; Graner, M. W. Exosome proteomics reveals transcriptional regulator proteins with potential to mediate downstream pathways. *Cancer Sci.* **2014**, *105* (11), 1384−92.
(35) Martínez-Solano, L.; Reales-Calderón, J. A.; Nombela, C.; Molero, G.; Gil, C. Proteomics of RAW 264.7 macrophages upon interaction with heat-inactivated *Candida albicans* cells unravel an anti-inflammatory response. *Proteomics* **2009**, *9* (11), 2995−3010.
(36) Reales-Calderon, J. A.; Martinez-Solano, L.; Martinez-Gomariz, M.; Nombela, C.; Molero, G.; Gil, C. Sub-proteomic study on macrophage response to *Candida albicans* unravels new proteins involved in the host defense against the fungus. *J. Proteomics* **2012**, *75* (15), 4734−46.
(37) Mizoguchi, E. Chitinase 3-like-1 exacerbates intestinal inflammation by enhancing bacterial adhesion and invasion in colonic epithelial cells. *Gastroenterology* **2006**, *130* (2), 398−411.
(38) Volck, B.; Price, P. A.; Johansen, J. S.; Sorensen, O.; Benfield, T. L.; Nielsen, H. J.; Calafat, J.; Borregaard, N. YKL-40, a mammalian member of the Chitinase family, is a matrix protein of specific granules in human neutrophils. *Proc. Assoc. Am. Physicians* **1998**, *110* (4), 351−360.
(39) Rehli, M.; Niller, H. H.; Ammon, C.; Langmann, S.; Schwarzfischer, L.; Andreesen, R.; Krause, S. W. Transcriptional regulation of CHI3L1, a marker gene for late stages of macrophage differentiation. *J. Biol. Chem.* **2003**, *278* (45), 44058−67.
(40) Lee, J. H.; Kim, S. S.; Kim, I. J.; Song, S. H.; Kim, Y. K.; In Kim, J.; Jeon, Y. K.; Kim, B. H.; Kwak, I. S. Clinical implication of plasma and urine YKL-40, as a proinflammatory biomarker, on early stage of nephropathy in type 2 diabetic patients. *J. Diabetes Complications* **2012**, *26* (4), 308−12.
(41) Di Rosa, M.; Malaguarnera, G.; De Gregorio, C.; Drago, F.; Malaguarnera, L. Evaluation of CHI3L-1 and CHIT-1 expression in differentiated and polarized macrophages. *Inflammation* **2013**, *36* (2), 482−92.
(42) Johansen, J. S. Studies on serum YKL-40 as a biomarker in diseases with inflammation, tissue remodelling, fibroses and cancer. *Dan. Med. Bull.* **2006**, *53* (2), 172−209.
(43) Cario, E.; Gerken, G.; Podolsky, D. K. Toll-like receptor 2 controls mucosal inflammation by regulating epithelial barrier function. *Gastroenterology* **2007**, *132* (4), 1359−74.
(44) Heimesaat, M. M.; Fischer, A.; Siegmund, B.; Kupz, A.; Niebergall, J.; Fuchs, D.; Jahn, H. K.; Freudenberg, M.; Loddenkemper, C.; Batra, A.; Lehr, H. A.; Liesenfeld, O.; Blaut, M.; Gobel, U. B.; Schumann, R. R.; Bereswill, S. Shift towards pro-inflammatory intestinal bacteria aggravates acute murine colitis via Toll-like receptors 2 and 4. *PLoS One* **2007**, *2* (7), e662.
(45) Barone, R.; Simpore, J.; Malaguarnera, L.; Pignatelli, S.; Musumeci, S. Plasma chitotriosidase activity in acute *Plasmodium falciparum* malaria. *Clin. Chim. Acta* **2003**, *331* (1−2), 79−85.
(46) Soria, G.; Ben-Baruch, A. The inflammatory chemokines CCL2 and CCL5 in breast cancer. *Cancer Lett.* **2008**, *267* (2), 271−285.
(47) Devalaraja, M. N.; Richmond, A. Multiple chemotactic factors: fine control or redundancy? *Trends Pharmacol. Sci.* **1999**, *20* (4), 151−156.
(48) Mantovani, A. The chemokine system: redundancy for robust outputs. *Immunology Today* **1999**, *20* (6), 254−257.
(49) Renkema, G. H.; Boot, R. G.; Muijsers, A. O.; Donkerkoopman, W. E.; Aerts, J. M. F. G. Purification and Characterization of Human Chitotriosidase, a Novel Member of the Chitinase Family of Proteins. *J. Biol. Chem.* **1995**, *270* (5), 2198−2202.
(50) Cozzarini, E.; Bellin, M.; Norberto, L.; Polese, L.; Musumeci, S.; Lanfranchi, G.; Paoletti, M. G. CHIT1 and AMCase expression in human gastric mucosa: correlation with inflammation and *Helicobacter pylori* infection. *Eur. J. Gastroenterol. Hepatol.* **2009**, *21* (10), 1119−26.
(51) Nair, M. G.; Gallagher, L. J.; Taylor, M. D.; Loke, P.; Coulson, P. S.; Wilson, R. A.; Maizels, R. M.; Allen, J. E. Chitinase and Fizz family members are a generalized feature of nematode infection with selective Upregulation of Ym1 and F10.1 by antigen-presenting cells. *Infect. Immun.* **2005**, *73* (1), 385−394.
(52) Di Rosa, M.; De Gregorio, C.; Malaguarnera, G.; Tuttobene, M.; Biazzo, F.; Malaguarnera, L. Evaluation of AMCase and CHIT-1 expression in monocyte macrophages lineage. *Mol. Cell. Biochem.* **2013**, *374* (1−2), 73−80.
(53) Shen, C. R.; Juang, H. H.; Chen, H. S.; Yang, C. J.; Wu, C. J.; Lee, M. H.; Hwang, Y. S.; Kuo, M. L.; Chen, Y. S.; Chen, J. K.; Liu, C. L. The Correlation between Chitin and Acidic Mammalian Chitinase in Animal Models of Allergic Asthma. *Int. J. Mol. Sci.* **2015**, *16* (11), 27371−27377.
(54) Boulland, M. L.; Marquet, J.; Molinier-Frenkel, V.; M?ller, P.; Guiter, C.; Lasoudris, F.; Copie-Bergman, C.; Baia, M.; Gaulard, P.; Leroy, K.; Castellano, F. Human IL4I1 is a secreted L-phenylalanine oxidase expressed by mature dendritic cells that inhibits T-lymphocyte proliferation. *Blood* **2007**, *110* (1), 220−227.
(55) Marquet, J.; Lasoudris, F.; Cousin, C.; Puiffe, M. L.; Martin-Garcia, N.; Baud, V.; Chereau, F.; Farcet, J. P.; Molinier-Frenkel, V.; Castellano, F. Dichotomy between factors inducing the immunosuppressive enzyme IL-4-induced gene 1 (IL4I1) in B lymphocytes and mononuclear phagocytes. *Eur. J. Immunol.* **2010**, *40* (9), 2557−2568.

DOI: 10.1021/acs.jproteome.6b00605
J. Proteome Res. XXXX, XXX, XXX−XXX

(56) Yue, Y. P.; Huang, W.; Liang, J. J.; Guo, J.; Ji, J.; Yao, Y. L.; Zheng, M. Z.; Cai, Z. J.; Lu, L. R.; Wang, J. L. IL4I1 Is a Novel Regulator of M2Macrophage Polarization That Can Inhibit T Cell Activation via L-Tryptophan and Arginine Depletion and IL-10 Production. *PLoS One* **2015**, *10* (11), e0142979.
(57) Benes, P.; Maceckova, V.; Zdrahal, Z.; Konecna, H.; Zahradnickova, E.; Muzik, J.; Smarda, J. Role of vimentin in regulation of monocyte/macrophage differentiation. *Differentiation* **2006**, *74* (6), 265−276.
(58) Mor-Vaknin, N.; Punturieri, A.; Sitwala, K.; Markovitz, D. M. Vimentin is secreted by activated macrophages. *Nat. Cell Biol.* **2002**, *5* (1), 59−63.
(59) Perlson, E.; Michaelevski, I.; Kowalsman, N.; Ben-Yaakov, K.; Shaked, M.; Seger, R.; Eisenstein, M.; Fainzilber, M. Vimentin binding to phosphorylated Erk sterically hinders enzymatic dephosphorylation of the kinase. *J. Mol. Biol.* **2006**, *364* (5), 938−44.
(60) Mor-Vaknin, N.; Punturieri, A.; Sitwala, K.; Faulkner, N.; Legendre, M.; Khodadoust, M. S.; Kappes, F.; Ruth, J. H.; Koch, A.; Glass, D.; Petruzzelli, L.; Adams, B. S.; Markovitz, D. M. The DEK nuclear autoantigen is a secreted chemotactic factor. *Mol. Cell. Biol.* **2006**, *26* (24), 9484−9496.
(61) Saha, A. K.; Kappes, F.; Mundade, A.; Deutzmann, A.; Rosmarin, D. M.; Legendre, M.; Chatain, N.; Al-Obaidi, Z.; Adams, B. S.; Ploegh, H. L.; Ferrando-May, E.; Mor-Vaknin, N.; Markovitz, D. M. Intercellular trafficking of the nuclear oncoprotein DEK. *Proc. Natl. Acad. Sci. U. S. A.* **2013**, *110* (17), 6847−6852.
(62) Etienne-Manneville, S.; Hall, A. Rho GTPases in cell biology. *Nature* **2002**, *420* (6916), 629−35.
(63) Medrano-Fernandez, I.; Reyes, R.; Olazabal, I.; Rodriguez, E.; Sanchez-Madrid, F.; Boussiotis, V. A.; Reche, P. A.; Cabanas, C.; Lafuente, E. M. RIAM (Rap1-interacting adaptor molecule) regulates complement-dependent phagocytosis. *Cell. Mol. Life Sci.* **2013**, *70* (13), 2395−410.
(64) Cammas, L.; Wolfe, J.; Choi, S. Y.; Dedhar, S.; Beggs, H. E. Integrin-linked kinase deletion in the developing lens leads to capsule rupture, impaired fiber migration and non-apoptotic epithelial cell death. *Invest. Ophthalmol. Visual Sci.* **2012**, *53* (6), 3067−81.

DOI: 10.1021/acs.jproteome.6b00605
J. Proteome Res. XXXX, XXX, XXX−XXX

SCIENTIFIC REPORTS

OPEN

Trk1-mediated potassium uptake contributes to cell-surface properties and virulence of *Candida glabrata*

Received: 30 January 2019
Accepted: 25 April 2019
Published online: 17 May 2019

Vicent Llopis-Torregrosa[1], Catarina Vaz[2], Lucia Monteoliva[2], Kicki Ryman[3], Ylva Engstrom[3], Attila Gacser[4,5], Concha Gil[2], Per O. Ljungdahl[3] & Hana Sychrová[1]

The absence of high-affinity potassium uptake in *Candida glabrata*, the consequence of the deletion of the *TRK1* gene encoding the sole potassium-specific transporter, has a pleiotropic effect. Here, we show that in addition to changes in basic physiological parameters (e.g., membrane potential and intracellular pH) and decreased tolerance to various cell stresses, the loss of high affinity potassium uptake also alters cell-surface properties, such as an increased hydrophobicity and adherence capacity. The loss of an efficient potassium uptake system results in diminished virulence as assessed by two insect host models, *Drosophila melanogaster* and *Galleria mellonella*, and experiments with macrophages. Macrophages kill *trk1*Δ cells more effectively than wild type cells. Consistently, macrophages accrue less damage when co-cultured with *trk1*Δ mutant cells compared to wild-type cells. We further show that low levels of potassium in the environment increase the adherence of *C. glabrata* cells to polystyrene and the propensity of *C. glabrata* cells to form biofilms.

The incidence of fungal infections of the *Candida* genus has increased in recent decades, and among them *Candida glabrata* is classified as the second most commonly isolated yeast in the majority of patient populations studied[1–4]. The reasons for this upswing are on the one side medical progress by itself, which has increased life expectancy, but also the niches where opportunistic fungi can develop. The use of antibiotics, catheters or transplantation therapies has generated a susceptible population that has helped fungal pathogens come to the front line of clinical problems in developed countries[5,6]. The success of various yeast species as pathogens depends on their ability to adapt to the environmental stresses they encounter within the diverse niches they occupy in the human host[7]. For many years, pathogenic yeasts were assumed to passively contribute to the establishment of infection, but nowadays, it is well known that these organisms dynamically participate in the disease process through mechanisms of aggression, called virulence factors. Among these factors, the ability to evade host defenses, adherence, biofilm formation and the production of tissue-damaging hydrolytic enzymes play a crucial role[8,9].

Candida glabrata, a member of the WGD (Whole Genome Duplication) yeast family and a close relative of *Saccharomyces cerevisiae*, is an opportunistic yeast pathogen that is distantly related to the CTG clade of yeast (yeast species translating the CUG codon as serine instead of leucine), which includes most of the pathogenic *Candida* species[10]. Its high stress resistance and high adhesion capacity are characteristics that make *C. glabrata* a serious pathogen for humans[11]. The ability of *C. glabrata* to respond to changes in environmental conditions with rapid transcriptional reprogramming, together with its robust resistance to both nutrient starvation and oxidative stress[12], are properties that provide *C. glabrata* a competitive advantage when nutrient availability is low, such as on mucosal surfaces or within phagosomes after engulfment by phagocytic cells. In the latter case, *Candida* cells

[1]Department of Membrane Transport, Institute of Physiology of the Czech Academy of Sciences, 14220, Prague 4, Czech Republic. [2]Department of Microbiology and Parasitology, Faculty of Pharmacy, Complutense University of Madrid and IRYCIS, Madrid, Spain. [3]Department of Molecular Biosciences, The Wenner-Gren Institute, Stockholm University, SE-10691, Stockholm, Sweden. [4]Department of Microbiology, University of Szeged Interdisciplinary Excellence Centre, Szeged, Hungary. [5]MTA-SZTE "Lendület" "Mycobiome" Research Group, University of Szeged, Szeged, Hungary. Correspondence and requests for materials should be addressed to H.S. (email: hana.sychrova@fgu.cas.cz)

are also exposed to reactive oxygen species and reactive nitrogen species[13], moreover, host immune cells also activate intracellular ion currents that might expose *Candida* cells to cationic and osmotic stresses[14]. Given this situation, it is not surprising that *C. glabrata*, as well as other *Candida spp*., have evolved a robust tolerance to cationic/osmotic, oxidative and nitrosative stresses[15,16].

Adherence is one of the crucial steps in the establishment of fungal infections, and it is a feature that enables *C. glabrata* to adhere to host epithelial tissues and other surfaces, e.g., catheters. This trait is coupled to virulence, and is mediated by cell-wall associated proteins termed adhesins, which belong to diverse protein families. Several studies have demonstrated that *C. glabrata* has a large repertoire of adhesins[17,18], which facilitate its ability to colonize humans. Another factor, considered important for virulence, and related to adherence, is cell-surface hydrophobicity (CSH), which depends on the cell-wall composition and architecture. The relative CSH of *C. glabrata* is thought to be more extensive than that of *Candida albicans*, the best studied yeast pathogen[19]. After the adhesion to host tissues or other surfaces within the host, yeast cells grow and develop a biofilm, i.e., a population of cells embedded within a self-synthesized extracellular matrix[20]. *C. glabrata* biofilms, composed of a compact monolayer or multilayer of only blastospores[21], are extremely resistant to antifungal therapies, being able to withstand much higher concentrations of antifungal drugs than planktonic cells, and thus making *C. glabrata* biofilm infections extremely challenging to treat[22].

In addition to virulence factors, such as adhesion and biofilm formation, fitness traits such as rapid adaptation to fluctuations in environmental pH, metabolic flexibility, powerful nutrient acquisition systems and robust stress response machineries, influence fungal pathogenicity and support the ability of *Candida spp*. to infect diverse host niches. Many studies have shown that the disruption of various signaling and/or metabolic pathways has led to a diminished virulence and pathogenicity of yeast cells[23]. Also important in the establishment of the infection, is the expression of efficient and robust systems for the uptake of different compounds serving as carbon or nitrogen sources, or providing necessary metal ions, such as iron or zinc[24–27].

Potassium is the most abundant metal cation in all organisms. Due to its low toxicity and high ability to bind water, it has many general physiological functions in all cells. Consistent with its importance, cells spend a lot of energy to accumulate potassium in relatively high concentrations. In general, it is indispensable for establishing intracellular turgor, which is necessary for cell growth and expansion, and for the compensation of negative charges of many macromolecules, including DNA, RNA and polyphosphates. In yeast, potassium fluxes and accumulation are also indispensable for the regulation of intracellular pH and membrane potential, for the activation of various enzymes, for protein synthesis and many other functions[28–30]. Yeast cells have three types of potassium uptake systems, which allow cells to concentrate potassium to a 200–300 mM concentration from the environment with as low as micromolar concentrations of potassium salts[28–31]. All three types of transporters exist in *Candida* species[32]. They share the same basic function (the uptake of potassium) but are very different from the mechanistic, structural and phylogenetic points of view. Moreover, none of them has a homologue in mammalian cells. *C. albicans* has all three types of these transporters, i.e., the Trk uniporter, Hak potassium-proton symporter and Acu potassium-influx ATPase[33]. This might be an advantage in proliferating in host niches with relatively low potassium concentrations, or in formation and rapid growth of hyphae, a process which needs a high intracellular turgor[34].

The *C. glabrata* genome has only a single potassium-uptake system encoded by *TRK1*. This is surprising, since most yeast species have at least two types of potassium uptake systems (usually Trk and Hak, reviewed in[29]) and the closely related *S. cerevisiae* has two *TRK* genes[35,36]. The existence of only one potassium-uptake system in *C. glabrata* and the need of yeast cells to accumulate high intracellular K^+ concentrations to ensure cell growth and division, turned our attention to the characterization of *C. glabrata* Trk1 and the phenotypes of its absence[37]. We showed that *TRK1* indeed encodes an efficient potassium uptake system in *C. glabrata* cells. The expression of *CkTRK1* is low and constitutive, similarly as the expression of *TRK1* in *S. cerevisiae*[28]. The deletion of *TRK1* has a pleiotropic effect on the cell physiology, not only affecting the ability of *trk1Δ* mutants to grow at low potassium concentrations, but also their tolerance to toxic alkali-metal cations and cationic drugs, as well as the ability to maintain their membrane potential and intracellular pH. Taken together, our current understanding is that the sole potassium uptake system of *C. glabrata* is critical to its physiology and fitness, and suggests that potassium uptake may affect virulence. In this report we compare *C. glabrata* strains lacking *TRK1 (trk1Δ)* with its wild-type parent, focusing on traits related to virulence, such as cell surface properties, the ability to cause infections in two insect host models and challenge to phagocytosis by macrophages.

Results

Lack of Trk1 increases cell surface hydrophobicity and adherence capacity. The yeast cell wall has a highly dynamic structure, and its composition is tightly controlled not only during the cell cycle, but also in the different growth phases and during the adaptation to environmental changes. Alterations in cell-wall composition have consequences such as the modification of CSH or altered susceptibilities to cell-wall targeted drugs[17]. To elucidate whether the observed changes in membrane potential and susceptibility to cationic drugs of the *trk1Δ* mutant[37] are also reflected in the cell surface properties, we compared the CSH of wild-type and *trk1Δ* cells. The relative CSHs were estimated with cells grown under two conditions – in the presence of 100 mM KCl (a concentration at which *trk1Δ* cells can grow but clearly experience low-potassium stress, Fig. 1A) and 250 mM KCl (a concentration at which both the wild type and *trk1Δ* strains grow similarly, Fig. 1B). As shown in Fig. 1C, the mutant strain exhibited a higher hydrophobicity at both of the tested KCl concentrations. As expected, the CSH of the mutant was higher than that of the wild type when cells were grown with 100 mM KCl, but strikingly, a significantly higher CSH was observed for the *trk1Δ* cells in 250 mM KCl, i.e., a concentration close to the physiological intracellular concentration (approx. 280 mM in exponentially growing *C. glabrata* cells[38]). This latter observation suggested that the absence of Trk1-mediated transport leads to permanent changes in the cell wall, and consequently, to changes in cell surface hydrophobicity. Changes in cell-wall or plasma-membrane composition may be

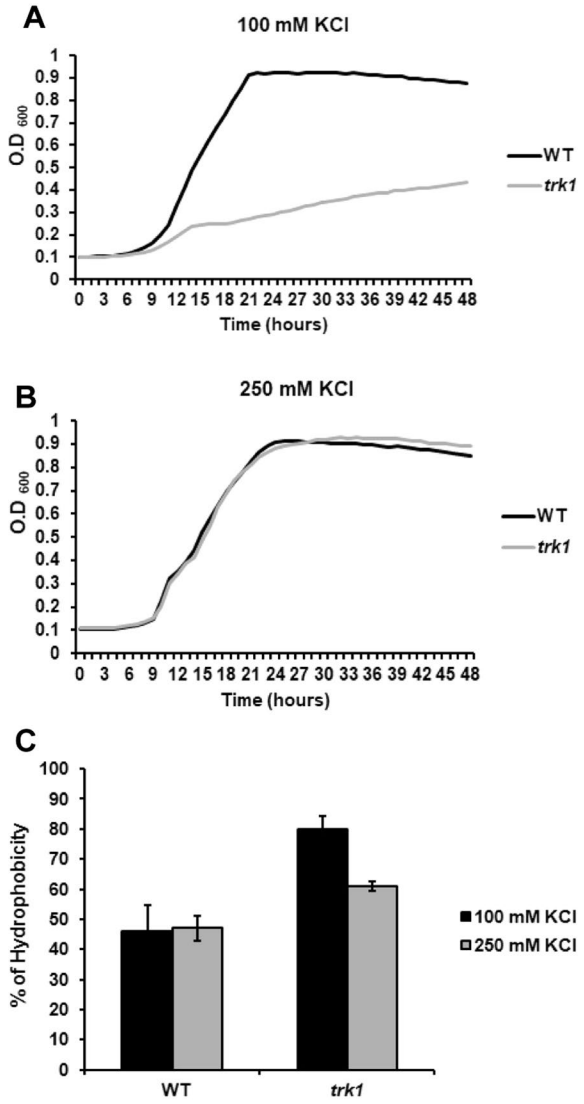

Figure 1. Hydrophobicity of *C. glabrata* cell surface depends on Trk1 function. The growth of cells was monitored in YNB-F medium supplemented with 100 mM (**A**) or 250 mM (**B**) KCl. The relative hydrophobicity (**C**) of the wild-type and *trk1Δ* cells grown in YNB-F media supplemented with 100 or 250 mM KCl was estimated as described in Methods.

reflected in increased cell sensitivity to compounds such as Congo red or SDS. For this reason, we tested whether the *trk1*Δ mutant exhibited alterations in growth when these two compounds were added to the media. No significant differences were observed between the growth of the wild-type strain and the mutant on solid media supplemented with 250 mM KCl and SDS (up to 0.05%) or Congo red (up to 400 µg/ml) (data non-shown).

Alterations in potassium fluxes and homeostasis may affect the adhesion capacity of *C. glabrata* to polystyrene. We therefore compared the adhesion properties of the wild-type and the *trk1*Δ strains grown in the presence of 100 or 250 mM KCl. As shown in Fig. 2A, the adhesion capacity of the wild type was almost the same under both growth conditions. On the other hand, the adhesion capacity of the mutant changed with the availability of potassium in the growth medium. As compared to wild-type cells, the *trk1*Δ cells adhered similarly at 250 mM KCl, but when grown in 100 mM KCl, their adhesion capacity was significantly increased. Thus, the higher CSH of the *trk1*Δ mutant (Fig. 1C) was not accompanied by an increased adhesion when the cells were grown at 250 mM KCl. To verify the differences, the same experiments were performed with another independently constructed *trk1*Δ mutant and the same results were obtained (data shown only for one of the two mutant strains).

These results led us to test the specific role of potassium in cell adherence. Cells were grown in 100 mM KCl (non-stress conditions for the wild-type strain, low-potassium stress for the *trk1*Δ mutant), and then shifted to YNB-F without the addition of any salt (YNB-F contains 15 µM K^+) or supplemented with either 100 mM KCl, 100 mM NaCl, or 100 mM $CaCl_2$. The results (Fig. 2B) show that when cells were shifted from YNB-F with 100 mM KCl to YNB-F lacking salt (−), both wild-type and *trk1Δ* cells increased their adhesion to polystyrene significantly, and to a similar level. This increase was also present for both strains when cells were transferred to media with 100 mM NaCl or $CaCl_2$. The results suggest that *C. glabrata* adherence is a potassium-specific phenotype.

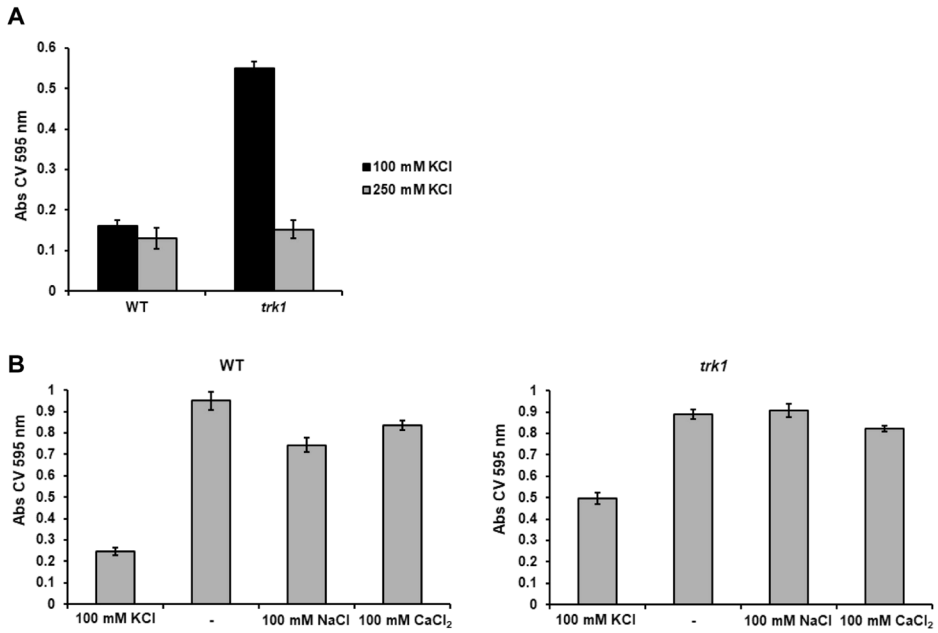

Figure 2. *C. glabrata* adherence capacity depends on amount of potassium in environment. (**A**) The adherence of the wild-type and *trk1Δ* cells grown in YNB-F media supplemented with 100 or 250 mM KCl to polystyrene was estimated as described in Methods. (**B**) Cells pregrown in YNB-F media supplemented with 100 mM KCl were transferred to YNB-F media without extra added KCl (−) or supplemented with NaCl or $CaCl_2$ as indicated, and their adherence capacity was estimated as described in Methods.

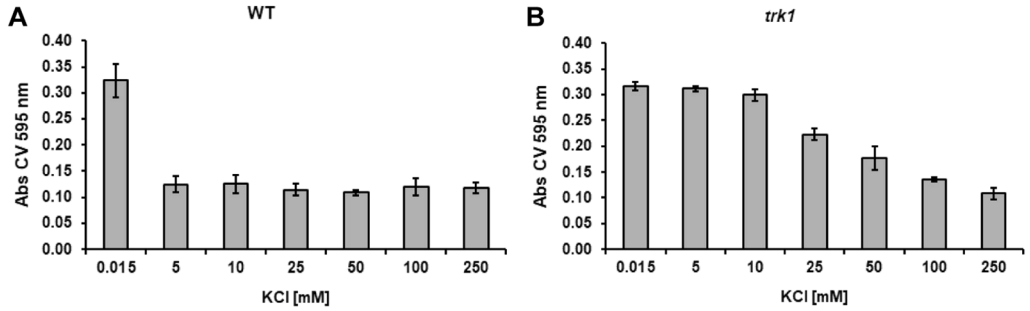

Figure 3. Limited external potassium increases biofilm formation. Wild-type and *trk1Δ* cells were pregrown in YNB-F supplemented with 250 mM KCl, then the adherence step in the same medium occurred for 2 h, non-adhered cells were washed out, fresh YNB-F medium supplemented with KCl as indicated was added, and the biofilm formation was estimated after 48 h as described in Methods.

Potassium influences formation of biofilms. It is believed that the formation of mature biofilms and the production of extracellular matrix is strongly dependent on species, strain, and environmental conditions such as pH, medium composition and oxygen availability[39]. As we observed a potassium-dependent increase in the adherence ability of *C. glabrata* cells, we speculated that the formation of a biofilm might also be dependent on the availability of potassium cations. Cells were pre-grown in YNB-F supplemented with 250 mM KCl, i.e. under conditions in which both strains exhibited similar adherence (Fig. 2A), transferred to polystyrene plates, and after a two-hour incubation, the medium was replaced with a series of media containing KCl at concentrations ranging from 15 µM to 250 mM. For the wild-type strain, a significant biofilm was formed only when grown in YNB-F without added potassium (0.015 mM; Fig. 3A); similar low levels of biofilm formation were observed at KCl concentrations between 5–250 mM. By contrast, the *trk1*Δ mutant formed biofilms over a wide range of KCl concentrations; significant biofilms formed even at 100 mM KCl (Fig. 3B). At the higher KCl concentrations tested, the *trk1*Δ mutant produced significantly larger biofilms than the wild type. These results suggested that potassium availability and its transport to cells have a direct effect on biofilm formation. The capacity of *C. glabrata* to form biofilms was inversely proportional to the K^+ concentration, suggesting that cellular stress resulting from potassium limitation promotes biofilm formation.

Absence of Trk1 makes *C. glabrata* less virulent in insect models. The higher cell-surface hydrophobicity, as well as the higher adherence and biofilm formation of *trk1*Δ cells in the presence of a standard potassium concentration suggested that the mutant cells might be more virulent than the wild-type. On the other hand,

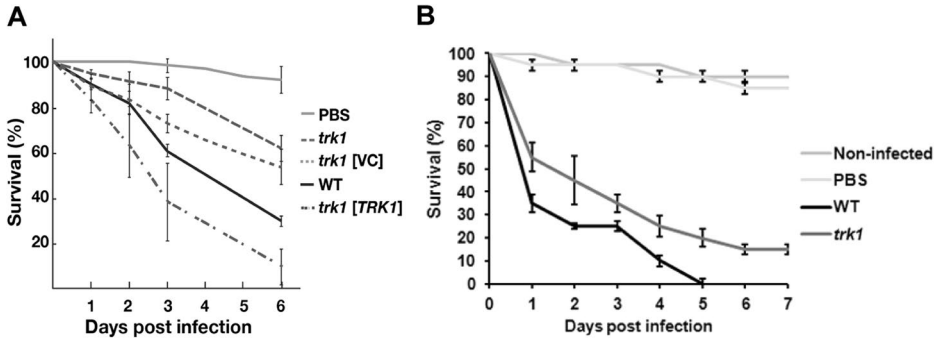

Figure 4. *C. glabrata* cells lacking Trk1 are less virulent in insect models. *D. melanogaster* $Bom^{\Delta 55C}$ flies (**A**) were infected with *C. glabrata* wild-type or *trk1* mutant strains without a plasmid vector (*trk1*), with an empty vector control (*trk1* [VC]), or with a vector expressing *TRK1* (*trk1* [*TRK1*]). Survival was monitored for the indicated period of days. Survival curves were obtained from the Cox proportional hazards model with data from 4 biological replicates (N = 4; bars represent standard error). (**B**) Survival of *G. mellonella* larvae infected with *C. glabrata* wild-type or *trk1* mutant strains was monitored for the indicated period of days. Data from 3 biological replicates (N = 3; bars represent standard error). PBS was used to control wounding.

the inability of the *trk1*Δ mutant to proliferate in media with a potassium concentration close to the concentrations in the host (a few mM extracellularly) would correspond to a lower virulence of mutants lacking an active potassium uptake system. To elucidate the relationship between the absence of Trk1 and virulence, we performed a series of experiments using two insect models, *Drosophila melanogaster* and *Galleria mellonella*. These invertebrate models are capable of reproducing clinical features seen in human infections with remarkable fidelity[40–42].

When introduced into *D. melanogaster*, fungal cells activate the Toll signaling pathway, triggering a robust induction of innate immune effectors, including the family of twelve *Bomanin* genes. The Bomanins, small secreted peptides, bestow resistance to multiple microbial pathogens, including *C. glabrata*. In contrast to wild-type flies, $Bom^{\Delta 55C}$ flies lacking10 Bomanins exhibit decreased survival upon *C. glabrata* infection[43], similar to mutational inactivation of the essential Toll pathway in MyD88 flies[44]. Figure 4A shows the killing curves obtained with $Bom^{\Delta 55C}$ flies infected with wild-type and *trk1*Δ *C. glabrata* strains. It is clearly evident that flies infected with the mutant strain survived better than those infected with the wild type. The introduction of plasmid encoded *TRK1*, but not the empty plasmid (VC; vector control), into the *trk1*Δ mutant restored full virulence. When the MyD88 flies were used, similar results were observed, i.e. lower virulence of the *trk1*Δ mutant (data not shown). For the assays with *G. mellonella*[45], two temperatures were used: 30 and 37 °C. We obtained similar results in both cases, and those obtained from assays at 37 °C are shown in Fig. 4B. Although both *Candida* strains killed the larvae quite efficiently, it was evident that the infection with *trk1*Δ cells was less severe than that with the wild-type *C. glabrata* cells.

Together, the virulence assays in the insect hosts confirm that the loss of Trk1-mediated high-affinity potassium uptake results in attenuated virulence of *C. glabrata*. Clearly, the *trk1*Δ mutant failed to accumulate sufficient potassium for cell growth and division within the host.

Absence of Trk1 results in increased clearance of *C. glabrata* cells by macrophages. The reduced virulence of *trk1*Δ mutant cells prompted us to examine the host-pathogen interaction with THP-1 macrophages. Macrophages are immune cells important in the recognition and destruction of pathogens[46,47]. These primary immune cells contain, as all mammalian cells, a high concentration of potassium (>100 mM). However, the levels of potassium in phagosomes have not been determined. Initially, the internal phagosome microenvironment should mirror the low extracellular concentration until it fuses with lysosomes, at which point the potassium levels should increase. Thus, there are two possibilities. The initial low levels of potassium may compromise growth of *trk1*Δ cells, which may affect survival. Alternatively, lysosomal fusion is rapid and *trk1*Δ cells experience sufficiently high levels of potassium to enable growth at rates comparable to wild-type.

Our initial observations regarding the growth and division of *C. glabrata* cells interacting with macrophages indicated that the *trk1*Δ strain exhibited slower growth in comparison to wild type (Fig. 5A). The growth of one hundred *C. glabrata* cells interacting with macrophages was monitored during 6 hours. Thirty percent of wild-type cells had duplicated, whereas only 20% of *trk1*Δ cells had duplicated. The lower level of growth of *trk1*Δ mutant cells suggested that the interaction between the macrophages and both *C. glabrata* strains differ and that a high affinity potassium uptake is required for proper yeast proliferation in this condition. These findings prompted us to perform further experiments.

To assess fungal cell-induced damage to macrophages during co-culturing we measured LDH release (% cytotoxity, Fig. 5B). *C. albicans*, known to cause high levels of damage, was used as a control[48]. The *trk1*Δ mutant caused almost no damage to macrophages as compared to wild type (the difference was already observable after 8 h, and clearly obvious after 24 h, Fig. 5B). Both *C. glabrata* strains caused less damage than *C. albicans*, particularly at the earlier timepoint, which correlates with the different strategies that these fungi employ after being engulfed by macrophages. *C. albicans* rapidly forms hyphae, damages macrophages and escapes, while *C. glabrata* seems to be adapted to longer stays inside the macrophages[47].

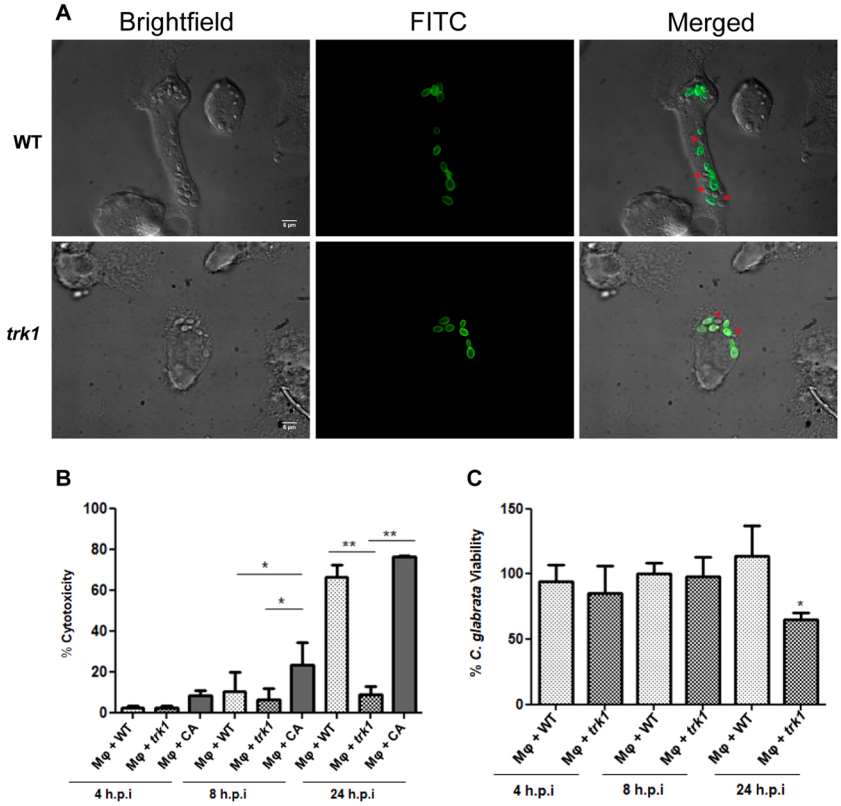

Figure 5. *C. glabrata* wild-type and *trk1Δ* cells interaction with human THP1 macrophages. (**A**) THP1 macrophages were incubated with FITC stained (green) *C. glabrata* cells, and fluorescence microcopy was used to evaluate yeast cell interaction with macrophages within 6 hours of incubation. The dye is not transferred to the daughter cells, allowing to differentiate mother cells (green) and daughter cells (red asterisks) in the merged channel. (**B**) Cytotoxicity mediated by *C. glabrata* wild-type (WT) and *trk1Δ* cells in THP1 macrophages was evaluated by LDH measurement. *C. albicans* wild-type strain SC5314 (CA) was used as a positive control. (**C**) Candidacidal activity of THP1 macrophages against *C. glabrata* wild type (WT) and *trk1Δ* was evaluated and expressed as a percentage of yeast viability. A lower viability of the yeast cells represents a higher candidacidal activity of the macrophages.

These results suggested that the candidacidal activity of the macrophages towards the *trk1*Δ strain may be higher. This was confirmed in the experiments shown in Fig. 5C. The macrophages killed *trk1*Δ cells more effectively than wild type, which was statistically significant after 24 h. These finding indicates that the loss of high-affinity potassium uptake impairs growth of *C. glabrata* inside macrophages and makes fungal cells more sensitive to killing by macrophages.

Cytokine production upon interaction of macrophages with *C. glabrata* cells. Cytokine production and secretion by macrophages is important in mediating the response of the immune system and to the outcome of microbial infections[49]. We assessed the cytokine profiles of macrophages after co-culture with the *C. glabrata* strains. We measured the release of 3 pro-inflammatory (IL-12, TNF-α and IL-1 β) and 1 anti-inflammatory (IL-10) cytokines. We were unable to detect secretion of IL-12 nor IL-10 cytokines in our experiments (data not shown). TNF-α was secreted, but there was no difference in secretion levels between control macrophages and macrophages with *C. glabrata* wild-type or *trk1*Δ cells (data not shown). The secretion of pro-inflammatory cytokine IL-1β was elevated similarly in the presence of either wild-type or *trk1*Δ (Supplementary Fig. 1). These largely negative results are in agreement with previous reports regarding *C. glabrata* macrophage interactions[50], with the cytokine patterns in murine infections[51] and with the previously described low level induction of MAP kinase phosphorylation[52].

Discussion

In our previous work we showed how the deletion of *TRK1*, encoding the sole potassium transporter in *C. glabrata*, has a pleiotropic effect on cell physiology, affecting the membrane potential, the intracellular pH and the tolerance to cationic drugs[37]. Based on this knowledge, we hypothesized that the altered physiological parameters of the mutant would also effect *C. glabrata* virulence. To test this notion we performed a series of experiments to document whether a *C. glabrata* strain lacking Trk1 exhibits altered virulence characteristics and a reduced capacity to induce virulent infections in insect hosts models and to kill and evade macrophages.

Initially, we focused on two closely related aspects known to be important determinants in virulence, cell-surface hydrophobicity (CSH) and adhesion capacity[17,18]. As shown in Fig. 1C, we observed a significant difference in CSH when comparing the wild-type strain and *trk1*Δ mutant. The wild type exhibited no differences in CSH at the two tested potassium concentrations (100 and 250 mM), suggesting that the composition of the cell wall and physico-chemical properties of the cell surface do not change in this KCl concentration range. It is worth noting that wild-type grows well at both much lower and higher extracellular potassium concentrations[37,38]. In comparison to the wild-type, the *trk1*Δ strain exhibited a significant increase in its CSH (Fig. 1C). Moreover, there was a clear increase in the CSH of the mutant at 100 mM KCl compared to its CSH at 250 mM KCl in the growth media. The obtained results suggest that the deletion of *TRK1* causes a basal stress that has persistent consequences on the composition of the cell wall, thus influencing the hydrophobicity of mutant cells even under conditions supporting an apparently normal growth rate (Fig. 1B). A similar situation was found when measuring the membrane potential of *C. glabrata* wild-type and *trk1*Δ cells grown in the presence of 250 mM KCl. Mutant cells were always relatively hyperpolarized, indicating that the deletion of *TRK1* affects the physiology parameters permanently and not only under low-potassium stress[37].

As with the CSH, the adherence of the wild-type cells did not seem to be significantly influenced at the two KCl concentrations used (100 and 250 mM; Fig. 2A). In striking contrast, although the adherence capacity of the *trk1*Δ mutant grown in the presence of 250 mM KCl was very similar to that of the wild type, the *trk1*Δ exhibited a dramatic increase in its adhesion capacity when a suboptimal 100 mM concentration of KCl was used (Fig. 2A). To elucidate whether the observed phenotypes of higher adhesion were potassium-specific or related to a general concentration of cations in the growth media, we tested adhesion in low K^+ media supplemented with Na^+ and Ca^+. Surprisingly, we observed a significant increase in the cell adhesion to polystyrene plates for both wild type and *trk1*Δ strains (Fig. 2B). This result means that the low concentration of potassium, and not the presence of other cations, is responsible for the observed increase in adhesion capacity. Consistent with this conclusion, the *trk1*Δ strain exhibited significantly more adhesion than wild type in media containing 100 mM KCl. As far as we know, this is the first time that the dependence of *C. glabrata* adhesion capacity on the amount of potassium cations in the external medium has been demonstrated.

The observed increase in the adherence of the wild-type strain in YNB-F without extra added KCl made us hypothesize that this phenomenon might have consequences in biofilm formation, enabling the cells to cope better with the limited amount of available potassium, as the extracellular matrix may trap and concentrate the potassium. To test this hypothesis, an experiment was performed at different concentrations of potassium (Fig. 3). At low KCl (15 μM) concentrations the biofilm formation of wild type correlated with the higher adherence, which is not surprising, since adhesion is the first phase of biofilm formation[20]. As shown in Fig. 3, the biofilm biomass of the wild-type strain was greatly reduced when potassium levels increased. By contrast, the *trk1*Δ strain persisted in establishing biofilms even up to 100 mM KCl; the progressive decrease in the formation of a biofilm in parallel with an increase in potassium concentration reinforces the idea that the change from planktonic cells to cells that form biofilms depends on the intracellular potassium supply. The fact that biofilm formation is strongly dependent on potassium, suggests that biofilm formation is a stress response and that growth in biofilms enables cells to maintain a critical concentrations of this essential alkali metal cation.

As was shown in our previous work[37], the *trk1*Δ mutant exhibits several physiological parameters that reduce its growth and fitness, which likely affect its virulence properties. For this reason, we examined whether the phenotypes resulting from *TRK1* deletion would also have an effect on the virulence of the mutant strain. The results obtained with experiments carried out in two model host systems, *D. melanogaster* and *G. mellonella* (Fig. 4), provided support for this notion; the *trk1*Δ strain exhibited significantly attenuated virulence compared to the wild type in $Bom^{\Delta 55C}$ flies. Although *D. melanogaster* is considered to be the most suitable insect model alternative to murine infection models[42], the use of *G. mellonella* gave similar results.

In summary, our data show that the deletion of *TRK1* has a pleiotropic effect on the physiology of *C. glabrata*, which affects its ability to colonize infected hosts. The reason for impaired virulence of the mutant strain lacking a high-affinity potassium-specific transporter is likely due to the inability to take up and maintain physiological intracellular levels of potassium, an essential cation. The resulting stress and impaired growth of the *trk1*Δ mutant enables the host immune system to be more effective at overcoming the infection and clearing the fungal cells from the host. Consistently, the experiments carried out with macrophages demonstrated that in comparison to wild type, *trk1*Δ strain grew less efficiently within phagosomes (Fig. 5A), inflicted less damage to the macrophages (Fig. 5B), and was more readily killed (Fig. 5C). Macrophages are known to actively sequester micronutrients from invading microorganisms[53], and the lack of Trk1 as the sole high-affinity and specific potassium uptake system may represent an additional handicap that promotes the higher susceptibility of the mutant to being killed by the macrophage. Additionally, we previously demonstrated that the *trk1Δ* mutant is sensitive to low external pH[37], which is another aspect that may contribute to the observed increased fungicidal capacity of the macrophages against the mutant, since one of the strategies of the defense cells for fighting invading microorganisms is the acidification of their phagosomes[52]. A high-affinity potassium uptake seems to be crucial for *C. glabrata* physiology and virulence thus highlighting the unique K^+ transporter in *C. glabrata* cells as a potential target for the development of a new antifungal drug.

Methods

Yeast strains and growth media. The *C. glabrata* reference strain ATCC 2001 and its derivative lacking the *TRK1* gene[37] were used in this study. *C. albicans* SC5314 was used for LDH measurements. Yeast cells were propagated in YPD (1% yeast extract, 2% peptone, 2% glucose, 2% agar for solid media) or YNB-F (0.17% YNB without amino acids, ammonium sulfate and potassium (ForMedium) supplemented with 0.4% ammonium sulfate, 2% glucose and adjusted to pH 5.8 with NH_4OH; potassium concentration approx. 15 μM) media at 30 °C. When necessary, the media were supplemented with indicated amount of KCl.

Cell surface hydrophobicity (CSH). CSH was determined as the relative distribution of yeast cells in a two-phase system consisting of an aqueous phase and the organic solvent hexadecane[17,54]. When cultures in YNB-F supplemented with 250 or 100 mM KCl reached $OD_{600} = 1.5$, cells were harvested, washed twice with distilled water, adjusted to $OD_{600} = 1$. Aliquots (1.5 ml) were transferred to a glass tube with (A_1) and without (A_0) 100 µl of hexadecane. Glass tubes were then mixed by gentle vortexing for 30 seconds. The two phases were allowed to separate for 2 minutes at room temperature, 1 ml of the aqueous phase of each tube was carefully transferred to a cuvette and the OD_{600} was measured. The percentage of hydrophobicity was calculated as Hydrophobicity (%) = [1 − (A1/A0)] × 100.

***In vitro* adhesion capacity.** Overnight cultures grown in YNB-F supplemented with 250 or 100 mM KCl ($OD_{600} \approx 1.5$) were adjusted to $OD_{600} = 1$ with fresh growth medium. Three wells of a flat-bottom polystyrene 96-well microtiter plate were filled with 200 µl of each cell suspension (adapted from[18]). Growth media without cells were used as negative controls. Adhesion was allowed to occur at 30 °C for 2 hours. After removing the medium, non-adherent cells were removed by washing three times with sterile water. Adhered cells were fixed with 200 µl of methanol, and plates were incubated at room temperature for 10 minutes. After washing three times with water to eliminate methanol, cells were stained with crystal violet (CV). 200 µl of 1% CV solution were added to each well, and plates were incubated at 37 °C for 20 minutes. After staining, the excess of CV was removed by washing three times with water. After adding 200 µl of 33% acetic acid to solubilize cell-bound CV, the staining intensity was measured as the OD_{595} using a 96-well plate reader (BioTek). The obtained values were normalized after subtracting the background level of CV staining without cells. For the potassium specificity assay, wild-type and *trk1*Δ cells were grown in YNB-F supplemented with 100 mM KCl till the cultures reached an OD_{600} of around 1. Cells were harvested, washed twice and resuspended to $OD_{600} = 0.4$ in YNB-F without KCl addition, or in YNB-F supplemented with 100 mM KCl, NaCl or $CaCl_2$. After this step, the adhesion protocol described above was followed.

Biofilm formation. For the study of biofilm formation, a modified version of the protocol of[55] was used. Both strains were grown in YNB-F supplemented with 250 mM KCl at 30 °C overnight, then adjusted to $OD_{600} = 0.4$ with fresh medium. For adhesion, three wells of a polystyrene microtiter plate were filled with 200 µl of the cell suspension for each set of biofilm formation conditions. After two hours of incubation at 30 °C, the medium was removed, free cells were washed out twice with water, and YNB-F supplemented with various concentrations of KCl (15 µM–250 mM) was added to the adhered cells. Plates were further incubated at 37 °C for 48 hours, and the quantification of the biofilm formation was performed after the staining with CV described above. As a control after the adhesion phase, the number of adhered cells of wild-type and *trk1*Δ mutant grown in 250 mM KCl was estimated by CV staining as described above to ensure that the number of adhered cells was the same for both strains. No significant differences were observed in the initial number of adhered cells.

Virulence in insect models. For testing the virulence of *C. glabrata* strains, *Drosophila melanogaster* flies and *Galleria mellonella* larvae were used. *D. melanogaster* stocks were maintained on instant mashed potato agar medium at 25 °C. $Bom^{\Delta 55C}$ flies, carry a 9 kb TALEN-induced deletion that removes a cluster of 10 *Bom* genes on chromosome 2[43]. The *MyD88* mutant strain lacks an adaptor protein functioning downstream of Tl receptor[44,56].

The overnight yeast precultures were diluted in fresh YPD to $OD_{600} = 0.15$ and incubated at 30 °C until the OD_{600} reached 1.0. Aliquots of the cultures (1 ml) were harvested, washed once with phosphate-buffered saline (PBS; pH 7) and resuspended in 1 ml of PBS. Male and female flies, 1–5 days old, were injected with approximately 50 nl of fungal cell suspensions (approx. 500 cells/fly) using a fine glass capillary needle with a micro-injector (TriTech Research, USA). Cohorts of 30 flies were injected and maintained in separate vials. Four biological replicas (independently prepared fungal preparations derived from individual colonies) and 12 technical replicates per strain were conducted. Infected flies were maintained at 29 °C for up to six days after infection and the number of surviving flies was noted on a daily basis.

G. mellonella larvae were from Mous Live Bait, The Netherlands. One day before the infection experiment, ten groups of ten *G. mellonella* larvae were placed in ten Petri dishes containing sawdust and incubated at 30 or 37 °C to acclimatize them to the conditions of the experiment. *C. glabrata* cells were grown in 15 ml of YPD supplemented with 100 mM KCl overnight. The day of infection, 10 ml of the *C. glabrata* cultures were harvested, washed twice with PBS and resuspended in 2 ml of PBS. After measuring OD_{600}, cell suspensions of both strains containing approx. 5×10^7 cells/100 µl were prepared, and 10 µl, i.e. 5×10^6 cells, were injected into one of the last pro-legs of the larvae with an insulin 29 G U-100 needle. Twenty individuals per yeast strain were infected. Three biological replicas were conducted. Untouched larvae and larvae injected with 10 µl PBS were used as controls. Larvae were kept in Petri dishes with sawdust, and live larvae were scored daily for 7 days. Larvae were considered dead when not responding to touch.

Interaction with macrophages. To quantify yeast replication upon interaction with macrophages, *C. glabrata* strains were grown in YNB430 F supplemented with 250 mM KCl and labelled with 100 µg/ml FITC (Sigma-Aldrich) in carbonate buffer (0.1 M Na_2CO_3, pH 9.0) for 30 min at 37 °C, followed by washing with PBS. TPH-1 macrophages were allowed to adhere to coverslips within a 24-well plate, infected at a MOI (multiplicity of infection; macrophage:yeast) 2:1 with labelled yeast strains for 30 min, washed to remove unbound yeast cells, and incubated at 37 °C and 5% CO_2 for 6 hours. Cells were fixed with 4% paraformaldehyde at 37 °C for 10 min. As FITC is not transferred to daughter cells, it was possible to differentiate mother and daughter cells. Replication was quantified by fluorescence microscopy scoring FITC-stained and not-stained cells for at least 100 yeast cells.

THP-1 cell culture and macrophage differentiation. The human acute monocytic leukemia cell line (THP-1) was cultured in DMEM medium supplemented with antibiotics (penicillin 10000 U/ml-streptomycin 10000 U/ml and 10% heat-inactivated fetal bovine serum (FBS) at 37 °C in a humidified atmosphere containing

5% CO_2. THP1 cells were centrifuged and resuspended in fresh DMEM. Phorbol 12-myristate 13-acetate (PMA) was added at a final concentration of 0.03 µg/ml and cells were counted. Then, 1×10^5 THP-1 cells were seeded onto 24-well plastic plates and 5×10^4 cells were seeded onto a 96-well plate and left to differentiate for 48 hours. The medium was replaced with fresh medium on the day of the interaction. DMEM without phenol red supplemented with 1% of FBS was used for the LDH measurements,. For the assays of candidacidal activity and cytokine production, DMEM with phenol red and 10% FBS was used.

C. glabrata-macrophage co-culture. For the interaction studies, THP-1 macrophages were incubated with *C. glabrata* cells at a MOI 1:1 and for the durations: 4 h, 8 h and 24 h.

Macrophage damage assay. A colorimetric assay based on the measurement of LDH activity released by damaged cells was used (Roche). Experiments were performed in 96-well plate and the manufacturer's instructions were followed. Briefly, Lysis buffer was added to the positive control cells 15 minutes before the end of the incubation time. To determine LDH activity, 100 µl of reaction mixture, (catalyst and dye solution) was added to each well on the 96-well plate and incubated for up to 30 min at room temperature and protected from the light. After this, 50 µl of stop solution was added to each well and absorbance measured at 490 nm. Cytotoxicity was calculated as follows:

$$Cytotoxicity\ (\%) = \frac{experimental\ value - low\ control}{high\ control - low\ control} \times 100$$

Three biological replicates were performed.

Candidacidal activity. The candidacidal activity of the macrophages was estimated by colony-forming units (CFUs) counting by comparing both *C. glabrata* strains with and without interaction with macrophages. 24-well plates were used for this assay. Briefly, the DMEM of each condition was collected, sterile H_20 was added to each well and a syringe plunger was used to destroy the macrophages and to resuspend *C. glabrata* cells in each well. From the total volume collected, dilutions were made and wild-type cells were plated on YPD agar and *trk1Δ* cells on YPD agar supplemented with 100 mM KCl. Candidacidal activity was calculated by comparing the CFUs counted for *Candida* cells growing without the presence of the macrophages and the CFUs counted the interacting cells. Four biological replicates were performed.

Determination of cytokine production. For cytokines measurements, macrophages from the THP1 cell line were incubated for 4, 8 and 24 hours in 24-well plates. Briefly, supernatants from THP-1 macrophages (untreated, LPS (1000 ng/ml), or *Candida*-treated) were collected. Afterwards, they were tested for cytokine production by ELISA using matched paired antibodies specific for IL-12p40, TNF-α IL-10 and IL-1β (Immunotools), and according to the manufacturer's instructions. Cytokine production was measured spectrophotometrically at 450 nm in a total of 3 biological replicates.

Statistical analysis. Statistical analysis was performed by doing a paired t-test. *p-value < 0.05, **p-value < 0.01.

References

1. Azie, N. *et al*. The PATH (Prospective Antifungal Therapy) Alliance (R) registry and invasive fungal infections: update 2012. *Diagn. Microbiol. Infect. Dis.* **73**, 293–300 (2012).
2. Diekema, D., Arbefeville, S., Boyken, L., Kroeger, J. & Pfaller, M. The changing epidemiology of healthcare-associated candidemia over three decades. *Diagn. Microbiol. Infect. Dis.* **73**, 45–48 (2012).
3. Khatib, R., Johnson, L. B., Fakih, M. G., Riederer, K. & Briski, L. Current trends in candidemia and species distribution among adults: *Candida glabrata* surpasses *C. albicans* in diabetic patients and abdominal sources. *Mycoses* **59**, 781–786 (2016).
4. Tortorano, A. M. *et al*. Candidaemia in Europe: epidemiology and resistance. *Int. J. Antimicrob. Agents* **27**, 359–366 (2006).
5. Brown, G. D. *et al*. Hidden killers: human fungal infections. *Sci. Transl. Med.* **4**, 165rv113 (2012).
6. Pfaller, M. A. & Diekema, D. J. Epidemiology of invasive mycoses in North America. *Crit. Rev. Microbiol.* **36**, 1–53 (2010).
7. Brown, A. J. P., Haynes, K. & Quinn, J. Nitrosative and oxidative stress responses in fungal pathogenicity. *Curr. Opin. Microbiol.* **12**, 384–391 (2009).
8. Rodrigues, C. F., Silva, S. & Henriques, M. *Candida glabrata*: a review of its features and resistance. *Eur. J. Clin. Microbiol. Infect. Dis.* **33**, 673–688 (2014).
9. Silva, S. *et al*. *Candida glabrata*, *Candida parapsilosis* and *Candida tropicalis*: biology, epidemiology, pathogenicity and antifungal resistance. *FEMS Microbiol. Rev.* **36**, 288–305 (2012).
10. Papon, N., Courdavault, V., Clastre, M. & Bennett, R. J. Emerging and emerged pathogenic *Candida* species: Beyond the *Candida albicans* paradigm. *PLoS Pathogens* **9**, 3550–3550 (2013).
11. Gabaldon, T. & Carrete, L. The birth of a deadly yeast: tracing the evolutionary emergence of virulence traits in *Candida glabrata*. *FEMS Yeast Res.* **16**, fov110 (2016).
12. Roetzer, A., Gabaldon, T. & Schuller, C. *From* Saccharomyces cerevisiae to *Candida glabrata* in a few easy steps: important adaptations for an opportunistic pathogen. *FEMS Microbiol. Lett.* **314**, 1–9 (2011).
13. Mansour, M. K. & Levitz, S. M. Interactions of fungi with phagocytes. *Curr. Opin. Microbiol.* **5**, 359–365 (2002).
14. Steinberg, B. E. *et al*. A cation counterflux supports lysosomal acidification. *J. Cell Biol.* **189**, 1171–1186 (2010).
15. Kaloriti, D. *et al*. Combinatorial stresses kill pathogenic *Candida* species. *Med. Mycol.* **50**, 699–709 (2012).
16. Nikolaou, E. *et al*. Phylogenetic diversity of stress signalling pathways in fungi. *BMC Evolutionary Biology* **9**, Artn 4410 (2009).
17. de Groot, P. W., Bader, O., de Boer, A. D., Weig, M. & Chauhan, N. Adhesins in human fungal pathogens: glue with plenty of stick. *Eukaryot. Cell* **12**, 470–481 (2013).
18. Gomez-Molero, E. *et al*. Proteomic analysis of hyperadhesive *Candida glabrata* clinical isolates reveals a core wall proteome and differential incorporation of adhesins. *FEMS Yeast Res.* **15**, fov098 (2015).
19. Luo, G. & Samaranayake, L. P. *Candida glabrata*, an emerging fungal pathogen, exhibits superior relative cell surface hydrophobicity and adhesion to denture acrylic surfaces compared with *Candida albicans*. *APMIS* **110**, 601–610 (2002).

20. Lopez, D., Vlamakis, H. & Kolter, R. Biofilms. *Cold Spring Harb. Perspect Biol.* **2**, a000398 (2010).
21. Araujo, D., Henriques, M. & Silva, S. Portrait of *Candida* species biofilm regulatory network genes. *Trend. Microbiol.* **25**, 62–75 (2017).
22. Rodrigues, C. F., Rodrigues, M. E., Silva, S. & Henriques, M. *Candida glabrata* biofilms: How far have Wwe come? *J. Fungi (Basel)* **3**, jof3010011 (2017).
23. Mayer, F. L., Wilson, D. & Hube, B. *Candida albicans* pathogenicity mechanisms. *Virulence* **4**, 119–128 (2013).
24. Almeida, R. S., Wilson, D. & Hube, B. *Candida albicans* iron acquisition within the host. *FEMS Yeast Res.* **9**, 1000–1012 (2009).
25. Citiulo, F. *et al*. *Candida albicans* scavenges host zinc via Pra1 during endothelial invasion. *PLoS Pathogens* **8**, ARTN e1002777 (2012).
26. Ene, I. V. *et al*. Host carbon sources modulate cell wall architecture, drug resistance and virulence in a fungal pathogen. *Cell Microbiol.* **14**, 1319–1335 (2012).
27. Hood, M. I. & Skaar, E. P. Nutritional immunity: transition metals at the pathogen-host interface. *Nat. Rev. Microbiol.* **10**, 525–537 (2012).
28. Arino, J., Ramos, J. & Sychrova, H. Alkali metal cation transport and homeostasis in yeasts. *Microbiol. Mol. Biol. Reviews* **74**, 95–120 (2010).
29. Arino, J., Ramos, J. & Sychrova, H. Monovalent cation transporters at the plasma membrane in yeasts. *Yeast*, https://doi.org/10.1002/yea.3355 (2018).
30. Ramos, J., Arino, J. & Sychrova, H. Alkali-metal-cation influx and efflux systems in nonconventional yeast species. *FEMS Microbiol. Lett.* **317**, 1–8 (2011).
31. Rodriguez-Navarro, A. & Benito, B. Sodium or potassium efflux ATPase a fungal, bryophyte, and protozoal ATPase. *Biochim. Biophys. Acta* **1798**, 1841–1853 (2010).
32. Huseĸova, B., Elicharova, H. & Sychrova, H. Pathogenic *Candida* species differ in the ability to grow at limiting potassium concentrations. *Canad. J. Microbiol.* **62**, 394–401 (2016).
33. Elicharova, H., Huseĸova, B. & Sychrova, H. Three *Candida albicans* potassium uptake systems differ in their ability to provide *Saccharomyces cerevisiae trk1trk2* mutants with necessary potassium. *FEMS Yeast Res.* **16**, fow039 (2016).
34. Watanabe, H., Azuma, M., Igarashi, K. & Ooshima, H. Relationship between cell morphology and intracellular potassium concentration in *Candida albicans*. *J. Antibiot. (Tokyo)* **59**, 281–287 (2006).
35. Navarrete, C. *et al*. Lack of main K^+ uptake systems in *Saccharomyces cerevisiae* cells affects yeast performance in both potassium-sufficient and potassium-limiting conditions. *FEMS Yeast Res* **10**, 508–517 (2010).
36. Petrezselyova, S., Ramos, J. & Sychrova, H. Trk2 transporter is a relevant player in K^+ supply and plasma-membrane potential control in *Saccharomyces cerevisiae*. *Folia Microbiol. (Praha)* **56**, 23–28 (2011).
37. Llopis-Torregrosa, V., Huseĸova, B. & Sychrova, H. Potassium uptake mediated by Trk1 is crucial for *Candida glabrata* growth and fitness. *PLoS One* **11**, e0153374 (2016).
38. Krauke, Y. & Sychrova, H. Cnh1 Na^+/H^+ antiporter and Ena1 Na^+-ATPase play different roles in cation homeostasis and cell physiology of *Candida glabrata*. *FEMS Yeast Res.* **11**, 29–41 (2011).
39. Silva, S. *et al*. Adherence and biofilm formation of non-*Candida albicans Candida* species. *Trends Microbiol.* **19**, 241–247, https://doi.org/10.1016/j.tim.2011.02.003 (2011).
40. Binder, U., Maurer, E. & Lass-Florl, C. *Galleria mellonella*: An invertebrate model to study pathogenicity in correctly defined fungal species. *Fung. Biol.* **120**, 288–295 (2016).
41. Borman, A. M. Of mice and men and larvae: *Galleria mellonella* to model the early host-pathogen interactions after fungal infection. *Virulence* **9**, 9–12 (2018).
42. Brunke, S. *et al*. Of mice, flies - and men? Comparing fungal infection models for large-scale screening efforts. *Dis. Mod. Mechan.* **8**, 473–486 (2015).
43. Clemmons, A. W., Lindsay, S. A. & Wasserman, S. A. An effector peptide family required for *Drosophila* Toll-mediated immunity. *PLoS Pathog.* **11**, doi:ARTN e1004876 (2015).
44. Horng, T. & Medzhitov, R. *Drosophila* MyD88 is an adapter in the Toll signaling pathway. *Proc. Natl. Acad. Sc.i USA* **98**, 12654–12658 (2001).
45. Kloezen, W., van Helvert-van Poppel, M., Fahal, A. H. & van de Sande, W. W. A *Madurella mycetomatis* grain model in *Galleria mellonella* larvae. *PLoS Negl. Trop. Dis.* **9**, e0003926 (2015).
46. Bourgeois, C., Majer, O., Frohner, I. E., Tierney, L. & Kuchler, K. Fungal attacks on mammalian hosts: pathogen elimination requires sensing and tasting. *Curr. Opin. Microbiol.* **13**, 401–408 (2010).
47. Kasper, L., Seider, K. & Hube, B. Intracellular survival of *Candida glabrata* in macrophages: immune evasion and persistence. *FEMS Yeast Res.* **15**, fov042 (2015).
48. Marcil, A., Harcus, D., Thomas, D. Y. & Whiteway, M. *Candida albicans* killing by RAW 264.7 mouse macrophage cells: effects of *Candida* genotype, infection ratios, and gamma interferon treatment. *Infect. Immun.* **70**, 6319–6329 (2002).
49. Arango Duque, G. & Descoteaux, A. Macrophage cytokines: involvement in immunity and infectious diseases. *Front Immunol* **5**, 491, https://doi.org/10.3389/fimmu.2014.00491 (2014).
50. Seider, K. *et al*. The facultative intracellular pathogen *Candida glabrata* subverts macrophage cytokine production and phagolysosome maturation. *J. Immunol.* **187**, 3072–3086 (2011).
51. Jacobsen, I. D. *et al*. *Candida glabrata* persistence in mice does not depend on host immunosuppression and is unaffected by fungal amino acid auxotrophy. *Infect. Immun.* **78**, 1066–1077 (2010).
52. Kasper, L. *et al*. Identification of *Candida glabrata* genes involved in pH modulation and modification of the phagosomal environment in macrophages. *PLoS One* **9**, e96015 (2014).
53. Skaar, E. P. & Raffatellu, M. Metals in infectious diseases and nutritional immunity. *Metallomics* **7**, 926–928 (2015).
54. Van Raamsdonk, M., Vandermei, H. C., Desoet, J. J., Busscher, H. J. & Degraaff, J. Effect of polyclonal and monoclonal-antibodies on surface-properties of *Streptococcus-Sobrinus*. *Infect. Immun.* **63**, 1698–1702 (1995).
55. Li, X. G., Yan, Z. & Xu, J. P. Quantitative variation of biofilms among strains in natural populations of Candida albicans. *Microbiology-SGM* **149**, 353–362 (2003).
56. Tauszig-Delamasure, S., Bilak, H., Capovilla, M., Hoffmann, J. A. & Imler, J. L. *Drosophila* MyD88 is required for the response to fungal and Gram-positive bacterial infections. *Nat. Immunol.* **3**, 91–97 (2002).

Acknowledgements

We gratefully acknowledge Steven A. Wasserman, San Diego, USA for providing the $Bom^{\Delta 55C}$ *Drosophila melangaster* strain. This work was supported by the EC FP7-PEOPLE-2013-ITN ImResFun (606786) (H.S.; A.G.; C.G.; P.O.L.), BIO2015-65147-R from Spanish Ministry of Economy and Competitiveness (C.G.), Swedish Research Council VR-2015-04202 (P.O.L.) and Swedish Cancer Society CAN2014/449 (Y.E.). This work was also supported by the Czech Science Foundation (GA CR 16-03398S) and the Ministry of Education, Youth and Sports of CR within the LQ1604 National Sustainability Program II (Project BIOCEV-FAR) and "BIOCEV"

(CZ.1.05/1.1.00/02.0109) (H.S.), and by NKFIH K 123952 and GINOP2-3-2-15-2016-00015 (A.G.). O. Zimmermannová is acknowledged for the critical reading of the manuscript.

Author Contributions

V.L.-T., C.V. and K.R. performed the experiments, A.G., C.G., L.M., Y.E. and P.L. supervised the experimental work, V.L.-T., C.V. and K.R. prepared the figures, C.V. contributed to the manuscript writing. H.S. and V.L.-T. wrote and complied the main manuscript. C.G., A.G. and P.O.L. critically reviewed the manuscript. All authors contributed to the conception and planning of the study, and reviewed the manuscript.

Additional Information

Supplementary information accompanies this paper at https://doi.org/10.1038/s41598-019-43912-1.

Competing Interests: The authors declare no competing interests.

Publisher's note: Springer Nature remains neutral with regard to jurisdictional claims in published maps and institutional affiliations.